Course Notes:
United States Particle Accelerator School

Beam Physics with Intense Space-Charge

J.J. Barnard and S.M. Lund

Lawrence Livermore National Laboratory
Livermore, CA 94550
and
Accelerator Fusion Research Division
Ernest Orlando Lawrence Berkeley National Laboratory
Berkeley, CA 94720

June 2008

Presented at
Annapolis MD, 16-27 Jnue 2008

This work was supported by the Director, Office of Science, Office of Fusion Energy Sciences, of the U.S. Department of Energy under Contract No. DE-AC02-05CH11231, and the U.S. Department of Energy, Lawrence Livermore National Laboratory under Contract DE-AC52-07NA27344

LLNL-AR-407617

Beam Physics with Intense Space-Charge

Lecturers:
John J. Barnard and Steven M. Lund
Lawrence Livermore National Laboratory
Lawrence Berkeley National Laboratory

Grader:
Christos Papadopoulous
University of Maryland

Course Notes:
United States Particle Accelerator School
Held 16-27 June, 2008
Annapolis, Maryland
Sponsored by University of Maryland at College Park

Prepared under the auspices of the US Department of Energy at the Lawrence Livermore and Lawrence Berkeley National Laboratories under Contracts No. DE-AC52-07NA27344 and DE-AC02-05CH11231.

Beam Physics with Intense Space Charge

Instructors: John Barnard and Steven Lund, Lawrence Livermore National Laboratory

Purpose and Audience

The purpose of this course is to provide a comprehensive introduction to the physics of beams with intense space charge. This course is suitable for graduate students and researchers interested in accelerator systems that require sufficient high intensity where mutual particle interactions in the beam can no longer be neglected. *Prerequisites: undergraduate level Electricity and Magnetism and Classical Mechanics. Some familiarity with plasma physics, special relativity, and basic accelerator physics is recommended but not required.*

Objectives

This course is intended to give the student a broad overview of the dynamics of beams with strong space charge. The emphasis is on theoretical and analytical methods of describing the acceleration and transport of beams. Some aspects of numerical and experimental methods will also be covered. Students will become familiar with standard methods employed to understand the transverse and longitudinal evolution of beams with strong space charge. The material covered will provide a foundation to design practical architectures.

Instructional Method

Lectures will be given during morning sessions, followed by afternoon discussion sessions, which will engage the student on the material covered in lecture. Daily problem sets will be assigned that will be expected to be completed outside of scheduled class sessions. Problem sets will generally be due the morning of the next lecture session. A final take home exam will be given on the second Thursday, and will cover the contents of the entire course. Two instructors will be available for guidance during evening homework sessions.

Course Content

In this course, we will introduce you to the physics of intense charged particle beams, focusing on the role of space charge. The topics include: particle equations of motion, the paraxial ray equation, and the Vlasov equation; 4-D and 2-D equilibrium distribution functions (such as the Kapchinskij-Vladimirskij, thermal equilibrium, and Neuffer distributions), reduced moment and envelope equation formulations of beam evolution; transport limits and focusing methods; the concept of emittance and the calculation of its growth from mismatches in beam envelope and from space-charge non-uniformities using system conservation constraints; the role of space-charge in producing beam halos; longitudinal space-charge effects including small amplitude and rarefaction waves; stable and unstable oscillation modes of beams (including envelope and kinetic modes); the role of space charge in the injector; and algorithms to calculate space-charge effects in particle codes. Examples of intense beams will be given primarily from the ion and proton accelerator communities with applications from, for example, heavy-ion fusion, spallation neutron sources, nuclear waste transmutation, etc.

Reading Requirements

Extensive class notes will be provided that will serve as the primary reference. *(To be provided by the USPAS)* "The Theory and Design of Charged Particle Beams" Second Edition, Updated and Expanded by Martin Reiser, Wiley & Sons 2008.

Credit Requirements

Students will be evaluated based on performance: final exam (20 % of course grade), homework assignments (80 % of course grade).

```
US Particle Accelerator School
  sponsored by University of Maryland at College Park
Annapolis, Maryland
Monday June 16 - Friday June 27, 2008

LLNL: UCRL-?TBD?
LBNL: LBNL-?TBD?

"Beam Physics with Intense Space Charge"

Lecturers:
John J. Barnard and Steven M. Lund
Lawrence Livermore National Laboratory

Grader:
Christos Papadopoulous
University of Maryland


List of file format suffixes:
  .txt  => ascii text
  .pdf  => Adobe Acrobat pdf
  .html => html
  .ppt  => Microsoft Power Point (produced by OpenOffice Conversion)
  .xls  => Microsoft Excel       (produced on OpenOffice Conversion)
  .odp  => Open Document Presentation (Open Office)
  .odw  => Open Document Writer       (Open Office)
  .ods  => Open Document Spread Sheet (Open Office)

Author abbreviations:
   JJB - Notes by J.J. Barnard
   SML - Notes by S.M. Lund
 4
Class material can be found in the following files and directories:

00.cover.pdf
00.cover.ppt
  Cover used in paper printing of class material.

00.outline.txt
00.outline.pdf
  Outline and file list (this file).

00.overview.txt
00.overview.pdf
  Class overview in text and pdf formats.

00.schedule.pdf
00.schedule.xls
  Actual schedule of class lectures.

01.intro.pdf   (JJB)
  Introductory lecture surveying basic concepts.

02.env_eqns.pdf  (JJB)
  Introduction to envelope equations.

03.curr_lims.pdf (JJB)
  Introduction to current limits.

04.tpe.pdf  (SML)
  Transverse particle equations of motion.

05.ted_full.pdf  (SML)  full version
05.ted.pdf              slides
05.ted_ho.pdf           slides -- hand out version
05.ted_app_a.pdf        handwritten notes -- Appendix A
05.ted_app_b.pdf        handwritten notes -- Appendix B
```



```
  Transverse equilibrium distributions.

06.pr_full.pdf  (SML)   full version
06.pr.pdf               slides
06.pr_ho.pdf            slides -- hand out version
06.pr_sup.pdf           handwritten note supplement
  Transverse particle resonances with application to rings.

07.inj_long_I.pdf  (JJB)
  Injectors and longitudinal physics, part I.

08.long_II.pdf  (JJB)
  Longitudinal physics, part II.

09.long_III.pdf  (JJB)
  Longitudinal physics, part III.

10.tce_full.pdf  (SML)  full version
10.tce.pdf              slides
10.tce_ho.pdf           slides -- hand out version
10.tce_sec9.pdf         handwritten note supplement -- Sec 9
  Centroid and envelope evolution including envelope modes and stability.

11.env_modes_halo.pdf  (JJB)
  Continuous focusing envelope modes and beam halo.

12.tks_full.pdf  (SML)  full version
12.tks.pdf              slides
12.tks_ho.pdf           slides -- hand out version
12.tks_sup.pdf          handwritten note supplement
  Transverse kinetic stability: conservation constraints, kinetic stability
  bounds, normal modes on a KV beam, and other beam stability topics.

13.press_scat_elec.pdf  (JJB)
  Vacuum, scattering, and electron effects.

14.apps.pdf  (JJB)
  Applications: Heavy ion fusion overview and final focus.

15.st_full.pdf  (SML)   full version
15.st.pdf               slides
15.st_ho.pdf            slides -- hand out version
15.st_sup.pdf           handwritten note supplement
  Numerical simulations of beams.

16.summary_jjb.pdf  (JJB)
  Summary of lectures by J.J. Barnard.

grades_evaluations  (directory)
  Note: This directory is only distributed to the instructors.

  evaluations.pdf
    Student evaluations of class.

  grade_sheet.pdf
    Formal grade sheet turned in to the USPAS.

  homeworkandgrades.xls
    All grades on problem sets and final.

  students.pdf
    Listing of students and institutions, and credit status
     both preliminary and final.

audio (directory)
  Note: This directory is not included in most distributions (large file size)


movies  (directory)
```

```
  Note: This directory is not included in most distributions (large file size)

  ESQfastrise_zx.mpg
    3D injector simulation with a fast rise voltage pulse.

  ESQslowrise_zx.mpg
    3D injector simulation with a slow rise voltage pulse.

  hcx.mov
    Simulation of the HCX experiment from the source.

  hollow_movie.mpg
    Simulation on the evolution of a nonuniform density beam.


photos  (directory)


problems (directory)
  Note: This directory is only distributed to the instructors.

  All files pdf scans of handwritten problems and solutions

  01_set1_probs.pdf    Problem  Set #1
  01_set1_sols.pdf     Solution Set #1

  02_set2_probs.pdf    Problem  Set #2
  02_set2_sols.pdf     Solution Set #2

  03_set3_probs.pdf    Problem  Set #3
  03_set3_sols.pdf     Solution Set #3

  04_set4_probs.pdf    Problem  Set #4
5 04_set4_sols.pdf     Solution Set #4

  05_set5_probs.pdf    Problem  Set #5
  05_set5_sols.pdf     Solution Set #5

  06_set6_probs.pdf    Problem  Set #6
  06_set6_sols.pdf     Solution Set #6

  07_set7_probs.pdf    Problem  Set #7
  07_set7_sols.pdf     Solution Set #7

  08_set8_probs.pdf    Problem  Set #8
  08_set8_sols.pdf     Solution Set #8

  09_final_probs.pdf   Final Exam Problems  (Final Exam counts for 2 sets)
  09_final_sols.pdf    Final Exam Solutions

  collections directory containing:

  SML: Collections of problems and solutions sorted by topic
       (only a subset were used in this class) problems _prob and
       solutions _sol files

  tpe_prob.pdf  Transverse particle equations of motion
  tpe_sol.pdf

  ted_prob.pdf  Transverse equilibrium distributions
  ted_sol.pdf

  pr_prob.pdf   Circular accelerators and resonance effects in rings
  pr_sol.pdf

  tce_prob.pdf  Transverse centroid and envelope descriptions of beam evolution
  tce_sol.pdf

  st_prob.pdf   Simulation techniques for intense beams
```



```
  st_sol.pdf

simulations (directory)
  Note:  This directory not included in most distributions.  Material
  used in class demonstrations of simulations.

  ag-slice.py
     Python input script for example WARP PIC code simulations.   This file
     was used in one interactive class session to carry out example
     simulations by making simple variants of this example run.  See script
     header for instructions on running this script and viewing the output
     files.

  ag-slice.000.cgm
     cgm output file produced by WARP simulation ag-slice.py


uspas (directory)
  Note: This directory is not included in most distributions.  The information
  contained is available on the usaps web site:  http://uspas.fnal.gov

  uspas.pdf
    Information on the school.

  uspas_local.pdf
    Local school info.

  participants.pdf
    Full list of school participants.

Course Outline:

Note:  This outline and the distribution files are arranged in logical
presentation order.  In the actual class, there were deviations from
this order due to practical constraints.  The actual order of material
presented can be found in 00_schedule.pdf.

"Beam Physics with Intense Space-Charge"


Lecturers: John J. Barnard and Steven M. Lund
Lawrence Livermore National Laboratory

Simulations and Grading: Christos Papadopoulous
University of Maryland

1.  Introduction to the Physics of Beams and Basic Parameters  (JJB)
01.intro.pdf  pdf scan, handwritten notes and slides

  1.1 Particle equations of motion
  1.2 Dimensionless parameters: Perveance, phase advance, space charge
      tune depression
  1.3 Plasma physics of beams: collisions, Debye Length
  1.4 Klimontovich equation, Vlasov equation, Liouville's theorem
  1.4 Emittance and brightness


2.  Envelope Equations-I  (JJB)
02.env_eqns.pdf  pdf scan, handwritten notes and slides

  2.1 Paraxial Ray Equation
  2.2 Envelope equations for axially symmetric beams
  2.3 Cartesian equations of motion
      2.3.1 Quadrupole focusing
      2.3.2 Space charge force for elliptical beams
  2.4 Envelope equations for elliptically symmetric beams


3.  Current Limits in Accelerators and Centroid equations-I (JJB)
```

```
03.curr_lims.pdf  pdf scan, handwritten notes and slides

  3.1 Axisymmetric beams
     3.1.1 Solenoids
     3.1.2 Einzel Lenses
  3.2 Elliptically symmetric beams
     3.2.1 Derivation of space charge term in envelope equation with
           elliptical symmetry
     3.2.2 Current limit for quadrupoles using Fourier transforms
  3.3 Current limit for continuous focusing
     3.3.1 Calculation of sigma_0 (using matrix multiplication)
     3.3.2 Comparison of quadrupole current limit (from Fourier transform,
     and matrix methods)
  3.4 Centroid equations (first order moments)
     3.4.1 Space charge and focusing forces
  3.5 Image forces (effect on centroid and envelope)


4.  Transverse Particle Equations of Motion (SML)
04.tpe.pdf      pdf conversion of Open Office document
04.tpe_ho.pdf   04.tpe.pdf in handout form (4 slides per page)
04.tpe_full.pdf 04.tpe_ho.pdf oriented for 2-sided printing

  4.1  Particle Equations of Motion
    4.1.A Introduction: The Lorentz Force Equation
    4.1.B Applied Fields
    4.1.C Machine Lattice
    4.1.D Self Fields
    4.1.E Equations of Motion in s and the Paraxial Approximation
    4.1.F Summary: Transverse Particle Equations of Motion
    4.1.G Overview of Analysis to Come
    4.1.H Bent Coordinate System and Particle Equations of Motion with
          Dipole Bends and Axial Momentum Spread
 64.2  Transverse Particle Equations of Motion in Linear Focusing Channels
    4.1.A Introduction
    4.2.B Continuous Focusing
    4.2.C Alternating Gradient Quadrupole Focusing - Electric Quadrupoles
    4.2.D Alternating Gradient Quadrupole Focusing - Magnetic Quadrupoles
    4.2.E Solenoidal Focusing
    4.2.F Summary of Transverse Particle Equations of Motion
    Appendix A: Quadrupole Skew Coupling
    Appendix A: The Larmor Transform to Express Solenoidal Focused
                Particle Equations of Motion in Uncoupled Form
  4.3  Description of Applied Focusing Fields
    4.3.A Overview
    4.3.B Magnetic Field Expansions for Focusing and Bending
    4.3.C Hard Edge Equivalent Models
    4.3.D 2D Transverse Multipole Magnetic Moments
    4.3.E Good Field Radius
    4.3.F Example Permanent Magnet Assemblies
  4.4 Transverse Particle Equations of Motion with Nonlinear Applied Fields
    4.4.A Overview
    4.4.B Approach 1: Explicit 3D Form
    4.4.C Approach 2: Perturbed Form
  4.5  Linear Equations of Motion Without Space-Charge, Acceleration, and
       Momentum Spread
    4.5.A Hill's equation
    4.5.B Transfer Matrix Form of the Solution to Hill's Equation
    4.5.C Wronskian Symmetry of Hill's Equation
    4.5.D Stability of Solutions to Hill's Equation in a Periodic Lattice
  4.6  Hill's Equation: Floquet's Theorem and the Phase-Amplitude Form
       of the Particle Orbit
    4.6.A Introduction
    4.6.B Floquet's Theorem
    4.6.C Phase-Amplitude Form of the Particle Orbit
    4.6.D Summary: Phase-Amplitude Form of the Solution to Hill's Equation
    4.6.E Points on the Phase-Amplitude Formulation
    4.6.F Relation Between the Principal Orbit Functions and the
          Phase-Amplitude Form Orbit Functions
```



```
    4.6.G Undepressed Particle Phase Advance
    Appendix C: Calculation of w(s) from Principal Orbit Functions
  4.7  Hill's Equation: The Courant-Snyder Invariant and the
       Single-Particle Emittance
    4.7.A Introduction
    4.7.B Derivation of the Courant-Snyder Invariant
    4.7.C Lattice Maps
  4.8 Hill's Equation: The Betatron Formulation of the Particle Orbit
      and Maximum Orbit Excursions
    4.8.A Formulation
    4.8.B Maximum Orbit Excursions
  4.9  Momentum Spread Effects and Bending
    4.9.A Overview
    4.9.B Chromatic Effects
    4.9.B Dispersive Effects
  4.10 Acceleration and Normalized Emittance
    4.10.A Introduction
    4.10.B Transformation to Normal Form
    4.10.C Phase-Space Relations Between Transformed and Untransformed Systems
    Appendix D: Accelerating Fields and Calculation of Changes in gamma*beta
  Contact Information
  References
  Acknowledgments


5.  Transverse Equilibrium Distribution Functions (SML)
05.ted.pdf         pdf conversion of Open Office document
05.ted_ho.pdf      05.ted.pdf in handout form (4 slides per page)
05.ted_app.pdf     appendix A and B, pdf scan, handwritten notes

05.ted_full.pdf    combined file:  05.ted_ho.pdf, 05.ted_app_a.pdf,
                                   05.ted_app_b.pdf
                   oriented for printing

  5.1  Vlasov Model
    Vlasov-Poisson System
    Review: Lattices: Continuous, Solenoidal, and Quadrupole
    Review: Undepressed Particle Phase Advance
  5.2  Vlasov Equilibria
    Equilibrium Conditions
    Single Particle Constants of the Motion
    Discussion: Plasma Physics Approach to Beam Physics
  5.3 The KV Equilibrium Distribution
    Hill's Equation with Linear Space-Charge Forces
    Review: Courant-Snyder Invariants
    Courant-Snyder Invariants for a Uniform Density Elliptical Beam
    KV Envelope Equations
    Canonical Form of the KV Distribution Function
    Matched Envelope Structure
    Depressed Particle Orbits
    rms Equivalent Beams
    Discussions/Comments on the KV Model
  Appendix A: Self-Fields of a Uniform Density Elliptical Beam in Free Space
    (handwritten notes)
    Derivation #1: Direct
    Derivation #2: Simplified
  Appendix B: Canonical Transforms of the KV Distribution
    (handwritten notes)
    Canonical Transforms
    Simplified Moment Calculations
  5.4  The Continuous Focusing Limit of the KV Distribution
    Reduction of Elliptical Model
    Wavenumbers of Particle Oscillations
    Distribution Form
    Discussion
  5.5  Continuous Focusing Equilibrium Distributions
    Equilibrium Form
    Poisson's Equation
    Moments and rms Equivalent Beam Envelope Equation
```

```
    Example Distributions
  5.6  Continuous Focusing: The Waterbag Equilibrium Distribution
    Distribution Form
    Poisson's Equation
    Solution in Terms of Accelerator Parameters
    Equilibrium Properties
  5.7  Continuous Focusing: The Thermal Equilibrium Distribution
    Overview
    Distribution Form
    Poisson's Equation
    Solution in Terms of Accelerator Parameters
    Equilibrium Properties
  5.8  Continuous Focusing: Debye Screening in a Thermal Equilibrium Beam
    Poisson's Equation for the Perturbed Potential Due to a Test Particle
    Solution for Characteristic Debye Screening
  5.9  Continuous Focusing: The Density Inversion Theorem
    Relation of Density Profile to the Full Distribution Function
    Example Application to the KV Distribution
  5.10 Comments on the Plausibility of Smooth, non-KV Vlasov Equilibria
       in Periodic Focusing Lattice
    Discussion
  Contact Information
  References


6.  Transverse Particle Resonances with Application to Circular Accelerators
    (SML)
06.pr.pdf         pdf conversion of Open Office document
06.pr_ho.pdf      06.pr.pdf in handout form (4 slides per page)
06.pr_sup.pdf     pdf scan, handwritten notes for slides not
                            yet converted to Open Office

06.pr_full.pdf    combined file: 06.pr_ho.pdf, 06.pr_sup.pdf
                  oriented for printing

  6.1 Overview
    Hill's Equation Review: Betatron Form of Phase-Amplitude Solution
    Transform Approach
    Random and Systematic Perturbations Acting on Orbits
  6.2 Floquet Coordinates
    Transformation of Hill's Equation to a Simple Harmonic Oscillator
    Phase-Space Structure of Solution
    Expression of the Courant-Snyder Invariant
    Phase-Space Area Transform
  6.3 Perturbed Hill's Equation in Floquet Coordinates
    Transformation Result for x-Equation
  6.4 Sources and Forms of Perturbation Terms
    Power Series Expansion of Perturbations
    Connection to Multipole Errors
  6.5 Perturbed Solution: Resonances
    Fourier Expansion of Perturbations and Resonance Terms
    Resonance Conditions
  6.6 Machine Operating Points: Restrictions Resulting from Resonances
    Tune Restrictions from Low Order Resonances
  6.7 Space-Charge Effects
    Coherent and Incoherent Tune Shifts
    Laslett Limit
  Contact Information
  References
  Acknowledgments

7.  Injectors and Longitudinal Physics Part I (JJB)
07.inj_long_I.pdf  pdf scan, handwritten notes and slides

  7.1  Diodes and Injectors
    7.1.1 Space-charge limited flow and child-Langmuir law
    7.1.2 Pierce electrodes
    7.1.3 Transients in injectors and Lampel-Tiefenback solution
  7.2 Injector Choices
```



```
8.  Longitudinal Physics Part II (JJB)
08.long_II.pdf  pdf scan, handwritten notes and slides

  8.1  Acceleration -- introduction
  8.2  Space charge of short bunches (in rf-accelerators)
  8.3  Space charge of long bunches (g-factor model)
  8.4  Longitudinal 1D Vlasov equation
  8.5  Longitudinal fluid equation
  8.4  Longitudinal space charge waves
  8.5  Longitudinal rarefaction waves and bunch end control


9.  Longitudinal Physics Part III (JJB)
09.long_III.pdf  pdf scan, handwritten notes and slides

  9.1  Longitudinal cooling from acceleration
  9.2  Longitudinal resistive instability
  9.3  Bunch compression
  9.4  Longitudinal envelope equation
  9.4  Neuffer distribution function


10. Transverse Centroid and Envelope Descriptions of Beam Evolution (SML)

10.tce.pdf       pdf conversion of Open Office document
10.tce_ho.pdf    10.tce.pdf in handout form (4 slides per page)
10.tce_sec9.pdf  pdf scan, handwritten notes and slides for sec9 (2006 uspas)

10.tce_full.pdf  combined pdf file: 10.tce_ho.pdf, 10.tce_sec9.pdf
                 oriented for printing

  10.1  Overview
  10.2  Derivation of Centroid and Envelope Equations of Motion
    Statistical Averages
    Particle Equations of Motion
    Distribution Assumptions
    Self-Field Calculation: Direct and Image
    Coupled Centroid and Envelope Equations of Motion
  10.3  Centroid Equations of Motion
    Single Particle Limit: Oscillation and Stability Properties
    Effect of Driving Errors
    Effect of Image Charges
  10.4  Envelope Equations of Motion
    KV Envelope Equations
    Applicability of Model
    Properties of Terms
  10.5  Matched Envelope Solutions
    Construction of Matched Solution
    Symmetries of Matched Envelope: Interpretation via KV Envelope Equations
    Examples
  10.6  Envelope Perturbations
    Perturbed Equations
    Matrix Form: Stability and EigenMode Symmetries
    Decoupled Modes
    General Mode Limits
   10.7 Envelope Modes in Continuous Focusing
    Normal Modes: Breathing and Quadrupole Modes
    Driven Modes
   10.8  Envelope Modes in Periodic Focusing Channels
    Solenoidal Focusing
    Quadrupole Focusing
    Mode Launching
   10.9  Transport Limit Scaling Based on Envelope Models
         (see handwritten notes)
    Overview
    Example Calculation for a Periodic FODO Quadrupole Transport Channel
    Discussion on Application of Formulas in Design
```

```
    Results of More Detailed Models
  10.10 Centroid and Envelope Descriptions via
        1st Order Coupled Moment Equations
    Formulation
    Example Illustration - Familiar KV Envelope Model
 Contact Information
 References


11. Continuous Focusing Envelope Modes and Beam Halo  (JJB)
11.env_modes_halo.pdf  pdf scan, handwritten notes and slides

  11.1 Envelope modes of unbunched beams in continuous focusing
  11.2 Envelope modes of bunched beams in continuous focusing
  11.3 Halos from mismatched beams
    11.3.1 What is halo? Why do we care
    11.3.2 Qualitative picture of halo formation: mismatches
           resonantly drive particles to large amplitude
    11.3.3 Core/particle models
    11.3.4 Amplitude phase analysis


12. Transverse Kinetic Stability (SML)
12.tks.pdf       pdf conversion of Open Office document
12.tks_ho.pdf    12.tks.pdf in handout form (4 slides per page)
12.tks_sup.pdf   pdf scan, handwritten notes supplementing Sec. 4

12.tks_full.pdf  combined pdf file: 12.tks_ho.pdf, 12.tks_sup.pdf
                 oriented for printing

  12.1 Overview: Machine Operating Points
    Notions of Beam Stability
    Tiefenback Experimental Results for Quadrupole Transport
∞12.2 Overview: Collective Modes and Transverse Kinetic Stability
    Possibility of Collective Internal Modes
    Vlasov Model Review
    Plasma Physics Approach to Understanding Higher Order Instability
  12.3 Linearized Vlasov Equation
    Equilibrium and Perturbations
    Linear Vlasov Equation
    Method of Characteristics
    Discussion
  12.4 Collective Modes on a KV Equilibrium Beam
    KV Equilibrium
    Linearized Equations of Motion
    Solution of Equations
    Mode Properties
    Physical Mode Components Based on Fluid Model
    Periodic Focusing Results
  12.5 Global Conservation Constraints
    Conserved Quantities
    Implications
  12.6 Kinetic Stability Theorem
    Effective Free Energy
    Free Energy Expansion in Perturbations
    Perturbation Bound and a Sufficient Condition for Stability
    Interpretation and Example Applications
  12.7 rms Emittance Growth and Nonlinear Forces
    Equations of Motion
    Coupling of Nonlinear Forces to rms Emittance Evolution
  12.8 rms emittance Growth and Nonlinear Space-Charge Forces
    Equations of Motion
    rms Equivalent Beam Forms
    Wangler's Theorem
  12.9 Uniform Density Beams and Extreme Energy States
    Variational Formulation
    Self-Field Energy Minimization
  12.10 Collective Relaxation and rms Emittance Growth
    Conservation Constraints
```



```
    Relaxation Processes
    Emittance Growth Bounds from Space-Charge Nonuniformities
  12.11 Halo Induced Mechanism of Higher-Order Instability
    Halo Model for an Elliptical Beam
    Pumping Mechanism
    Stability Properties
  12.12 Phase Mixing and Landau Damping in Beams
    (to be added in future versions)
  Contact Information
  References


13. Pressure, Scattering, and Electron Effects (JJB)
13.press_scat_elec.pdf  pdf scan, handwritten notes and slides

  13.1 Beam/beam Coulomb collisions
  13.2 Beam/residual-gas scattering
  13.3 Charge-changing processes
  13.4 Wall effects
    13.4.1 gas pressure instability
  13.5 Electron cloud processes
    13.5.1 Multiple-bunch beam-induced multipacting
    13.5.2 Single-bunch beam-induced multipacting
  13.6 Electron-ion instability


14. Applications: Heavy Ion Fusion and Final Focus (JJB)
14.apps.pdf  pdf scan, handwritten notes and slides

  14.1 An application of intense beams: Heavy Ion Fusion
    14.1.1 Requirements
    14.1.2 Targets for inertial confinement fusion
    14.1.3 Accelerator
    14.1.4 Drift compression
    14.1.5 Final focus
  14.2 Final focus
    14.2.1 Predicting spot size using envelope equation
           and estimate of effects from chromaticity
  14.3 Experiments for Heavy Ion Fusion


15. Numerical Simulations (SML)
15.st.pdf        pdf conversion of Open Office document
15.st_ho.pdf     15.st.pdf in handout form (4 slides per page)
15.st_sup.pdf    pdf scan, handwritten notes supplementing unfinished sections

15.st_full.pdf   combined file: 15.st_ho.pdf, 15.st_sup.pdf
                 oriented for printing

  15.1 Why Numerical Simulation?
  15.2 Classes of Intense Beam Simulations
    15.2.A Overview
    15.2.B Particle Methods
    15.2.C Distribution Methods
    15.2.D Moment Methods
    15.2.E Hybrid Methods
  15.3 Overview of Basic Numerical Methods
    15.3.A Discretizations
    15.3.B Discrete Numerical Operations
      - Derivatives
      - Quadrature
      - Irregular Grids and Axisymmetric Systems
    15.3.C Time Adavnce
      - Overview
      - Euler and Runge-Kutta Advances
      - Solution of Moment Methods
  15.4 Numerical Methods for Particle and Distribution Methods
    14.4.A Overview
    14.4.B Integration of Equations of Motion
```

```
      - Leapfrog Advance for Electric Forces
      - Leapfrog Advance for Electric and Magnetic Forces
      - Numerical Errors and Stability of the Leapfrog Method
      - Illustrative Examples
    15.4.C Field Solution
      - Electrostatic Overview
      - Green's Function Approach
      - Gidded Field Solution: Equation and Boundary Condtions
      - Methods of Gridded Field Solution
      - Spectral Methods and the FFT
    15.4.D Weighting: Depositing Particles on the Field Mesh and
           Interopolating Fields to the Particles
      - Overview of Approaches
      - Approaches: Nearest Grid Point, Cloud in Cell, Area, Splines
    15.4.E Computational Cycle for Particle in Cell Simulations
   15.5 Diagnostics
   15.6 Initial Distribution and Particle Loading
   15.7 Numerical Convergence
   15.8 Practial Considerations
      15.8.A Overview
      15.8.B Fast Memory
      15.8.C Run Time
      15.8.D Machine Architectures
   15.9 Overview of the WARP Code
   15.10 Example Simulations
  Contact Information
  Acknowledgments
  References


16. Summary of Lectures by John J. Barnard (JJB)
16.summary_jjb.pdf  pdf scan, handwritten notes and slides

 16.1 Emittance and phase space review
  16.2 Particle equations of motion (radial and Cartesian)
  16.3 Summary of 6 statistical envelope equations and two equations based
       on particular distribution functions
  16.4 Current limits
  16.5 Using envelope equations to estimate spot size
  16.6 Longitudinal dynamics summary
  16.7 Instability summary
  16.8 Halo summary
  16.9 Electron, gas, pressure, and scattering effects summary
  16.10 Summary of HIF
```

Sponsored by the University of Maryland at College Park
US Particle Accelerator School, June 16-27, 2008, Annapolis, Maryland

Course Instructors: John J. Barnard (JB) and Steven M. Lund (SL), Lawrence Livermore National Laboratory
Recitations and Grading: Christos Papadopoulous (CP), University of Maryland

	Monday 6/16	Tuesday 6/17	Wednesday 6/18	Thursday 6/19	Friday 6/20
9:00 am - 10:30 am	Class Organization Introduction Envelope Equations JB	Envelope Equations Current Limits JB	Injectors/Longitudinal Beam Physics I JB	Longitudinal Beam Physics II JB	Longitudinal Beam Physics III JB
10:30 am - 12:00 noon	Transverse Particle Equations of Motion I SI	Transverse Particle Equations of Motion II SL	Transverse Distribution Functions I SL	Transverse Distribution Functions II SL	Resonances SL
12:00 noon - 1:00 pm	Lunch	Lunch	Lunch	Lunch	Lunch
1:00 pm - 2:00 pm	Transverse Particle Equations of Motion I SI	Transverse Particle Eqns. of Motion II SL	Tran. Dist. Functions I SL	Tran. Dist. Funcs. II SL	Simulation Techniques I SL
2:00pm - 3:00 pm	Carry Over	Carry Over + Recitation CP	Carry Over + Recitation CP	Carry Over + Recitation CP	Carry Over + Recitation CP
3:00 pm 4:00 pm					

6:00 pm - ?	Homework 1	Homework 2	Homework 3	Homework 4	Homework 5

	Monday 6/23	Tuesday 6/24	Wednesday 6/25	Thursday 6/26	Friday 6/27
9:00 am 10:30 am	Modes in Continuous Focusing and Halo JB	Pressure/Scattering/ Electron Effects JB	Heavy Ion Fusion/ Final Focusing JB	Review of Material JB	To Be Determined
10:30 am - 12:00 noon	Transverse Centroid and Envelope Equations SL	Transverse Centroid and Envelope Equations I SL	Transverse Kinetic Stability I SL	Simulation Techniques II SL	Final Exam Review JB/SL/CP
12:00 noon - 1:00 pm	Lunch	Lunch	Lunch	Lunch	
1:00 pm - 2:00 pm	Tran. Cen. Env. Eqns. I SL	Tran. Cen. Env. Eqns. II SL	Tran. Kin. Stability II SL	Simulation Techs. III SL	
2:00pm - 3:00 pm	Carry Over + Recitation CP	Carry Over + Recitation CP	Carry Over + Recitation CP	Carry Over + Recitation CP	
3:00 pm - 4:00 pm					

6:00 pm - ?	Homework 6	Homework 7	Homework 8	Take-home final

Carry Over: Over time lectures will be caught up prior to the Recitation to avoid falling behind schedule
Homework: Collaboration with other students in class and hints from grader or instructors are allowed. (80% of grade)
Take-Home Final: No collaboration allowed (20% of grade)

John Barnard
Steven Lund
USPAS
June 2008

I. Introduction

(related reading in parentheses)

Particle motion (Reiser 2.1)
Equation of motion (Reiser 2.1)
Dimensionless quantities (Reiser 4.2)

Plasma physics of beams (Reiser 3.2, 4.1)

Emittance and brightness (Reiser 3.1 - 3.2)

PARTICLE EQUATIONS OF MOTION / DIMENSIONLESS QUANTITIES

CONSIDER THE LORENTZ FORCE ON A PARTICLE UNDER THE INFLUENCE OF ELECTRIC AND MAGNETIC FORCES.

$$\frac{d\underline{p}}{dt} = q\left(\underline{E} + \underline{v}\times\underline{B}\right) \qquad [\text{SI units}]$$

$$\underline{p} = \gamma m \underline{v} \qquad \gamma^2 = \frac{1}{1-\beta^2} \qquad \beta = \frac{v}{c}$$

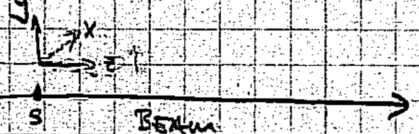

CONSIDER THE X-COMPONENT OF THE MOTION (TRANSVERSE TO THE STREAMING MOTION OF THE PARTICLE)

TRANSFORM TO S AS THE INDEPENDENT VARIABLE:

$$dt = \frac{ds}{v_z} \quad \Rightarrow \quad v_x = \frac{dx}{dt} = v_z x' \qquad ' = \frac{d}{ds}$$

$$m v_z \frac{d}{ds}\left(\gamma v_z x'\right) = q\left(\underline{E} + \underline{v}\times\underline{B}\right)_x$$

$$\gamma m v_z^2 x'' + x' m v_z \frac{d}{ds}\left(\gamma v_z\right) = q\left(\underline{E} + \underline{v}\times\underline{B}\right)_x$$

$$\Rightarrow \quad x'' + \left[\frac{1}{\gamma v_z}\frac{d}{ds}\left(\gamma v_z\right)\right]x' = \frac{q}{\gamma m v_z^2}\left(\underline{E} + \underline{v}\times\underline{B}\right)_x$$

NOW CONSIDER AN UNBUNCHED BEAM OF UNIFORM DENSITY ρ AND CIRCULAR CROSS SECTION (with $r \le r_b$)

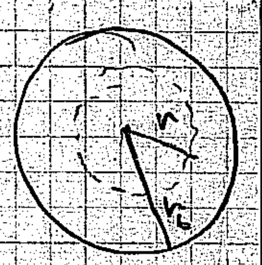

$$\nabla \cdot E = \frac{\rho}{\epsilon_0}$$

$$2\pi r E_r = \pi r^2 \frac{\rho}{\epsilon_0} \quad \text{(Gauss' theorem)}$$

$$\lambda = \pi r_b^2 \rho$$

$$E_r = \frac{\rho}{2\epsilon_0} r = \frac{\lambda}{2\pi\epsilon_0}\frac{r}{r_b^2} \qquad E_x = E_r \cos\theta = E_r\left(\frac{x}{r}\right) = \frac{\lambda}{2\pi\epsilon_0}\frac{x}{r_b^2}$$

Similarly $\nabla \times B = \mu_0 J$

$$2\pi r B_\theta = \mu_0 \rho v_z \pi r^2 \quad \text{(Stokes theorem)}$$

$$B_\theta = \frac{\mu_0 \lambda v_z}{2\pi}\frac{r}{r_b^2} \qquad B_y = \frac{\mu_0 \lambda v_z}{2\pi}\frac{x}{r_b^2} \qquad (B_z = 0)$$

Let $(E + v \times B)_x = (E_x - v_z B_y)^{self} + (E_x + v_y B_z - v_z B_y)^{ext}$

$$\Rightarrow \quad x'' + \left[\frac{1}{\gamma v_z}\frac{d}{ds}\gamma v_z\right] x' = \frac{q}{\gamma m v_z^2}\frac{\lambda}{2\pi\epsilon_0}\frac{x}{r_b^2}\left[1 - \mu_0\epsilon_0 v_z^2\right] + \frac{q}{\gamma m v_z^2}(E + v \times B)_x^{ext}$$

USING $\mu_0 \epsilon_0 = \frac{1}{c^2}$

Assuming $\beta_x^2 + \beta_y^2 \ll \frac{1}{\gamma^2} \Rightarrow \gamma^2 \simeq \frac{1}{1 - v_z^2/c^2}$ (PARAXIAL APPROXIMATION)

($\Rightarrow \tilde{\beta}_x^2 + \tilde{\beta}_y^2 \ll 1$, HERE ~ INDICATES VALUE IN COMOVING FRAME [NON-RELATIVISTIC MOTION IN COMOVING FRAME].)

LUMPING EXTERNAL FORCE INTO A LINEAR FIELD:

$$x'' + \frac{1}{\gamma v_z}\frac{d}{ds}(\gamma v_z)\,x' \simeq \frac{q}{\gamma^3 m v_z^2}\frac{\lambda}{2\pi\epsilon_0}\frac{x}{r_b^2} - \underbrace{K(z)\,x}_{\text{EXTERNAL FORCES}}$$

$$\equiv Q\frac{x}{r_b^2} - K(z)\,x$$

$$Q = \frac{q\lambda}{2\pi\epsilon_0\gamma^3 m v_z^2} = \text{GENERALIZED PERVEANCE} \longrightarrow \begin{cases} \dfrac{\lambda}{4\pi\epsilon_0 V} & \text{for } \gamma^2 v_z^2 \ll c^2 \\[2ex] \dfrac{\lambda}{2\pi\epsilon_0 V\left(\frac{qV}{mc^2}\right)^2} & \text{for } \gamma^2 v_z^2 \gg \end{cases}$$

$$= \frac{(q/e)}{(m/m_{amu})}\frac{2I}{I_0}\frac{1}{\gamma^3\beta^3} \qquad I_0 = \frac{4\pi\epsilon_0 m_{amu} c^3}{e} \cong 31\ \text{MA}$$

here $qV \equiv (\gamma - 1)mc^2$

Also note in non-relativistic limit $Q = \left(\frac{m}{2q}\right)^{1/2}\frac{1}{4\pi\epsilon_0 c}\left(\frac{I}{V^{3/2}}\right)$

(same scaling as original term perveance characterizing in pierces).

$$Q \simeq \frac{\Phi_{SELF}}{V} = \frac{\int_0^{r_b}(E_r - v_z B_\theta)\,dr}{V} = \frac{\text{POTENTIAL ENERGY OF BEAM PARTICLE}}{\text{KINETIC ENERGY OF " "}}$$

SOMETIMES PERIODIC FOCUSING IS EMPLOYED

$$K(z) = K(z+S)$$

$$S = \text{PERIOD}$$

FOR SOME PURPOSES A SUITABLE CONSTANT CAN BE FOUND WHICH CAPTURES SLOW VARIATION OF THE PARTICLE MOTION. (SMOOTH FOCUSING APPROX.)

$$\Rightarrow \boxed{x'' + \frac{1}{\gamma v_z}\frac{d}{ds}(\gamma v_z)\,x' = Q\frac{x}{r_b^2} - k_{\beta 0}^2 x}$$

$k_{\beta 0} \equiv$ "UNDEPRESSED BETATRON FREQUENCY" $\qquad \sigma_0 \equiv k_{\beta 0} S$ = UNDEPRESSED PHASE ADVANCE

If $\frac{dv_z}{dz} = 0$ [drifting beams]

$$x'' = -\left[k_{\beta 0}^2 - \frac{Q}{r_b^2}\right] x$$

$$= -k_{\beta 0}^2 \underbrace{\left[1 - \frac{Q}{k_{\beta 0}^2 r_b^2}\right]}_{\equiv \left(\frac{\sigma}{\sigma_0}\right)^2 = (\text{"TUNE DEPRESSION"})^2} x \quad = -k_\beta^2\, x$$

k_β: "DEPRESSED BETATRON FREQUENCY"

EFFECT OF SPACE CHARGE IS TO LOWER FREQUENCY OF HARMONIC OSCILLATIONS

$\frac{\sigma}{\sigma_0} = 0 \Rightarrow$ FULLY TUNE DEPRESSED

$\frac{\sigma}{\sigma_0} = 1 \Rightarrow$ NO SPACE-CHARGE DEPRESSION

Space charge reduces betatron phase advance

Without space charge: $X = X_i \cos\left[k_{\beta 0}(s-s_i)\right] + \frac{X_i'}{k_{\beta 0}} \sin\left[k_{\beta 0}(s-s_i)\right]$

Particle orbit

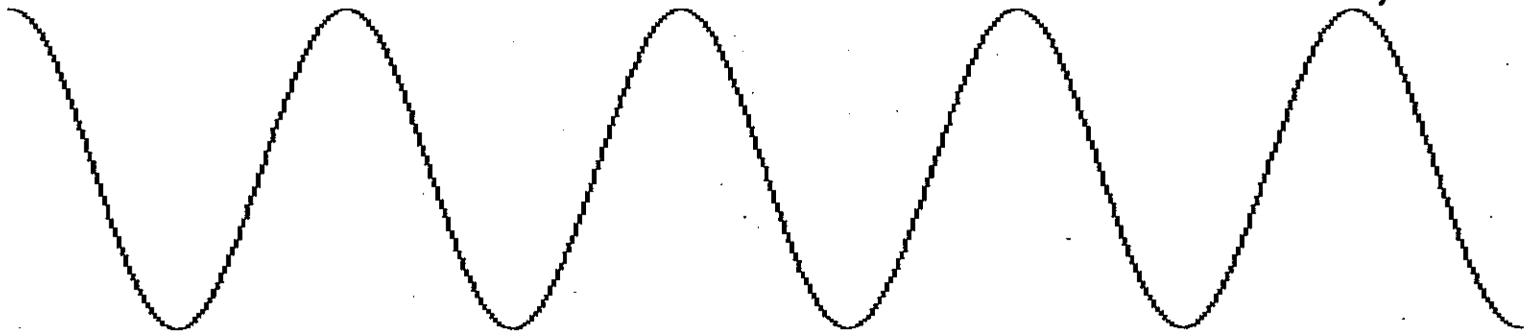

With space charge:

Particle orbit

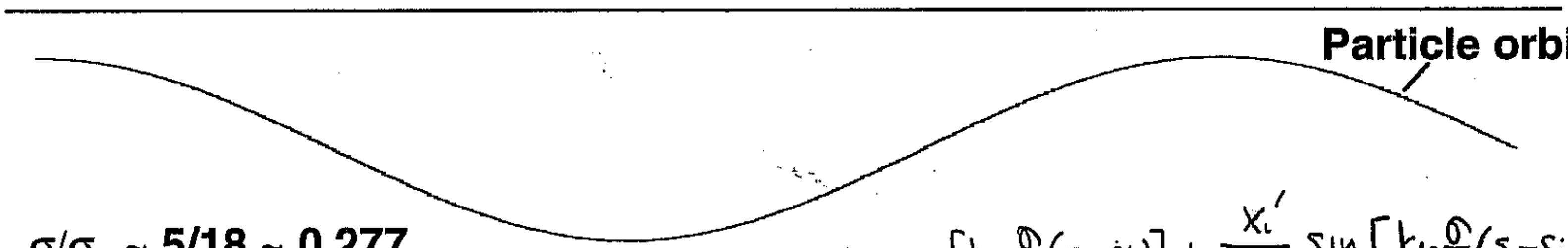

$\sigma/\sigma_0 \sim 5/18 \sim 0.277$

$X = X_i \cos\left[k_{\beta 0}\frac{\sigma}{\sigma_0}(s-s_i)\right] + \frac{X_i'}{\left(\frac{\sigma}{\sigma_0}\right)k_{\beta 0}} \sin\left[k_{\beta 0}\frac{\sigma}{\sigma_0}(s-s_i)\right]$

Beam envelope

J. BARNARD (5)

BENDING BEAMS

RETURNING TO PARTICLE EQUATION WITH ARBITRARY $\underline{E}$, & $\underline{B}$:

$$x'' + \left[\frac{1}{\gamma v_z}\frac{d}{ds}(\gamma v_z)\right] x' = \frac{q}{\gamma m v_z^2}\left(\underline{E} + \underline{v}\times\underline{B}\right)_x$$

IF EXTERNAL FORCE IS PROPORTIONAL TO $-x$

$\Rightarrow$ FOCUSING (HARMONIC OSCILLATIONS)

HOWEVER, IF $\underline{E} + \underline{v}\times\underline{B}$ = CONSTANT

$\Rightarrow$ BENDING

EXAMPLE: If $B = B_y \hat{e}_y$

$\vec{v} = v_0 \hat{e}_z + v_x \hat{e}_x$ where $v_0 \gg v_x$

$$\Rightarrow \quad x'' = \frac{q B_y}{\gamma m v_z} = \frac{B_y}{[B\rho]}$$

$[B\rho] \equiv$ RIGIDITY $= \dfrac{\gamma m v_z}{q} = \dfrac{p}{q}$

$$x' = \frac{B_y}{[B\rho]} z + x_0'$$

$$x = \frac{B_y}{[B\rho]}\frac{z^2}{2} + x_0' z + x_0$$

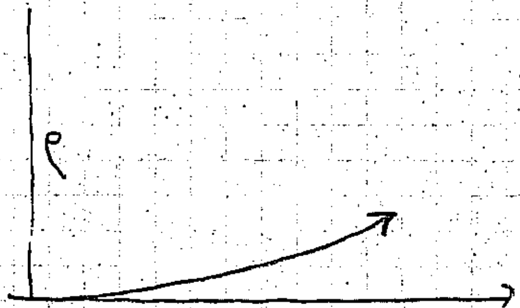

ρ = RADIUS OF CURVATURE OF ARC $= \dfrac{[B\rho]}{B_y}$

(BENDING CAN ALSO BE CARRIED OUT WITH ELECTRIC FIELDS E_x = CONST).

J. BARNARD (b)

PLASMA PHYSICS OF BEAMS

PHYSICS OF SPACE-CHARGE ≡ PHYSICS OF SELF-FIELDS

≡ PLASMA PHYSICS OF PARTICLE BEAMS

PLASMA PARAMETER

$$q\bar{\Phi}_{IP} = \frac{1}{4\pi\epsilon_0}\frac{q^2}{r}$$

$$\simeq \frac{1}{4\pi\epsilon_0} n_0^{1/3} q^2$$

AVERAGE POTENTIAL ENERGY $q\bar{\Phi}_{IP}$ OF PARTICLE DUE TO ITS NEAREST NEIGHBOR (q = charge of particle)

IF $q\bar{\Phi}_{IP} << k_B T$ $\Rightarrow$ PLASMA (weakly coupled plasma)

DEFINE $$\lambda_D = \frac{(kT/m)^{1/2}}{(n_0 q^2/\epsilon_0 m)^{1/2}} = \frac{V_{TH}}{\omega_p} = \left(\frac{kT\epsilon_0}{n_0 q^2}\right)^{1/2} = \text{DEBYE LENGTH}$$

= SHIELDING DISTANCE EVEN IN NON-NEUTRAL PLASMA

DEFINE $\Lambda = \frac{4\pi}{3} n_0 \lambda_D^3$ ≡ PLASMA PARAMETER

$$\sim \left(\frac{k_B T}{q\bar{\Phi}_{IP}}\right)^{3/2} >> 1$$

J. Barnard (7)

REF. "INTRO. TO PLASMA THEORY", D.R. NICHOLSON WILEY, 1983.

KLIMONTOVICH EQUATION

Let $N(\underline{x},\underline{v},t) = \sum_{i=1}^{N_0} \delta(\underline{x}-\underline{X}_i(t))\delta(\underline{v}-\underline{V}_i(t))$

N_0 particles; $\underline{X}_i$, $\underline{V}_i$ are position and velocity of ith particle

$\dot{\underline{X}}_i = \underline{V}_i \qquad m\dot{\underline{V}}_i = q\underline{E}^m[\underline{X}_i(t),t] + q[\underline{V}_i \times \underline{B}^m[\underline{X}_i(t),t]]$ (non-relativistic)

$N(x,v,t)$ = "density" of particles in phase space

$$\int N \, d^3x \, d^3v = N_0$$

Let $u = x - X_i(t)$

$\frac{\partial}{\partial x} f(u) = f'(u)$

$\frac{\partial}{\partial t} f(u) = f'(u)(-\dot{X}(t))$

$= -\dot{X}(t)\frac{\partial}{\partial x} f(u)$

Taking derivative:

$$\frac{\partial N}{\partial t}(x,v,t) = -\sum_{i=1}^{N} \dot{\underline{X}}_i(t)\cdot\nabla_x\left[\delta(\underline{x}-\underline{X}_i(t))\delta(\underline{v}-\underline{V}_i(t))\right]$$
$$-\sum_{i=1}^{N_0} \dot{\underline{V}}_i(t)\cdot\nabla_v\left[\delta(\underline{x}-\underline{X}_i(t))\delta(\underline{v}-\underline{V}_i(t))\right]$$

MAXWELL'S EQUATIONS:

$$\nabla\cdot\underline{E}^m = \left(\frac{1}{\epsilon_0}\right)\overbrace{q\int dv\, N(x,v,t)}^{\rho^m} \qquad \nabla\cdot\underline{B}^m = 0$$

$$\nabla\times\underline{E}^m = -\frac{\partial\underline{B}^m}{\partial t} \qquad \nabla\times\underline{B}^m = \mu_0\underbrace{q\int d\underline{v}\,\underline{v}\,N(x,v,t)}_{J^m} + \frac{\partial E^m}{\partial t}$$

$$\Rightarrow \frac{\partial N}{\partial t}(x,v,t) = -\sum_{i=1}^{N_0}\underline{V}_i(t)\cdot\nabla_x\left[\delta(\underline{x}-\underline{X}_i(t))\delta(\underline{v}-\underline{V}_i(t))\right]$$
$$-\sum_{i=1}^{N_0}\left(\left(\frac{q}{m}\right)E^m + \left(\frac{q}{m}\right)[\underline{V}_i\times\underline{B}^m[X_i(t),t]]\right)\cdot\nabla_v\left[\delta(x-X_i)\delta(v-V_i(t))\right]$$

Note that $\underline{V}_i(t)\delta(\underline{v}-\underline{V}_i(t)) = \underline{v}\,\delta(\underline{v}-V_i(t))$ so,

∇_x = spatial gradient

∇_v = gradient w.r.t. 3 velocity variables

$$\Rightarrow \frac{\partial N}{\partial t}(x,\underline{v},t) = -\underline{v}\cdot\nabla_x\sum_{i=1}^{N_0}\delta(\underline{x}-\underline{X}_i(t))\delta(\underline{v}-\underline{V}_i(t))$$
$$-\left(\frac{q}{m}E^m(\underline{x},t) + \frac{q}{m}(\underline{v}\times\underline{B}^m(\underline{x},t))\right)\cdot\nabla_v\sum_{i=1}^{N_0}\delta(\underline{x}-\underline{X}_i(t))\delta(v-V_i(t))$$

$$\boxed{\frac{\partial N}{\partial t}(x,\underline{v},t) = -\underline{v}\cdot\nabla_x N(\underline{x},v,t) + \frac{q}{m}(E^m + v\times B^m)\cdot\nabla_v N(\underline{x},\underline{v},t)}$$

Klimontovich Equation

Total derivative along an orbit:

$$\frac{D}{Dt} = \frac{\partial}{\partial t} + \left.\frac{dx}{dt}\right|_{\text{ORBIT}} \cdot \nabla_x + \left.\frac{dv}{dt}\right|_{\text{ORBIT}} \cdot \nabla_v$$

$$\Rightarrow \boxed{\frac{D}{Dt} N(\underline{x}, \underline{v}, t) = 0}$$

Note that $N = 0$ or ∞, nothing in between.

Let $$f(x, v, t) = \frac{\int^{\Delta x^3, \Delta v^3} N(\underline{x}, \underline{v}, t)\, d^3x\, d^3v}{\Delta x^3 \Delta v^3}$$

over some box in phase space. Δx & Δv are the size of box

$$\equiv \langle N(\underline{x}, \underline{v}, t) \rangle$$

Assume $n^{-1/3} \ll \Delta x \ll \lambda_D$ so that $f(x, v, t)$ is smooth function.

Then
$$N = f + \delta f \qquad f = \langle N \rangle \qquad \langle \delta f \rangle = 0$$
$$E^m = E + \delta E \qquad E = \langle E^m \rangle \qquad \langle \delta E \rangle = 0$$
$$B^m = B + \delta B \qquad B = \langle B^m \rangle \qquad \langle \delta B \rangle = 0$$

$$\Rightarrow \underbrace{\frac{\partial f}{\partial t} + \underline{v} \cdot \nabla_x f + \frac{q}{m}(\underline{E} + \underline{v} \times \underline{B}) \cdot \nabla_v f}_{\text{"SMOOTHLY VARYING PART"}} = \underbrace{-\frac{q}{m} \langle (\delta \underline{E} + \underline{v} \times \delta \underline{B}) \cdot \nabla_v \delta f \rangle}_{\text{AVERAGE OF "SPIKEY" QUANTITIES}}$$

"DISCRETE PARTICLE EFFECTS" OR "COLLISIONS"

If collisions are neglected (set RHS to zero):

$\boxed{\text{Vlasov - EQUATION}}$

$$\frac{\partial f}{\partial t} + \underline{v} \cdot \nabla_x f + \frac{q}{m}(\underline{E} + \underline{v} \times \underline{B}) \cdot \nabla_v f = 0$$

$$\Rightarrow \boxed{\frac{Df}{Dt} = 0}$$

PHASE SPACE DENSITY CONSTANT ON TRAJECTORIES. (LIOUVILLE'S THEOREM)

THE RHS IS DUE TO COLLISIONS WITH NON-SMOOTH FIELDS:

VERY HEURISTICALLY

$$-\frac{q}{m}\left\langle\left(\delta \underline{E} + \underline{v} \times \delta \underline{B}\right) \cdot \nabla_v \delta f\right\rangle \sim \nu_c f$$

$$\nu_c \sim \sigma n v$$

$\sigma \sim \pi r_c^2$ where r_c is given by $kT \sim \dfrac{q^2}{4\pi\varepsilon_0 r_c}$

(for large angle collisions)

$$\Rightarrow \nu_c \sim \pi\left(\frac{q^2}{4\pi\varepsilon_0 kT}\right)^2 n_0 \left(\frac{kT}{m}\right)^{1/2} \longleftarrow$$

(VERY ROUGH, BUT MAIN SCALING IS CORRECT, WITH LOGARITHMIC CORRECTION FACTORS)

ON LHS OF VLASOV EQUATION:

$$\frac{q}{m} E \nabla_v f \sim \left(\frac{q \lambda_D n_0}{\varepsilon_0}\right) \frac{f}{v_{TH}} \qquad \text{where } v_{TH} \sim \sqrt{\frac{kT}{m}}$$

$$\frac{\text{COLLISION TERM}}{\text{LHS}} \sim \frac{1}{16 \cdot \lambda_D^3 n_0} = \frac{1}{16 \Lambda}$$

Accelerator beams are non-neutral plasmas

Accelerator beams for Heavy Ion Fusion

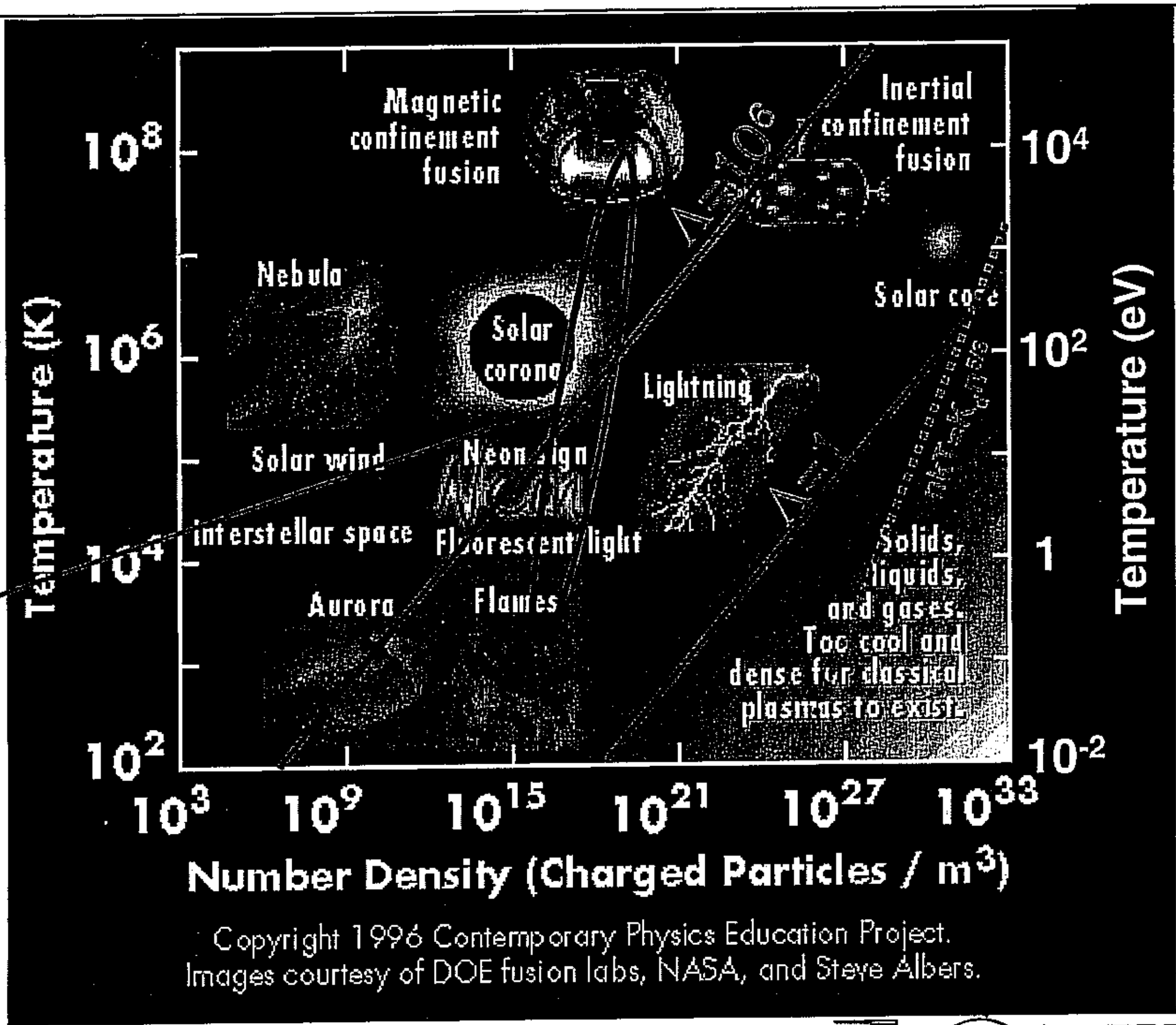

J. BARNARD (II)

DESCRIPTION OF THE BEAM

LIOUVILLE'S THEOREM: $\frac{df}{dt} = 0$ along a trajectory in phase space,

Let $dN = f\, dx\, dy\, dz\, dp_x\, dp_y\, dp_z$

The continuity equation in phase space is:

$$\frac{\partial f}{\partial t} + \underline{\nabla} \cdot (f\underline{v}) = 0$$

where $\underline{v} = \frac{d}{dt}\begin{pmatrix} q_1 \\ q_2 \\ q_3 \\ p_1 \\ p_2 \\ p_3 \end{pmatrix}$ & $\underline{\nabla} \cdot \underline{a} = \frac{\partial a_1}{\partial q_1} + \frac{\partial a_2}{\partial q_2} + \frac{\partial a_3}{\partial q_3} + \frac{\partial a_{p_1}}{\partial p_1} + \frac{\partial a_{p_2}}{\partial p_2} + \frac{\partial a_{p_3}}{\partial p_3}$

($\underline{v}$ & $\underline{\nabla}\cdot$ are the 6-D velocity & divergence, respectively).

If the system is governed by a Hamiltonian $H(\underline{q}, \underline{p}, t)$

$$\dot{q}_i = \frac{\partial H}{\partial p_i} \qquad \dot{p}_i = \frac{-\partial H}{\partial q_i}$$

Now, $\underline{\nabla} \cdot \underline{v} = \sum_{i=1}^{3} \frac{\partial \dot{q}_i}{\partial q_i} + \frac{\partial \dot{p}_i}{\partial p_i} = \sum_{i=1}^{3} \frac{\partial^2 H}{\partial q_i \partial p_i} - \frac{\partial^2 H}{\partial p_i \partial q_i} = 0$

$$\Rightarrow \frac{\partial f}{\partial t} + f \underbrace{\underline{\nabla} \cdot \underline{v}}_{0} + \underline{v} \cdot \nabla \underline{f} = 0$$

$$\Rightarrow \boxed{\left.\frac{df}{dt}\right|_{\substack{6D \\ \text{trajectory}}} = 0}$$

Emittance & Brightness

LIOUVILLE'S EQUATION OR VLASOV EQUATION $\Rightarrow \dfrac{dN}{dx\,dy\,dz\,dp_x\,dp_y\,dp_z} = \text{const}$

IF $x'' = f(x)$ AND NOT FUNCTIONS (y & z)
$y'' = f(y) =$ " " " (x, & z)
$z'' = f(z) =$ " " " (x, & y)

THEN $\dfrac{dN}{dx\,dp_x} = \text{const}$; $\dfrac{dN}{dy\,dp_y} = \text{const}$ & $\dfrac{dN}{dz\,dp_z} = \text{const}$

separately.

1ST DEFINITION:
EMITTANCE: USE TRACE-SPACE OF ALL PARTICLES IN A GIVEN SLICE OF BEAM.

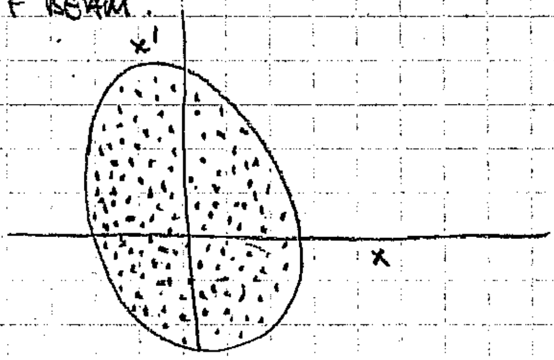

INSTEAD OF p_x USE $x' = \dfrac{v_x}{v_z}$ (FOR NON-ACCELERATING PARAXIAL BEAM, x' PROPORTIONAL TO MOMENTUM)

EMITTANCE $\equiv \dfrac{1}{\pi}$ · AREA OF SMALLEST ELLIPSE WHICH ENCLOSES ALL PARTICLES. (TRACE-SPACE DEFINITION)

(INTUITIVELY, PRODUCT OF WIDTH IN x, TIMES WIDTH IN x', SO IT IS ESSENTIALLY (WITHIN FACTOR OF π) = PHASE SPACE AREA OF BEAM.

2ND DEFINITION INVOLVES STATISTICAL AVERAGES OF 2ND ORDER QUANTITIES (SUCH AS rms).

$$\epsilon_x \equiv 4\left(\langle x^2\rangle\langle x'^2\rangle - \langle xx'\rangle^2\right)^{1/2}$$

For an upright uniform beam (in phase space): $\langle x^2\rangle = \dfrac{r_x^2}{4}$ $\langle x'^2\rangle = \dfrac{x'^2_{max}}{4}$
& $\langle xx'\rangle = 0$

$$\Rightarrow \epsilon_x = r_x\, x'_{max} = \frac{\text{Area}}{\pi}$$

NORMALIZED EMITTANCE

For a beam that is accelerating, return to x, p_x as definition of phase space area:

$$p_x = \gamma m v_x = \gamma m v_z x' \qquad \text{AGAIN, assuming } v \simeq v_z$$

$$\Rightarrow \epsilon_{Nx} \equiv 4\gamma\beta\left(\langle x^2\rangle\langle x'^2\rangle - \langle x x'\rangle^2\right)^{1/2} = \gamma\beta\,\epsilon_x$$

$$= \frac{4}{m}\left(\langle x^2\rangle\langle p_x^2\rangle - \langle x p_x\rangle^2\right)^{1/2}$$

SINCE EMITTANCE IS THE AVERAGE PHASE SPACE AREA OF BEAM (AVERAGING OVER EMPTY SPACE) THE EMITTANCE IN GENERAL GROWS AS A BEAM FILAMENTS (ENGULFING EMPTY SPACE).

BRIGHTNESS

THE DENSITY OF PARTICLES IN 6-D PHASE SPACE IS

$$\frac{dN}{dx\,dy\,dz\,dp_x\,dp_y\,dp_z} = f \longleftarrow \text{MICROSCOPIC DENSITY}$$

DEFINE A QUANTITY $\bar{f}$ WHICH IS THE PHASE-SPACE DENSITY IN AN AVERAGE SENSE

$$\bar{f} = \left\langle \frac{dN}{dx\,dp_x\,dy\,dp_y\,dz\,dp_z} \right\rangle = \frac{(I\Delta t)/q}{\pi^3 \epsilon_{Nx}\epsilon_{Ny}\epsilon_{Nz}}$$

Note $f(\underline{x},\underline{p})$ = constant along a trajectory, whereas $\bar{f}$ usually is a decreasing function of z.

NORMALIZED BRIGHTNESS $B_N \equiv \dfrac{I}{\epsilon_{Nx}\epsilon_{Ny}}$

IS A USEFUL MEASURE OF 4D AVERAGE PHASE SPACE DENSITY, (if Δt = constant, & $\perp$,$\parallel$ motion is uncoupled.)

For non-accelerating beams the unnormalized brightness B (also if Δt = const. & $\perp$,$\parallel$ motion uncoupled)

$$\Rightarrow B \equiv \frac{I}{\epsilon_x \epsilon_y} \qquad \text{MEASURES PHASE SPACE DENSITY.}$$

Emittance constant for linear force profile & matched beams

Linear force profile ($x'' = -k^2 x$) => Phase space area preserved, ellipse stays elliptical.

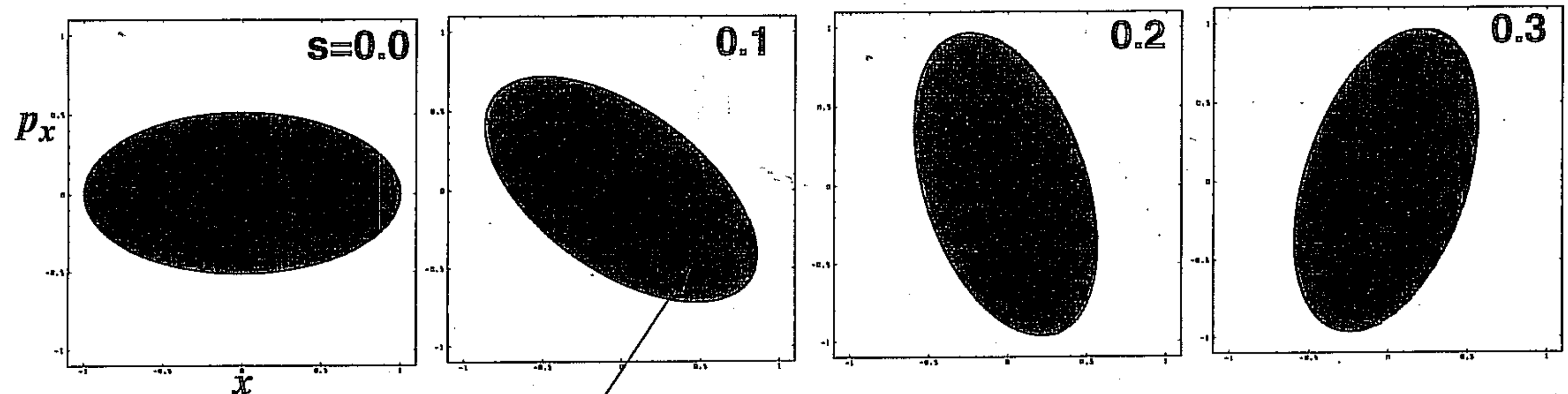

Emittance = phase space area

Emittance constant if forces linear

Here, width of beam is oscillating or "mismatched."

Non-linear forces (e.g. $x'' = -k^2x + \varepsilon x^3$) $\Rightarrow$ position-dependent frequency

$\Rightarrow$ phase mixing, increasing effective area $\Rightarrow$ Emittance increases if forces non-linear

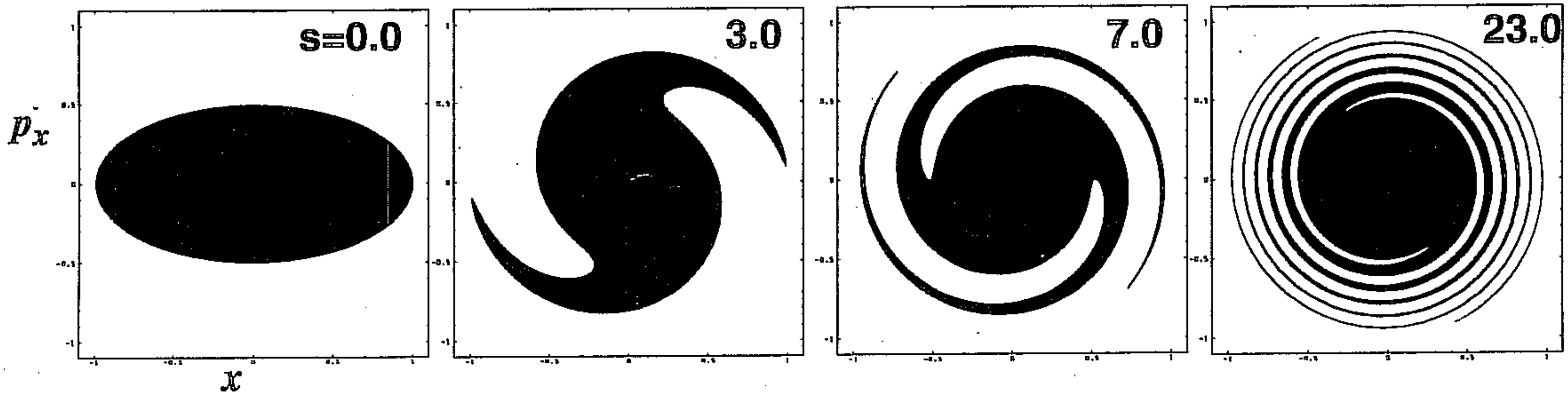

J. Barnard (14)

John Barnard
Steven Lund
USPAS
June 2008

II. Envelope Equations

Paraxial Ray Equation

Envelope equations for axially symmetric beams

Cartesian equation of motion

Envelope equations for elliptically symmetric beams

Roadmap:

John Barnard
Steven Lund
USPAS
June 2008

Single particle equation with Lorentz force
q(E + v x B)

$\Downarrow$

Make use of:

1. Paraxial (near-axis) approximation
   ($r \ll 1/k_{\beta 0}$ and $x' = v_x/v_z \ll 1$)

2. Conservation of canonical angular momentum

3. Axisymmetry f(r,z)

$\Downarrow$

Paraxial Ray Equation for Single Particle

Next take statistical averages over the distribution function

$\Rightarrow$ Moment equations

Express some of the moments in terms of the rms radius and emittance

$\Rightarrow$ Envelope equations (axi-symmetric case)

Some focusing systems have quadrupolar symmetry
Rederive envelope equations in cartesian coordinates
(x,y,z) rather than radial (r,z)

J. BARNARD ①

START WITH NEWTON'S EQUATION WITH THE LORENTZ FORCE:

$$\frac{d\underline{p}}{dt} = q\left(\underline{E} + \underline{v}\times\underline{B}\right)$$

In cartesian coordinates:

$$\frac{d}{dt}(\gamma m\dot{x}) = \dot{\gamma} m\dot{x} + \gamma m\ddot{x} = q\left(E_x + \dot{y}B_z - \dot{z}B_y\right)$$

$$\frac{d}{dt}(\gamma m\dot{y}) = \dot{\gamma} m\dot{y} + \gamma m\ddot{y} = q\left(E_y + \dot{z}B_x - \dot{x}B_z\right)$$

$$\frac{d}{dt}(\gamma m\dot{z}) = \dot{\gamma} m\dot{z} + \gamma m\ddot{z} = q\left(E_z + \dot{x}B_y - \dot{y}B_x\right)$$

In cylindrical coordinates: $\left(\text{use } \frac{d\hat{e}_r}{dt} = \hat{e}_\theta\dot{\theta}\ ;\quad \frac{d\hat{e}_\theta}{dt} = -\hat{e}_r\dot{\theta}\right)$

$$\frac{d}{dt}(\gamma m\dot{r}) - \gamma m r\dot{\theta}^2 = q\left(E_r + r\dot{\theta}B_z - \dot{z}B_\theta\right) \qquad (\mathrm{I})$$

$$\frac{1}{r}\frac{d}{dt}(\gamma m r^2\dot{\theta}) = q\left(E_\theta + \dot{z}B_r - \dot{r}B_z\right) \qquad (\mathrm{II})$$

$$\frac{d}{dt}(\gamma m\dot{z}) = q\left(E_z + \dot{r}B_\theta - r\dot{\theta}B_r\right) \qquad (\mathrm{III})$$

When $\frac{\partial}{\partial\theta} = 0$:

$$\underline{E} = -\underline{\nabla}\Phi - \frac{\partial\underline{A}}{\partial t} = \hat{e}_r\left[-\frac{\partial\Phi}{\partial r} - \frac{\partial A_r}{\partial t}\right] + \hat{e}_\theta\left[-\frac{\partial A_\theta}{\partial t}\right] + \hat{e}_z\left[-\frac{\partial\Phi}{\partial z} - \frac{\partial A_z}{\partial t}\right]$$

$$\underline{B} = \nabla\times\underline{A} = \hat{e}_r\left[\frac{-\partial}{\partial z}A_\theta\right] + \hat{e}_\theta\left[\frac{\partial A_r}{\partial z} - \frac{\partial A_z}{\partial r}\right] + \hat{e}_z\left[\frac{1}{r}\frac{\partial}{\partial r}(rA_\theta)\right]$$

$$qr\left(E_\theta + \dot{z}B_r - \dot{r}B_z\right) = q\left(-\frac{\partial rA_\theta}{\partial t} - \dot{z}\frac{\partial rA_\theta}{\partial z} - \dot{r}\frac{\partial}{\partial r}(rA_\theta)\right)$$

$$= -q\left[\frac{\partial}{\partial t} + \underline{v}\cdot\frac{\partial}{\partial\underline{x}}\right](rA_\theta)$$

$$= -q\frac{d(rA_\theta)}{dt} \qquad (\mathrm{IV})$$

Eqtn II & IV $\Longrightarrow$ $\displaystyle\frac{d}{dt}\left(\gamma m r^2\dot{\theta} + qrA_\theta\right) = 0$

$$\underline{p} = p_r \hat{e}_r + p_\theta^* \hat{e}_\theta + p_z \hat{e}_z$$

where
$$p_r = \gamma m \dot{r}$$
$$p_\theta^* = \gamma m r \dot{\theta}$$
$$p_z = \gamma m \dot{z}$$

$$\frac{d\underline{p}}{dt} = \dot{p}_r \hat{e}_r + p_r \dot{\hat{e}}_r + \dot{p}_\theta^* \hat{e}_\theta + p_\theta^* \dot{\hat{e}}_\theta + \dot{p}_z \hat{e}_z$$

$$\Rightarrow \frac{d\underline{p}}{dt} = (\dot{p}_r - p_\theta^* \dot{\theta})\, \hat{e}_r + (p_r \dot{\theta} + \dot{p}_\theta^*)\, \hat{e}_\theta + \dot{p}_z \hat{e}_z$$

WHERE WE HAVE USED:

$$\frac{d\hat{e}_r}{dt} = \hat{e}_\theta \dot{\theta} \quad \& \quad \frac{d\hat{e}_\theta}{dt} = -\hat{e}_r \dot{\theta}$$

$$\Rightarrow \frac{d\underline{p}}{dt} = \left[\frac{d}{dt}(\gamma m \dot{r}) - \frac{d}{dt}(\gamma m \dot{r} \dot{\theta}^2)\right] \hat{e}_r$$
$$+ \Big[\underbrace{\gamma m \dot{r} \dot{\theta} + \frac{d}{dt}(\gamma m r \dot{\theta})}_{= \frac{1}{r} \frac{d}{dt}(\gamma m r^2 \dot{\theta})}\Big] \hat{e}_\theta$$
$$+ \frac{d}{dt}(\gamma m \dot{z})\, \hat{e}_z$$

(NOTE: ON THIS PAGE $P_\theta^* \equiv \theta$-component of MECHANICAL MOMENTUM NOT TO BE CONFUSED WITH $P_\theta = \gamma m r^2 \dot{\theta} + q r A_\theta \equiv \theta$-component OF <u>CANONICAL</u> <u>ANGULAR</u> MOMENTUM)

CONSERVATION OF CANONICAL ANGULAR MOMENTUM

J. BARNARD (2)

DEFINE $p_\theta = \gamma m r^2 \dot{\theta} + q r A_\theta$

$$\frac{d}{dt} p_\theta = 0$$

(CONSERVATION OF CANONICAL ANGULAR MOMENTUM)

NOTE THAT THE FLUX ENCLOSED BY A CIRCLE OF RADIUS r

$$\psi = \int \underline{B} \cdot d\underline{A} = \int (\nabla \times \underline{A}) \cdot dA = \oint \underline{A} \cdot d\underline{l} = 2\pi r A_\theta$$

$$p_\theta = \gamma m r^2 \dot{\theta} + \frac{q}{2\pi} \psi$$

IS CONSERVED ALONG AN ORBIT IN AXISYMMETRIC GEOMETRIES

"EXTERNAL" (REISER SECTION 3.3)

ELECTRIC & MAGNETIC FIELDS WITH RADIAL SYMMETRY

J. BARNARD

(B)

CONSIDER THE EXTERNAL FIELD: (TIME STEADY VACUUM SOLUTION)

$$\nabla \times \underline{B} = 0 \quad \& \quad \nabla \times \underline{E} = 0$$

$$\nabla \cdot \underline{B} = 0 \quad \& \quad \nabla \cdot \underline{E} = 0 \quad \Rightarrow \quad \underline{E} \ \& \ \underline{B} = -\nabla \Phi$$

Let $\Phi = \sum_{\nu=0}^{\infty} f_{2\nu}(z) r^{2\nu} \qquad \nabla^2 \Phi = 0 \Rightarrow \Phi = \sum_{\nu=0} \frac{(-1)^\nu}{\nu!} \frac{\partial^{2\nu} f(0,z)}{\partial z^{2\nu}} \left(\frac{r}{2}\right)^{2\nu}$

$$\Rightarrow \Phi = \Phi(0,z) - \frac{1}{4}\frac{\partial^2 \Phi(0,z)}{\partial z^2} r^2 + \frac{1}{64}\frac{\partial^4 \Phi(0,z)}{\partial z^4} r^4$$

Let $B_z(0,z) = B(z)$ & Let $\Phi(0,z) = V(z)$

$$B_z(r,z) = B(z) - \frac{r^2}{4}\frac{\partial^2 B}{\partial z^2} + \frac{r^4}{64}\frac{\partial^4 B}{\partial z^4} + \ldots$$

$$B_r(r,z) = -\frac{r}{2}\frac{\partial B}{\partial z} + \frac{r^3}{16}\frac{\partial^3 B}{\partial z^3} + \ldots$$

$$\Phi(r,z) = V(z) - \frac{1}{4}V'' r^2 + \frac{r^4}{64}\frac{\partial^4 V}{\partial z^4}$$

$$\Rightarrow \quad E_r = \frac{1}{2}V'' r - \frac{r^3}{16}\frac{\partial^4 V}{\partial z^4}$$

Also, $\psi \cong \pi r^2 B(z)$

$$\nabla^2 \phi = \frac{1}{r}\frac{\partial}{\partial r}\left(r\frac{\partial \phi}{\partial r}\right) + \frac{\partial^2 \phi}{\partial z^2} = 0$$

$$f(r,z) = \sum_{\nu=0}^{\infty} f_{2\nu}(z)\, r^{2\nu} = f_0 + f_2 r^2 + f_4 r^4$$

$$\sum_{\nu=1}^{\infty} \left[2\nu + 2\nu(\nu-1)\right] f_{2\nu}\, r^{2\nu-2} + \sum_{\nu=0}^{\infty} f''_{2\nu}\, r^{2\nu} = 0$$

PARAXIAL RAY EQUATION

(I) $\Rightarrow$ $\frac{d}{dt}(\gamma m \dot{r}) - \gamma m r \dot{\theta}^2 = q\left(\frac{V''}{2} r + r\dot{\theta} B\right) + q\left(E_r^{self} - v_z B_\theta^{self}\right)$.

INERTIAL — CENTRIFUGAL — E_r external — $v_\theta B_z$ external — SELF FIELDS

Now use s as independent variable $v_z dt = ds$

$$v_z \frac{d}{ds}(\gamma m v_z r') - \gamma m v_z^2 r \theta'^2 = q\left(\frac{V''}{2} r + r v_z \theta' B\right) + q\left(E_r^{self} - v_z B_\theta^{self}\right)$$

EXPANDING 1st term and $v_z \cong v$; AND DIVIDING BY $\gamma m v^2$:

$$r'' - r\theta'^2 + \frac{\gamma'}{\beta^2\gamma} r' = \frac{q}{\gamma m \beta^2 c^2}\left(\frac{V''}{2} r + r\beta c\,\theta' B + E_r^{self} - v_z B_\theta^{self}\right) \qquad (P1)$$

Using CANONICAL MOMENTUM, eliminate θ' via

$$\theta' = \frac{p_\theta - \frac{q\psi}{2\pi}}{\gamma m r^2 \beta c} = \frac{p_\theta}{\gamma m r^2 \beta c} - \frac{qB}{2\gamma\beta m c} \equiv \frac{p_\theta}{\gamma m r^2 \beta c} - \frac{\omega_c}{2\gamma\beta c}$$

where we define $\omega_c \equiv \frac{qB}{m}$.

ADDING THE TWO θ' TERMS IN THE EQUATION (P1)

$$-r\theta'^2 - \frac{r\omega_c\theta'}{\gamma\beta c} = \frac{-p_\theta^2}{\gamma^2 m^2 r^3 \beta^2 c^2} + \frac{p_\theta \omega_c}{\gamma^2 m \beta^2 c^2 r} - \frac{r\omega_c^2}{4\gamma^2\beta^2 c^2}$$

$$- \frac{p_\theta \omega_c}{\gamma^2 m \beta^2 c^2 r} + \frac{r\omega_c^2}{2\gamma^2\beta^2 c^2}$$

$$= \frac{-p_\theta^2}{\gamma^2 m^2 r^3 \beta^2 c^2} + \frac{r\omega_c^2}{2\gamma^2\beta^2 c^2}$$

So equation (P1) becomes:

$$r'' + \frac{\gamma'}{\beta^2\gamma} r' = \frac{q}{\gamma m \beta^2 c^2}\left(\frac{V''}{2} r\right) + \frac{r\omega_c^2}{2\gamma^2\beta^2 c^2} + \frac{p_\theta^2}{\gamma^2 m^2 r^3 \beta^2 c^2} + \frac{q}{\gamma m \beta^2 c^2}\left[E_r^{self} - v_z B_\theta^{self}\right] \quad (P2)$$

Now $\gamma' mc^2 = q\frac{\underline{E}\cdot\underline{v}}{v_z}$ so $\gamma'' = \left(V'' + \frac{\partial^2\phi^{self}}{\partial z^2}\right)\frac{q}{mc^2}$

CALCULATING $\frac{q}{\gamma m \beta^2 c^2}\left[\frac{V''}{2} r + E_r^{self} - v_z B_\theta^{self}\right]$:

$$\nabla^2\phi^{self} = -\frac{\rho}{\varepsilon_0} \quad \Rightarrow \quad \frac{1}{r}\frac{\partial}{\partial r}\left(r\frac{\partial\phi}{\partial r}\right) = -\frac{\rho}{\varepsilon_0} - \frac{\partial^2\phi^{self}}{\partial z^2}$$

$$\Rightarrow \frac{\partial}{\partial r}\left(r\frac{\partial\phi}{\partial r}\right) = -\frac{r\rho(r)}{\varepsilon_0} - \frac{r\,\partial^2\phi^{self}}{\partial z^2}$$

$$r\frac{\partial\phi}{\partial r} = -\frac{1}{2\pi\varepsilon_0}\int_0^r 2\pi r\,\rho(r)\,dr - \frac{r^2}{2}\frac{\partial^2\phi}{\partial z^2}$$

$$= -\frac{1}{2\pi\varepsilon_0}\lambda(r) - \frac{r^2}{2}\frac{\partial^2\phi^{self}}{\partial z^2}$$

$$\Rightarrow E_r^{self} = \frac{\lambda(r)}{2\pi\varepsilon_0 r} + \frac{r}{2}\frac{\partial^2\phi^{self}}{\partial z^2}$$

$$\nabla \times \underline{B} = \mu_0 \underline{J} \quad \Rightarrow \quad 2\pi r B_\theta = \mu_0\int_0^r 2\pi r\, J_z(r)\,dr = \mu_0 v_z \lambda(r)$$

$$B_\theta^{self} = \frac{\mu_0 v_z \lambda(r)}{2\pi r} = \frac{v_z}{c^2}\frac{\lambda(r)}{2\pi\varepsilon_0 r}$$

$$\left[\frac{V''}{2} r + E_r^{self} - v_z B_\theta^{self}\right] = \left[\frac{r}{2}\underbrace{\left(V'' + \frac{\partial^2\phi^{self}}{\partial z^2}\right)}_{-\frac{mc^2}{q}\gamma''} + \underbrace{\left(1 - \frac{v_z^2}{c^2}\right)}_{1/\gamma^2}\frac{\lambda(r)}{2\pi\varepsilon_0 r}\right]$$

So equation (P2) becomes: "THE PARAXIAL RAY EQUATION:"

$$\underbrace{r'' + \frac{\gamma'}{\beta^2\gamma} r'}_{\text{INERTIAL}} + \underbrace{\frac{\gamma''}{2\beta^2\gamma} r}_{\substack{E_r \\ \text{(CONVERGENCE OF} \\ \text{FIELD LINES)}}} + \underbrace{\left(\frac{\omega_c}{2\gamma\beta c}\right)^2 r}_{\substack{V_\theta B_z \\ -\text{ CENTRIFUGAL}}} - \underbrace{\left(\frac{p_\theta}{\gamma\beta m c}\right)^2 \frac{1}{r^3}}_{\text{CENTRIFUGAL}} - \underbrace{\frac{q}{\gamma^3 m v_z^2} \frac{\lambda(r)}{2\pi\epsilon_0 r}}_{\substack{\text{SELF} \\ \text{FIELD}}} = 0$$

J. Barnard

(6)

Moment Equations

Vlasov eqtn: $\frac{\partial f}{\partial s} + x' \frac{\partial f}{\partial x} + x'' \frac{\partial f}{\partial x'} + y' \frac{\partial f}{\partial y} + y'' \frac{\partial f}{\partial y'} = 0$

Let $g = g(x, x', y, y')$; $N = \iiiint f \, dx\, dx'\, dy\, dy'$

Multiply Vlasov equation by g & $\frac{1}{N} \iiiint dx\, dx'\, dy\, dy'$

$$\int dx\, dx'\, dy\, dy' \left[g \frac{\partial f}{\partial s} + g x' \frac{\partial f}{\partial x} + g x'' \frac{\partial f}{\partial x'} + g y' \frac{\partial f}{\partial y} + g y'' \frac{\partial f}{\partial y'} \right] = 0$$

INTEGRATE BY PARTS

$$\Rightarrow \frac{d}{ds} \langle g \rangle + \underbrace{\frac{1}{N} \iiint g f \Big|_{x=-\infty}^{\infty}}_{\to 0} - \underbrace{\frac{1}{N} \iiiint \frac{\partial g}{\partial x} f x'}_{= \langle x' \frac{\partial g}{\partial x} \rangle} + \cdots = 0$$

$$\Rightarrow \frac{d}{ds} \langle g \rangle = \langle x' \frac{\partial g}{\partial x} \rangle + \langle x'' \frac{\partial g}{\partial x'} \rangle + \langle y' \frac{\partial g}{\partial y} \rangle + \langle y'' \frac{\partial g}{\partial y'} \rangle$$

But $\frac{dg}{ds} = \frac{\partial g}{\partial x} x' + \frac{\partial g}{\partial x'} x'' + \frac{\partial g}{\partial y} y' + \frac{\partial g}{\partial y'} y''$

$$\Rightarrow \frac{d}{ds} \langle g \rangle = \langle g' \rangle$$

So $\frac{d}{ds} \langle x^2 \rangle = 2 \langle x x' \rangle$

$\frac{d}{ds} \langle x'^2 \rangle = 2 \langle x' x'' \rangle$ etc...

$\frac{d}{ds} \langle x x' \rangle = \langle x x'' \rangle + \langle x'^2 \rangle$

ENVELOPE EQUATION FOR AXISYMMETRIC BEAMS

LET $r_b^2 = 2\langle r^2\rangle = 2(\langle x^2\rangle + \langle y^2\rangle) = 4\langle x^2\rangle$ for an axisymmetric beam

$$2 r_b r_b' = 4\langle r r'\rangle \quad \Rightarrow \quad r_b' = \frac{2\langle r r'\rangle}{r_b}$$

$$r_b'' = \frac{2\langle r r''\rangle + 2\langle r'^2\rangle}{r_b} - \frac{2\langle r r'\rangle}{r_b^2}\left(\frac{2\langle r r'\rangle}{r_b}\right)$$

$$= 2\frac{\langle r r''\rangle}{r_b} + \frac{4\langle r^2\rangle\langle r'^2\rangle - 4\langle r r'\rangle^2}{r_b^3}$$

WHAT IS $\langle r r''\rangle$?

(7.1)

RECALL EQUATION P1 (ON PATH TO PARAXIAL RAY EQUATION):

$$r'' - r\theta'^2 + \frac{\gamma'}{\beta^2\gamma} r' = \frac{q}{\gamma m \beta^2 c^2}\left(\frac{V''}{2} r + r\beta c \theta' B + E_r^{self} - v_\theta B_z^{self} \right)$$

P1 may be rewritten:

$$r'' - r\theta'^2 + \frac{\gamma'}{\beta^2\gamma} r' = \frac{q}{\gamma m \beta^2 c^2}\left[\frac{-mc^2}{q}\gamma'' \frac{r}{2} + \frac{\lambda(r)}{\gamma^2 2\pi\epsilon_0 r} + r\beta c\theta' B \right]$$

$\Rightarrow$

$$\boxed{r'' + \frac{\gamma'}{\beta^2\gamma} r' + \frac{\gamma''}{2\beta^2\gamma} r - \frac{q}{\gamma^3 m v_z^2}\frac{\lambda(r)}{2\pi\epsilon_0 r} - \frac{\omega_c}{\gamma\beta c}\theta' r - r\theta'^2 = 0}$$

What is $\langle r r'' \rangle$?

$$\langle r r'' \rangle + \frac{-\omega_c}{\gamma\beta c}\langle \theta' r^2 \rangle - \langle r^2 \theta'^2 \rangle + \cdots = 0$$

$$\langle p_\theta \rangle^2 = \gamma^2 m^2 \beta^2 c^2 \langle r^2\theta' \rangle^2 + \frac{\omega_c^2}{4} m^2 \langle r^2 \rangle^2 + \omega_c \gamma m^2 \beta c \langle r^2\theta' \rangle \langle r^2 \rangle$$

$$\Rightarrow \frac{-\omega_c}{\gamma\beta c}\langle \theta' r^2 \rangle = \frac{-\omega_c}{\gamma\beta c}\left[\frac{\langle p_\theta \rangle^2}{\omega_c \gamma m^2 \beta c \langle r^2 \rangle} - \frac{\omega_c \langle r^2 \rangle}{4\gamma\beta c} - \frac{\gamma\beta c}{\omega_c}\frac{\langle r^2\theta' \rangle^2}{\langle r^2 \rangle} \right]$$

$$\Rightarrow \langle r r'' \rangle - \frac{\langle p_\theta \rangle^2}{\gamma^2 m^2 \beta^2 c^2 \langle r^2 \rangle} + \frac{\omega_c^2 \langle r^2 \rangle}{4\gamma^2 \beta^2 c^2} - \frac{\langle r^2\theta' \rangle^2}{\langle r^2 \rangle} + \langle r^2\theta'^2 \rangle + \cdots = 0$$

$$\Rightarrow \langle r r'' \rangle = \frac{\gamma'}{\beta^2\gamma}\langle r r'\rangle + \frac{\gamma''}{2\beta^2\gamma}\langle r^2\rangle - \frac{q}{\gamma^3 m v_z^2}\frac{\langle\lambda(r)\rangle}{2\pi\epsilon_0} +$$

$$\frac{\langle p_\theta\rangle^2}{(\gamma m\beta c)^2\langle r^2\rangle} - \frac{\omega_c^2\langle r^2\rangle}{4(\gamma\beta c)^2} - \frac{\langle r^2\theta'\rangle^2}{\langle r^2\rangle} + \langle r^2\theta'^2\rangle$$

$$r_b'' = \frac{2\langle r r''\rangle}{r_b} + \frac{4\langle r^2\rangle\langle r'^2\rangle - 4\langle r r'\rangle}{r_b^3}$$

$$= \frac{\gamma'}{\beta^2\gamma}\frac{2\langle r r'\rangle}{r_b} + \frac{\gamma''}{2\beta^2\gamma}\frac{2\langle r^2\rangle}{r_b} - \frac{2q}{\gamma^3 m v_z^2}\frac{\langle\lambda(r)\rangle}{2\pi\epsilon_0}\frac{1}{r_b}$$

$$+ \frac{\langle p_\theta\rangle^2}{(\gamma m\beta c)^2}\frac{2}{\langle r^2\rangle r_b} - \frac{\omega_c^2}{4(\gamma\beta c)^2}\frac{2\langle r^2\rangle}{r_b} - \frac{2\langle r^2\theta'\rangle^2}{r_b\langle r^2\rangle}$$

$$+ \frac{2\langle r^2\theta'^2\rangle}{r_b} + \frac{4\langle r^2\rangle\langle r'^2\rangle - 4\langle r r'\rangle^2}{r_b^3}$$

USING $r_b^2 \equiv 2\langle r^2\rangle$ & $r_b' = \dfrac{2\langle r r'\rangle}{r_b}$

ENVELOPE EQUATION

$$\Rightarrow \boxed{r_b'' + \frac{\gamma'}{\beta^2\gamma}r_b' + \frac{\gamma''}{2\beta^2\gamma}r_b + \left(\frac{\omega_c}{2\gamma\beta c}\right)^2 r_b + \frac{-4\langle p_\theta\rangle^2}{(\gamma m\beta c)^2 r_b^3} - \frac{\epsilon_r^2}{r_b^3} - \frac{Q}{r_b} = 0}$$

WHERE $\epsilon_r^2 = 4(\langle r^2\rangle\langle r'^2\rangle - \langle r r'\rangle^2 + \langle r^2\rangle\langle r^2\theta'^2\rangle - \langle r^2\theta'\rangle^2)$

ENVELOPE EQUATION -- CONTINUED

$$\boxed{r_b'' + \frac{\gamma'}{\beta^2\gamma} r_b' + \frac{\gamma''}{2\beta^2\gamma} r_b + \left(\frac{\omega_c}{2\gamma\beta c}\right)^2 r_b - \frac{4\langle p_\theta\rangle^2}{(\gamma m\beta c)^2 r_b^3} - \frac{\varepsilon_r^2}{r_b^3} - \frac{Q}{r_b} = 0}$$

COMPARE WITH THE SINGLE PARTICLE PARAXIAL RAY EQUATION:

$$\underbrace{r'' + \frac{\gamma'}{\beta^2\gamma} r'}_{\text{INERTIAL}} + \underbrace{\frac{\gamma''}{2\beta^2\gamma} r}_{E_r} + \underbrace{\left(\frac{\omega_c}{2\gamma\beta c}\right)^2 r}_{v_\theta B_z\text{ - CENTRIFUGAL}} - \underbrace{\left(\frac{p_\theta}{\gamma m\beta c}\right)^2 \frac{1}{r^3}}_{\text{CENTRIFUGAL}} - \underbrace{\frac{q}{\gamma^3 m v_z^2}\frac{\lambda(r)}{2\pi\varepsilon_0 r}}_{E_r - v_z B_\theta \text{ self field}} = 0$$

$$\varepsilon_r^2 = 4\left(\langle r^2\rangle\langle r'^2\rangle - \langle rr'\rangle^2 + \langle r^2\rangle\langle r^2\theta'^2\rangle - \langle r^2\theta'\rangle^2\right)$$

NOTE THAT FOR AXISYMMETRIC BEAMS ($\rho = \rho(r)$ ONLY)

$$\langle r^2\rangle = \langle x^2\rangle + \langle y^2\rangle = 2\langle x^2\rangle$$

$$\Rightarrow 2\langle rr'\rangle = 4\langle xx'\rangle$$

$$\text{\& } \langle x'^2\rangle + \langle y'^2\rangle = 2\langle x'^2\rangle = \langle r'^2\rangle + \langle r^2\theta'^2\rangle$$

DEFINE $\varepsilon_x^2 = 16\left(\langle x^2\rangle\langle x'^2\rangle - \langle xx'\rangle^2\right)$

$$\Rightarrow \boxed{\varepsilon_r^2 = \varepsilon_x^2 - 4\langle r^2\theta'\rangle^2}$$

EXAMPLES OF
SYSTEMS WITH AXIAL SYMMETRY

- PERIODIC SOLENOIDS

- EINZEL LENSES

- CONTINUOUS FOCUSING

EXAMPLES OF
SYSTEMS WITHOUT AXIAL SYMMETRY

- ELECTRIC OR MAGNETIC QUADRUPOLE

$\Rightarrow$ USE CARTESIAN COORDINATES WITH
ELLIPTICAL SPACE CHARGE SYMMETRY

(11)

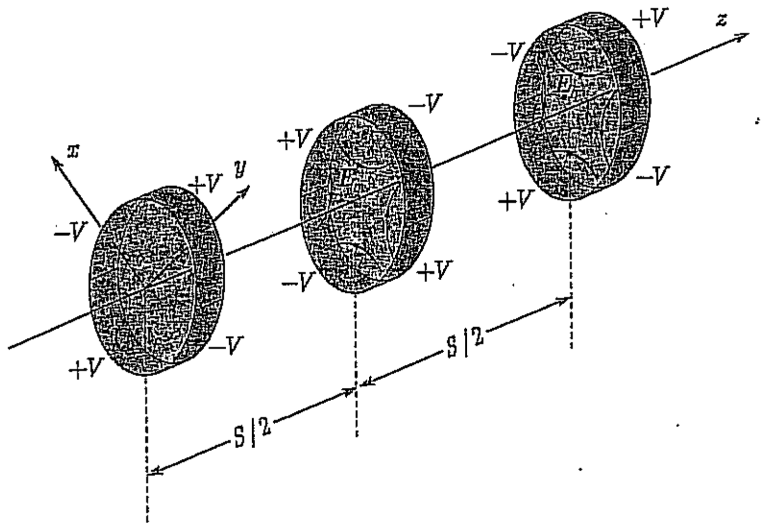

Figure 3.3. Schematic of conductor configuration with applied voltages producing an alternating-gradient quadrupole electric field with axial periodicity length S.

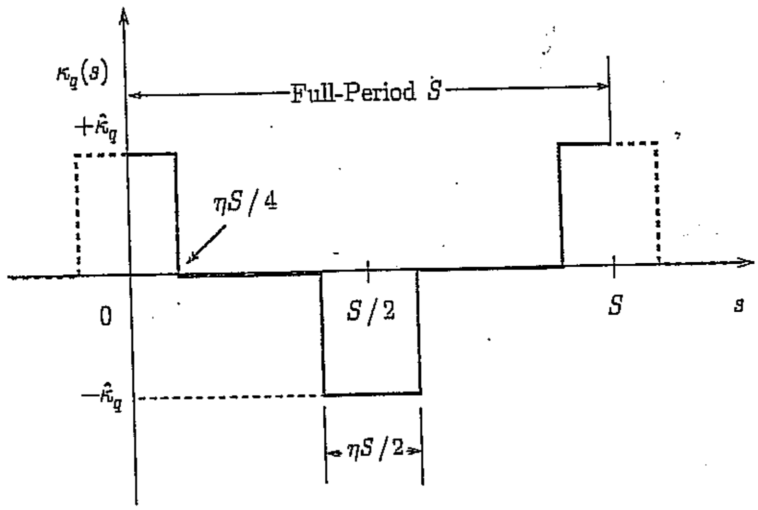

Figure 3.7. Alternating step-function model of a periodic quadrupole lattice with filling factor η for the lens elements. The figure shows a plot of the quadrupole coupling coefficient $\kappa_q(s)$ versus s for one full period (S) of the lattice. Such a configuration is often called a FODO transport lattice (acronym for focusing-off-defocusing-off).

FIGURES FROM DAVIDSON & QIN 2003

(12)

figure from
Davidson & Qin, 2003.

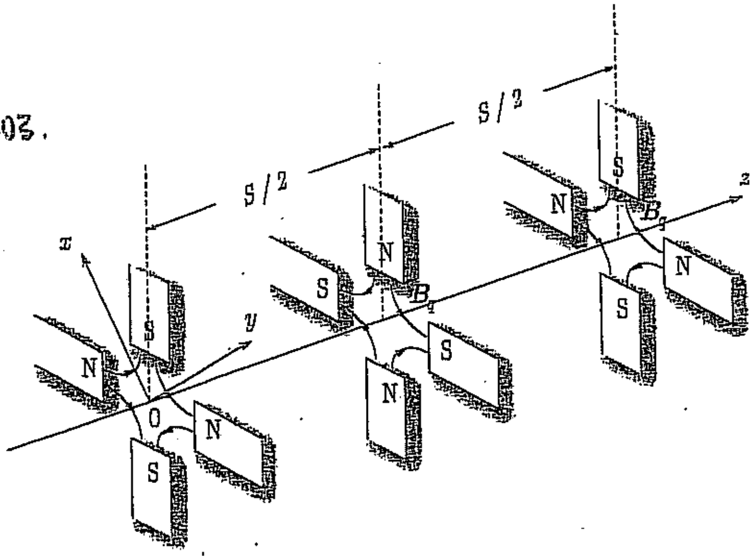

Figure 3.1. Schematic of magnet sets producing an alternating-gradient quadrupole field with axial periodicity length S.

J. BARNARD

13

FROM REISER, p. 112

$E_x = -E' x$

$E_y = E' y$

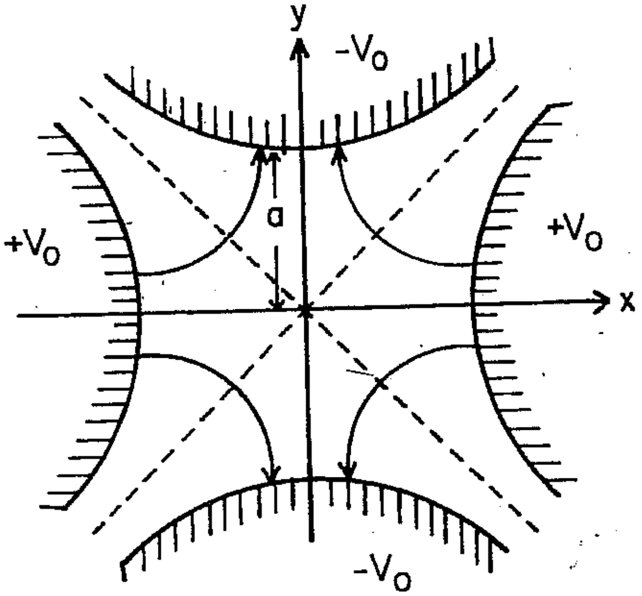

$F_x = -q E' x$

$F_y = q E' y$

ELECTROSTATIC QUADS

Figure 3.15. Electrodes and force lines in an electrostatic quadrupole.

$B_x = B' y$

$B_y = B' x$

$F_x = -q V_z B' x$

$F_y = q V_x B' y$

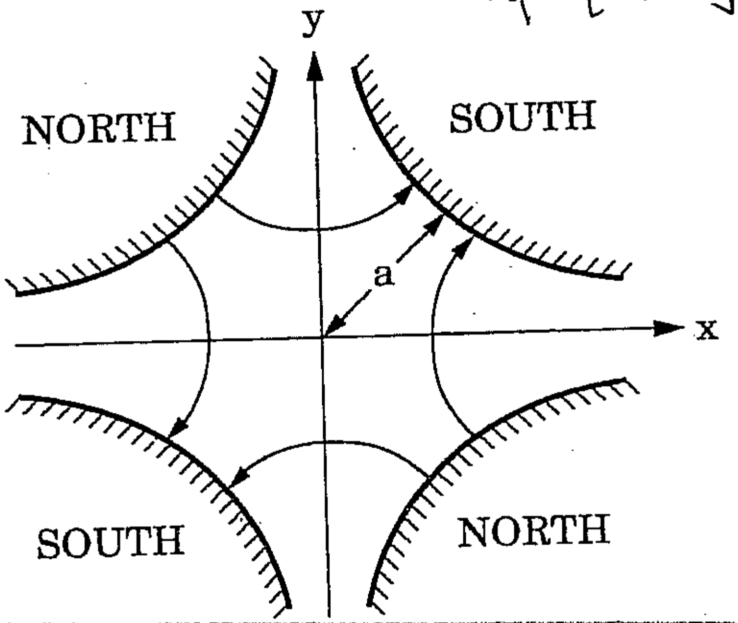

MAGNETIC QUADS

J. BARNARD

(14)

QUADRUPOLE FOCUSING

Now, relax radial symmetry:

For $\nabla \cdot E = 0$ or $\nabla \times B = 0$

EXPAND FIELD IN CYLINDRICAL "MULTIPOLES":

$$E_r, B_r = \sum_{n=1}^{\infty} f_n r^{n-1} \cos(n\theta)$$

$E_x = E_r \cos\theta - E_\theta \sin\theta$
$E_y = E_r \sin\theta + E_\theta \cos\theta$

$$E_\theta, B_\theta = \sum_{n=1}^{\infty} -f_n r^{n-1} \sin(n\theta)$$

$$n=1 \Rightarrow \text{dipole} \begin{cases} E_r = f_1 \cos\theta \\ E_\theta = -f_1 \sin\theta \end{cases} \Rightarrow \begin{matrix} E_x = f_1 \\ E_y = 0 \end{matrix}$$

$$n=2 \Rightarrow \text{quadrupole} \begin{cases} E_r = f_2 r \cos 2\theta \\ E_\theta = -f_2 r \sin 2\theta \end{cases} \Rightarrow \begin{matrix} E_x = f_2 x \\ E_y = -f_2 y \end{matrix}$$

NOTE: ABOVE EXPANSION IS VALID WHEN E or $B \neq$ function(z). FOR MAGNETS OF FINITE AXIAL EXTENT, FOR EACH FUNDAMENTAL n-pole, A SET OF HIGHER ORDER MULTIPOLES WITH SAME AZIMUTHAL SYMMETRY ARE REQUIRED TO SATISFY $\nabla^2\phi = 0$.

FOR EXAMPLE FOR A FUNDAMENTAL QUADRUPOLE THE FIELD MAY BE EXPANDED:

$$E_r = \sum_{\nu=0}^{\infty} f_{2,\nu}(z) [1+\nu] r^{1+2\nu} \cos[2\theta]$$

$$E_\theta = \sum_{\nu=0}^{\infty} -f_{2,\nu}(z) r^{1+2\nu} \sin[2\theta]$$

$$E_z = \sum_{\nu=0}^{\infty} \frac{1}{2} \frac{df_{2,\nu}}{dz} r^{2+2\nu} \cos 2\theta$$

with $f_{2,\nu+1}(z) = \dfrac{-1}{4(\nu+1)(\nu+3)} \dfrac{d^2 f_{2,\nu}(z)}{dz^2}$

SEE LUND, S. M. (1996) FOR EXAMPLE. HIF note 96-LLNL.

Heavy ion accelerators use alternating gradient quadrupoles to focus (confine) the beams (non-neutral plasmas)

Space-charge forces and thermal forces act to expand beam

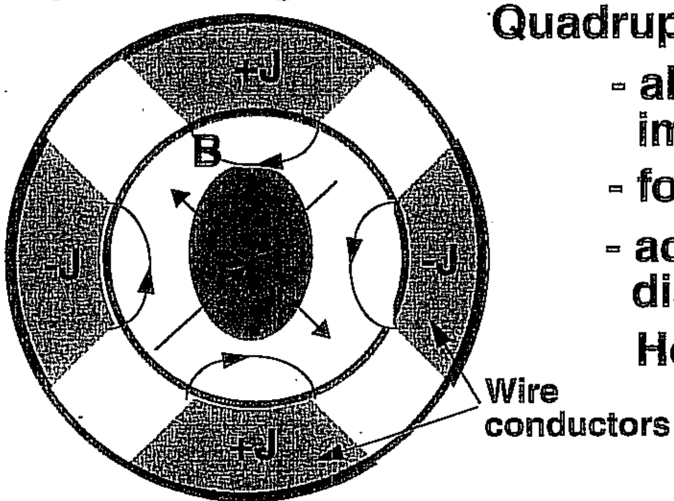

Magnetic quad

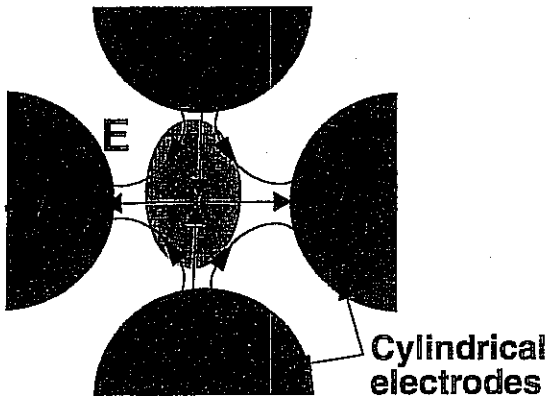

Electric quad

Quadrupoles (magnetic or electric):

- alternately provide inward then outward impulse
- focus in one plane and defocus in other
- act as linear lenses. (Force proportional to distance from axis).

Horizontal (x) plane:

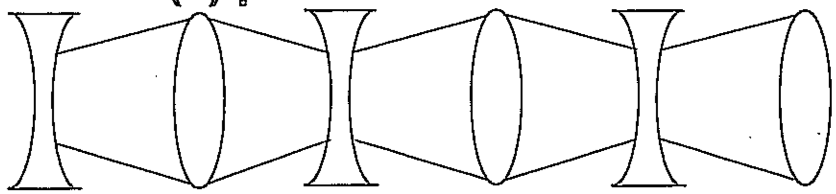

Vertical (y) plane:

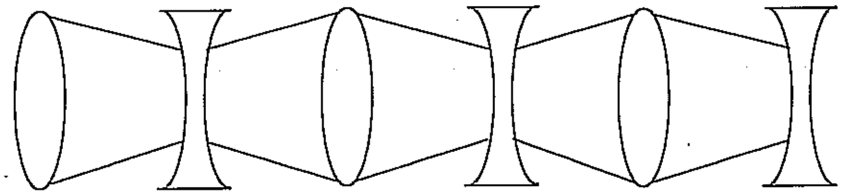

Average displacement
is larger in focusing lenses
so the net effect is focusing.

J. Barnard
16

Space charge reduces betatron phase advance

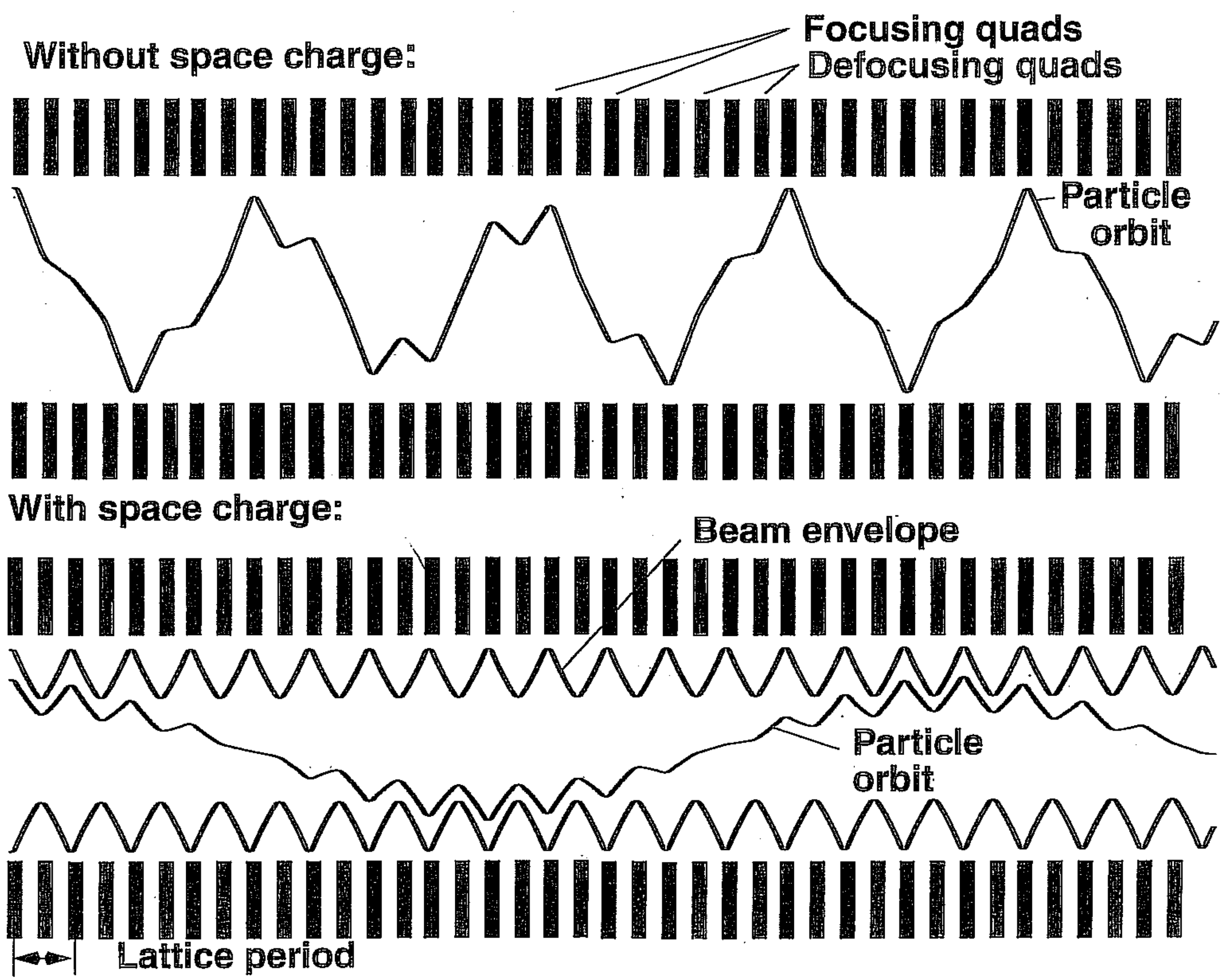

J. BARNARD (6)
(17)

John Barnard
Steven Lund
USPAS
June 2008

Current limits

A. Axisymmetric
   1. Solenoids
   2. Einzel lens
B. Quadrupolar
   1. Derivation of envelope equations with elliptic symmetry
   2. Current limit using fourier transform method

②

YESTERDAY, WE DERIVED THE PARAXIAL RAY EQUATION FOR PARTICLES IN AXISYMMETRIC SYSTEMS:

$$\underbrace{r'' + \frac{\gamma'}{\beta^2\gamma} r'}_{\text{INERTIAL}} + \underbrace{\frac{\gamma''}{2\beta^2\gamma}}_{E_r} + \underbrace{\left(\frac{\omega_c}{2\gamma\beta c}\right)^2 r}_{\substack{V_\theta B_z \\ -\text{CENTRIFUGAL}}} - \underbrace{\left(\frac{p_\theta}{\gamma\beta mc}\right)^2 \frac{1}{r^3}}_{\text{CENTRIPETAL}} - \underbrace{\frac{q}{\gamma^3 m v_z^2}\frac{\lambda(r)}{2\pi\epsilon_0 r}}_{\text{SELF-FIELD}} = 0$$

$$\theta' = \frac{p_\theta}{\gamma m r^2 \beta c} - \frac{\omega_c}{2\gamma\beta c} \quad \leftarrow \text{CONSTANCY \& DEFINITION OF CANONICAL MOMENTUM}$$

ENVELOPE EQUATION FOR AXISYMMETRIC BEAM

$$r_b'' + \frac{\gamma' r_b'}{\beta^2\gamma} + \frac{\gamma''}{2\beta^2\gamma} r_b + \left(\frac{\omega_c}{2\gamma\beta c}\right)^2 r_b - \frac{4\langle p_\theta\rangle^2}{(\gamma m\beta c)^2 r_b^3} - \frac{\varepsilon_r^2}{r_b^3} - \frac{Q}{r_b} = 0$$

$$\varepsilon_r^2 \equiv 4\left(\langle r^2\rangle\langle r'^2\rangle - \langle rr'\rangle^2 + \langle r^2\rangle\langle r^2\theta'^2\rangle - \langle r^2\theta'\rangle^2\right)$$

3

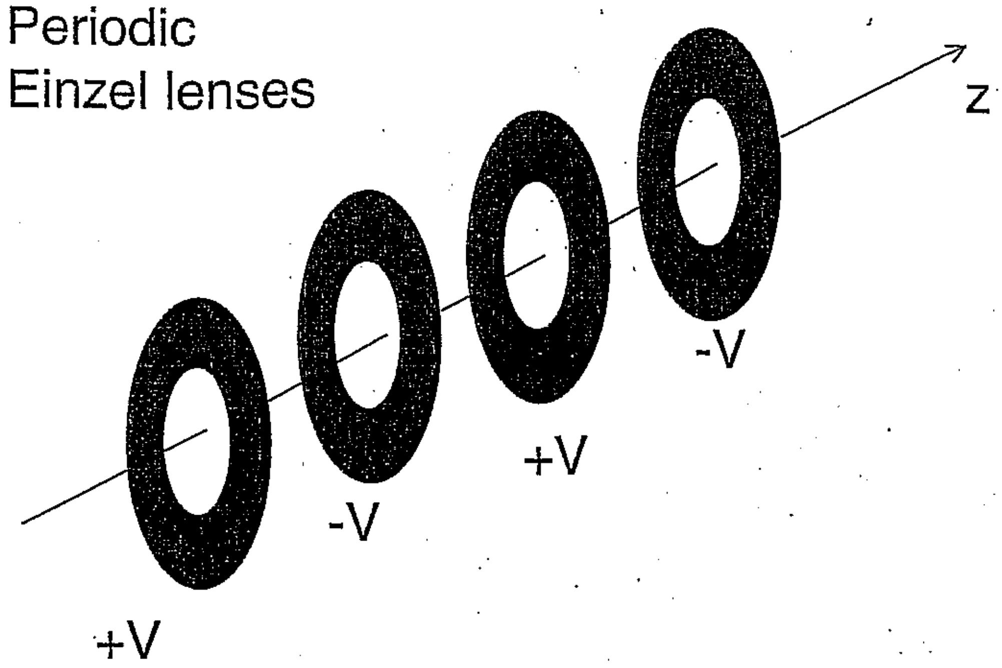

PERIODIC SOLENOIDS

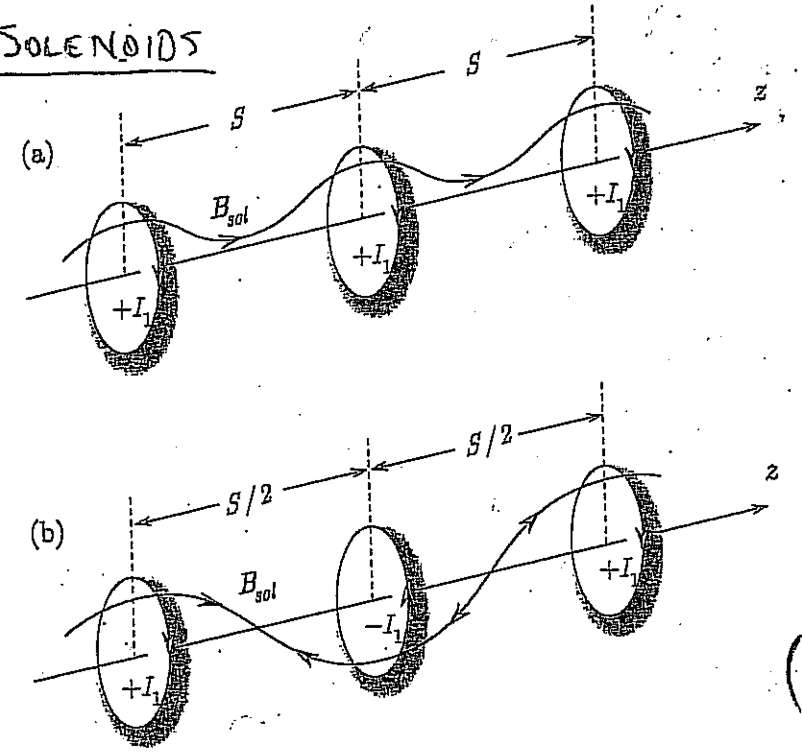

(FIGURE FROM DAVIDSON & QIN, 2003) p. 55 "PHYSICS OF INTENSE CHARGED PARTICLE BEAMS IN HIGH ENERGY ACCELERATORS"

Figure 3.2. Schematic of magnet sets producing a periodic focusing solenoidal field with axial periodicity length S. In Fig. 3.2 (a), successive coils are spaced by S and have the same current polarity $+I_1, +I_1, \cdots$. In Fig. 3.2 (b), successive coils are spaced by $S/2$ and have alternating current polarities $+I_1, -I_1, +I_1, \cdots$.

SOLENOIDAL FOCUSING

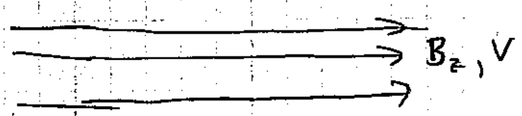

Let $\gamma' = \gamma'' = 0$

FOR MAXIMUM TRANSPORT $P_\theta = 0$ & $\varepsilon_r^2 = 0$

$$\Rightarrow \quad r_b'' + \left(\frac{\omega_c}{2\gamma\beta c}\right)^2 r_b = \frac{Q}{r_b}$$

FOR A MATCHED BEAM:

$$Q_{max} = \left(\frac{\omega_c}{2\gamma\beta c}\right)^2 r_b^2$$

HEURISTICALLY:

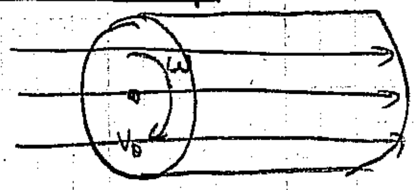

$V_\theta = \omega r$

$$\underset{\substack{\uparrow \\ \text{centrifugal} \\ \text{force}}}{m\omega^2 r} + \underset{\substack{\uparrow \\ \text{SPACE} \\ \text{CHARGE FORCE}}}{Q m V_z^2 \left(\frac{r}{r_b^2}\right)} = \underset{\substack{\uparrow \\ \text{MAGNETIC FORCE} \\ \text{INWARD}}}{q \overset{q\,\omega r\, B}{\overset{\shortparallel}{V_\theta}} B_z}$$

$$\Rightarrow \quad \omega^2 + \frac{QV^2}{r_b^2} = \omega\,\omega_c$$

$\omega\omega_c - \omega^2$ = MAXIMUM WHEN $\omega = \dfrac{\omega_c}{2}$

$$\Rightarrow \quad Q_{max} = \left(\frac{\omega_c^2}{4}\right)\left(\frac{r_b^2}{V^2}\right)$$

SOLENOIDAL FOCUSING - CONTINUED

IN REALITY BEAM ACQUIRES V_θ AS BEAM ENTERS SOLENOID:

CONSIDER SIMPLE STEP FUNCTION APPROXIMATION TO SOLENOID FIELD:

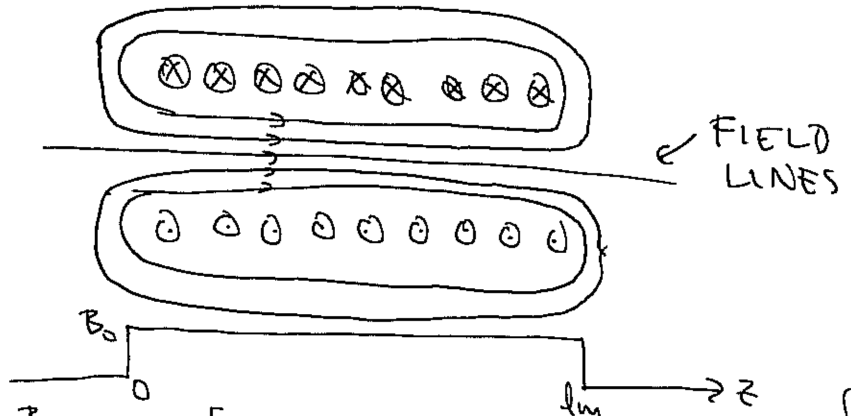

LET $B_z = B_0\left[\Theta(z) + \Theta(l_m - z) - 1\right] = \begin{cases} 0 & z<0 \\ B_0 & 0<z<l_m \\ 0 & z>l_m \end{cases}$

$$\frac{\partial B_z}{\partial z} = B_0\left[\delta(z) + \delta(l_m - z)\right]$$

here $\Theta(z) = \begin{cases} 1 & z>0 \\ 0 & z<0 \end{cases}$

As we found earlier $\nabla \cdot B = 0 \Rightarrow$

$$B_r(r,z) \simeq -\frac{r}{2}\frac{\partial B_z}{\partial z} + \cdots = -\frac{r}{2} B_0\left[\delta(z) + \delta(l_m - z)\right]$$

$$\Delta p_\theta^* = q\int v_z B_r\, dt = \int_{-\infty}^{0+\epsilon} q B_r\, dz = -\frac{rqB_0}{2}$$

$$\Rightarrow v_\theta = r\frac{qB_0}{2m} = \frac{r\omega_c}{2}$$

EINZEL LENS

J. BARNARD

5

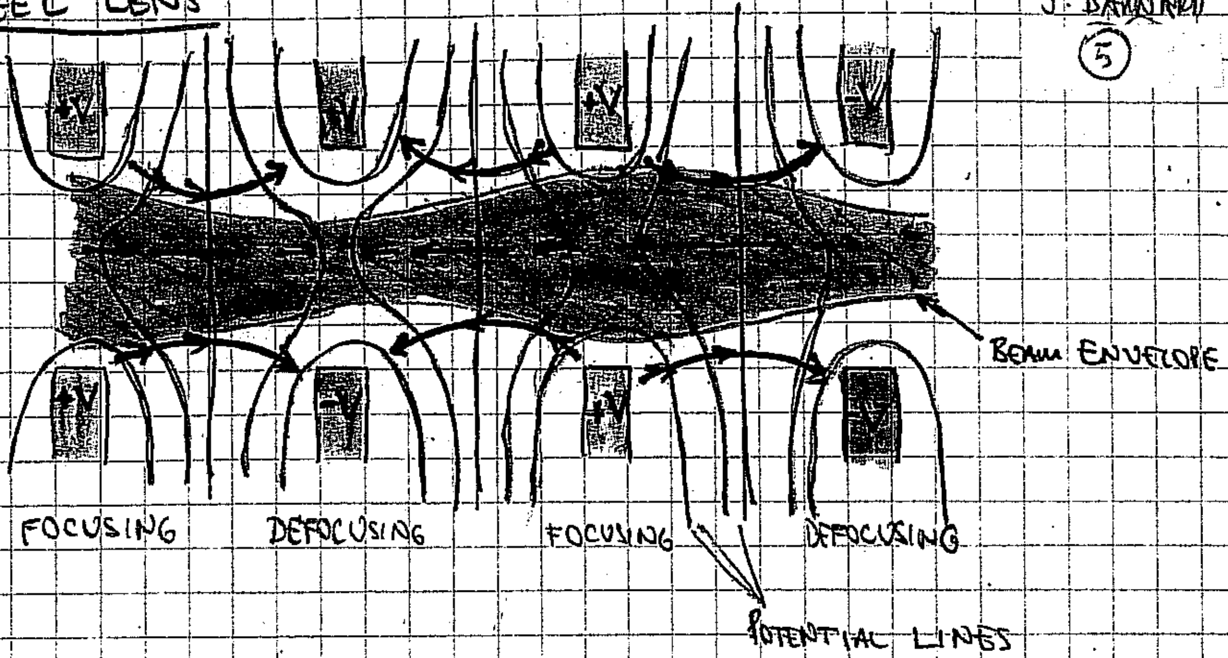

FOCUSING OCCURS AT LARGE radius THAN DEFOCUSING

⇒ NET INWARD FORCE

J. BARNARD

6

EINZEL LENS – ANALYSIS (DERIVATION FROM ED LEE)

NOW, LET $\omega_c = \langle P_\theta \rangle = \varepsilon_r^2 = 0$

$$\Rightarrow \quad r_b'' + \frac{\gamma'}{\beta^2\gamma} r_b' + \frac{\gamma''}{2\beta^2\gamma} r_b - \frac{Q}{r_b} = 0$$

ALSO ASSUME $\beta \ll 1$, NON-RELATIVISTIC BEAM $\Rightarrow \gamma' \simeq \beta\beta'$, $\gamma'' \simeq \beta'^2 + \beta''\beta$

$$r_b'' + \frac{\beta'}{\beta} r_b' + \left[\frac{1}{2}\frac{\beta'^2}{\beta^2} + \frac{1}{2}\frac{\beta''}{\beta}\right] r_b - \frac{Q}{r_b} = 0$$

To eliminate r_b' term try substitution

$$r_b = \left(\frac{\beta_0}{\beta}\right)^{1/2} R$$

$$r_b' = \left(\frac{\beta_0}{\beta}\right)^{1/2} R' - \frac{1}{2}\left(\frac{\beta}{\beta_0}\right)^{-3/2} \frac{R}{\beta_0}\beta'$$

$$r_b'' = \left(\frac{\beta_0}{\beta}\right)^{1/2} R'' - \left(\frac{\beta}{\beta_0}\right)^{-\frac{3}{2}} \frac{R'}{\beta_0}\beta' + \frac{3}{4}\left(\frac{\beta}{\beta_0}\right)^{-\frac{5}{2}} \frac{R}{\beta_0^2}\beta'^2 - \frac{1}{2}\left(\frac{\beta}{\beta_0}\right)^{-\frac{3}{2}} \frac{R}{\beta_0}\beta''$$

$$\Rightarrow \left(\frac{\beta_0}{\beta}\right)^{1/2} R'' + \frac{3}{4}\left(\frac{\beta}{\beta_0}\right)^{-\frac{5}{2}} \frac{\beta'^2}{\beta_0^2} R = \frac{Q}{R}\left(\frac{\beta}{\beta_0}\right)^{1/2}$$

$$\Rightarrow \quad \boxed{R'' = \frac{Q}{R}\left(\frac{\beta}{\beta_0}\right) - \frac{3}{4}\left(\frac{\beta'}{\beta}\right)^2 R}$$

EINZEL LENS - CONTINUED

MODEL: LET $\phi = \phi_0 \cos\left(\frac{\pi z}{L}\right)$

$$\frac{1}{2} m v^2 + q\phi = \text{constant}$$

$$\Rightarrow v^2 = v_0^2 + \frac{2q\phi}{m}\cos\left(\frac{\pi z}{L}\right)$$

$$v' = \frac{-q\phi_0}{mv}\left(\frac{\pi}{L}\right)\sin\left(\frac{\pi z}{L}\right)$$

If $\left(\frac{2q\phi_0}{m}\right) << v_0^2$: $\left(\frac{\beta'}{\beta}\right)^2 \cong \left(\frac{q\phi_0}{mv_0^2}\right)^2\left(\frac{\pi}{L}\right)^2 \sin^2\left(\frac{\pi z}{L}\right)$

FOR EQUILIBRIUM LOOK AT D.C. COMPONENT: $\sin^2(x) = \frac{1}{2} - \frac{1}{2}\cos 2x$

$$R'' = 0 \Rightarrow \frac{Q}{\overline{R}} = \frac{3}{4}\overline{\left(\frac{\beta'}{\beta}\right)^2}\ \overline{R}$$

$$R \equiv \left(\frac{\beta}{\beta_0}\right)^{1/2} r_b \Rightarrow \overline{R} = r_b$$

$$\overline{\left(\frac{\beta'}{\beta}\right)^2} = \frac{1}{2}\left(\frac{q\phi_0}{mv_0^2}\right)^2\left(\frac{\pi}{L}\right)^2$$

$$\Rightarrow Q_{max} = \frac{3\pi^2}{8}\left(\frac{q\phi_0}{mv_0^2}\right)^2\left(\frac{r_b}{L}\right)^2$$

J. BARNARD

7,5

FROM REISER, p.112

$E_x = -E'x$

$E_y = E'y$

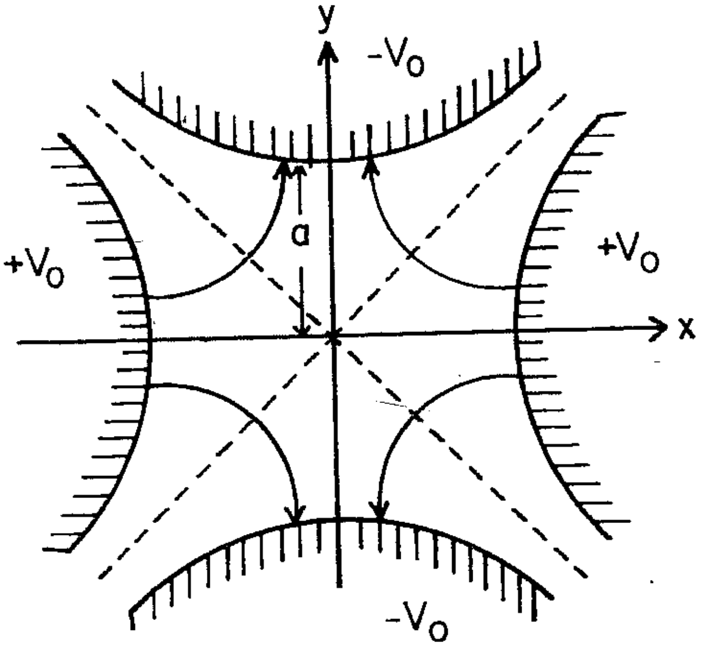

$F_x = -qE'x$

$F_y = qE'y$

ELECTROSTATIC QUADS

Figure 3.15. Electrodes and force lines in an electrostatic quadrupole.

$B_x = B'y$

$B_y = B'x$

$F_x = -qV_z B'x$

$F_y = qV_z B'y$

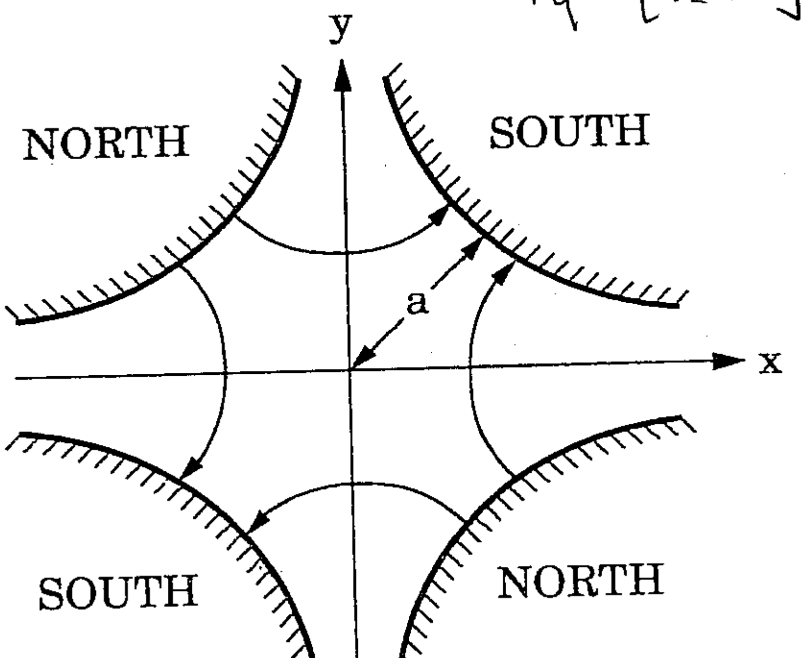

MAGNETIC QUADS

EQUATION OF MOTION

RETURN TO X, Y COORDINATES

$$x'' + \frac{1}{\gamma V_z}\frac{d}{ds}(\gamma V_z)x' = \frac{-q}{\gamma^3 m V_z^2}\frac{\partial\varphi}{\partial x} \pm \begin{cases} \frac{qB'}{\gamma m V_z^2}x & \text{for magnetic quads} \\ \frac{qE'}{\gamma m V_z^2}x & \text{for electric quads}\end{cases}$$

$$\text{Let } \frac{\gamma m V_z}{q} = \frac{p}{q} \equiv [B\rho] \equiv \text{RIGIDITY}$$

$$y'' + \frac{1}{\gamma V_z}\frac{d}{ds}(\gamma V_z)y' = \frac{-q}{\gamma^3 m V_z^2}\frac{\partial\varphi}{\partial y} \mp \begin{cases} \frac{B'}{[B\rho]}y & \text{magnetic} \\ \frac{qE'}{\gamma m V_z^2}y & \text{electric}\end{cases}$$

ENVELOPE EQUATION

$$r_x^2 = 4\langle x^2\rangle; \quad r_y^2 = 4\langle y^2\rangle$$

$$r_x' = \frac{4\langle xx'\rangle}{r_x}$$

$$r_x'' = \frac{4\langle xx''\rangle}{r_x} + \frac{\varepsilon_x^2}{r_x^3}; \qquad \varepsilon_x^2 = 16(\langle x^2\rangle\langle x'^2\rangle - \langle xx'\rangle^2)$$

$$r_y'' = \frac{4\langle yy''\rangle}{r_y} + \frac{\varepsilon_y^2}{r_y^3} \qquad \varepsilon_y^2 = 16(\langle y^2\rangle\langle y'^2\rangle - \langle yy'\rangle^2)$$

for magnetic focusing:

$$r_x'' + \frac{1}{\gamma V_z}\frac{d}{ds}(\gamma V_z)r_x' + \frac{4q}{\gamma^3 m V_z^2}\frac{\langle x\frac{\partial\varphi}{\partial x}\rangle}{r_x} \mp \frac{B'}{[B\rho]}r_x - \frac{\varepsilon_x^2}{r_x^3} = 0$$

$$r_y'' + \frac{1}{\gamma V_z}\frac{d}{ds}(\gamma V_z)r_y' + \frac{4q}{\gamma^3 m V_z^2}\frac{\langle y\frac{\partial\varphi}{\partial y}\rangle}{r_y} \pm \frac{B'}{[B\rho]}r_x - \frac{\varepsilon_y^2}{r_y^3} = 0$$

(for electric focusing $\frac{B'}{[B\rho]} \to \frac{qE'}{\gamma m V_z^2}$)

(9)

SPACE CHARGE TERM WITH ELLIPTICAL SYMMETRY

#4: ELLIPTICAL SYMMETRY: $\rho = \rho\left(\frac{x^2}{r_x^2} + \frac{y^2}{r_y^2}\right)$

CAN BE SHOWN THAT $\left\langle x \frac{\partial\phi}{\partial x} \right\rangle = \frac{-\lambda}{4\pi\epsilon_0} \frac{r_x}{r_x + r_y}$

$$\left\langle y \frac{\partial\phi}{\partial y} \right\rangle = \frac{-\lambda}{4\pi\epsilon_0} \frac{r_y}{r_x + r_y}$$

DEFINING $Q = \frac{2q\lambda}{4\pi\epsilon_0 \gamma^3 m v_z^2}$

$$\Rightarrow \boxed{\begin{aligned} r_x'' + \frac{1}{\gamma v_z}\frac{d}{ds}(\gamma v_z) r_x' - \frac{2Q}{r_x + r_y} \mp \frac{B'}{[B\rho]} r_x - \frac{\epsilon_x^2}{r_x^3} = 0 \\ r_y'' + \frac{1}{\gamma v_z}\frac{d}{ds}(\gamma v_z) r_y' - \frac{2Q}{r_x + r_y} \pm \frac{B'}{[B\rho]} r_y - \frac{\epsilon_y^2}{r_y^3} \end{aligned}}$$

(for Electric Focusing $\frac{B'}{[B\rho]} \to \frac{qE'}{\gamma m v_z^2}$).

SPACE CHARGE TERM WITH ELLIPTICAL SYMMETRY II

J. BARNARD

(10)

ELLIPTICAL SYMMETRY: $\rho = \rho\left(\frac{x^2}{r_x^2} + \frac{y^2}{r_y^2}\right)$

CAN BE SHOWN THAT $\left\langle x \frac{\partial\varphi}{\partial x}\right\rangle = \frac{-\lambda}{4\pi\varepsilon_0}\,\frac{r_x}{r_x + r_y}$

(Sacherer, 1971)

& $\left\langle y \frac{\partial\varphi}{\partial y}\right\rangle = \frac{-\lambda}{4\pi\varepsilon_0}\,\frac{r_y}{r_x + r_y}$

OUTLINE OF PROOF: (from R. Ryne)

Let $\chi = \frac{x^2}{r_x^2+s} + \frac{y^2}{r_y^2+s}$

DEFINE $\eta(\chi)$ such that $\rho(x,y) = \left.\frac{d\eta(\chi)}{d\chi}\right|_{s=0} = \left.\hat{\rho}(\chi)\right|_{s=0}$

So $\rho = \hat{\rho}\left(\frac{x^2}{r_x^2} + \frac{y^2}{r_y^2}\right) = \left.\hat{\rho}(\chi)\right|_{s=0}$

DEFINE $\Psi(x,y) = \frac{-r_x r_y}{4\varepsilon_0}\int_0^\infty \frac{\eta(\chi)\, ds}{\sqrt{r_x^2+s}\,\sqrt{r_y^2+s}}$

It follows that $\frac{\partial^2\Psi}{\partial x^2} + \frac{\partial^2\Psi}{\partial y^2} = -\frac{\rho}{\varepsilon_0}$ AND SO IS A SOLUTION OF POISSON'S EQUATION

(since $\Psi \to 0$ as $x, y \to \infty$)

WHAT IS $\left\langle x \frac{\partial\Psi}{\partial x}\right\rangle$?

$$\left\langle x \frac{\partial\Psi}{\partial x}\right\rangle = \frac{-r_x r_y}{4\lambda\varepsilon_0}\int_{-\infty}^{\infty} dx \int_{-\infty}^{\infty} dy\, x\,\rho(x,y)\int_0^\infty \frac{\eta'\,\frac{\partial\chi}{\partial x}\, ds}{\sqrt{r_x^2+s}\,\sqrt{r_y^2+s}}$$

where $\lambda = \int_{-\infty}^{\infty} dx \int_{-\infty}^{\infty} dy\, \rho(x,y)$

So $$\left\langle x \frac{\partial \psi}{\partial x} \right\rangle = \frac{-2 r_x r_y}{4 \lambda \varepsilon_0} \int_{-\infty}^{\infty} dx \int_{-\infty}^{\infty} dy \; x^2 \hat{\rho}\left(\frac{x^2}{r_x^2} + \frac{y^2}{r_y^2}\right) \int_0^{\infty} \frac{\hat{\rho}\left(\frac{x^2}{r_x^2+s} + \frac{y^2}{r_y^2+s}\right) ds}{(r_x^2+s)^{3/2}(r_y^2+s)^{1/2}}$$

Let $$r\cos\theta = \frac{x}{\sqrt{r_x^2+s}} \qquad r\sin\theta = \frac{y}{\sqrt{r_y^2+s}}$$

$$\det J = \sqrt{r_x^2+s}\,\sqrt{r_y^2+s}\; r$$ where J is the Jacobian $dx\,dy = \det J \cdot dr\,d\theta$

$$\Rightarrow \left\langle x \frac{\partial \psi}{\partial x} \right\rangle = \frac{-r_x r_y}{\lambda 2 \varepsilon_0} \int_0^{\infty} dr \int_0^{2\pi} d\theta \int_0^{\infty} ds \; r^3 \hat{\rho}(r^2)\, \rho\left(\frac{r_x^2+s}{r_x^2} r^2\cos^2\theta + \frac{r_y^2+s}{r_y^2} r^2 \sin^2\theta\right) \cdot \cos^2\theta$$

Let $$r'^2 = \frac{r_x^2+s}{r_x^2} r^2\cos^2\theta + \frac{r_y^2+s}{r_y^2} r^2\sin^2\theta$$
$$= r^2\left[1 + s\left(\frac{\cos^2\theta}{r_x^2} + \frac{\sin^2\theta}{r_y^2}\right)\right]$$

with r fixed $$2r'dr' = r^2\left(\frac{\cos^2\theta}{r_x^2} + \frac{\sin^2\theta}{r_y^2}\right) ds$$

$$\Rightarrow \left\langle x \frac{\partial \psi}{\partial x} \right\rangle = \frac{-r_x r_y}{2 \lambda \varepsilon_0} \int_0^{\infty} dr \int_0^{2\pi} d\theta \int_r^{\infty} dr' \frac{2r'dr'\, r^3 \rho(r^2)\hat{\rho}(r'^2)}{r^2\left(\frac{\cos^2\theta}{r_x^2} + \frac{\sin^2\theta}{r_y^2}\right)} \cos^2\theta$$

$$\int_0^{2\pi} \frac{\cos^2\theta \; d\theta}{\frac{\cos^2\theta}{r_x^2} + \frac{\sin^2\theta}{r_y^2}} = \frac{2\pi r_x^2 r_y}{r_x + r_y}$$

$$\Rightarrow \left\langle x \frac{\partial \psi}{\partial x} \right\rangle = \frac{-r_x^3 r_y^2}{\lambda 2\pi \varepsilon_0 (r_x + r_y)} \int_0^{\infty} dr\, 2\pi r\, \hat{\rho}(r^2) \int_r^{\infty} dr'\, 2\pi r' \hat{\rho}(r'^2)$$

Recall $$\lambda = \int_{-\infty}^{\infty}\int_{-\infty}^{\infty} dx\,dy\, \rho(x,y) = \int_{-\infty}^{\infty}\int_{-\infty}^{\infty} dx\,dy\, \hat{\rho}\left(\frac{x^2}{r_x^2} + \frac{y^2}{r_y^2}\right)$$

Let $$\frac{x}{r_x} = r\cos\theta \qquad \frac{y}{r_y} = r\sin\theta \qquad \det J = r_x r_y r$$
$$\Rightarrow \lambda = \int_0^{\infty} dr \int_0^{2\pi} d\theta\, \rho(r^2)\, r_x r_y r = 2\pi r_x r_y \int_0^{\infty} dr\, r\, \hat{\rho}(r^2)$$

(12)

$$\text{Now}\quad \int_0^\infty dr\, r\,\rho(r^2)\int_0^r dr'\, r'\,\rho(r'^2) = \frac{1}{2}\underbrace{\int_0^\infty dr\, r\,\rho(r^2)}_{\lambda/2\pi r_x r_y}\ \underbrace{\int_0^\infty dr'\, r'\,\rho(r'^2)}_{\lambda/2\pi r_x r_y}$$

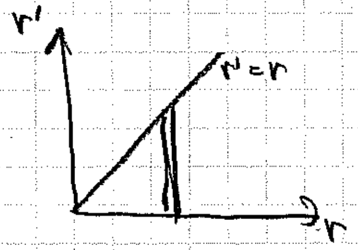

(by symmetry & consideration of diagram at left)

$$\Rightarrow\quad \left\langle x\,\frac{\partial\psi}{\partial x}\right\rangle = \frac{-\lambda}{4\pi\epsilon_0}\,\frac{r_x}{r_x+r_y}$$

CURRENT LIMIT FOR QUADRUPOLES

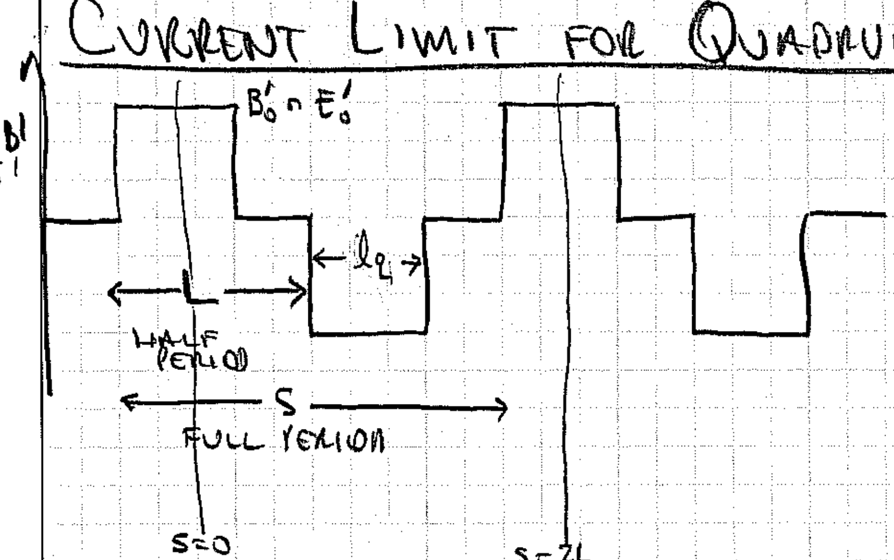

$$k = \begin{cases} \dfrac{B_0'}{[B\rho]} & \text{MAGNETIC} \\ \dfrac{qE_0'}{\gamma m v_z^2} & \text{ELECTRIC} \end{cases}$$

$$r_x'' + k f(s)\, r_x - \frac{2Q}{r_x + r_y} = 0$$

(NOTE WE HAVE SET $\epsilon = 0$).

$$r_y'' - k f(s)\, r_y - \frac{2Q}{r_x + r_y} = 0$$

$$f(s) = \begin{cases} 1 & 0 < s < \eta L/2 \\ -1 & L - \frac{\eta L}{2} < s < L + \eta L/2 \\ 1 & 2L - \eta L/2 < s < 2L \\ 0 & \text{otherwise} \end{cases}$$

$$\frac{1}{L}\int_0^{2L} f(s)\cos\left(\frac{\pi s}{L}\right) ds = \left(\frac{4}{\pi}\right)\sin\left(\frac{\pi\eta}{2}\right)$$ = fourier amplitude at fundamental lattice frequency

Let $r_x = r_b\left(1 + \delta\cos\left(\frac{\pi s}{L}\right)\right)$

$r_y = r_b\left(1 - \delta\cos\left(\frac{\pi s}{L}\right)\right)$

Let $k f(s) \rightarrow k\left(\frac{4}{\pi}\right)\sin\left(\frac{\eta\pi}{2}\right)\cos\left(\frac{\pi s}{L}\right)$

COLLECTING "FAST" TERMS AND "SLOW" TERMS

$$\left[-\frac{\pi^2}{L^2} r_b \delta + k r_b\left(\frac{4\sin\left(\frac{\eta\pi}{2}\right)}{\pi}\right)\right]\cos\left(\frac{\pi s}{L}\right) = 0 \quad \text{(fast)}$$

$$\delta k r_b\left(\frac{2\sin\left(\frac{\eta\pi}{2}\right)}{\pi}\right) = \frac{Q}{r_b} \quad \text{(slow)}$$

Fast $\Rightarrow \delta = \frac{4kL^2}{\pi^3}\sin\left(\frac{\eta\pi}{2}\right)$ & $Q_{max} \cong \frac{2\eta^2 k^2 L^2}{\pi^2}\left(\frac{\sin\left(\frac{\eta\pi}{2}\right)}{\left(\frac{\eta\pi}{2}\right)}\right)^2 r_b^2$

CONTINUOUS FOCUSING

$$r_x'' = -k_{p0}^2 r_x + \frac{2Q}{r_x + r_y} - \frac{\epsilon^2}{r_x^3}$$

$$r_y'' = -k_{p0}^2 r_y + \frac{2Q}{r_x + r_y} - \frac{\epsilon^2}{r_y^3}$$

CURRENT LIMIT BALANCES PERVEANCE & EXTERNAL FOCUSING ($r_x = r_y = r_b$):

$$k_{p0}^2 r_b = \frac{Q_{max}}{r_b}$$

Effective k_{p0}^2 FOR QUADRUPOLES FOUND FROM DOMINANT FOURIER COMPONENT

$$k_{p0}^2 = \frac{2\eta^2 k^2 L^2}{\pi^2} \left(\frac{\sin\left(\frac{\eta\pi}{2}\right)}{\frac{\eta\pi}{2}} \right)^2 \qquad \text{where } k = \frac{B'}{[B\rho]}$$

FOR CONTINUOUS FOCUSING: $k_{p0}^2 = \frac{\sigma_0^2}{4L^2}$

ELIMINATING L:

$$Q_{max} = \frac{\eta k \sigma_0}{\sqrt{2}\pi} \left(\frac{\sin\frac{\eta\pi}{2}}{\frac{\eta\pi}{2}} \right) r_b^2 \leftarrow$$

PERVEANCE LIMIT FOR FODO QUADRUPOLES

Envelope instabilities set upper limit on "single particle" phase advance σ_0

Experimental data (Tiefenback, 1986) from LBL's Single Beam Transport Experiment (SBTE)

$\sigma_0 < 85^o$

79

Experimental limits on beam stability in terms of σ and σ_0

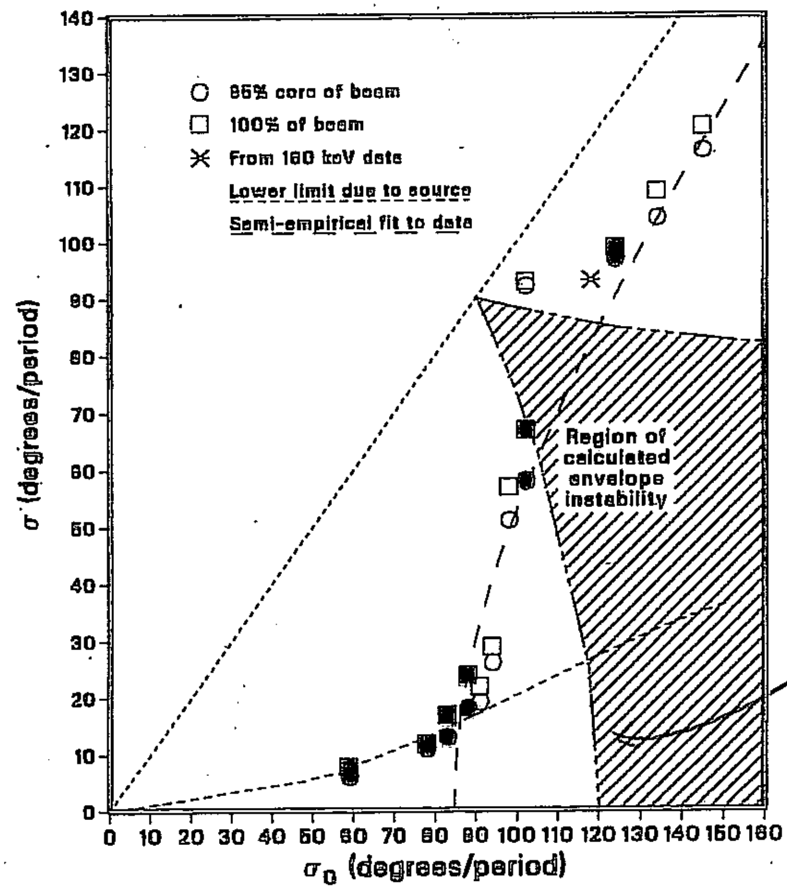

SEE LUND & CHAWLA 2006, NIMPR-A, FOR HIGHER ORDER PARTICLE-LATTICE RESONANCES WHICH CLARIFIES $\sigma_0 = 85^\circ$ LIMIT

SEE STRUCKMEIER & REISER, PARTICLE ACCELERATORS 14, 227, (1984) & LUND & BUKH, PRSTAB, 7 024801 (2004)

J. BARNARD

QUADRUPOLE CURRENT LIMIT — CONTINUED

$$Q_{max} \cong \frac{\eta k \theta_0}{\sqrt{2}\pi}\left(\frac{\sin\frac{\eta\pi}{2}}{\frac{\eta\pi}{2}}\right) r_b^2$$

here $k = \begin{cases} \dfrac{dB/dx}{[B\ell]} \sim \dfrac{B}{[B\ell]\, r_p} & \text{(MAGNETIC QUAD FODO)} \\ \dfrac{q\, dE/dx}{\gamma m v_z^2} \sim \dfrac{2 q V_q}{\gamma m v_z^2\, r_p^2} & \text{where } V_q = \frac{1}{2}\frac{dE}{dx} r_p^2 \text{ (ELECTRIC QUAD FODO)} \end{cases}$

So

$$Q_{max} \cong \frac{\eta \theta_0}{\sqrt{2}\pi}\left(\frac{\sin\frac{\eta\pi}{2}}{\frac{\eta\pi}{2}}\right)\begin{cases} \dfrac{B\, r_b}{[B\ell]}\left[\dfrac{r_b}{r_p}\right] & \text{(MAGNETIC QUAD)} \\ \dfrac{2 q V_q}{\gamma m v_z^2}\left[\dfrac{r_b^2}{r_p^2}\right] & \text{(ELECTRIC QUAD)} \end{cases}$$

Summary of Current Limits From Different Focusing Methods

Einzel Lens

$$Q_{max} \cong \frac{3\pi^2}{8}\left(\frac{q\phi_0}{m v_0^2}\right)^2\left(\frac{r_b}{L}\right)^2$$

Solenoids

$$Q_{max} = \left(\frac{\omega_c r_b}{2\gamma\beta c}\right)^2$$

Quadrupole Focusing

$$Q_{max} \cong \frac{\eta\,\omega_0}{\sqrt{2\pi}}\left(\frac{\sin\frac{\eta\pi}{2}}{\frac{\eta\pi}{2}}\right)\begin{bmatrix}\frac{B r_b}{[B\rho]} & \left[\frac{r_b}{r_p}\right] \\ \frac{2qV_q}{\gamma m v_z^2} & \left[\frac{r_b^2}{r_p^2}\right]\end{bmatrix}$$

MAGNETIC

Electric

For Non-Relativistic Beams

$$\lambda_{max} \propto \frac{\phi_0^2}{V} \qquad \lambda_{max} \propto \frac{q}{m} B^2 r_p^2 \qquad \lambda_{max} \propto \begin{cases} B_1 V^{1/2} r_p \\ V_q \end{cases}$$

Note
ϕ_0 = Voltage between Einzel lences
V_q = Voltage on a quad relative to ground
V = particle energy / q

Transverse Particle Equations of Motion*

Steven M. Lund
Lawrence Livermore National Laboratory (LLNL)

Steven M. Lund and John J. Barnard
"Beam Physics with Intense Space-Charge"

US Particle Accelerator School

University of Maryland, held at Annapolis, MD
16-27 June, 2008
(Version 20080624)

* Research supported by the US Dept. of Energy at LLNL and LBNL under contract Nos. DE-AC52-07NA27344 and DE-AC02-05CH11231.

Transverse Particle Equations: Outline

Particle Equations of Motion: Detailed Outline

Detailed Outline - 2

Detailed Outline - 3

Detailed Outline - 4

Detailed Outline - 5

S1: Particle Equations of Motion

S1A: Introduction: The Lorentz Force Equation

The *Lorentz force equation* of a charged particle is given by (SI Units):

$$\boxed{\frac{d}{dt}\mathbf{p}_i(t) = q_i\left[\mathbf{E}(\mathbf{x}_i,t) + \mathbf{v}_i(t)\times\mathbf{B}(\mathbf{x}_i,t)\right]}$$

$i =$ particle index
$t =$ time

$m_i, \quad q_i$ .... particle mass, charge

$\mathbf{x}_i(t)$ .... particle coordinate

$\mathbf{p}_i(t) = m\gamma_i(t)\mathbf{v}_i(t)$ .... particle momentum

$\mathbf{v}_i(t) = \dfrac{d}{dt}\mathbf{x}_i(t) = c\vec{\beta}_i(t)$ .... particle velocity

$\gamma_i(t) = \dfrac{1}{\sqrt{1-\beta_i^2(t)}}$ .... particle gamma factor

	Total		Applied		Self
Electric Field:	$\mathbf{E}(\mathbf{x},t)$	$=$	$\mathbf{E}^a(\mathbf{x},t)$	$+$	$\mathbf{E}^s(\mathbf{x},t)$
Magnetic Field:	$\mathbf{B}(\mathbf{x},t)$	$=$	$\mathbf{B}^a(\mathbf{x},t)$	$+$	$\mathbf{B}^s(\mathbf{x},t)$

S1B: Applied Fields

Transverse Focusing Optics:

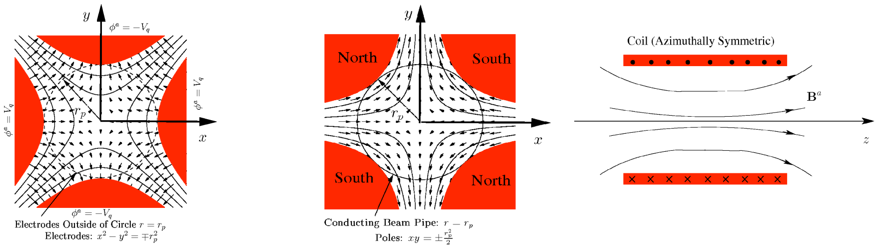

Dipole Bends:

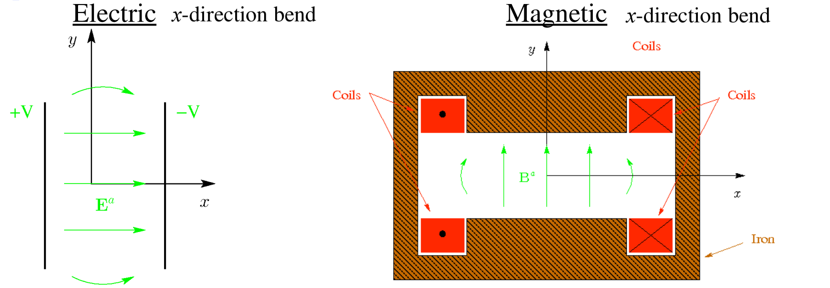

Longitudinal Acceleration:

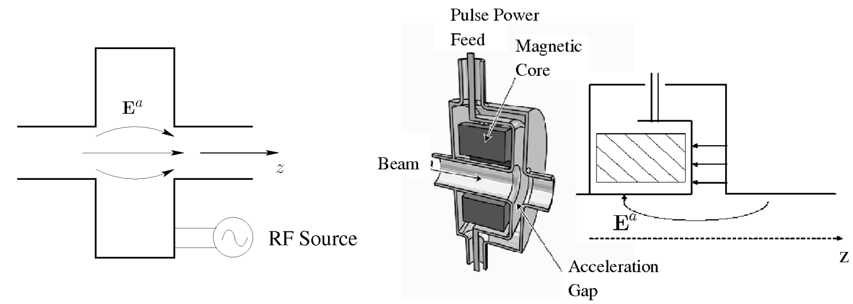

S1C: Machine Lattice

Applied field structures are often arraigned in a regular (periodic) lattice for beam transport/acceleration:

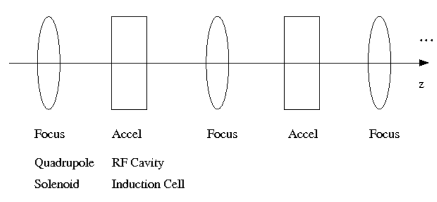

- Sometimes functions like bending/focusing are combined into a single element

Example – Linear FODO lattice (symmetric quadrupole doublet)

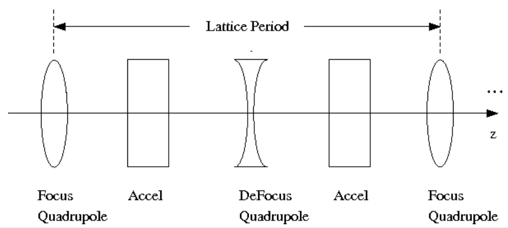

Lattices for rings and some beam insertion/extraction sections also incorporate bends and more complicated periodic structures:

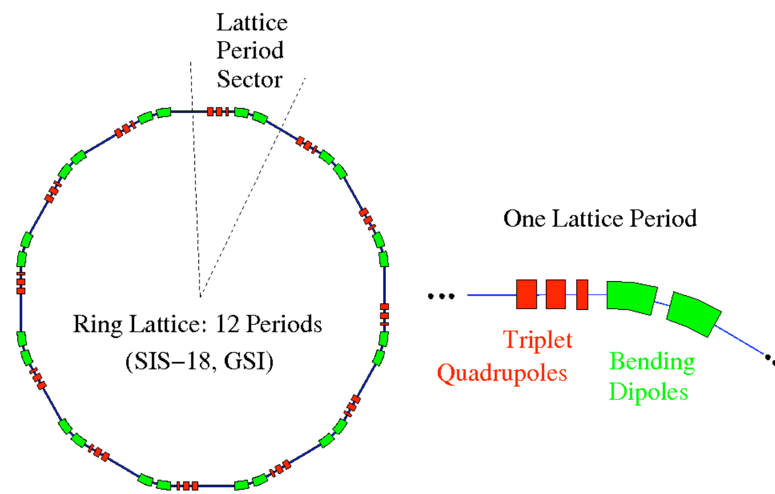

S1D: Self fields

Self-fields are generated by the distribution of beam particles:

- Charges
- Currents

Particle at Rest (pure electrostatic)

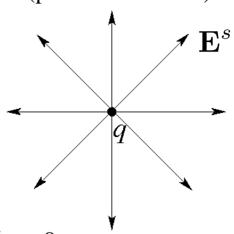

$\mathbf{B}^s = 0$

Particle in Motion

Obtain from Lorentz boost of rest-frame field: see Jackson, *Classical Electrodynamics*

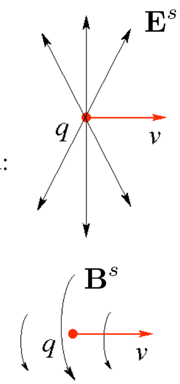

- Superimpose for all particles in the beam distribution
- Accelerating particles also radiate
  - We neglect electromagnetic radiation in this class (see: J.J. Barnard, Intro Lectures)

The electric ($\mathbf{E}$) and magnetic ($\mathbf{B}$) fields satisfy the Maxwell Equations. The linear structure of the Maxwell equations can be exploited to resolve the field into Applied and Self-Field components:

Applied Fields (often quasi-static)

- Generated by elements in lattice

$$\nabla \cdot \mathbf{E}^a = \frac{\rho^a}{\epsilon_0} \qquad \nabla \times \mathbf{B}^a = \mu_0 \mathbf{J}^a + \frac{1}{c^2}\frac{\partial}{\partial t}\mathbf{E}^a$$

$$\nabla \times \mathbf{E}^a = -\frac{\partial}{\partial t}\mathbf{B}^a \qquad \nabla \cdot \mathbf{B}^a = 0$$

$$\rho^a = \text{applied charge density} \qquad \frac{1}{\mu_0\epsilon_0} = c^2$$
$$\mathbf{J}^a = \text{applied current density}$$

$$+ \text{ Boundary Conditions on } \mathbf{E}^a \text{ and } \mathbf{B}^a$$

- Boundary conditions depend on the total fields $\mathbf{E}$, $\mathbf{B}$ and if separated into Applied and Self-Field components, care is required

/// Aside: Notation:

$$\nabla \equiv \hat{\mathbf{x}}\frac{\partial}{\partial x} + \hat{\mathbf{y}}\frac{\partial}{\partial y} + \hat{\mathbf{z}}\frac{\partial}{\partial z}$$

Cartesian Representation

$$= \hat{\mathbf{r}}\frac{\partial}{\partial r} + \frac{\hat{\theta}}{r}\frac{\partial}{\partial \theta} + \hat{\mathbf{z}}\frac{\partial}{\partial z}$$

Cylindrical Representation
$x = r\cos\theta$
$y = r\sin\theta$

$$= \frac{\partial}{\partial \mathbf{x}}$$

Abbreviated Representation

$$= \frac{\partial}{\partial \mathbf{x}_\perp} + \hat{\mathbf{z}}\frac{\partial}{\partial z}$$

Resolved Abbreviated Rep.
Resolved into Perpendicular $(\perp)$ and Parallel (z) components

$$\mathbf{x} = \hat{\mathbf{x}}x + \hat{\mathbf{y}}y + \hat{\mathbf{z}}z$$
$$= \mathbf{x}_\perp + \hat{\mathbf{z}}z \qquad \mathbf{x}_\perp \equiv \hat{\mathbf{x}}x + \hat{\mathbf{y}}y$$

///

Self-Fields (dynamic, evolve with beam)

- Generated by particles in the beam

$$\nabla \cdot \mathbf{E}^s = \frac{\rho^s}{\epsilon_0} \qquad \nabla \times \mathbf{B}^s = \mu_0 \mathbf{J}^s + \frac{1}{c^2}\frac{\partial}{\partial t}\mathbf{E}^s$$

$$\nabla \times \mathbf{E}^s = -\frac{\partial}{\partial t}\mathbf{B}^s \qquad \nabla \cdot \mathbf{B}^s = 0$$

$$\rho^s = \text{beam charge density} = \sum_{i=1}^{N} q_i \delta[\mathbf{x} - \mathbf{x}_i(t)]$$

$$\mathbf{J}^s = \text{beam current density} = \sum_{i=1}^{N} q_i \mathbf{v}_i(t)\delta[\mathbf{x} - \mathbf{x}_i(t)]$$

i = particle index (N particles)
q_i = particle charge
$\mathbf{x}_i$ = particle coordinate
$\mathbf{v}_i$ = particle velocity

$\delta(\mathbf{x}) \equiv \delta(x)\delta(y)\delta(z)$
$\delta(x) \equiv$ Dirac-delta function
$\sum_{i=1}^{N} \cdots =$ sum over beam particles

$$+ \text{ Boundary Conditions on } \mathbf{E}^s \text{ and } \mathbf{B}^s$$
from material structures, radiation conditions, etc.

In accelerators, there is ideally a single species of particle:

$$\boxed{\begin{aligned} q_i &\rightarrow q \\ m_i &\rightarrow m \end{aligned}}$$

Large Simplification!

Multi-species results in more complex collective effects

Motion of particles within axial slices of the "bunch" are highly directed:

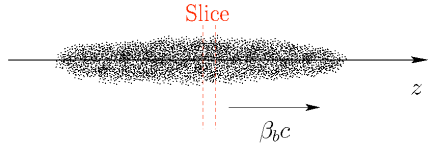

$$\beta_b(z)c \equiv \frac{1}{N'}\sum_{i=1}^{N'} \mathbf{v}_i \cdot \hat{\mathbf{z}}$$

= Mean axial velocity of N' particles in beam slice

$$\frac{d}{dt}\mathbf{x}_i(t) = \mathbf{v}_i(t) = \hat{\mathbf{z}}\beta_b(z)c + \delta\mathbf{v}_i$$

$$|\delta\mathbf{v}_i| \ll |\beta_b|c \qquad \text{Paraxial Approximation}$$

There are typically many particles:

$$\rho^s = \sum_{i=1}^{N} q_i \delta[\mathbf{x} - \mathbf{x}_i(t)] \qquad \mathbf{J}^s = \sum_{i=1}^{N} q_i \mathbf{v}_i(t)\delta[\mathbf{x} - \mathbf{x}_i(t)]$$

$$\simeq \rho(\mathbf{x}, t) \quad \text{continuous charge-density} \qquad \simeq \beta_b c \rho(\mathbf{x}, t)\hat{\mathbf{z}} \quad \text{continuous axial current-density}$$

The beam evolution is typically sufficiently slow (for heavy ions) where we can neglect radiation and approximate the self-field Maxwell Equations as:

- See: J. J. Barnard, Intro. Lectures: Electrostatic Approximation

$$\mathbf{E}^s = -\nabla\phi$$

$$\mathbf{B}^s = \nabla \times \mathbf{A} \qquad \mathbf{A} = \hat{\mathbf{z}}\frac{\beta_b}{c}\phi$$

$$\nabla^2\phi = \frac{\partial}{\partial\mathbf{x}} \cdot \frac{\partial}{\partial\mathbf{x}}\phi = -\frac{\rho^s}{\epsilon_0}$$

$+$ Boundary Conditions on ϕ

Vast Reduction of self-field model:

But still complicated!

Resolve the Lorentz force acting on beam particles into Applied and Self-Field terms:

$$\mathbf{F}_i(\mathbf{x}_i, t) = q\mathbf{E}(\mathbf{x}_i, t) + q\mathbf{v}_i(t) \times \mathbf{B}(\mathbf{x}_i, t)$$

$$\mathbf{F}_i = \mathbf{F}_i^a + \mathbf{F}_i^s$$

$$\mathbf{E} = \mathbf{E}^a + \mathbf{E}^s$$

$$\mathbf{B} = \mathbf{B}^a + \mathbf{B}^s$$

Applied:

$$\boxed{\mathbf{F}_i^a = q\mathbf{E}_i^a + q\mathbf{v}_i \times \mathbf{B}_i^a}$$

$$\mathbf{E}^a(\mathbf{x}_i, t) \equiv \mathbf{E}_i^a \quad \text{etc.}$$

Self-Field:

$$\boxed{\mathbf{F}_i^s = q\mathbf{E}_i^s + q\mathbf{v}_i \times \mathbf{B}_i^s}$$

The self-field force can be simplified:

- See also: J.J. Barnard, Intro. Lectures

Plug in self-field forms:

$$\mathbf{F}_i^s = q\mathbf{E}_i^s + q\mathbf{v}_i \times \mathbf{B}_i^s \qquad \cdots\Big|_i \equiv \cdots\Big|_{\mathbf{x}=\mathbf{x}_i}$$

$$\simeq q\left[-\left.\frac{\partial\phi}{\partial\mathbf{x}}\right|_i + (\beta_b c\hat{\mathbf{z}} + \underbrace{\delta\mathbf{v}_i}_{0\ \text{Neglect: Paraxial}}) \times \left.\left(\frac{\partial}{\partial\mathbf{x}} \times \hat{\mathbf{z}}\frac{\beta_b}{c}\phi\right)\right|_i\right]$$

Resolve into transverse (x and y) and longitudinal (z) components. After some algebra, find:

$$\mathbf{F}_i^s = \underbrace{-\frac{q}{\gamma_b^2}\left.\frac{\partial\phi}{\partial\mathbf{x}_\perp}\right|_i}_{\text{Transverse}} \underbrace{- \hat{\mathbf{z}}q\left.\frac{\partial\phi}{\partial z}\right|_i}_{\text{Longitudinal}}$$

$$\gamma_b \equiv \frac{1}{\sqrt{1-\beta_b^2}} \qquad \text{Axial relativistic gamma of beam}$$

/// Aside: Singular Self Fields

In *free space*, the beam potential generated from the singular charge density:

$$\rho^s = \sum_{i=1}^{N} q_i \delta[\mathbf{x} - \mathbf{x}_i(t)]$$

is

$$\phi(\mathbf{x}) = \frac{q}{4\pi\epsilon_0}\sum_{i=1}^{N}\frac{1}{|\mathbf{x} - \mathbf{x}_i|}$$

Thus, the force of a particle at $\mathbf{x} = \mathbf{x}_i$'s:

$$\mathbf{F}_i = -q\left.\frac{\partial\phi}{\partial\mathbf{x}}\right|_i = \frac{q^2}{4\pi\epsilon_0}\sum_{j=1}^{N}\frac{(\mathbf{x}_i - \mathbf{x}_j)}{|\mathbf{x}_i - \mathbf{x}_j|^{3/2}}$$

Which diverges due to the $i = j$ term. This divergence is essentially "erased" when the continuous charge density is applied:

$$\rho^s = \sum_{i=1}^{N} q_i \delta[\mathbf{x} - \mathbf{x}_i(t)] \quad \longrightarrow \quad \rho(\mathbf{x}, t)$$

- Effectively removes effect of collisions
- See: J.J. Barnard, Intro Lectures for more details
  - Find collisionless Vlasov model of evolution is often adequate ///

The particle equations of motion in $\mathbf{x}_i - \mathbf{v}_i$ phase-space variables become:

Transverse

$$\frac{d}{dt}\mathbf{x}_{\perp i} = \mathbf{v}_{\perp i}$$

$$\frac{d}{dt}(m\gamma_i \mathbf{v}_{\perp i}) \simeq \underbrace{q\mathbf{E}^a_{\perp i} + q\beta_b c\hat{\mathbf{z}} \times \mathbf{B}^a_{\perp i} + qB^a_{zi}\mathbf{v}_{\perp i} \times \hat{\mathbf{z}}}_{\text{Applied}} \underbrace{- q\frac{1}{\gamma_b^2}\frac{\partial \phi}{\mathbf{x}_\perp}\Big|_i}_{\text{Self}}$$

Longitudinal

$$\frac{d}{dt}z_i = v_{zi}$$

$$\frac{d}{dt}(m\gamma_i v_{zi}) \simeq \underbrace{qE^a_{zi} - q(v_{xi}B^a_{yi} - v_{yi}B^a_{xi})}_{\text{Applied}} \underbrace{- q\frac{\partial \phi}{\partial z}\Big|_i}_{\text{Self}}$$

In the remainder of this (and most other) lectures, we analyze Transverse Dynamics. Longitudinal Dynamics will be covered in J.J. Barnard lectures

- Except near injector, acceleration is typically slow
  - Fractional change in γ_b, β_b small over characteristic transverse dynamical scales such as lattice period and betatron oscillation periods
- Regard γ_b, β_b as specified functions given by the "acceleration schedule"

S1E: Equations of Motion in *s* and the Paraxial Approximation

In transverse accelerator dynamics, it is convenient to employ the axial coordinate (s) of the particle in the accelerator as the independent variable:

$$\boxed{s \equiv s_i + \int_{t_i}^{t} d\tilde{t}\; v_{zi}(\tilde{t})}$$

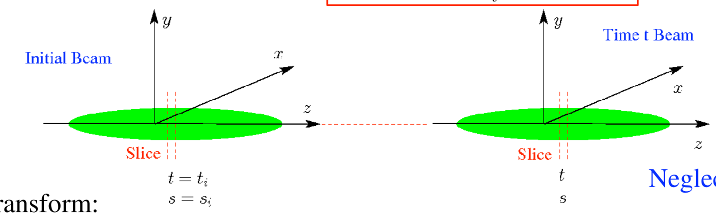

Transform:

$$v_{zi} = \frac{ds}{dt} \quad \Longrightarrow \quad v_{xi} = \frac{dx_i}{dt} = \frac{ds}{dt}\frac{dx_i}{ds} = v_{zi}\frac{dx_i}{ds} = (\beta_b c + \delta v_{zi})\frac{dx_i}{ds}$$

Neglect: Paraxial 0

$$\simeq \beta_b c \frac{dx_i}{ds}$$

Denote:

$$\boxed{{}' \equiv \frac{d}{ds} \qquad \begin{aligned} v_{xi} &= \frac{dx_i}{dt} \simeq \beta_b c x_i' \\ v_{yi} &= \frac{dy_i}{dt} \simeq \beta_b c y_i' \end{aligned}}$$

In the paraxial approximation, x' and y' can be interpreted as the (small magnitude) angles that the particles make the with the z-axis:

$$\boxed{\begin{aligned} x - \text{angle} &= \frac{v_{xi}}{v_{zi}} \simeq \frac{v_{xi}}{\beta_b c} = x_i' \\ y - \text{angle} &= \frac{v_{yi}}{v_{zi}} \simeq \frac{v_{yi}}{\beta_b c} = y_i' \end{aligned}}$$

The angles will be *small* in the paraxial approximation:

$$v_{xi}^2,\; v_{yi}^2 \ll \beta_b^2 c^2 \quad \Longrightarrow \quad x_i'^2,\; y_i'^2 \ll 1$$

Since the spread of axial momentum/velocities is small in the paraxial approximation, a thin axial slice of the beam maps to a thin axial slice and s can also be thought of as the axial coordinate of the slice in the accelerator lattice

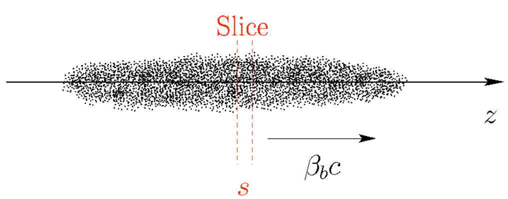

$$\beta_b \equiv \sum_{\substack{i=1 \\ \text{slice}}}^{N'} \frac{v_{zi}}{c}$$

$$\boxed{s \simeq s_i + \int_{t_i}^{t} d\tilde{t}\; \beta_b(\tilde{t})}$$

Transverse particle equations of motion:

$$\underbrace{\frac{d}{dt}(m\gamma_i \mathbf{v}_{\perp i})}_{\text{Term 1}} \simeq q\mathbf{E}^a_{\perp i} + q\beta_b c\hat{\mathbf{z}} \times \mathbf{B}^a_{\perp i} + \underbrace{qB^a_{zi}\mathbf{v}_{\perp i} \times \hat{\mathbf{z}}}_{\text{Term 2}} - q\frac{1}{\gamma_b^2}\frac{\partial \phi}{\mathbf{x}_\perp}\Big|_i$$

Transform Terms 1 and 2 in the particle equation of motion:

Term 1: $$\frac{d}{dt}\left(m\gamma_i \frac{d\mathbf{x}_{\perp i}}{dt}\right) = m v_{zi}\frac{d}{ds}\left(\gamma_i v_{zi}\frac{d}{ds}\mathbf{x}_{\perp i}\right)$$

$$= \underbrace{m\gamma_i v_{zi}^2 \frac{d^2}{ds^2}\mathbf{x}_{\perp i}}_{\text{Term 1A}} + \underbrace{m\left(\frac{d}{ds}\mathbf{x}_{\perp i}\right)\frac{d}{ds}(\gamma_i v_{zi})}_{\text{Term 1B}}$$

Approximate:

Term 1A: $$m\gamma_i v_{zi}^2 \frac{d^2}{ds^2}\mathbf{x}_{\perp i} \simeq m\gamma_b \beta_b^2 c^2 \frac{d^2}{ds^2}\mathbf{x}_{\perp i} = m\gamma_b\beta_b^2 c^2 \mathbf{x}''_{\perp i}$$

Term 1B: $$m\left(\frac{d}{ds}\mathbf{x}_{\perp i}\right) v_{zi}\frac{d}{ds}(\gamma_i v_{zi}) \simeq m\left(\frac{d}{ds}\mathbf{x}_{\perp i}\right)\beta_b c \frac{d}{ds}(\gamma_b\beta_b c)$$

$$\simeq m\beta_b c^2 (\gamma_b \beta_b)' \mathbf{x}'_{\perp i}$$

Using the approximations 1A and 1B gives for Term 1:

$$\boxed{m\frac{d}{dt}\left(\gamma_i \frac{d\mathbf{x}_{\perp i}}{dt}\right) \simeq m\gamma_b\beta_b^2c^2\left[\mathbf{x}''_{\perp i} + \frac{(\gamma_b\beta_b)'}{(\gamma_b\beta_b)}\mathbf{x}'_{\perp i}\right]}$$

Similarly we approximate in Term 2:

$$\boxed{qB^a_{zi}\mathbf{v}_{\perp i}\times\hat{\mathbf{z}} \simeq qB^a_{zi}\beta_b c\mathbf{x}'_{\perp i}\times\hat{\mathbf{z}}}$$

Using the reduced expressions for Terms 1 and 2 obtains the reduced transverse equation of motion:

$$\boxed{\begin{aligned}\mathbf{x}''_{\perp i} + \frac{(\gamma_b\beta_b)'}{(\gamma_b\beta_b)}\mathbf{x}'_{\perp i} &= \frac{q}{m\gamma_b\beta_b^2c^2}\mathbf{E}^a_{\perp i} + \frac{q}{m\gamma_b\beta_b c}\hat{\mathbf{z}}\times\mathbf{B}^a_{\perp i}\\ &+ \frac{qB^a_{zi}}{m\gamma_b\beta_b c}\mathbf{x}'_{\perp i}\times\hat{\mathbf{z}} - \frac{q}{\gamma_b^3\beta_b^2c^2}\left.\frac{\partial\phi}{\partial\mathbf{x}_\perp}\right|_i\end{aligned}}$$

- Will be analyzed extensively in lectures that follow in various limits to better understand structure of solutions

S1F: Summary: Transverse Particle Equations of Motion

$$\boxed{\begin{aligned}\mathbf{x}''_\perp + \frac{(\gamma_b\beta_b)'}{(\gamma_b\beta_b)}\mathbf{x}'_\perp &= \frac{q}{m\gamma_b\beta_b^2c^2}\mathbf{E}^a_\perp + \frac{q}{m\gamma_b\beta_b c}\hat{\mathbf{z}}\times\mathbf{B}^a_\perp + \frac{qB^a_z}{m\gamma_b\beta_b c}\mathbf{x}'_\perp\times\hat{\mathbf{z}}\\ &- \frac{q}{\gamma_b^3\beta_b^2c^2}\frac{\partial}{\partial\mathbf{x}_\perp}\phi\\ \mathbf{E}^a &= \text{Applied Electric Field} \qquad {}' \equiv \frac{d}{ds} \qquad \gamma_b \equiv \frac{1}{\sqrt{1-\beta_b^2}}\\ \mathbf{B}^a &= \text{Applied Magnetic Field}\\ \nabla^2\phi &= \frac{\partial}{\partial\mathbf{x}}\cdot\frac{\partial}{\partial\mathbf{x}}\phi = -\frac{\rho}{\epsilon_0}\\ &+ \text{Boundary Conditions on } \phi\end{aligned}}$$

- Drop particle i subscripts (in most cases) henceforth to simplify notation
- Neglects axial energy spread, bending, and electromagnetic radiation
- γ_b factors different in applied and self-field terms:

  In $-\frac{q}{m\gamma_b^3\beta_b^2c^2}\frac{\partial}{\partial\mathbf{x}}\phi$, contibutions to γ_b^3:

  $\gamma_b \Longrightarrow$ Kinematics

  $\gamma_b^2 \Longrightarrow$ Self-Magnetic Field Corrections (leading order)

S1G: Overview: Analysis to Come

Much of accelerator physics centers on understanding the evolution of beam particles in 4-dimensional x-x' and y-y' phase space.

Typically, restricted 2-dimensional phase-space projections in x-x' and/or y-y' are analyzed to simplify interpretations:

- When forces are linear particles tend to move on ellipses of constant area
  - Ellipse may elongate/shrink and rotate as beam evolves in lattice
- Nonlinear force components distort orbits and cause undesirable effects
  - Growth of effective phase-space area

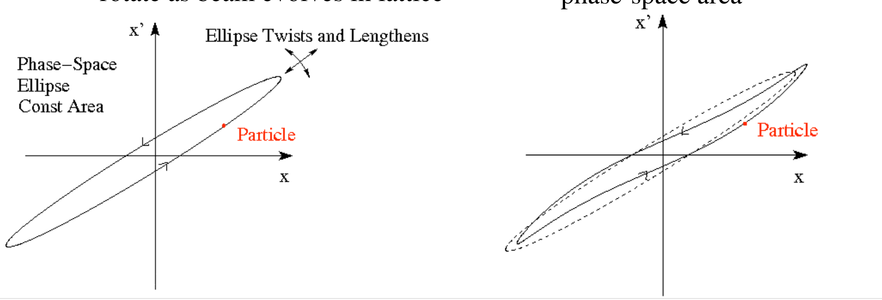

The "effective" phase-space volume of a distribution of beam particles is of fundamental interest

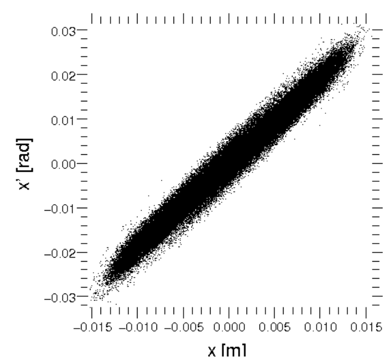

Effective area measure in x-x' phase-space is the x-emittance ε_x

Statistical "Area" $\sim \pi\varepsilon_x$

$$\varepsilon_x = 4[\langle x^2\rangle_\perp\langle x'^2\rangle_\perp - \langle xx'\rangle_\perp^2]^{1/2}$$

We will find in statistical beam descriptions that:

Larger/Smaller beam phase-space areas (Larger/Smaller emittances) $\Longrightarrow$ Harder/Easier to focus beam on small final spots

Much of advanced accelerator physics centers on understanding and controling emittance growth due to nonlinear forces arising from both space-charge and the applied focusing. In the remainder of the next few lectures we will review the physics of transverse particle dynamics of particles moving in linear applied fields. Later we will generalize concepts to include forces from space-charge and

S1H: Bent Coordinate System and Particle Equations of Motion with Dipole Bends and Axial Momentum Spread

The previous equations of motion can be applied to dipole bends provided the *x,y,z* coordinate system is fixed. In practice, it can prove more convenient to employ coordinates that follow the beam in a bend.

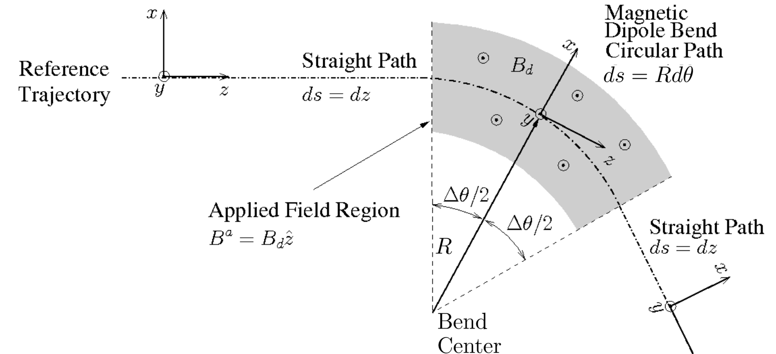

$R =$ Bend Radius
$s =$ Reference Trajectory Coordinate

In this perspective, dipoles are adjusted given the design momentum of the reference particle to bend the orbit through a radius *R*.

- Bends usually only in one plane (say *x*)
  - Implemented by a dipole applied field: E^a_x or B^a_y
- Easy to apply material analogously for *y*-plane bends, if necessary

Denote:

$$\boxed{p_0 = m\gamma_b\beta_b c = \text{design momentum}}$$

Then a magnetic *x*-bend through a radius *R* is specified by:

$$\boxed{\begin{aligned}&\mathbf{B}^a = B^a_y\hat{\mathbf{y}} = \text{const in bend}\\ &\frac{1}{R} = \frac{qB^a_y}{p_0}\end{aligned}}$$

Analogous formula for Electric Bend will be derived in problem set

The particle rigidity is defined as ($[B\rho]$ read as one symbol called "B-Rho"):

$$\boxed{[B\rho] \equiv \frac{p_0}{q} = \frac{m\gamma_b\beta_b c}{q}}$$

is often applied to express the bend result as:

$$\boxed{\frac{1}{R} = \frac{B^a_y}{[B\rho]}}$$

Comments on bends:

- *R* can be positive or negative depending on sign of $B^a_y/[B\rho]$
- For straight sections, $R \rightarrow \infty$ (or equivalently, $B^a_y = 0$)
- Lattices often made from discrete element dipoles and straight sections with separated function optics
  - Bends sometimes provide "edge focus" in a ring
  - Sometimes elements for bending/focusing are combined
- For a ring, dipoles strengths are tuned with particle rigidity/momentum so the reference orbit makes a closed path lap through the circular machine
  - Dipoles adjusted as particles gain energy to maintain closed path
  - In a Synchrotron dipoles and focusing elements are adjusted together to maintain focusing and bending properties with energy gain. This is the origin of the name "Synchrotron."
- Total bending strength of a ring in Tesla-meters limits the ultimately achievable particle energy/momentum in the ring

/// Example: Typical separated function lattice in a Synchrotron

Focus Elements in Red

Bending Elements in Green

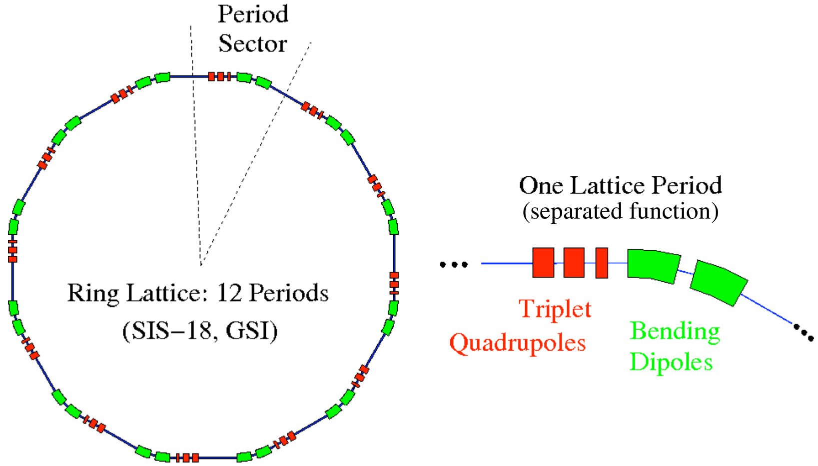

For "off-momentum" errors:

$$\boxed{\begin{aligned} p_s &= p_0 + \delta p \\ p_0 &= m\gamma_b\beta_b c = \text{design momentum} \\ \delta p &= \text{off- momentum} \end{aligned}}$$

This will modify the particle equations of motion, particularly in cases where there are bends since particles with different momenta will be bent at different radii

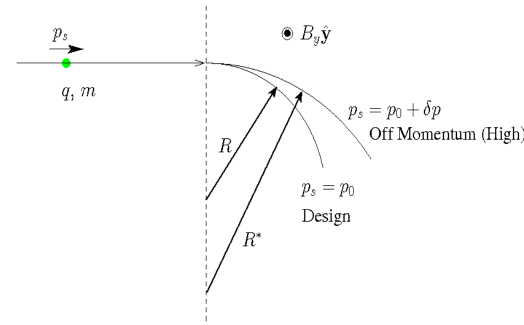

- Not usual to have acceleration in bends
  - Dipole bends and quadrupole focusing are sometimes combined

Transverse particle equations of motion including "off-momentum" effects:

- See texts such as Edwards and Syphers for guidance on derivation steps
- Full derivation is beyond needs/scope of this class

$$x'' + \frac{(\gamma_b\beta_b)'}{(\gamma_b\beta_b)}x' + \left[\frac{1}{R^2(s)}\frac{1-\delta}{1+\delta}\right]x = \frac{\delta}{1+\delta}\frac{1}{R(s)} + \frac{q}{m\gamma_b\beta_b^2c^2}\frac{E_x^a}{(1+\delta)^2}$$
$$- \frac{q}{m\gamma_b\beta_b c}\frac{B_y^a}{1+\delta} + \frac{q}{m\gamma_b\beta_b c}\frac{B_s^a}{1+\delta}y' - \frac{q}{m\gamma_b^3\beta_b^2c^2}\frac{1}{1+\delta}\frac{\partial\phi}{\partial x}$$
$$y'' + \frac{(\gamma_b\beta_b)'}{(\gamma_b\beta_b)}y' = \frac{q}{m\gamma_b\beta_b^2c^2}\frac{E_y^a}{(1+\delta)^2} + \frac{q}{m\gamma_b\beta_b c}\frac{B_x^a}{1+\delta}$$
$$- \frac{q}{m\gamma_b\beta_b c}\frac{B_s^a}{1+\delta}x' - \frac{q}{m\gamma_b^3\beta_b^2c^2}\frac{1}{1+\delta}\frac{\partial\phi}{\partial y}$$

$p_0 = m\gamma_b\beta_b c =$ Design Momentum

$\delta \equiv \frac{\delta p}{p_0} =$ Fractional Momentum Error

$$\frac{1}{R(s)} = \frac{B_y^a(s)|_{\text{Dipole}}}{[B\rho]} \qquad [B\rho] = \frac{p_0}{q}$$

Comments:

- Design bends only in x and $B_y^a,\ E_x^a$ contain *no* dipole terms (design orbit)
  - Dipole components set via the design bend radius $R(s)$
- Equations contain only low-order terms in momentum spread δ

Comments continued:

- Equations are often applied linearized in δ
- Achromatic focusing lattices are often designed using equations with momentum spread to obtain focal points independent of δ to some order
- x and y equations differ significantly due to bends modifying the x-equation when $R(s)$ is finite
- It will be shown in the problems that for electric bends:

$$\frac{1}{R(s)} = \frac{E_x^a(s)}{\beta_b c[B\rho]}$$

- Applied fields for focusing: $\mathbf{E}_\perp^a,\ \mathbf{B}_\perp^a,\ B_s^a$ must be expressed in the bent x,y,s system of the reference orbit
  - Includes error fields in dipoles
- Self fields may also need to be solved taking into account bend terms
  - Often can be neglected in Poisson's Equation

∇^2 Operator Modified

(add equation in future versions)

S2: Transverse Particle Equations of Motion in Linear Focusing Channels

S2A: Introduction

$$x'' + \frac{(\gamma_b\beta_b)'}{(\gamma_b\beta_b)}x' = \frac{q}{m\gamma_b\beta_b^2c^2}E_x^a - \frac{q}{m\gamma_b\beta_b c}B_y^a + \frac{q}{m\gamma_b\beta_b c}B_z^a y' - \frac{q}{m\gamma_b^3\beta_b^2c^2}\frac{\partial\phi}{\partial x}$$

$$y'' + \frac{(\gamma_b\beta_b)'}{(\gamma_b\beta_b)}y' = \frac{q}{m\gamma_b\beta_b^2c^2}E_y^a + \frac{q}{m\gamma_b\beta_b c}B_x^a - \frac{q}{m\gamma_b\beta_b c}B_z^a x' - \frac{q}{m\gamma_b^3\beta_b^2c^2}\frac{\partial\phi}{\partial y}$$

Equations previously derived under assumptions:
- No bends (fixed *x*-*y*-*z* coordinate system with no local bends)
- Paraxial equations ($x'^2, y'^2 \ll 1$)
- No dispersive effects (β_b same all particles), acceleration allowed ($\beta_b \neq \text{const}$)
- Electrostatic and leading-order (in β_b) self-magnetic interactions

The applied focusing fields

$$\begin{array}{ll} \text{Electric:} & E_x^a,\ E_y^a\ E_z^a \\ \text{Magnetic:} & B_x^a,\ B_y^a\ B_z^a \end{array}$$

must be specified as a function of s and the transverse particle coordinates x and y to complete the description
- Consistent change in axial velocity ($\beta_b c$) due to E_z^a must be evaluated
  - Typically due to RF cavities and/or induction cells
- Restrict analysis to fields from applied focusing structures

Intense beam accelerators and transport lattices are designed to optimize *linear* applied focusing forces with terms:

$$\begin{array}{lll} \text{Electric:} & E_x^a \simeq (\text{function of } s) \times (x \text{ or } y) \\ & E_y^a \simeq (\text{function of } s) \times (x \text{ or } y) \\ \text{Magnetic:} & B_x^a \simeq (\text{function of } s) \times (x \text{ or } y) \\ & B_y^a \simeq (\text{function of } s) \times (x \text{ or } y) \\ & B_z^a \simeq (\text{function of } s) \end{array}$$

Common situations that realize these linear applied focusing forms will be overviewed:
- Continuous Focusing (see: S2B)
- Quadrupole Focusing
  - Electric (see: S2C)
  - Magnetic (see: S2D)
- Solenoidal Focusing (see: S2E)

Other situations that will not be covered (typically more nonlinear optics):
- Enzil Lens (see: J.J. Barnard, Intro Lectures)
- Plasma Lens
- Wire guiding

S2B: Continuous Focusing

Assume constant electric field applied focusing force:

$$\mathbf{B}^a = 0$$
$$\mathbf{E}_\perp^a = E_x^a\hat{\mathbf{x}} + E_y^a\hat{\mathbf{y}} = -\frac{m\gamma_b\beta_b^2c^2k_{\beta0}^2}{q}\mathbf{x}_\perp \qquad k_{\beta0}^2 \equiv \text{const} > 0$$
$$E_z^a = 0 \qquad [k_{\beta0}^2] = \frac{\text{rad}}{\text{m}^2}$$

Continuous focusing equations of motion:
- Insert field components into linear applied field equations and collect terms

$$\mathbf{x}_\perp'' + \frac{(\gamma_b\beta_b)'}{(\gamma_b\beta_b)}\mathbf{x}_\perp' + k_{\beta0}^2\mathbf{x}_\perp = -\frac{q}{m\gamma_b^3\beta_b^2c^2}\frac{\partial}{\partial\mathbf{x}_\perp}\phi$$

Even this simple model can become complicated
- Space charge: ϕ must be calculated consistent with beam evolution
- Acceleration: acts to damp orbits (see: S10)

Simple model in limit of no acceleration ($\gamma_b\beta_b \simeq \text{const}$) and negligible space-charge ($\phi \simeq \text{const}$):

$$\boxed{\mathbf{x}''_\perp + k^2_{\beta 0}\mathbf{x}_\perp = 0} \quad \Longrightarrow \text{orbits simple harmonic oscillatons}$$

General solution is elementary:

$$\boxed{\begin{aligned} \mathbf{x}_\perp &= \mathbf{x}_\perp(s_i)\cos[k_{\beta 0}(s-s_i)] + [\mathbf{x}'_\perp(s_i)/k_{\beta 0}]\sin[k_{\beta 0}(s-s_i)] \\ \mathbf{x}'_\perp &= -k_{\beta 0}\mathbf{x}_\perp(s_i)\sin[k_{\beta 0}(s-s_i)] + \mathbf{x}'_\perp(s_i)\cos[k_{\beta 0}(s-s_i)] \\ \\ \mathbf{x}_\perp(s_i) &= \text{Initial coordinate} \\ \mathbf{x}'_\perp(s_i) &= \text{Initial angle} \end{aligned}}$$

/// Example: Particle Orbits in Continuous Focusing

Particle phase-space in x-x' with only applied field

$$k_{\beta 0} = 2\pi \text{ rad/m} \qquad x(0) = 1 \text{ mm}$$
$$\phi \simeq 0 \quad \gamma_b\beta_b = \text{const} \qquad x'(0) = 0$$

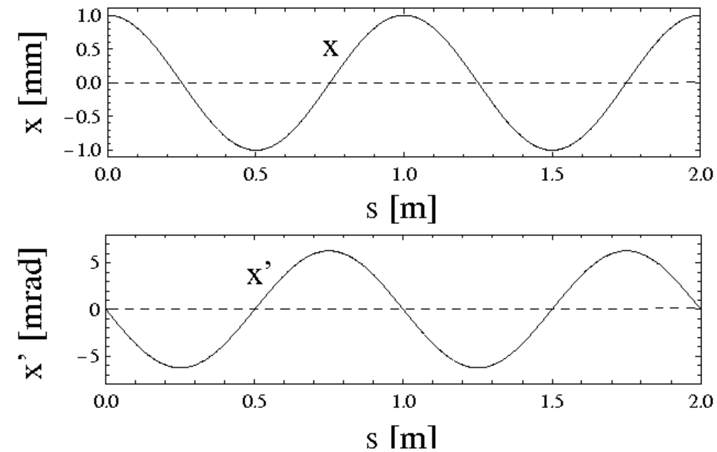

- Orbits in the applied field are just simple harmonic oscillators ///

Problem with continuous focusing model:

The continuous focusing model is realized by a stationary ($m \to \infty$) partially neutralizing uniform background of charges filling the beam pipe. To see this apply Maxwell's equations to the applied field to calculate an applied charge density:

$$\boxed{\rho^a = \epsilon_0 \frac{\partial}{\partial \mathbf{x}} \cdot \mathbf{E}^a = -\frac{2m\epsilon_0\gamma_b\beta_b^2 c^2 k^2_{\beta 0}}{q} = \text{const}}$$

- Unphysical model, but commonly employed since it represents the average action of more physical focusing fields in a simpler to analyze model
  - Demonstrate later in simple examples and problems given
- Continuous focusing can provide reasonably good estimates for more realistic periodic focusing models if $k^2_{\beta 0}$ is appropriately identified in terms of "equivalent" parameters *and* the periodic system is stable.
  - See lectures that follow and homework problems for examples

In more realistic models, one requires that *quasi-static* focusing fields in the machine aperture satisfy the vacuum Maxwell equations

$$\boxed{\begin{aligned} \nabla \cdot \mathbf{E}^a &= 0 & \qquad \nabla \cdot \mathbf{B}^a &= 0 \\ \nabla \times \mathbf{E}^a &= 0 & \qquad \nabla \times \mathbf{B}^a &= 0 \end{aligned}}$$

- Require in the region of the beam
- Applied field sources outside of the beam region

The vacuum Maxwell equations constrain the 3D form of applied fields resulting from spatially localized lenses. The following cases can be exploited to optimize linear focusing strength in physically realizable systems while keeping the model relatively simple:

1) Alternating Gradient Quadrupoles with transverse orientation
   - Electric Quadrupoles (see: S2C)
   - Magnetic Quadrupoles (see: S2D)

2) Solenoidal Magnetic Fields with longitudinal orientation (see: S2E)

S2C: Alternating Gradient Quadrupole Focusing
Electric Quadrupoles

In the axial center of a long electric quadrupole, model the fields as 2D transverse

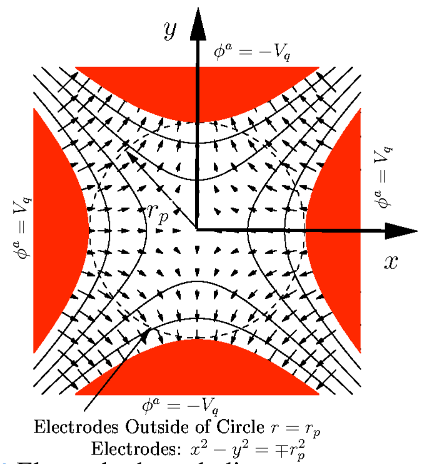

- Electrodes hyperbolic
- Structure infinitely extruded along z

2D Transverse Fields

$$\mathbf{B}^a = 0$$

$$E_x^a = -Gx$$
$$E_y^a = Gy$$
$$E_z^a = 0$$

$$G \equiv \frac{2V_q}{r_p^2} = -\frac{\partial E_x^a}{\partial x} = \frac{\partial E_y^a}{\partial y}$$
$$= \text{Electric Gradient}$$

V_q = Pole Voltage

r_p = Pipe Radius (clear aperture)

Quadrupoles actually have finite axial length in z. Model this by taking the gradient G to vary in s, i.e., $G = G(s)$ with $s = z - z_{\text{center}}$ (straight section)

- Variation is called the fringe-field of the focusing element
- Variation will violate the Maxwell Equations in 3D
  - Provides a reasonable first approximation in many applications
- Usually quadrupole is long, and $G(s)$ will have a flat central region and rapid variation near the ends

$s = z - z_{\text{center}}$

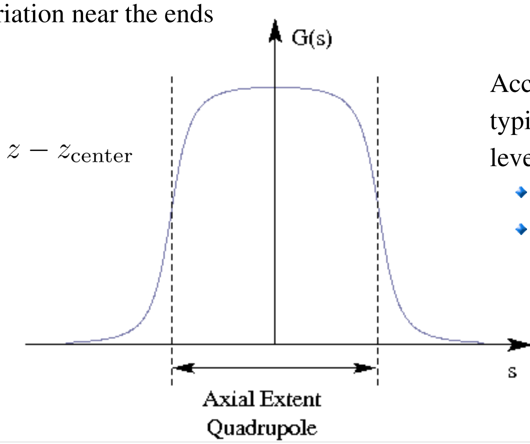

Accurate fringe calculation typically requires higher level modeling:
- 3D analysis
- Detailed geometry

For many applications the actual quadrupole fringe function $G(s)$ is replaced by a simpler function to allow more idealized modeling

- Replacements should be made in an "equivalent" parameter sense to be detailed later (see: lectures on Transverse Centroid and Envelope Modeling)
- Fringe functions sometimes replaced by piecewise constant $G(s)$
  - Often called "hard-edge" approximation
- See S3 and Lund and Bukh, PRSTAB 7 924801 (2004), Appendix C for more details on equivalent models

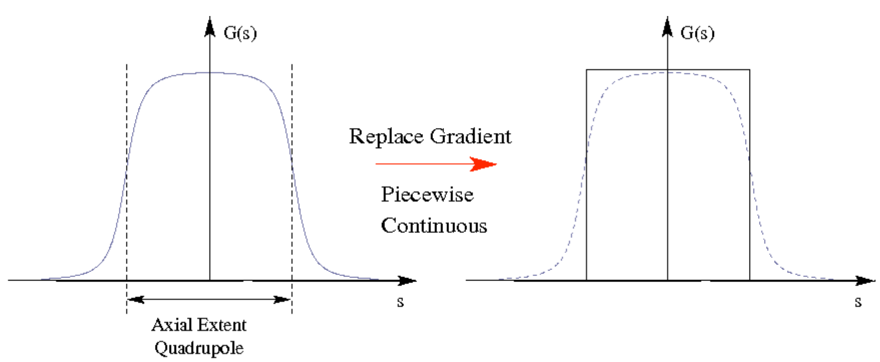

Electric quadrupole equations of motion:

- Insert applied field components into linear applied field equations and collect terms

$$\boxed{\begin{aligned} x'' + \frac{(\gamma_b\beta_b)'}{(\gamma_b\beta_b)}x' + \kappa(s)x &= -\frac{q}{m\gamma_b^3\beta_b^2c^2}\frac{\partial\phi}{\partial x} \\ y'' + \frac{(\gamma_b\beta_b)'}{(\gamma_b\beta_b)}y' - \kappa(s)y &= -\frac{q}{m\gamma_b^3\beta_b^2c^2}\frac{\partial\phi}{\partial y} \\ \kappa(s) = \frac{qG}{m\gamma_b\beta_b^2c^2} &= \frac{G}{\beta_b c[B\rho]} \\ G = -\frac{\partial E_x^a}{\partial y} = \frac{\partial E_y^a}{\partial x} = \frac{2V_q}{r_p^2} \qquad & [B\rho] = \frac{m\gamma_b\beta_b c}{q} \end{aligned}}$$

- For positive/negative κ the applied forces are Focusing/deFocusing in the x- and y-planes
- The x- and y-equations are decoupled

Quadrupoles must be arranged in a lattice where the particles traverse a sequence of optics with alternating gradient to focus strongly in all directions

- Alternating gradient necessary to provide focusing in both *x*- and *y*-planes
- Alternating Gradient Focusing often abbreviated "AG" and is sometimes called "Strong Focusing"
- Parameters should be tuned with particle properties and oscillation phases for proper operation
  - F (Focus) in plane placed where excursions (on average) are small
  - D (deFocus) placed where excursions (on average) are large
  - O (drift) allows axial separation between elements

Example Quadrupole FODO periodic lattices with piecewise constant κ

- FODO: [Focus drift(O) DeFocus Drift(O)] has equal length drifts and same length F and D quadrupoles

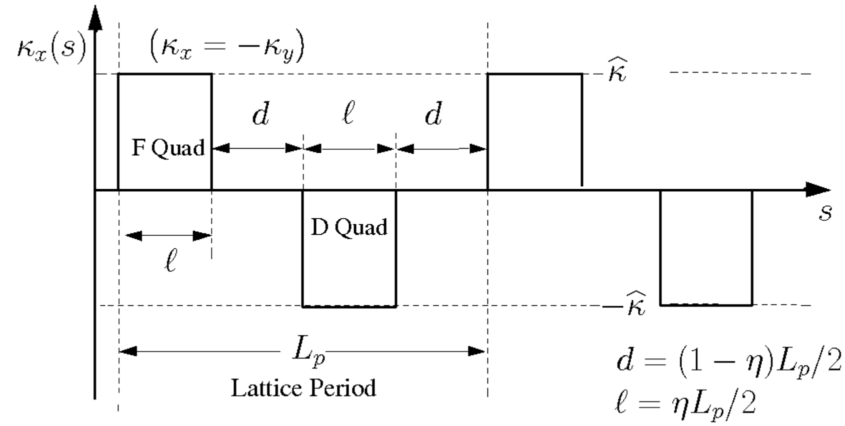

$$\eta = \text{Occupancy} \in (0, 1]$$

/// Example: Particle Orbits in a FODO Periodic Quadrupole Focusing Lattice:

Particle phase-space in *x*-*x'* with only hard-edge applied field

$L_p = 0.5$ m $\quad \kappa = \pm 50$ in Quads $\quad x(0) = 1$ mm

$\eta = 0.5 \quad \phi \simeq 0 \quad \gamma_b\beta_b = \text{const} \quad x'(0) = 0$

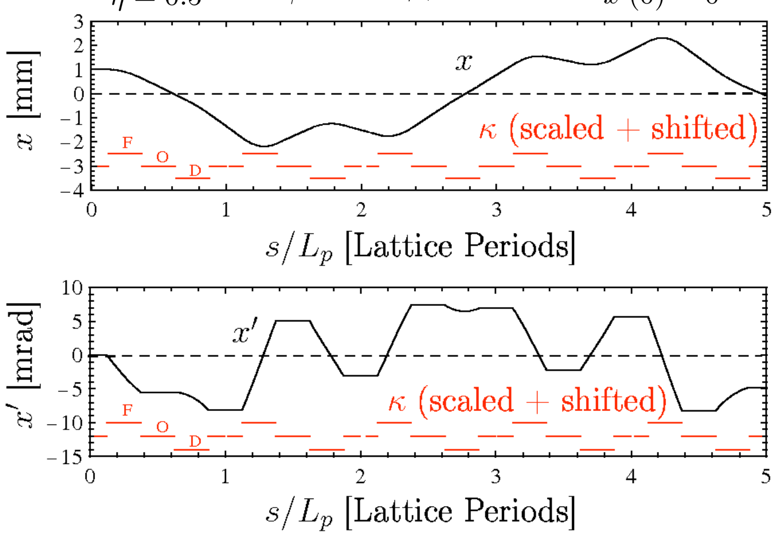

///

Comments on Orbits:

- Orbits strongly deviate from simple harmonic form due to AG focusing
  - Multiple harmonics present
- Orbit tends to be farther from axis in focusing quadrupoles and closer to axis in defocusing quadrupoles to provide net focusing
- Will find later that if the focusing is sufficiently strong that the orbit can become unstable (see: S5)
- *y*-orbit has the same properties as *x*-orbit due to the periodic structure and AG focusing
- If quadrupoles are rotated about their z-axis of symmetry, then the *x*- and *y*-equations become cross-coupled. This is called quadrupole skew coupling (see: Appendix A)

Some properties of particle orbits in quadruoples with $\kappa = \text{const}$ will be analyzed in the problem sets

S2D: Alternating Gradient Quadrupole Focusing
Magnetic Quadrupoles

In the axial center of a long magnetic quadrupole, model fields as 2D transverse

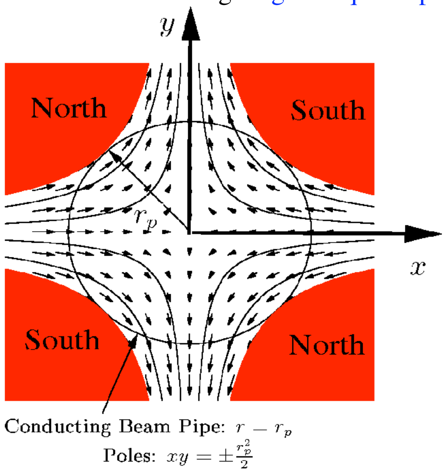

2D Transverse Fields

$$\mathbf{E}^a = 0$$

$$B_x^a = Gy$$
$$B_y^a = Gx$$
$$B_z^a = 0$$

$$G \equiv \frac{B_q}{r_p} = \frac{\partial B_x^a}{\partial y} = \frac{\partial B_y^a}{\partial x}$$
$$= \text{Magnetic Gradient}$$

$$B_q = |\mathbf{B}^a|_{r=r_p} = \text{Pole Field}$$
$$r_p = \text{Pipe Radius}$$

- Magnetic (ideal iron) poles hyperbolic
- Structure infinitely extruded along z

Analogously to the electric quadrupole case, take $G = G(s)$

- Same comments made on electric quadrupole fringe in S2C are directly applicable to magnetic quadrupoles

Magnetic quadrupole equations of motion:

- Insert field components into linear applied field equations and collect terms

$$x'' + \frac{(\gamma_b\beta_b)'}{(\gamma_b\beta_b)}x' + \kappa(s)x = -\frac{q}{m\gamma_b^3\beta_b^2c^2}\frac{\partial\phi}{\partial x}$$
$$y'' + \frac{(\gamma_b\beta_b)'}{(\gamma_b\beta_b)}y' - \kappa(s)y = -\frac{q}{m\gamma_b^3\beta_b^2c^2}\frac{\partial\phi}{\partial y}$$
$$\kappa(s) = \frac{qG}{m\gamma_b\beta_b c} = \frac{G}{[B\rho]}$$
$$G = \frac{\partial B_x^a}{\partial y} = \frac{\partial B_y^a}{\partial x} = \frac{B_q}{r_p} \qquad [B\rho] = \frac{m\gamma_b\beta_b c}{q}$$

- Equations identical to the electric quadrupole case in terms of $\kappa(s)$
- All comments made on electric quadrupole focusing lattice are immediately applicable to magnetic quadruples: just apply different κ definition in design

S2E: Solenoidal Focusing

The field of an ideal magnetic solenoid is invariant under transverse rotations about it's axis of symmetry (z) can be expanded in terms of the on-axis field as as:

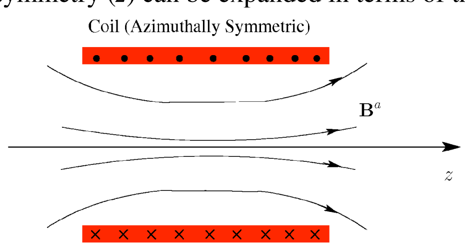

$$\mathbf{E}^a = 0$$
$$\mathbf{B}_\perp^a = \frac{1}{2}\sum_{\nu=1}^{\infty}\frac{(-1)^\nu}{\nu!(\nu-1)!}\frac{\partial^{2\nu-1}B_{z0}(z)}{\partial z^{2\nu-1}}\left(\frac{|\mathbf{x}_\perp|}{2}\right)^{2\nu-2}\mathbf{x}_\perp$$
$$B_z^a = B_{z0}(z) + \sum_{\nu=1}^{\infty}\frac{(-1)^\nu}{(\nu!)^2}\frac{\partial^{2\nu}B_{z0}(z)}{\partial z^{2\nu}}\left(\frac{|\mathbf{x}_\perp|}{2}\right)^{2\nu}$$
$$B_{z0}(z) \equiv B_z(\mathbf{x}_\perp = 0, z) = \text{On-Axis Field}$$

See Reiser, *Theory and Design of Charged Particle Beams*, Sec. 3.3.1

For modeling, we truncate the expansion using only leading-order terms to obtain:

- Corresponds to linear dynamics in the equations of motion

$$B_x = -\frac{1}{2}\frac{\partial B_{z0}(z)}{\partial z}x$$
$$B_y = -\frac{1}{2}\frac{\partial B_{z0}(z)}{\partial z}y \qquad B_{z0}(z) \equiv B_z(\mathbf{x}_\perp = 0, z)$$
$$B_z = B_{z0}(z) \qquad = \text{On-Axis Field}$$

Note that this truncated expansion is divergence free:

$$\nabla\cdot\mathbf{B}^a = -\frac{1}{2}\frac{\partial B_{z0}}{\partial z}\frac{\partial}{\partial\mathbf{x}_\perp}\cdot\mathbf{x}_\perp + \frac{\partial}{\partial z}B_{z0} = 0$$

but not curl free within the vacuum aperture:

(add analysis in future versions)

Solenoid equations of motion:

- Insert field components into linear applied field equations and collect terms

$$x'' + \frac{(\gamma_b\beta_b)'}{(\gamma_b\beta_b)}x' - \frac{\omega_c'(s)}{2\gamma_b\beta_b c}y - \frac{\omega_c(s)}{\gamma_b\beta_b c}y' = -\frac{q}{m\gamma_b^3\beta_b^2c^2}\frac{\partial\phi}{\partial x}$$
$$y'' + \frac{(\gamma_b\beta_b)'}{(\gamma_b\beta_b)}y' + \frac{\omega_c'(s)}{2\gamma_b\beta_b c}x + \frac{\omega_c(s)}{\gamma_b\beta_b c}x' = -\frac{q}{m\gamma_b^3\beta_b^2c^2}\frac{\partial\phi}{\partial y}$$

$$\omega_c(s) = \frac{qB_{z0}(s)}{m} = \text{Cyclotron Frequency}$$
(in applied axial magnetic field)

- Equations are linearly cross-coupled in the applied field terms
  - x equation depends on y, y'
  - y equation depends on x, x'

It can be shown (see: Appendix B) that the linear cross-coupling in the applied field can be removed by an s-varying transformation to a rotating "Larmor" frame:

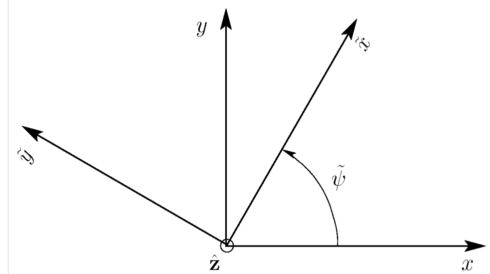

~ used to denote rotating frame variables

$$\tilde{x} = \quad x\cos\tilde{\psi}(s) + y\sin\tilde{s}$$
$$\tilde{y} = -x\sin\tilde{\psi}(s) + y\cos\tilde{s}$$
$$\tilde{\psi}(s) = \int_{s_i}^{s} d\bar{s}\, k_L(\bar{s})$$
$$k_L(s) \equiv \frac{\omega_c(s)}{2\gamma_b\beta_b c}$$
= Larmor wave number

$s = s_i$ defines initial condition

If the beam space-charge is *axisymmetric*:

$$\frac{\partial\phi}{\partial\mathbf{x}_\perp} = \frac{\partial\phi}{\partial r}\frac{\partial r}{\partial\mathbf{x}_\perp} = \frac{\partial\phi}{\partial r}\frac{\mathbf{x}_\perp}{r}$$

then the space-charge term also decouples under the Larmor transformation and the equations of motion can be expressed in fully uncoupled form:

$$\tilde{x}'' + \frac{(\gamma_b\beta_b)'}{(\gamma_b\beta_b)}\tilde{x}' + \kappa(s)\tilde{x} = -\frac{q}{m\gamma_b^3\beta_b^2c^2}\frac{\partial\phi}{\partial r}\frac{\tilde{x}}{r}$$
$$\tilde{y}'' + \frac{(\gamma_b\beta_b)'}{(\gamma_b\beta_b)}\tilde{y}' + \kappa(s)\tilde{y} = -\frac{q}{m\gamma_b^3\beta_b^2c^2}\frac{\partial\phi}{\partial r}\frac{\tilde{y}}{r}$$
$$\kappa(s) \equiv \left[\frac{\omega_c(s)}{2\gamma_b\beta_b c}\right]^2 = k_L^2(s)$$

Will demonstrate this in problems for the simple case of: $\omega_c(s) = \text{const}$

- Because Larmor frame equations are in the same form as continuous and quadrupole focusing with a different κ, for solenoidal focusing we implicitly work in the Larmor frame and simplify notation by dropping the tildes:

$$\tilde{\mathbf{x}}_\perp \rightarrow \mathbf{x}_\perp$$

/// Aside: Notation:

A common theme of this class will be to introduce new effects and generalizations while keeping formulations looking as similar as possible to the the most simple representations given. When doing so, we will often use "tildes" to denote transformed variables to stress that the new coordinates have, in fact, a more complicated form that must be interpreted in the context of the analysis being carried out. Some examples:

- Larmor frame transformations for Solenoidal focusing
  See: Appendix B
- Normalized variables for analysis of accelerating systems
  See: S10
- Coordinates expressed relative to the beam centroid
  See: S.M. Lund, lectures on Transverse Centroid and Envelope Model

///

Solenoid periodic lattices can be formed similarly to the quadrupole case

- Drifts placed between solenoids of finite axial length
  - Allows space for diagnostics, pumping, acceleration cells, etc.
- Analogous equivalence cases to quadrupole
  - Piecewise constant κ often used
- Fringe can be more important for solenoids

Simple hard-edge solenoid lattice with piecewise constant κ

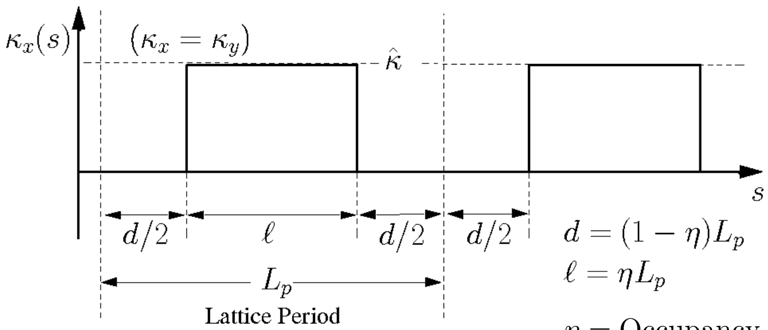

$$d = (1-\eta)L_p$$
$$\ell = \eta L_p$$
$$\eta = \text{Occupancy} \in (0, 1]$$

/// Example: Larmor Frame Particle Orbits in a Periodic Solenoidal Focusing Lattice: $\tilde{x} - \tilde{x}'$ phase-space for hard edge elements and applied fields

$L_p = 0.5$ m $\quad \kappa = 20$ in Solenoids $\quad \tilde{x}(0) = 1$ mm

$\eta = 0.5 \quad \phi \simeq 0 \quad \gamma_b\beta_b = \text{const} \quad \tilde{x}'(0) = 0$

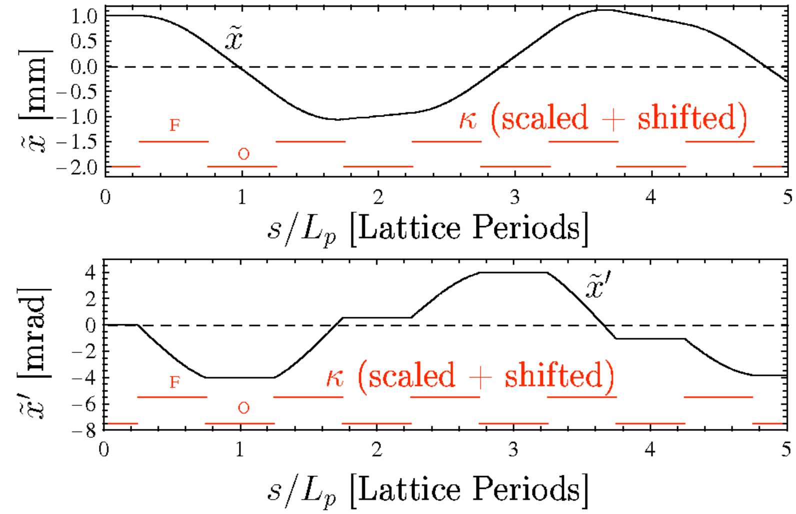

///

Comments on Orbits:

- Larmor-frame orbits strongly deviate from simple harmonic form due to periodic focusing
  - Multiple harmonics present
  - Less complicated that quadrupole AG focusing case when interpreted in the Larmor frame due to the optic being focusing in both planes
- Orbits can be transformed back into the Laboratory frame using Larmor transform (see: Appendix B)
  - Laboratory frame orbit exhibits more complicated x-y plane coupled oscillatory structure
- Will find later that if the focusing is sufficiently strong that the orbit can become unstable (see: S5)
- y-orbits have same properties as the x-orbits due to the equations being decoupled and identical in form in each plane

///

Some properties of particle orbits in solenoids with $\kappa = \text{const}$ will be analyzed in the problem sets

S2F: Summary of Transverse Particle Equations of Motion

In linear applied focusing channels, without momentum spread or radiation, the particle equations of motion in both the x- and y-planes expressed as:

$$\boxed{\begin{aligned} x'' + \frac{(\gamma_b\beta_b)'}{(\gamma_b\beta_b)}x' + \kappa_x(s)x &= -\frac{q}{m\gamma_b^3\beta_b^2c^2}\frac{\partial}{\partial x}\phi \\ y'' + \frac{(\gamma_b\beta_b)'}{(\gamma_b\beta_b)}y' + \kappa_y(s)y &= -\frac{q}{m\gamma_b^3\beta_b^2c^2}\frac{\partial}{\partial y}\phi \\ \kappa_x(s) &= x\text{-focusing function of lattice} \\ \kappa_y(s) &= y\text{-focusing function of lattice} \end{aligned}}$$

Common focusing functions:

Continuous:
$$\kappa_x(s) = \kappa_y(s) = k_{\beta 0}^2 = \text{const}$$

Quadrupole (Electric or Magnetic):
$$\kappa_x(s) = -\kappa_y(s) = \kappa(s)$$

Solenoidal (equations must be interpreted in Larmor Frame: see Appendix B):
$$\kappa_x(s) = \kappa_y(s) = \kappa(s)$$

It is instructive to review the structure of solutions of the transverse particle equations of motion in the absence of:

Space-charge: $\dfrac{\partial \phi}{\partial x} \sim \dfrac{\partial \phi}{\partial y} \sim 0$

Acceleration: $\gamma_b \beta_b \simeq \text{const} \qquad \Longrightarrow \dfrac{(\gamma_b \beta_b)'}{(\gamma_b \beta_b)} \simeq 0$

In this simple limit, the x and y-equations are of the same Hill's Equation form:

$$\boxed{\begin{aligned} x'' + \kappa_x(s) x &= 0 \\ y'' + \kappa_y(s) y &= 0 \end{aligned}}$$

- These equations are central to transverse dynamics in conventional accelerator physics (weak space-charge and acceleration)
    - Will study how solutions change with space-charge in later lectures

In many cases beam transport lattices are designed where the applied focusing functions are periodic:

$$\boxed{\begin{aligned} \kappa_x(s + L_p) &= \kappa_x(s) \\ \kappa_y(s + L_p) &= \kappa_y(s) \end{aligned} \qquad L_p = \text{Lattice Period}}$$

Common, simple examples of periodic lattices:

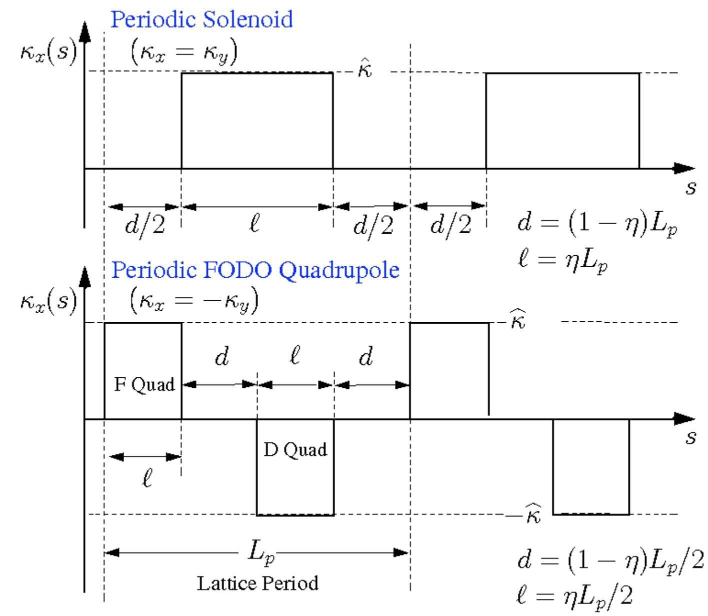

However, the focusing functions need not be periodic:
- Often take periodic or continuous in this class for simplicity of interpretation

Focusing functions can vary strongly in many common situations:
- Matching and transition sections
- Strong acceleration
- Significantly different elements can occur within periods of lattices in rings
    - "Panofsky" type wide aperture quadrupoles for beam insertion and extraction in a ring

Example of Non-Periodic Focusing Functions: Beam Matching Section

Maintains alternating-gradient structure but not quasi-periodic

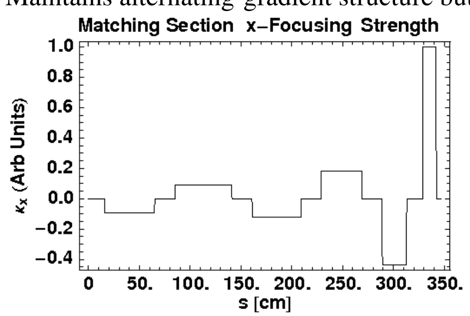

Example corresponds to High Current Experiment Matching Section (hard edge equivalent) at LBNL (2002)

Equations presented in this section apply to a single particle moving in a beam under the action of linear applied focusing forces. In the remaining sections, we will (mostly) neglect space-charge ($\phi \rightarrow 0$) as is conventional in the standard theory of low-intensity accelerators.
- What we learn from treatment will later aid analysis of space-charge effects
    - Appropriate variable substitutions will be made to apply results
- Important to understand basic applied field dynamics since space-charge complicates
    - Results in plasma-like collective response

/// Example: We will see in Transverse Centroid and Envelope Descriptions of Beam Evolution that the linear particle equations of motion can be applied to analyze the evolution of a beam when image charges are neglected

$$\begin{aligned} x &\rightarrow x_c \equiv \langle x \rangle_\perp \quad x - \text{centroid} \\ y &\rightarrow y_c \equiv \langle y \rangle_\perp \quad y - \text{centroid} \end{aligned}$$

///

Appendix A: Quadrupole Skew Coupling

Consider a quadrupole actively rotated through an angle ψ about the z-axis:

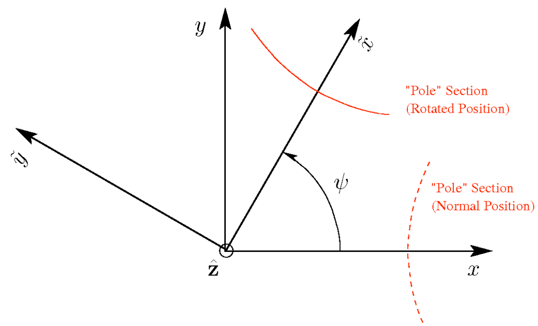

Transforms

$$\tilde{x} = \quad x\cos\psi + y\sin\psi$$
$$\tilde{y} = -x\sin\psi + y\cos\psi$$

$$x = \quad \tilde{x}\cos\psi - \tilde{y}\sin\psi$$
$$y = \quad \tilde{x}\sin\psi + \tilde{y}\cos\psi$$

Normal Orientation Fields

Electric

$$E_x^a = -Gx$$
$$E_y^a = \quad Gy$$

Magnetic

$$B_x^a = Gy$$
$$B_y^a = Gx$$

$$G = G(s)$$
$$= \text{Field Gradient (Electric or Magnetic)}$$

A1

Rotated Fields

Electric

$$E_x^a = E_{\tilde{x}}^a \cos\psi - E_{\tilde{y}}^a \sin\psi \qquad E_{\tilde{x}}^a = -G\tilde{x} = -G(\;x\cos\psi + y\sin\psi)$$
$$E_y^a = E_{\tilde{x}}^a \sin\psi + E_{\tilde{y}}^a \cos\psi \qquad E_{\tilde{y}}^a = \quad G\tilde{y} = \quad G(-x\sin\psi + y\cos\psi)$$

Combine equations, collect terms, and apply trigonometric identities to obtain:

$$\boxed{\begin{aligned} E_x^a &= -G\cos(2\psi)x - G\sin(2\psi)y \\ E_y^a &= -G\sin(2\psi)x + G\cos(2\psi)y \end{aligned}} \qquad \begin{aligned} 2\sin\psi\cos\psi &= \sin(2\psi) \\ \cos^2\psi - \sin^2\psi &= \cos(2\psi) \end{aligned}$$

Magnetic

$$B_x^a = B_{\tilde{x}}^a \cos\psi - B_{\tilde{y}}^a \sin\psi \qquad B_{\tilde{x}}^a = G\tilde{y} = G(-x\sin\psi + y\cos\psi)$$
$$B_y^a = B_{\tilde{x}}^a \sin\psi + B_{\tilde{y}}^a \cos\psi \qquad B_{\tilde{y}}^a = G\tilde{x} = G(\;x\cos\psi + y\sin\psi)$$

Combine equations, collect terms, and apply trigonometric identities to obtain:

$$\boxed{\begin{aligned} B_x^a &= -G\sin(2\psi)x + G\cos(2\psi)y \\ B_y^a &= \quad G\cos(2\psi)x + G\sin(2\psi)y \end{aligned}}$$

A2

For *both* electric and magnetic focusing quadrupoles, these field component projections can be inserted in the linear field Eqns of motion to obtain:

Skew Coupled Quadrupole Equations of Motion

$$x'' + \frac{(\gamma_b\beta_b)'}{(\gamma_b\beta_b)}x' + \kappa\cos(2\psi)x + \kappa\sin(2\psi)y = -\frac{q}{m\gamma_b^3\beta_b^2c^2}\frac{\partial\phi}{\partial x}$$
$$y'' + \frac{(\gamma_b\beta_b)'}{(\gamma_b\beta_b)}y' - \kappa\cos(2\psi)y + \kappa\sin(2\psi)x = -\frac{q}{m\gamma_b^3\beta_b^2c^2}\frac{\partial\phi}{\partial y}$$
$$\kappa = \begin{cases} \frac{G}{\beta_b c[B\rho]}, & \text{Electric Focusing} \\ \frac{G}{[B\rho]}, & \text{Magnetic Focusing} \end{cases}$$

System is skew coupled:

- x-equation depends on y, y' and y-equation on x, x' for $\psi \neq 0, \pi, 2\pi, \cdots$

Skew-coupling considerably complicates dynamics

- Unless otherwise specified, we consider only quadrupoles with "normal" orientation with $\psi = 0$
- Skew coupling errors or intentional skew couplings can be important
  - Leads to transfer of oscillations energy between x and y-planes
  - Invariants much more complicated to construct/interpret

A3

The skew coupled equations of motion can be alternatively derived by actively rotating the quadrupole equation of motion in the form:

$$x'' + \frac{(\gamma_b\beta_b)'}{(\gamma_b\beta_b)}x' + \kappa(s)x = -\frac{q}{m\gamma_b^3\beta_b^2c^2}\frac{\partial\phi}{\partial x}$$
$$y'' + \frac{(\gamma_b\beta_b)'}{(\gamma_b\beta_b)}y' - \kappa(s)y = -\frac{q}{m\gamma_b^3\beta_b^2c^2}\frac{\partial\phi}{\partial y}$$

- Steps are then identical whether quadrupoles are electric *or* magnetic

A4

Appendix B: The Larmor Transform to Express Solenoidal Focused Particle Equations of Motion in Uncoupled Form

Solenoid equations of motion:

$$x'' + \frac{(\gamma_b\beta_b)'}{(\gamma_b\beta_b)}x' - \frac{\omega_c'(s)}{2\gamma_b\beta_b c}y - \frac{\omega_c(s)}{\gamma_b\beta_b c}y' = -\frac{q}{m\gamma_b^3\beta_b^2c^2}\frac{\partial\phi}{\partial x}$$
$$y'' + \frac{(\gamma_b\beta_b)'}{(\gamma_b\beta_b)}y' + \frac{\omega_c'(s)}{2\gamma_b\beta_b c}x + \frac{\omega_c(s)}{\gamma_b\beta_b c}x' = -\frac{q}{m\gamma_b^3\beta_b^2c^2}\frac{\partial\phi}{\partial y}$$

$$\omega_c(s) = \frac{qB_{z0}(s)}{m} = \text{Cyclotron Frequency}$$
(in applied axial magnetic field)

To simplify algebra, introduce the complex coordinate

$$\underline{z} \equiv x + iy \qquad i \equiv \sqrt{-1}$$

Note* context clarifies use of i (particle index, initial cond, complex i)

Then the two equations can be expressed as a single complex equation

$$\underline{z}'' + \frac{(\gamma_b\beta_b)'}{(\gamma_b\beta_b)}\underline{z}' + i\frac{\omega_c'(s)}{2\gamma_b\beta_b c}\underline{z} + i\frac{\omega_c(s)}{\gamma_b\beta_b c}\underline{z}' = -\frac{q}{m\gamma_b^3\beta_b^2c^2}\left(\frac{\partial\phi}{\partial x} + i\frac{\partial\phi}{\partial y}\right)$$

B1

If the potential is also axisymmetric with $\phi = \phi(r)$:

$$\frac{\partial\phi}{\partial x} + i\frac{\partial\phi}{\partial y} = \frac{\partial\phi}{\partial r}\frac{\underline{z}}{r} \qquad r \equiv \sqrt{x^2+y^2}$$

then the complex form equation of motion reduces to:

$$\underline{z}'' + \frac{(\gamma_b\beta_b)'}{(\gamma_b\beta_b)}\underline{z}' + i\frac{\omega_c'(s)}{2\gamma_b\beta_b c}\underline{z} + i\frac{\omega_c(s)}{\gamma_b\beta_b c}\underline{z}' = -\frac{q}{m\gamma_b^3\beta_b^2c^2}\frac{\partial\phi}{\partial r}\frac{\underline{z}}{r}$$

Following Wiedemann, Vol II, pg 82, introduce a transformed complex variable that is a local (s-varying) rotation:

$$\tilde{\underline{z}} \equiv \underline{z}e^{-i\tilde{\psi}(s)} = \tilde{x} + i\tilde{y}$$

$\tilde{\psi}(s)$ = phase-function (real-valued)

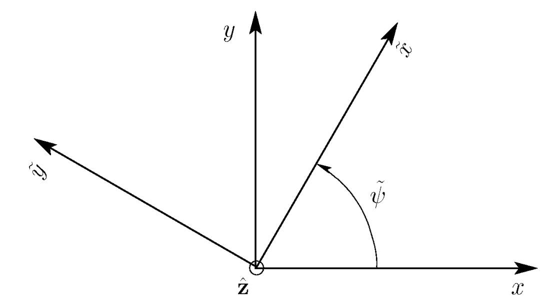

B2

Then: $\underline{z} = \tilde{\underline{z}}e^{i\tilde{\psi}}$

$$\underline{z}' = \left(\tilde{\underline{z}}' + i\tilde{\psi}'\tilde{\underline{z}}\right)e^{i\tilde{\psi}}$$
$$\underline{z}'' = \left(\tilde{\underline{z}}'' + 2i\tilde{\psi}'\tilde{\underline{z}}' + i\tilde{\psi}''\tilde{\underline{z}} - \tilde{\psi}'^2\tilde{\underline{z}}\right)e^{i\tilde{\psi}}$$

and the complex form equations of motion become:

$$\tilde{\underline{z}}'' + \left[i\left(2\tilde{\psi}' + \frac{\omega_c}{\gamma_b\beta_b c}\right) + \frac{(\gamma_b\beta_b)'}{(\gamma_b\beta_b)}\right]\tilde{\underline{z}}'$$
$$+ i\left[-\tilde{\psi}'^2 - \frac{\omega_c}{\gamma_b\beta_b c}\tilde{\psi}' + i\left(\tilde{\psi}'' + \frac{\omega_c'(s)}{2\gamma_b\beta_b c} + \frac{(\gamma_b\beta_b)'}{(\gamma_b\beta_b)}\tilde{\psi}'\right)\right]\tilde{\underline{z}}$$
$$= -\frac{q}{m\gamma_b^3\beta_b^2c^2}\frac{\partial\phi}{\partial r}\frac{\tilde{\underline{z}}}{r}$$

Free to choose the form of $\tilde{\psi}$ Can choose to eliminate imaginary terms in [....] by taking:

$$\tilde{\psi}' \equiv -\frac{\omega_c}{2\gamma_b\beta_b c} \qquad \Longrightarrow \qquad \tilde{\psi}'' = -\frac{\omega_c'}{2\gamma_b\beta_b c} + \frac{\omega_c}{2c}\frac{(\gamma_b\beta_b)'}{(\gamma_b\beta_b)^2}$$

B3

B4

Using these results, the complex form equations of motion reduce to:

$$\tilde{\underline{z}}'' + \frac{(\gamma_b\beta_b)'}{(\gamma_b\beta_b)}\tilde{\underline{z}}' + \left(\frac{\omega_c}{2\gamma_b\beta_b c}\right)^2\tilde{\underline{z}} = -\frac{q}{m\gamma_b^3\beta_b^2c^2}\frac{\partial\phi}{\partial r}\frac{\tilde{\underline{z}}}{r}$$

Or using $\tilde{\underline{z}} = \tilde{x} + i\tilde{y}$, the equations can be expressed in decoupled $\tilde{x},\ \tilde{y}$ variables in the Larmor Frame as:

$$\tilde{x} + \frac{(\gamma_b\beta_b)'}{(\gamma_b\beta_b)}\tilde{x}' + \kappa_s(s)\tilde{x} = -\frac{q}{m\gamma_b^3\beta_b^2c^2}\frac{\partial\phi}{\partial r}\frac{\tilde{x}}{r}$$
$$\tilde{y} + \frac{(\gamma_b\beta_b)'}{(\gamma_b\beta_b)}\tilde{y}' + \kappa_s(s)\tilde{y} = -\frac{q}{m\gamma_b^3\beta_b^2c^2}\frac{\partial\phi}{\partial r}\frac{\tilde{y}}{r}$$

$$\kappa_s(s) \equiv k_L^2(s) \qquad k_L(s) \equiv \frac{\omega_c(s)}{2\gamma_b\beta_b c} \qquad \omega_c(s) \equiv \frac{qB_{z0}(s)}{m}$$
$$= \text{Larmor Wave-Number}$$

Equations of motion are uncoupled but must be interpreted in the rotating Larmor frame

- Same form as quadrupoles but with focusing function same sign in each plane

The rotational transformation to the Larmor Frame can be effected by integrating the equation for $\tilde{\psi}' = -\frac{\omega_c}{2\gamma_b\beta_b}$

$$\boxed{\tilde{\psi}(s) = -\frac{1}{2\gamma_b\beta_b c}\int_{s_i}^{s} d\tilde{s}\, \omega_c(\tilde{s}) \quad = -\int_{s_i}^{s} d\tilde{s}\, k_L(\tilde{s})}$$

Here, s_i is some value of s where the initial conditions are taken.

- Take $s = s_i$ where axial field is zero for simplest interpretation (see: pg B6)

Because

$$\boxed{\tilde{\psi}' = -\frac{\omega_c}{2\gamma_b\beta_b}}$$

the local $\tilde{x} - \tilde{y}$ Larmor frame is rotating at ½ of the local s-varying cyclotron frequency

- If $B_{z0} = \text{const}$, then the Larmor frame is uniformly rotating as is well known from elementary textbooks (see problem sets)

B5

The complex form phase-space transformation and inverse transformations are:

$$\begin{aligned} &\underline{z} = \tilde{\underline{z}} e^{i\tilde{\psi}} && \tilde{\underline{z}} = \underline{z} e^{-i\tilde{\psi}} \\ &\underline{z}' = \left(\tilde{\underline{z}}' + i\tilde{\psi}'\tilde{\underline{z}}\right) e^{i\tilde{\psi}} && \tilde{\underline{z}}' = \left(\underline{z}' - i\tilde{\psi}'\underline{z}\right) e^{-i\tilde{\psi}} \end{aligned}$$

$$\underline{z} = x + iy \qquad \tilde{\underline{z}} = \tilde{x} + i\tilde{y} \qquad \tilde{\psi}' = -\frac{\omega_c}{2\gamma_b\beta_b c} = -k_L$$
$$\underline{z}' = x' + iy' \qquad \tilde{\underline{z}}' = \tilde{x}' + i\tilde{y}'$$

Apply to:

- Project initial conditions from lab-frame when integrating equations
- Project integrated solution back to lab-frame to interpret solution

If the initial condition $s = s_i$ is taken outside of the magnetic field where $B_{z0}(s_i) = 0$, then:

$$\begin{aligned} &\tilde{x}(s = s_i) = x(s = s_i) && \tilde{x}'(s = s_i) = x'(s = s_i) \\ &\tilde{y}(s = s_i) = y(s = s_i) && \tilde{y}'(s = s_i) = y'(s = s_i) \\ &\tilde{\underline{z}}(s = s_i) = \underline{z}(s = s_i) && \tilde{\underline{z}}'(s = s_i) = \underline{z}'(s = s_i) \end{aligned}$$

B6

The solution in the laboratory frame can be expressed in component form using the real and imaginary parts of the complex form transformations to obtain:

$$\boxed{\begin{pmatrix} x \\ x' \\ y \\ y' \end{pmatrix} = \begin{pmatrix} \cos\tilde{\psi} & 0 & -\sin\tilde{\psi} & 0 \\ k_L \sin\tilde{\psi} & \cos\tilde{\psi} & k_L\cos\tilde{\psi} & -\sin\tilde{\psi} \\ \sin\tilde{\psi} & 0 & \cos\tilde{\psi} & 0 \\ -k_L\cos\tilde{\psi} & \sin\tilde{\psi} & k_L\sin\tilde{\psi} & \cos\tilde{\psi} \end{pmatrix} \begin{pmatrix} \tilde{x} \\ \tilde{x}' \\ \tilde{y} \\ \tilde{y}' \end{pmatrix}}$$

Here we used the transforms and

$$\tilde{\psi}' = -\frac{\omega_c}{2\gamma_b\beta_b} = -k_L \qquad \begin{aligned} \tilde{\underline{z}} &= \tilde{x} + i\tilde{y} \\ \tilde{\underline{z}}' &= \tilde{x}' + i\tilde{y}' \end{aligned}$$

B7

S3: Description of Applied Focusing Fields

S3A: Overview

Applied fields for focusing, bending, and acceleration enter the equations of motion via:

$$\mathbf{E}^a = \text{Applied Electric Field}$$
$$\mathbf{B}^a = \text{Applied Magnetic Field}$$

Generally, these fields are produced by sources (often static or slowly varying in time) located outside an aperture or so-called pipe radius $r = r_p$. For example, the electric and magnetic quadrupoles of S2:

Electric Quadrupole

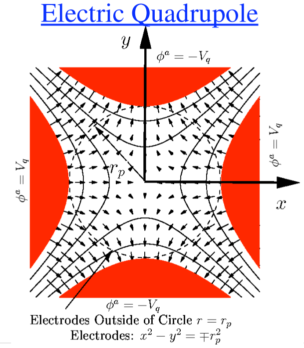

Hyperbolic material surfaces outside pipe radius $r = r_p$

Magnetic Quadrupole

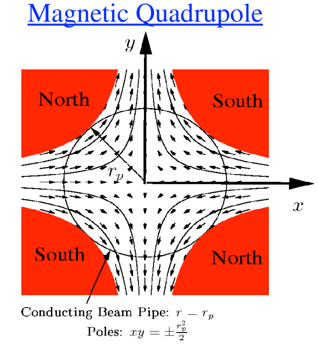

The fields of such classes of magnets obey the vacuum Maxwell Equations within the aperture:

$$\boxed{\begin{aligned} \nabla \cdot \mathbf{E}^a &= 0 & \nabla \cdot \mathbf{B}^a &= 0 \\ \nabla \times \mathbf{E}^a &= -\frac{\partial}{\partial t}\mathbf{B}^a & \nabla \times \mathbf{B}^a &= \frac{1}{c^2}\frac{\partial}{\partial t}\mathbf{E}^a \end{aligned}}$$

If the fields are static or sufficiently slowly varying (quasistatic) where the time derivative terms can be neglected, then the fields in the aperture will obey the static vacuum Maxwell equations:

$$\boxed{\begin{aligned} \nabla \cdot \mathbf{E}^a &= 0 & \nabla \cdot \mathbf{B}^a &= 0 \\ \nabla \times \mathbf{E}^a &= 0 & \nabla \times \mathbf{B}^a &= 0 \end{aligned}}$$

In general, optical elements are tuned to limit the strength of nonlinear field terms so the beam experiences primarily linear applied fields.
- Linear fields allow better preservation of beam quality

Removal of *all* nonlinear fields cannot be accomplished
- 3D structure of the Maxwell equations precludes for finite geometry optics
- Even in finite geometries deviations from optimal structures and symmetry will result in nonlinear fields

As an example of this, when an ideal 2D iron magnet with infinite hyperbolic poles is truncated radially for finite 2D geometr, this leads to nonlinear focusing fields even in 2D:
- Truncation necessary along with confinement of return flux in yoke

Cross-Sections of Iron Quadrupole Magnets

Ideal (infinite geometry)

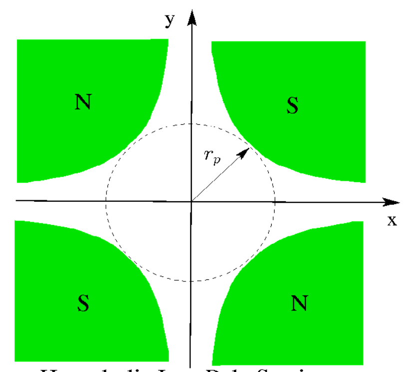

Hyperbolic Iron Pole Sections (infinite)

Practical (finite geometry)

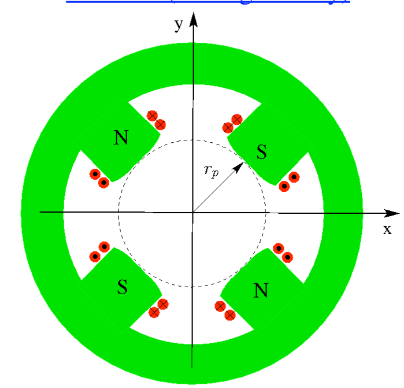

Shaped Iron Pole Sections (finite)

The design of optimized electric and magnetic optics for accelerators is a specialized topic with a vast literature. It is not be possible to cover this topic in this brief survey. In the remaining part of this section we will overview a limited subset of material on magnetic optics including:
- (see: S3B) Magnetic field expansions for focusing and bending
- (see: S3C) Hard edge equivalent models
- (see: S3D) 2D multipole models and nonlinear field scalings
- (see: S3E) Good field radius

Much of the material presented can be immediately applied to static Electric Optics since the vacuum Maxwell equations are the same for static Electric $\mathbf{E}^a$ and Magnetic $\mathbf{B}^a$ fields in vacuum.

S3B: Magnetic Field Expansions for Focusing and Bending

Transverse magnetic forces enter the transverse equations of motion (see: S1, S2) via:

Force: $\mathbf{F}^a_\perp \simeq q\beta_b c\hat{\mathbf{z}} \times \mathbf{B}^a_\perp$

Field: $\mathbf{B}^a_\perp = \hat{\mathbf{x}}B^a_x + \hat{\mathbf{y}}B^a_y$

Combined these give:

$$\boxed{\begin{aligned} F^a_x &\simeq -q\beta_b c B^a_y \\ F^a_y &\simeq \quad q\beta_b c B^a_x \end{aligned}}$$

Field components entering these expressions can be expanded about $\mathbf{x}_\perp = 0$
- Element center and design orbit taken to be $\mathbf{x}_\perp = 0$

$$B^a_x = \overset{1}{B^a_x(0)} + \overset{2}{\frac{\partial B^a_x}{\partial y}(0)y} + \overset{3}{\frac{\partial B^a_x}{\partial x}(0)x} \qquad \text{Nonlinear Focus}$$
$$+ \frac{1}{2}\frac{\partial^2 B^a_x}{\partial x^2}(0)x^2 + \frac{\partial^2 B^a_x}{\partial x \partial y}(0)xy + \frac{1}{2}\frac{\partial B^a_x}{\partial y^2}(0)y^2 + \cdots$$
$$B^a_y = \overset{1}{B^a_y(0)} + \overset{2}{\frac{\partial B^a_y}{\partial x}(0)x} + \overset{3}{\frac{\partial B^a_y}{\partial y}(0)y} \qquad \text{Nonlinear Focus}$$
$$+ \frac{1}{2}\frac{\partial^2 B^a_y}{\partial x^2}(0)x^2 + \frac{\partial^2 B^a_y}{\partial x \partial y}(0)xy + \frac{1}{2}\frac{\partial B^a_y}{\partial y^2}(0)y^2 + \cdots$$

Terms:
1: Dipole Bend
2: Normal Quad Focus
3: Skew Quad Focus

Sources of undesired nonlinear applied field components include:

- Intrinsic finite 3D geometry and the structure of the Maxwell equations
- Systematic errors or sub-optimal geometry associated with practical trade-offs in fabricating the optic
- Random construction errors in individual optical elements
- Alignment errors of magnets in the lattice giving field projections in unwanted directions
- Excitation errors effecting the field strength
  - Currents in coils not correct and/or unbalanced

More advanced treatments exploit less simple power-series expansions to express symmetries more clearly:

- Maxwell equations constrain structure of solutions
- Forms appropriate for bent coordinate systems in dipole bends can become complicated

S3C: Hard Edge Equivalent Models

Real 3D magnets can often be modeled with sufficient accuracy by 2D hard-edge "equivalent" magnets that give the same approximate focusing impulse to the particle as the full 3D magnet

- Objective is to provide same approximate applied focusing "kick" to particles with different gradient focusing gradient functions $G(s)$

See Figure Next Slide

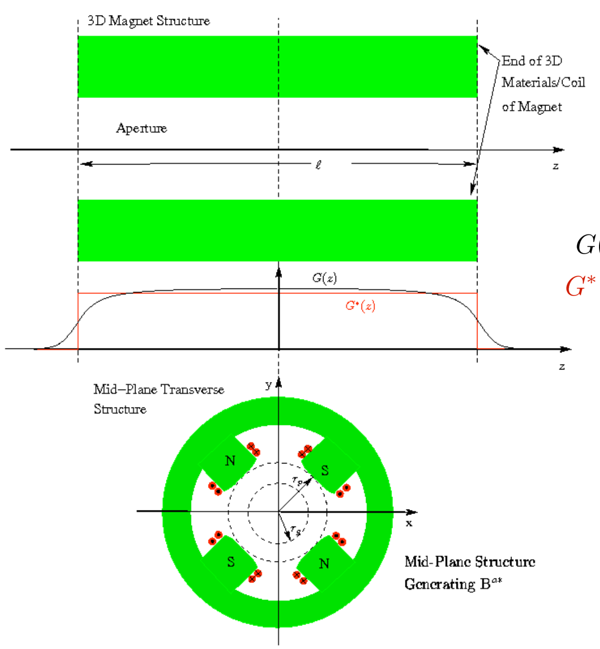

$G(z)$ = 3D Field Gradient

$G^*(z)$ = Hard-Edge Equivalent Field Gradient

Many prescriptions exist for calculating the effective axial length and strength of hard-edge equivalent models

- See Review: Lund and Bukh, PRSTAB 7 204801 (2004), Appendix C

Here we overview a simple equivalence method that has been shown to work

For a relatively long, but finite axial length magnet with 3D gradient function:

$$G(z) \equiv \left.\frac{\partial B_x^a}{\partial y}\right|_{x=y=0}$$

Take hard-edge equivalent parameters:

- Assume $z = 0$ at the axial magnet mid-plane

Gradient: $$G^* \equiv G(z=0)$$

Axial Length: $$\ell \equiv \frac{1}{G(z=0)} \int_{-\infty}^{\infty} dz\, G(z)$$

- More advanced equivalences can be made based more on particle optics
  - Disadvantage of such methods is "equivalence" changes with particle energy and must be revisited as optics are tuned

S3D: 2D Transverse Multipole Magnetic Fields

In many cases, it is sufficient to characterize the field errors in 2D hard-edge equivalent as:

$$\boxed{\begin{aligned} B_x(x,y) &= \frac{1}{\ell}\int_{-\infty}^{\infty} dz\; B_x^a(x,y,z) \\ B_y(x,y) &= \frac{1}{\ell}\int_{-\infty}^{\infty} dz\; B_y^a(x,y,z) \end{aligned}}$$

2D Effective Fields 3D Fields

Operating on the vacuum Maxwell equations with: $\int_{-\infty}^{\infty}\frac{dz}{\ell}\cdots$

yields the (exact) 2D Transverse Maxwell equations :

$$\boxed{\begin{aligned} \frac{\partial B_x(x,y)}{\partial x} &= -\frac{\partial B_y(x,y)}{\partial y} \\ \frac{\partial B_x(x,y)}{\partial y} &= \frac{\partial B_y(x,y)}{\partial x} \end{aligned}}$$

These equations are recognized as the Cauchy-Riemann conditions for a complex field variable:

$$\boxed{\underline{B} = B_y + iB_x \qquad i \equiv \sqrt{-1}}$$

to be an analytical function of the complex variable:

$$\boxed{\underline{z} = x + iy \qquad i \equiv \sqrt{-1}}$$

Notation: Underlines denote complex variables

- Note that the x and y components are exchanged from the "usual" complex ordering in the field variable $\underline{B}$. This is not a typo.
- The coordinate $\underline{z}$ has the usual ordering

It follows that $\underline{B}(\underline{z})$ can be analyzed using the full power of the highly developed theory of analytical functions of a complex variable.

Expand $\underline{B}(\underline{z})$ as a Laurent Series within the vacuum aperture as:

$$\underline{B}(\underline{z}) = B_y + iB_x = \sum_{n=1}^{\infty} \underline{B}_n \left(\frac{\underline{z}}{r_p}\right)^{n-1}$$

$\underline{B}_n = \text{const (complex)}$

$n = \text{Multipole Index}$ $\quad r_p = \text{Aperture "Pipe" Radius}$

The $\underline{B}_n$ are called "multipole coefficients" and give the structure of the field. The multipole coefficients can be resolved into real and imaginary parts as:

$$\boxed{\begin{aligned} &\underline{B}_n = b_n + ia_n \\ &\qquad a_n \Longrightarrow \text{"Normal" Multipoles} \\ &\qquad b_n \Longrightarrow \text{"Skew" Multipoles} \end{aligned}}$$

Some algebra identifies the polynomial symmetries of the terms as:

Index n	Name	Normal Field Components $B_x r_p^{n-1}/b_n$	$B_y r_p^{n-1}/b_n$	Skew Field Components $B_x r_p^{n-1}/a_n$	$B_y r_p^{n-1}/b_n$
$n=1$	Dipole	0	1	1	0
$n=2$	Quadrupole	y	x	x	$-y$
$n=3$	Sextupole	$2xy$	x^2-y^2	x^2-y^2	$-2xy$
$n=4$	Octupole	$3x^2y-y^3$	x^3-3xy^2	x^3-3xy^2	$-3x^2y+y^3$
$\vdots$	$\vdots$	$\vdots$	$\vdots$	$\vdots$	$\vdots$

Comments:

- Reason for pole names most apparent from polar representation (see following pages) and sketches of the magnetic pole structure
- Caution: In Europe, poles are often labeled with index n -1

Magnetic Pole Symmetries (normal orientation):

Dipole (n=1) Quadrupole (n=2) Sextupole (n=3)

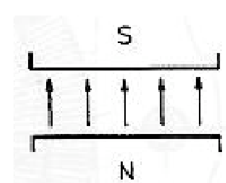

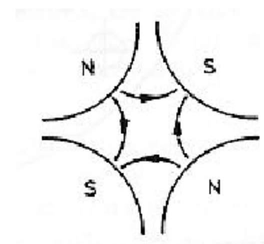

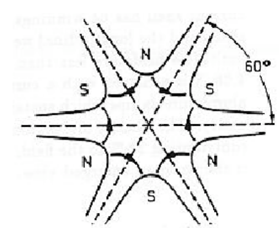

- Actively rotate structures clockwise through an angle of $\pi/(2n)$ for skew component symmetries

Higher order multipole coefficients (larger *n* values) leading to nonlinear focusing forces decrease rapidly within the aperture. To see this use a polar representation for $\underline{z}$, $\underline{B}_n$

$$\boxed{\begin{aligned} \underline{z} = x + iy = re^{i\theta} \qquad & r = \sqrt{x^2+y^2} \\ & \theta = \arctan[y, x] \\ \underline{B}_n = |\underline{B}_n| e^{i\psi_n} \qquad & \psi_n = \text{Real Const} \end{aligned}}$$

Thus, the nth order multipole terms scale as

$$\boxed{\underline{B}_n \left(\frac{\underline{z}}{r_p}\right)^{n-1} = |\underline{B}_n| \left(\frac{r}{r_p}\right)^{n-1} e^{i[(n-1)\theta + \psi_n]}}$$

- Unless the coefficient $|\underline{B}_n|$ is very large, high order terms in *n* will become small rapidly as r_p decreases
- Better field quality can be obtained for a given magnet design by simply making the clear bore r_p larger, or alternatively using smaller bundles (more tight focus) of particles
  - Larger bore machines/magnets cost more. So designs become trade-off between cost and performance.
  - Stronger focusing can also be unstable (see: S5)

S3E: Good Field Radius

Often a magnet design will have a so-called "good-field" radius $r = r_g$ that the maximum field errors are specified on.

- In superior designs the good field radius can be around ~70% or more of the clear bore aperture to the beginning of material structures of the magnet.
- Beam particles should evolve with radial excursions with $r < r_g$

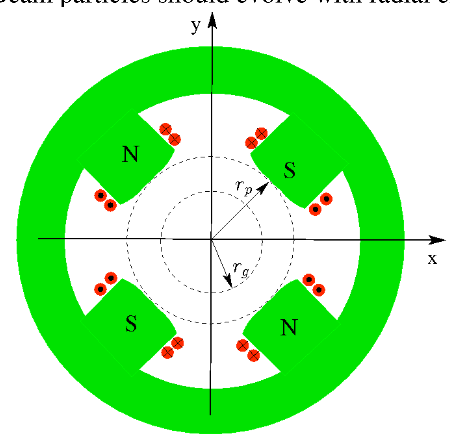

r_p = Clear Bore Radius
$\sim$ Pole Radius Typical

r_g = Good Field Radius
$\sim 70\%\ r_p$ Typical

Comments:

- Particle orbits are designed to remain within radius r_g
- Field error statements are readily generalized to 3D since:

$$\begin{aligned} \nabla \cdot \mathbf{B}^a = 0 \\ \nabla \times \mathbf{B}^a = 0 \end{aligned} \quad \Longrightarrow \quad \nabla^2 \mathbf{B}^a = 0$$

and therefore each component of $\mathbf{B}^a$ satisfies a Laplace equation within the vacuum aperture. Therefore, field errors decrease when moving within a source-free region.

S3F: Example Permanent Magnet Assemblies

A few examples of practical permanent magnet assemblies with field contours are provided to illustrate error field structures in practical devices

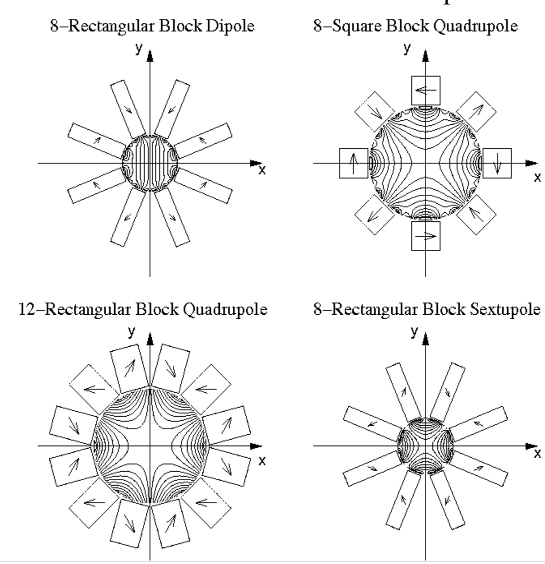

For more info on permanent magnet design see: Lund and Halbach, Fusion Engineering Design, **32-33**, 401-415 (1996)

S4: Transverse Particle Equations of Motion with Nonlinear Applied Fields — S4A: Overview

In S1 we showed that the particle equations of motion can be expressed as:

$$\mathbf{x}''_\perp + \frac{(\gamma_b\beta_b)'}{(\gamma_b\beta_b)}\mathbf{x}'_\perp = \frac{q}{m\gamma_b\beta_b^2c^2}\mathbf{E}^a_\perp + \frac{q}{m\gamma_b\beta_b c}\hat{\mathbf{z}}\times\mathbf{B}^a_\perp + \frac{qB^a_z}{m\gamma_b\beta_b c}\mathbf{x}'_\perp\times\hat{\mathbf{z}} - \frac{q}{\gamma_b^3\beta_b^2c^2}\frac{\partial}{\partial\mathbf{x}_\perp}\phi$$

When momentum spread is neglected and results are interpreted in a Cartesian coordinate system (no bends). In S2, we showed that these equations can be further reduced when the applied focusing fields are linear to:

$$x'' + \frac{(\gamma_b\beta_b)'}{(\gamma_b\beta_b)}x' + \kappa_x(s)x = -\frac{q}{m\gamma_b^3\beta_b^2c^2}\frac{\partial}{\partial x}\phi$$
$$y'' + \frac{(\gamma_b\beta_b)'}{(\gamma_b\beta_b)}y' + \kappa_y(s)y = -\frac{q}{m\gamma_b^3\beta_b^2c^2}\frac{\partial}{\partial y}\phi$$

where

$\kappa_x(s) = x\text{-focusing function of lattice}$

$\kappa_y(s) = y\text{-focusing function of lattice}$

describe the linear applied focusing forces and the equations are implicitly analyzed in the rotating Larmor frame when $B^a_z \neq 0$.

Lattice designs attempt to minimize nonlinear applied fields. However, the 3D Maxwell equations show that there will *always* be some finite nonlinear applied fields for an applied focusing element with finite extent. Applied field nonlinearities also result from:

- Design idealizations
- Fabrication and material errors

The largest source of nonlinear terms will depend on the case analyzed.

Nonlinear applied fields must be added back in the idealized model when it is appropriate to analyze their effects

- Common problem to address when carrying out large-scale numerical simulations to design/analyze systems

There are two basic approaches to carry this out:

Approach 1: Explicit 3D Formulation

Approach 2: Perturbations About Linear Applied Field Model

S4B: Approach 1: Explicit 3D Formulation

This is the simplest. Just employ the full 3D equations of motion expressed in terms of the applied field components $\mathbf{E}^a,\ \mathbf{B}^a$ and avoid using the focusing functions $\kappa_x,\ \kappa_y$

Comments:

- Most easy to apply in computer simulations where many effects are simultaneously included
  - Simplifies comparison to experiments when many details matter for high level agreement
- Simplifies simultaneous inclusion of transverse and longitudinal effects
  - Accelerating field E^a_z can be included to calculate changes in $\beta_b,\ \gamma_b$
  - Transverse and longitudinal dynamics cannot be fully decoupled in high level modeling – especially try when acceleration is strong in systems like injectors
- Can be applied with time based equations of motion (see: S1)
  - Helps avoid unit confusion and continuously adjusting complicated equations of motion to identify the axial coordinate *s* appropriately

S4C: Approach 2: Perturbations About Linear Applied Field Model

Exploit the linearity of the Maxwell equations to take:

$$\mathbf{E}^a_\perp = \mathbf{E}^a_\perp|_L + \delta\mathbf{E}^a_\perp$$
$$\mathbf{B}^a = \mathbf{B}^a|_L + \delta\mathbf{B}^a$$

where

$\mathbf{E}^a_\perp|_L,\ \mathbf{B}^a|_L$ are the linear field components incorporated in $\kappa_x,\ \kappa_y$

to express the equations of motion as:

$$x'' + \frac{(\gamma_b\beta_b)'}{(\gamma_b\beta_b)}x' + \kappa_x x = \frac{q}{m\gamma_b\beta_b^2c^2}\delta E^a_x - \frac{q}{m\gamma_b\beta_b c}\delta B^a_y + \frac{q}{m\gamma_b\beta_b c}\delta B^a_z y' - \frac{q}{m\gamma_b^3\beta_b^2c^2}\frac{\partial\phi}{\partial x}$$

$$y'' + \frac{(\gamma_b\beta_b)'}{(\gamma_b\beta_b)}y' + \kappa_y y = \frac{q}{m\gamma_b\beta_b^2c^2}\delta E^a_y + \frac{q}{m\gamma_b\beta_b c}\delta B^a_x - \frac{q}{m\gamma_b\beta_b c}\delta B^a_z x' - \frac{q}{m\gamma_b^3\beta_b^2c^2}\frac{\partial\phi}{\partial y}$$

This formulation can be most useful to understand the effect of deviations from the usual linear model where intuition is developed

Comments:

- Best suited to non-solenoidal focusing
  - Simplified Larmor frame analysis for solenoidal focusing is only valid for axisymmetric potentials $\phi = \phi(r)$ which may not hold in the presence of non-ideal perturbations.
  - Applied field perturbations $\delta \mathbf{E}^a_\perp, \ \delta \mathbf{B}^a$ would also need to be projected into the Larmor frame
- Applied field perturbations $\delta \mathbf{E}^a_\perp, \ \delta \mathbf{B}^a$ will not necessarily satisfy the 3D Maxwell Equations by themselves
  - Follows because the linear field components $\mathbf{E}^a_\perp|_L, \ \mathbf{B}^a|_L$ will not, in general, satisfy the 3D Maxwell equations by themselves

S5: Linear Transverse Particle Equations of Motion without Space-Charge, Acceleration, and Momentum Spread

S5A: Hill's Equation

Neglect:

- Space-charge effects: $\partial \phi / \partial \mathbf{x} \simeq 0$
- Nonlinear applied focusing and bends: $\mathbf{E}^a, \ \mathbf{B}^a$ have only linear focus terms
- Acceleration: $\gamma_b \beta_b \simeq \text{const}$
- Momentum spread effects: $v_{zi} \simeq \beta_b c$

Then the transverse particle equations of motion reduce to Hill's Equation:

$$\boxed{x''(s) + \kappa(s) x(s) = 0}$$

$$\begin{aligned} x &= \perp \text{ particle coordinate} \\ &\quad \text{(i.e., } x \text{ or } y \text{ or possibly combinations of coordinates)} \\ s &= \text{Axial coordinate of reference particle} \\ {}' &= \frac{d}{ds} \\ \kappa(s) &= \text{Lattice focusing function (linear fields)} \end{aligned}$$

For a periodic lattice:

$$\boxed{\begin{aligned} \kappa(s + L_p) &= \kappa(s) \\ L_p &= \text{Lattice Period} \end{aligned}}$$

/// Example: Hard-Edge Periodic Focusing Function

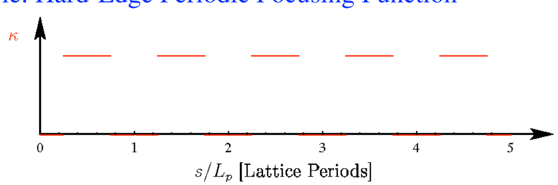

///

For a ring (i.e., circular accelerator), one also has the "superperiod" condition:

$$\boxed{\begin{aligned} \kappa(s + \mathcal{C}) &= \kappa(s) \\ \mathcal{C} = \mathcal{N} L_p &= \text{Ring Circumfrance} \\ \mathcal{N} &= \text{Superperiod Number} \end{aligned}}$$

- Distinction matters when there are (field) construction errors in the ring
  - Repeat with superperiod but not lattice period
  - See lectures on: Particle Resonances

/// Example: Period and Superperiod distinctions for errors in a ring

* Magnet with systematic defect will be felt every lattice period

X Magnet with random (fabrication) defect felt once per lap

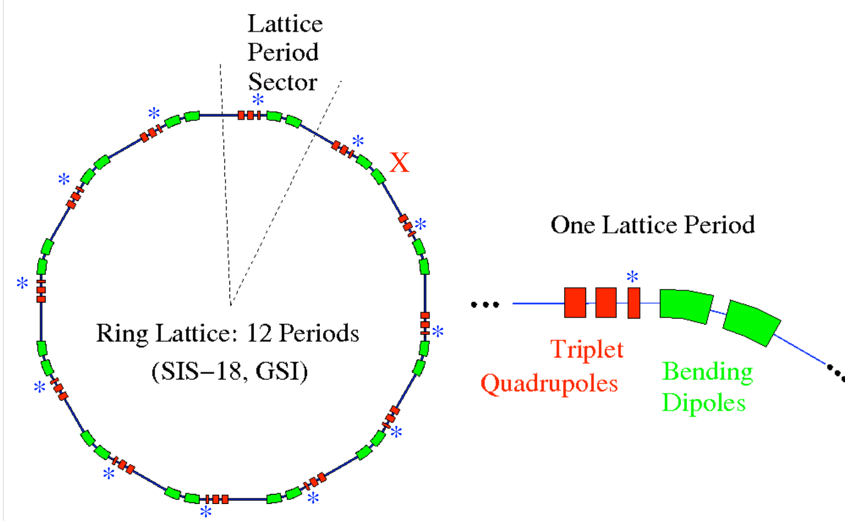

///

S5B: Transfer Matrix Form of the Solution to Hill's Equation

Hill's equation is linear. The solution with initial condition:

$$\boxed{\begin{aligned} x(s = s_i) &= x(s_i) \\ x'(s = s_i) &= x'(s_i) \end{aligned}} \qquad s = s_i = \text{Axial location of initial condition}$$

can be uniquely expressed in matrix form (**M** is the transfer matrix) as:

$$\boxed{\begin{aligned} \begin{bmatrix} x(s) \\ x'(s) \end{bmatrix} &= \mathbf{M}(s|s_i) \cdot \begin{bmatrix} x(s_i) \\ x'(s_i) \end{bmatrix} \\ &= \begin{bmatrix} C(s|s_i) & S(s|s_i) \\ C'(s|s_i) & S'(s|s_i) \end{bmatrix} \cdot \begin{bmatrix} x(s_i) \\ x'(s_i) \end{bmatrix} \end{aligned}}$$

Where $C(s|s_i)$ and $S(s|s_i)$ are "cosine-like" and "sine-like" principal trajectories satisfying:

$$\boxed{\begin{aligned} &C''(s|s_i) + \kappa(s)C(s|s_i) = 0 \qquad C(s_i|s_i) = 1 \quad C'(s_i|s_i) = 0 \\ &S''(s|s_i) + \kappa(s)S(s|s_i) = 0 \qquad S(s_i|s_i) = 0 \quad S'(s_i|s_i) = 1 \end{aligned}}$$

Transfer matrices will be worked out in the problems for a few simple focusing systems discussed in S2 with the additional assumption of piecewise constant $\kappa(s)$

1) Drift: $\kappa = 0$

$$\mathbf{M}(s|s_i) = \begin{bmatrix} 1 & s - s_i \\ 0 & 1 \end{bmatrix}$$

2) Continuous Focusing: $\kappa = k_{\beta 0}^s = \text{const} > 0$

$$\mathbf{M}(s|s_i) = \begin{bmatrix} \cos[k_{\beta 0}(s - s_i)] & \frac{1}{k_{\beta 0}} \sin[k_{\beta 0}(s - s_i)] \\ -k_{\beta 0} \sin[k_{\beta 0}(s - s_i)] & \cos[k_{\beta 0}(s - s_i)] \end{bmatrix}$$

3) Solenoidal Focusing: $\kappa = \hat{\kappa} = \text{const} > 0$

Results are expressed within the rotating Larmor Frame
(same as continuous focusing with reinterpretation of variables)

$$\mathbf{M}(s|s_i) = \begin{bmatrix} \cos[\sqrt{\hat{\kappa}}(s - s_i)] & \frac{1}{\sqrt{\hat{\kappa}}} \sin[\sqrt{\hat{\kappa}}(s - s_i)] \\ -\sqrt{\hat{\kappa}} \sin[\sqrt{\hat{\kappa}}(s - s_i)] & \cos[\sqrt{\hat{\kappa}}(s - s_i)] \end{bmatrix}$$

4) Quadrupole Focusing-Plane: $\kappa = \hat{\kappa} = \text{const} > 0$

(Obtain from continuous focusing case)

$$\mathbf{M}(s|s_i) = \begin{bmatrix} \cos[\sqrt{\hat{\kappa}}(s - s_i)] & \frac{1}{\sqrt{\hat{\kappa}}} \sin[\sqrt{\hat{\kappa}}(s - s_i)] \\ -\sqrt{\hat{\kappa}} \sin[\sqrt{\hat{\kappa}}(s - s_i)] & \cos[\sqrt{\hat{\kappa}}(s - s_i)] \end{bmatrix}$$

5) Quadrupole DeFocusing-Plane: $\kappa = -\hat{\kappa} = \text{const} < 0$

(Obtain from quadrupole focusing case with $\hat{\kappa} \rightarrow i\hat{\kappa} \quad i = \sqrt{-1}$)

$$\mathbf{M}(s|s_i) = \begin{bmatrix} \cosh[\sqrt{\hat{\kappa}}(s - s_i)] & \frac{1}{\sqrt{\hat{\kappa}}} \sinh[\sqrt{\hat{\kappa}}(s - s_i)] \\ \sqrt{\hat{\kappa}} \sinh[\sqrt{\hat{\kappa}}(s - s_i)] & \cosh[\sqrt{\hat{\kappa}}(s - s_i)] \end{bmatrix}$$

6) Thin Lens: $\kappa(s) = \frac{1}{f}\delta(s - s_0)$

$$\begin{aligned} s_0 &= \text{const} = \text{Axial Location Lens} \\ f &= \text{const} = \text{Focal Length} \\ \delta(x) &= \text{Dirac-Delta Function} \end{aligned}$$

$$\mathbf{M}(s_0^+|s_0^-) = \begin{bmatrix} 1 & 0 \\ -\frac{1}{f} & 1 \end{bmatrix}$$

S5C: Wronskian Symmetry of Hill's Equation

An important property of this linear motion is a Wronskian invariant/symmetry:

$$\boxed{\begin{aligned} W(s|s_i) &\equiv \det \mathbf{M}(s|s_i) = \det \begin{bmatrix} C(s|s_i) & S(s|s_i) \\ C'(s|s_i) & S'(s|s_i) \end{bmatrix} \\ &= C(s|s_i)S'(s|s_i) - C'(s|s_i)S(s|s_i) = 1 \end{aligned}}$$

/// Proof: Abbreviate Notation $C \equiv C(s|s_i)$ etc.

Multiply Equations of Motion for C and S by S and C, respectively:

$$\begin{aligned} -S(C'' + \kappa C) &= 0 \\ +C(S'' + \kappa S) &= 0 \end{aligned}$$

Add Equations:

$$CS'' - SC'' + \kappa(\cancelto{0}{CS - SC}) = 0$$

$$\Longrightarrow \frac{dW}{ds} = 0 \qquad \Longrightarrow W = \text{const}$$

Apply initial conditions:

$$W(s) = W(s_i) = C_i S_i' - C_i' S_i = 1 \cdot 1 - 0 \cdot 0 = 1$$ ///

/// Example: Continuous Focusing: Transfer Matrix and Wronskian

$$\kappa(s) = k_{\beta 0}^2 = \text{const} > 0$$

Principal orbit equations are simple harmonic oscillators with solution:

$$C(s|s_i) = \cos[k_{\beta 0}(s - s_i)] \qquad C'(s|s_i) = -k_{\beta 0} \sin[k_{\beta 0}(s - s_i)]$$

$$S(s|s_i) = \frac{\sin[k_{\beta 0}(s - s_i)]}{k_{\beta 0}} \qquad S'(s|s_i) = \cos[k_{\beta 0}(s - s_i)]$$

Transfer matrix gives the familiar solution:

$$\begin{bmatrix} x(s) \\ x'(s) \end{bmatrix} = \begin{bmatrix} \cos[k_{\beta 0}(s - s_i)] & \frac{\sin[k_{\beta 0}(s-s_i)]}{k_{\beta 0}} \\ -k_{\beta 0} \sin[k_{\beta 0}(s - s_i)] & \cos[k_{\beta 0}(s - s_i)] \end{bmatrix} \cdot \begin{bmatrix} x(s_i) \\ x'(s_i) \end{bmatrix}$$

Wronskian invariant is elementary:

$$W = \cos^2[k_{\beta 0}(s - s_i)] + \sin^2[k_{\beta 0}(s - s_i)] = 1$$

///

S5D: Stability of Solutions to Hill's Equation in a Periodic Lattice

The transfer matrix must be the same in any period of the lattice:

$$\mathbf{M}(s + L_p|s_i + L_p) = \mathbf{M}(s|s_i)$$

For a propagation distance $s - s_i$ satisfying

$$NL_p \leq s - s_i \leq (N+1)L_p \qquad N = 0, 1, 2, \cdots$$

the transfer matrix can be resolved as

$$\boxed{\begin{aligned} \mathbf{M}(s|s_i) &= \mathbf{M}(s - NL_p|s_i) \cdot \mathbf{M}(s_i + NL_p|s_i) \\ &= \underbrace{\mathbf{M}(s - NL_p|s_i)}_{\text{Residual}} \cdot \underbrace{[\mathbf{M}(s_i + L_p|s_i)]^N}_{N \text{ Full Periods}} \end{aligned}}$$

For a lattice to have stable orbits, both $x(s)$ and $x'(s)$ should remain bounded on propagation through an arbitrary number N of lattice periods. This is equivalent to requiring that the elements of **M** remain bounded on propagation through any number of lattice periods: $\mathbf{M}^N \equiv [\mathbf{M}^N{}_{ij}]$

$$\boxed{\lim_{N \to \infty} \left| \mathbf{M}^N{}_{ij} \right| < \infty \quad \Longrightarrow \text{Stable Motion}}$$

Clarification of stability notion: Unstable Orbit

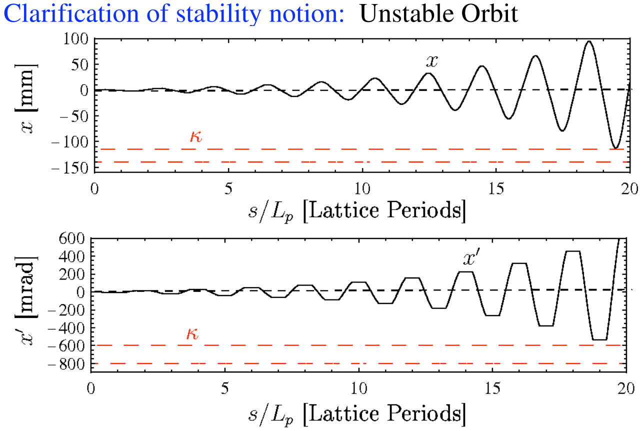

$L_p = 0.5$ m

$\eta = 0.5$

$$\kappa = \begin{cases} 48 & \text{where } \kappa \neq 0 \\ 0 & \text{otherwise} \end{cases}$$

$x(0) = 1$ mm

$x'(0) = 0$

For energetic particle: $H = \frac{1}{2}x'^2 + \frac{1}{2}\kappa x^2 \quad \sim \text{Large, but } \neq \text{const}$

where $|x'|$ small, $|x|$ large

where $|x|$ small, $|x'|$ large

The matrix criterion corresponds to our intuitive notion of stability: as the particle advances there are no large oscillation excursions in position and angle.

To analyze the stability condition, examine the eigenvectors/eigenvalues of **M** for transport through one lattice period:

$$\boxed{\begin{aligned} &\mathbf{M}(s_i + L_p|s_i) \cdot \mathbf{E} \equiv \lambda \mathbf{E} \\ &\mathbf{E} = \text{Eigenvector} \\ &\lambda = \text{Eigenvalue} \end{aligned}}$$

- Eigenvectors and Eigenvalues are generally complex
- Eigenvectors and Eigenvalues generally vary with s_i
- Two independent Eigenvalues and Eigenvectors
  - Degeneracies special case

Derive the two independent eigenvectors/eigenvalues through analysis of the characteristic equation: Abbreviate Notation

$$\mathbf{M}(s_i + L_p|s_i) = \begin{bmatrix} C(s_i + L_p|s_i) & S(s_i + L_p|s_i) \\ C'(s_i + L_p|s_i) & S'(s_i + L_p|s_i) \end{bmatrix} \equiv \begin{bmatrix} C & S \\ C' & S' \end{bmatrix}$$

Nontrivial solutions exist when:

$$\det \begin{bmatrix} C - \lambda & S \\ C' & S' - \lambda \end{bmatrix} = \lambda^2 + (C + S')\lambda + (CS' - SC') = 0$$

But we can apply the Wronskian condition:

$$CS' - SC' = 1$$

and we make the notational definition

$$C + S' = \text{Tr}\,\mathbf{M} \equiv 2\cos\sigma_0$$

The characteristic equation then reduces to:

$$\boxed{\lambda^2 - 2\lambda\cos\sigma_0 + 1 = 0 \qquad \cos\sigma_0 \equiv \frac{1}{2}\text{Tr}\,\mathbf{M}(s_i + L_p|s_i)}$$

- The use of $2\cos\sigma_0$ to denote Tr $\mathbf{M}$ is in anticipation of later results (see S6) where σ_0 is identified as the phase-advance of a stable orbit

There are two solutions to the characteristic equation that we denote $\lambda_\pm$

$$\boxed{\begin{aligned} \lambda_\pm &= \cos\sigma_0 \pm \sqrt{\cos^2\sigma_0 - 1} = \cos\sigma_0 \pm i\sin\sigma_0 = e^{\pm i\sigma_0} \\ \mathbf{E}_\pm &= \text{Corresponding Eigenvectors} \qquad i \equiv \sqrt{-1} \end{aligned}}$$

- Note that: $\lambda_+\lambda_- = 1$
  $\lambda_+ = 1/\lambda_-$

Consider a vector of initial conditions:

$$\begin{bmatrix} x(s_i) \\ x'(s_i) \end{bmatrix} = \begin{bmatrix} x_i \\ x'_i \end{bmatrix}$$

The eigenvectors $\mathbf{E}_\pm$ span two-dimensional space. So any initial condition vector can be expanded as:

$$\boxed{\begin{aligned} \begin{bmatrix} x_i \\ x'_i \end{bmatrix} &= \alpha_+\mathbf{E}_+ + \alpha_-\mathbf{E}_- \\ \alpha_\pm &= \text{Complex Constants} \end{aligned}}$$

Then using $\mathbf{M}\mathbf{E}_\pm = \lambda_\pm\mathbf{E}_\pm$

$$\boxed{\mathbf{M}^N(s_i + L_p|s_i)\begin{bmatrix} x_i \\ x'_i \end{bmatrix} = \alpha_+\lambda_+^N\mathbf{E}_+ + \alpha_-\lambda_-^N\mathbf{E}_-}$$

Therefore, if $\lim_{N\to\infty} \lambda^N$ is bounded, then the motion is stable. This will always be the case if $|\lambda_\pm| \leq 1$, corresponding to σ_0 real with $|\cos\sigma_0| \leq 1$

This implies for stability or the orbit that we must have:

$$\boxed{\begin{aligned} \frac{1}{2}\,|\text{Trace}\,\mathbf{M}(s_i + L_p|s_i)| &= \frac{1}{2}|C(s_i + L_p|s_i) + S'(s_i + L_p|s_i)| \\ &= |\cos\sigma_0| \leq 1 \end{aligned}}$$

In a periodic focusing lattice, this important stability condition places restrictions on the lattice structure (focusing strength) that are generally interpreted in terms of phase advance limits (see: S6).

- Accelerator lattices almost always tuned for single particle stability to maintain beam control
  - Even for intense beams, beam centroid approximately obeys single particle equations of motion when image charges are negligible
- Space-charge and nonlinear applied fields can further limit particle stability
  - Resonances: see: Particle Resonances ....
  - Envelope Instability: see: Transverse Centroid and Envelope ....
  - Higher Order Instability: see: Transverse Kinetic Stability
- We will show (see: S6) that for stable orbits σ_0 can be interpreted as the phase-advance of single particle oscillations

/// Example: Continuous Focusing Stability

$$\kappa(s) = k_{\beta 0}^2 = \text{const} > 0$$

Principal orbit equations are simple harmonic oscillators with solution:

$$C(s|s_i) = \cos[k_{\beta 0}(s - s_i)] \qquad C'(s|s_i) = -k_{\beta 0}\sin[k_{\beta 0}(s - s_i)]$$

$$S(s|s_i) = \frac{\sin[k_{\beta 0}(s - s_i)]}{k_{\beta 0}} \qquad S'(s|s_i) = \cos[k_{\beta 0}(s - s_i)]$$

Stability bound then gives:

$$\begin{aligned} \frac{1}{2}\,|\text{Trace}\,\mathbf{M}(s_i + L_p|s_i)| &= \frac{1}{2}|C(s_i + L_p|s_i) + S'(s_i + L_p|s_i)| \\ &= |\cos(k_{\beta 0}(s - s_i)| \leq 1 \end{aligned}$$

- Always satisfied for real $k_{\beta 0}$
- Confirms known result using formalism: continuous focusing stable
  - Energy not pumped into or out of particle orbit ///

The simplest example of the stability criterion applied to periodic lattices will be given in the problem sets: Stability of a periodic thin lens lattice

- Analytically find that lattice unstable when focusing kicks sufficiently strong

More advanced treatments

- See: Dragt, *Lectures on Nonlinear Orbit Dynamics*, AIP Conf Proc 87 (1982)

show that symplectic 2x2 transfer matrices associated with Hill's Equation have only two possible classes of eigenvalue symmetries:

1) Stable

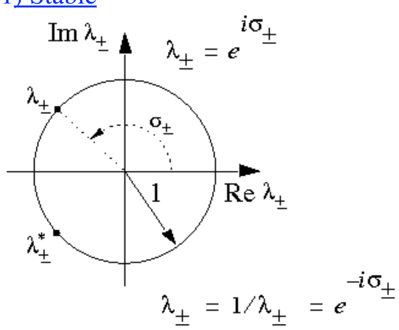

Occurs for:

$$0 \leq \sigma_0 \leq 180^\circ/\text{period}$$

2) Unstable, Lattice Resonance

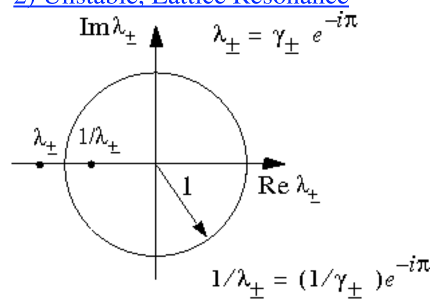

Occurs in bands when focusing strength is increased beyond

$$\sigma_0 = 180^\circ/\text{period}$$

- Limited class of possibilities simplifies analysis of focusing lattices

S6: Hill's Equation: Floquet's Theorem and the Phase-Amplitude Form of the Particle Orbit

S6A: Introduction

In this section we consider Hill's Equation:

$$\boxed{x''(s) + \kappa(s)x(s) = 0}$$

subject to a periodic applied focusing function

$$\boxed{\begin{aligned}&\kappa(s + L_p) = \kappa(s)\\ &L_p = \text{Lattice Period}\end{aligned}}$$

- Many results will also hold in more complicated form for a non-periodic $\kappa(s)$

S6B: Floquet's Theorem

Floquet's Theorem (proof: see standard Mathematics and Mathematical Physics Texts)

The solution to Hill's Equation $x(s)$ has two linearly independent solutions that can be expressed as:

$$x_1(s) = w(s)e^{i\mu s}$$
$$x_2(s) = w(s)e^{-i\mu s}$$

$$i = \sqrt{-1}$$
$$\begin{aligned}\mu &= \frac{1}{2}\text{Tr}\,\mathbf{M}(s_i + L_p|s_i) = \cos\sigma_0\\ &= \text{const} = \text{Characteristic Exponent}\end{aligned}$$

Where $w(s)$ is a periodic function:

$$w(s + L_p) = w(s)$$

- Theorem as written only applies for **M** with non-degenerate eigenvalues. But a similar theorem applies in the degenerate case.
- A similar theorem is also valid for non-periodic

S6C: Phase-Amplitude Form of Particle Orbit

As a consequence of Floquet's Theorem, any (stable or unstable) nondegenerate solution to Hill's Equation can be expressed in phase-amplitude form as:

$$\boxed{\begin{aligned}x(s) &= A(s)\cos\psi(s) \qquad & A(s) &= \text{Amplitude Function}\\ A(s + L_p) &= A(s) & \psi(s) &= \text{Phase Function}\end{aligned}}$$

Derive equations of motion for $A,\ \psi$ by taking derivatives of the phase-amplitude form for $x(s)$:

$$\begin{aligned}x &= A\cos\psi\\ x' &= A'\cos\psi - A\psi'\sin\psi\\ x'' &= A''\cos\psi - A'\psi'\sin\psi - A\psi''\sin\psi - A\psi'^2\cos\psi\end{aligned}$$

then substitute in Hill's Equation:

$$\boxed{x'' + \kappa x = \left[A'' + \kappa A - A\psi'^2\right]\cos\psi - \left[2A'\psi' + A\psi''\right]\sin\psi = 0}$$

$$\boxed{x'' + \kappa x = \left[A'' + \kappa A - A\psi'^2\right]\cos\psi - \left[2A'\psi' + A\psi''\right]\sin\psi = 0}$$

We are free to introduce an additional constraint between A and ψ:

- Two functions A, ψ to represent one function x allows a constraint

Choose:

Eq. (1) $\quad \boxed{2A'\psi' + A\psi'' = 0} \quad \Longrightarrow \quad$ Coefficient of $\sin\psi$ zero

Then to satisfy Hill's Equation for all ψ the, coefficient of $\cos\psi$ must also vanish giving:

Eq. (2) $\quad \boxed{A'' + \kappa A - A\psi'^2 = 0} \quad \Longrightarrow \quad$ Coefficient of $\cos\psi$ zero

Eq. (1) Analysis (coefficient of $\sin\psi$): $\quad 2A'\psi' + A\psi'' = 0$

Simplify:

$$2A'\psi' + A\psi'' = \frac{(A^2\psi')'}{A} = 0 \qquad A \neq 0$$

Will show later that this assumption met for all s

$$\Longrightarrow \quad (A^2\psi')' = 0$$

Integrate once:

$$\boxed{A^2\psi' = \text{const}}$$

One commonly rescales the amplitude $A(s)$ in terms of an auxiliary amplitude functions $w(s)$:

$$\boxed{A(s) = A_i w(s) \qquad A_i = \text{const} = \text{Initial Amplitude}}$$

such that

$$\boxed{w^2\psi' \equiv 1}$$

This equation can then be integrated to obtain the phase-function of the particle:

$$\boxed{\psi(s) = \psi_i + \int_{s_i}^{s} \frac{d\tilde{s}}{w^2(\tilde{s})} \qquad \psi_i = \text{const} = \text{Initial Phase}}$$

Eq. (2) Analysis (coefficient of $\cos\psi$): $\quad A'' + \kappa A - A\psi'^2 = 0$

With the choice of amplitude rescaling, $w^2\psi' = 1$ and Eq. (2) becomes:

$$\boxed{w'' + \kappa w - \frac{1}{w^3} = 0}$$

Floquet's theorem tells us that we are free to restrict w to be a periodic solution:

$$\boxed{w(s + L_p) = w(s)}$$

Reduced Expressions for x and x':

Using $A = A_i w$ and $w^2\psi' = 1$:

$$x = A\cos\psi$$
$$x' = A'\cos\psi - A\psi'\sin\psi$$

$$\Longrightarrow \quad \boxed{\begin{aligned} x &= A_i w\cos\psi \\ x' &= A_i w'\cos\psi - \frac{A_i}{w}\sin\psi \end{aligned}}$$

S6D: Summary: Phase-Amplitude Form of Solution to Hill's Eqn

$$x(s) = A_i w(s)\cos\psi(s) \qquad A_i = \text{const} = \text{Initial Amplitude}$$

$$x'(s) = A_i w'(s)\cos\psi(s) - \frac{A_i}{w(s)}\sin\psi(s) \qquad \psi_i = \text{const} = \text{Initial Phase}$$

where $w(s)$ and $\psi(s)$ are amplitude- and phase-functions satisfying:

Amplitude Equations

$$w''(s) + \kappa(s)w(s) - \frac{1}{w^3(s)} = 0$$
$$w(s + L_p) = w(s)$$

Phase Equations

$$\psi'(s) = \frac{1}{w^2(s)}$$
$$\psi(s) = \psi_i + \int_{s_i}^{s} \frac{d\tilde{s}}{w^2(\tilde{s})}$$
$$\psi(s) = \psi_i + \Delta\psi(s)$$

Initial ($s = s_i$) amplitudes are constrained by the particle initial conditions as:

$$x(s = s_i) = A_i w_i \cos\psi_i$$
$$x'(s = s_i) = A_i w_i'\cos\psi_i - \frac{A_i}{w_i}\sin\psi_i$$

or

$$\boxed{\begin{aligned} A_i\cos\psi_i &= x(s = s_i)/w_i & w_i &\equiv w(s = s_i) \\ A_i\sin\psi_i &= x(s = s_i)w_i' - x'(s = s_i)w_i & w_i' &\equiv w'(s = s_i) \end{aligned}}$$

S6E: Points on the Phase-Amplitude Formulation

1) $w(s)$ can be taken as positive definite

$$w(s) > 0$$

/// Proof: Sign choices in w:

Let $w(s)$ be positive at some point. Then the equation:

$$w'' + \kappa w - \frac{1}{w^3} = 0$$

Insures that w can never vanish or change sign. This follows because whenever w becomes small, $w'' \simeq 1/w^3 \gg 0$ can become arbitrarily large to turn w before it reaches zero. Thus, to fix phases, we conveniently require that $w > 0$. ///

- Proof verifies assumption made in analysis that $A = A_i w \neq 0$
- Conversely, one could choose w negative and it would always remain negative for analogous reasons. This choice is *not* commonly made.
- Sign choice removes ambiguity in relating initial conditions $x(s_i),\ x'(s_i)$ to $A_i,\ \psi_i$

2) $w(s)$ is a unique periodic function

- Can be proved using a connection between w and the principal orbit functions C and S (see: Appendix C and S7)
- $w(s)$ can be regarded as a special, periodic function describing the lattice

3) The amplitude parameters

$$w_i = w(s = s_i)$$
$$w'_i = w'(s_i)$$

depend *only* on the periodic lattice properties and are *independent* of the particle initial conditions $x(s_i),\ x'(s_i)$

4) The phase-advance

$$\Delta\psi(s) = \int_{s_i}^{s} \frac{d\tilde{s}}{w^2(\tilde{s})}$$

depends on the choice of initial condition s_i . However, the phase-advance through one lattice period

$$\Delta\psi(s_i + L_p) = \int_{s_i}^{s_i+L_p} \frac{d\tilde{s}}{w^2(\tilde{s})}$$

Will be independent of s_i since w is a periodic function with period L_p

- Will show that (see later in this section)

  $$\Delta\psi(s_i + L_p) \equiv \sigma_0$$

  is the undepressed phase advance of particle oscillations

5) $w(s)$ has dimensions [[w]] = Sqrt[meters]

- Can prove inconvenient in applications and motivates the use of an alternative "betatron" function

  $$\beta(s) \equiv w^2(s)$$

  with dimension [[β]] = meters (see: S7 and S8)

6) On the surface, what we have done: Transform the linear Hill's Equation to a form where a solution to nonlinear axillary equations for w and are needed via the phase-amplitude method seems insane ..... why do it?

- Method will help identify the useful Courant-Snyder invariant which will aid interpretation of the dynamics (see: S7)
- Decoupling of initial conditions in the phase-amplitude method will help simplify understanding of bundles of particles in the distribution

S6F: Relation between Principal Orbit Functions and Phase-Amplitude Form Orbit Functions

The transfer matrix **M** of the particle orbit can be expressed in terms of the principal orbit functions C and S as (see: S4):

$$\boxed{\begin{bmatrix} x(s) \\ x'(s) \end{bmatrix} = \mathbf{M}(s|s_i) \cdot \begin{bmatrix} x(s_i) \\ x'(s_i) \end{bmatrix} = \begin{bmatrix} C(s|s_i) & S(s|s_i) \\ C'(s|s_i) & S'(s|s_i) \end{bmatrix} \cdot \begin{bmatrix} x(s_i) \\ x'(s_i) \end{bmatrix}}$$

Use of the phase-amplitude forms and some algebra identifies (see problem sets):

$$C(s|s_i) = \frac{w(s)}{w_i}\cos\Delta\psi(s) - w'_i w(s)\sin\Delta\psi(s)$$
$$S(s|s_i) = w_i w(s)\sin\Delta\psi(s)$$
$$C'(s|s_i) = \left(\frac{w'(s)}{w_i} - \frac{w'_i}{w(s)}\right)\cos\Delta\psi(s) - \left(\frac{1}{w_i w(s)} + w'_i w'(s)\right)\sin\Delta\psi(s)$$
$$S'(s|s_i) = \frac{w_i}{w(s)}\cos\Delta\psi(s) + w_i w'(s)\sin\Delta\psi(s)$$
$$\Delta\psi(s) \equiv \int_{s_i}^{s} \frac{d\tilde{s}}{w^2(\tilde{s})} \qquad w_i \equiv w(s = s_i) \qquad w'_i \equiv w'(s = s_i)$$

/// Aside: Alternatively, it can be shown (see: Appendix C) that $w(s)$ can be related to the principal orbit functions calculated over one Lattice period by:

$$\boxed{\begin{aligned} w^2(s) = \beta(s) &= \sin\sigma_0 \frac{S(s|s_i)}{S(s_i+L_p|s_i)} \\ &+ \frac{S(s_i+L_p|s_i)}{\sin\sigma_0}\left[C(s|s_i) + \frac{\cos\sigma_0 - C(s|s_i)}{S(s_i+L_p|s_i)} S(s|s_i)\right]^2 \\ \sigma_0 &\equiv \int_{s_i}^{s} \frac{d\tilde{s}}{w^2(\tilde{s})} \end{aligned}}$$

The formula for σ_0 in terms of principal orbit functions is useful:

- σ_0 (phase advance, see: S6G) is often specified for the lattice and the focusing function $\kappa(s)$ is tuned to achieve the specified value
- Shows that $w(s)$ can be constructed from two principal orbit integrations over one lattice period
  - Integrations must generally be done numerically for C and S
  - No root finding required for initial conditions to construct periodic $w(s)$
  - s_i can be anywhere in the lattice period and $w(s)$ will be independent of the specific choice of s_i

- The form of $w^2(s)$ suggests an underlying Courant-Snyder Invariant (see: S7 and Appendix C)
- $w^2 = \beta$ can be applied to calculate max beam particle excursions in the absence of space-charge effects (see: S8)
  - Useful in machine design
  - Exploits Courant-Snyder Invariant

///

S6G: Undepressed Particle Phase Advance

We can now concretely connect σ_0 for a stable obit to the advance in particle oscillation phase $\Delta\psi$ through one lattice period:

From S5D:

$$\boxed{\cos\sigma_0 \equiv \frac{1}{2}\text{Tr }\mathbf{M}(s_i+L_p|s_i)}$$

Apply the principal orbit representation of $\mathbf{M}$

$$\text{Tr }\mathbf{M}(s_i+L_p|s_i) = C(s_i+L_p|s_i) + S'(s_i+L_p|s_i)$$

and use the phase-amplitude identifications of C and S' calculated in S6F:

$$\begin{aligned} \text{Tr }\mathbf{M}(s_i+L_p|s_i) &= \frac{1}{2}\left(\frac{w(s_i+L_p)}{w_i} + \frac{w_i}{w(s_i+L_p)}\right)\cos\Delta\psi(s_i+L_p) \\ &+ \frac{1}{2}\left(w_i w'(s_i+L_p) - w'_i w(s_i+L_p)\right)\sin\Delta\psi(s_i+L_p) \end{aligned}$$

By periodicity:

$$\begin{aligned} w(s_i+L_p) &= w(s_i) = w_i \\ w'(s_i+L_p) &= w'(s_i) = w'_i \end{aligned} \quad \Longrightarrow \quad \begin{aligned} &\text{coefficient of } \cos\Delta\psi = 1 \\ &\text{coefficient of } \sin\Delta\psi = 0 \end{aligned}$$

Applying these results gives:

$$\boxed{\cos\sigma_0 = \cos\Delta\psi(s_i+L_p) = \frac{1}{2}\text{Tr }\mathbf{M}(s_i+L_p|s_i)}$$

Thus, σ_0 is identified as the phase advance of a stable particle orbit through one lattice period:

$$\boxed{\sigma_0 = \Delta\psi(s_i+L_p) = \int_{s_i}^{s_i+L_p} \frac{ds}{w^2(s)}}$$

- Again verifies that σ_0 is independent of s_i since w(s) is periodic with period L_p
- The stability criterion (see: S5)

$$\frac{1}{2}|\text{Tr }\mathbf{M}(s_i+L_p|s_i)| = |\cos\sigma_0| < 1$$

is concretely connected to the particle phase advance through one lattice period providing a useful physical interpretation

Discussion:

The phase advance σ_0 is an extremely useful dimensionless measure to characterize the focusing strength of a periodic lattice. Much of conventional accelerator physics centers on focusing strength and the suppression of resonance effects. The phase advance is a natural parameter to employ in many situations to allow ready interpretation of results in a generalizable manner.

We present phase advance formulas for σ_0 for several simple classes of lattices to help build intuition on focusing strength:

1) Continuous Focusing
2) Periodic Solenoidal Focusing
3) Periodic Quadrupole Doublet Focusing
   - FODO Quadrupole Limit

Several of these will be derived in the problem sets

- Lattices analyzed as "hard-edge" with piecewise-constant $\kappa(s)$ and lattice period L_p
- Results are summarized only with derivations guided in the problem sets.

4) Thin Lens Limits
   - Useful for analysis of scaling properties

1) Continuous Focusing

"Lattice period" L_p is an arbitrary length for phase accumulation

$\kappa(s) = k_{\beta 0}^2 = \text{const} > 0$

Parameters:

$L_p = \text{Lattice Period}$
$k_{\beta 0}^2 = \text{Strength}$

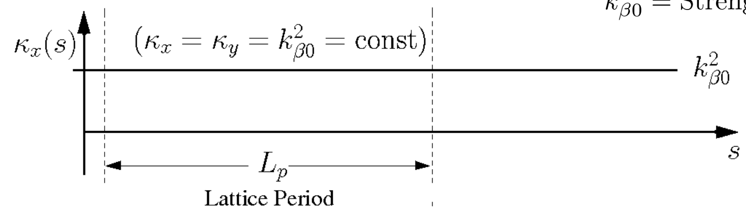

Calculation gives:

$$\boxed{\sigma_0 = k_{\beta 0} L_p}$$

- Always stable
  - Energy cannot pump into or out of particle orbit

Rescaled Principal Orbit Evolution:

$L_p = 0.5$ m
$\sigma_0 = \pi/3 = 60°$
$k_{\beta 0} = (\pi/6)$ rad/m

1: $x(0) = 1$ mm, $x'(0) = 0$ mrad

2: $x(0) = 0$ mm, $x'(0) = 1$ mrad

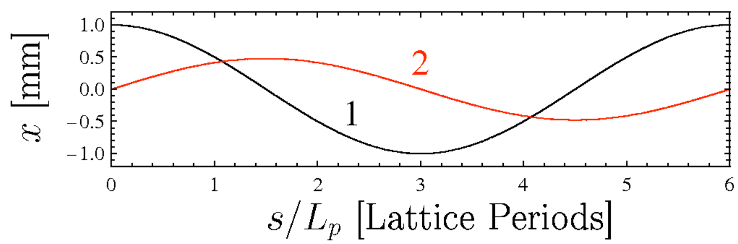

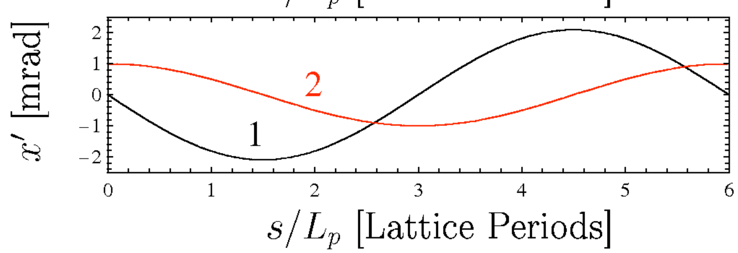

Phase-Space Evolution (see also S7):

- Phase-space ellipse stationary and aligned along x, x' axes for continuous focusing

$$w = \sqrt{1/k_{\beta 0}} = \text{const}$$

$$w' = 0$$

$$\gamma = \frac{1}{w^2} = k_{\beta 0} = \text{const}$$

$$\alpha = -ww' = 0$$

$$\beta = w^2 = 1/k_{\beta 0} = \text{const}$$

$$k_{\beta 0} x^2 + x'^2/k_{\beta 0} = \epsilon = \text{const}$$

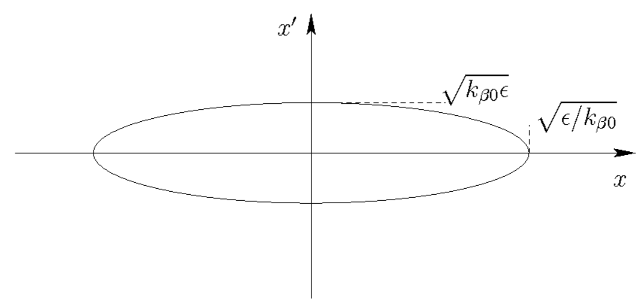

2) Periodic Solenoidal Focusing

Results are interpreted in the rotating Larmor frame (see S2 and Appendix A)

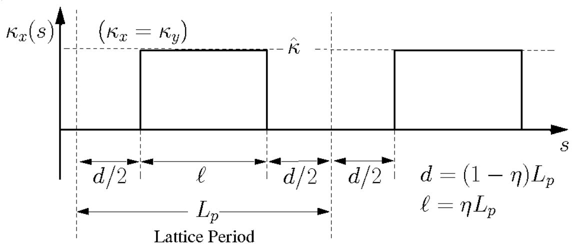

Parameters:

L_p = Lattice Period

$\eta \in (0, 1]$ = Occupancy

$\hat{\kappa}$ = Strength

Characteristics:

ηL_p = Optic Length

$(1-\eta)L_p$ = Drift Length

Calculation gives:

$$\boxed{\cos\sigma_0 = \cos(2\Theta) - \frac{1-\eta}{\eta}\Theta\sin(2\Theta) \qquad \Theta \equiv \frac{\eta}{2}\sqrt{\hat{\kappa}}L_p}$$

- Can be unstable when $\hat{\kappa}$ becomes large
  - Energy can pump into or out of particle orbit

Rescaled Larmor-Frame Principal Orbit Evolution:

$L_p = 0.5$ m

$\sigma_0 = \pi/3 = 60°$ ($\kappa = 8.558$ m^{-2})

$\eta = 0.5$

1: $\tilde{x}(0) = 1$ mm, $\tilde{x}'(0) = 0$ mrad

2: $\tilde{x}(0) = 0$ mm, $\tilde{x}'(0) = 1$ mrad

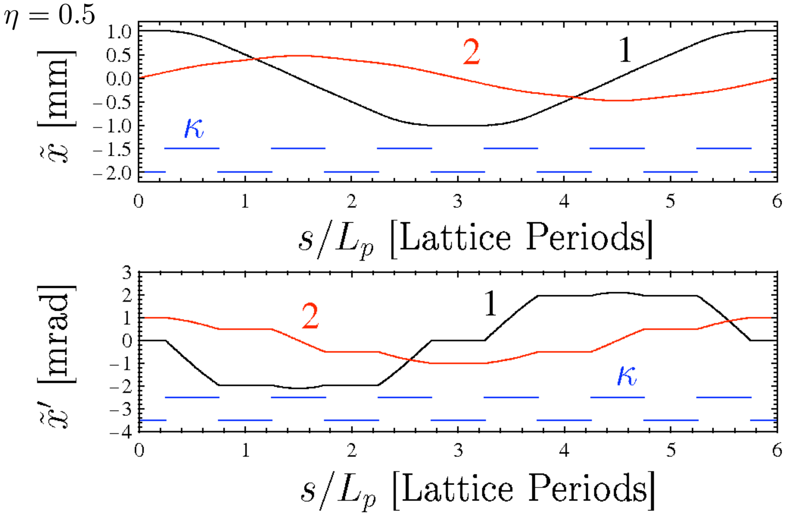

- Principal orbits in $\tilde{y} - \tilde{y}'$ phase-space are identical

Phase-Space Evolution in the Larmor frame (see also: S7):

- Phase-Space ellipse rotates and evolves in periodic lattice
- $\tilde{y} - \tilde{y}'$ phase-space properties same as in $\tilde{x} - \tilde{x}'$
  - Phase-space structure in x-x', y-y' phase space is complicated

$$\gamma\tilde{x}^2 - 2\alpha\tilde{x}\tilde{x}' + \beta\tilde{x}'^2 = \epsilon = \text{const}$$

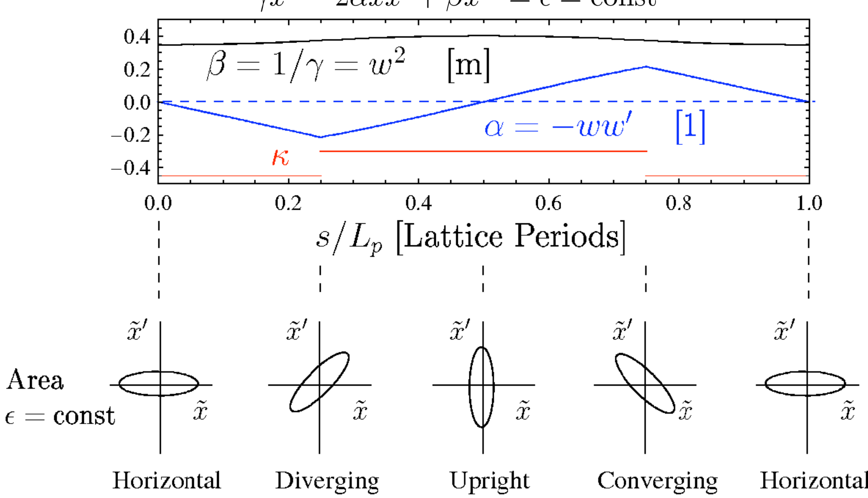

Comments on periodic solenoid results:

- Larmor frame analysis greatly simplifies results
  - 4D coupled orbit in x-x', y-y' phase-space will be much more intricate in structure
- Phase-Space ellipse rotates and evolves in periodic lattice
- Periodic structure of lattice changes orbits from simple harmonic

3) Periodic Quadrupole Doublet Focusing

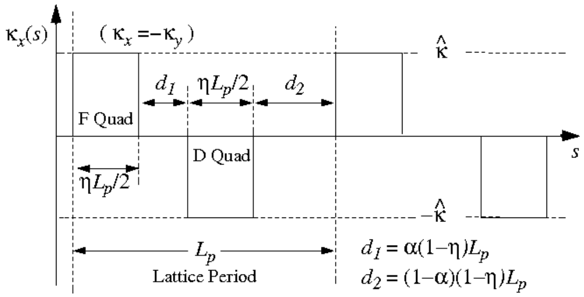

Parameters:
L_p = Lattice Period
$\eta \in (0,1]$ = Occupancy
$\alpha \in [0,1]$ = Syncopation
$\hat{\kappa}$ = Strength

Characteristics:
$\eta L_p/2$ = F/D Len
$\alpha(1-\eta)L_p$ = Drift Len d_1
$(1-\alpha)(1-\eta)L_p$ = Drift Len d_2

Calculation gives:

$$\cos\sigma_0 = \cos\Theta\cosh\Theta + \frac{1-\eta}{\eta}\Theta(\cos\Theta\sinh\Theta - \sin\Theta\cosh\Theta) - 2\alpha(1-\alpha)\frac{(1-\eta)^2}{\eta^2}\Theta^2\sin\Theta\sinh\Theta \qquad \Theta \equiv \frac{\eta}{2}\sqrt{|\hat{\kappa}|}L_p$$

- Can be unstable when $\hat{\kappa}$ becomes large
  - Energy can pump into or out of particle orbit

Comments on Parameters:

- The "syncopation" parameter α measures how close the Focusing (F) and DeFocusing (D) quadrupoles are to each other in the lattice

$$\alpha \in [0,1] \qquad \begin{array}{lll} \alpha = 0 & \Longrightarrow & d_1 = 0 \qquad d_2 = (1-\eta)L_p \\ \alpha = 1 & \Longrightarrow & d_1 = (1-\eta)L_p \quad d_2 = 0 \end{array}$$

The range $\alpha \in [1/2, 1]$ can be mapped to $\alpha \in [0, 1/2]$ by simply relabeling quantities. Therefore, we can take:

$\alpha \in [0, 1/2]$

- The special case of a doublet lattice with $\alpha = 1/2$ corresponds to equal drift lengths between the F and D quadrupoles and is called a FODO lattice

$$\alpha = 1/2 \qquad \Longrightarrow \qquad d_1 = d_2 \equiv d = (1-\eta)L_p/2$$

Phase advance constraint will be derived for FODO case in problems (algebra much simpler than doublet case)

Special Case Doublet Focusing: Periodic Quadrupole FODO Lattice

Parameters:
L_p = Lattice Period
$\eta \in (0,1]$ = Occupancy
$\hat{\kappa}$ = Strength

Characteristics:
$\eta L_p/2 = \ell$ = F/D Len
$(1-\eta)L_p/2 = d$ = Drift Len

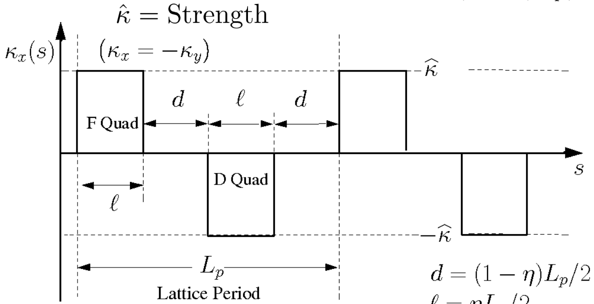

Phase advance formula reduces to:

$$\cos\sigma_0 = \cos\Theta\cosh\Theta + \frac{1-\eta}{\eta}\Theta(\cos\Theta\sinh\Theta - \sin\Theta\cosh\Theta) - \frac{(1-\eta)^2}{2\eta^2}\Theta^2\sin\Theta\sinh\Theta \qquad \Theta \equiv \frac{\eta}{2}\sqrt{|\hat{\kappa}|}L_p$$

- Analysis shows FODO provides stronger focus for same integrated field gradients than doublet due to symmetry

Rescaled Principal Orbit Evolution:

$L_p = 0.5$ m
$\sigma_0 = \pi/3 = 60^\circ$ ($\kappa = 39.24\ \mathrm{m}^{-2}$)
$\eta = 0.5$

1: $x(0) = 1$ mm, $x'(0) = 0$ mrad
2: $x(0) = 0$ mm, $x'(0) = 1$ mrad

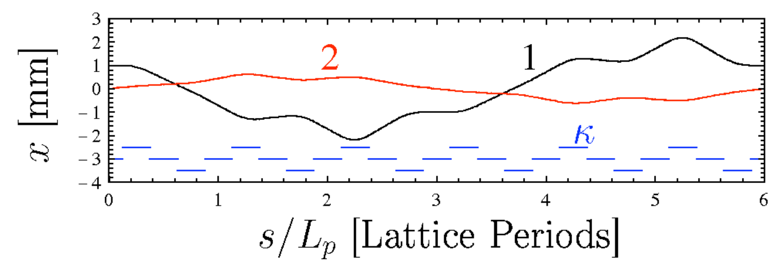

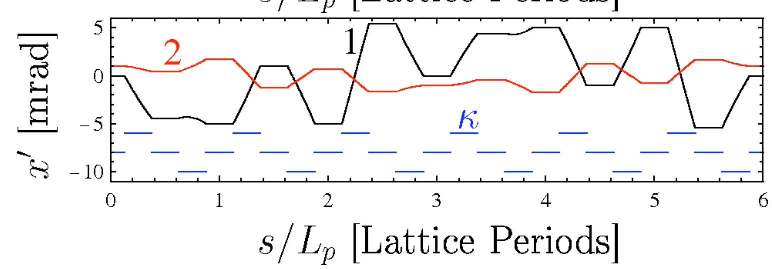

Phase-Space Evolution (see also: S7):

$$\gamma x^2 - 2\alpha x x' + \beta x'^2 = \epsilon = \text{const}$$

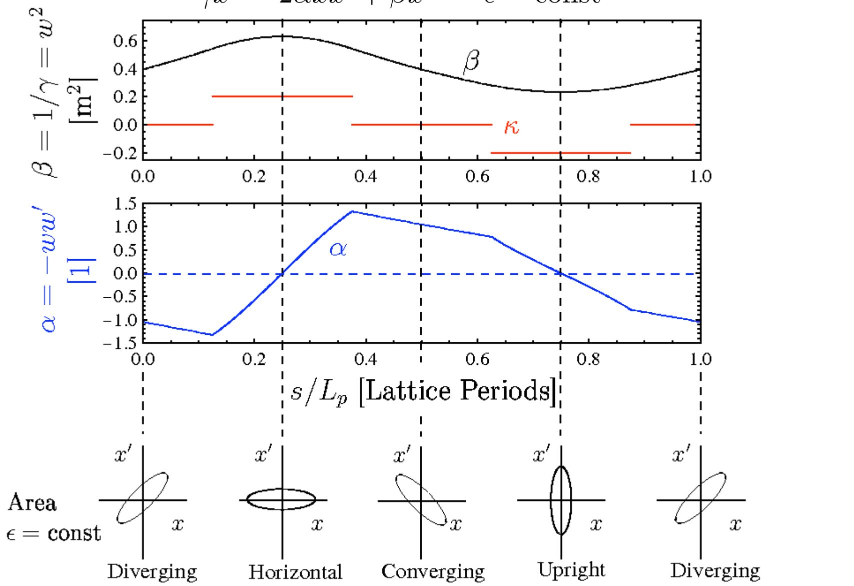

Comments on periodic FODO quadrupole results:

- Phase-Space ellipse rotates and evolves in periodic lattice
  - Evolution more intricate for Alternating Gradient (AG) focusing than for solenoidal focusing in the Larmor frame
- Harmonic content of orbits larger for AG focusing than solenodial focusing
- Orbit and phase space evolution analogous in *y-y'* plane
  - Simply related by an shift in *s* of the lattice

Contrast of Principal Orbits for different focusing:

- Use previous examples with "equivalent" focusing strength $\sigma_0 = 60^\circ$
- Note that periodic focusing adds harmonic structure

1) Continuous Focusing

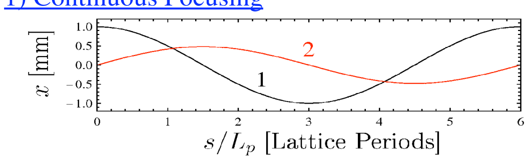

Simple Harmonic Oscillator

2) Periodic Solenoidal Focusing (Larmor Frame)

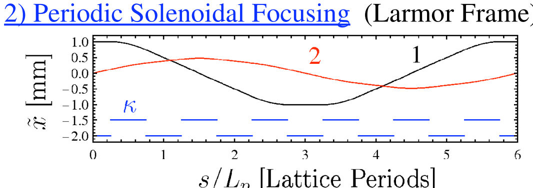

Simple harmonic oscillations modified with additional harmonics due to periodic focus

3) Periodic FODO Quadrupole Doublet Focusing

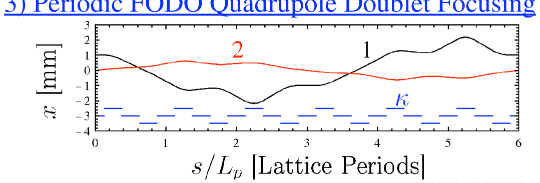

Simple harmonic oscillations more strongly modified due to periodic AG focus

4) Thin Lens Limits

Convenient to simply understand analytic scaling

$$\boxed{\begin{aligned} \kappa_x(s) &= \frac{1}{f}\delta(s - s_0) \\ s_0 &= \text{Optic Location} = \text{const} \\ f &= \text{focal length} = \text{const} \end{aligned}}$$

Transfer Matrix:

$$\begin{pmatrix} x \\ x' \end{pmatrix}_{s=s_0^+} = \begin{bmatrix} 1 & 0 \\ -1/f & 1 \end{bmatrix} \cdot \begin{pmatrix} x \\ x' \end{pmatrix}_{s=s_0^-}$$

Graphical Interpretation:

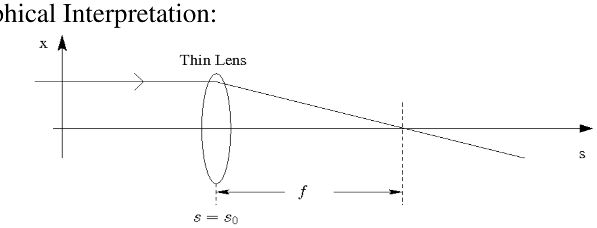

The thin lens limit of "thick" hard-edge solenoid and quadrupole focusing lattices presented can be obtained by taking:

Solenoids: $\hat{\kappa} \equiv \dfrac{1}{\eta f L_p}$ then take $\lim\limits_{\eta \to 0}$

Quadrupoles: $\hat{\kappa} \equiv \dfrac{2}{\eta f L_p}$ then take $\lim\limits_{\eta \to 0}$

This obtains when applied in the previous formulas:

$$\boxed{\cos\sigma_0 = \begin{cases} 1 - \frac{1}{2}\frac{L_p}{f}, & \text{thin-lens periodic solenoid} \\ 1 - \frac{\alpha}{2}(1-\alpha)\left(\frac{L_p}{f}\right)^2, & \text{thin-lens quadrupole doublet} \end{cases}}$$

These formulas can also be derived directly from the drift and thin lens transfer matrices as

Periodic Solenoid

$$\cos\sigma_0 = \frac{1}{2}\mathrm{Tr}\begin{bmatrix} 1 & L_p \\ 0 & 1 \end{bmatrix}\begin{bmatrix} 1 & 0 \\ -\frac{1}{f} & 1 \end{bmatrix} = 1 - \frac{1}{2}\frac{L_p}{f}$$

Periodic Quadrupole Doublet

$$\cos\sigma_0 = \frac{1}{2}\mathrm{Tr}\begin{bmatrix} 1 & 0 \\ -\frac{1}{f} & 1 \end{bmatrix}\begin{bmatrix} 1 & \alpha L_p \\ 0 & 1 \end{bmatrix}\begin{bmatrix} 1 & 0 \\ \frac{1}{f} & 1 \end{bmatrix}\begin{bmatrix} 1 & (1-\alpha)L_p \\ 0 & 1 \end{bmatrix} = 1 - \frac{\alpha}{2}(1-\alpha)\left(\frac{L_p}{f}\right)^2$$

Expanded phase advance formulas (thin lens type limit and similar) can be useful in system design studies

- Desirable to derive simple formulas relating magnet parameters to σ_0
  - Clear analytic scaling trends clarify design trade-offs
- For hard edge periodic lattices, expand formula for $\cos\sigma_0$ to leading order in $\Theta = \sqrt{|\hat{\kappa}|}\eta L_p/2$

/// Example: Periodic Quadrupole Doublet Focusing:

- Expand previous formula

$$\cos\sigma_0 = 1 - \frac{(\eta\hat{\kappa}L_p^2)^2}{32}\left[\left(1 - \frac{2}{3}\eta\right) - 4\left(\alpha - \frac{1}{2}\right)^2(1-\eta)^2\right]$$

where:

$$\hat{\kappa} = \begin{cases} \frac{\hat{G}}{[B\rho]}, & \text{Magnetic Quadrupoles} \\ \frac{\hat{G}}{\beta_b c[B\rho]}, & \text{Electric Quadrupoles} \end{cases} \qquad \hat{G} = \text{Hard-Edge Field Gradient}$$

Using these results, plot the Field Gradient and Integrated Gradient for quadrupole doublet focusing needed for $\sigma_0 = 80^\circ$ per lattice period

Gradient ~ $|\hat{\kappa}|L_p^2 \sim \hat{G}$

Integrated Gradient ~ $\eta|\hat{\kappa}|L_p^2/2 \sim \hat{G}\ell$

$\sigma_0 = 80^\circ$ /(Lattice Period) Quadrupole Doublet

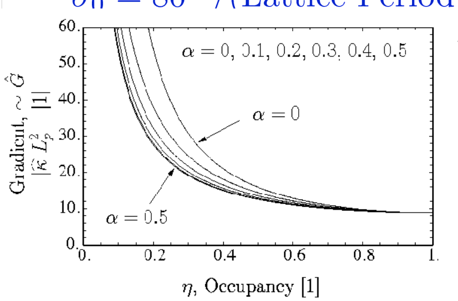

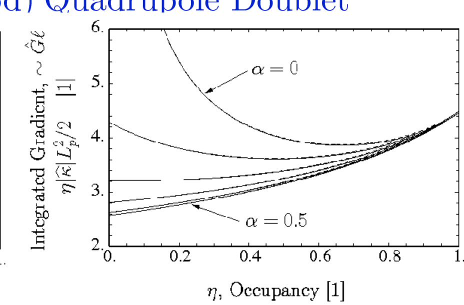

- Exact (non-expanded) solutions plotted dashed (almost overlay)
- Gradient and integrated gradient required depend only weakly on syncopation factor α when α is near ½
- Stronger gradient required for low occupancy η but integrated gradient varies little with η

///

Appendix C: Calculation of $w(s)$ from Principal Orbit Functions

Evaluate principal orbit expressions of the transfer matrix through one lattice period using

$$w(s_i + L_p) = w_i$$
$$w'(s_i + L_p) = w'_i$$

and

$$\Delta\psi(s_i + L_p) = \int_{s_i}^{s_i + L_p} \frac{ds}{w^2(s)} = \sigma_0$$

to obtain (see principal orbit formulas expressed in phase-amplitude form):

$$C(s_i + L_p|s_i) = \cos\sigma_0 - w_i w'_i \sin\sigma_0$$
$$S(s_i + L_p|s_i) = w_i^2 \sin\sigma_0$$
$$C'(s_i + L_p|s_i) = -\left(\frac{1}{w_i^2} + w_i w'_i\right)\sin\sigma_0$$
$$S'(s_i + L_p|s_i) = \cos\sigma_0 + w_i w'_i \sin\sigma_0$$

C1

Giving:

$$\boxed{\begin{aligned} w_i &= \sqrt{\frac{S(s_i + L_p|s_i)}{\sin\sigma_0}} \\ w'_i &= \frac{\cos\sigma_0 - C(s_i + L_p|s_i)}{\sqrt{S(s_i + L_p|s_i)\sin\sigma_0}} \end{aligned}}$$

Or in terms of the betatron formulation (see: S7 and S8) with

$\beta = w^2, \; \beta' = 2ww'$

$$\boxed{\begin{aligned} \beta_i &= w_i^2 = \frac{S(s_i + L_p|s_i)}{\sin\sigma_0} \\ \beta'_i &= 2w_i w'_i = \frac{2[\cos\sigma_0 - C(s_i + L_p|s_i)]}{\sin\sigma_0} \end{aligned}}$$

Next, calculate w from the principal orbit expression in phase-amplitude form:

$$\frac{S}{w_i w} = \sin\Delta\psi \qquad\qquad S \equiv S(s|s_i) \;\; \text{etc.}$$

$$\frac{w_i}{w}C + \frac{w'_i}{w}S = \cos\Delta\psi$$

C2

Square and add equations:

$$\left(\frac{S}{w_i w}\right)^2 + \left(\frac{w_i C}{w} + \frac{w'_i S}{w}\right)^2 = 1$$

- This result reflects the structure of the underlying Courant-Snyder invariant (see: S7)

Gives:

$$w^2 = \left(\frac{S}{w_i}\right)^2 + (w_i C + w'_i S)^2$$

Use $w_i, \; w'_i$ previously identified and write out result:

$$\boxed{\begin{aligned} w^2(s) = \beta(s) = \sin\sigma_0 & \frac{S^2(s|s_i)}{S(s_i + L_p|s_i)} \\ & + \frac{S(s_i + L_p|s_i)}{\sin\sigma_0}\left[C(s|s_i) + \frac{\cos\sigma_0 - C(s_i + L_p|s_i)}{S(s_i + L_p|s_i)}S(s|s_i)\right]^2 \end{aligned}}$$

- Formula shows that for a given σ_0 (used to specify lattice focusing strength), *w*(*s*) is given by two linear principal orbits calculated over one lattice period
  - Easy to apply numerically

C3

An alternative way to calculate *w*(*s*) is as follows. 1st apply the phase-amplitude formulas for the principal orbit functions with:

$$s_i \rightarrow s$$
$$s \rightarrow s + L_p$$

$$\Longrightarrow \quad \begin{aligned} C(s + L_p|s) &= \cos\sigma_0 - w(s)w'(s)\sin\sigma_0 \\ S(s + L_p|s) &= w^2(s)\sin\sigma_0 \end{aligned}$$

$$\boxed{w^2(s) = \beta(s) = \frac{S(s + L_p|s)}{\sin\sigma_0} = \frac{\mathbf{M}_{12}(s + L_p|s)}{\sin\sigma_0}}$$

- Formula requires calculation of $S(s + L_p|s)$ at every value of *s* within lattice period
- Previous formula requires one calculation of $C(s|s_i), \; S(s|s_i)$ for $s_i \leq s \leq s_i + L_p$ and any value of s_i

C4

Matrix algebra can be applied to simplify this result:

$$\begin{aligned} \mathbf{M}(s + L_p|s) &= \mathbf{M}(s + L_p|s_i + L_p)\cdot\mathbf{M}(s_i + L_p|s) \\ &= \mathbf{M}(s|s_i)\cdot\mathbf{M}(s_i + L_p|s)\cdot[\mathbf{M}(s|s_i)\cdot\mathbf{M}^{-1}(s|s_i)] \\ &= \mathbf{M}(s|s_i)\cdot\mathbf{M}(s_i + L_p|s_i)\cdot\mathbf{M}^{-1}(s|s_i) \end{aligned}$$

$$\boxed{\mathbf{M}(s + L_p|s) = \mathbf{M}(s|s_i)\cdot\mathbf{M}(s_i + L_p|s_i)\cdot\mathbf{M}^{-1}(s|s_i)}$$

- Using this result with the previous formula allows the transfer matrix to be calculated only once per period from any initial condition
- Using:

$$\mathbf{M} = \begin{pmatrix} C & S \\ C' & S' \end{pmatrix} \qquad \mathbf{M}^{-1} = \begin{pmatrix} S' & -S \\ -C' & C \end{pmatrix}$$

Apply Wronskian condition:

$\det\mathbf{M} = 1$

The matrix formula can be shown to the equivalent to the previous one

- Methodology applied in: Lund, Chilton, and Lee, PRSTAB **9** 064201 (2006) to construct a fail-safe iterative matched envelope including space-charge

C5

S7: Hill's Equation: The Courant-Snyder Invariant and Single Particle Emittance

S7A: Introduction

Constants of the motion can simplify the interpretation of dynamics in physics

- Desirable to identify constants of motion for Hill's equation for improved understanding of focusing in accelerators
- Constants of the motion are not immediately obvious for Hill's Equation due to s-varying focusing forces related to $\kappa(s)$ can add and remove energy from the particle
  - Wronskian symmetry is one useful symmetry
  - Are there other symmetries?

/// Illustrative Example: Continuous Focusing/Simple Harmonic Oscillator

Equation of motion:

$$x'' + k_{\beta 0}^2 x = 0 \qquad k_{\beta 0}^2 = \text{const} > 0$$

Constant of motion is the well-know Hamiltonian/Energy:

$$H = \frac{1}{2}x'^2 + \frac{1}{2}k_{\beta 0}^2 x^2 = \text{const}$$

which shows that the particle moves on an ellipse in x-x' phase-space with:

- Location of particle on ellipse set by initial conditions
- All initial conditions with same energy/H give same ellipse

$$\text{Max/Min}[x] \Leftrightarrow x' = 0$$
$$\text{Max/Min}[x] = \pm\sqrt{2H/k_{\beta 0}^2}$$
$$\text{Max/Min}[x'] \Leftrightarrow x = 0$$
$$\text{Max/Min}[x'] = \pm\sqrt{2H}$$

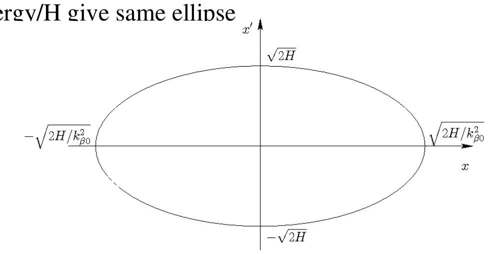

///

Question:

For Hill's equation:

$$x'' + \kappa(s)x = 0$$

does a quadratic invariant exist that can aid interpretation of the dynamics?

Answer we will find:

Yes, the Courant-Snyder invariant

Comments:

- Very important in accelerator physics
  - Helps interpretation of linear dynamics
- Named in honor of Courant and Synder who popularized it's use in Accelerator physics while co-discovering alternating gradient (AG) focusing in a single seminal (and very elegant) paper:

  Courant and Snyder, *Theory of the Alternating Gradient Synchrotron*, Annals of Physics **3**, 1 (1958).
  - Christofolos also understood AG focusing in the same period using a more heuristic analysis

S7B: Derivation of Courant-Snyder Invariant

The phase amplitude method described in S6 makes identification of the invariant elementary. Use the phase amplitude form of the orbit:

$$\boxed{\begin{aligned} x(s) &= A_i w(s)\cos\psi(s) \\ x'(s) &= A_i w'(s)\cos\psi(s) - \frac{A_i}{w(s)}\sin\psi(s) \end{aligned}}$$

$A_i,\ \psi_i = \psi(s_i)$ set by initial at $s = s_i$

where

$$w'' + \kappa(s)w - \frac{1}{w^3} = 0$$

Re-arrange the phase-amplitude trajectory equations:

$$\frac{x}{w} = A_i\cos\psi$$
$$wx' - w'x = A_i\sin\psi$$

square and add the equations to obtain the Courant-Snyder invariant:

$$\boxed{\begin{aligned} \left(\frac{x}{w}\right)^2 + (wx' - w'x)^2 &= A_i^2(\cos^2\psi + \sin^2\psi) \\ &= A_i^2 = \text{const} \end{aligned}}$$

Comments on the Courant-Snyder Invariant:

- Simplifies interpretation of dynamics (will show how shortly)
- Extensively used in accelerator physics
- Quadratic structure in *x*-*x*' defines a rotated ellipse in *x*-*x*' phase space.
- Because $w^2\left(\frac{x}{w}\right)' = wx' - w'x$

  the Courant-Snyder invariant can be alternatively expressed as:

$$\left(\frac{x}{w}\right)^2 + \left[w^2\left(\frac{x}{w}\right)'\right]^2 = \text{const}$$

- *Cannot* be interpreted as a conserved energy!

The point that the Courant-Snyder invariant is *not* a conserved energy should be elaborated on. The equation of motion:

$$x'' + \kappa(s)x = 0$$

Is derivable from the Hamiltonian

$$H = \frac{1}{2}x'^2 + \frac{1}{2}\kappa x^2 \quad\Longrightarrow\quad \begin{aligned}\frac{d}{ds}x &= \frac{\partial H}{\partial x'} = x' \\ \frac{d}{ds}x' &= -\frac{\partial H}{\partial x} = -\kappa x\end{aligned} \quad\Longrightarrow\quad x'' + \kappa x = 0$$

H is the energy:

$$H = \frac{1}{2}x'^2 + \frac{1}{2}\kappa x^2 = T + V \qquad \begin{aligned}T &= \frac{1}{2}x'^2 &&= \text{Kinetic "Energy"} \\ V &= \frac{1}{2}\kappa x^2 &&= \text{Potential "Energy"}\end{aligned}$$

Apply the chain-Rule with *H* = *H*(*x*,*x*';*s*):

$$\frac{dH}{ds} = \frac{\partial H}{\partial s} + \frac{\partial H}{\partial x}\frac{dx}{ds} + \frac{\partial H}{\partial x'}\frac{dx'}{ds}$$

Apply the equation of motion:

$$\frac{d}{ds}x = \frac{\partial H}{\partial x'} \qquad \frac{d}{ds}x' = -\frac{\partial H}{\partial x}$$

$$\frac{dH}{ds} = \frac{\partial H}{\partial s} - \frac{dx'}{ds}\frac{dx}{ds} + \frac{dx}{ds}\frac{dx'}{ds} = \frac{\partial H}{\partial s} = \frac{1}{2}\kappa' x^2 \neq 0$$

$$\Longrightarrow \boxed{H \neq \text{const}}$$

- Energy of a "kicked" oscillator with $\kappa(s) \neq \text{const}$ is not conserved
- Energy should not be confused with the Courant-Snyder invariant

/// Aside: Only for the special case of continuous focusing (i.e., a simple Harmonic oscillator) are the Courant-Snyder invariant and energy simply related:

Continuous Focusing: $\kappa(s) = k_{\beta 0}^2 = \text{const}$

$$\Longrightarrow \quad H = \frac{1}{2}x'^2 + \frac{1}{2}k_{\beta 0}^2 x^2 = \text{const}$$

w equation: $w'' + k_{\beta 0}^2 w - \frac{1}{w^3} = 0$

$$\Longrightarrow \quad w = \sqrt{\frac{1}{k_{\beta 0}}} = \text{const}$$

Courant-Snyder Invariant: $\left(\frac{x}{w}\right)^2 + (wx' - w'x)^2 = \text{const}$

$$\begin{aligned}\Longrightarrow \quad \left(\frac{x}{w}\right)^2 + (wx' - w'x)^2 &= k_{\beta 0}x^2 + \frac{x'^2}{k_{\beta 0}} \\ &= \frac{2}{k_{\beta 0}}\left(\frac{1}{2}x'^2 + \frac{1}{2}\kappa x^2\right) \\ &= \frac{2H}{k_{\beta 0}} = \text{const}\end{aligned}$$

///

Interpret the Courant-Snyder invariant:

$$\boxed{\left(\frac{x}{w}\right)^2 + (wx' - w'x)^2 = A_i^2 = \text{const}}$$

by expanding and isolating terms quadratic terms in *x*-*x*' phase-space variables:

$$\left[\frac{1}{w^2} + w'^2\right]x^2 + 2[-ww']xx' + [w^2]x'^2 = A_i^2 = \text{const}$$

The three coefficients in [...] are functions of *w* and *w*' only and therefore are *functions of the lattice only* (not particle initial conditions). They are commonly called "Twiss Parameters" and are expressed denoted as:

$$\boxed{\begin{aligned}&\gamma x^2 + 2\alpha x x' + \beta x'^2 = A_i^2 = \text{const} \\ &\gamma(s) \equiv \frac{1}{w^2(s)} = \frac{1+\alpha^2(s)}{\beta(s)} \\ &\beta(s) \equiv w^2(s) \\ &\alpha(s) \equiv -w(s)w'(s)\end{aligned}}$$

- Only 2 of the three Twiss parameters are "independent"

  (i.e., *w*, *w*' determine all 3)

The area of the invariant ellipse is:

- Apply standard formulas from Analytic Geometry or calculate

$$\boxed{\text{Area} = \int_{\text{ellipse}} dx dx' = \frac{\pi A_i^2}{\sqrt{\gamma\beta - \alpha^2}} = \pi A_i^2 \equiv \pi\epsilon}$$

where ϵ is the single-particle emittance:

- Emittance is the area of the orbit in *x*-*x*' phase-space divided by π

$$\boxed{\gamma x^2 + 2\alpha x x' + \beta x'^2 = \epsilon}$$

See problem sets for critical point calculation

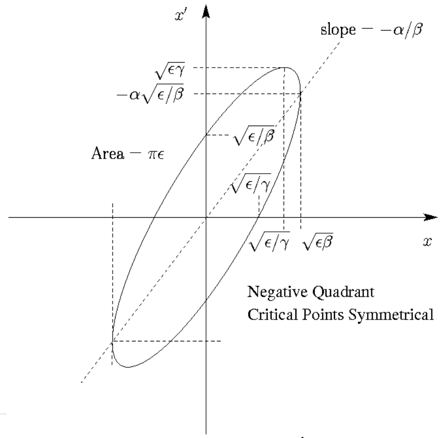

/// Aside: Emittance Units and choices of definition:

x has dimensions of length and *x*' is a dimensionless angle. So *x*-*x*' phase-space area and ϵ has dimensions [[ϵ]] = length. A common choice of units is millimeters (mm) and milliradians (mrad), e.g.,

$$\epsilon = 10 \text{ mm-mrad}$$

The definition of the emittance employed is not unique and different workers use a wide variety of symbols. Some common notational choices:

- $\pi\epsilon \longrightarrow \epsilon \qquad \epsilon \longrightarrow \varepsilon \qquad \epsilon \longrightarrow E$
- Write the emittance values in units with a π, e.g.,

$$\epsilon = 10.5\ \pi - \text{mm-mrad}$$

Use caution! Understand conventions being used before applying results!

///

Properties of Courant-Snyder Invariant:

- The ellipse will rotate and change shape as the particle advances through the focusing lattice, but the instantaneous area of the ellipse ($\pi\epsilon = \text{const}$) remains constant.
- The location of the particle on the ellipse and the size (area) of the ellipse depends on the initial conditions of the particle.
- The orientation of the ellipse is independent of the particle initial conditions. All particles move on nested ellipses.
- Quadratic in the *x*-*x*' phase-space coordinates, but is *not* the transverse particle energy (which is not conserved).

S7C: Lattice Maps

The Courant-Snyder invariant helps us understand the phase-space evolution of the particles. Knowing how the ellipse transforms (twists and rotates without changing area) is equivalent to knowing the dynamics of a *bundle* of particles.

To see this:

General *s*:

$$\gamma x^2 + 2\alpha x x' + \beta x'^2 = \epsilon$$

Initial $s = s_i$:

$$\gamma_i x_i^2 + 2\alpha_i x_i x_i' + \beta_i x_i'^2 = \epsilon$$

$$\beta_i \equiv \beta(s = s_i) \qquad x_i \equiv x(s = s_i)$$
$$\alpha_i \equiv \alpha(s = s_i) \qquad x_i' \equiv x'(s = s_i)$$
$$\gamma_i \equiv \gamma(s = s_i)$$

Apply the components of the transport matrix:

$$\begin{bmatrix} x \\ x' \end{bmatrix} = \mathbf{M}(s|s_i) \cdot \begin{bmatrix} x_i \\ x_i' \end{bmatrix} = \begin{bmatrix} C(s|s_i) & S(s|s_i) \\ C'(s|s_i) & S'(s|s_i) \end{bmatrix} \cdot \begin{bmatrix} x_i \\ x_i' \end{bmatrix}$$

Invert 2x2 matrix and apply det **M** = 1 (Wronskian):

$$\Longrightarrow \quad \begin{bmatrix} x_i \\ x_i' \end{bmatrix} = \begin{bmatrix} S' & -S \\ -C' & C \end{bmatrix} \cdot \begin{bmatrix} x \\ x' \end{bmatrix} \qquad C \equiv C(s|s_i), \text{ etc.}$$

Insert expansion for $x_i,\ x'_i$ in the initial ellipse expression, collect factors of x^2, xx', and x'^2, and equate to general s ellipse expression:

$$\begin{aligned}&[\gamma_i S'^2 - 2\alpha_i S'C' + \beta_i C'^2]x^2 \\ &+2[-\gamma_i SS' + \alpha_i(CS' + SC') - \beta_i CC']xx' \\ &+[\gamma_i S^2 - 2\alpha_i SC + \beta_i C^2]x'^2 \\ &= \gamma x^2 + 2\alpha x x' + \beta x'^2\end{aligned}$$

Collect coefficients of x^2, xx', and x'^2 and summarize in matrix form:

$$\boxed{\begin{bmatrix}\gamma \\ \alpha \\ \beta\end{bmatrix} = \begin{bmatrix} S'^2 & -2C'S' & C'^2 \\ -SS' & CS'+SC' & -CC' \\ S^2 & -2CS & C^2\end{bmatrix}\cdot\begin{bmatrix}\gamma_i \\ \beta_i \\ \alpha_i\end{bmatrix}}$$

This result can be applied to illustrate how a bundle of particles will evolve from an initial location in the lattice subject to the linear focusing optics in the machine using only principal orbits C, S, C', and S'

- Principal orbits will generally need to be calculated numerically
  - Intuition can be built up using simple analytical results (hard edge etc)

/// Example: Ellipse Evolution in a simple kicked focusing lattice

Drift: $\begin{bmatrix} C & S \\ C' & S'\end{bmatrix} = \begin{bmatrix} 1 & s-s_i \\ 0 & 1\end{bmatrix}$

$$\begin{aligned}\gamma &= \gamma_i \\ \alpha &= -\gamma_i(s-s_i) + \alpha_i \\ \beta &= \gamma_i(s-s_i)^2 - 2\alpha_i(s-s_i) + \beta_i\end{aligned}$$

Thin Lens: focal length f $\begin{bmatrix} C & S \\ C' & S'\end{bmatrix} = \begin{bmatrix} 1 & 0 \\ -1/f & 1\end{bmatrix}$

$$\begin{aligned}\gamma &= \gamma_i + 2\alpha_i/f + \beta_i/f^2 \\ \alpha &= -\beta_i/f + \alpha_i \\ \beta &= \beta_i\end{aligned}$$

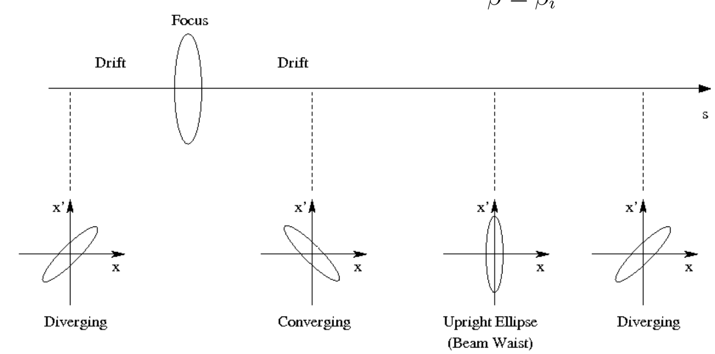

For further examples of phase-space ellipse evolutions in standard lattices, see: S6G ///

S8: Hill's Equation: The Betatron Formulation of the Particle Orbit and Maximum Orbit Excursions S8A: Formulation

The phase-amplitude form of the particle orbit analyzed in S6 of

$$\boxed{x(s) = A_i w(s)\cos\psi(s)} \qquad [[w]] = (\text{meters})^{1/2}$$

is not a unique choice. Here, w has dimensions [[w]] = (meters)^(1/2), which can render it inconvenient in applications. Due to this and the utility of the Twiss parameters used in describing orientation of the phase-space ellipse associated with the Courant-Snyder invariant (see: S7) on which the particle moves, it is convenient to define an alternative, Betatron representation of the orbit with:

$$x(s) = \sqrt{\epsilon}\sqrt{\beta(s)}\cos\psi(s)$$

Betatron function: $\beta(s) \equiv w^2(s)$

Emittance: $\epsilon \equiv A_i^2 = \text{const}$

Phase: $\psi(s) = \psi_i + \int_{s_i}^{s}\frac{d\tilde{s}}{\beta(\tilde{s})} = \psi_i + \Delta\psi(s)$

- The betatron function has dimensions [[β]] = meters

Comments:

- Use of the symbol β for the betatron function does not result in confusion with relativistic factors such as β_b since the context of use will make clear
  - Relativistic factors often absorbed in lattice focusing function and do not directly appear in the dynamical descriptions
- The initial phase ψ_i will differer in the w- and betatron phase-amplitude forms in order to match initial conditions in x and x' at
  - We do not distinguish for reasons of notational simplicity
- The change in phase $\Delta\psi$ is the same for both formulations:

$$\Delta\psi(s) = \int_{s_i}^{s}\frac{d\tilde{s}}{w^2(\tilde{s})} = \int_{s_i}^{s}\frac{d\tilde{s}}{\beta(\tilde{s})}$$

Add material on initial condition correspondence in future editions of notes

From the equation for w:

$$w''(s) + \kappa(s)w(s) - \frac{1}{w^3(s)} = 0$$

$$w(s + L_p) = w(s) \qquad w(s) > 0$$

the betatron function is described by:

$$\boxed{\begin{aligned} &\frac{1}{2}\beta(s)\beta'(s) - \frac{1}{4}\beta'^2(s) + \kappa(s)\beta^2(s) = 1 \\ &\beta(s + L_p) = \beta(s) \qquad \beta(s) > 0 \end{aligned}}$$

- The betatron function can, analogously to the w-function, as a special function defined by the periodic lattice
- Again, the equation is nonlinear and must generally be solved numerically

S8B: Maximum Orbit Excursions

From the orbit equation

$$x = \sqrt{\epsilon\beta}\cos\psi$$

the maximum and minimum possible particle excursions occur where:

$$\cos\psi = +1 \quad \longrightarrow \quad \text{Max}[x] = \sqrt{\epsilon\beta(s)} = \sqrt{\epsilon}w(s)$$

$$\cos\psi = -1 \quad \longrightarrow \quad \text{Min}[x] = -\sqrt{\epsilon\beta(s)} = -\sqrt{\epsilon}w(s)$$

Thus, the max radial extent of *all* particle oscillations $\text{Max}[x] \equiv x_m$ in the beam distribution occurs for the particle with the max single particle emittance since the particles move on nested ellipses:

$$\boxed{\begin{aligned} &\text{Max}[\epsilon] \equiv \epsilon_m \\ &x_m(s) = \sqrt{\epsilon_m\beta(s)} = \sqrt{\epsilon_m}w(s) \end{aligned}}$$

- Assumes sufficient numbers of particles to populate all possible phases
- x_m corresponds to the min possible machine aperture to prevent particle losses
  - Practical aperture choice influenced by: resonance effects due to nonlinear applied fields, space-charge, scattering, finite particle lifetime, ...

From:

$$w''(s) + \kappa(s)w(s) - \frac{1}{w^3(s)} = 0$$

$$w(s + L_p) = w(s) \qquad w(s) > 0$$

We immediately obtain an equation for the maximum locus (envelope) of radial particle excursions $x_m = \sqrt{\epsilon_m}w$ as:

$$\boxed{\begin{aligned} &x_m''(s) + \kappa(s)x_m(s) - \frac{\epsilon_m^2}{x_m^3(s)} = 0 \\ &x_m(s + L_p) = x_m(s) \qquad x_m(s) > 0 \end{aligned}}$$

Comments:

- Equation is analogous to the statistical envelope equation derived by J.J. Barnard in the Intro Lectures when a space-charge term is added and the max single particle emittance is interpreted as a statistical emittance
  - correspondence will become more concrete in later lectures
- This correspondence will be developed more extensively in later lectures on Transverse Centroid and Envelope Descriptions of Beam Evolution and Transverse Equilibrium Distributions

S9: Momentum Spread Effects and Bending

S9A: Formulation

Except for brief digressions in S1 and S4, we have concentrated on particle dynamics where all particles have the design longitudinal momentum:

$$\boxed{p_s = m\gamma_b\beta_b c = \text{const}}$$

Realistically, there will always be a finite spread of particle momentum within a beam slice, so we take:

$$\boxed{\begin{aligned} &p_s = p_0 + \delta p \\ &p_0 \equiv m\gamma_b\beta_b c = \text{Design Momentum} \\ &\delta p \equiv \text{Off Momentum} \end{aligned}}$$

Typical values of momentum spread in a beam with a single species of particles with conventional sources and accelerating structures:

$$\frac{|\delta p|}{p_0} \sim 10^{-2} \rightarrow 10^{-6}$$

The spread of particle momentum can modify particle orbits, particularly when dipole bends are present since the bend radius depends strongly on the particle momentum

To better understand this effect, we analyze the particle equations of motion with leading-order momentum spread (see: S1) effects retained:

$$x''(s) + \left[\frac{1}{R^2(s)}\frac{1-\delta}{1+\delta} + \frac{\kappa_x(s)}{(1+\delta)^n}\right] x(s) = \frac{\delta}{1+\delta}\frac{1}{R(s)}$$

$$y''(s) + \frac{\kappa_y(s)}{(1+\delta)^n} y(s) = 0$$

$R(s) =$ Local Bend Radius
for design momentum p_0
($R \rightarrow \infty$ in straight sections)

Magnetic Dipole Bend

$$\frac{1}{R(s)} = \frac{B_y^a|_{\text{dipole}}}{[B\rho]}$$

$$[B\rho] = \frac{p_0}{q}$$

$$\delta \equiv \frac{\delta p}{p_0}$$

$\kappa_{x,y} =$ Focusing Functions (using design momentum)

$$n = \begin{cases} 1, & \text{Magnetic Quadrupoles} \\ 2, & \text{Solenoids, Electric Quadrupoles} \end{cases}$$

Neglects:
- Space-charge: $\phi \rightarrow 0$
- Nonlinear applied focusing: $\mathbf{E}^a$, $\mathbf{B}^a$ contain only linear focus terms
- Acceleration: $p_0 = m\gamma_b\beta_b = \text{const}$

In the equations of motion, it is important to understand that B_y^a of the magnetic bends are set from the radius R required by the design particle orbit (see: S1 for details)
- Equations must be modified slightly for electric bends (see S1)
- y-plane bends also require modification

The focusing strengths are defined with respect to the design momentum:

$$\kappa_x = \begin{cases} \frac{qG}{m\gamma_b\beta_b^2c^2}, & G = \text{Electric Quadrupole Gradient} \\ \frac{qG}{m\gamma_b\beta_b c}, & G = \text{Magnetic Quadrupole Gradient} \\ \frac{qB_{z0}}{4m\gamma_b^2\beta_b^2c^2}, & B_{z0} = \text{Solenoidal Magnetic Field} \end{cases}$$

γ_b, β_b calculated from p_0

Terms in the equations of motion associated with momentum spread (δ) can be lumped into two classes:

1) Chromatic -- Associated with Focusing
2) Dispersive -- Associated with Dipole Bends

S9B: Chromatic Effects

Present in both x- and y-equations of motion and result from applied focusing strength changing with deviations in momentum:

$$x''(s) + \frac{\kappa_x(s)}{(1+\delta)^n} x(s) = 0$$

$$y''(s) + \frac{\kappa_y(s)}{(1+\delta)^n} y(s) = 0$$

$R \rightarrow \infty$

to neglect bending terms

$\kappa_{x,y} =$ Focusing Functions
with γ_b, β_b calculated from p_0

- Generally of lesser importance (smaller corrections) relative to dispersive terms (S9C) *except* where the beam is focused onto a target (small spot) or when momentum spreads are large
- Lectures by J.J. Barnard on Heavy Ion Fusion and Final Focusing will overview consequences of chromatic effects in final focus optics

S9C: Dispersive Effects

Present in only the x-equation of motion and result from bending. Neglecting chromatic terms:

$$x''(s) + \underbrace{\left[\frac{1}{R^2(s)}\frac{1-\delta}{1+\delta} + \kappa_x(s)\right]}_{\text{Term 1}} x(s) = \underbrace{\frac{\delta}{1+\delta}\frac{1}{R(s)}}_{\text{Term 2}}$$

Particles are bent at different radii when the momentum deviates from the design value ($\delta \neq 0$) leading to changes in the particle orbit
- Dispersive terms contain the bend radius R

Generally, the bend radii R are large and δ is small, and we can take to leading order:

Term 1: $\left[\frac{1}{R^2}\frac{1-\delta}{1+\delta} + \kappa_x\right] x \simeq \kappa_x x$

Term 2: $\frac{\delta}{1+\delta}\frac{1}{R} \simeq \frac{\delta}{R}$

The equations of motion then become:

$$\boxed{\begin{aligned} x''(s) + \kappa_x(s)x(s) &= \frac{\delta}{R(s)} \\ y''(s) + \kappa_y(s)y(s) &= 0 \end{aligned}}$$

- The y-equation is not changed from the usual Hill's Equation

Generally, the *x*-equation is solved for periodic lattices by exploiting the linear structure of the equation and linearly resolving:

$$\boxed{\begin{aligned} &x(s) = x_h(s) + x_p(s) \\ &\qquad x_h \equiv \text{Homogeneous Solution} \\ &\qquad x_p \equiv \text{Particular Solution} \end{aligned}}$$

where x_h is the *general* solution to the Hill's Equation:

$$\boxed{x_h''(s) + \kappa_x(s)x_h(s) = 0}$$

and x_p is the *periodic* solution to:

$$\boxed{\begin{aligned} &x_p = \delta \cdot D && D''(s) + \kappa_x(s)D(s) = \frac{1}{R(s)} \\ &D \equiv \text{Disperson Function} && D(s + L_p) = D(s) \end{aligned}}$$

This convenient resolution of the orbit $x(s)$ can *always* be made because the homogeneous solution will be adjusted to match any initial condition

Note that δD provides a measure of the offset of the particle orbit relative to the design orbit resulting from a small deviation of momentum (δ)

- $x(s) = 0$ defines the design orbit
- $[[D]] = \text{meters}$
  $\delta \cdot D = \text{Orbit offset in meters}$

/// Example: Simple piecewise constant focusing and bending lattice

$L_p = 0.5$ m $\quad \kappa = 20$ in Focusing
$\eta = 0.5 \quad R = 15$ m, in bend, 25% Occupancy

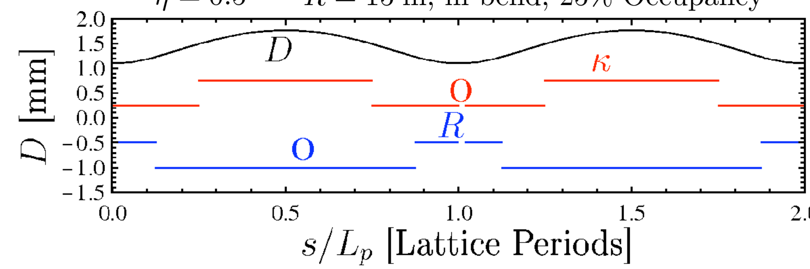

///

/// Example: Dispersion broadens the *x*-distribution

Uniform Bundle of particles D = 0

Same Bundle of particles D $\neq$ 0

- Gaussian distribution of momentum spread distorts the x-y distribution extents in x but not in y

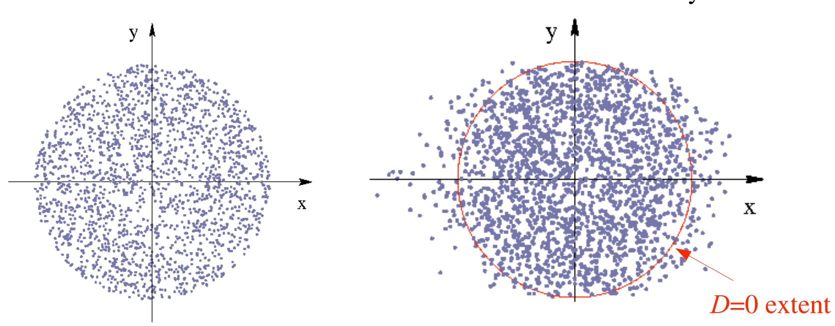

///

Many rings are designed to focus the dispersion function $D(s)$ to small values in straight sections even though the lattice has strong bends

- Desirable since it allows smaller beam sizes at locations near where $D = 0$ and these locations can be used to insert and extract (kick) the beam into and out of the ring with minimal losses
  - Since average value of D is dictated by ring size and focusing strength (see example next page) this variation in values can lead to D being larger in other parts of the ring
- Quadrupole triplet focusing lattices are often employed in rings since the optics allows sufficient flexibility to tune D without dramatically changing particle phase advances

/// Example: Continuous Focusing in a Continuous Bend

$$\kappa_x(s) = k_{\beta 0}^2 = \text{const}$$
$$R(s) = R = \text{const}$$

Dispersion equation becomes:

$$D'' + k_{\beta 0}^2 D = \frac{1}{R}$$

With solution:

$$D = \frac{1}{k_{\beta 0}^2 R} = \text{const}$$

From this result we can crudely estimate the average value of the dispersion function in a ring with periodic focusing by taking:

$$\begin{aligned} R &= \text{Avg Radius Ring} \\ L_p &= \text{Lattice Period (Focusing)} \\ \sigma_{0x} &= x\text{-Plane Phase Advance} \end{aligned}$$

$$\Longrightarrow \quad k_{\beta 0} \sim \frac{\sigma_0}{L_p} \qquad \Longrightarrow \quad D \sim \frac{L_p^2}{\sigma_0^2 R}$$

///

S10: Acceleration and Normalized Emittance

S10A: Introduction

If the beam is accelerated longitudinally, the x-particle equation of motion (see: S1 and S2) is:

$$\boxed{x'' + \frac{(\gamma_b\beta_b)'}{(\gamma_b\beta_b)}x' + \kappa_x x = -\frac{q}{m\gamma_b^3\beta_b^2c^2}\frac{\partial\phi}{\partial x}}$$

Analogous equation holds in y

Neglects:
- Nonlinear applied focusing fields
- Momentum spread effects

Comments:
- γ_b, β_b are regarded as prescribed functions of s set by the acceleration schedule of the machine
- Variations in γ_b, β_b due to acceleration must be included in and/or compensated by adjusting the strength of the optics via κ_x, κ_y
  - Scaling different for electric and magnetic optics (see: S2)

Comments Continued:
- In typical accelerating systems, changes in $\gamma_b\beta_b$ are slow and the fractional changes in the orbit induced by acceleration are small
  - Exception near an injector since the beam is often not yet energetic
- The acceleration term:

$$\frac{(\gamma_b\beta_b)'}{(\gamma_b\beta_b)} > 0$$

will act to damp particle oscillations (see following slides for motivation)

Even with acceleration, we will find that there is a Courant-Snyder invariant (normalized emittance) that is valid in an analogous context as in the case without acceleration provided phase-space coordinates are chosen to compensate for the damping of particle oscillations

Acceleration Factor: Characteristics of

Relativistic Factor

$$\boxed{\gamma_b\beta_b \simeq \begin{cases} \gamma_b, & \text{Relativistic Limit} \\ \beta_b, & \text{Nonrelativistic Limit} \end{cases}} \qquad \gamma_b \equiv \frac{1}{\sqrt{1-\beta_b^2}}$$

Beam/Particle Kinetic Energy:

$$\boxed{\mathcal{E}_b(s) = (\gamma_b - 1)mc^2 = \text{Beam Kinetic Energy}}$$

- Function of s specified by Acceleration schedule for transverse dynamics
- See Appendix D for calculation of $\mathcal{E}_b$ and $\gamma_b\beta_b$ from longitudinal dynamics and J.J. Barnard lectures on Longitudinal Dynamics

Approximate energy gain from average gradient:

$$\boxed{\mathcal{E}_b \simeq \mathcal{E}_i + G(s - s_i)} \qquad \begin{aligned} \mathcal{E}_i &= \text{const} = \text{Initial Energy} \\ G &= \text{const} = \text{Average Gradient} \end{aligned}$$

- Real energy gain will be rapid when going through discreet acceleration gaps

$$\boxed{\mathcal{E}_b \simeq \begin{cases} \gamma_b mc^2, & \text{Relativistic Limit} \\ \frac{1}{2}m\beta_b^2c^2, & \text{Nonrelativistic Limit} \end{cases}}$$

Identify relativistic factor with average gradient energy gain:

Relativistic Limit:

$$\gamma_b \simeq \frac{\mathcal{E}_b}{mc^2} = \frac{\mathcal{E}_i}{mc^2} + \frac{G}{mc^2}(s - s_i)$$

$$\Longrightarrow \boxed{\frac{(\gamma_b\beta_b)'}{(\gamma_b\beta_b)} \simeq \frac{\gamma_b'}{\gamma_b} \simeq \frac{1}{\left(\frac{\mathcal{E}_i}{G} - s_i\right) + s} \sim \frac{1}{s}}$$

Nonrelativistic Limit:

$$\beta_b \simeq \sqrt{2\frac{\mathcal{E}_b}{mc^2}} = \sqrt{2\frac{\mathcal{E}_i}{mc^2} + 2\frac{G}{mc^2}(s - s_i)}$$

$$\Longrightarrow \boxed{\frac{(\gamma_b\beta_b)'}{(\gamma_b\beta_b)} \simeq \frac{\beta_b'}{\beta_b} = \frac{1/2}{\left(\frac{\mathcal{E}_i}{G} - s_i\right) + s} \sim \frac{1}{2s}}$$

- Expect Relativistic and Nonrelativistic motion to have similar solutions
  - Parameters for each case will often be quite different

/// Aside: Acceleration and Continuous Focusing Orbits with $\kappa_x = k_{\beta 0}^2 = \text{const}$

Assume relativistic motion and negligible space-charge:

$$\frac{(\gamma_b\beta_b)'}{(\gamma_b\beta_b)} \simeq \frac{\gamma_b'}{\gamma_b} = \frac{1}{\left(\frac{\mathcal{E}_i}{G} - s_i\right) + s} \qquad \frac{\partial\phi}{\partial x} \simeq 0$$

Then the equation of motion reduces to:

$$\boxed{x'' + \frac{1}{\left(\frac{\mathcal{E}_i}{G} - s_i\right) + s}x' + k_{\beta 0}^2 x = 0}$$

This equation is the equation of a Bessel Function of order zero:

$$\frac{d^2x}{d\xi^2} + \frac{1}{\xi}\frac{dx}{d\xi} + x = 0 \qquad \xi = k_{\beta 0}s + k_{\beta 0}\left(\frac{\mathcal{E}_i}{G} - s_i\right)$$

$$x = C_1 J_0(\xi) + C_2 Y_0(\xi)$$

$$x' = -C_1 k_{\beta 0} J_1(\xi) - C_2 k_{\beta 0} Y_1(\xi)$$

$C_1 = \text{const}$ $\quad C_2 = \text{const}$

$J_n =$ Order n Bessel Func (1st kind)

$Y_n =$ Order n Bessel Func (2nd kind)

Solving for the constants in terms of the particle initial conditions:

$$\begin{bmatrix} x_i \\ x_i' \end{bmatrix} = \begin{bmatrix} J_0(\xi_i) & Y_0(\xi_i) \\ -k_{\beta 0}J_1(\xi_i) & -k_{\beta 0}Y_1(\xi_i) \end{bmatrix} \cdot \begin{bmatrix} C_1 \\ C_2 \end{bmatrix}$$

$$x_i \equiv x(s = s_i) \qquad \xi_i \equiv k_{\beta 0}\frac{\mathcal{E}_i}{G} = \xi(s = s_i)$$
$$x_i' \equiv x'(s = s_i)$$

Invert matrix to solve for constants in terms of initial conditions:

$$\Longrightarrow \begin{bmatrix} C_1 \\ C_2 \end{bmatrix} = \frac{1}{\Delta}\begin{bmatrix} -k_{\beta 0}Y_1(\xi_i) & -Y_0(\xi_i) \\ k_{\beta 0}J_1(\xi_i) & J_0(\xi_i) \end{bmatrix} \cdot \begin{bmatrix} x_i \\ x_i' \end{bmatrix}$$

$$\Delta \equiv k_{\beta 0}[Y_0(\xi_i)J_1(\xi_i) - J_0(\xi_i)Y_1(\xi_i)]$$

Comments:

- Bessel functions behave like damped harmonic oscillators
  - See any texts on Mathematical Physics or Applied Mathematics
- Nonrelativistic limit solution is *not* described by a Bessel Function solution
  - Properties of solution will be similar though (similar special function)
  - The coefficient in the damping term $\propto x'$ has a factor of 2 difference, preventing exact Bessel function form

Using this solution, plot the orbit for (contrived parameters for illustration only):

$$k_{\beta 0} = \frac{\sigma_0}{L_p} \qquad \sigma_0 = 90^\circ/\text{Period} \qquad \mathcal{E}_i = 1000 \text{ MeV}$$
$$L_p = 0.5 \text{ m} \qquad G = 100 \text{ MeV/m}$$
$$x(0) = 10 \text{ mm} \qquad s_i = 0$$
$$x'(0) = 0 \text{ mrad}$$

$$\frac{\gamma_{bi}}{\gamma_b} = \frac{1}{1 + (G/\mathcal{E}_i)(s - s_i)}$$

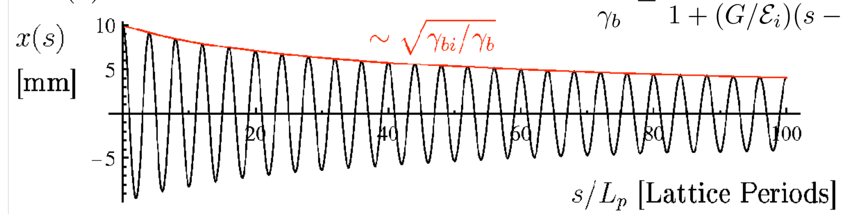

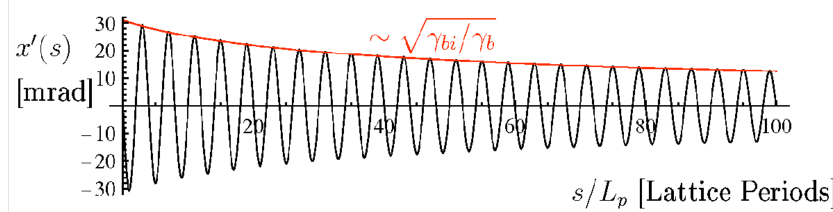

- Solution shows damping: phase volume scaling $\sim 1/(\gamma_b\beta_b) \simeq 1/\gamma_b$ ///

S10B: Transformation to Normal Form

"Guess" transformation to apply motivated by conjugate variable arguments (see: J.J. Barnard, Intro. Lectures)

$$\boxed{\tilde{x} \equiv \sqrt{\gamma_b\beta_b}\,x}$$

Then:

$$x = \frac{1}{\sqrt{\gamma_b\beta_b}}\tilde{x}$$
$$x' = \frac{1}{\sqrt{\gamma_b\beta_b}}\tilde{x}' - \frac{1}{2}\frac{(\gamma_b\beta_b)'}{(\gamma_b\beta_b)^{3/2}}\tilde{x}$$
$$x'' = \frac{1}{\sqrt{\gamma_b\beta_b}}\tilde{x}'' - \frac{(\gamma_b\beta_b)'}{(\gamma_b\beta_b)^{3/2}}\tilde{x}' + \left[\frac{3}{4}\frac{(\gamma_b\beta_b)'^2}{(\gamma_b\beta_b)^{5/2}} - \frac{1}{2}\frac{(\gamma_b\beta_b)''}{(\gamma_b\beta_b)^{3/2}}\right]\tilde{x}$$

The inverse phase-space transforms will also be useful later:

$$\tilde{x} = \sqrt{\gamma_b\beta_b}\,x$$
$$\tilde{x}' = \sqrt{\gamma_b\beta_b}\,x' + \frac{1}{2}\frac{(\gamma_b\beta_b)'}{\sqrt{\gamma_b\beta_b)}}x$$

Applying these results, the particle x- equation of motion with acceleration becomes:

$$\tilde{x}'' + \left[\kappa_x + \frac{1}{4}\frac{(\gamma_b\beta_b)'^2}{(\gamma_b\beta_b)^2} - \frac{1}{2}\frac{(\gamma_b\beta_b)''}{(\gamma_b\beta_b)}\right]\tilde{x} = -\frac{q}{m\gamma_b^2\beta_b c^2}\frac{\partial\phi}{\partial\tilde{x}}$$

Note:

- Factor of $\gamma_b\beta_b$ difference from untransformed expression in the space-charge coupling coefficient

It is instructive to also transform the Possion equation associated with the space-charge term:

$$\left(\frac{\partial^2}{\partial x^2} + \frac{\partial^2}{\partial y^2}\right)\phi = -\frac{\rho}{\epsilon_0}$$

Transform:

$$\frac{\partial^2}{\partial x^2} = \left(\frac{\partial\tilde{x}}{\partial x}\frac{\partial}{\partial\tilde{x}}\right)\left(\frac{\partial\tilde{x}}{\partial x}\frac{\partial}{\partial\tilde{x}}\right) = \gamma_b\beta_b\frac{\partial^2}{\partial\tilde{x}^2}$$
$$\frac{\partial^2}{\partial y^2} = \left(\frac{\partial\tilde{y}}{\partial y}\frac{\partial}{\partial\tilde{y}}\right)\left(\frac{\partial\tilde{y}}{\partial y}\frac{\partial}{\partial\tilde{y}}\right) = \gamma_b\beta_b\frac{\partial^2}{\partial\tilde{y}^2}$$

Using these results, Poisson's equation becomes:

$$\left(\frac{\partial^2}{\partial\tilde{x}^2} + \frac{\partial^2}{\partial\tilde{y}^2}\right)\phi = -\frac{\rho}{\gamma_b\beta_b\epsilon_0}$$

Or defining a transformed potential $\tilde{\phi}$

$$\tilde{\phi} = \gamma_b\beta_b\phi$$
$$\left(\frac{\partial^2}{\partial\tilde{x}^2} + \frac{\partial^2}{\partial\tilde{y}^2}\right)\tilde{\phi} = -\frac{\rho}{\epsilon_0}$$

Applying these results, the x-equation of motion with acceleration becomes:

$$\tilde{x}'' + \left[\kappa_x + \frac{1}{4}\frac{(\gamma_b\beta_b)'^2}{(\gamma_b\beta_b)^2} - \frac{1}{2}\frac{(\gamma_b\beta_b)''}{(\gamma_b\beta_b)}\right]\tilde{x} = -\frac{q}{m\gamma_b^3\beta_b^2c^2}\frac{\partial\tilde{\phi}}{\partial\tilde{x}}$$

- Usual form of the space-charge coefficient with $\gamma_b^3\beta_b^2$ rather than $\gamma_b^2\beta_b$ is restored when expressed in terms of the transforme $\tilde{\phi}$ otential

An additional step can be taken to further stress the correspondence between the transformed system with acceleration and the untransformed system in the absence of acceleration.

Denote an effective focusing strength:

$$\tilde{\kappa}_x \equiv \kappa_x + \frac{1}{4}\frac{(\gamma_b\beta_b)'^2}{(\gamma_b\beta_b)^2} - \frac{1}{2}\frac{(\gamma_b\beta_b)''}{(\gamma_b\beta_b)}$$

$\tilde{\kappa}_x$ incorporates acceleration terms beyond $\gamma_b,\ \beta_b$ factors already included in the definition of κ_x (see: S2):

$$\kappa_x = \begin{cases} \frac{qG}{m\gamma_b\beta_b^2c^2}, & G = \text{Electric Quadrupole Gradient} \\ \frac{qG}{m\gamma_b\beta_b c}, & G = \text{Magnetic Quadrupole Gradient} \\ \frac{qB_{z0}}{4m\gamma_b^2\beta_b^2c^2} & B_{z0} = \text{Solenoidal Magnetic Field} \end{cases}$$

The transformed equation of motion with acceleration then becomes:

$$\tilde{x}'' + \tilde{\kappa}_x\tilde{x} = -\frac{q}{m\gamma_b^3\beta_b^2c^2}\frac{\partial\tilde{\phi}}{\partial\tilde{x}}$$

The transformed equation with acceleration has the same form as the equation in the absence of acceleration. If space-charge is negligible ($\phi \rightarrow 0$) we have:

Accelerating System — Non-Accelerating System

$$\tilde{x}'' + \tilde{\kappa}_x \tilde{x} = 0 \qquad \Longleftrightarrow \qquad x'' + \kappa_x x = 0$$

Therefore, *all previous analysis* on phase-amplitude methods and Courant-Snyder invariants associated with Hill's equation in *x-x*' phase-space can be immediately applied to $\tilde{x} - \tilde{x}'$ phase-space for an accelerating beam

$$\boxed{\begin{aligned} &\left(\frac{\tilde{x}}{\tilde{w}_x}\right)^2 + (\tilde{w}_x \tilde{x}' - \tilde{w}_x' \tilde{x})^2 = \tilde{\epsilon} = \text{const} \\ &\tilde{w}_x'' + \tilde{\kappa}\tilde{w}_x - \frac{1}{\tilde{w}_x^3} = 0 \\ &\tilde{w}_x(s + L_p) = \tilde{w}_x(s) \\ &\pi\tilde{\epsilon} = \text{Area traced by orbit} = \text{const} \\ &\qquad \text{in } \tilde{x}\text{-}\tilde{x}' \text{ phase-space} \end{aligned}}$$

- Focusing field strengths need to be adjusted to maintain periodicity of κ_x in the presence of acceleration
  - Not possible to do exactly, but can be approximate for weak acceleration

S10C: Phase Space Relation Between Transformed and UnTransformed Systems

It is instructive to relate the transformed phase-space area in tilde variables to the usual *x-x*' phase area:

$$d\tilde{x} \otimes d\tilde{x}' = |J| dx \otimes dx'$$

where *J* is the Jacobian:

$$J \equiv \det \begin{bmatrix} \frac{\partial \tilde{x}}{\partial x}, & \frac{\partial \tilde{x}}{\partial x'} \\ \frac{\partial \tilde{x}'}{\partial x} & \frac{\partial \tilde{x}'}{\partial x'} \end{bmatrix}$$

$$= \det \begin{bmatrix} \sqrt{\gamma_b \beta_b} & 0 \\ \frac{1}{2}\frac{(\gamma_b\beta_b)'}{\sqrt{\gamma_b\beta_b}} & \sqrt{\gamma_b\beta_b} \end{bmatrix} = \gamma_b \beta_b$$

Apply the inverse transforms derived previously

Thus:

$$\boxed{d\tilde{x} \otimes d\tilde{x}' = \gamma_b \beta_b \, dx \otimes dx'}$$

Based on this area transform, if we define the (instantaneous) phase space area of the orbit trance in *x-x*' to be $\pi\epsilon_x$ "regular emittance", then this emittance is related to the "normalized emittance" $\tilde{\epsilon}_x$ in $\tilde{x} - \tilde{x}'$ phase-space by:

$$\boxed{\begin{aligned} \tilde{\epsilon}_x &= \gamma_b \beta_b \epsilon_x \\ &\equiv \text{Normalized Emittance} \equiv \epsilon_{nx} \end{aligned}}$$

- Factor $\gamma_b \beta_b$ compensates for acceleration induced damping in particle orbits
- Normalized emittance is very important in design of lattices to transport accelerating beams
  - Designs usually made assuming conservation of normalized emittance
- Same result that J.J. Barnard motivated in the Intro. Lectures using alternative methods

Appendix D: Accelerating Fields and Calculation of Changes in gamma*beta

The transverse particle equation of motion with acceleration was derived in a Cartesian system by approximating (see: S1):

$$\frac{d}{dt}\left(m\gamma\frac{d\mathbf{x}_\perp}{dt}\right) \simeq \quad q\mathbf{E}_\perp^a + q\beta_b c\hat{\mathbf{z}} \times \mathbf{B}_\perp^a + qB_z^a \mathbf{v}_\perp \times \hat{\mathbf{z}} \quad - q\frac{1}{\gamma_b^2}\frac{\partial \phi}{\mathbf{x}_\perp}$$

using

$$m\frac{d}{dt}\left(\gamma\frac{d\mathbf{x}_\perp}{dt}\right) \simeq m\gamma_b\beta_b^2 c^2 \left[\mathbf{x}_\perp'' + \frac{(\gamma_b\beta_b)'}{(\gamma_b\beta_b)}\mathbf{x}_\perp'\right]$$

to obtain:

$$\boxed{\begin{aligned} \mathbf{x}_\perp'' + \frac{(\gamma_b\beta_b)'}{(\gamma_b\beta_b)}\mathbf{x}_\perp' = \frac{q}{m\gamma_b\beta_b^2c^2}\mathbf{E}_\perp^a + \frac{q}{m\gamma_b\beta_b c}\hat{\mathbf{z}} \times \mathbf{B}_\perp^a + \frac{qB_z^a}{m\gamma_b\beta_b c}\mathbf{x}_\perp' \times \hat{\mathbf{z}} \\ - \frac{q}{\gamma_b^3\beta_b^2c^2}\frac{\partial}{\partial \mathbf{x}_\perp}\phi \end{aligned}}$$

D1

Changes in $\gamma_b\beta_b$ are calculated from the longitudinal particle equation of motion:

$$\boxed{\underbrace{\frac{d}{dt}\left(m\gamma\frac{dz}{dt}\right)}_{\text{Term 1}} \simeq \underbrace{qE_z^a}_{\text{Term 2}} \underbrace{- q(v_xB_y^a - v_yB_x^a)}_{\text{Term 3}} - q\frac{\partial\phi}{\partial z}}$$

Using steps similar to those in S1, we approximate terms:

$$\frac{dz}{dt} = v_z \simeq \beta_b c \qquad \gamma \simeq \gamma_b$$

$$\frac{d}{dt} \simeq \beta_b c\frac{d}{ds}$$

Term 1: $\displaystyle \frac{d}{dt}\left(\gamma\frac{dz}{dt}\right) \simeq c^2\beta_b(\gamma_b\beta_b)'$

Term 2: $\displaystyle \frac{q}{m}E_z^a \simeq -\frac{q}{m}\frac{\partial\phi^a}{\partial s}\Big|_{x=y=0}$

- ϕ^a is a quasi-static approximation accelerating potential (see next pages)

Term 3: $\displaystyle -q(v_xB_y^a - v_yB_x^a) = -q\left(\frac{dx}{dt}B_y^a - \frac{dy}{dt}B_x^a\right) \simeq 0$

- Transverse magnetic fields typically only weakly change particle energy and terms can be neglected relative to others

D2

The longitudinal particle equation of motion for $\gamma_b,\ \beta_b$ then reduces to:

$$\boxed{\beta_b(\gamma_b\beta_b)' \simeq -\frac{q}{mc^2}\frac{\partial\phi^a}{\partial s}\Big|_{x=y=0}}$$

Some algebra then shows that:

$$\gamma_b' = \left(\frac{1}{\sqrt{1-\beta_b^2}}\right)' = \gamma_b^3\beta_b\beta_b'$$

$$\Longrightarrow \quad \beta_b(\gamma_b\beta_b)' = \beta_b^2\gamma_b' + \gamma_b\beta_b\beta_b'$$
$$= (1+\gamma_b^2\beta_b^2)\gamma_b\beta_b\beta_b' = \gamma_b^3\beta_b\beta_b'$$
$$= \gamma_b'$$

Giving:

$$\boxed{\gamma_b' = -\frac{q}{mc^2}\frac{\partial\phi^a}{\partial s}\Big|_{x=y=0}}$$

Which can then be integrated to obtain:

$$\boxed{\gamma_b = \frac{q}{mc^2}\phi^a(r=0,z=s) + \text{const} \qquad \beta_b = \sqrt{1+1/\gamma_b^2}}$$

D3

We denote the on-axis accelerating potential as:

$$\boxed{V(s) \equiv \phi^a(x=y=0,z=s)}$$

- Can represent RF or induction accelerating gap fields
- See: J.J. Barnard lectures for more details

Giving:

$$\boxed{\gamma_b = \frac{q}{mc^2}V(s) + \text{const} \qquad \beta_b = \sqrt{1+1/\gamma_b^2}}$$

These equations can be solved for the consistent variation of $\gamma_b(s),\ \beta_b(s)$ in the transverse equations of motion:

$$\mathbf{x}_\perp'' + \frac{(\gamma_b\beta_b)'}{(\gamma_b\beta_b)}\mathbf{x}_\perp' = \frac{q}{m\gamma_b\beta_b^2c^2}\mathbf{E}_\perp^a + \frac{q}{m\gamma_b\beta_b c}\hat{\mathbf{z}}\times\mathbf{B}_\perp^a + \frac{qB_z^a}{m\gamma_b\beta_b c}\mathbf{x}_\perp'\times\hat{\mathbf{z}}$$
$$-\frac{q}{\gamma_b^3\beta_b^2c^2}\frac{\partial}{\partial\mathbf{x}_\perp}\phi$$

D4

Nonrelativistic limit results

In the nonrelativistic limit:

$$\gamma_b \simeq 1 + \frac{1}{2}\beta_b^2 \qquad \beta_b^2 \ll 1$$

Giving the familiar result of a nonrelativistic particle gaining energy when falling down a potential gradient:

$$\boxed{\frac{1}{2}m\beta_b^2c^2 \simeq q\phi^a(r=0,z=s) + \text{const} \qquad \beta_b^2 \ll 1}$$

Using this result, in the nonrelativistic limit we can take in the transverse particle equation of motion:

$$\frac{(\gamma_b\beta_b)'}{(\gamma_b\beta_b)} \simeq \frac{1}{2}\frac{V'}{V}$$

D5

Quasistatic potential expansion

In the quasistatic approximation, the accelerating potential can be expanded in the axisymmetric limit as:

- See: J.J. Barnard, Intro Lectures; and Reiser, *Theory and Design of Charged Particle Beams*, (1994, 2008) Sec. 3.3.

$$\boxed{\phi^a = V(z) - \frac{1}{4}\frac{\partial^2}{\partial z^2}V(z)(x^2+y^2) + \frac{1}{64}\frac{\partial^4}{\partial z^4}V(z)(x^2+y^2)^2 + \cdots}$$

The longitudinal acceleration also result in a transverse focusing field

$$\mathbf{E}^a_\perp = \mathbf{E}^a_\perp|_{\text{foc}} - \frac{\partial \phi^a}{\partial \mathbf{x}_\perp}$$

$$\mathbf{E}^a_\perp|_{\text{foc}} = \text{Fields from Focusing Optics}$$

$$-\frac{\partial \phi^a}{\partial \mathbf{x}_\perp} = \frac{1}{2}\frac{\partial^2}{\partial z^2}V(z)\mathbf{x}_\perp = \text{Focusing Field from Acceleration}$$

- Results can be used to cast acceleration terms in more convenient forms. See J.J. Barnard lectures for more details.

D6

These slides will be corrected and expanded for reference and any future editions of the US Particle Accelerator School class:
Beam Physics with Intense Space Charge, by J.J. Barnard and S.M. Lund

Corrections and suggestions are welcome. Contact:

Steven M. Lund
Lawrence Berkeley National Laboratory
BLDG 47 R 0112
1 Cyclotron Road
Berkeley, CA 94720-8201

SMLund@lbl.gov
(510) 486 – 6936

Please do not remove author credits in any redistributions of class material.

References: For more information see:

Earlier versions of course notes posted online (present will also be posted with corrections):
J. Barnard and S. Lund, *Intense Beam Physics*, US Particle Accelerator School Notes, http://uspas.fnal.gov/lect_note.html (2006, 2004)

Basic introduction on many of the topics covered:
M. Reiser, *Theory and Design of Charged Particle Beams*, Wiley (1994, revised 2008)

Review by author (with similar perspective to notes) with material on phase advances, lattice focusing strength, etc.
S.M. Lund and B. Bukh, Stability Properties of the Transverse Envelope Equations Describing Intense Ion Beam Transport, Phys. Rev. Special Topics – Accelerators and Beams (2004).

Hill's Equation, Floquet's theorem, Courant-Snyder invariants, and dispersion functions:
H. Wiedermann, *Particle Accelerator Physics*, Springer-Verlag (1995)

Particle equations of motion with bends and momentum spread:
D.A. Edwards and M.J. Syphers, *An Introduction to the Physics of High Energy Accelerators*, Wiley (1993).

Original, classic paper on strong focusing and Courant-Snyder invariants applied to accelerator physics. Remains one of the best formulated treatments to date:
E.D. Courant and H. S. Snyder, Theory of the Alternating Gradient Synchrotron, Annals Physics **3**, 1 (1958).

More mathematical treatment of transfer matrices and stability
A. Dragt, *Lectures on Nonlinear Orbit Dynamics*, in "Physics of High Energy Accelerators," edited by R.A. Carrigan, F.R. Hudson, and M. Month (AIP Conf. Proc. No. 87, New York, 1982), p. 147.

Phase-amplitude methods, Larmor frame:
J.D. Lawson, *The Physics of Charged Particle Beams*, Oxford University Priess (1977).

Solenoidal focusing and the Larmor frame:
H. Wiedemann, *Particle Accelerator Physics II: Nonlinear and Higher Order Beam Dynamics*, Springer (1995).

Acknowledgments:

Klaus Halbach educated one of the authors (S.M. Lund) on the use of complex variable theory to simplify analysis of multipole fields employed in S3: Description of Applied Focusing Fields.

Considerable help was provided by Guliano Franchetti (GSI) in educating one of the authors (S.M. Lund) in phase-amplitude methods described in this lecture.

Edward P. Lee (LBNL) helped formulate parts of material presented in S10: Acceleration and Normalized Emittance.

Transverse Equilibrium Distribution Functions*

Steven M. Lund
Lawrence Livermore National Laboratory (LLNL)

Steven M. Lund and John J. Barnard
"Beam Physics with Intense Space-Charge"

US Particle Accelerator School

University of Maryland, held at Annapolis, MD
16-27 June, 2008
(Version 20080625)

* Research supported by the US Dept. of Energy at LLNL and LBNL under contract Nos. DE-AC52-07NA27344 and DE-AC02-05CH11231.

Transverse Equilibrium Distribution Functions: Outline

Transverse Equilibrium Dist. Functions: Detailed Outline

Detailed Outline - 2

Detailed Outline - 3

Detailed Outline - 4

S1: Transverse Vlasov-Poisson Model: for a coasting, single species beam with electrostatic self-fields propagating in a linear focusing lattice:

$\mathbf{x}_\perp, \ \mathbf{x}'_\perp$ transverse particle coordinate, angle

$q, \ m$ charge, mass

$\gamma_b, \ \beta_b$ axial relativistic factors

$f_\perp(\mathbf{x}_\perp, \mathbf{x}'_\perp, s)$ single particle distribution

$H_\perp(\mathbf{x}_\perp, \mathbf{x}'_\perp, s)$ single particle Hamiltonian

Vlasov Equation (see J.J. Barnard, Introductory Lectures):

$$\frac{d}{ds}f_\perp = \frac{\partial f_\perp}{\partial s} + \frac{d\mathbf{x}_\perp}{ds}\cdot\frac{\partial f_\perp}{\partial \mathbf{x}_\perp} + \frac{d\mathbf{x}'_\perp}{ds}\cdot\frac{\partial f_\perp}{\partial \mathbf{x}'_\perp} = 0$$

Particle Equations of Motion:

$$\frac{d}{ds}\mathbf{x}_\perp = \frac{\partial H_\perp}{\partial \mathbf{x}'_\perp} \qquad \frac{d}{ds}\mathbf{x}'_\perp = -\frac{\partial H_\perp}{\partial \mathbf{x}_\perp}$$

Hamiltonian (see S.M. Lund, lectures on Transverse Particle Equations of Motion):

$$H_\perp = \frac{1}{2}\mathbf{x}'^{\,2}_\perp + \frac{1}{2}\kappa_x(s)x^2 + \frac{1}{2}\kappa_y(s)y^2 + \frac{q}{m\gamma_b^3\beta_b^2c^2}\phi$$

Poisson Equation:

$$\left(\frac{\partial^2}{\partial x^2} + \frac{\partial^2}{\partial y^2}\right)\phi = -\frac{q}{\epsilon_0}\int d^2\mathbf{x}'_\perp \ f_\perp$$

+ boundary conditions on ϕ

Hamiltonian expression of the Vlasov equation:

$$\frac{d}{ds}f_\perp = \frac{\partial f_\perp}{\partial s} + \frac{d\mathbf{x}_\perp}{ds}\cdot\frac{\partial f_\perp}{\partial \mathbf{x}_\perp} + \frac{d\mathbf{x}'_\perp}{ds}\cdot\frac{\partial f_\perp}{\partial \mathbf{x}'_\perp} = 0$$

$$= \frac{\partial f_\perp}{\partial s} + \frac{\partial H_\perp}{\partial \mathbf{x}'_\perp}\cdot\frac{\partial f_\perp}{\partial \mathbf{x}_\perp} - \frac{\partial H_\perp}{\partial \mathbf{x}_\perp}\cdot\frac{\partial f_\perp}{\partial \mathbf{x}'_\perp} = 0$$

Using the equations of motion:

$$\frac{d}{ds}\mathbf{x}_\perp = \frac{\partial H_\perp}{\partial \mathbf{x}'_\perp} = \mathbf{x}'_\perp$$

$$\frac{d}{ds}\mathbf{x}'_\perp = -\frac{\partial H_\perp}{\partial \mathbf{x}_\perp} = -\left(\kappa_x x\hat{\mathbf{x}} + \kappa_y y\hat{\mathbf{y}} + \frac{q}{m\gamma_b^3\beta_b^2c^2}\frac{\partial\phi}{\partial \mathbf{x}_\perp}\right)$$

$$\boxed{\frac{\partial f_\perp}{\partial s} + \mathbf{x}'_\perp\cdot\frac{\partial f_\perp}{\partial \mathbf{x}_\perp} - \left(\kappa_x x\hat{\mathbf{x}} + \kappa_y y\hat{\mathbf{y}} + \frac{q}{m\gamma_b^3\beta_b^2c^2}\frac{\partial\phi}{\partial \mathbf{x}_\perp}\right)\cdot\frac{\partial f_\perp}{\partial \mathbf{x}'_\perp} = 0}$$

In formal dynamics, a "Poisson Bracket" notation is frequently employed:

$$\frac{d}{ds}f_\perp = \frac{\partial f_\perp}{\partial s} + \frac{\partial H_\perp}{\partial \mathbf{x}'_\perp}\cdot\frac{\partial f_\perp}{\partial \mathbf{x}_\perp} - \frac{\partial H_\perp}{\partial \mathbf{x}_\perp}\cdot\frac{\partial f_\perp}{\partial \mathbf{x}'_\perp} = 0$$

$$\equiv \frac{\partial f_\perp}{\partial s} + \underbrace{\{H_\perp, f_\perp\}}_{\text{Poisson Bracket}} = 0$$

Comments on Vlasov-Poisson Model

- Collisionless Vlasov-Poisson model good for intense beams with many particles
  - Collisions negligible, see: J.J. Barnard, Intro. Lectures
- Vlasov-Poisson model can be solved as an initial value problem

$$1)\ f_\perp(\mathbf{x}_\perp, \mathbf{x}'_\perp, s = s_i) = \text{Initial "condition" (function) specified}$$

$$2)\ \text{Vlasov-Poisson model solved for subsequent evolution in } s \text{ for } f_\perp(\mathbf{x}_\perp, \mathbf{x}'_\perp, s) \text{ for } s \geq s_i$$

- The coupling to the self-field via the Poisson equation makes the Vlasov-Poisson model *highly* nonlinear

$$\rho = q \int d^2x'_\perp\, f_\perp \qquad \left(\frac{\partial^2}{\partial x^2} + \frac{\partial^2}{\partial y^2}\right)\phi = -\frac{\rho}{\epsilon_0}$$

- Vlasov-Poisson system is written without acceleration, but the transforms developed to identify the normalized emittance in the lectures on Transverse Particle Equations of Motion can be exploited to generalize all result presented to (weakly) accelerating beams (interpret in tilde variables)
- For solenoidal focusing the system must be interpreted in the rotating Larmor Frame, see: lectures on Transverse Particle Equations of Motion

Review: Focusing lattices, continuous and periodic (simple piecewise constant):

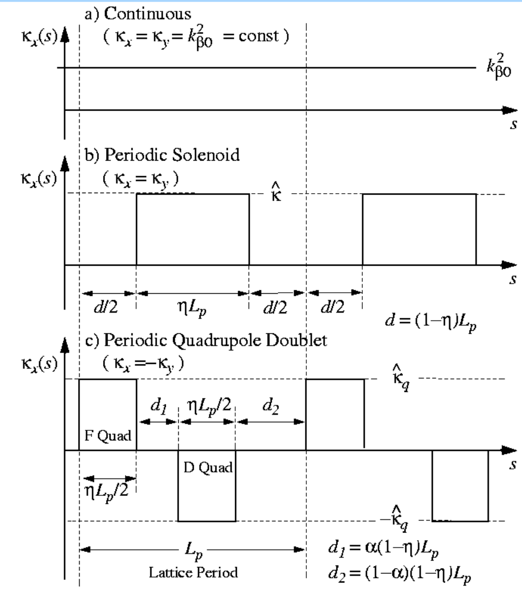

Lattice Period L_p

Occupancy η

$\eta \in [0, 1]$

Solenoid description carried out implicitly in Larmor frame

[see: S.M. Lund, lectures on Transverse Particle Equations]

Syncopation Factor α

$$\alpha \in [0, \frac{1}{2}]$$

$$\alpha = \frac{1}{2} \implies FODO$$

Example Hamiltonians:

Continuous focusing $\kappa_x = \kappa_y = k_{\beta 0}^2 = \text{const}$

$$H_\perp = \frac{1}{2}\mathbf{x}'^2_\perp + \frac{1}{2}k_{\beta 0}^2\mathbf{x}_\perp^2 + \frac{q}{m\gamma_b^3\beta_b^2c^2}\phi$$

Solenoidal focusing (in Larmor frame variables) $\kappa_x = \kappa_y = \kappa(s)$

$$H_\perp = \frac{1}{2}\mathbf{x}'^2_\perp + \frac{1}{2}\kappa\mathbf{x}_\perp^2 + \frac{q}{m\gamma_b^3\beta_b^2c^2}\phi$$

Quadrupole focusing $\kappa_x = -\kappa_y = \kappa(s)$

$$H_\perp = \frac{1}{2}\mathbf{x}'^2_\perp + \frac{1}{2}\kappa x^2 - \frac{1}{2}\kappa y^2 + \frac{q}{m\gamma_b^3\beta_b^2c^2}\phi$$

Review: Undepressed particle phase advance ! $_0$ is typically employed to characterize the applied focusing strength of periodic lattices:

see: S.M. Lund lectures on Transverse Particle Equations of Motion

x-orbit without space-charge satisfies Hill's equation

$$x''(s) + \kappa_x(s)x(s) = 0$$

$$\begin{pmatrix} x(s) \\ x'(s) \end{pmatrix} = \mathbf{M}_x(s\,|\,s_i)\cdot\begin{pmatrix} x(s_i) \\ x'(s_i) \end{pmatrix} \qquad \mathbf{M}_x = \text{2 x 2 Transfer Matrix from } s = s_i \text{ to } s$$

Undepressed phase advance

$$\boxed{\cos\sigma_{0x} = \frac{1}{2}\text{Tr}\ \mathbf{M}_x(s_i + L_p|s_i)}$$

- Subscript used stresses -plane value and zero (= 0) space-charge effects

Single particle (and centroid) stability requires:

$$\frac{1}{2}\text{Tr}\ \mathbf{M}_x(s_i + L_p|s_i) < 1 \longrightarrow \boxed{\sigma_{0x} < 180^\circ}$$

[Courant and Snyder, Annals of Phys. 3, 1 (1958)]

Analogous equations hold in the *y*-plane

The undepressed phase advance can also be equivalently calculated from:

$$w_{0x}'' + \kappa_x w_{0x} - \frac{1}{w_{0x}^3} = 0 \qquad w_{0x}(s+L_p) = w_{0x}(s)$$
$$w_{0x} > 0$$
$$\sigma_{0x} = \int_{s_i}^{s_i+L_p} \frac{ds}{w_{0x}^2}$$

- Subscript stresses -plane value and zero (= 0) space-charge effects

S2: Vlasov Equilibria: Plasma physics-like approach is to resolve the system into an equilibrium + perturbation and analyze stability

Equilibrium constructed from single-particle constants of motion C_i

$$\boxed{f_\perp = f_\perp(\{C_i\}) \geq 0 \quad \Longrightarrow \quad \text{equilibrium}}$$

$$\frac{d}{ds} f_\perp(\{C_i\}) = \sum_i \frac{\partial f_\perp}{\partial C_i} \overbrace{\cancel{\frac{dC_i}{ds}}}^{0} = 0$$

Comments:

- Equilibrium is an exact solution to Vlasov's equation that *does not change* in 4D phase-space as advances
  - Projections of the distribution can evolve in in general cases
- Requirement of positive $f_\perp(\{C_i\})$ results from single particle species
- Particle conversation constraints are in the presence of (possibly -varying) applied and space-charge forces
  - Highly non-trivial!
  - Only one exact solution known for -varying focusing using Courant-Snyder invariants: the KV distribution to be analyzed in this lecture

/// Example: Continuous focusing $f_\perp = f_\perp(H_\perp)$

$$H_\perp = \frac{1}{2}\mathbf{x}_\perp'^{\,2} + \frac{1}{2}k_{\beta 0}^2 \mathbf{x}_\perp^2 + \frac{q}{m\gamma_b^3\beta_b^2c^2}\phi$$

no explicit dependence

$$\frac{df_\perp}{ds} = \frac{\partial f_\perp}{\partial s} + \frac{\partial H_\perp}{\partial \mathbf{x}_\perp'} \cdot \frac{\partial f_\perp}{\partial \mathbf{x}_\perp} - \frac{\partial H_\perp}{\partial \mathbf{x}_\perp} \cdot \frac{\partial f_\perp}{\partial \mathbf{x}_\perp'}$$

see problem sets for detailed argument

$$= \frac{\partial f_\perp}{\partial H_\perp} \overbrace{\cancel{\frac{\partial H_\perp}{\partial s}}}^{0} + \frac{\partial f_\perp}{\partial H_\perp}\left(\frac{\partial H_\perp}{\partial \mathbf{x}_\perp'} \cdot \frac{\partial H_\perp}{\partial \mathbf{x}_\perp} \overbrace{\cancel{-}}^{0} \frac{\partial H_\perp}{\partial \mathbf{x}_\perp} \cdot \frac{\partial H_\perp}{\partial \mathbf{x}_\perp'} \right) = 0$$

Showing that $f_\perp = f_\perp(H_\perp)$ exactly satisfies Vlasov's equation for continuous focusing

- Also, for physical solutions must require: $f_\perp(H_\perp) \geq 0$
  - To be appropriate for single species with positive density
- Huge variety of equilibrium function choices $f_\perp(H_\perp)$ can be made to generate many radically different equilibria
  - Infinite variety in function space
- Does *NOT* apply to systems with -varying focusing $\kappa_x \rightarrow k_{\beta 0}^2$
  - Can provide a rough guide if we can approximate: ///

Typical single particle constants of motion:

Transverse Hamiltonian for continuous focusing:

$$H_\perp = \frac{1}{2}\mathbf{x}_\perp'^{\,2} + \frac{1}{2}k_{\beta 0}^2 \mathbf{x}_\perp^2 + \frac{q}{m\gamma_b^3\beta_b^2c^2}\phi = \text{const}$$
$$k_{\beta 0}^2 = \text{const}$$

- Not valid for periodic focusing systems!

Angular momentum for systems invariant under azimuthal rotation:

$$\boxed{P_\theta = xy' - yx' = \text{const}}$$

- Subtle point: This form is really a Canonical Angular Momentum and applies to solenoidal magnetic focusing when the variables are expressed in the rotating Larmor frame (i.e., in the ™tilde∫ variables)
  - see: S.M. Lund, lectures on Transverse Particle Equations

Axial kinetic energy for systems with no acceleration:

$$\boxed{\mathcal{E} = (\gamma_b - 1)mc^2 = \text{const}}$$

- Trivial for a coasting beam with $\gamma_b\beta_b = \text{const}$

More on other classes of constraints later ...

Plasma physics approach to beam physics:

Resolve:

$$\boxed{f(\mathbf{x}_\perp, \mathbf{x}'_\perp, s) = f_\perp(\{C_i\}) + \delta f_\perp(\mathbf{x}_\perp, \mathbf{x}'_\perp, s)}$$

equilibrium perturbation $f_\perp \gg |\delta f_\perp|$

and carry out equilibrium + stability analysis

Comments:

- Attraction is to parallel the impressive successes of plasma physics
  - Gain insight into preferred state of nature
- Beams are born off a source and may not be close to an equilibrium condition
  - Appropriate single particle constants of the motion unknown for periodic focusing lattices other than the (unphysical) KV distribution
- Intense beam self-fields and finite radial extent vastly complicate equilibrium description and analysis of perturbations
  - It is not clear if smooth Vlasov equilibria exist in periodic focusing
  - Higher model detail vastly complicates picture!
- If system can be tuned to more closely resemble a relaxed, equilibrium, one might expect less deleterious effects based on plasma physics analogies

S3: The KV Equilibrium Distribution

[Kapchinskij and Vladimirskij, Proc. Int. Conf. On High Energy Accel., p. 274 (1959); and Review: Lund, Kikuchi, and Davidson, PRSTAB, to be published, (2008)]

Assume a uniform density elliptical beam in a periodic focusing lattice

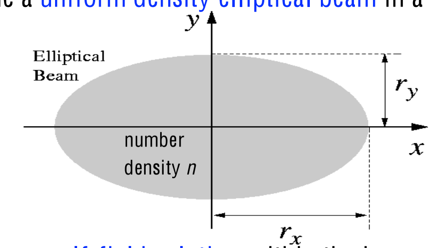

Line-Charge:

$$\lambda = qn(s)\pi r_x(s) r_y(s)$$
$$= \text{const}$$

Free-space self-field solution within the beam (see: Appendix A) is:

$$\phi = -\frac{\lambda}{2\pi\epsilon_0}\left[\frac{x^2}{(r_x+r_y)r_x} + \frac{y^2}{(r_x+r_y)r_y}\right] + \text{const}$$

$$-\frac{\partial\phi}{\partial x} = \frac{\lambda}{\pi\epsilon_0}\frac{x}{(r_x+r_y)r_x}$$
$$-\frac{\partial\phi}{\partial y} = \frac{\lambda}{\pi\epsilon_0}\frac{y}{(r_x+r_y)r_y}$$

valid only within the beam!

The particle equations of motion:

$$x'' + \kappa_x x = -\frac{q}{m\gamma_b^3\beta_b^2c^2}\frac{\partial\phi}{\partial x}$$
$$y'' + \kappa_y y = -\frac{q}{m\gamma_b^3\beta_b^2c^2}\frac{\partial\phi}{\partial y}$$

become within the beam:

$$x''(s) + \left\{\kappa_x(s) - \frac{2Q}{[r_x(s)+r_y(s)]r_x(s)}\right\}x(s) = 0$$
$$y''(s) + \left\{\kappa_y(s) - \frac{2Q}{[r_x(s)+r_y(s)]r_y(s)}\right\}y(s) = 0$$

Here, is the dimensionless perveance defined by:

$$\boxed{Q = \frac{q\lambda}{2\pi\epsilon_0 m\gamma_b^3\beta_b^2c^2} = \text{const}}$$

- Same measure of space-charge intensity used by J.J. Barnard in Intro. Lectures
- Properties/interpretations of the perveance will be extensively developed in in this and subsequent lectures

If we regard the envelope radii $r_x,\ r_y$ as specified functions of , then these equations of motion are Hill's equations familiar from elementary accelerator physics:

$$x''(s) + \kappa_x^{\text{eff}}(s)x(s) = 0$$
$$y''(s) + \kappa_y^{\text{eff}}(s)y(s) = 0$$
$$\kappa_x^{\text{eff}}(s) = \kappa_x(s) - \frac{2Q}{[r_x(s)+r_y(s)]r_x(s)}$$
$$\kappa_y^{\text{eff}}(s) = \kappa_y(s) - \frac{2Q}{[r_x(s)+r_y(s)]r_y(s)}$$

Suggests Procedure:

- Calculate Courant-Snyder invariants under assumptions made
- Construct a distribution function of Courant-Snyder invariants that generates the uniform density elliptical beam projection assumed
  - Nontrivial step: guess and show that it works

Resulting distribution will be an equilibrium that does not evolve in in 4D phase-space, but lower-dimensional phase-space projections can evolve in

Review (1): The Courant-Snyder invariant of Hill's equation

[Courant and Snyder, Annl. Phys. 3, 1 (1958)]

Hill's equation describes a zero space-charge particle orbit in linear applied focusing fields:

$$\boxed{x''(s) + \kappa(s)x(s) = 0}$$

As a consequence of Floquet's theorem, the solution can be cast in phase-amplitude form:

$$x(s) = A_i w(s)\cos\psi(s)$$

where $w(s)$ is the periodic amplitude function satisfying

$$w''(s) + \kappa(s)w(s) - \frac{1}{w^3(s)} = 0$$

$$w(s + L_p) = w(s) \qquad w(s) > 0$$

$\psi(s)$ is a phase function given by

$$\psi(s) = \psi_i + \int_{s_i}^{s} \frac{d\tilde{s}}{w^2(\tilde{s})}$$

A_i and ψ_i are constants set by initial conditions at $s = s_i$

Review (2): The Courant-Snyder invariant of Hill's equation

From this formulation, it follows that

$$x(s) = A_i w(s)\cos\psi(s)$$

$$x'(s) = A_i w'(s)\cos\psi(s) - \frac{A_i}{w(s)}\sin\psi(s)$$

or

$$\frac{x}{w} = A_i\cos\psi$$

$$wx' - w'x = A_i\sin\psi$$

square and add equations to obtain the Courant-Snyder invariant

$$\boxed{\left(\frac{x}{w}\right)^2 + (wx' - w'x)^2 = A_i^2 = \text{const}}$$

- Simplifies interpretation of dynamics
- Extensively used in accelerator physics

Phase-amplitude description of particles evolving within a uniform density beam:

Phase-amplitude form of -orbit equations:

$$x(s) = A_{xi}w_x(s)\cos\psi_x(s)$$

$$x'(s) = A_{xi}w_x'(s)\cos\psi_x(s) - \frac{A_{xi}}{w_x(s)}\sin\psi_x(s)$$

initial conditions yield:

$$(s = s_i)$$

$$A_{xi} = \text{const}$$

$$\psi_{xi} = \psi_x(s = s_i) = \text{const}$$

where

$$w_x''(s) + \kappa_x(s)w_x(s) - \frac{2Q}{[r_x(s) + r_y(s)]r_x(s)}w_x(s) - \frac{1}{w_x^3(s)} = 0$$

$$w_x(s + L_p) = w_x(s) \qquad w_x(s) > 0$$

$$\psi_x(s) = \psi_{xi} + \int_{s_i}^{s} \frac{d\tilde{s}}{w_x^2(\tilde{s})}$$

identifies the Courant-Snyder invariant

$$\boxed{\left(\frac{x}{w_x}\right)^2 + (w_x x' - w_x' x)^2 = A_{xi}^2 = \text{const}}$$

Analogous equations hold for the *y*-plane

The KV envelope equations:

Define *maximum* Courant-Snyder invariants:

$$\boxed{\begin{aligned}\varepsilon_x &\equiv \text{Max}(A_{xi}^2)\\ \varepsilon_y &\equiv \text{Max}(A_{yi}^2)\end{aligned}}$$

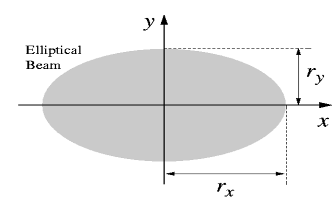

These values must correspond to the beam-edge:

$$r_x(s) = \sqrt{\varepsilon_x}w_x(s)$$

$$r_y(s) = \sqrt{\varepsilon_y}w_y(s)$$

The equations for w_x and w_y can then be rescaled to obtain the familiar KV envelope equations for the matched beam envelope

$$r_x''(s) + \kappa_x(s)r_x(s) - \frac{2Q}{r_x(s) + r_y(s)} - \frac{\varepsilon_x^2}{r_x^3(s)} = 0$$

$$r_y''(s) + \kappa_y(s)r_y(s) - \frac{2Q}{r_x(s) + r_y(s)} - \frac{\varepsilon_y^2}{r_y^3(s)} = 0$$

$$r_x(s + L_p) = r_x(s) \qquad r_x(s) > 0$$

$$r_y(s + L_p) = r_y(s) \qquad r_y(s) > 0$$

Use variable rescalings to denote - and -plane Courant-Snyder invariants as:

$$\left(\frac{x}{w_x}\right)^2 + (w_x x' - w_x' x)^2 = A_{xi}^2 = \text{const}$$

$$\boxed{\begin{aligned} \left(\frac{x}{r_x}\right)^2 + \left(\frac{r_x x' - r_x' x}{\varepsilon_x}\right)^2 &= C_x = \text{const} \\ \left(\frac{y}{r_y}\right)^2 + \left(\frac{r_y y' - r_y' y}{\varepsilon_y}\right)^2 &= C_y = \text{const} \end{aligned}}$$

Kapchinskij and Vladimirskij constructed a delta-function distribution of a linear combination of these Courant-Snyder invariants that generates the correct uniform density elliptical beam needed for consistency with the assumptions:

$$f_\perp = \frac{\lambda}{q\pi^2 \varepsilon_x \varepsilon_y} \delta\left[C_x + C_y - 1\right]$$

- Delta function means the sum of the x- and y-invariants is a constant
- Other forms cannot generate the needed uniform density elliptical beam projection (see: S9)

The KV equilibrium is constructed from the Courant-Snyder invariants:

KV equilibrium distribution:

$$\boxed{\begin{aligned} f_\perp(\mathbf{x}_\perp, \mathbf{x}'_\perp, s) = \frac{\lambda}{q\pi^2 \varepsilon_x \varepsilon_y} \delta \Bigg[\left(\frac{x}{r_x}\right)^2 &+ \left(\frac{r_x x' - r_x' x}{\varepsilon_x}\right)^2 + \\ \left(\frac{y}{r_y}\right)^2 &+ \left(\frac{r_y y' - r_y' y}{\varepsilon_y}\right)^2 - 1 \Bigg] = \text{const} \\ \delta(x) = \ &\text{Dirac delta function} \end{aligned}}$$

This distribution generates (see: proof in Appendix B) the correct uniform density elliptical beam:

$$\boxed{n = \int d^2x'_\perp \; f_\perp = \begin{cases} \frac{\lambda}{q\pi r_x r_y}, & x^2/r_x^2 + y^2/r_y^2 < 1 \\ 0, & x^2/r_x^2 + y^2/r_y^2 > 1 \end{cases}}$$

Obtaining this form consistent with the assumptions, thereby demonstrating full self-consistency of the KV equilibrium distribution.

- Full 4-D form of the distribution does not evolve in
- Projections of the distribution can (and generally do!) evolve in

/// Comment on notation of integrals:

- 2nd forms useful for systems with azimuthal spatial or annular symmetry

Spatial

$$\int d^2x_\perp \cdots \equiv \int_{-\infty}^{\infty} dx \int_{-\infty}^{\infty} dy \ \cdots$$

$$= \int_0^\infty dr\, r \int_{-\pi}^{\pi} d\theta \ \cdots$$

Cylindrical Coordinates:
$x = r\cos\theta$
$y = r\sin\theta$

Angular

$$\int d^2x'_\perp \cdots \equiv \int_{-\infty}^{\infty} dx' \int_{-\infty}^{\infty} dy' \ \cdots$$

$$= \int_0^\infty dr'\, r' \int_{-\pi}^{\pi} d\theta' \ \cdots$$

Angular
Cylindrical Coordinates:
$x' = r'\cos\theta'$
$y' = r'\sin\theta'$

Comment on angle integral representation:

$$\theta' \neq \frac{d}{ds}\theta \qquad [[r']] = \text{Angle} \qquad r' \in [0, \infty)$$

$$[[\theta']] = \text{rad} \qquad \theta' \in [-\pi, \pi]$$

$$x' = r'\cos\theta' \qquad [[x']] = \text{Angle} \qquad x' \in (-\infty, \infty)$$

$$y' = r'\sin\theta' \qquad [[y']] = \text{Angle} \qquad y' \in (-\infty, \infty)$$

Comment on notation of integrals (continued):

Axisymmetry simplifications

Spatial: for some function $f(\mathbf{x}_\perp^2) = f(r^2)$

$$\int d^2x_\perp \; f(\mathbf{x}_\perp^2) = 2\pi \int_0^\infty dr\, r f(r^2) = \pi \int_0^\infty dr^2 \; f(r^2) = \pi \int_0^\infty dw \; f(w)$$

Cylindrical Coordinates:
$x = r\cos\theta$
$y = r\sin\theta$
$w = r^2$

Angular: for some function $g(\mathbf{x}_\perp'^2) = g(r'^2)$

$$\int d^2x'_\perp \; g(\mathbf{x}_\perp'^2) = 2\pi \int_0^\infty dr'\, r' g(r'^2) = \pi \int_0^\infty dr'^2 \; g(r'^2) = \pi \int_0^\infty du \; g(u)$$

Angular Cylindrical Coordinates:
$x' = r'\cos\theta'$
$y' = r'\sin\theta'$
$u = r'^2$

///

Moments of the KV distribution can be calculated directly from the distribution to further aid interpretation: [see: Appendix B for details]

Full 4D average: $\langle \cdots \rangle_\perp \equiv \dfrac{\int d^2x_\perp \int d^2x'_\perp \; \cdots f_\perp}{\int d^2x_\perp \int d^2x'_\perp \; f_\perp}$

Restricted angle average: $\langle \cdots \rangle_{\mathbf{x}'_\perp} \equiv \dfrac{\int d^2x'_\perp \; \cdots f_\perp}{\int d^2x'_\perp \; f_\perp}$

Envelope edge radius:

$$r_x = 2\langle x^2 \rangle_\perp^{1/2}$$

rms edge emittance (maximum Courant-Snyder invariant):

$$\varepsilon_x = 4[\langle x^2\rangle_\perp \langle x'^2\rangle_\perp - \langle xx'\rangle_\perp^2]^{1/2} = \text{const}$$

Coherent flows (within the beam, zero otherwise):

$$\langle x' \rangle_{\mathbf{x}'_\perp} = r'_x \frac{x}{r_x}$$

Angular spread (x-temperature, within the beam, zero otherwise):

$$T_x \equiv \langle (x' - \langle x' \rangle_{\mathbf{x}'_\perp})^2 \rangle_{\mathbf{x}'_\perp} = \frac{\varepsilon_x^2}{2r_x^2}\left(1 - \frac{x^2}{r_x^2} - \frac{y^2}{r_y^2}\right)$$

Summary of 1st and 2nd order moments of the KV distribution:

Moment	Value
$\int d^2x'_\perp \; x' f_\perp$	$r'_x \frac{x}{r_x} n$
$\int d^2x'_\perp \; y' f_\perp$	$r'_y \frac{y}{r_y} n$
$\int d^2x'_\perp \; x'^2 f_\perp$	$\left[r_x'^2 \frac{x^2}{r_x^2} + \frac{\varepsilon_x^2}{2r_x^2}\left(1 - \frac{x^2}{r_x^2} - \frac{y^2}{r_y^2}\right)\right] n$
$\int d^2x'_\perp \; y'^2 f_\perp$	$\left[r_y'^2 \frac{y^2}{r_y^2} + \frac{\varepsilon_y^2}{2r_y^2}\left(1 - \frac{x^2}{r_x^2} - \frac{y^2}{r_y^2}\right)\right] n$
$\int d^2x'_\perp \; xx' f_\perp$	$\frac{r'_x}{r_x} x^2 n$
$\int d^2x'_\perp \; yy' f_\perp$	$\frac{r'_y}{r_y} y^2 n$
$\int d^2x'_\perp \; (xy' - yx') f_\perp$	0
$\langle x^2 \rangle_\perp$	$\frac{r_x^2}{4}$
$\langle y^2 \rangle_\perp$	$\frac{r_y^2}{4}$
$\langle x'^2 \rangle_\perp$	$\frac{r_x'^2}{4} + \frac{\varepsilon_x^2}{4r_x^2}$
$\langle y'^2 \rangle_\perp$	$\frac{r_y'^2}{4} + \frac{\varepsilon_y^2}{4r_y^2}$
$\langle xx' \rangle_\perp$	$\frac{r_x r'_x}{4}$
$\langle yy' \rangle_\perp$	$\frac{r_y r'_y}{4}$
$\langle xy' - yx' \rangle_\perp$	0
$16[\langle x^2\rangle_\perp \langle x'^2\rangle_\perp - \langle xx'\rangle_\perp^2]$	ε_x^2
$16[\langle y^2\rangle_\perp \langle y'^2\rangle_\perp - \langle yy'\rangle_\perp^2]$	ε_y^2

All 1st and 2nd order moments not listed vanish, i.e.,

$$\int d^2x'_\perp \; xy f_\perp = 0$$

$$\langle xy \rangle_\perp = 0$$

see reviews by:

(limit of results presented) Lund and Bukh, PRSTAB 024801 (2004), Appendix A

S.M. Lund, T. Kikuchi, and R.C. Davidson, PRSTAB, to be published (2008)

Canonical transformation illustrates KV distribution structure:

[Davidson, Physics of Nonneutral Plasmas, Addison-Wesley (1990), and Appendix B]

Phase-space transformation:

$$X = \frac{\sqrt{\varepsilon_x}}{r_x} x \qquad X' = \frac{r_x x' - r'_x x}{\sqrt{\varepsilon_x}}$$

$$dx\; dy = \frac{r_x r_y}{\sqrt{\varepsilon_x \varepsilon_y}} dX\; dY$$

$$dx'\; dy' = \frac{\sqrt{\varepsilon_x \varepsilon_y}}{r_x r_y} dX'\; dY'$$

$$dx\; dy\; dx'\; dy' = dX\; dY\; dX'\; dY'$$

Courant-Snyder invariants in the presence of beam space-charge are then simply:

$$X^2 + X'^2 = \text{const}$$

and the KV distribution takes the simple, *symmetrical* form:

$$f_\perp(x, y, x', y', s) = f_\perp(X, Y, X', Y') = \frac{\lambda}{q\pi^2 \varepsilon_x \varepsilon_y} \delta\left[\frac{X^2 + X'^2}{\varepsilon_x} + \frac{Y^2 + Y'^2}{\varepsilon_y} - 1\right]$$

from which the density and other projections can be (see: Appendix B) calculated more easily:

$$n = \int d^2x'_\perp \; f_\perp = \frac{\lambda}{q\pi r_x r_y} \int_0^\infty dU^2 \; \delta\left[U^2 - \left(1 - \frac{x^2}{r_x^2} - \frac{y^2}{r_y^2}\right)\right]$$

$$= \begin{cases} \frac{\lambda}{q\pi r_x r_y}, & x^2/r_x^2 + y^2/r_y^2 < 1 \\ 0, & x^2/r_x^2 + y^2/r_y^2 > 1 \end{cases}$$

KV Envelope equation

The envelope equation reflects low-order force balances

$$r_x'' + \kappa_x r_x - \frac{2Q}{r_x + r_y} - \frac{\varepsilon_x^2}{r_x^3} = 0$$

$$r_y'' + \kappa_y r_y - \frac{2Q}{r_x + r_y} - \frac{\varepsilon_y^2}{r_y^3} = 0$$

Terms:	Applied Focusing	Space-Charge Defocusing	Thermal Defocusing
	Lattice	Perveance	Emittance

Matched Solution:

$$r_x(s + L_p) = r_x(s)$$
$$r_y(s + L_p) = r_y(s)$$

Comments:
- Envelope equation is a projection of the 4D invariant distribution
  - Envelope evolution equivalently given by moments of the 4D equilibrium distribution
- Most important basic design equation for transport lattices with high space-charge intensity
  - Simplest consistent model incorporating applied focusing, space-charge defocusing, and thermal defocusing forces
  - Starting point of almost all practical machine design!

Comments Continued:
- Beam envelope matching will be covered in much more detail in S.M. Lund lectures on Centroid and Envelope Description of Beams
  Requires specific initial conditions for periodic evolution

  $$r_x(s_i),\ r_y(s_i) \qquad r_x'(s_i),\ r_y'(s_i)$$

- Instabilities of envelope equations are well understood and real (to be covered: see S.M. Lund lectures on Centroid and Envelope Description of Beams)
  - Must be avoided for reliable machine operation

The matched solution to the KV envelope equations reflects the symmetry of the focusing lattice and must in general be calculated numerically

$$r_x(s + L_p) = r_x(s)$$
$$r_y(s + L_p) = r_y(s)$$
$$\varepsilon_x = \varepsilon_y$$

Parameters

$$L_p = 0.5 \text{ m}, \quad \sigma_0 = 80^\circ, \quad \eta = 0.5$$
$$\varepsilon_x = 50 \text{ mm-mrad}$$
$$\sigma/\sigma_0 = 0.2$$

Solenoidal Focusing

$(Q = 6.6986 \times 10^{-4})$

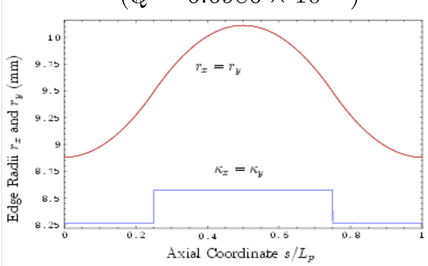

FODO Quadrupole Focusing

$(Q = 6.5614 \times 10^{-4})$

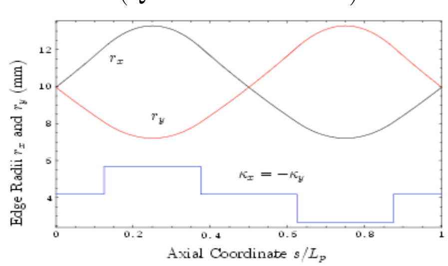

The matched beam is the most radially compact solution to the envelope equations rendering it highly important for beam transport

Some phase-space projections of a matched KV equilibrium beam in a periodic FODO quadrupole transport lattice

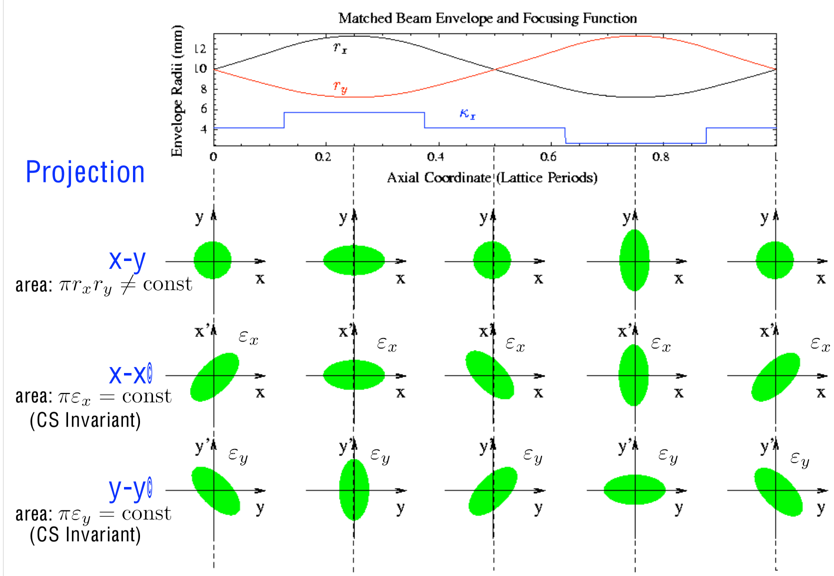

KV model shows that particle orbits in the presence of space-charge can be strongly modified ± space charge slows the orbit response:

Matched envelope:

$$r_x''(s) + \kappa_x(s)r_x(s) - \frac{2Q}{r_x(s)+r_y(s)} - \frac{\varepsilon_x^2}{r_x^3(s)} = 0$$
$$r_y''(s) + \kappa_y(s)r_y(s) - \frac{2Q}{r_x(s)+r_y(s)} - \frac{\varepsilon_y^2}{r_y^3(s)} = 0$$
$$r_x(s+L_p) = r_x(s) \qquad r_x(s) > 0$$
$$r_y(s+L_p) = r_y(s) \qquad r_y(s) > 0$$

Equation of motion for x-plane ™depressed∫ orbit in the presence of space-charge:

$$x''(s) + \kappa_x(s)x(s) - \frac{2Q}{[r_x(s)+r_y(s)]r_x(s)}x(s) = 0$$

All particles have the *same value* of depressed phase advance (similar Eqns in):

$$\sigma_x \equiv \psi_x(s_i+L_p) - \psi_x(s_i) = \varepsilon_x \int_{s_i}^{s_i+L_p} \frac{ds}{r_x^2(s)}$$

Contrast: Review, the undepressed particle phase advance calculated in the lectures on Transverse Particle Equations of Motion

The undepressed phase advance in defined as the phase advance of a particle in the absence of space-charge (= 0):

- Denote by σ_{0x} to distinguished from the ™depressed∫ phase advance σ_x in the presence of space-charge

$$w_{0x}'' + \kappa_x w_{0x} - \frac{1}{w_{0x}^3} = 0 \qquad w_{0x}(s+L_p) = w_{0x}(s)$$
$$w_{0x} > 0$$
$$\sigma_{0x} = \int_{s_i}^{s_i+L_p} \frac{ds}{w_{0x}^2}$$

This can be equivalently calculated from the matched envelope with = 0:

$$r_{0x}'' + \kappa_x r_{0x} - \frac{\varepsilon_x^2}{r_{0x}^3} = 0 \qquad r_{0x}(s+L_p) = r_{0x}(s)$$
$$r_{0x} > 0$$
$$\sigma_{0x} = \varepsilon_x \int_{s_i}^{s_i+L_p} \frac{ds}{r_{0x}^2}$$

- Value of ε_x is arbitrary (answer for σ_{0x}'s independent)

Depressed particle -plane orbits within a matched KV beam in a periodic FODO quadrupole channel for the matched beams previously shown

Solenoidal Focusing (Larmor frame orbit):

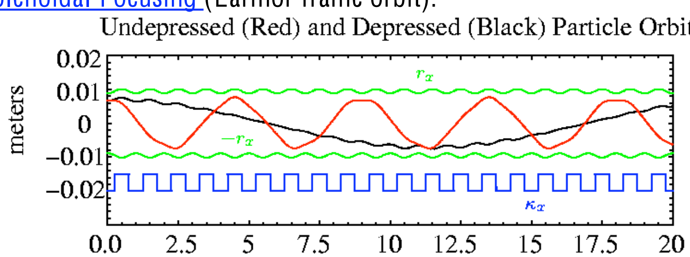

-plane orbit: $y = 0 = y'$

FODO Quadrupole Focusing:

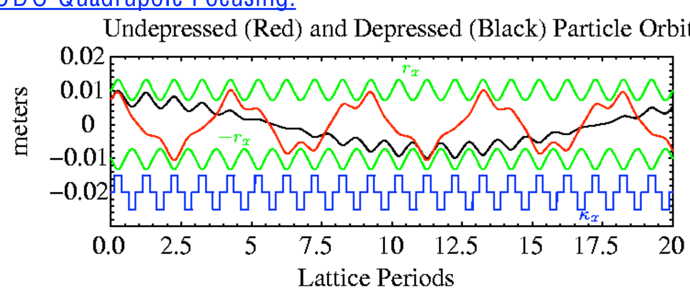

-plane orbit: $y = 0 = y'$

Depressed particle phase advance provides a convenient measure of space-charge strength

For simplicity take (plane symmetry in average focusing and emittance)

$$\sigma_{0x} = \sigma_{0y} \equiv \sigma_0 \qquad \varepsilon_x = \varepsilon_y \equiv \varepsilon$$

Depressed phase advance within a matched beam

$$\sigma = \varepsilon \int_{s_i}^{s_i+L_p} \frac{ds}{r_x^2(s)} = \varepsilon \int_{s_i}^{s_i+L_p} \frac{ds}{r_y^2(s)}$$

$$\lim_{Q\to 0} \sigma = \sigma_0$$

Normalized space charge strength

$$0 \leq \sigma/\sigma_0 \leq 1$$

$\sigma/\sigma_0 \to 0$ Cold Beam (space-charge dominated) $\varepsilon \to 0$

$\sigma/\sigma_0 \to 1$ Warm Beam (kinetic dominated) $Q \to 0$

For example matched envelope presented earlier:

Undepressed phase advance: $\sigma_0 = 80°$ repeat periods 4.5

Depressed phase advance: $\sigma = 16°$ $\rightarrow \sigma/\sigma_0 = 0.2$ 22.5

Periods for 360 degree phase advance

Solenoidal Focusing (Larmor frame orbit):

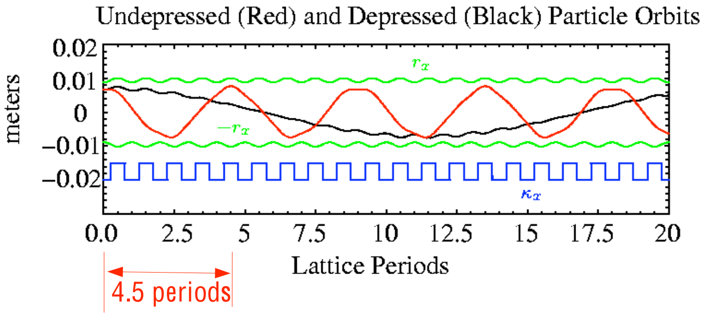

-plane orbit = 0 =

Comment:

All particles in the distribution will, of course, always move in response to both applied and self-fields. You cannot turn off space-charge for an undepressed orbit. It is a convenient conceptual construction to help understand focusing properties.

The rms equivalent beam model helps interpret general beam evolution in terms of an ™equivalent∫ local KV distribution

For the same focusing lattice, replace any beam charge $\rho(x,y)$ density by a uniform density KV beam in each axial slice (s) using averages calculated from the actual ™real∫ beam distribution with:

$$\langle \cdots \rangle_\perp \equiv \frac{\int d^2x_\perp \int d^2x'_\perp \; \cdots f_\perp}{\int d^2x_\perp \int d^2x'_\perp \; f_\perp} \qquad f_\perp = \text{ real distribution}$$

rms equivalent beam:

Quantity	KV Equiv.	Calculated from Distribution
Perveance	Q	$= q^2 \int d^2x_\perp \int d^2x'_\perp \; f_\perp \; / [2\pi\epsilon_0 \gamma_b^3 \beta_b^2 c^2]$
x-edge radius	r_x	$= 2\langle x^2 \rangle_\perp^{1/2}$
y-edge radius	r_y	$= 2\langle y^2 \rangle_\perp^{1/2}$
x-emittance	ε_x	$= 4[\langle x^2\rangle_\perp \langle x'^2\rangle_\perp - \langle xx'\rangle_\perp]^{1/2}$
y-emittance	ε_y	$= 4[\langle y^2\rangle_\perp \langle y'^2\rangle_\perp - \langle yy'\rangle_\perp]^{1/2}$

Comments on rms equivalent beam concept:

- The emittances will generally evolve in
  - Means that the equivalence must be recalculated in every slice as the emittances evolve
  - For reasons to be analyzed later (see S.M. Lund lectures on Kinetic Stability of Beams), this evolution is often small
- Concept is highly useful
  - KV equilibrium properties well understood and are approximately correct to model lowest order ™real∫ beam properties
  - See, Reiser, *Theory and Design of Charged Particle Beams* (1994, 2008) for a detailed discussion of rms equivalence

Sacherer expanded the concept of rms equivalency by showing that the equivalency works exactly for beams with elliptic symmetry space-charge

[Sacherer, IEEE Trans. Nucl. Sci. 18, 1101 (1971), J.J. Barnard, Intro. Lectures]

For any beam with elliptic symmetry charge density in each transverse slice:

$$\boxed{\rho = \rho\left(\frac{x^2}{r_x^2} + \frac{y^2}{r_y^2}\right)}$$

Based on:

$$\langle x \frac{\partial \phi}{\partial x} \rangle_\perp = -\frac{\lambda}{4\pi\epsilon_0} \frac{r_x}{r_x + r_y}$$

see J.J. Barnard intro. lectures

the KV envelope equations

$$r''_x(s) + \kappa_x(s) r_x(s) - \frac{2Q}{r_x(s) + r_y(s)} - \frac{\varepsilon_x^2(s)}{r_x^3(s)} = 0$$

$$r''_y(s) + \kappa_y(s) r_y(s) - \frac{2Q}{r_x(s) + r_y(s)} - \frac{\varepsilon_y^2(s)}{r_y^3(s)} = 0$$

remain valid when (averages taken with the full distribution):

$$Q = \frac{q\lambda}{2\pi\epsilon_0 m \gamma_b^3 \beta_b^2 c^2} = \text{const} \qquad \lambda = q\int d^2x_\perp \; \rho \; = \; \text{const}$$

$$r_x = 2\langle x^2 \rangle_\perp^{1/2} \qquad \varepsilon_x = 4[\langle x^2\rangle_\perp \langle x'^2\rangle_\perp - \langle xx'\rangle_\perp^2]^{1/2}$$

$$r_y = 2\langle y^2 \rangle_\perp^{1/2} \qquad \varepsilon_y = 4[\langle y^2\rangle_\perp \langle y'^2\rangle_\perp - \langle yy'\rangle_\perp^2]^{1/2}$$

The emittances must, in general, evolve in s under this model

(see SM Lund lectures on *Transverse Kinetic Stability*)

Further comments on the KV equilibrium: Distribution Structure

KV equilibrium distribution:

$$\boxed{f_\perp \sim \delta[\text{Courant-Snyder invariants}]}$$

Forms a highly singular hyper-shell in 4D phase-space

Schematic:

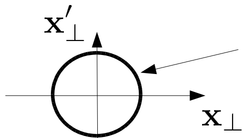

- Singular distribution has large ™Free-Energy∫ to drive many instabilities
  - Low order envelope modes are physical and highly important (see: lectures by S.M. Lund on Centroid and Envelope Descriptions of Beams)
- Perturbative analysis shows strong collective instabilities
  - Hofmann, Laslett, Smith, and Haber, Part. Accel. 13, 145 (1983)
  - Higher order instabilities (collective modes) have unphysical aspects due to (delta-function) structure of distribution and must be applied with care (see: lectures by S.M. Lund on Kinetic Stability of Beams)
  - Instabilities can cause problems if the KV distribution is employed as an initial beam state in self-consistent simulations

Preview: lecture on Centroid and Envelope Descriptions of Beams: Instability bands of the KV envelope equation are well understood in periodic focusing channels and must be avoided in machine operation

Envelope Mode Instability Growth Rates

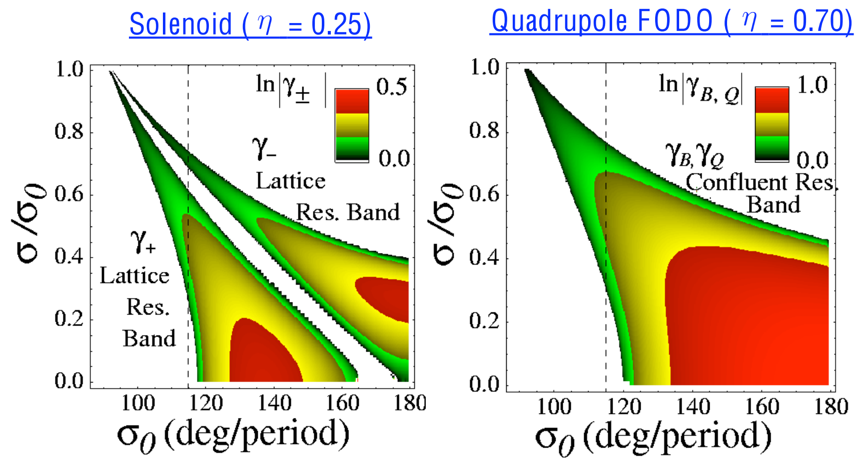

[S.M. Lund and B. Bukh, PRSTAB 024801 (2004)]

Further comments on the KV equilibrium: 2D Projections

All 2D projections of the KV distribution are uniformly filled ellipses

- Not very different from what is often observed in experimental measurements and self-consistent simulations of stable beams with strong space-charge
- Falloff of distribution at ™edges∫ can be rapid, but smooth, for strong space-charge

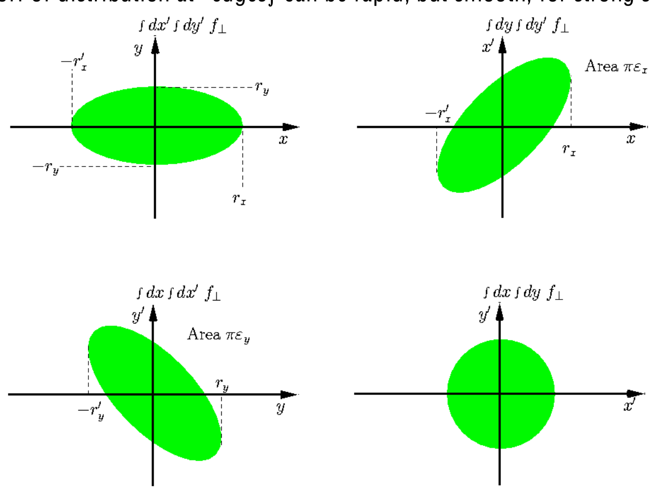

Further comments on the KV equilibrium: Angular Spreads: Coherent and Incoherent

Angular spreads within the beam:

Coherent (flow):

$$\langle x' \rangle_{\mathbf{x}'_\perp} \equiv \frac{\int d^2x'_\perp \; x'_\perp \; f_\perp}{\int d^2x'_\perp \; f_\perp} = r'_x \frac{x}{r_x}$$

Incoherent (temperature):

$$\langle (x' - r'_x x/r_x)^2 \rangle_{\mathbf{x}'_\perp} = \frac{\varepsilon_x^2}{2r_x^2}\left(1 - \frac{x^2}{r_x^2} - \frac{y^2}{r_y^2}\right)$$

$$\widehat{T}_x \equiv \frac{\varepsilon_x^2}{2r_x^2}$$

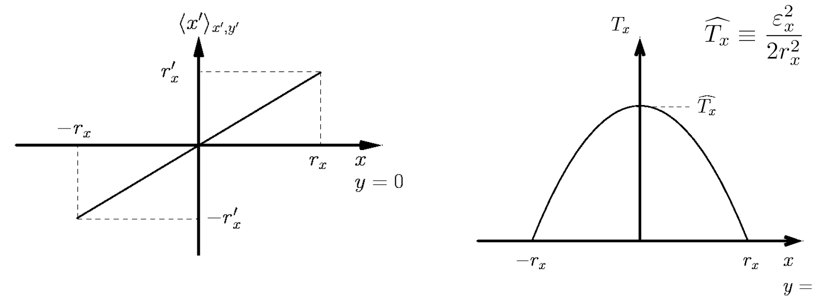

- Coherent flow required for periodic focusing to conserve charge
- Temperature must be zero at the beam edge since the distribution edge is sharp
- Parabolic temperature profile is consistent with linear grad P pressure forces in a fluid model interpretation of the (kinetic) KV distribution

Further comments on the KV equilibrium:

The KV distribution is the *only* exact equilibrium distribution formed from Courant-Snyder invariants of linear forces valid for periodic focusing channels:

- Low order properties of the distribution are physically appealing
- Illustrates relevant Courant-Snyder invariants in simple form
  - Later arguments demonstrate that these invariants should be a reasonable approximation for beams with strong space charge
- KV distribution does not have a 3D generalization [see F. Sacherer, Ph.d. thesis, 1968]

Strong Vlasov instabilities associated with the KV model render the distribution inappropriate for use in evaluating machines at high levels of detail:

- Instabilities are not all physical and render interpretation of results difficult
  - Difficult to separate physical from nonphysical effects in simulations

Possible Research Problem (unsolved in 40+ years!):

Can a valid Vlasov equilibrium be constructed for a *smooth* (non-singular), nonuniform density distribution in a linear, periodic focusing channel?

- Not clear what invariants can be used or if any can exist
  - Nonexistence proof would also be significant
- Lack of a smooth equilibrium does not imply that real machines cannot work!

Because of a lack of theory for a smooth, self-consistent distribution that would be more physically appealing than the KV distribution we will examine smooth distributions in the idealized continuous focusing limit (after an analysis of the continuous limit of the KV theory):

- Allows more classic ™plasma physics∫ like analysis
- Illuminates physics of intense space charge
- Lack of continuous focusing in the laboratory will prevent over generalization of results obtained

A 1D analog to the KV distribution called the ™Neuffer Distribution∫ is useful in longitudinal physics

- Based on linear forces with a ™g-factor∫ model
- Distribution is not singular in 1D
- See: J.J. Barnard, lectures on Longitudinal Physics

Appendix A: Self-Fields of a Uniform Density Elliptical Beam in Free-Space

See handwritten notes

Appendix B: Canonical Transformation of the KV Distribution

See handwritten notes

S4: Continuous Focusing limit of the KV Equilibrium Distribution

Continuous focusing, axisymmetric beam

$$\boxed{\begin{aligned}&\kappa_x(s)=\kappa_y(s)=k_{\beta 0}^2=\text{const}\\&\varepsilon_x=\varepsilon_y\equiv\varepsilon\\&r_x=r_y\equiv r_b\end{aligned}}$$

Undepressed betatron wavenumber

KV envelope equation

$$r_x'' + \kappa_x r_x - \frac{2Q}{r_x+r_y} - \frac{\varepsilon_x^2}{r_x^3} = 0$$

$$r_y'' + \kappa_y r_y - \frac{2Q}{r_x+r_y} - \frac{\varepsilon_y^2}{r_y^3} = 0$$

immediately reduces to:

$$r_b'' + k_{\beta 0}^2 r_b - \frac{Q}{r_b} - \frac{\varepsilon^2}{r_b^3} = 0$$

with solution

$$\boxed{r_b = \left(\frac{Q+\sqrt{4k_{\beta 0}^2\varepsilon^2+Q^2}}{2k_{\beta 0}^2}\right)^{1/2} = \text{const}}$$

Similarly, the particle equations of motion within the beam are:

$$x'' + \left\{\kappa_x - \frac{2Q}{[r_x+r_y]r_x}\right\}x = 0$$

$$y'' + \left\{\kappa_y - \frac{2Q}{[r_x+r_y]r_y}\right\}y = 0$$

reduce to

$$\mathbf{x}_\perp'' + k_\beta^2\mathbf{x}_\perp = 0 \qquad \boxed{k_\beta \equiv \sqrt{k_{\beta 0}^2 - \frac{Q}{r_b^2}} = \text{const}}$$

Depressed betatron wavenumber

with solution

$$\boxed{\mathbf{x}_\perp(s) = \mathbf{x}_{\perp i}\cos[k_\beta(s-s_i)] + \frac{\mathbf{x}_{\perp i}'}{k_\beta}\sin[k_\beta(s-s_i)]}$$

Space-charge tune depression (rate of phase advance same everywhere, L_p arb.)

$$\frac{k_\beta}{k_{\beta 0}} = \frac{\sigma}{\sigma_0} = \left(1-\frac{Q}{k_{\beta 0}^2 r_b^2}\right)^{1/2} \qquad 0 \le \frac{\sigma}{\sigma_0} \le 1$$

$$\varepsilon \to 0 \qquad Q \to 0$$

$$\Rightarrow\ k_{\beta 0}^2 r_b^2 = Q$$

envelope equation

Continuous Focusing KV Equilibrium ± Undepressed and depressed particle orbits in the -plane

$$k_\beta = \frac{\sigma}{\sigma_0}k_{\beta 0} \qquad \frac{\sigma}{\sigma_0} = 0.2 \qquad = 0 =$$

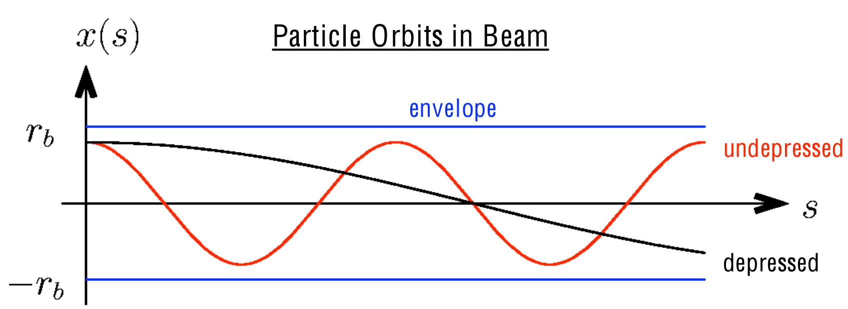

Much simpler in details than the periodic focusing case, but qualitatively similar in that space-charge ™depresses∫ the rate of particle phase advance

Continuous Focusing KV Beam ± Equilibrium Distribution Form

Using

$$\lambda = q\pi\hat{n}r_b^2 \qquad \hat{n} = \text{const} \qquad \text{density within the beam}$$

for the beam line charge and

$$\delta(\text{const}\cdot x) = \frac{\delta(x)}{\text{const}}$$

the full elliptic beam KV distribution can be expressed as :

- See next slide for steps involved in the form reduction

$$\boxed{\begin{aligned}f_\perp &= \frac{\lambda}{q\pi^2\varepsilon_x\varepsilon_y}\delta\left[\left(\frac{x}{r_x}\right)^2 + \left(\frac{r_x x' - r_x' x}{\varepsilon_x}\right)^2 + \left(\frac{y}{r_y}\right)^2 + \left(\frac{r_y y' - r_y' y}{\varepsilon_y}\right)^2 - 1\right]\\ &= \frac{\hat{n}}{2\pi}\delta(H_\perp - H_{\perp b})\end{aligned}}$$

where

$$H_\perp = \frac{1}{2}\mathbf{x}_\perp'^2 + \frac{\varepsilon^2}{2r_b^4}\mathbf{x}_\perp^2$$

-- Hamiltonian (on-axis value 0 ref)

$$= \frac{1}{2}\mathbf{x}_\perp'^2 + \frac{1}{2}k_{\beta 0}^2\mathbf{x}_\perp^2 + \frac{q\phi}{m\gamma_b^3\beta_b^2c^2}$$

$$H_{\perp b} \equiv \frac{\varepsilon^2}{2r_b^2} = \text{const}$$

-- Hamiltonian at beam edge

/// Aside: Steps of derivation

Using:

$$\varepsilon_x = \varepsilon_y \equiv \varepsilon \qquad \lambda = q\pi\hat{n}r_b^2 = \text{const}$$

$$r_x = r_y \equiv r_b = \text{const}$$

$$f_\perp = \frac{\lambda}{q\pi^2\varepsilon_x\varepsilon_y}\delta\left[\left(\frac{x}{r_x}\right)^2 + \left(\frac{r_x x' - r_x' x}{\varepsilon_x}\right)^2 + \left(\frac{y}{r_y}\right)^2 + \left(\frac{r_y y' - r_y' y}{\varepsilon_y}\right)^2 - 1\right]$$

$$= \frac{\hat{n}r_b^2}{\pi\varepsilon^2}\delta\left(\frac{x^2}{r_b^2} + \frac{y^2}{r_b^2} + \frac{r_b^2 x'^2}{\varepsilon^2} + \frac{r_b^2 y'^2}{\varepsilon^2} - 1\right)$$

Using:

$$\delta(\text{const}\cdot x) = \frac{\delta(x)}{\text{const}}$$

$$f_\perp = \frac{\hat{n}}{2\pi}\delta\left(\frac{1}{2}\mathbf{x}_\perp'^2 + \frac{\varepsilon^2}{2r_b^4}\mathbf{x}_\perp^2 - \frac{\varepsilon^2}{2r_b^2}\right)$$

The solution for the potential for the uniform density beam inside the beam is:

$$\frac{1}{r}\frac{\partial}{\partial r}r\frac{\partial\phi}{\partial r} = -\frac{\lambda}{\pi\epsilon_0 r_b^2} \quad\longrightarrow\quad \phi = -\frac{\lambda}{4\pi\epsilon_0 r_b^2}\mathbf{x}_\perp^2 + \text{const}$$

The Hamiltonian becomes:

$$H_\perp = \frac{1}{2}\mathbf{x}_\perp'^2 + \frac{1}{2}k_{\beta 0}^2\mathbf{x}_\perp^2 + \frac{q\phi}{m\gamma_b^3\beta_b^2c^2}$$

$$= \frac{1}{2}\mathbf{x}_\perp'^2 + \frac{1}{2}k_{\beta 0}^2\mathbf{x}_\perp^2 - \frac{q\lambda}{4\pi m\gamma_b^3\beta_b^2c^2}\mathbf{x}_\perp^2 + \text{const} \qquad Q \equiv \frac{q\lambda}{2\pi\epsilon_0 m\gamma_b^3\beta_b^2c^2}$$

$$= \frac{1}{2}\mathbf{x}_\perp'^2 + \frac{1}{2}k_{\beta 0}^2\mathbf{x}_\perp^2 - \frac{Q}{2r_b^2}\mathbf{x}_\perp^2 + \text{const} \qquad = \text{const}$$

From the equilibrium envelope equation:

$$k_{\beta 0}^2 = \frac{Q}{r_b^2} + \frac{\varepsilon^2}{r_b^4}$$

The Hamiltonian reduces to:

$$H_\perp = \frac{1}{2}\mathbf{x}_\perp'^2 + \frac{\varepsilon^2}{2r_b^4}\mathbf{x}_\perp^2 + \text{const}$$

with edge value (turning point with zero angle):

$$H_{\perp b} \equiv \frac{\varepsilon^2}{2r_b^2} + \text{const}$$

Giving (constants are same in Hamiltonian and edge value and subtract out):

$$f_\perp = \frac{\hat{n}}{2\pi}\delta\left(\frac{1}{2}\mathbf{x}_\perp'^2 + \frac{\varepsilon^2}{2r_b^4}\mathbf{x}_\perp^2 - \frac{\varepsilon^2}{2r_b^2}\right) = \frac{\hat{n}}{2\pi}\delta\left(H_\perp - H_{\perp b}\right)$$

///

Equilibrium distribution

$$\boxed{f_\perp(H_\perp) = \frac{\hat{n}}{2\pi}\delta(H_\perp - H_{\perp b})} \qquad H_{\perp b} = \frac{\varepsilon^2}{2r_b^2} = \text{const}$$

$$\hat{n} = \text{const}$$

then it is straightforward to explicitly calculate (see homework problems)

Density: $$n = \int d^2x_\perp' \, f_\perp = \begin{cases} \hat{n}, & 0 \le r < r_b \\ 0, & r_b < r \end{cases}$$

Temperature: $$T_x = \gamma_b m\beta_b^2c^2\frac{\int d^2x_\perp' \, x'^2 f_\perp}{\int d^2x_\perp' \, f_\perp} = \begin{cases} \widehat{T_x}(1 - r^2/r_b^2), & 0 \le r < r_b \\ 0, & r_b < r \end{cases}$$

Density

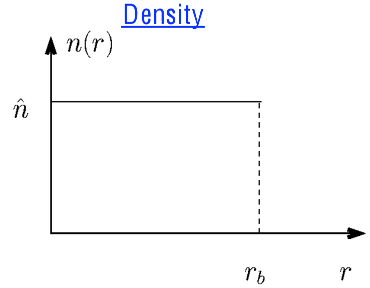

Temperature

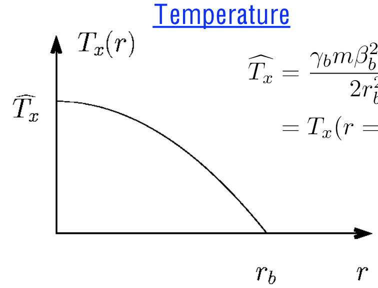

$$\widehat{T_x} = \frac{\gamma_b m\beta_b^2c^2\varepsilon^2}{2r_b^2} = T_x(r=0)$$

Continuous Focusing KV Beam ± Comments

For continuous focusing, $H_\perp$ is a single particle constant of the motion (see problem sets), so it is not surprising that the KV equilibrium form reduces to a delta function form of $f_\perp(H_\perp)$

- Because of the delta-function distribution form, all particles in the continuous focusing KV beam have the same transverse energy with $H_\perp = H_{\perp b} = \text{const}$

Several textbook treatments of the KV distribution derive continuous focusing versions and then just write down (if at all) the periodic focusing version based on Courant-Snyder invariants. This can create a false impression that the KV distribution is a Hamiltonian-type invariant in the general form.

- For non-continuous focusing channels there is no simple relation between Courant-Snyder type invariants and $H_\perp$

S5: Equilibrium Distributions in Continuous Focusing Channels

Take

$$\boxed{\kappa_x(s) = \kappa_y(s) = k_{\beta 0}^2 = \text{const}}$$

- Real transport channels have *s*-varying focusing functions
- For a rough correspondence to physical lattices take: $k_{\beta 0} = \sigma_0/L_p$

A valid family of equilibria can be constructed for any choice of function:

$$\boxed{f_\perp = f_\perp(H_\perp) \geq 0} \qquad H_\perp = \frac{1}{2}\mathbf{x}_\perp'^2 + \frac{1}{2}k_{\beta 0}^2\mathbf{x}_\perp^2 + \frac{q\phi}{m\gamma_b^3\beta_b^2c^2}$$

must be calculated consistently from the (generally nonlinear) Poisson equation:

$$\boxed{\left(\frac{\partial^2}{\partial x^2} + \frac{\partial^2}{\partial y^2}\right)\phi = -\frac{q}{\epsilon_0}\int d^2x_\perp' \; f_\perp(H_\perp)}$$

- Solutions generated will be steady-state $(\partial/\partial s = 0)$
- When $f_\perp = f_\perp(H_\perp)$, the Poisson equation *only* has axisymmetric solutions with $\partial/\partial\theta = 0$ [see: Lund, PRSTAB 10, 064203 (2007)]

The Hamiltonian is only equivalent to the Courant-Snyder invariant in continuous focusing (see: Transverse Particle Equations). In periodic focusing channels $\kappa_x(s)$ and $\kappa_y(s)$ vary in *s* and the Hamiltonian is *not* a constant of the motion.

The axisymmetric Poisson equation simplifies to:

$$\frac{1}{r}\frac{\partial}{\partial r}\left(r\frac{\partial\phi}{\partial r}\right) = -\frac{qn}{\epsilon_0} = -\frac{q}{\epsilon_0}\int d^2x_\perp' \; f_\perp(H_\perp)$$

Introduce a streamfunction

$$\boxed{\psi(r) = \frac{1}{2}k_{\beta 0}^2 r^2 + \frac{q\phi}{m\gamma_b^3\beta_b^2c^2}} \qquad r = \sqrt{x^2+y^2}$$

then

$$\boxed{H_\perp = \frac{1}{2}\mathbf{x}_\perp'^2 + \psi}$$

and system axisymmetry can be exploited to calculate the beam density (see earlier aside slides on integral symmetries for steps) as:

$$\boxed{n(r) = \int d^2x_\perp' \; f_\perp(H_\perp) \; = 2\pi\int_\psi^\infty dH_\perp \; f_\perp(H_\perp)}$$

The Poisson equation can then be expressed in terms of the stream function as:

$$\boxed{\frac{1}{r}\frac{\partial}{\partial r}\left(r\frac{\partial\psi}{\partial r}\right) = 2k_{\beta 0}^2 - \frac{2\pi q^2}{m\epsilon_0\gamma_b^3\beta_b^2c^2}\int_{\psi(r)}^\infty dH_\perp \; f_\perp(H_\perp)}$$

To characterize a choice of equilibrium function $f_\perp(H_\perp)$, the (transformed) Poisson equation must be solved

- Equation is, in general, *highly* nonlinear rendering the procedure difficult

Some general features of equilibria can still be understood:

- Apply rms equivalent beam picture and interpret in terms of moments
- Calculate equilibria for a few types of very different functions to understand the likely range of characteristics

Moment properties of continuous focusing equilibrium distributions

Equilibria with *any* valid equilibrium $f_\perp(H_\perp)$ satisfy the rms equivalent beam matched beam envelope equation:

$$\boxed{k_{\beta 0}^2 r_b - \frac{Q}{r_b} - \frac{\varepsilon^2}{r_b^3} = 0}$$

- Describes average radial force balance of particles
- Uses the result (see J.J. Barnard, Intro. Lectures): $\langle x\partial\phi/\partial x\rangle_\perp = -\lambda/(8\pi\epsilon_0)$

where

$$Q = \frac{q\lambda}{2\pi\epsilon_0 m\gamma_b^3\beta_b^2c^2} = \text{const} \qquad \lambda = q\int d^2x_\perp \int d^2x_\perp' \; f_\perp(H_\perp)$$

$$r_b^2 = 2\langle r^2\rangle_\perp = \frac{\int_0^\infty dr\; r^3 \int_\psi^\infty dH_\perp \; f_\perp(H_\perp)}{\int_0^\infty dr\; r\int_\psi^\infty dH_\perp \; f_\perp(H_\perp)}$$

$$\varepsilon^2 = 2r_b^2\langle \mathbf{x}_\perp'^2\rangle_\perp = 2r_b^2\frac{\int_0^\infty dr\; r\int_\psi^\infty dH_\perp \; (H_\perp - \psi)f_\perp(H_\perp)}{\int_0^\infty dr\; r\int_\psi^\infty dH_\perp \; f_\perp(H_\perp)}$$

$$\langle\cdots\rangle_\perp = \frac{\int d^2x_\perp \int d^2x_\perp' \; \cdots f_\perp(H_\perp)}{\int d^2x_\perp \int d^2x_\perp' \; f_\perp(H_\perp)}$$

Parameters used to define the equilibrium function

$$f_\perp(H_\perp)$$

should be cast in terms of

$$Q, \;\; \varepsilon, \;\; r_b$$

for use in accelerator applications. The rms equivalent beam equations can be used to carry out needed parameter eliminations. Such eliminations can be highly nontrivial due to the nonlinear form of the equations.

A kinetic temperature can also be calculated

$$T_x = \langle x'^2 \rangle_{\mathbf{x}'_\perp} \qquad \langle \cdots \rangle_{\mathbf{x}'_\perp} \equiv \frac{\int d^2x'_\perp \cdots f_\perp}{\int d^2x'_\perp \, f_\perp}$$

$$\boxed{n(r)T_x(r) = \frac{1}{2}\int d^2x'_\perp \; \mathbf{x}'^2_\perp f_\perp(H_\perp) \; = 2\pi \int_\psi^\infty dH_\perp \; (H_\perp - \psi) f_\perp(H_\perp)}$$

which is also related to the emittance,

$$\langle x'^2 \rangle_\perp = \frac{\int d^2x_\perp \, nT_x}{\int d^2x_\perp n} \qquad \boxed{\varepsilon^2 = 16\langle x^2\rangle_\perp \langle x'^2\rangle_\perp = 4r_b^2 \frac{\int d^2x_\perp \, nT}{\int d^2x_\perp \, n}}$$

Choices of continuous focusing equilibrium distributions:

Common choices for $f_\perp(H_\perp)$ analyzed in the literature:

1) KV (already covered)

$$\boxed{f_\perp \propto \delta(H_\perp - H_{\perp b})}$$

$$H_{\perp b} = \text{const}$$

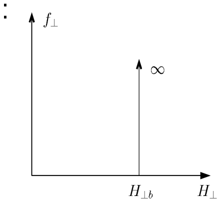

2) Waterbag (to be covered)

[see M. Reiser, *Charged Particle Beams*, (1994, 2008)]

$$\boxed{f_\perp \propto \Theta(H_{\perp b} - H_\perp)}$$

$$\Theta(x) = \begin{cases} 0, & x < 0 \\ 1, & 0 < x \end{cases}$$

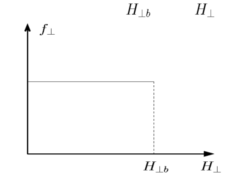

3) Thermal (to be covered)

[see M. Reiser; Davidson, *Noneutral Plasmas*, 1990]

$$\boxed{f_\perp \propto \exp(-H_\perp/T)}$$

$$T = \text{const} > 0$$

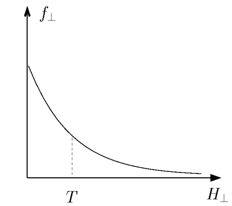

Infinity of choices can be made for an infinity of papers!

- Fortunately, range of behavior can be understood with a few reasonable choices

Preview of what we will find: When relative space-charge is strong, all smooth equilibrium distributions expected to look similar

Constant charge and focusing: $Q = 10^{-4} \qquad k_{\beta 0}^2 = \text{const}$

Vary relative space-charge strength: $\sigma/\sigma_0 = 0.1, \; 0.2, \; \cdots, \; 0.9$

Waterbag Distribution

$$f_\perp \propto \Theta(H_{\perp b} - H_\perp)$$

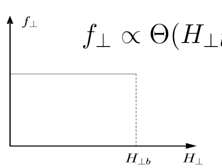

Thermal Distribution

$$f_\perp \propto \exp(-H_\perp/T)$$

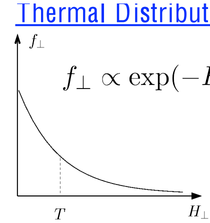

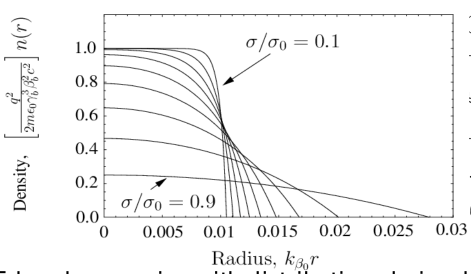

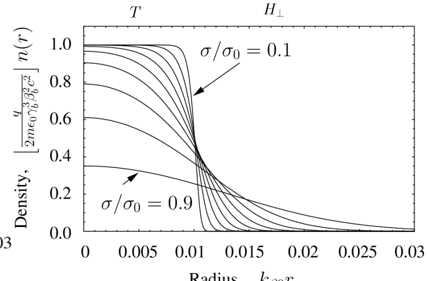

Edge shape varies with distribution choice, but cores similar when σ/σ_0 small

S6: Continuous Focusing: The Waterbag Equilibrium Distribution:

[Reiser, *Theory and Design of Charged Particle Beams*, Wiley (1994, 2008); and Review: Lund, Kikuchi, and Davidson, PRSTAB, to be published (2008)]

Waterbag distribution:

$$\boxed{\begin{aligned} & f_\perp(H_\perp) = f_0\Theta(H_b - H_\perp) && f_0 = \text{const} \\ & && H_b = \text{const} \;\; \text{Edge Hamiltonian} \\ & \Theta(x) = \begin{cases} 1, & x > 0 \\ 0, & x < 0 \end{cases} \end{aligned}}$$

The physical edge radius r_e of the beam will be related to the edge Hamiltonian:

$$\boxed{H_\perp|_{r=r_e} = H_b}$$

Note (generally): $r_e \neq r_b \equiv 2\langle x^2 \rangle_\perp^{1/2}$, $r_e > r_b$

Using previous formulas the equilibrium density can then be calculated as:

$$H_\perp = \mathbf{x}'^2_\perp/2 + \psi \qquad \psi = k_{\beta 0}^2 r^2/2 + \frac{q\phi}{m\gamma_b^3\beta_b^2c^2}$$

$$\boxed{n(r) = \int d^2x'_\perp \; f_\perp = 2\pi f_0 \begin{cases} H_b - \psi(r), & \psi < H_b, \\ 0, & \psi > H_b. \end{cases}}$$

The Poisson equation of the equilibrium can be expressed within the beam $(r < r_e)$ as:

$$\boxed{\begin{aligned}&\frac{1}{r}\frac{\partial}{\partial r}\left(r\frac{\partial \psi}{\partial r}\right) - k_0^2\psi = 2k_{\beta 0}^2 - k_0^2 H_b \\ &k_0^2 \equiv \frac{2\pi q^2 f_0}{\epsilon_0 m \gamma_b^3 \beta_b^2 c^2} = \text{const}\end{aligned}}$$

This is a modified Bessel function equation and the solution within the beam regular at the origin r = 0 and satisfying $\psi(r = r_e) = H_b$ is given by

$$\boxed{\psi(r) = H_b - 2\frac{k_{\beta 0}^2}{k_0^2}\left[1 - \frac{I_0(k_0 r)}{I_0(k_0 r_e)}\right]}$$

where $I_\ell(x)$ is a modified Bessel function of order ℓ

The density is then expressible within the beam $(r < r_e)$ as:

$$\boxed{\begin{aligned} n(r) &= 4\pi f_0 \frac{k_{\beta 0}^2}{k_0^2}\left[1 - \frac{I_0(k_0 r)}{I_0(k_0 r_e)}\right] \\ &= \frac{2\epsilon_0 m \gamma_b^2 \beta_b^2 c^2 k_{\beta 0}^2}{q^2}\left[1 - \frac{I_0(k_0 r)}{I_0(k_0 r_e)}\right]\end{aligned}}$$

Similarly, the local beam temperature within the beam can be calculated as:

$$\boxed{\begin{aligned} T_x(r) = \langle x'^2\rangle_{\mathbf{x}'_\perp} &= \frac{k_{\beta 0}^2}{k_0^2}\left[1 - \frac{I_0(k_0 r)}{I_0(k_0 r_e)}\right] \\ &\propto n(r)\end{aligned}}$$

The proportionality between the temperature ( ) and the density ( ) is a consequence of the waterbag equilibrium distribution choice and is *not* a general feature of continuous focusing.

The waterbag distribution expression can now be expressed as:

$$\boxed{f_\perp(\mathbf{x}_\perp, \mathbf{x}'_\perp) = f_0 \Theta\left(2\frac{k_{\beta 0}^2}{k_0^2}\left[1 - \frac{I_0(k_0 r)}{I_0(k_0 r_e)}\right] - \frac{1}{2}\mathbf{x}'^2_\perp\right)}$$

- The edge Hamiltonian value H_b has been eliminated
- Parameters are:

  f_0 .... distribution normalization

  $k_0 r_e$ .... scaled edge radius

  $k_{\beta 0}/k_0$ .... scaled focusing strength

Parameters preferred for accelerator applications:

$$k_{\beta 0}, \quad Q, \quad \varepsilon_x = \varepsilon_y = \varepsilon_b$$

Needed constraints to eliminate parameters in terms of our preferred set will now be derived.

Parameters constraints for the waterbag equilibrium beam

First calculate the beam line-charge:

$$\lambda = 2\pi q \int_0^{r_e} dr\, r n(r) = 4\pi^2 q f_0 \frac{k_{\beta 0}^2}{k_0^2} r_e^2 \left[1 - \frac{2}{k_0 r_e}\frac{I_1(k_0 r_e)}{I_0(k_0 r_e)}\right]$$

$$\boxed{\lambda = 2\pi q \int_0^{r_e} dr\, r n(r) = 4\pi^2 q f_0 \frac{k_{\beta 0}^2}{k_0^2} r_e^2 \frac{I_2(k_0 r_e)}{I_0(k_0 r_e)}}$$

here we have employed the modified Bessel function identities (ℓ integer):

$$\frac{d}{dx}[x^\ell I_\ell(x)] = x^\ell I_{\ell-1}(x),$$

$$-\frac{2\ell}{x} I_\ell(x) = I_{\ell+1}(x) - I_{\ell-1}(x),$$

Similarly, the beam rms edge radius can be explicitly calculated as:

$$r_b^2 = 2\langle r^2\rangle_\perp = 2\frac{\int_0^{r_e} dr\, r^3 n(r)}{\int_0^{r_e} dr\, r n(r)}$$

$$\boxed{\left(\frac{r_b}{r_e}\right)^2 = \frac{I_0(k_0 r_e)}{I_2(k_0 r_e)} - \frac{4}{(k_0 r_e)^2}\left[2 + (k_0 r_e)\frac{I_3(k_0 r_e)}{I_2(k_0 r_e)}\right]}$$

The perveance is then calculated as:

$$Q \equiv \frac{q\lambda}{2\pi\epsilon_0 m\gamma_b^3\beta_b^2c^2} = (k_{\beta 0}r_e)^2\frac{I_2(k_0r_e)}{I_0(k_0r_e)}$$

The edge and perveance equations can then be combined to obtain a parameter constraint relating k_0r_e to desired system parameters:

$$\frac{k_{\beta 0}^2r_b^2}{Q} = \frac{I_0^2(k_0r_e)}{I_2^2(k_0r_e)} - \frac{4}{(k_0r_e)^2}\left[2\frac{I_0(k_0r_e)}{I_2(k_0r_e)} + (k_0r_e)\frac{I_0(k_0r_e)I_3(k_0r_e)}{I_2^2(k_0r_e)}\right]$$

Here, any of the 3 system parameters on the LHS may be eliminated using the matched beam envelope equation to effect alternative parameterizations:

$$k_{\beta 0}^2r_b - \frac{Q}{r_b} - \frac{\varepsilon_b^2}{r_b^3} = 0 \longrightarrow \text{eliminate any of:} \quad k_{\beta 0}^2, \quad r_b \quad Q$$

The rms equivalent beam concept can also be applied to show that:

$$\frac{k_{\beta 0}^2r_b^2}{Q} = \frac{1}{1-(\sigma/\sigma_0)^2}$$

rms equivalent KV measure of σ/σ_0

- Space-charge really nonlinear and the Waterbag equilibrium has a spectrum of σ

The constraint is plotted over the full range of effective space-charge strength:

$$\frac{1}{1-(\sigma/\sigma_0)^2} = \frac{I_0^2(k_0r_e)}{I_2^2(k_0r_e)} - \frac{4}{(k_0r_e)^2}\left[2\frac{I_0(k_0r_e)}{I_2(k_0r_e)} + (k_0r_e)\frac{I_0(k_0r_e)I_3(k_0r_e)}{I_2^2(k_0r_e)}\right]$$

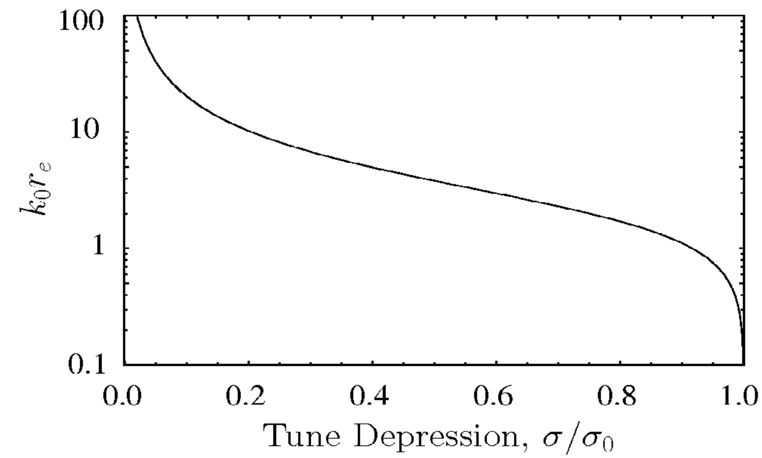

- Equilibrium parameter k_0r_e uniquely fixes effective space-charge strength

///Aside: Parameter choices and limits of the constraint equation

Some prefer to use an alternative space-charge strength measure to σ/σ_0 and use a so-called self-field parameter defined in terms of the on-axis plasma frequency of the distribution:

Self-field parameter:

$$s_b \equiv \frac{\hat{\omega}_p^2}{2\gamma_b^3\beta_b^2c^2k_{\beta 0}^2} \qquad \hat{\omega}_p^2 \equiv \frac{q^2\hat{n}}{m\epsilon_0} \qquad \begin{aligned}\hat{n} &= n(r=0)\\ &= \text{on-axis plasma density}\end{aligned}$$

For a KV equilibrium, s_b and σ/σ_0 are simply related:

$$s_b = 1 - \left(\frac{\sigma}{\sigma_0}\right)^2$$

For a waterbag equilibrium, s_b and k_0r_e (from which σ/σ_0 can be calculated) are related by:

$$s_b = 1 - \frac{1}{I_0(k_0r_e)}$$

Generally, for smooth (non-KV) equilibria, s_b turns out to be a logarithmically insensitive parameter for strong space-charge strength (see tables in S6 and S7) ///

Use parameter constraints to plot properties of waterbag equilibrium

1) Density and temperature profile at fixed line charge and focusing strength

$Q = 10^{-4}$ $\qquad k_{\beta 0}^2 = \text{const}$

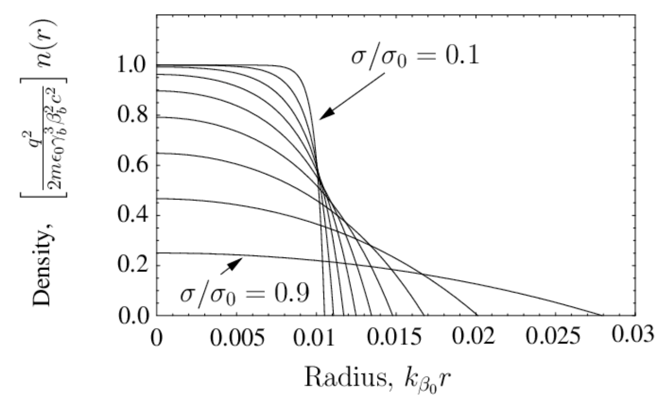

- Parabolic density for weak space-charge and flat in the core out to a sharp edge for strong space charge
- For the waterbag equilibrium, temperature ( ) is proportional to density ( ) so the same curves apply for ( )

2) Phase-space boundary of distribution at fixed line charge and focusing strength

$Q = 10^{-4}$ $\qquad k_{\beta 0}^2 = \text{const}$

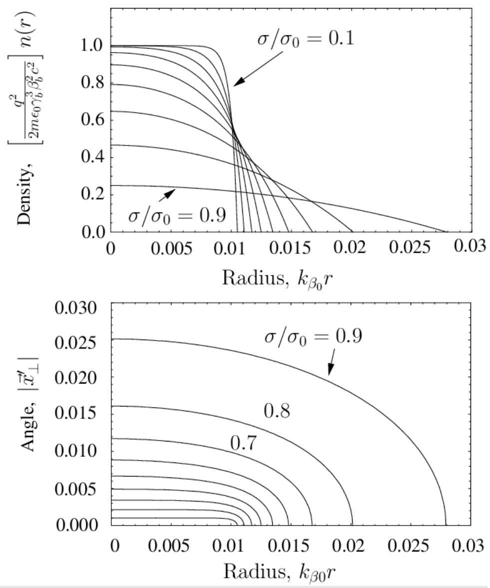

Density Profile

Edge of distribution in phase-space

3) Summary of scaled parameters for example plots:

σ/σ_0	s_b	$\frac{k_{\beta 0}^2 r_b^2}{Q}$	$k_0 r_e$	$\frac{r_e}{r_b}$	$\frac{k_0}{k_{\beta 0}}$	$10^3 \times k_{\beta 0}\varepsilon_b$
					$Q = 10^{-4}$	
0.9	0.2502	5.263	1.112	1.217	39.81	0.4737
0.8	0.4666	2.778	1.709	1.208	84.87	0.2222
0.7	0.6477	1.961	2.304	1.197	137.5	0.1373
0.6	0.7916	1.563	2.979	1.183	201.5	0.09375
0.5	0.8968	1.333	3.821	1.166	283.8	0.06667
0.4	0.9626	1.190	4.978	1.144	398.7	0.04762
0.3	0.9928	1.099	6.789	1.118	579.3	0.03297
0.2	0.9997	1.042	10.25	1.085	925.6	0.02083
0.1	1.0000	1.010	20.38	1.046	1938.	0.01010

140

S7: Continuous Focusing: The Thermal Equilibrium Distribution:

[Davidson, Physics of Nonneutral Plasma, Addison Wesley (1990) and Reiser, Theory and Design of Charged Particle Beams, Wiley (1994, 2008)]

In an infinitely long continuous focusing channel, collisions will eventually relax the beam to thermal equilibrium. The Fokker-Planck equation predicts that the unique Maxwell-Boltzmann distribution describing this limit is:

$$\lim_{s\to\infty} f_\perp \propto \exp\left(-\frac{H_{\rm rest}}{T}\right)$$

$H_{\rm rest} =$ single particle Hamiltonian of beam in rest frame (energy units)

$T = \text{const}$ Thermodynamic temperature (energy units)

Beam propagation time in transport channel is generally short relative to collision time, inhibiting full relaxation

- Collective effects may enhance relaxation rate
  - Wave spectrums likely large for real beams and enhanced by transient and nonequilibrium effects
  - Random errors acting on system may enhance and lock-in phase mixing

Continuous focusing thermal equilibrium distribution

Analysis of the rest frame transformation shows that the 2D Maxwell-Boltzmann distribution (careful on frame for temperature definition!) is:

$$f_\perp(H_\perp) = \frac{m\gamma_b\beta_b^2c^2\hat{n}}{2\pi T}\exp\left(-\frac{m\gamma_b\beta_b^2c^2H_\perp}{T}\right)$$

$$H_\perp = \frac{1}{2}\mathbf{x}_\perp'^2 + \frac{1}{2}k_{\beta 0}^2\mathbf{x}_\perp^2 + \frac{q\phi}{m\gamma_b^3\beta_b^2c^2} = \frac{1}{2}\mathbf{x}_\perp'^2 + \psi$$

$T = \text{const}$ Temperature (energy units, lab frame)

$n(r=0) = \hat{n} = \text{const}$ on-axis density

$\phi(r=0) = 0$ (reference choice)

The density can then be conveniently calculated in terms of a scaled stream function:

$$n(r) = \int d^2x'_\perp \; f_\perp \; = \hat{n}e^{-\tilde{\psi}}$$

$$\tilde{\psi}(r) \equiv \frac{m\gamma_b\beta_b^2c^2\psi}{T} = \frac{1}{T}\left(\frac{m\gamma_b\beta_b^2c^2k_{\beta 0}^2}{2}r^2 + \frac{q\phi}{\gamma_b^2}\right)$$

and the - and -temperatures are equal and spatially uniform with:

$$T_x = \gamma_b m\beta_b^2c^2\frac{\int d^2x'_\perp \; x'^2 \; f_\perp}{\int d^2x'_\perp \; f_\perp} = T = \text{const}$$

Scaled Poisson equation for continuous focusing thermal equilibrium

To describe the thermal equilibrium density profile, the Poisson equation must be solved. In terms of the scaled streamfunction:

$$\boxed{\begin{aligned} &\frac{1}{\rho}\frac{\partial}{\partial \rho}\left(\rho\frac{\partial\tilde{\psi}}{\partial\rho}\right) = 1 + \Delta - e^{-\tilde{\psi}} \\ &\tilde{\psi}(\rho = 0) = 0 \qquad \frac{\partial\tilde{\psi}}{\partial\rho}(\rho = 0) = 0 \end{aligned}}$$

Here,

$$\lambda_D = \left(\frac{\epsilon_0 T}{q^2\hat{n}}\right)^{1/2}$$ Debye length formed from the peak, on-axis beam density

$$\rho = \frac{r}{\gamma_b \lambda_D}$$ Scaled radial coordinate in rel. Debye lengths

$$\hat{\omega}_p \equiv \left(\frac{q^2\hat{n}}{\epsilon_0 m}\right)^{1/2}$$ Plasma frequency formed from on-axis beam density $\longrightarrow$ $$\lambda_D = \left(\frac{T}{\hat{\omega}_p^2 m}\right)^{1/2}$$

$$\Delta = \frac{2\gamma_b^3\beta_b^2 c^2 k_{\beta 0}^2}{\hat{\omega}_p^2} - 1$$ Dimensionless parameter relating the ratio of applied to space-charge defocusing forces

- Equation is highly nonlinear, but can be solved (approximately) analytically
- Scaled solutions depend only on the single dimensionless parameter #

Numerical solution of scaled thermal equilibrium Poisson equation in terms of a normalized density

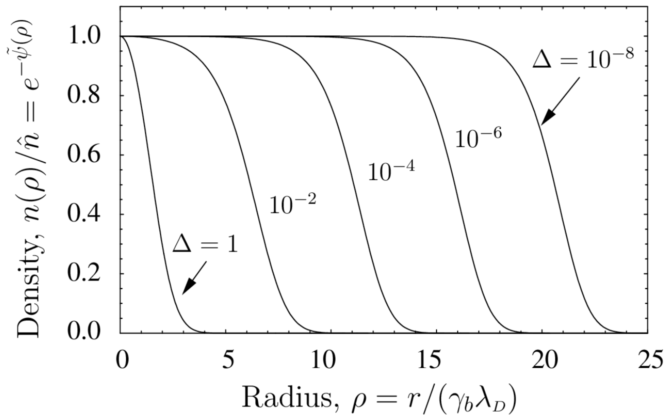

- Equation is highly nonlinear and must, in general, be solved numerically
  - Dependance on # is very sensitive
  - For small #, the beam is nearly uniform in the core
- Edge fall-off is always in a few Debye lengths when # is small
  - Edge becomes very sharp at fixed beam line-charge

/// Aside: Approximate Analytical Solution for the Thermal Equilibrium Density/Potential

Using the scaled density

$$N \equiv \frac{n}{\hat{n}} = e^{-\tilde{\psi}}$$

the equilibrium Poisson equation can be equivalently expressed as:

$$\boxed{\begin{aligned} &\frac{\partial^2 N}{\partial\rho^2} - \frac{1}{N}\left(\frac{\partial N}{\partial\rho}\right)^2 + \frac{1}{\rho}\frac{\partial N}{\partial\rho} = N^2 - (1+\Delta)N \\ &N(\rho = 0) = 1 \\ &\left.\frac{\partial N}{\partial\rho}\right|_{\rho=0} = 0 \end{aligned}}$$

This equation has been analyzed to construct limiting form analytical solutions for both large and small Δ [see: Startsev and Lund, PoP 15, 043101 (2008)]

- *Large* Δ solution => warm beam => Gaussian-like radial profile
- *Small* Δ solution => cold beam => Flat core, bell shaped profile
  - Highly nonlinear structure, but approx solution has very high accuracy out to where the density becomes exponentially small!

Large Δ solution:

$$N \simeq \exp\left[-\frac{1+\Delta}{4}\rho^2\right]$$

- Accurate for $\Delta \gtrsim 0.1$ [For full error spec. see: PoP 15, 043101 (2008)]

Small Δ solution:

$$N \simeq \frac{(1 + \frac{1}{2}\Delta + \frac{1}{24}\Delta^2)^2}{\{1 + \frac{1}{2}\Delta I_0(\rho) + \frac{1}{24}[\Delta I_0(\rho)]^2\}^2}$$

$I_0(x) =$ 0th order Modified Bessel Function of 1st kind

- Highly accurate for $\Delta \lesssim 0.1$ [For full error spec. see: PoP 15, 043101 (2008)]

Special numerical methods have also been developed to calculate or $\tilde{\psi} = -\ln N$ to arbitrary accuracy for *any* value of Δ, *however small*
[see: Lund, Kikuchi, and Davidson, PRSTAB, to be published, (2008) Appendices F, G]

- Extreme flatness of solution for small $\Delta \lesssim 10^{-8}$ creates numerical precision problems that require special numerical methods to address
- Method was used to verify accuracy of small Δ solution above

///

Parameters constraints for the thermal equilibrium beam

Parameters employed in $f_\perp(H_\perp)$ to specify the equilibrium are (+ kinematic factors): $\hat{n}, \quad T, \quad \Delta$

Parameters preferred for accelerator applications:

$$k_{\beta 0}, \quad Q, \quad \varepsilon_x = \varepsilon_y = \varepsilon_b$$

Needed constraints can be calculated directly from the equilibrium:

$$\boxed{\begin{aligned} Q &= \left(\frac{T}{\gamma_b m \beta_b^2 c^2}\right) \int_0^\infty d\rho \rho \, e^{-\tilde{\psi}} \\ k_{\beta 0}^2 \varepsilon_b &= 4\left(\frac{T}{\gamma_b m \beta_b^2 c^2}\right)\left[4\left(\frac{T}{\gamma_b m \beta_b^2 c^2}\right) + Q\right] \\ k_{\beta 0}^2 &= \left(\frac{T}{\gamma_b m \beta_b^2 c^2}\right) \frac{1+\Delta}{2(\gamma_b \lambda_D)^2} \end{aligned}}$$

Integral function of Δ only

Also useful,

$$\boxed{\begin{aligned} \varepsilon_b^2 &= 16 \frac{T}{\gamma_b m \beta_b^2 c^2} \langle x^2 \rangle_\perp^2 = 4\left(\frac{T}{\gamma_b m \beta_b^2 c^2}\right) r_b^2 \\ r_b^2 &= 4\langle x^2 \rangle_\perp = \frac{1}{k_{\beta 0}^2}\left[4\left(\frac{T}{\gamma_b m \beta_b^2 c^2}\right) + Q\right] \end{aligned}}$$

Example of derivation steps applied to derive previous constraint equations:

Line charge: $$\lambda = \frac{\gamma_b^2 T}{2q} \int_0^\infty d\rho \, \rho e^{-\tilde{\psi}}$$

rms edge radius: $$r_b^2 = 4\langle x^2 \rangle_\perp = 2\gamma_b^2 \lambda_D^2 \frac{\int_0^\infty d\rho \, \rho^3 e^{-\tilde{\psi}}}{\int_0^\infty d\rho \, \rho e^{-\tilde{\psi}}}$$

rms edge emittance:

$$\varepsilon_b^2 = \varepsilon_x^3 = 16[\langle x^2 \rangle_\perp \langle x'^2 \rangle_\perp - \cancelto{0}{\langle x x' \rangle_\perp^2}]$$

$$= 16 \frac{T}{\gamma_b m \beta_b^2 c^2} \langle x^2 \rangle_\perp = 4\left(\frac{T}{\gamma_b m \beta_b^2 c^2}\right) r_b^2$$

Matched envelope equation:

$$\cancelto{0}{r_b''} + k_{\beta 0}^2 r_b - \frac{Q}{r_b} - \frac{\varepsilon_b^2}{r_b^3} = 0$$

These constraints must, in general, be solved numerically

- Useful to probe system sensitivities in relevant parameters

Examples:

1) rms equivalent beam tune depression as a function of #

$$\frac{\sigma}{\sigma_0} = \sqrt{1 - \frac{Q}{k_{\beta_0}^2 r_b^2}} = \left\{1 - \frac{[\int_0^\infty d\rho \, \rho e^{-\tilde{\psi}}]^2}{(1+\Delta)\int_0^\infty d\rho \rho^3 e^{-\tilde{\psi}}}\right\}^{1/2}$$

R.H.S function of # only

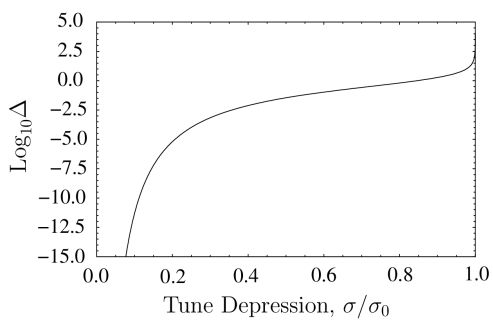

rms equivalent KV measure of σ/σ_0

- Space-charge really nonlinear and the Thermal equilibrium has a spectrum of σ

- Small rms equivalent tune depression corresponds to *extremely* small values of #
  - Special numerical methods generally must be employed to calculate equilibrium

2) Density profile at fixed line charge and focusing strength

$Q = 10^{-4}$ $\quad k_{\beta 0}^2 = \text{const}$

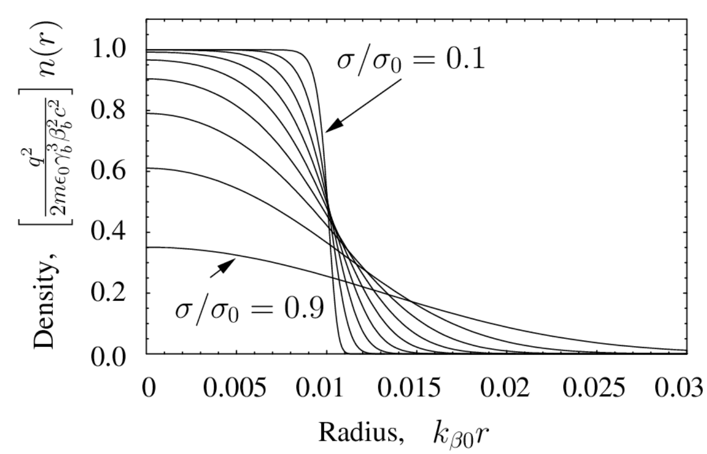

- Density profile changes with scaled T
  - Low values yields a flat-top => $\sigma/\sigma_0 \to 0$
  - High values yield a Gaussian like profile => $\sigma/\sigma_0 \to 1$

3) Distribution contours at fixed line charge and focusing strength

$Q = 10^{-4}$ $\quad k_{\beta 0}^2 = \text{const}$

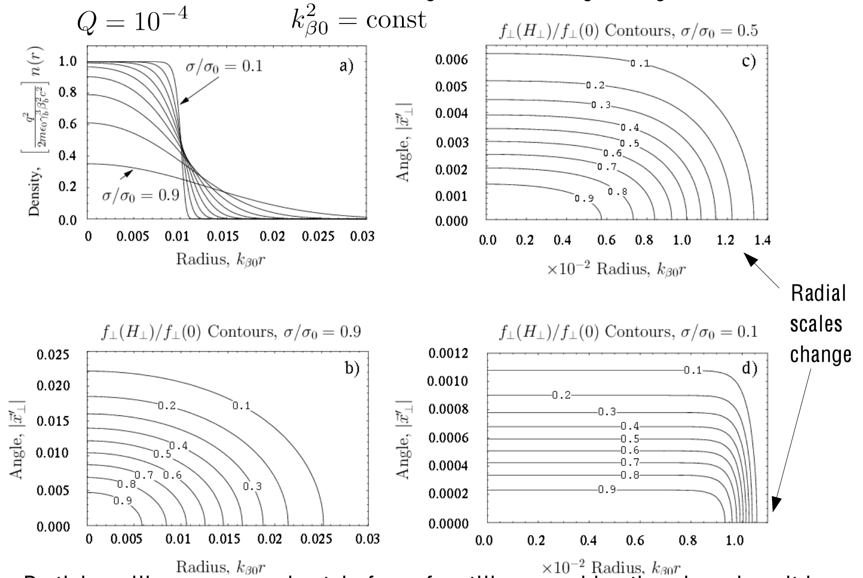

- Particles will move approximately force-free till approaching the edge where it is rapidly bent back (see Debye screening analysis this lecture)

Scaled parameters for examples 2) and 3)

			$Q = 10^{-4}$		
σ/σ_0	Δ	s_b	$k_{\beta 0}\gamma_b\lambda_D$	$\frac{T}{m\gamma_b\beta_b^2c^2}$	$10^3 \times k_{\beta 0}\varepsilon_b$
0.9	1.851	0.3508	12.33	1.065×10^{-4}	0.4737
0.8	6.382×10^{-1}	0.6104	6.034	4.444×10^{-5}	0.2222
0.7	2.649×10^{-1}	0.7906	3.898	2.402×10^{-5}	0.1373
0.6	1.059×10^{-1}	0.9043	2.788	1.406×10^{-5}	0.09375
0.5	3.501×10^{-2}	0.9662	2.077	8.333×10^{-6}	0.06667
0.4	7.684×10^{-3}	0.9924	1.549	4.762×10^{-6}	0.04762
0.3	6.950×10^{-4}	0.9993	1.112	2.473×10^{-6}	0.03297
0.2	6.389×10^{-6}	1.0000	0.7217	1.042×10^{-6}	0.02083
0.1	4.975×10^{-12}	1.0000	0.3553	2.525×10^{-7}	0.01010

Comments on continuous focusing thermal equilibria

From these results it is not surprising that the KV model works well for real beams with strong space-charge (i.e, rms equivalent σ/σ_0 small) since the edges of a smooth thermal distribution become sharp

- Thermal equilibrium likely overestimates the edge with since T = const, whereas a real distribution likely becomes colder near the edge

However, the beam edge contains strong nonlinear terms that will cause deviations from the KV model

- Nonlinear terms can radically change the stability properties (stabilize fictitious higher order KV modes)
- Smooth distributions contain a spectrum of particle oscillation frequencies that are amplitude dependent

S8: Continuous Focusing: Debye Screening in a Thermal Equilibrium Beam

[Davidson, *Physics of Nonneutral Plasmas*, Addison Wesley (1990)]

We will show that space-charge and the applied focusing forces of the lattice conspire together to Debye screen interactions in the core of a beam with high space-charge intensity

- Will systematically derive the Debye length employed by J.J. Barnard in the Introductory Lectures
- The applied focusing forces are analogous to a stationary neutralizing species in a plasma

// Review:

Free-space field of a ™bare∫ test line-charge λ_t at the origin $r = 0$

$$\rho(r) = \lambda_t \frac{\delta(r)}{2\pi r} \qquad \frac{1}{r}\frac{\partial}{\partial r}\left(r\frac{\partial\phi}{\partial r}\right) = -\frac{\lambda_t}{2\pi\epsilon_0}\frac{\delta(r)}{r}$$

solution (use Gauss' theorem) shows long-range interaction

$$\boxed{\begin{aligned}\phi &= -\frac{\lambda_t}{2\pi\epsilon_0}\ln(r) + \text{const} \\ E_r &= -\frac{\partial\phi}{\partial r} = \frac{\lambda_t}{2\pi\epsilon_0 r}\end{aligned}}$$

//

Place a *small* test line charge at $r = 0$ in a thermal equilibrium beam:

$$\frac{1}{r}\frac{\partial}{\partial r}\left(r\frac{\partial \phi}{\partial r}\right) = -\frac{q}{\epsilon_0}\int d^2x'_\perp\ f_\perp(H_\perp)\ -\ \frac{\lambda_t}{2\pi\epsilon_0}\frac{\delta(r)}{r}$$

Thermal Equilibrium Test Line-Charge

Set:

$$\phi = \phi_0 + \delta\phi$$

$\phi_0 =$ Thermal Equilibrium potential with no test line-charge

$\delta\phi =$ Perturbed potential from test line-charge

Assume thermal equilibrium adapts adiabatically to the test line-charge:

$$n(r) = \int d^2x'_\perp\ f_\perp(H_\perp)\ = \hat{n}e^{-\tilde{\psi}} \simeq \hat{n}e^{-\tilde{\psi}_0(r)}e^{-q\delta\phi/(\gamma_b^2 T)}$$

$$\simeq \hat{n}e^{-\tilde{\psi}_0(r)}\left(1 - \frac{q\delta\phi}{\gamma_b^2 T}\right) \qquad \left|\frac{q\delta\phi}{\gamma_b^2 T}\right| \ll 1$$

Yields:

$$\frac{1}{r}\frac{\partial}{\partial r}\left(r\frac{\partial \delta\phi}{\partial r}\right) = -\frac{q^2}{\epsilon_0\gamma_b^2 T}\hat{n}e^{-\tilde{\psi}_0(r)}\ -\ \frac{\lambda_t}{2\pi\epsilon_0}\frac{\delta(r)}{r}$$

Assume a relatively cold beam so the density is flat near the test line-charge:

$$\hat{n}e^{-\tilde{\psi}_0(r)} \simeq \hat{n}$$

This gives:

$$\boxed{\frac{1}{r}\frac{\partial}{\partial r}\left(r\frac{\partial \delta\phi}{\partial r}\right) - \frac{\delta\phi}{\gamma_b^2\lambda_D^2} = -\frac{\lambda_t}{2\pi\epsilon_0}\frac{\delta(r)}{r}}$$

$$\lambda_D = \left(\frac{\epsilon_0 T}{q^2\hat{n}}\right)^{1/2} =$$ Debye radius formed from peak, on-axis beam density

Derive a general solution by connecting solution very near the test charge with the general solution for r nonzero:

Near solution: $(r \rightarrow 0)$

$$\frac{\delta\phi}{\gamma_b^2\lambda_D^2}$$ Negligible ---> $$\frac{1}{r}\frac{\partial}{\partial r}\left(r\frac{\partial \delta\phi}{\partial r}\right) = -\frac{\lambda_t}{2\pi\epsilon_0}\frac{\delta(r)}{r}$$

The free-space solution can be immediately applied:

$$\boxed{\delta\phi \simeq -\frac{\lambda_t}{2\pi\epsilon_0}\ln(r) + \text{const} \qquad r \rightarrow 0}$$

General Exterior Solution: $(r \neq 0)$

The delta-function term vanishes giving:

$$\boxed{\frac{1}{\rho}\frac{\partial}{\partial \rho}\left(\rho\frac{\partial \delta\phi}{\partial \rho}\right) - \delta\phi = 0 \qquad \rho \equiv \frac{r}{\gamma_b\lambda_D}}$$

This is a modified Bessel equation of order 0 with general solution:

$$\delta\phi = C_1 I_0(\rho) + C_2 K_0(\rho)$$

$I_0(x) =$ Modified Bessel Func, 1st kind

$K_0(x) =$ Modified Bessel Func, 2nd kind

$C_1,\ \ C_2 = \text{constants}$

Connection and General Solution:

Use limiting forms:

$\rho \ll 1$

$$I_0(\rho) \rightarrow 1 + \Theta(\rho^2)$$

$$K_0(\rho) \rightarrow -[\ln(\rho/2) + 0.5772\cdots + \Theta(\rho^2)]$$

$\rho \gg 1$

$$I_0(\rho) \rightarrow \frac{e^\rho}{\sqrt{2\pi\rho}}[1 + \Theta(1/\rho)]$$

$$K_0(\rho) \rightarrow \sqrt{\frac{\pi}{2\rho}}[1 + \Theta(1/\rho)]$$

Comparison shows that we must choose for connection to the near solution and regularity at infinity:

$$\boxed{C_1 = 0 \qquad C_2 = \frac{\lambda_t}{2\pi\epsilon_0}}$$

General solution shows Debye screening of test charge in the core of the beam:

$$\delta\phi = \frac{\lambda_t}{2\pi\epsilon_0}K_0\left(\frac{r}{\gamma_b\lambda_D}\right)$$

$K_0(x)$ Order Zero Modified Bessel Function

$$\simeq \frac{\lambda_t}{2\sqrt{2\pi}\epsilon_0}\frac{1}{\sqrt{r/(\gamma_b\lambda_D)}}e^{-r/(\gamma_b\lambda_D)} \qquad r \gg \gamma_b\lambda_D$$

- Screened interaction does not require overall charge neutrality!
  - Beam particles redistribute to screen bare interaction
  - Beam behaves as a plasma and expect similar collective waves etc.
- Same result for all smooth equilibrium distributions and in 1D, 2D, and 3D
  - Reason why lower dimension models can get the ™right∫ answer for collective interactions in spite of the Coulomb force varying with dimension
- Explains why the radial density profile in the core of space-charge dominated beams are expected to be flat

S9: Continuous Focusing: The Density Inversion Theorem
Shows   and   dependencies are strongly connected in an equilibrium

For:

$$f_\perp = f_\perp(H_\perp)$$

$$H_\perp = \frac{1}{2}\mathbf{x}'^2_\perp + \frac{1}{2}k^2_{\beta 0}\mathbf{x}^2_\perp + \frac{q\phi}{m\gamma_b^3\beta_b^2c^2}$$
$$= \frac{1}{2}\mathbf{x}'^2_\perp + \psi(r) \qquad \psi \equiv \frac{1}{2}k^2_{\beta 0}r^2 + \frac{q\phi}{m\gamma_b^3\beta_b^2c^2}$$

calculate the beam density

$$n(r) = \int d^2x'_\perp\, f_\perp(H_\perp) = 2\pi\int_0^\infty dU\; f_\perp(U+\psi(r))$$

differentiate:

$$\frac{\partial n}{\partial \psi} = 2\pi\int_0^\infty dU\;\frac{\partial}{\partial\psi}f_\perp(U+\psi) = 2\pi\int_0^\infty dU\;\frac{\partial}{\partial U}f_\perp(U+\psi)$$

$$= 2\pi\underbrace{\lim_{U\to\infty} f_\perp(U+\psi)}_{0\text{ (bounded distribution)}} - 2\pi f_\perp(\psi)$$

$$\boxed{f_\perp(H_\perp) = -\frac{1}{2\pi}\frac{\partial n}{\partial\psi}\bigg|_{\psi=H_\perp} \qquad \psi(r) = \frac{1}{2}k^2_{\beta 0}r^2 + \frac{q\phi(r)}{m\gamma_b^3\beta_b^2c^2}}$$

Assume that $n(r)$ is specified, then the Poisson equation can be integrated:

$$\psi(r) - \frac{q\phi(r=0)}{m\gamma_b^3\beta_b^2c^2} = \frac{1}{2}k^2_{\beta 0}r^2 - \frac{q}{m\gamma_b^3\beta_b^2c^2\epsilon_0}\int_0^r\frac{d\tilde{r}}{\tilde{r}}\int_0^{\tilde{r}}d\tilde{\tilde{r}}\;\tilde{\tilde{r}}\;n(\tilde{\tilde{r}})$$

For $n(r)$ = const $\quad \displaystyle\int_0^r\frac{d\tilde{r}}{\tilde{r}}\int_0^{\tilde{r}}d\tilde{\tilde{r}}\;\tilde{\tilde{r}}\;n(\tilde{\tilde{r}}) \;\propto r^2$

This suggests that (r) is monotonic in r when $d\,n(r)/dr$ is monotonic. Apply the chain rule:

Density Inversion Theorem

$$\boxed{\begin{aligned} f_\perp(H_\perp) &= -\frac{1}{2\pi}\frac{\partial n}{\partial\psi}\bigg|_{\psi=H_\perp} = -\frac{1}{2\pi}\frac{\partial n(r)/\partial r}{\partial\psi(r)/\partial r}\bigg|_{\psi=H_\perp} \\ \psi(r) &= \frac{1}{2}k^2_{\beta 0}r^2 + \frac{q\phi}{m\gamma_b^3\beta_b^2c^2}\end{aligned}}$$

For specified monotonic $n(r)$ the density inversion theorem can be applied with the Poisson equation to calculate the corresponding equilibrium $f_\perp(H_\perp)$

Comments on density inversion theorem:

- Shows that the   and   dependence of the distribution are *inextricably linked* for an equilibrium distribution function $f_\perp(H_\perp)$
  - Not so surprising -- equilibria are highly constrained
- If $df_\perp(H_\perp)/dH_\perp \leq 0$ then the kinetic stability theorem (see: S.M. Lund, lectures on Transverse Kinetic Stability) shows that the equilibrium is also stable

// Example: Application of the inversion theorem to the KV equilibrium

$$n = \begin{cases}\hat{n}, & 0 \leq r < r_b \\ 0, & r_b < r\end{cases} \longrightarrow \frac{\partial n}{\partial r} = -\hat{n}\delta(r - r_b)$$

$$\frac{\partial n}{\partial\psi} = \frac{\partial n/\partial r}{\partial\psi/\partial r} = -\frac{\hat{n}\delta(r-r_b)}{\partial\psi/\partial r} = -\frac{\hat{n}\delta(r-r_b)}{\partial\psi/\partial r|_{r=r_b}} = -\hat{n}\delta(\psi(r)-\psi(r_b))$$

property of delta-function:

$$\delta(f(x)) = \sum_i\frac{\delta(x-x_i)}{|df/dx|_{x=x_i}}$$
$$f(x_i) = 0$$
$$x_i \text{is root of } f$$

use: $\quad \psi(r_b) = H_\perp|_{\mathbf{x}'_\perp=0} = H_{\perp b}$

$$\boxed{f_\perp(H_\perp) = -\frac{1}{2\pi}\frac{\partial n}{\partial\psi}\bigg|_{\psi=H_\perp} = \frac{\hat{n}}{2\pi}\delta(H_\perp - H_{\perp b})}$$

Expected
KV form

//

Similar application of derivatives with respect to Courant-Snyder invariants can ™derive∫ the needed form for the KV distribution of an elliptical beam without guessing.

S10: Comments on the Plausibility of Smooth, Vlasov Equilibria in Periodic Transport Channels

The KV and continuous models are the only (or related to simple transforms thereof) known exact beam equilibria. Both suffer from idealizations that render them inappropriate for use as initial distribution functions for detailed modeling of stability in real accelerator systems:

- KV distribution has an unphysical singular structure giving rise to collective instabilities with unphysical manifestations
  - Low order properties (envelope and some features of low-order plasma modes) are physical and very useful in machine design
- Continuous focusing is inadequate to model real accelerator lattices with periodic or -varying focusing forces
  - Kicked oscillator intrinsically different than a continuous oscillator

There is much room for improvement in this area, including study if smooth equilibria exist in periodic focusing and implications if no exact equilibria exist.

Large envelope flutter associated with strong focusing can result in a rapid high-order oscillating force imbalance acting on edge particles of the beam

Temperature Flutter

Elliptical rms Equivalent Beam

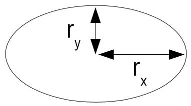

Example Systems	$(r_{max}/r_{min})^2$
AG Trans: σ_0 = 60°	~ 2.5
AG Trans: σ_0 = 100°	~ 4.9
Matching Section	~ 15 Possible

$$\varepsilon_x^2 \propto T_x r_x^2 \simeq \text{const} \implies T_x \propto \frac{1}{r_x^2}$$

Characteristic Plasma Frequency of Collective Effects

Continuous Focusing Estimate

$$\sigma_{\text{plasma}} \sim \frac{L_p}{r_b}\sqrt{2Q} \qquad \text{Typical: } \sigma_{\text{plasma}} \sim 105^\circ/\text{period}$$

- Temperature asymmetry in beam will rapidly fluctuate with lattice periodicity
  - Converging plane => Warmer
  - Diverging plane => Colder
- Collective plasma wave response slower than lattice frequency
  - Beam edge will not be able to adapt rapidly enough
  - Collective waves will be launched from lack of local force balance near the edge

The continuous focusing equilibrium distribution suggests that varying Debye screening together with envelope flutter would require a rapidly adapting beam edge in a smooth, periodic equilibrium beam distribution

$$f_\perp = \frac{m\gamma_b\beta_b^2c^2\hat{n}}{2\pi T}\exp\left(-\frac{m\gamma_b\beta_b^2c^2H_\perp}{T}\right)$$

Continuous Focusing Thermal Equilibrium Beam

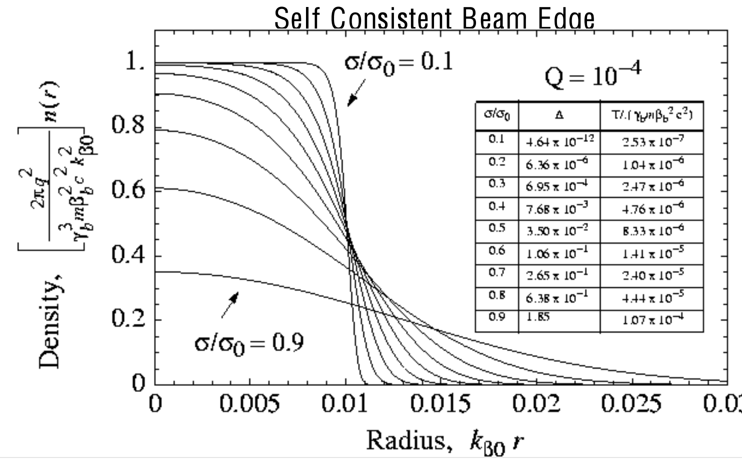

σ/σ_0	Δ	$T/(\gamma_b m\beta_b^2c^2)$
0.1	4.64×10^{-12}	2.53×10^{-7}
0.2	6.36×10^{-6}	1.04×10^{-6}
0.3	6.95×10^{-4}	2.47×10^{-6}
0.4	7.68×10^{-3}	4.76×10^{-6}
0.5	3.50×10^{-2}	8.33×10^{-6}
0.6	1.06×10^{-1}	1.41×10^{-5}
0.7	2.65×10^{-1}	2.40×10^{-5}
0.8	6.38×10^{-1}	4.44×10^{-5}
0.9	1.85	1.07×10^{-4}

It is clear from these considerations that if smooth ™equilibrium∫ beam distributions exist for periodic focusing, then they are highly nontrivial

Would a nonexistence of an equilibrium distribution be a problem:

- Real beams are born off a source that can be simulated
  - Propagation length can be relatively small in linacs
- Transverse confinement can exist without an equilibrium
  - Particles can turn at large enough radii forming an edge
  - Edge can oscillate from lattice period to lattice period without pumping to large excursions

→ Might not preclude long propagation with preserved statistical beam quality

Even approximate equilibria would help sort out complicated processes:

- Reduce transients and fluctuations can help understand processes in simplest form
  - Allows more ™plasma physics∫ type analysis and advances
- Beams in Vlasov simulations are often observed to ™settle down∫ to a fairly regular state after an initial transient evolution
  - Extreme phase mixing leads to an effective relaxation

These slides will be corrected and expanded for reference and any future editions of the US Particle Accelerator School class: *Beam Physics with Intense Space Charge*, by J.J. Barnard and S.M. Lund

Corrections and suggestions are welcome. Contact:

Steven M. Lund
Lawrence Berkeley National Laboratory
BLDG 47 R 0112
1 Cyclotron Road
Berkeley, CA 94720-8201

SMLund@lbl.gov
(510) 486 ± 6936

References: For more information see:

M. Reiser, *Theory and Design of Charged Particle Beams*, Wiley (1994, 2008)

R. Davidson, *Theory of Nonneutral Plasmas*, Addison-Wesley (1989)

R. Davidson and H. Qin, Physics of Intense Charged Particle Beams in High Energy Accelerators, World Scientific (2001).

H. Wiedermann, *Particle Accelerator Physics*, Springer-Verlag (1995)

J. Barnard and S. Lund, *Intense Beam Physics*, US Particle Accelerator School Notes, http://uspas.fnal.gov/lect_note.html (2006)

F. Sacherer, *Transverse Space-Charge Effects in Circular Accelerators*, Univ. of California Berkeley, Ph.D Thesis (1968).

S. Lund and B. Bukh, Review Article: *Stability Properties of the Transverse Envelope Equations Describing Intense Beam Transport*, PRST-Accel. and Beams 7, 024801 (2004).

D. Nicholson, *Introduction to Plasma Theory*, Wiley (1983)

I. Kaphinskij and V. Vladimirskij, in *Proc. Of the Int. Conf. On High Energy Accel. and Instrumentation* (CERN Scientific Info. Service, Geneva, 1959) p. 274

J.J. Barnard and S.M. Lund
USPAS June 2008

Appendix A
Self Fields of a Uniform Density Elliptical Beam in Free Space

$$\boxed{\left(\frac{\partial^2}{\partial x^2}+\frac{\partial^2}{\partial y^2}\right)\phi = \begin{cases} -\dfrac{\lambda}{\pi\varepsilon_0 r_x r_y}; & \dfrac{x^2}{r_x^2}+\dfrac{y^2}{r_y^2} < 1 \\ 0; & \dfrac{x^2}{r_x^2}+\dfrac{y^2}{r_y^2} > 1 \end{cases} \qquad \frac{\partial\phi}{\partial r} \sim \frac{\lambda}{2\pi\varepsilon_0 r} \quad \text{as } r\to\infty.}$$

The solution to this system to an arb. constant has been formally constructed by Landau & Lifshitz and others (gravitational field analog) as:

$$\boxed{\phi = -\frac{\lambda}{4\pi\varepsilon_0}\left\{\int_0^{\xi}\frac{ds}{[(r_x^2+s)(r_y^2+s)]^{1/2}} + \int_{\xi}^{\infty}\frac{ds}{[(r_x^2+s)(r_y^2+s)]^{1/2}}\left(\frac{x^2}{r_x^2+s}+\frac{y^2}{r_y^2+s}\right)\right\} + \text{const.}}$$

where

$$\begin{cases} \xi = 0; & \text{when } (x/r_x)^2+(y/r_y)^2 < 1 \\ \xi:\ \text{root of } \dfrac{x^2}{r_x^2+\xi}+\dfrac{y^2}{r_y^2+\xi} = 1, & \text{when } (x/r_x)^2+(y/r_y)^2 > 1 \end{cases}$$

Trivially for $x=y=0$

$$\phi(x=y=0) = \text{const.}$$

Calculate:

$$\frac{\partial\phi}{\partial x} = -\frac{\lambda}{4\pi\varepsilon_0}\left\{\int_{\xi}^{\infty}\frac{ds}{[(r_x^2+s)(r_y^2+s)]^{1/2}}\frac{2x}{r_x^2+s} - \frac{1}{[(r_x^2+\xi)(r_y^2+\xi)]^{1/2}}\left[1-\frac{x^2}{r_x^2+\xi}-\frac{y^2}{r_y^2+\xi}\right]\frac{\partial\xi}{\partial x}\right\}$$

$$\left.\begin{array}{l} \text{If } \xi\neq 0 \Rightarrow 1 = \dfrac{x^2}{r_x^2+\xi}+\dfrac{y^2}{r_y^2+\xi} \\ \xi = 0 \Rightarrow \dfrac{\partial\xi}{\partial x} = 0 \end{array}\right\} \Rightarrow \text{2nd term vanishes}$$

$$\boxed{\begin{aligned}\frac{\partial\phi}{\partial x} &= -\frac{\lambda}{2\pi\varepsilon_0}\int_{\xi}^{\infty}\frac{ds}{[(r_x^2+s)(r_y^2+s)]^{1/2}}\,\frac{x}{r_x^2+s}\\ &\text{by symmetry}\\ \frac{\partial\phi}{\partial y} &= -\frac{\lambda}{2\pi\varepsilon_0}\int_{\xi}^{\infty}\frac{ds}{[(r_x^2+s)(r_y^2+s)]^{1/2}}\,\frac{y}{r_y^2+s}\end{aligned}}$$

Differentiating again and using the chain rule:

$$\left(\frac{\partial^2}{\partial x^2}+\frac{\partial^2}{\partial y^2}\right)\phi = -\frac{\lambda}{2\pi\varepsilon_0}\left\{\int_{\xi}^{\infty}\frac{ds}{[(r_x^2+s)(r_y^2+s)]^{1/2}}\left[\frac{1}{r_x^2+s}+\frac{1}{r_y^2+s}\right] - \frac{1}{[(r_x^2+\xi)(r_y^2+\xi)]^{1/2}}\left[\frac{x\,\partial\xi/\partial x}{r_x^2+\xi}+\frac{y\,\partial\xi/\partial y}{r_y^2+\xi}\right]\right\}$$

Must show that the r.h.s. reduces to the needed forms for:

<u>case 1</u> exterior ξ satisfies: $\dfrac{x^2}{r_x^2+\xi}+\dfrac{y^2}{r_y^2+\xi}=1$

<u>case 2</u> interior $\xi=0$

<u>case 1</u> (exterior: $x^2/r_x^2+y^2/r_y^2>1$)

Differentiate $\dfrac{x^2}{r_x^2+\xi}+\dfrac{y^2}{r_y^2+\xi}=1$

$$\Rightarrow\quad \frac{\partial\xi}{\partial x} = \frac{2x}{(r_x^2+\xi)\left[\frac{x^2}{(r_x^2+\xi)^2}+\frac{y^2}{(r_y^2+\xi)^2}\right]}$$

$$\frac{\partial\xi}{\partial y} = \frac{2y}{(r_y^2+\xi)\left[\frac{x^2}{(r_x^2+\xi)^2}+\frac{y^2}{(r_y^2+\xi)^2}\right]}$$

$$\Rightarrow\quad \frac{x\,\partial\xi/\partial x}{r_x^2+\xi}+\frac{y\,\partial\xi/\partial y}{r_y^2+\xi} = 2\left[\frac{x^2}{(r_x^2+\xi)^2}+\frac{y^2}{(r_y^2+\xi)^2}\right]\frac{1}{\left[\frac{x^2}{(r_x^2+\xi)^2}+\frac{y^2}{(r_y^2+\xi)^2}\right]} = 2$$

Also need Integrals like: $\quad W^2 \equiv s + r_y^2$

$$I_x(\xi) \equiv \int_{\xi}^{\infty}\frac{ds}{[(r_x^2+s)(r_y^2+s)]^{1/2}}\,\frac{1}{r_x^2+s} = 2\int_{\sqrt{r_x^2+\xi}}^{\infty}\frac{dW}{(r_x^2-r_y^2+W^2)^{3/2}}$$

This integral can be done using tables:

$$I_x(\xi) = \left.\frac{2W}{(r_x^2-r_y^2)\sqrt{r_x^2-r_y^2+W^2}}\right|_{W=\sqrt{r_x^2+\xi}}^{W\to\infty} = \frac{2}{r_x^2-r_y^2} - \frac{2\sqrt{r_y^2+\xi}}{(r_x^2-r_y^2)\sqrt{r_x^2+\xi}}$$

Similarly:

$$I_y(\xi) \equiv \int_\xi^\infty \frac{ds}{[(r_x^2+s)(r_y^2+s)]^{1/2}}\frac{1}{(r_y^2+s)} = \frac{2}{r_y^2-r_x^2} - \frac{2\sqrt{r_x^2+\xi}}{(r_y^2-r_x^2)\sqrt{r_y^2+\xi}}$$

$$\int_0^\infty \frac{ds}{[(r_x^2+s)(r_y^2+s)]^{1/2}}\left[\frac{1}{r_x^2+s}+\frac{1}{r_y^2+s}\right] = I_x(\xi)+I_y(\xi)$$

$$= \frac{2}{r_x^2-r_y^2}\left(\frac{\sqrt{r_x^2+\xi}}{\sqrt{r_y^2+\xi}} - \frac{\sqrt{r_y^2+\xi}}{\sqrt{r_x^2+\xi}}\right) = \frac{2}{[(r_x^2+\xi)(r_y^2+\xi)]^{1/2}}$$

Using these results:

$$\left(\frac{\partial^2}{\partial x^2}+\frac{\partial^2}{\partial y^2}\right)\phi = -\frac{\lambda}{2\pi\varepsilon_0}\left\{\frac{2}{[(r_x^2+\xi)(r_y^2+\xi)]^{1/2}} - \frac{2}{[(r_x^2+\xi)(r_y^2+\xi)]^{1/2}}\right\}$$

$$= 0 \quad \text{checks.} \checkmark$$

<u>Case 2</u> (Interior: $x^2/r_x^2 + y^2/r_y^2 < 1$)

$$\xi = 0 \Rightarrow \frac{x\,\partial\xi/\partial x}{r_x^2+\xi} + \frac{y\,\partial\xi/\partial y}{r_y^2+\xi} = 0$$

$$\Rightarrow I_x(\xi=0) = \cancel{I_y(\xi=0)} = \frac{2}{(r_x+r_y)r_x} \quad \text{and} \quad I_y(\xi=0) = \frac{2}{(r_x+r_y)r_y}$$

Using these results:

$$\left(\frac{\partial^2}{\partial x^2}+\frac{\partial^2}{\partial y^2}\right)\phi = -\frac{\lambda}{2\pi\varepsilon_0}\left\{\frac{2}{r_x r_y} - 0\right\} = \frac{-\lambda}{\varepsilon_0\pi r_x r_y} = -\frac{q\hat{n}}{\varepsilon_0} \quad \text{checks} \checkmark$$

Finally, check the limiting form outside the beam for r large $\Rightarrow \xi$ large.

$$-\frac{\partial\phi}{\partial x} = \frac{\lambda}{2\pi\varepsilon_0}x I_x(\xi) \qquad \lim_{r\to\infty} I_x(\xi) = \frac{1}{\xi} = \frac{1}{r^2}$$

$$-\frac{\partial\phi}{\partial y} = \frac{\lambda}{2\pi\varepsilon_0}y I_y(\xi) \qquad \lim_{r\to\infty} I_y(\xi) = \frac{1}{\xi} = \frac{1}{r^2}$$

Thus:

$$\lim_{r\to\infty} -\frac{\partial\phi}{\partial x} = \frac{\lambda}{2\pi\varepsilon_0}\frac{x}{r^2}$$ ✓

$$\lim_{r\to\infty} -\frac{\partial\phi}{\partial y} = \frac{\lambda}{2\pi\varepsilon_0}\frac{y}{r^2}$$ ✓

These have the correct limiting forms for a line charge at the origin. Completing the verification of the general formula.

In the beam $\left(x^2/r_x^2 + y^2/r_y^2 < 1,\ \xi = 0\right)$, the formula reduces to:

$$\phi = -\frac{\lambda}{4\pi\varepsilon_0}\left\{ x^2 I_x(\xi=0) + y^2 I_y(\xi=0) \right\} + \text{const.}$$

$$= -\frac{\lambda}{4\pi\varepsilon_0}\left\{ \frac{2x^2}{r_x(r_x+r_y)} + \frac{2y^2}{r_y(r_x+r_y)} \right\} + \text{const.}$$

$$\boxed{\phi = -\frac{\lambda}{2\pi\varepsilon_0}\left\{ \frac{x^2}{r_x(r_x+r_y)} + \frac{y^2}{r_y(r_x+r_y)} \right\} + \text{const.}}$$

The case of an axisymmetric beam with

$$r_x = r_y = r_b$$

is easy to construct explicitly and is included in the homework problems.

There is also an alternative way to do this field calculation, that is less direct but more efficient. We carry out this proof now since steps involved are useful for other purposes.

S. M. Lund A5/

A density profile with elliptic symmetry can be expressed as:

$$n(x,y) = n\left(\frac{x^2}{r_x^2} + \frac{y^2}{r_y^2}\right)$$

Here we do not assume a specific uniform density profile and we leave $n(x^2/r_x^2 + y^2/r_y^2)$ arbitrary outside of having elliptic symmetry. The solution to the 2D Poisson equation in free-space

$$\left(\frac{\partial^2}{\partial x^2} + \frac{\partial^2}{\partial y^2}\right)\phi = -\frac{qn}{\varepsilon_0}$$

is then given by

$$\phi = -\frac{q r_x r_y}{4\varepsilon_0}\int_0^\infty d\xi \frac{\eta(\varkappa)}{\sqrt{r_x^2+\xi}\sqrt{r_y^2+\xi}}$$

$$\varkappa \equiv \frac{x^2}{r_x^2+\xi} + \frac{y^2}{r_y^2+\xi}$$

where $\eta(\varkappa)$ is a function defined such that:

$$n(x,y) = \left.\frac{d\eta(\varkappa)}{d\varkappa}\right|_{\xi=0}$$

This choice for $\eta(\varkappa)$ can always be made.

We first prove that this solution is valid by direct substitution:

$$\psi = \frac{x^2}{r_x^2+\xi} + \frac{y^2}{r_y^2+\xi} \implies \frac{\partial\psi}{\partial x} = \frac{2x}{r_x^2+\xi}\,;\quad \frac{\partial^2\psi}{\partial x^2} = \frac{2}{r_x^2+\xi}$$

$$\frac{\partial\psi}{\partial y} = \frac{2y}{r_y^2+\xi}\,;\quad \frac{\partial^2\psi}{\partial y^2} = \frac{2}{r_y^2+\xi}$$

Substitute in Poisson's equation and use the chain rule and results above:

$$\left(\frac{\partial^2}{\partial x^2}+\frac{\partial^2}{\partial y^2}\right)\phi = \frac{-q r_x r_y}{4\epsilon_0}\int_0^\infty d\xi\,\frac{\left(\frac{d^2\eta}{d\psi^2}\right)\left(\frac{4x^2}{(r_x^2+\xi)^2}+\frac{4y^2}{(r_y^2+\xi)^2}\right)+\left(\frac{d\eta}{d\psi}\right)\left(\frac{2}{r_x^2+\xi}+\frac{2}{r_y^2+\xi}\right)}{\sqrt{r_x^2+\xi}\,\sqrt{r_y^2+\xi}}$$

Note: $$d\psi = -\left[\frac{x^2}{(r_x^2+\xi)^2}+\frac{y^2}{(r_y^2+\xi)}\right]d\xi$$

so the first integral can be simplified by partial integration:

$$\int_0^\infty d\xi\,\frac{\left(\frac{d^2\eta}{d\psi^2}\right)\left(\frac{4x^2}{(r_x^2+\xi)^2}+\frac{4y^2}{(r_y^2+\xi)^2}\right)}{\sqrt{r_x^2+\xi}\,\sqrt{r_y^2+\xi}} = -4\int_0^\infty d\xi\,\frac{\frac{d^2\eta}{d\psi^2}\frac{d\psi}{d\xi}}{\sqrt{r_x^2+\xi}\,\sqrt{r_y^2+\xi}}$$

$$= -4\int_0^\infty d\xi\,\frac{\frac{d}{d\xi}\left(\frac{d\eta}{d\psi}\right)}{\sqrt{r_x^2+\xi}\,\sqrt{r_y^2+\xi}} = -4\int_0^\infty d\xi\,\frac{d}{d\xi}\left[\frac{\frac{d\eta}{d\psi}}{\sqrt{r_x^2+\xi}\,\sqrt{r_y^2+\xi}}\right] + 4\int_0^\infty d\xi\,\frac{d\eta}{d\psi}\frac{d}{d\xi}\frac{1}{\sqrt{r_x^2+\xi}\,\sqrt{r_y^2+\xi}}$$

$$= \left.\frac{-4\frac{d\eta}{d\psi}}{\sqrt{r_x^2+\xi}\,\sqrt{r_y^2+\xi}}\right|_{\xi\to 0}^{\xi\to\infty} - 2\int_0^\infty d\xi\,\frac{\frac{d\eta}{d\psi}\left(\frac{1}{r_x^2+\xi}+\frac{1}{r_y^2+\xi}\right)}{\sqrt{r_x^2+\xi}\,\sqrt{r_y^2+\xi}}$$

$$= \frac{4}{r_x r_y}\left.\frac{d\eta}{d\psi}\right|_{\xi=0} - 2\int_0^\infty d\xi\,\frac{\frac{d\eta}{d\psi}\left(\frac{1}{r_x^2+\xi}+\frac{1}{r_y^2+\xi}\right)}{\sqrt{r_x^2+\xi}\,\sqrt{r_y^2+\xi}}$$

term will cancel 2nd Integral

Thus:

$$\left(\frac{\partial^2}{\partial x^2}+\frac{\partial^2}{\partial y^2}\right)\phi = -\frac{q \cancel{r_x r_y}}{\cancel{4}\epsilon_0}\frac{\cancel{4}}{\cancel{r_x r_y}}\frac{d\eta(\mathcal{X})}{d\mathcal{X}}\bigg|_{\xi=0}$$

But $\displaystyle \frac{d\eta(\mathcal{X})}{d\mathcal{X}}\bigg|_{\xi=0} = n(x,y)$ by definition.

$$\Rightarrow \left(\frac{\partial^2}{\partial x^2}+\frac{\partial^2}{\partial y^2}\right)\phi = -\frac{q\,n(x,y)}{\epsilon_0}$$ verifying the result.

For a uniform density ellipse we take:

$$\eta(\mathcal{X}) = \frac{\lambda}{q\pi r_x r_y}\begin{cases}\mathcal{X} & ; \mathcal{X}<1\\ 1 & ; \mathcal{X}>1\end{cases} \Rightarrow \frac{d\eta(\mathcal{X})}{d\mathcal{X}} = \begin{cases}\frac{\lambda}{q\pi r_x r_y} & ; \mathcal{X}<1\\ 0 & ; \mathcal{X}>1\end{cases}$$

Thus

$$\frac{d\eta(\mathcal{X})}{d\mathcal{X}}\bigg|_{\xi=0} = \begin{cases}\frac{\lambda}{q\pi r_x r_y} & ; \mathcal{X}|_{\xi=0}<1\\ 0 & ; \mathcal{X}|_{\xi=0}\end{cases} = \begin{cases}\frac{\lambda}{q\pi r_x r_y} & ; \frac{x^2}{r_x^2}+\frac{y^2}{r_y^2}<1\\ 0 & ; \frac{x^2}{r_x^2}+\frac{y^2}{r_y^2}>1\end{cases}$$

$$\therefore \frac{d\eta(\mathcal{X})}{d\mathcal{X}}\bigg|_{\xi=0} = n(x,y)$$ for a uniform density elliptical beam with radii r_x, r_y and density $\lambda/(q\pi r_x r_y)$

Apply these results to calculate ϕ interior to a uniform density elliptical beam.

$$\phi = -\frac{q r_x r_y}{4\epsilon_0}\int_0^\infty d\xi\,\frac{\eta(\mathcal{X})}{\sqrt{r_x^2+\xi}\sqrt{r_y^2+\xi}}$$

$$\mathcal{X} = \frac{x^2}{r_x^2+\xi}+\frac{y^2}{r_y^2+\xi}$$ if $\displaystyle \frac{x^2}{r_x^2}+\frac{y^2}{r_y^2}<1$, then

$$\mathcal{X} = \frac{x^2}{r_x^2+\xi}+\frac{y^2}{r_y^2+\xi}<1 \quad \text{for all } 0\le\xi<\infty$$

Using this and the result above for $\eta(\mathcal{X})$, ϕ inside the elliptical beam is:

$$\phi = -\frac{q r_x r_y}{4\epsilon_0}\int_0^\infty d\xi\,\frac{\lambda}{q\pi r_x r_y}\left[\frac{x^2}{(r_x^2+\xi)^{3/2}(r_y^2+\xi)^{1/2}}+\frac{y^2}{(r_x^2+\xi)^{1/2}(r_y^2+\xi)^{3/2}}\right]$$

$$\phi = \frac{-\lambda}{4\pi\varepsilon_0}\left\{ x^2\int_0^\infty d\xi \frac{1}{(r_x^2+\xi)^{3/2}(r_y^2+\xi)^{1/2}} + y^2\int_0^\infty d\xi \frac{1}{(r_x^2+\xi)^{1/2}(r_y^2+\xi)^{3/2}} \right\}$$

Using Mathematica or Integral tables:

$$\int_0^\infty d\xi \frac{1}{(r_x^2+\xi)^{3/2}(r_y^2+\xi)^{1/2}} = \frac{2}{r_x(r_x+r_y)}$$

$$\int_0^\infty d\xi \frac{1}{(r_x^2+\xi)^{1/2}(r_y^2+\xi)^{3/2}} = \frac{2}{r_y(r_x+r_y)}$$

Hence

$$\phi = \frac{-\lambda}{2\pi\varepsilon_0}\left\{ \frac{x^2}{r_x(r_x+r_y)} + \frac{y^2}{r_y(r_x+r_y)} \right\} + \text{const}$$

since an overall constant can always be added to ϕ
(The integral has a reference choice $\phi(x=y=0)=0$ built in.).

The steps introduced in this proof can also be used to show that:

$$\left\langle x\frac{\partial\phi}{\partial x}\right\rangle_\perp = \frac{-\lambda}{4\pi\varepsilon_0}\frac{r_x}{r_x+r_y}$$

$$\left\langle y\frac{\partial\phi}{\partial y}\right\rangle_\perp = \frac{-\lambda}{4\pi\varepsilon_0}\frac{r_y}{r_x+r_y}$$

$\lambda = q\int d^2x\, n$

$r_x \equiv 2\langle x^2\rangle^{1/2}$

$r_y \equiv 2\langle y^2\rangle^{1/2}$

for any elliptic symmetry density profile $n(x,y) = n(x^2/r_x^2 + y^2/r_y^2)$. In the intro. lectures these results were employed to show that the KV envelope equations with evolving emittances can be applied to elliptic symmetry beams. This result was first demonstrated by Sacherer: [IEEE Trans Nucl. Sci. 18, 1105 (1971)]

J.J. Barnard and S.M. Lund
USPAS June 2008

Appendix B
Canonical Transformation of the KV Distribution

The single-particle equations of motion can be derived from the Hamiltonian: $\left(\frac{d\vec{x}_\perp}{ds} = \frac{\partial H}{\partial \vec{x}_\perp'},\ \frac{d\vec{x}_\perp'}{ds} = -\frac{\partial H}{\partial \vec{x}_\perp} \right)$

$$\boxed{\begin{aligned} H_\perp(x,y,x',y',s) = {} & \frac{1}{2}x'^2 + \left[\kappa_x(s) - \frac{2Q}{r_x(s)[r_x(s)+r_y(s)]}\right]\frac{x^2}{2} \\ & + \frac{1}{2}y'^2 + \left[\kappa_y(s) - \frac{2Q}{r_y(s)[r_x(s)+r_y(s)]}\right]\frac{y^2}{2} \end{aligned}}$$

Perform a canonical transform to new variables X, Y, X', Y' using the generating function

$$F_2(x,y,X',Y') = \frac{x}{w_x}\left[X' + \frac{x w_x'}{2}\right] + \frac{y}{w_y}\left[Y' + \frac{y w_y'}{2}\right]$$

Then:

$$\boxed{\begin{aligned} X &= \frac{\partial F_2}{\partial X'} = \frac{x}{w_x} \\ Y &= \frac{\partial F_2}{\partial Y'} = \frac{y}{w_y} \end{aligned}}$$

Ref:
R.C. Davidson, "Physics of Nonneutral Plasmas", Addison-Wesley, 1990

$$x' = \frac{\partial F_2}{\partial x} = \frac{1}{w_x}\left(X' + x w_x'\right)$$

$$y' = \frac{\partial F_2}{\partial y} = \frac{1}{w_y}\left(Y' + y w_y'\right)$$

and solving for X', Y':

$$\boxed{\begin{aligned} X' &= w_x x' - x w_x' \\ Y' &= w_y y' - y w_y' \end{aligned}}$$

Comment!
Here, $X' \neq \frac{d}{ds}X$, X' merely denotes the conjugate variable to X.
Also, X, X' both have dim. meters$^{1/2}$

The Courant-Snyder invariants are then simply expressed:

$$\boxed{\begin{aligned} \epsilon_x &= X^2 + X'^2 = \text{const} \\ \epsilon_y &= Y^2 + Y'^2 = \text{const} \end{aligned}}$$

One can show from the transformations that:

$$\boxed{\begin{aligned} dx\,dy &= w_x w_y \, dX\,dY \\ dx'dy' &= \frac{dX'dY'}{w_x w_y} \\ dx\,dy\,dx'dy' &= dX\,dY\,dX'dY' \;^{*} \end{aligned}}$$

* Property of canonical transforms in general. — Results from structure of Generating Function

Therefore, the distribution in transformed phase space variables is the same as for the original variables:

$$\boxed{\begin{aligned} f_\perp(X,Y,X',Y',s) &= f_\perp(x,y,x',y',s) \\ &= \frac{\lambda}{q\pi^2\varepsilon_x\varepsilon_y}\,\delta\left[\frac{X^2+X'^2}{\varepsilon_x}+\frac{Y^2+Y'^2}{\varepsilon_y}-1\right] \end{aligned}}$$

Now examine the density:

$$n(x,y) = \int dx'dy'\, f_\perp = \int \frac{dX'dY'}{w_x w_y} f_\perp$$

$$U_x = X'/\sqrt{\varepsilon_x}\,, \quad U_y = Y'/\sqrt{\varepsilon_y}$$

$$r_x = \sqrt{\varepsilon_x}\, w_x\,, \quad r_y = \sqrt{\varepsilon_y}\, w_y \qquad dU_x dU_y = \frac{dX'dY'}{\sqrt{\varepsilon_x\varepsilon_y}}$$

$$\boxed{n = \frac{\lambda}{q\pi^2 r_x r_y}\int dU_x dU_y\, \delta\left[U_x^2+U_y^2-\left(1-\frac{X^2}{\varepsilon_x}-\frac{Y^2}{\varepsilon_y}\right)\right]}$$

Exploit the cylindrical symmetry:

$$U_\perp^2 = U_x^2 + U_y^2$$

$$dU_x dU_y = d\psi\, U_\perp dU_\perp = d\psi \frac{dU_\perp^2}{2}$$

$$n(x,y) = \frac{\lambda}{q\pi^2 r_x r_y}\int_0^{2\pi} d\psi \int_0^{\infty} \frac{dU_\perp^2}{2}\, \delta\left[U_\perp^2 - \left(1 - \frac{x^2}{r_x^2} - \frac{y^2}{r_y^2}\right)\right]$$

Thus:

$$\boxed{\begin{aligned} n(x,y) &= \frac{\lambda}{q\pi r_x r_y}\int_0^{\infty} dU_\perp^2\, \delta\left[U_\perp^2 - \left(1 - \frac{x^2}{r_x^2} - \frac{y^2}{r_y^2}\right)\right] \\ &= \begin{cases} \dfrac{\lambda}{q\pi r_x r_y} = \hat{n} ; & \dfrac{x^2}{r_x^2} + \dfrac{y^2}{r_y^2} < 1 \\ 0 ; & \dfrac{x^2}{r_x^2} + \dfrac{y^2}{r_y^2} > 1 \end{cases} \end{aligned}}$$

Showing that the singular KV distribution yields the required uniform density beam of elliptical cross-section.

Note

$$\hat{n} = \frac{\lambda}{q\pi r_x r_y}$$

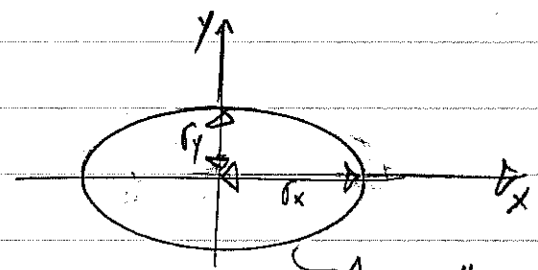

Area ellipse $= \pi r_x r_y$

$\lambda = q\hat{n}\pi r_x r_y$ for uniform density.

S. M. Lund B4

An interesting footnote to this appendix is that an infinity of Generating functions can be used to transform the KV distribution in standard quadratic form:

$$f_\perp \sim \delta\left[\bar{X}'^2 + \bar{Y}'^2 + \bar{X}^2 + \bar{Y}^2 - \text{const}\right]$$

to other sets of variables. This will generate other distributions with KV form for skew coupling and other effects. It would not be logical to label such distributions as "new" as has been done in the literature. However, identifying physically relevant transforms has practical value.

S. M. Lund B5/

Inverse transform:

$$x = w_x X$$

$$w_x x' = X' + x w_x' \quad \Rightarrow \quad x' = \frac{X'}{w_x} + w_x' X$$

$$\boxed{\begin{aligned} x &= w_x X & \qquad x' &= X'/w_x + w_x' X \\ y &= w_y Y & \qquad y' &= Y'/w_y + w_y' Y \end{aligned}}$$

Next,

$$\frac{d}{ds} X = \frac{x'}{w_x} - \frac{x\, w_x'}{w_x^2}$$

$$= \frac{X'}{w_x^2} + \cancel{\frac{w_x' X}{w_x}} - \cancel{\frac{w_x' X}{w_x}} = \frac{X'}{w_x^2}$$

Thus,

$$\boxed{\begin{aligned} \frac{d}{ds} X &= \frac{X'}{w_x^2} \\ \frac{d}{ds} Y &= \frac{Y'}{w_y^2} \end{aligned}}$$

$$\frac{d}{ds} X' = \cancel{w_x' x'} + w_x x'' - \cancel{x' w_x'} - x w_x''$$

$$\Rightarrow \boxed{\begin{aligned} x'' &= \frac{\frac{d}{ds} X'}{w_x} + w_x'' X \\ y'' &= \frac{\frac{d}{ds} Y'}{w_y} + w_y'' Y \end{aligned}}$$

Apply in Eqn of motion:

$$x'' + \kappa_x x - \frac{2Q\,x}{(r_x+r_y)\,r_x} = 0$$

$$\frac{\frac{d}{ds}X'}{w_x} + w_x'' X + \kappa_x w_x X - \frac{2Q\,w_x X}{(r_x+r_y)\,r_x} = 0$$

$$\frac{d}{ds}X' + w_x \overbrace{\left(w_x'' + \kappa_x w_x - \frac{2Q\,w_x}{(r_x+r_y)\,r_x} \right)}^{=\ \frac{1}{w_x^3}\ \text{from } w_x \text{ eqn}} X = 0$$

$$\boxed{\begin{array}{ll} \dfrac{d}{ds}X' + \dfrac{1}{w_x^2}X = 0, & \dfrac{d}{ds}X = \dfrac{X'}{w_x^2} \\[2ex] \dfrac{d}{ds}Y' + \dfrac{1}{w_y^2}Y = 0, & \dfrac{d}{ds}Y = \dfrac{Y'}{w_y^2} \end{array}}$$

Following Davidson, these eqns can be solved

$$X(s) = X_i \cos\psi_x(s) + X_i' \sin\psi_x(s)$$

$$\psi_x(s) = \int_{s_i}^{s} \frac{d\tilde{s}}{w_x^2(\tilde{s})} \quad ; \quad \psi_x'(s) = \frac{1}{w_x^2(s)}$$

etc. ⇒ This also demonstrates explicitly the C.S. Invariant

$$X^2 + X'^2 = \text{const.}$$

Note:
$$\frac{d}{ds}X = \frac{X'}{w_x^2}$$

Transformed Hamiltonian:

$$\boxed{\begin{aligned}
\frac{d}{ds}\mathcal{X} &= \frac{\partial \tilde{H}}{\partial \mathcal{X}'} = \frac{\mathcal{X}'}{w_x^2} \\
\frac{d}{ds}\mathcal{Y} &= \frac{\partial \tilde{H}}{\partial \mathcal{Y}'} = \frac{\mathcal{Y}'}{w_y^2} \\
\frac{d}{ds}\mathcal{X}' &= -\frac{\partial \tilde{H}}{\partial \mathcal{X}} = -\frac{1}{w_x^2}\mathcal{X} \\
\frac{d}{ds}\mathcal{Y}' &= -\frac{\partial \tilde{H}}{\partial \mathcal{Y}} = -\frac{1}{w_y^2}\mathcal{Y}
\end{aligned}}$$

$$\tilde{H} = \tilde{H}(\mathcal{X}, \mathcal{Y}, \mathcal{X}', \mathcal{Y}')$$

Transformed Hamiltonian

$$\Rightarrow \boxed{\tilde{H} = \frac{1}{2w_x^2}\mathcal{X}'^2 + \frac{1}{2w_y^2}\mathcal{Y}'^2 + \frac{1}{2w_x^2}\mathcal{X}^2 + \frac{1}{2w_y^2}\mathcal{Y}^2 + \text{const.}}$$

Note that $\tilde{H}$ is still explicitly s-dependant based on w_x and w_y lattice functions.

This Hamiltonian can also be found using results from the theory of canonical transforms:

$$\Rightarrow \tilde{H} = H + \frac{\partial F_2}{\partial s}$$

and the coordinate transform expressions.

Particle Resonances with Application to Circular Accelerators*

Steven M. Lund
Lawrence Livermore National Laboratory (LLNL)

Steven M. Lund and John J. Barnard
"Beam Physics with Intense Space-Charge"

US Particle Accelerator School

University of Maryland, held at Annapolis, MD
16-27 June, 2008
(Version 20080613)

* Research supported by the US Dept. of Energy at LLNL and LBNL under contract Nos. DE-AC52-07NA27344 and DE-AC02-05CH11231.

Particle Resonances: Outline

Particle Resonances: Detailed Outline

Particle Resonances: Detailed Outline - 2

S1: Overview

In our treatment of single particle orbits of lattices with s-varying focusing, we found that Hill's Equation describes the orbits to leading-order approximation:

$$x''(s) + \kappa_x(s)x(s) = 0$$
$$y''(s) + \kappa_y(s)y(s) = 0$$

where $\kappa_x(s), \quad \kappa_y(s)$
are functions that describe the linear applied focusing fields of the lattice

- Focusing functions can also incorporate linear space-charge forces
  - Self-consistent for special case of a KV distribution

In analyzing Hill's equations we employed phase-amplitude methods

- See: S.M. Lund lectures on Transverse Particle Equations, S8, on the betatron form of the solution

$$x(s) = A_{xi}\sqrt{\beta_x(s)}\cos\psi_x(s) \qquad A_{xi} = \text{const}$$
$$\frac{1}{2}\beta_x(s)\beta_x''(s) - \frac{1}{4}\beta_x'^2(s) + \kappa_x(s)\beta_x^2(s) = 1 \qquad \psi_x(s) = \psi_{xi} + \int_{s_i}^{s} \frac{d\bar{s}}{\beta_x(\bar{s})}$$
$$\beta_x(s+L_p) = \beta_x(s)$$

This formulation helped to simply identify the Courant-Snyder invariant:

$$\left(\frac{x}{w_x}\right)^2 + (w_x x' - w_x' x)^2 = A_x^2 = \text{const} \qquad w_x = \sqrt{\beta_x}$$

which helped to interpret the dynamics.

We will now exploit this formulation to better (analytically!) understand resonant instabilities in periodic focusing lattices. This is done by choosing coordinates such that stable unperturbed orbits described by Hill's equation:

$$x''(s) + \kappa_x(s)x(s) = 0$$

are mapped to a continuous oscillator

$$\tilde{x}''(\tilde{s}) + \tilde{k}_{\beta 0}^2\tilde{x}(\tilde{s}) = 0 \qquad \tilde{\cdots} = \text{Transformed Coordinate}$$
$$\tilde{k}_{\beta 0}^2 = \text{const} > 0$$

These transforms will help us more simply understand the action of perturbations (from applied field nonlinearities, ...) acting on the particle orbits:

$$x''(s) + \kappa_x(s)x(s) = \mathcal{P}_x(s; \mathbf{x}_\perp, \mathbf{x}_\perp', \vec{\delta})$$
$$y''(s) + \kappa_y(s)y(s) = \mathcal{P}_y(s; \mathbf{x}_\perp, \mathbf{x}_\perp', \vec{\delta})$$
$$\mathcal{P}_x, \ \mathcal{P}_y = \text{Perturbations}$$
$$\vec{\delta} = \text{Extra Coupling Variables}$$

For simplicity, we restrict analysis to:

$\gamma_b\beta_b = \text{const}$	No Acceleration
$\delta = 0$	No Axial Momentum Spread
$\phi = 0$	Neglect Space-Charge

- Comments on space-charge effects will be made in S7

We also take the applied focusing lattice to be periodic with:

$$\kappa_x(s+L_p) = \kappa_x(s) \qquad L_p = \text{Lattice Period}$$
$$\kappa_y(s+L_p) = \kappa_y(s)$$

For a ring we also have the superperiodicity condition:

$$\mathcal{P}_x(s+\mathcal{C}; \mathbf{x}_\perp, \mathbf{x}_\perp', \vec{\delta}) = \mathcal{P}_x(s; \mathbf{x}_\perp, \mathbf{x}_\perp', \vec{\delta})$$
$$\mathcal{P}_y(s+\mathcal{C}; \mathbf{x}_\perp, \mathbf{x}_\perp', \vec{\delta}) = \mathcal{P}_y(s; \mathbf{x}_\perp, \mathbf{x}_\perp', \vec{\delta})$$
$$\mathcal{C} = \mathcal{N}L_p = \text{Circumference Ring}$$
$$\mathcal{N} \equiv \text{Superperiodicity}$$

Perturbations can be Random and/or Systematic:

Random Errors in a ring will be felt once per particle lap in the ring rather than every lattice period

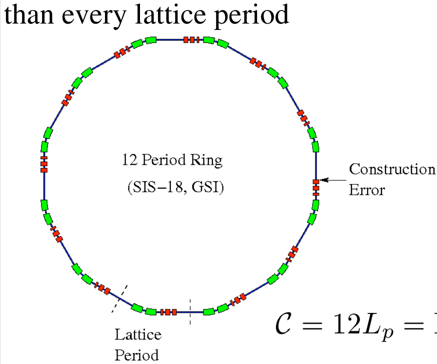

$$\mathcal{C} = 12L_p = \text{Ring Circumference}$$

Random Error Sources:

- Fabrication
- Assembly/Construction
- Material Defects
- ....

Systematic Errors can occur in both linear machines and rings and effect *every* lattice period in the same manner.

Example: FODO Lattice with the same error in each dipole of pair

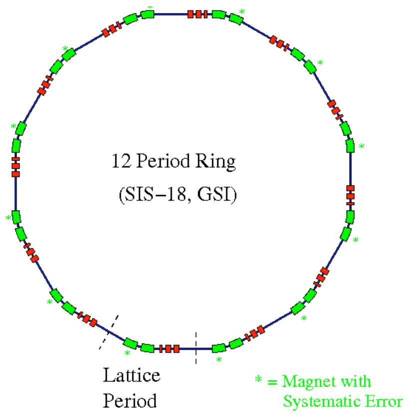

Systematic Error Sources:

- Design Flaw/Limit/Ideal
- Repeated Construction or Material Error
- ....

We will find that perturbations arising from both random and systematic error can drive resonance phenomena that destabilize particle orbits and limit machine performance

S2: Floquet Coordinates and Hill's Equation

Define for a *stable* solution to Hill's Equation

- Drop x subscripts and only analyze x-orbit for now to simplify

"Radial" Coordinate: (dimensionless) $\quad u \equiv \dfrac{x}{\sqrt{\beta}}$

"Angle" Coordinate: (dimensionless, normalized) $\quad \varphi \equiv \dfrac{1}{\nu_0}\displaystyle\int_{s_i}^{s} \frac{d\bar{s}}{\beta(\bar{s})} \equiv \frac{\Delta\psi(s)}{\nu_0}$

where

$$\beta = w^2 = \text{Betatron Amplitude Function}$$

$$\nu_0 \equiv \frac{\Delta\psi(\mathcal{N}L_p)}{2\pi} = \text{Number undepressed particle oscillations in ring } (\mathcal{N} = \text{Superperiod Number})$$

$$\psi = \text{Phase of } x\text{-orbit}$$

$$\Delta\psi(s) = \psi(s) - \psi(s_i)$$

- Can also take $\mathcal{N} = 1$ and then ν_0 is the number (usually fraction thereof) of undepressed particle oscillations in *one* lattice period

Comment:

φ can be interpreted as a normalized angle measured in the particle betatron phase advance:

Ring: ($\mathcal{N}$ = Superperiod #) $\implies$ φ advances by 2π on one transit around ring for analysis of Random Errors

Linac or Ring: ($\mathcal{N} = 1$) $\implies$ φ advances by 2π on transit through one lattice period for analysis of Systematic Errors in a ring *or* linac

Take φ as the independent coordinate:

$$\boxed{u = u(\varphi)}$$

and define a new "momentum" phase-space coordinate

$$\boxed{\dot{u} \equiv \frac{du}{d\varphi}} \qquad \boxed{\dot{} \equiv \frac{d}{d\varphi}}$$

These new variables will be applied to express Hill's equation in simpler form

From the definition

$$u \equiv \frac{x}{\sqrt{\beta}}$$

we have

$$x = \sqrt{\beta}u$$

$$x' = \frac{\beta'}{2\sqrt{\beta}}u + \sqrt{\beta}\frac{du}{d\varphi}\frac{d\varphi}{ds}$$

From:

$$\varphi \equiv \frac{1}{\nu_0}\int_{s_i}^{s}\frac{d\bar{s}}{\beta(\bar{s})} \quad \Longrightarrow \quad \boxed{\frac{d\varphi}{ds} = \frac{1}{\nu_0\beta}}$$

we obtain

$$x' = \frac{\beta'}{2\sqrt{\beta}}u + \frac{1}{\nu_0\sqrt{\beta}}\dot{u}$$

$$x'' = \frac{d}{ds}x' = \frac{\beta''}{2\sqrt{\beta}}u - \frac{\beta'^2}{4\beta^{3/2}}u - \cancel{\frac{\beta'}{2\nu_0\beta^{3/2}}\dot{u}} + \cancel{\frac{\beta'}{2\nu_0\beta^{3/2}}\dot{u}} + \frac{1}{\nu_0^2\beta^{3/2}}\ddot{u}$$

0 (cancels)

Summary:

$$x' = \frac{\beta'}{2\sqrt{\beta}}u + \frac{1}{\nu_0\sqrt{\beta}}\dot{u}$$
$$x'' = \frac{\beta''}{2\sqrt{\beta}}u - \frac{\beta'^2}{4\beta^{3/2}}u + \frac{1}{\nu_0^2\beta^{3/2}}\ddot{u}$$

Using these results, Hill's equation:

$$x''(s) + \kappa_x(s)x(s) = 0$$

becomes

$$\ddot{u} + \nu_0^2\left[\frac{\beta\beta''}{2} - \frac{\beta'^2}{4} + \kappa\beta^2\right]u = 0$$

But the betatron amplitude equation satisfies:

$$\frac{\beta\beta''}{2} - \frac{\beta'^2}{4} + \kappa\beta^2 = 1 \qquad \beta(s+L_p) = \beta(s)$$

Thus the terms in [...] = 1 and Hill's equation reduces to simple harmonic oscillator form:

$$\boxed{\ddot{u} + \nu_0^2 u = 0 \qquad \nu_0^2 = \text{const} > 0}$$

Transform has mapped a stable, time dependent solution to Hill's equation to a simple harmonic oscillator!

The general solution to the simple harmonic oscillator equation can be expressed as:

$$u(\varphi) = u_i\cos(\nu_0\varphi) + \frac{\dot{u}_i}{\nu_0}\sin(\nu_0\varphi)$$
$$\dot{u}(\varphi) = -u_i\nu_0\sin(\nu_0\varphi) + \dot{u}_i\cos(\nu_0\varphi)$$

$$u(\varphi=0) = u_i = \text{const}$$
$$\dot{u}(\varphi=0) = \dot{u}_i = \text{const}$$

u_i and $\dot{u}_i$ set by initial conditions at $s = s_i$ (phase choice $\varphi = 0$ at $s = s_i$)

The Floquet representation also simplifies the interpretation of the Courant-Snyder invariant:

$$\boxed{u^2 + \left(\frac{\dot{u}}{\nu_0}\right)^2 = u_i^2 + \left(\frac{\dot{u}_i}{\nu_0}\right)^2 \equiv \epsilon = \text{const}}$$

- Unperturbed phase-space in $u - \dot{u}/\nu_0$ is a unit circle!

Unperturbed phase-space ellipse:

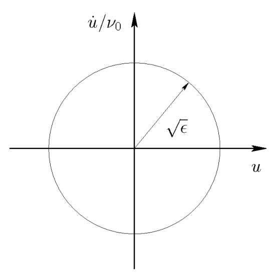

This simple structure will also allow more simple visualization of perturbations:

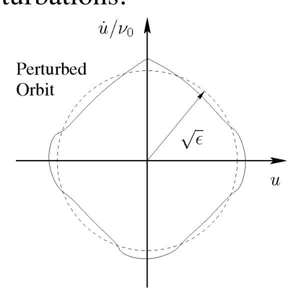

The $u - \dot{u}/\nu_0$ variables also preserve phase-space area

- Feature of the transform being symplectic (Hamiltonian Dynamics)

From previous results:

$$x = \sqrt{\beta}u \qquad \frac{d\varphi}{ds} = \frac{1}{\nu_0\beta}$$
$$x' = \frac{\beta'}{2\sqrt{\beta}}u + \sqrt{\beta}\frac{d\varphi}{ds}\dot{u} = \frac{\beta'}{2\sqrt{\beta}}u + \frac{1}{\nu_0\sqrt{\beta}}\dot{u}$$

Transform area elements by calculating the Jacobian:

$$dx \otimes dx' = |J| du \otimes d\dot{u}$$

$$J = \det\begin{vmatrix} \frac{\partial x}{\partial u} & \frac{\partial x}{\partial \dot{u}} \\ \frac{\partial x'}{\partial u} & \frac{\partial x'}{\partial \dot{u}} \end{vmatrix} = \det\begin{vmatrix} \sqrt{\beta} & 0 \\ \frac{\beta'}{2\sqrt{\beta}} & \frac{1}{\nu_0\sqrt{\beta}} \end{vmatrix} = \frac{1}{\nu_0}$$

$$\boxed{dx \otimes dx' = du \otimes \frac{d\dot{u}}{\nu_0}}$$

Thus the Courant-Snyder invariant ϵ is the usual single particle emittance

S3: Perturbed Hill's Equation in Floquet Coordinates

Return to the perturbed Hill's equation in S1:

$$\boxed{\begin{aligned} x''(s) + \kappa_x(s)x(s) &= \mathcal{P}_x(s; \mathbf{x}_\perp, \mathbf{x}'_\perp, \vec{\delta}) \\ y''(s) + \kappa_y(s)y(s) &= \mathcal{P}_y(s; \mathbf{x}_\perp, \mathbf{x}'_\perp, \vec{\delta}) \\ \mathcal{P}_x,\ \mathcal{P}_y &= \text{Perturbations} \\ \vec{\delta} &= \text{Extra Coupling Variables} \end{aligned}}$$

Drop the extra coupling variables and apply the Floquet transform in S2:

- Examine only x-equation, y-equation analogous

$$\boxed{\ddot{u} + \nu_0^2 u = \nu_0^2 \beta^{3/2} \mathcal{P}_x}$$

Here,

$$\mathcal{P}_x = \mathcal{P}(s(\varphi), \sqrt{\beta}u, y, \vec{\delta})$$

Transform y similarly to x

See Handwritten Notes From pg 12 Onward

S4: Sources and Forms of Perturbation Terms

S6: Solution of the Perturbed Hill's Equation: Resonances

S7: Machine Operating Points: Tune Restrictions Resulting from Resonances

S8: Space-Charge and Other Effects Altering Resonances

Ring operating points are generally chosen to be far from low-order resonance lines in *x-y* tune space. Processes that act to shift resonances closer towards the low-order lines can prove problematic:

- Oscillation amplitudes increase (spoiling beam quality and control)
- Particles can be lost

Tune shift limits of machine operation are often named "Laslett Limits" in honor of Jackson Laslett who first calculated tune shift limits for many processes:

- Image charges
- Image currents
- KV model self-fields internal to the beam
- ...

Processes shifting resonances can be grouped into two broad categories:

Coherent — Same for every particle in distribution
- Usually most dangerous

Incoherent — Different for particles in separate parts of the distribution
- Usually less dangerous

These slides will be corrected and expanded for reference and any future editions of the US Particle Accelerator School class:
Beam Physics with Intense Space Charge, by J.J. Barnard and S.M. Lund

Corrections and suggestions are welcome. Contact:

Steven M. Lund
Lawrence Berkeley National Laboratory
BLDG 47 R 0112
1 Cyclotron Road
Berkeley, CA 94720-8201

SMLund@lbl.gov
(510) 486 – 6936

References: For more information see:

E.D. Courant and H.S. Snyder, *Theory of the Alternating Gradient Synchrotron*, Annals of Physics **3**, 1 (1993).

A. Dragt, "Lectures on Nonlinear Orbit Dynamics," in *Physics of High Energy Accelerators*, edited by R.A. Carrigan, F.R. Hudson, and M. Month (AIP Conf. Proc. No. 87, 1982) p. 147.

D.A. Edwards and M.J. Syphers, *An Introduction to the Physics of High Energy Accelerators*, Wiley (1993).

M. Reiser, *Theory and Design of Charged Particle Beams*, Wiley (1994, 2008)

F. Sacherer, *Transverse Space-Charge Effects in Circular Accelerators*, Univ. of California Berkeley, Ph.D Thesis (1968)

H. Wiedemann, *Particle Accelerator Physics, Basic Principles and Linear Beam Dynamics,* Springer-Verlag (1993).

H. Wiedemann, *Particle Accelerator Physics II, Nonlinear and Higher-Order Beam Dynamics*, Springer-Verlag (1995).

Acknowledgments:

Considerable help was provided by Guliano Franchetti (GSI) in educating one of the authors (S.M. Lund) in methods described in this lecture.

Particle Resonace Notes – Supplement

We now analyze the effects of perturbations on the dynamics

$$\boxed{\ddot{U} + \nu_0^2 U = \nu_0^2 \beta^{3/2} P(x, y, s)} \; *$$

Expand the perturbation in a power series
- Can always be done for all physical applied field perturbations.

$$P(x,y,s) = P_0(y,s) + P_1(y,s)x + P_2(y,s)x^2 + \cdots$$

$$= \sum_{n=0}^{\infty} P_n(y,s)\, x^n$$

and take

$$x = \sqrt{\beta}\, U$$

to obtain

* P represents a perturbation due to:
  - Systematic or random field errors in magnets etc.
  - Alignment error induced field terms

  etc.

$$\boxed{\ddot{U} + \nu_0^2 U = \nu_0^2 \sum_{n=0}^{\infty} \beta^{\frac{n+3}{2}} P_n(y,s)\, U^n}$$

To more simply illustrate resonances we will take the particle to move in the x-plane only ($y = 0$ for all s). If this is not the case the formalism can be generalized by expanding the $P_n(y,s)$ in a power series in y and generalizing the notation for the Floquet coordinates to distinguish between the x- and y-planes, etc. The essential character of the more general analysis is illustrated by this simple case.

$$\boxed{y(s) \equiv 0 \quad \text{to simplify picture}}$$

In this special case $(y=0)$ we expand each coefficient in the power series in a Fourier series as:

Here I implicitly assume a ring and keep φ as a 2π "phase" path variable in the ring for both systematic and random errors.

$$\boxed{\begin{gathered} \mathcal{P}_n(y=0,s)\,\beta^{\frac{n+3}{2}} = \sum_{k=-\infty}^{\infty} C_{n,k}\, e^{ikP\varphi} \\ P = \begin{cases} 1 & \text{- A random perturbation (once in ring)} \\ N & \text{- A periodic perturbation (every period)} \end{cases} \\ C_{n,k} = \int_{-\pi/P}^{\pi/P} \frac{d\varphi}{2\pi/P}\, \mathcal{P}_n(y=0,s)\, \beta(s)^{\frac{n+3}{2}} \\ s = s(\varphi) \;; \quad \varphi = \int_{s_0}^{s} \frac{d\bar{s}}{\nu_0\,\beta(\bar{s})} \end{gathered}}$$

Then the perturbed equation of motion becomes:

$$\boxed{\ddot{U} + \nu_0^2 U = \nu_0^2 \sum_{n=0}^{\infty} \sum_{k=-\infty}^{\infty} C_{n,k}\, e^{ikP\varphi}\, U^n}$$

For the case of small amplitude perturbations this equation can be analyzed perturbatively to linear order as:

$$U = U_0 + \delta U \;; \quad |U_0| >> |\delta U|$$

where:

Simple Harmonic oscillator $\rightarrow$

$$\ddot{U}_0 + \nu_0^2 U_0 = 0$$

put unperturbed solution in perturbation

Simple Harmonic oscillator with driving terms. $\rightarrow$

$$\delta\ddot{U} + \nu_0^2\, \delta U \simeq \nu_0^2 \sum_{n=0}^{\infty} \sum_{k=-\infty}^{\infty} C_{n,k}\, e^{ipk\varphi}\, U_0^n$$

U_0 represents the unperturbed particle orbit. The general solution to the equation for U_0 can be expressed as:

$$\boxed{\begin{array}{l} U_0 = U_{0i} \cos(\nu_0 \varphi + \psi_i) \\ U_{0i},\ \psi_i \quad \text{initial conditions (constants)} \end{array}}$$

Then,

$$U_0^n = U_{0i}^n \left(\frac{e^{i(\nu_0\varphi + \psi_i)} + e^{-i(\nu_0\varphi+\psi_i)}}{2} \right)^n$$

$$= \frac{U_{0i}^n}{2^n} \sum_{m=0}^{n} \binom{n}{m} e^{i(n-m)(\nu_0\varphi+\psi_i)} e^{-im(\nu_0\varphi+\psi_i)}$$

Here, $\binom{n}{m} \equiv \frac{n!}{m!(n-m)!}$ is a binomial coefficient.

$$= \frac{U_{0i}^n}{2^n} \sum_{m=0}^{n} \binom{n}{m} e^{i(n-2m)\nu_0\varphi} e^{i(n-2m)\psi_i}$$

and the perturbed equation becomes:

$$\boxed{\delta \ddot{U} + \nu_0^2 \delta U \simeq \nu_0^2 \sum_{n=0}^{\infty} \sum_{k=\infty}^{\infty} \sum_{m=0}^{n} \binom{n}{m} C_{n,k}\, e^{i[(n-2m)\nu_0 + pk]\varphi} \times e^{i(n-2m)\psi_i}}$$

In general, can take $\delta U = \delta U_h + \delta U_p$ where $\delta \ddot{U}_h + \nu_0^2 \delta U_h = 0$ but in this case we can take $\delta U_h = 0$ since this part of the perturbative solution is contained in U_0. Thus only the particular solution need be found. From the properties of a driven harmonic oscillator, we know that no stable solution exists whenever the the frequency of the driving force equals that of the restoring force (resonant exchange). Thus we have the resonance condition: ← see Homework!

$$\boxed{\begin{gathered}(n-2m)\nu_0 + pk = \pm\nu_0 \\ n = 1, 2, 3, \ldots \quad ; \quad m = 0, 1, 2, \ldots n \\ k = -\infty, \ldots 0, \ldots \infty \\ p = \begin{cases} 1 & \text{A random perturbation (once per ring)} \\ N & \text{A periodic perturbation (every lattice period)} \end{cases}\end{gathered}}$$

For ν_0 satisfying this condition the perturbation will grow in amplitude. If the growth rate is sufficiently large, such tunes will be unreliable operating points of the machine and the corresponding perturbation must be corrected. Since this is a linear analysis, the purturbations may be analyzed in turn:

Examples:

$n=0$ (Dipole Perturbation)

$n=0 \Rightarrow m=0$ and the resonance condition becomes:

$$\nu_0 = \pm pk \qquad p\cdot k = \text{integer}$$

Therefore:

$$p = \begin{cases} 1; & \text{random pert in ring} \\ N; & \text{Periodic perturbation in lattice.} \end{cases} \qquad \boxed{\begin{aligned}\nu_0 \neq \text{integer} &= |p\cdot k| \quad \text{for dipole } (n=0) \\ &= p, p+1, \ldots \quad \text{perturbations}\end{aligned}}$$

$p=1$: Random error in ring (once per lap) $\Rightarrow$ $\nu_0 \neq 1, 2, 3, \ldots$

$p=N$: Systematic error (every lattice period) $\qquad \nu_0 \neq N, 2N, 3N, \ldots$

Systematic errors less restrictive.

$n=1$ Quadrupole Perturbation

The resonance conditions give: $\Rightarrow$ $n=1$, $m=0,1$

$$\nu_0 + pK = \pm\nu_0 \qquad (n=1, m=0)$$
$$-\nu_0 + pK = \pm\nu_0 \qquad (n=1, m=1)$$

$pK + \nu_0 = \nu_0$ represents a special case that can be eliminated by "renormalizing" the driving force of the oscillator and $pK = 2\nu_0$ implies that:

$p = \begin{cases} 1; & \text{random pert. in ring} \\ \mathcal{N}; & \text{periodic pert. in lattice} \end{cases}$

$$\boxed{\nu_0 \neq \text{half-integer} = |pK/2| \quad \text{for quadrupole } (n=1) \text{ perturbations.}}$$

$n=2$ Sextupole Perturbations $\Rightarrow$ $n=2$, $m=0,1,2$

The resonance conditions give:

$$2\nu_0 + pK = \pm\nu_0$$
$$pK = \pm\nu_0$$
$$-2\nu_0 + pK = \pm\nu_0$$

These conditions are equivalent to:

$p = \begin{cases} 1; & \text{random pert. in ring} \\ \mathcal{N}; & \text{periodic pert. in lattice} \end{cases}$

$$\boxed{\nu_0 \neq \begin{cases} \text{integer } (pK) \\ \text{half-integer } (pK/2) \\ \text{3rd-integer } (pK/3) \end{cases} \quad \text{for sextupole } (n=3) \text{ perturbations}}$$

The integer and half-integer restrictions were already obtained with respect to the dipole and quadrupole cases. The 3rd integer is a new restriction.

Other cases similar

// Aside Interpretation of low-order resonance conditions:

Dipole Errors

Consider a ring with 1 dipole error along the azimuth of a ring:

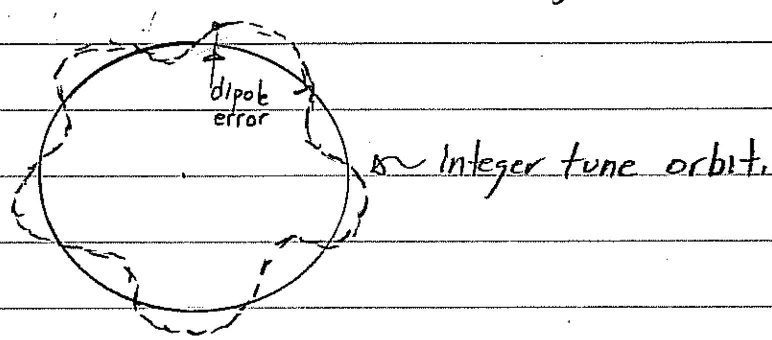

If the particle is oscillating with integer tune, then the particle will experience the error each time with the same phase of oscillation and the particle trajectory will "walk-off" lap to lap in phase-space. Since the machine aperture is finite the particle will be lost.

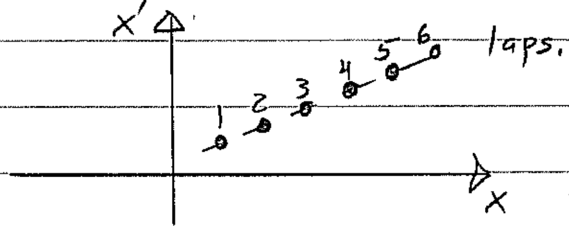

Quadrupole Errors

For a single quadrupole error along the azimuth of a ring, a similar qualitative argument leads one to conclude that if the particle oscillates with 1/2 integer tune that the orbit can "walk-off" lap-to-lap in phase space patterns as shown here:

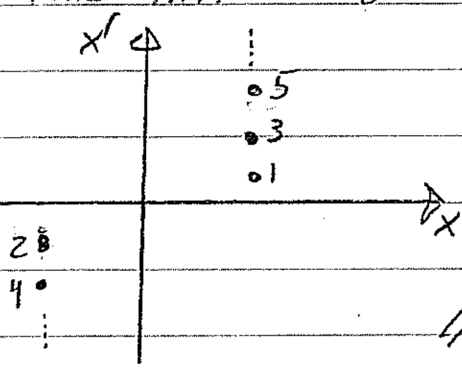

//

The general resonance condition for x-plane motion can be summarized as:

$$\boxed{M \nu_0 = N \qquad M, N \text{ integers of the same sign.}}$$

$M =$ order resonance

Generally higher order numbers are less dangerous.

- Longer coherence path for validity of theory and coefficients generally smaller $\therefore$ Higher order can "wash" out.

In the general case particle motion is not restricted to the x-plane ($y \neq 0$) and a more general resonance analysis shows that:

$$M_x \nu_{0x} + M_y \nu_{0y} = N$$

$\nu_{0x} =$ x-plane tune

$\nu_{0y} =$ y-plane tune

M_x, M_y, N integers of the same sign.

$$|M_x| + |M_y| = \text{order resonance.}$$

These restrictions are plotted order-by-order in $\nu_x - \nu_y$ plots to find allowed tunes where the machine can safely operate. Generally, lower order resonances are more dangeous, since small effects can invalidate the ideal analysis and "wash out" higher order resonances.

Typical tune plots for up to __3rd order__ resonances:

__$\mathcal{N}=1$ Superperiodicity__

Machine operating point is chosen to avoid resonance lines.

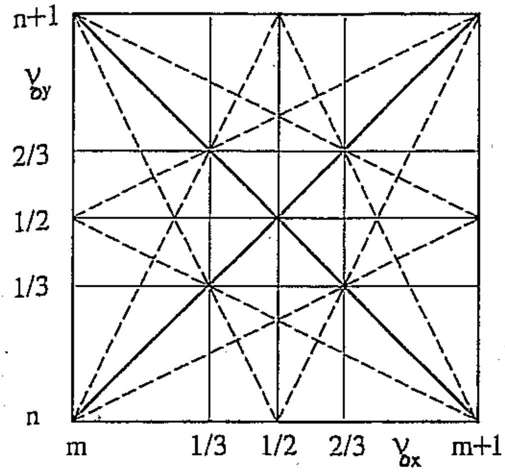

Applicable to field errors from __random construction errors.__

From Wiedemann

__$\mathcal{N}=4$ Superperiodicity__

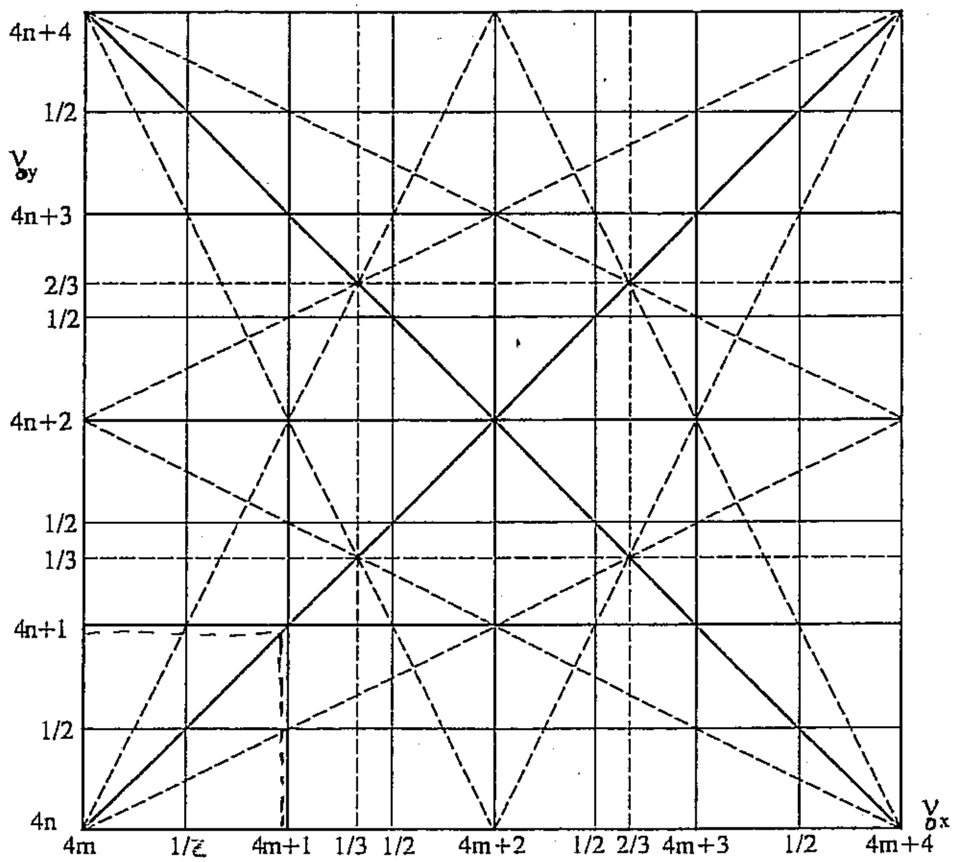

Applicable to __systematic lattice field errors__ in a 4-period ring.

Note __lesser density of resonance lines__ than __in the $\mathcal{N}=1$ case.__

Distinguishing between field errors from random construction ($p=1$) and systematic errors on the lattice ($p=\mathcal{N}$) is important.

Random errors ($p=1$)

- Errors always present and can give low order resonaces.
- Usually have weak amplitude coefficients and may be corrected.

Systematic errors ($p=\mathcal{N}$)

- Lead to higher order resonaces for large $\mathcal{N}$ and a lower density of resonance lines
  - Large symmetric rings ($\mathcal{N}$ large) have lesser restrictions from systematic errors
  - Practical issues such as construction cost and getting the beam into and out of the ring lead to smaller $\mathcal{N}$
- Amplitude coefficients can be large and the systematic resonances can be strong and thus can be dangerous.

In practice, resonances higher than 3rd order need rarely be considered.

- Effects outside model tend to wash out higher order resonances.

Effects of Space Charge on Resonances

Machine operating points are generally chosen far from low-order resonance lines. Coherent processes that shift tune values towards a low-order resonace are dangerous.

Coherent - same for each particle in distribution.

incoherent - different (random) for each particle in distribution.

Tune shift limits are often called "Laslett Limits" because he first calculated such limits for many processes

- Image charges
- Image currents
- space charge

⋮

For space-charge, the so-called Laslett limit is taken as:

$$\boxed{\nu_0 - \nu = \Delta\nu < 1/4}$$

ν_0 = tune at zero space charge

ν = KV distribution tune

This is probably over idealized and restrictive but is widely used to set ring current limits.

The Laslett condition is probably overly restrictive:

- Real space-charge is not coherent like a KV model
  - spectrum of β-tunes.
  - no equilibrium beam and oscillations may crack resonances.
- Simulations indicate that 10's → 100s of laps may pose little problems for strong space charge.
  - Univ. Maryland Ring may soon (~2007+) operate in such regime to test in the lab.

$\boxed{\text{This could be a good research area with new physics.}}$

John Barnard
Steven Lund
USPAS
June 2008

Injectors and longitudinal physics -- I

1. Child-Langmuir Law
   (Reiser 2.5.2, Appendix 1)
2. Pierce electrodes
3. Transients in injectors
4. Injector choices

(2)

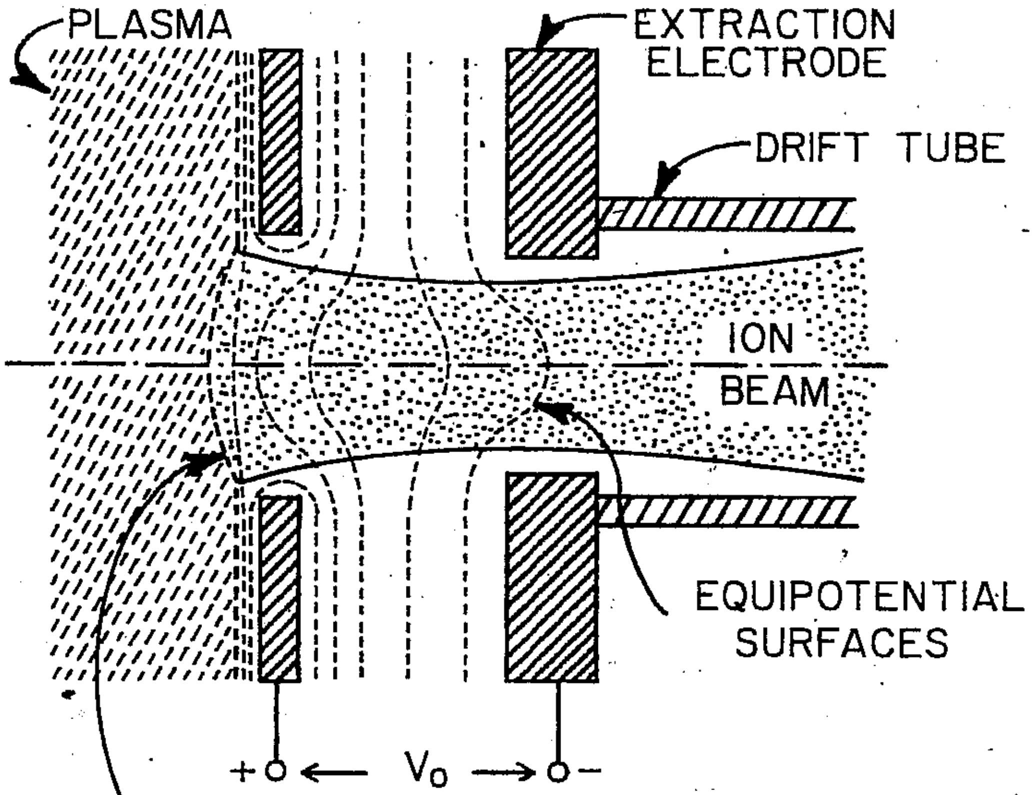

EMITTING SURFACE
(PLASMA "SHEATH" OR "MENISCUS")
OR "HOT PLATE"

Reiser, Figure 1.2

— DOPED TUNGSTEN
— ALUMINO-SILICATE

I CHILD-LANGMUIR EMISSION

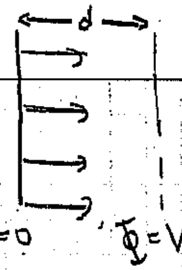

ASSUME EMISSION IS PLANAR 1-D:

$$J = \rho v_z \qquad (1)$$

$$\frac{1}{2} m v_z^2 = -q\Phi \qquad (2) \Rightarrow v_z = \left(\frac{-2q\Phi}{m}\right)^{1/2}$$

$$\frac{d^2\Phi}{dz^2} = \frac{\rho}{\varepsilon_0} \qquad (3)$$

(NOTE $\Phi = -\phi$ ACTUAL e.s. potential)

CONTINUITY EQUATION (1 D) $\quad \frac{\partial \rho}{\partial t} + \frac{\partial}{\partial z}\rho v_z = 0$

for time steady emission $\rho v_z = \text{constant} = J$

$$\Rightarrow \frac{d^2\Phi}{dz^2} = \frac{J}{\varepsilon_0 v_z} = \frac{J}{\varepsilon_0\left(\frac{-2q\Phi}{m}\right)^{1/2}}$$

MULTIPLYING BY $\frac{d\Phi}{dz}$ AND INTEGRATING:

$$\frac{\Phi'^2}{2} = \frac{J m^{1/2}}{\varepsilon_0 (2q)^{1/2}} 2\Phi^{1/2} + \text{const}$$

Assume $\Phi' = 0$ at $z = 0$ (Space-charge limited emission)

$\Phi = 0$ at $z=0 \Rightarrow \text{const} = 0$

$$\frac{d\Phi}{dz} = \left(\frac{4J}{\varepsilon_0}\right)^{1/2}\left(\frac{m\Phi}{2q}\right)^{1/4}$$

$$\Rightarrow \frac{4}{3}\Phi^{3/4} = \left(\frac{4J}{\varepsilon_0}\right)^{1/2}\left(\frac{m}{2q}\right)^{1/4} z \Rightarrow \Phi(x) = \left(\frac{3}{4}\right)^{4/3}\left(\frac{4J}{\varepsilon_0}\right)^{2/3}\left(\frac{m}{2q}\right)^{1/3} z^{4/3}$$

If $\Phi = V_0$ at $z = d$ $\Rightarrow$ $\Phi = V_0 \left(\frac{z}{d}\right)^{4/3}$

$$\Rightarrow \quad V_0 = \left(\frac{3}{4}\right)^{4/3} \left(\frac{4J}{\varepsilon_0}\right)^{2/3} \left(\frac{m}{2q}\right)^{1/3} d^{4/3}$$

$$\text{or} \quad J = \frac{4}{9}\varepsilon_0 \left(\frac{2q}{m}\right)^{1/2} \frac{V_0^{3/2}}{d^2}$$

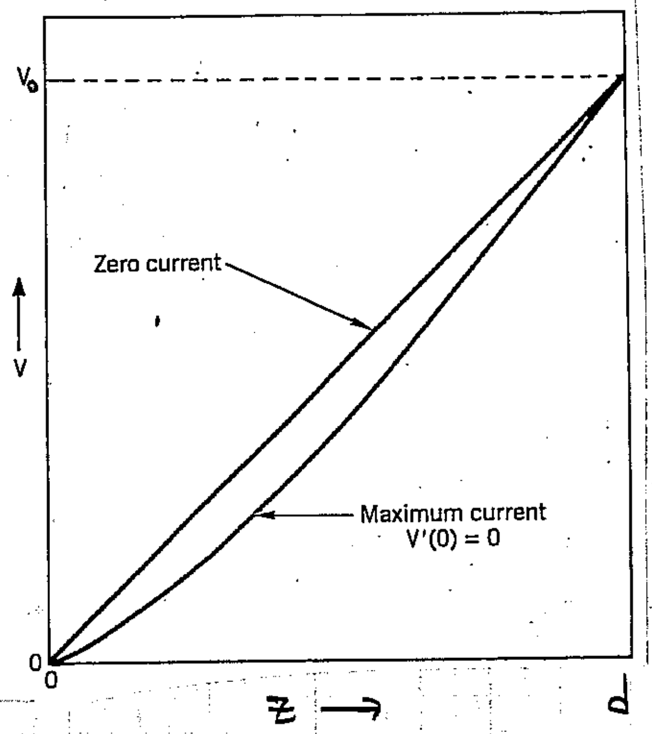

NOTE THAT IF WE MULTIPLY J BY THE BEAM AREA πr_b^2, AND DIVIDE BY $v = \left(\frac{2qV_0}{m}\right)^{1/2}$

$$\Rightarrow \lambda = \frac{4\pi\varepsilon_0 V}{9}\left(\frac{r_b^2}{d^2}\right) \qquad \text{RECALL} \quad Q \equiv \frac{\lambda}{4\pi\varepsilon_0 V} \quad \text{(NON-REL.)}$$

$$\Rightarrow Q = \frac{1}{9}\left(\frac{r_b^2}{d^2}\right) \quad \text{or as a function of } z: \quad Q(z) = \frac{1}{9}\left(\frac{r_b^2}{z^2}\right)$$

PERVEANCE

PIERCE COLUMN

$V \sim z^{4/3}$

$E \sim z^{1/3}$

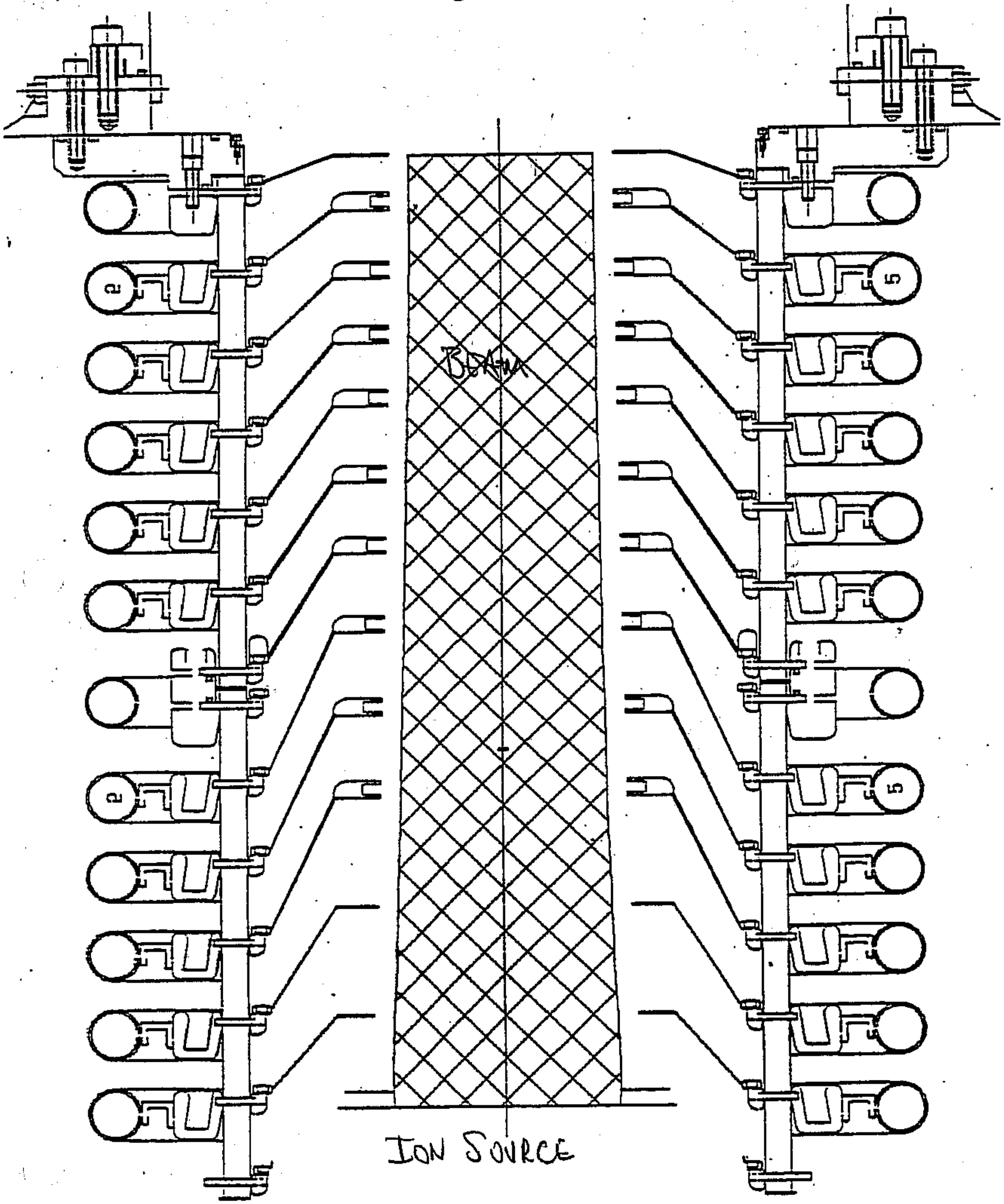

~~[illegible]~~, WE DERIVED THE PARAXIAL RAY EQUATION FOR PARTICLES IN AXISYMMETRIC SYSTEMS:

$$\underbrace{r'' + \frac{\gamma'}{\beta^2\gamma}\, r'}_{\text{INERTIAL}} + \underbrace{\frac{\gamma''}{2\beta^2\gamma}\, r}_{E_r} + \underbrace{\left(\frac{\omega_c}{2\gamma\beta c}\right)^2 r}_{v_\theta B_z \text{ - CENTRIFUGAL}} - \underbrace{\left(\frac{P_\theta}{\gamma\beta m c}\right)^2 \frac{1}{r^3}}_{\text{CENTRIFUGAL}} - \underbrace{\frac{q}{\gamma^3 m v_z^2}\,\frac{\lambda(r)}{2\pi\epsilon_0 r}}_{\text{SELF-FIELD}} = 0$$

$$\theta' = \frac{P_\theta}{\gamma m r^2 \beta c} - \frac{\omega_c}{2\gamma\beta c}$$ ← CONSTANCY & DEFINITION OF CANONICAL MOMENTUM

ENVELOPE EQUATION FOR AXISYMMETRIC BEAM

$$r_b'' + \frac{\gamma' r_b'}{\beta^2\gamma} + \frac{\gamma''}{2\beta^2\gamma}\, r_b + \left(\frac{\omega_c}{2\gamma\beta c}\right)^2 r_b - \frac{4\langle P_\theta\rangle^2}{(\gamma m\beta c)^2 r_b^3} - \frac{\epsilon_r^2}{r_b^3} - \frac{Q}{r_b} = 0$$

$$\epsilon_r^2 \equiv 4\left(\langle r^2\rangle\langle r'^2\rangle - \langle r r'\rangle^2 + \langle r^2\rangle\langle r^2\theta'^2\rangle - \langle r^2\theta'\rangle^2\right)$$

RETURNING TO PARAXIAL ENVELOPE EQUATION:

$$(\text{for } \beta \ll 1) \quad r_b'' + \frac{\beta'}{\beta} r_b' + \left[\frac{1}{2}\frac{\beta'^2}{\beta^2} + \frac{1}{2}\frac{\beta''}{\beta}\right] r_b - \frac{Q}{r_b} = 0$$

For $r_b'' = \frac{\beta'}{\beta} r_b' = 0$

If $\Phi = V_0 (z/d)^{4/3}$

$$v = C z^{2/3}$$

$$v' = \frac{2}{3} C z^{-1/3}$$

$$v'' = \frac{-2}{9} C z^{-4/3}$$

$$\Rightarrow \left[\frac{1}{2}\frac{\beta'^2}{\beta^2} + \frac{1}{2}\frac{\beta''}{\beta}\right] r_b^2 = Q$$

$$\left[\overset{\shortparallel}{\frac{2}{9}\frac{1}{z^2}} \qquad \overset{\shortparallel}{-\frac{1}{9}\frac{1}{z^2}} \right]$$

$$\Rightarrow Q(z) = \frac{1}{9}\frac{r_b^2}{z^2}$$

So Child-Langmuir flow satisfies the PARAXIAL ENVELOPE EQUATION FOR A CONSTANT BEAM RADIUS (AS IT SHOULD!)

PIERCE ELECTRODES: GOING BEYOND PARAXIAL APPROXIMATION

CONSIDER THE CASE A BEAM WHICH FILLS THE LOWER HALF-SPACE.

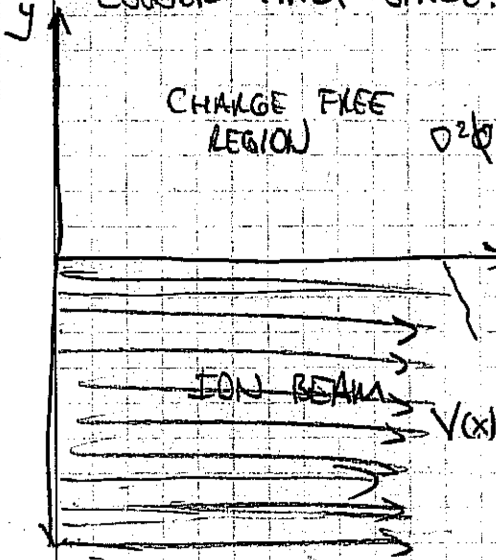

$$\frac{\partial^2\phi}{\partial x^2} + \frac{\partial^2\phi}{\partial y^2} = 0$$

$$V(x) = \left(\frac{J}{\chi}\right)^{2/3} x^{4/3}$$

$$\chi = \left(\frac{4\epsilon_0}{9}\right)\sqrt{\frac{2q}{m}}$$

FIND SOLUTION SUCH THAT

$$\frac{\partial\phi}{\partial y}(x, y=0) = 0$$

$$\& \quad \phi(x, y=0) = V(x)$$

PIERCE'S SOLUTION: LET THE POTENTIAL BE THE REAL PART OF

$$\phi + iW = V(x+iy) \equiv V(z) \qquad z \equiv x+iy$$

NOTE THAT FOR ANY $V(z)$ WITH derivatives that exist independent of direction (analytic) the real part of $V(z)$ satisfies Laplace's equation: $\frac{\partial^2 \mathrm{Re}[V]}{\partial x^2} + \frac{\partial^2 \mathrm{Re}[V]}{\partial y^2} = 0$.

$$\frac{\partial\phi}{\partial x} = \mathrm{Re}\left[\frac{dV}{dz}\right] \qquad \frac{\partial\phi}{\partial y} = \mathrm{Re}\left[i\frac{dV}{dz}\right]$$

$$\frac{\partial^2\phi}{\partial x^2} = \mathrm{Re}\left[\frac{d^2V}{dz^2}\right] \qquad \frac{\partial^2\phi}{\partial y^2} = -\mathrm{Re}\left[\frac{d^2V}{dz^2}\right] \Rightarrow \frac{\partial^2\phi}{\partial x^2} + \frac{\partial^2\phi}{\partial y^2} = \mathrm{Re}\left[\frac{d^2V}{dz^2}\right] - \mathrm{Re}\left[\frac{d^2V}{dz^2}\right] = 0$$

CHOOSE $V(z) = \left(\frac{J}{\chi}\right)^{2/3} (x+iy)^{4/3}$

By construction $\phi(x, y=0) = V(x)$ ✓

$$\phi = \mathrm{Re}\left[\left(\frac{J}{\chi}\right)^{2/3} (x+iy)^{4/3}\right]$$

Let $x+iy = r\exp[i\theta]$
$(x+iy)^{4/3} = r^{4/3}\exp\left[\frac{4i\theta}{3}\right]$

$$= \left(\frac{J}{\chi}\right)^{2/3} (x^2+y^2)^{2/3}\,\mathrm{Re}\left[\exp\left[i\,\frac{4}{3}\tan^{-1}\left(\frac{y}{x}\right)\right]\right]$$

$$\boxed{\phi(x,y) = \left(\frac{J}{\chi}\right)^{2/3} (x^2+y^2)^{2/3} \cos\left[\frac{4}{3}\tan^{-1}\left(\frac{y}{x}\right)\right]}$$

Note that $\phi(x,y) = \phi(x,-y) \Rightarrow \frac{\partial\phi}{\partial y}(x, y=0) = 0$

$\phi = 0$ EQUIPOTENTIAL:

$$\Rightarrow 0 = \cos\left[\frac{4}{3}\tan^{-1}\left(\frac{y}{x}\right)\right]$$

$$\Rightarrow \tan^{-1}\left(\frac{y}{x}\right) = \frac{3}{4}\left(\frac{\pi}{2}\right) = 67.5^\circ$$

FOR A GENERAL EQUIPOTENTIAL PASSING THROUGH X_0:

$$x_0^{4/3} = (x^2+y^2)^{2/3} \cos\left[\frac{4}{3}\tan^{-1}\left(\frac{y}{x}\right)\right]$$

EQUIPOTENTIALS FOR MATCHING TO A PLANAR BOUNDARY

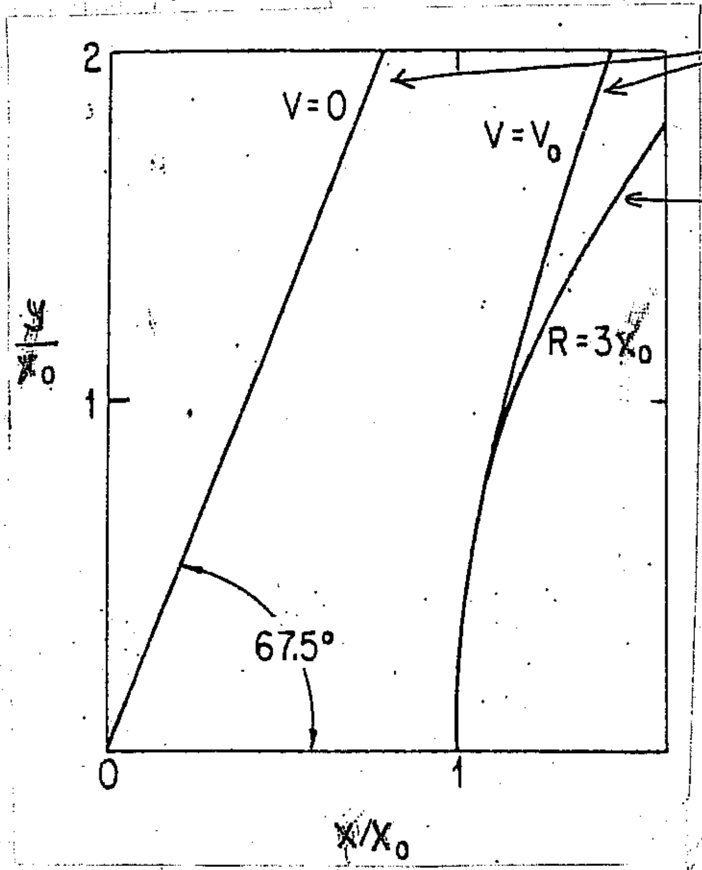

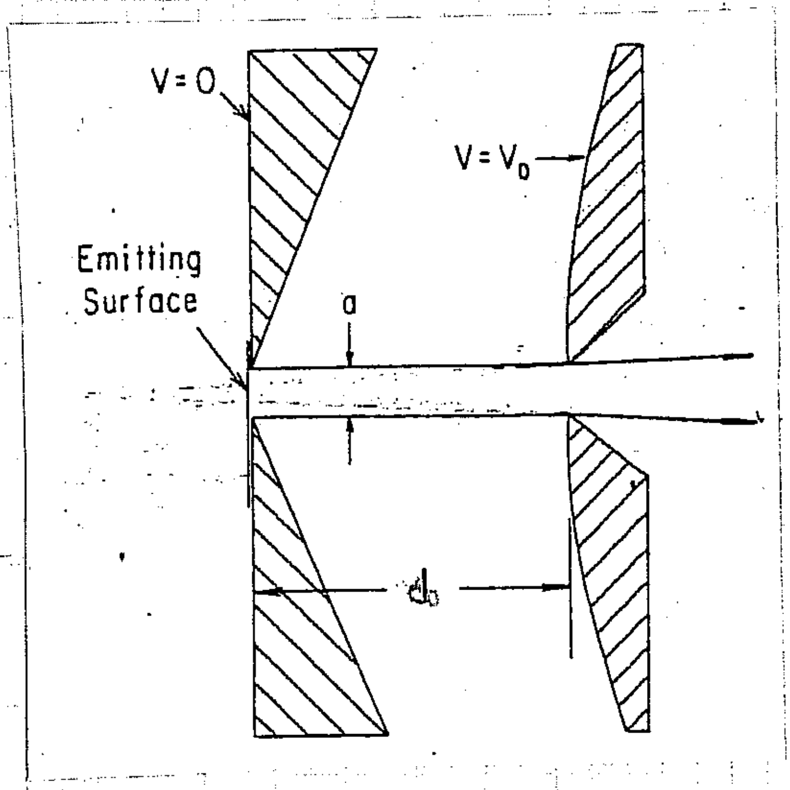

FIGURES FROM "LARGE ION BEAMS, FUNDAMENTALS OF GENERATION AND PROPAGATION" BY A.T. FORRESTER, WILEY, NY, 1988.

ELECTRODES FOR A LONG SLIT ION BEAM SYSTEM

PIERCE ELECTRODES FOR CIRCULAR BEAMS

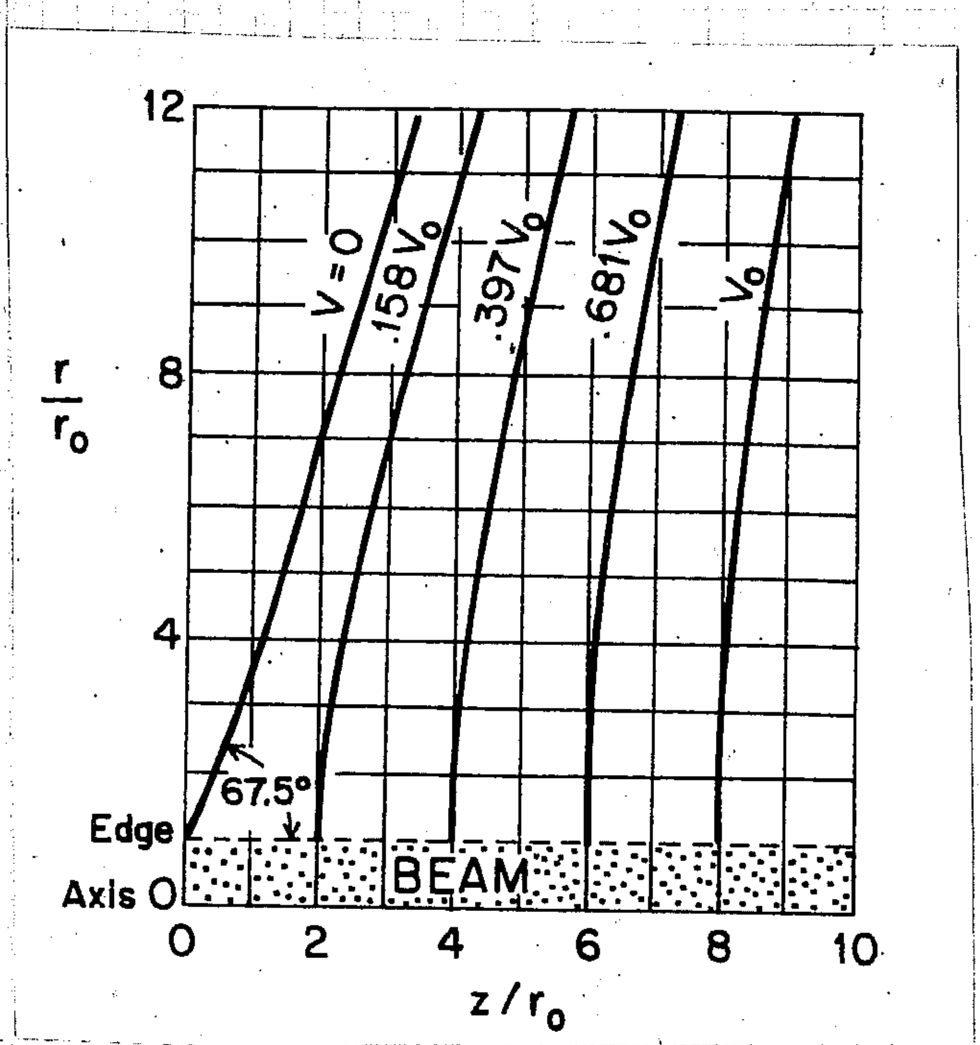

- SOLUTION is similar, but must be done numerically
- $\phi = 0$ is same as planar case

FIGURE FROM A.T. FORRESTER, "LARGE ION BEAMS, ..." WILEY, 1988

TRANSIENTS IN INJECTORS (LAMPEL & TIEFENBACK, Appl. Phys. Lett, 43, 57, 1983)

DURING TURN-ON THERE IS NO SPACE CHARGE IN FRONT OF BEAM, SO FIELDS MAY NOT BE GIVEN BY CHILD-LANGMUIR LAW. ⇒ CURRENT SPIKES POSSIBLE ⇒ ADVERSE TRANSVERSE COUPLING.

SOLUTION: ADJUST VOLTAGE ON DIODE SUCH THAT C-L FIELD OCCURS EVERYWHERE THERE IS BEAM.

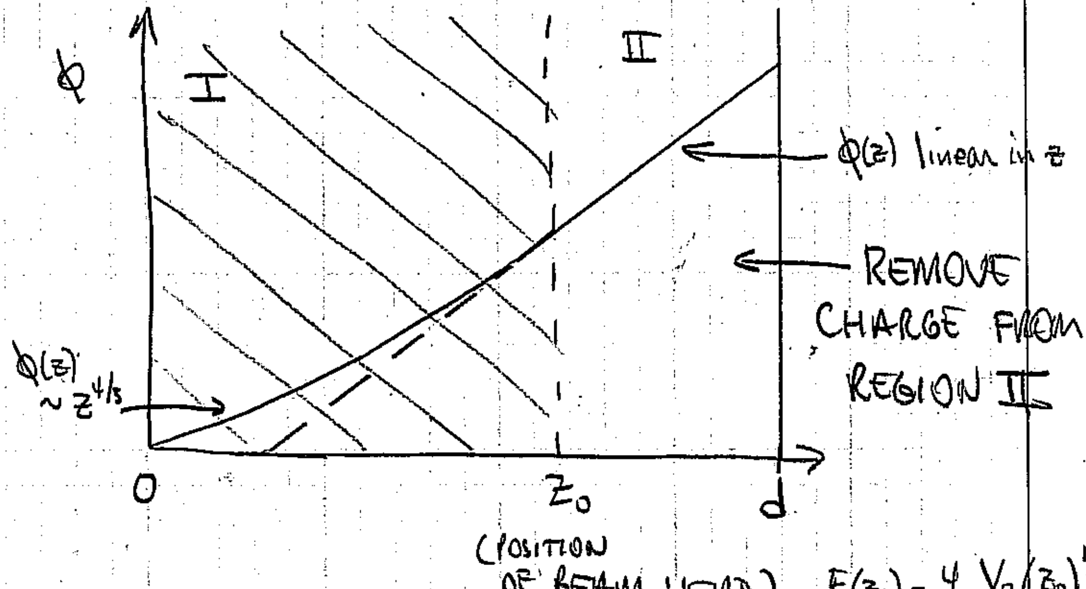

$$E(z_0) = \frac{4}{3}\frac{V_0}{d}\left(\frac{z_0}{d}\right)^{1/3}$$

$$\Phi(d) = \int_0^{z_0} E(z)\,dz + \int_{z_0}^{d} E(z)\,dz$$

$$= V_0\left(\frac{z_0}{d}\right)^{4/3} + \frac{4}{3}\frac{V_0}{d}\left(\frac{z_0}{d}\right)^{1/3}(d - z_0)$$

$$= V_0\left[\frac{4}{3}\left(\frac{z_0}{d}\right)^{1/3} - \frac{1}{3}\left(\frac{z_0}{d}\right)^{4/3}\right]$$

(NOTE V_0 IS THE DESIRED STEADY STATE VOLTAGE ACROSS DIODE].

SO IF WE KNOW $z_0(t)$ WE CAN DETERMINE $\Phi(t)$.

$$\frac{1}{2} m \dot{z}_0^2 = qV_0 \left(\frac{z_0}{d}\right)^{4/3}$$

(SINCE BY CONSTRUCTION, HEAD OF BEAM TRAVELS AT CHILD-LANGMUIR VELOCITY LIKE ALL PARTICLES).

$$\dot{z}_0 = \left(\frac{2qV_0}{m}\right)^{1/2} \left(\frac{z_0}{d}\right)^{2/3}$$

$$\frac{dz_0}{z_0^{2/3}} = \left(\frac{2qV_0}{m}\right)^{1/2} \frac{dt}{d^{2/3}}$$

$$\Rightarrow 3 z_0^{1/3} = \left(\frac{2qV_0}{m}\right)^{1/2} \frac{t}{d^{2/3}} \quad \Rightarrow \quad t = \frac{3(z_0 d^2)^{1/3}}{\left(\frac{2qV_0}{m}\right)^{1/2}}$$

Let $\tau = \dfrac{3d}{\left(\frac{2qV_0}{m}\right)^{1/2}}$ = transit time across diode

$$\Rightarrow \frac{t}{\tau} = \left(\frac{z_0}{d}\right)^{1/3}$$

$$\Phi(d, z_0) = V_0 \left[\frac{4}{3}\left(\frac{z_0}{d}\right)^{1/3} - \frac{1}{3}\left(\frac{z_0}{d}\right)^{4/3}\right]$$

$$\Rightarrow \Phi(d,t) = \begin{cases} V_0 \left[\frac{4}{3}\left(\frac{t}{\tau}\right) - \frac{1}{3}\left(\frac{t}{\tau}\right)^4\right] & \text{for } 0 < t < \tau \\ V_0 & \text{for } t > \tau \end{cases}$$

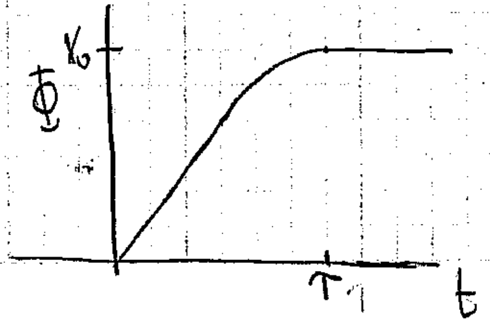

INJECTOR CHOICES (cf. Kwan et al, NIMPRA, 464, 379 (2001).

CHILD-LANGMUIR $\Rightarrow J = \chi \dfrac{V^{3/2}}{d^2}$

where $\chi = \frac{4}{9}\varepsilon_0\left(\frac{2q}{m}\right)^{1/2}$

SOME CONSTRAINTS:

(1) VOLTAGE BREAKDOWN

EMPIRICALLY $V \lesssim 100\,\text{kV} \begin{cases} \left(\dfrac{d}{1\,\text{cm}}\right) & \text{for } d \leq 1\,\text{cm} \\ \left(\dfrac{d}{1\,\text{cm}}\right)^{1/2} & \text{for } d \geq 1\,\text{cm} \end{cases}$

(2) BEAM OPTICS ABERRATIONS: $d \gtrsim 3 \text{ to } 4\ r_p$ (TYPICALLY)

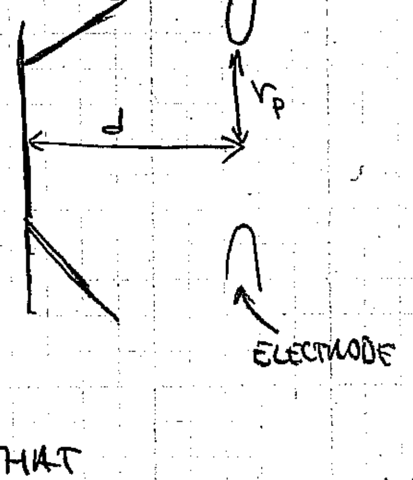

NOTE THAT

$$J \sim \frac{V^{3/2}}{d^2} \sim \begin{cases} V^{-1/2} & d<1\,\text{cm} \\ V^{-3/2} & d>1\,\text{cm} \end{cases} \qquad I \sim \pi r_p^2 J \sim \begin{cases} V^{3/2} \end{cases}$$

Thus current density decreases with size and voltage, but I increases.

Air
$V = 24S + 7\sqrt{S}$

from A. Faltens:

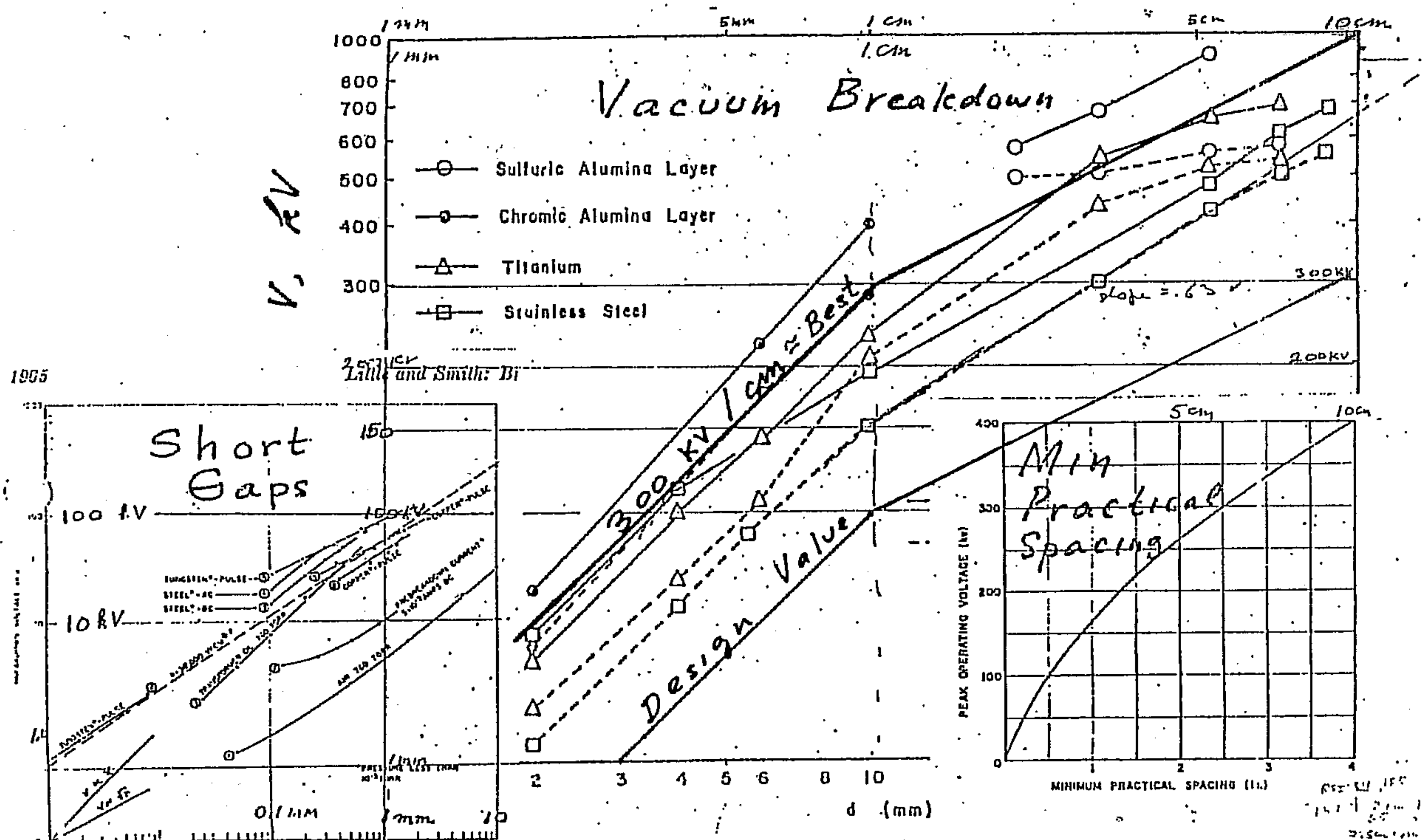

Figure 7.13 Log U - log d plot.

Fig. 1. Breakdown voltage-vs.-gap length for uniform-field and near-uniform-field geometry. Numbers on curves indicate the

15

MULTIPLE BEAMLET INJECTORS CAN HAVE HIGHER CURRENT DENSITY

DECREASING SIZE OF INJECTOR

traditional design using single large diameter source

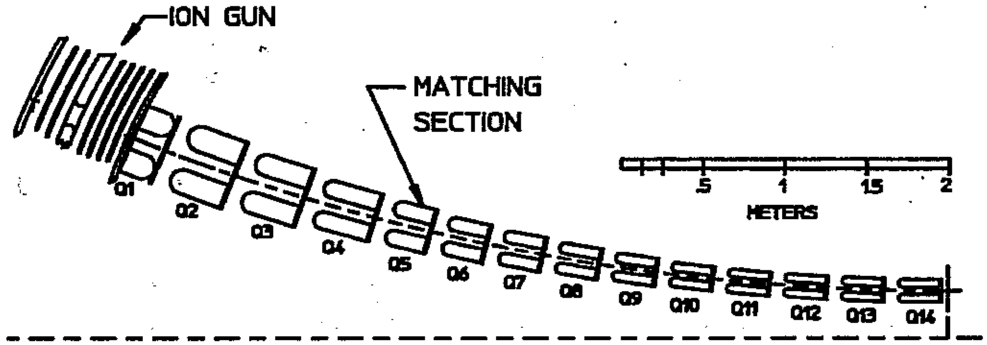

advanced design using multiple beamlets

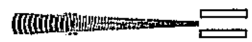

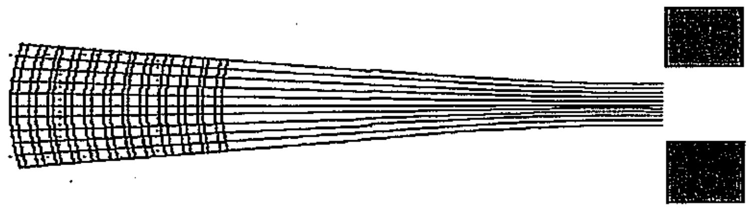

Each beamlet carries higher current density; But merging beamlets increases thermal spread.

Child-Langmuir $J_{CL} \propto \frac{V^{3/2}}{d^2}$

Breakdown limit $V \propto d^{1.0 \ to \ 0.5}$

$$J \propto V^{-1/2 \ to \ -5/2} \propto d^{-1/2 \ to \ -5/4}$$

Merge and match beamlets into an ESQ channel

The Heavy Ion Fusion Virtual National Laboratory

16

Simulations of merging-beamlet injector

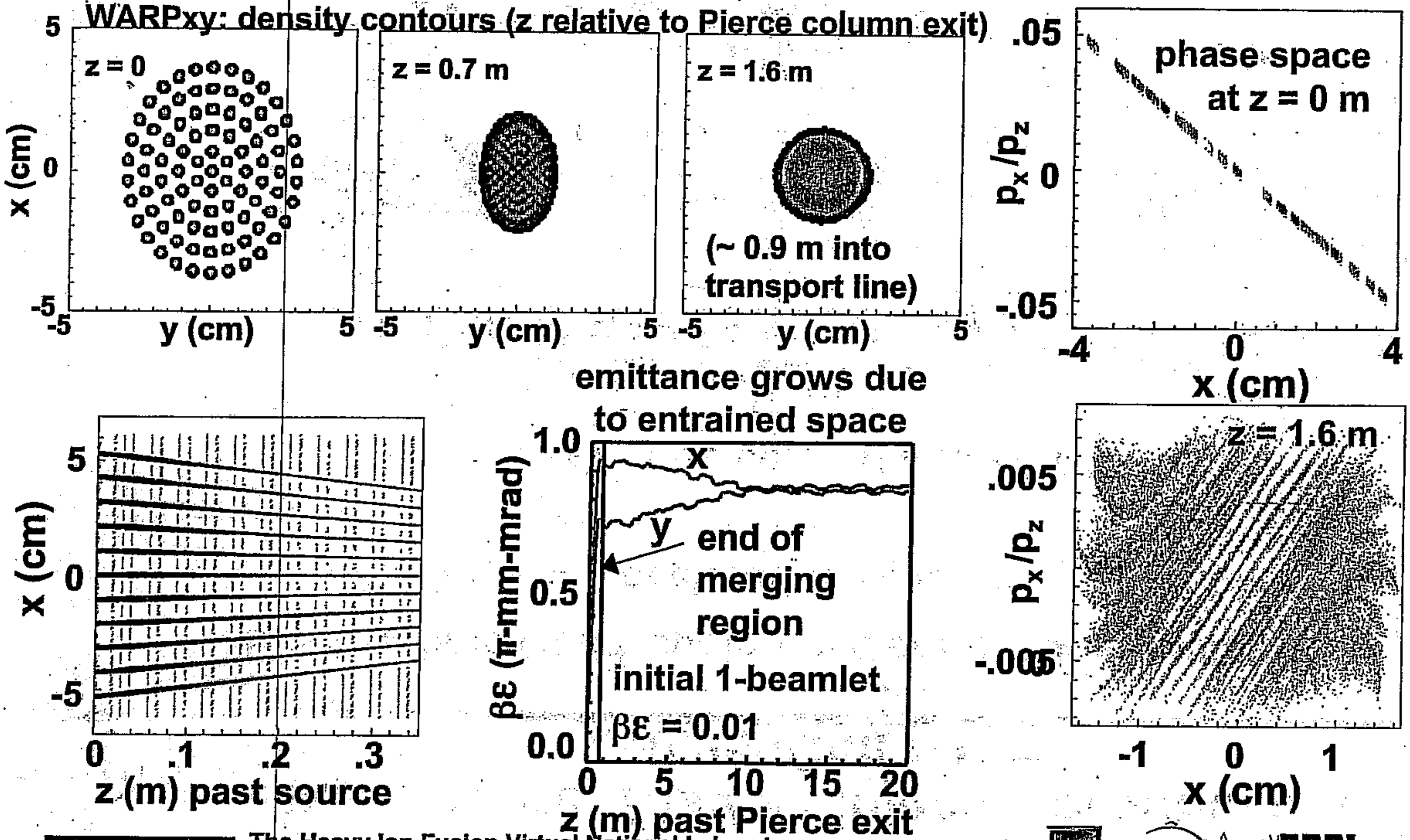

The Heavy Ion Fusion Virtual National Laboratory

PPPL

from D.P. Grote, E. Henestroza, J.W. Kwan, "Design & Simulation of the Multibeamlet

17

0.8 Ampere, 2 MV K+ Injector produced a λ=0.25μC/m beam

Electrostatic Quadrupole Accelerator for simultaneous focusing and acceleration of ion beams to 2 MV.

2.5 m, 2 MV, 2 μs column and ϕ6.7" source

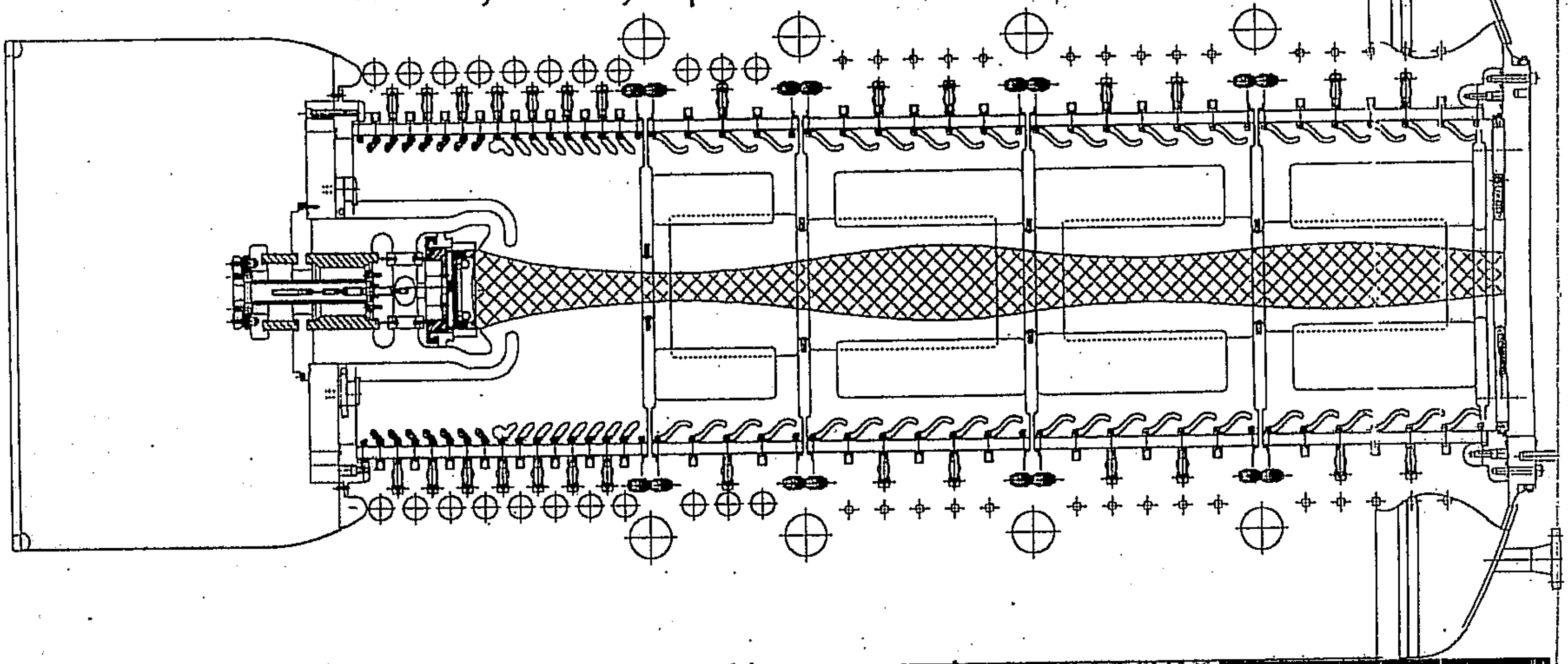

LAWRENCE BERKELEY NATIONAL LABORATORY

(18)

SCALING OF BRIGHTNESS IN INJECTORS

$$\epsilon_N = 4\beta \langle x^2 \rangle^{1/2} \langle x'^2 \rangle^{1/2} = \frac{4}{c}\left(\frac{r_b}{2}\right)\langle v_x^2 \rangle^{1/2}$$

$$\frac{1}{2} m v_x^2 = \frac{1}{2} kT$$

$$\epsilon_N = 2 r_b \sqrt{\frac{kT}{mc^2}}$$

$$\Rightarrow \quad B = \frac{I}{\epsilon_N^2} = \frac{\pi J}{4(kT/mc^2)} \sim \frac{J}{T}$$

$\Rightarrow$ FOR HIGH BRIGHTNESS & HIGH CURRENT MAY WISH TO ACCELERATE MANY BEAMLETS AND THEN MERGE TO FORM SINGLE BEAM.

MANY ISSUES NOT DISCUSSED HERE!

- SOURCES
- ELECTRON TRAPPING
- CONVERGING BEAMS
- MATCHING TO AN ESQ (e.g.)
- rf
- ...

John Barnard
Steven Lund
USPAS
June 2008

Injectors and longitudinal physics -- II

1. Acceleration - introduction
2. Space charge of short bunches (rf)
3. Space charge of long bunches
4. Longitudinal space charge waves
5. Longitudinal rarefaction waves and bunch ends

ACCELERATION

rf (radio-frequency)

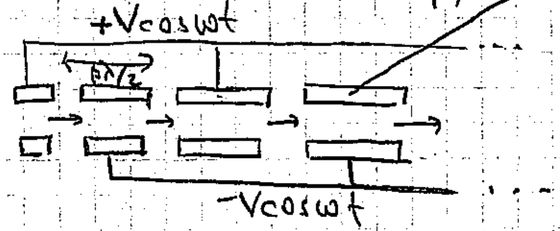

(Wideroe linac)
LOW FREQUENCIES (< 100 MHz)

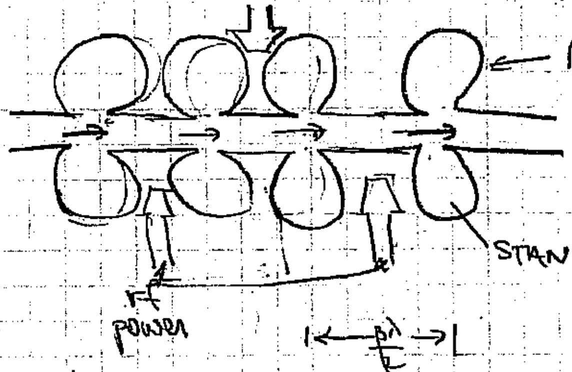

(COUPLED CAVITY Linac)
$0.4 < \beta < 1.0$

FREQUENCIES ~ 100's MHz – ~ 1 GHz

IN EACH GAP $E = E_m \sin \omega t$

Induction acceleration

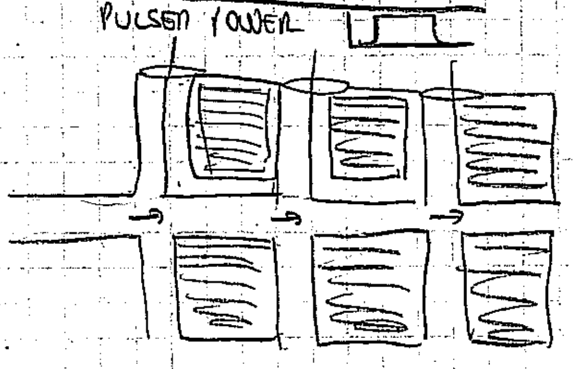

(INDUCTION LINAC)

$\nabla \times E = -\partial B / \partial t$

IN EACH GAP $E =$ CONSTANT
(OR SOME PRESCRIBED FUNCTION)

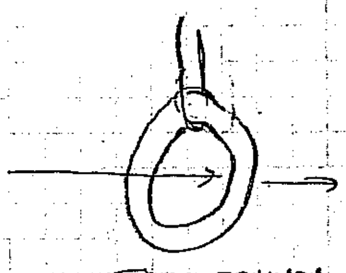

TRANSFORMER

rf longitudinal equation of motion

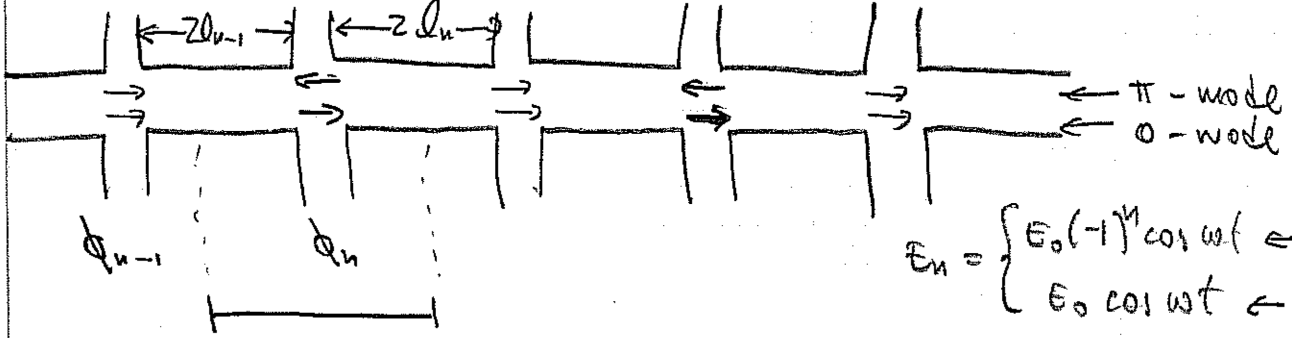

$$E_n = \begin{cases} E_0(-1)^n \cos\omega t & \leftarrow \pi\text{-mode} \\ E_0 \cos\omega t & \leftarrow 0\text{-mode} \end{cases}$$

L_n = center to center distance between drift tubes

$E_z = E_0 \cos(\phi_s)$ ← synchronous particle enters each gap at same phase

RESONANCE CONDITION ON SYNCHRONOUS PARTICLE:

$$\boxed{l_{n-1} = \frac{\beta_s \lambda}{2} \begin{Bmatrix} \frac{1}{2} \\ 1 \end{Bmatrix} \begin{matrix} \pi\text{-mode} \\ 0\text{-mode} \end{matrix} \qquad \lambda = \frac{2\pi}{\omega} c = \text{light travel distance in one} = c\Delta t_{rf} \text{ rf oscillation}}$$

(IT TAKES $\begin{Bmatrix} 1/2 \\ 1 \end{Bmatrix}$ OSCILLATION PERIOD TO TRAVEL BETWEEN GAPS).

$\beta_s = \frac{v_s}{c}$ = velocity of synchronous particle

PARTICLE PHASE RELATIVE TO rf at the n^{th} gap:

$$\phi_n = \phi_{n-1} + \omega \frac{2l_{n-1}}{\beta_{n-1} c} + \begin{Bmatrix} \pi & \pi\text{-mode} \\ 0 & 0\text{-mode} \end{Bmatrix}$$

$$\Delta(\phi - \phi_s)_n = 2\pi \beta_{s,n-1} \left(\frac{1}{\beta_{n-1}} - \frac{1}{\beta_{s,n-1}} \right) \begin{Bmatrix} 1/2 \\ 1 \end{Bmatrix} \begin{matrix} \pi\text{-mode} \\ 0\text{-mode} \end{matrix}$$

$$\cong -2\pi \frac{\delta\beta}{\beta_{s,n-1}} \begin{Bmatrix} 1/2 \\ 1 \end{Bmatrix}$$

A VELOCITY DIFFERENCE LEADS TO A PHASE DIFFERENCE!

$$\boxed{\Delta(\phi - \phi_s)_n \cong -2\pi \frac{W_{n-1} - W_{s,n-1}}{mc^2 \gamma^3_{s,n-1} \beta^2_{s,n-1}} \begin{Bmatrix} 1/2 \\ 1 \end{Bmatrix}}$$

$W = (\gamma - 1)mc^2$

$\frac{1}{\beta} - \frac{1}{\beta_s} \cong \frac{-\delta\beta}{\beta_s^2}$

$\delta W = \gamma_s^3 \beta_s mc^2 \delta\beta$

203

(4)

SIMILARLY, A PHASE DIFFERENCE PRODUCES AN ENERGY CHANGE (RELATIVE TO SYNCHRONOUS PARTICLE)

$$\boxed{\Delta(W - W_s)_n = qE_0 L_n (\cos\varphi_n - \cos\varphi_{s,n})}$$

$$L_n = \frac{(\beta_{s,n-1} + \beta_{s,n})\lambda}{2} \begin{Bmatrix} 1/2 \\ 1 \end{Bmatrix} =$$ CENTER-TO-CENTER DISTANCE BETWEEN DRIFT SECTIONS

$$(\Delta W_s = qE_0 L_n \cos\phi_s)$$

CONVERTING TO A CONTINUOUS VARIABLE:

$$\Delta(\phi - \phi_s) \rightarrow \frac{d\,\Delta\phi}{dn} \qquad \Delta(W - W_s) \rightarrow \frac{d\,\Delta W}{dn}$$

$$dn = \frac{ds}{\beta_s \lambda} \cdot \left\{ \begin{matrix} 2 \\ 1 \end{matrix} \right\}$$

$$\Rightarrow \boxed{\begin{aligned} \gamma_s^3 \beta_s^3 \frac{d\,\Delta\phi}{ds} &= -2\pi \frac{\Delta W}{mc^2 \lambda} \\ \frac{d\,\Delta W}{ds} &= qE_0 (\cos\phi - \cos\phi_s) \end{aligned}}$$

$$\frac{d}{ds}\left[\gamma_s^3 \beta_s \frac{d\,\Delta\phi}{ds}\right] = -2\pi \frac{qE_0}{mc^2\lambda}\left[\cos\phi - \cos\phi_s\right] \qquad \text{(I)}$$

NOW THE SPATIAL SEPARATION IS GIVEN BY:

$$\Delta z \equiv z - z_s = -\frac{\beta_s \lambda}{2\pi} \Delta\phi$$

$\Rightarrow$ ALSO, LET $\cos\phi - \cos\phi_s \simeq -\sin\phi_s \,\Delta\phi$ $\left[\text{for } \frac{2\pi\,\Delta z}{\beta\lambda} = \Delta\phi \ll 1\right]$

$$\Rightarrow \frac{d}{ds}\left[\gamma_s^3 \beta_s \frac{d}{ds}\left(\frac{\Delta z}{\beta_s}\right)\right] \cong -\frac{2\pi}{\lambda} \frac{qE_0}{mc^2} \sin\phi_s \frac{\Delta z}{\beta_s}$$

WHEN THE ACCELERATION RATE IS SMALL

$$\Rightarrow \frac{d^2}{ds^2}\Delta z \cong -\frac{2\pi}{\lambda} \frac{qE_0 \sin\phi_s}{\gamma_s^3 \beta_s mc^2} \Delta z$$

$$\equiv -k_{s0}^2 \,\Delta z \qquad \text{(synchrotron oscillations)}$$

(6)

RETURNING TO $\Delta W - \phi$ NOTATION

Let $w = \frac{\Delta W}{mc^2}$ $\quad A = \frac{2\pi}{\beta_s^3 \gamma_s^3 \lambda}$ $\quad B = \frac{qE_0}{mc^2}$

$$\boxed{\begin{aligned} \Rightarrow \quad w' &= B(\cos\phi - \cos\phi_s) \\ \phi' &= -Aw \\ \phi'' &= -AB(\cos\phi - \cos\phi_s) \end{aligned}}$$

MULTIPLYING BY ϕ' AND INTEGRATING:

$$\frac{\phi'^2}{2} = -AB(\sin\phi - \phi\cos\phi_s) + \text{const}$$

USING $\phi' = -Aw$ (& DIVIDING BY A)

$$\Rightarrow \underbrace{\frac{Aw^2}{2}}_{\text{kinetic energy}} + \underbrace{B(\sin\phi - \phi\cos\phi_s)}_{\text{potential energy}} = \text{CONST.}$$

$$\frac{dW_s}{ds} \sim qE_0\cos\phi_s$$

$$V(\phi) = B(\sin\phi - \phi\cos\phi_s)$$

$$\frac{dV}{d\phi} = B(\cos\phi - \cos\phi_s)$$

$$\frac{d^2V}{d\phi^2} = -B\sin\phi$$

$$> 0 \Rightarrow -\pi < \phi_s < 0$$

FOR LONGITUDINAL FOCUSING

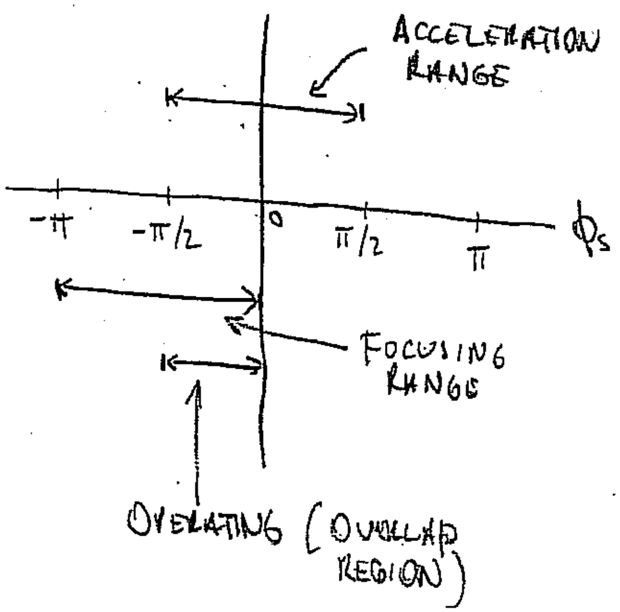

(7)

simultaneous acceleration and a potential well when $-\pi/2 \leq \phi_s \leq 0$. The stable region for the phase motion extends from $\phi_2 < \phi < -\phi_s$, where the lower phase limit ϕ_2 can be obtained numerically by solving for ϕ_2 using $H_\phi(\phi_2) = H_\phi(-\phi_s)$. Figure 6.3 shows longitudinal phase space and the longitudinal potential well. At the potential maximum, where $\phi = -\phi_s$, we

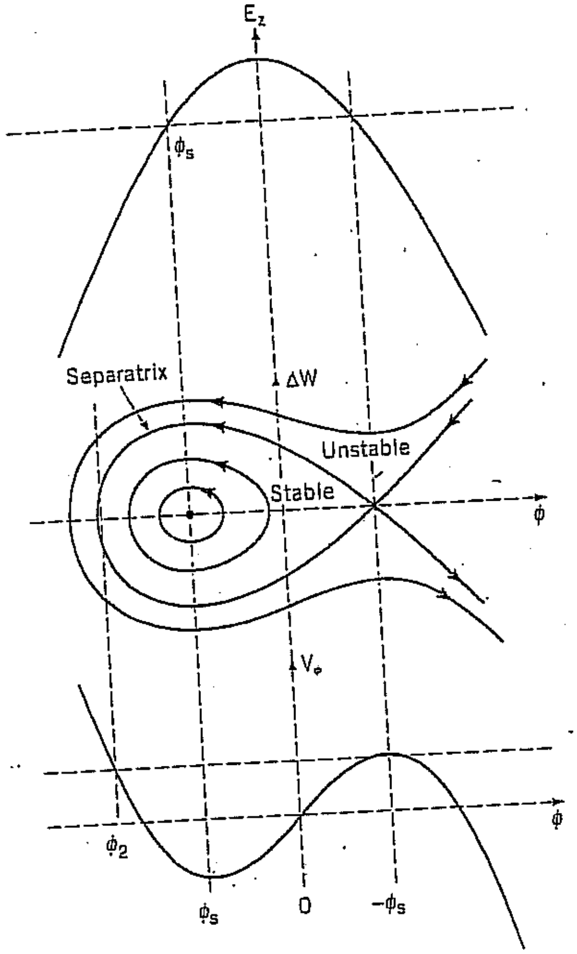

from T. Wangler's "PRINCIPLES of RF LINEAR ACCELERATORS"

Figure 6.3. At the top, the accelerating field is shown as a cosine function of the phase; the synchronous phase ϕ_s is shown as a negative number, which lies earlier than the crest where the field is rising in time. The middle plot shows some longitudinal phase-space trajectories, including the separatrix, the limiting stable trajectory, which passes through the unstable fixed point at $\Delta W = 0$, and $\phi = -\phi_s$. The stable fixed point lies at $\Delta W = 0$ and $\phi = \phi_s$, where the longitudinal potential well has its minimum, as shown in the bottom plot.

(8)

SPACE-CHARGE FIELD OF BUNCHED BEAMS

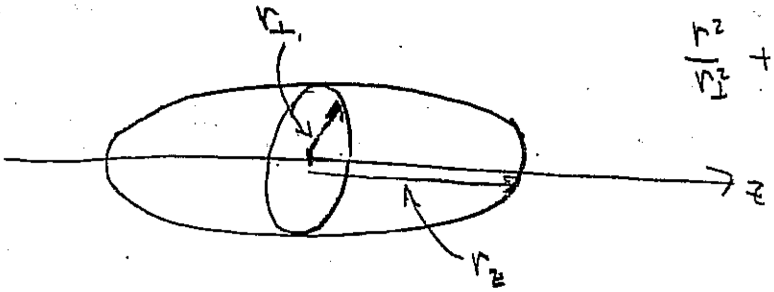

$$\frac{r^2}{r_\perp^2} + \frac{z^2}{r_z^2} = 1$$

BOUNDARY OF ELLIPSOID

THE POTENTIAL OF A UNIFORM DENSITY BUNCH IN FREE SPACE (A MACLAURIN SPHEROID) IS GIVEN BY:

(cf Landau & Lifshitz, Classical Theory of Fields, p 297)

$$\varphi = \frac{\rho}{4\epsilon_0}\left(\alpha_\perp r^2 + \alpha_\parallel z^2 - \delta\right)$$

where $\alpha_\perp = r_\perp^2 r_z \int_0^\infty \frac{ds}{(r_\perp^2+s)\,\Delta}$

$$\alpha_\parallel = r_\perp^2 r_z \int_0^\infty \frac{ds}{(r_z^2+s)\,\Delta}$$

$$\delta = r_\perp^2 r_z \int_0^\infty \frac{ds}{\Delta}$$

where $\Delta^2 = (r_\perp^2+s)^2(r_z^2+s)$

FOR NON-RELATIVISTIC BEAM:

$$E_z = -\frac{\partial\phi}{\partial z} = f\,\frac{\rho}{\epsilon_0}\,z$$

$$E_r = -\frac{\partial\phi}{\partial r} = \frac{(1-f)}{2}\,\frac{\rho}{\epsilon_0}\,r$$

$$f = f(\alpha) = \begin{cases} \dfrac{\alpha^2}{1-\alpha^2}\left[\dfrac{1}{\sqrt{1-\alpha^2}}\tanh^{-1}\sqrt{1-\alpha^2} - 1\right] & \alpha<1 \\ \dfrac{1}{3} & \alpha=1 \\ \dfrac{\alpha^2}{\alpha^2-1}\left[1 - \dfrac{1}{\sqrt{\alpha^2-1}}\tan^{-1}\sqrt{\alpha^2-1}\right] & \alpha>1 \end{cases} \qquad \alpha \equiv \frac{r_\perp}{r_z}$$

(9)

For Relativistic Beam

(cf. Lund & Barnard 1997 PAC97 Conf Proceedings)

$$\frac{d^2 X_\perp}{ds^2} = \frac{F_\perp}{\gamma_s \beta_s^2 mc^2} \qquad F_{\perp s} = \frac{-q}{\gamma_s^2}\frac{\partial\phi}{\partial X_\perp} = \frac{q\rho}{2\gamma_s^2 \epsilon_0}\left[1 - f(\alpha)\right] \underline{X_\perp}$$

$$\frac{d^2 \Delta z}{ds^2} = \frac{F_z}{\gamma_s^3 \beta_s^2 mc^2} \qquad F_{zs} = \frac{-q}{\gamma_s^2}\frac{\partial\phi}{\partial z} = \frac{q\rho}{\epsilon_0} f(\alpha)\,\Delta z$$

$$\alpha = \frac{r_\perp}{\gamma r_z} \qquad \left[\alpha = \frac{r_\perp}{(r_z \text{ in comoving frame})}\right]$$

Combining Focusing + Self Fields

$$\frac{d^2}{ds^2}\Delta z = -k_{s0}^2 \Delta z + \frac{q\rho\, f(\alpha)}{\gamma_s^3 \beta_s^2 mc^2 \epsilon_0}\Delta z \qquad \text{(LINEAR rf)}$$

Total field seen by particle is sum of rf and spacecharge

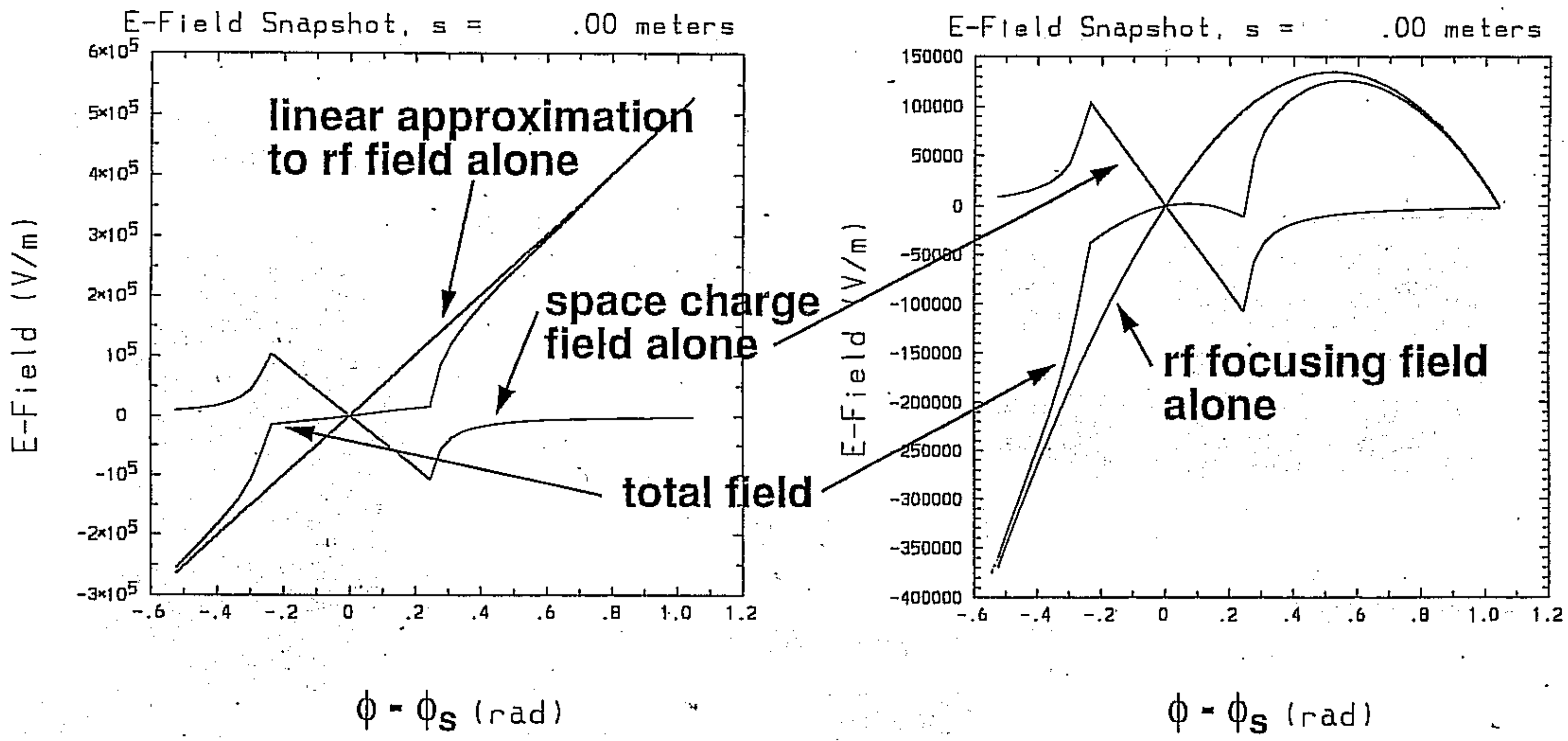

here $\phi - \phi_s = -(2\pi/\beta_s\lambda)\,\Delta z$, where $\beta_s c$ is the longitudinal velocity of the synchronous particle and $\lambda = c/\nu$ is the rf vacuum wavelength

Induction acceleration

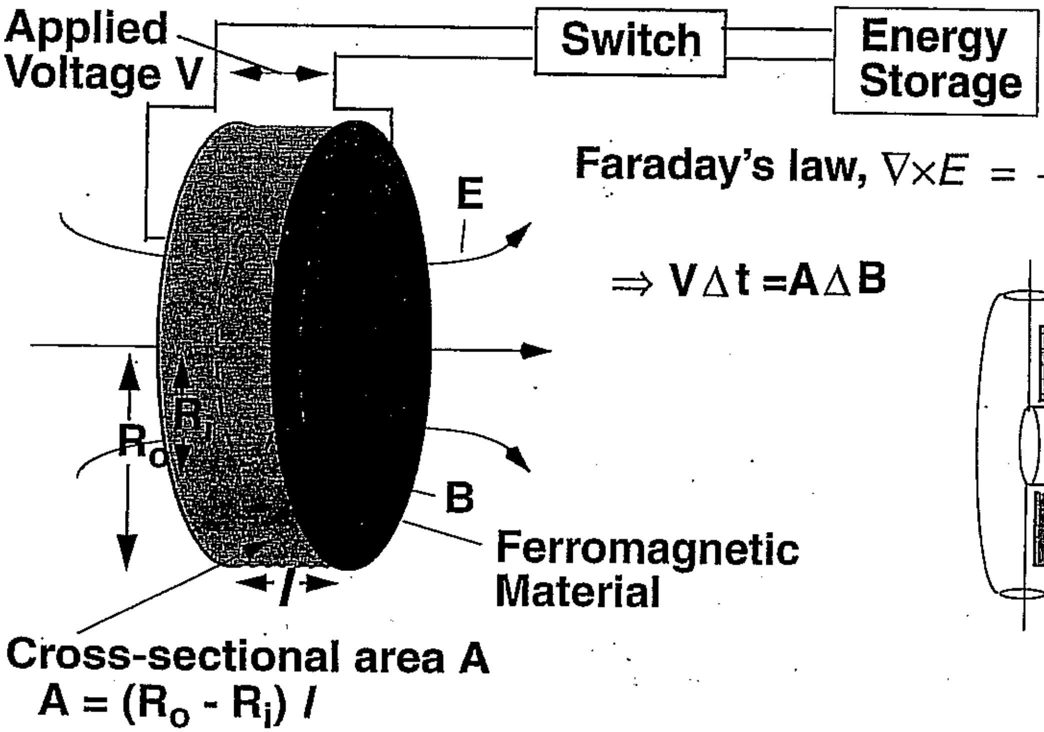

Faraday's law, $\nabla \times E = -\dfrac{\partial B}{\partial t}$

$\Rightarrow V \Delta t = A \Delta B$

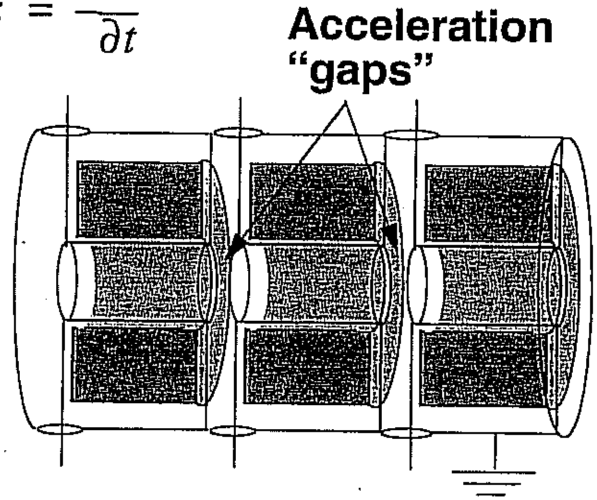

Volt-seconds per m: $(dV/dz)\,\Delta t = (R_o - R_i)\ \ \Delta B\ \ f_{radial}\ \ f_{longit.}$

$\sim 1\text{ m}\quad \sim 2.5\text{T}\quad \sim 0.8\quad \sim 0.8$

$\boxed{(dV/dz)\,\Delta t <\sim 1.6\text{ V-s/m}}$

11

Several types of waveform are needed to accelerate, compress, and confine the beam

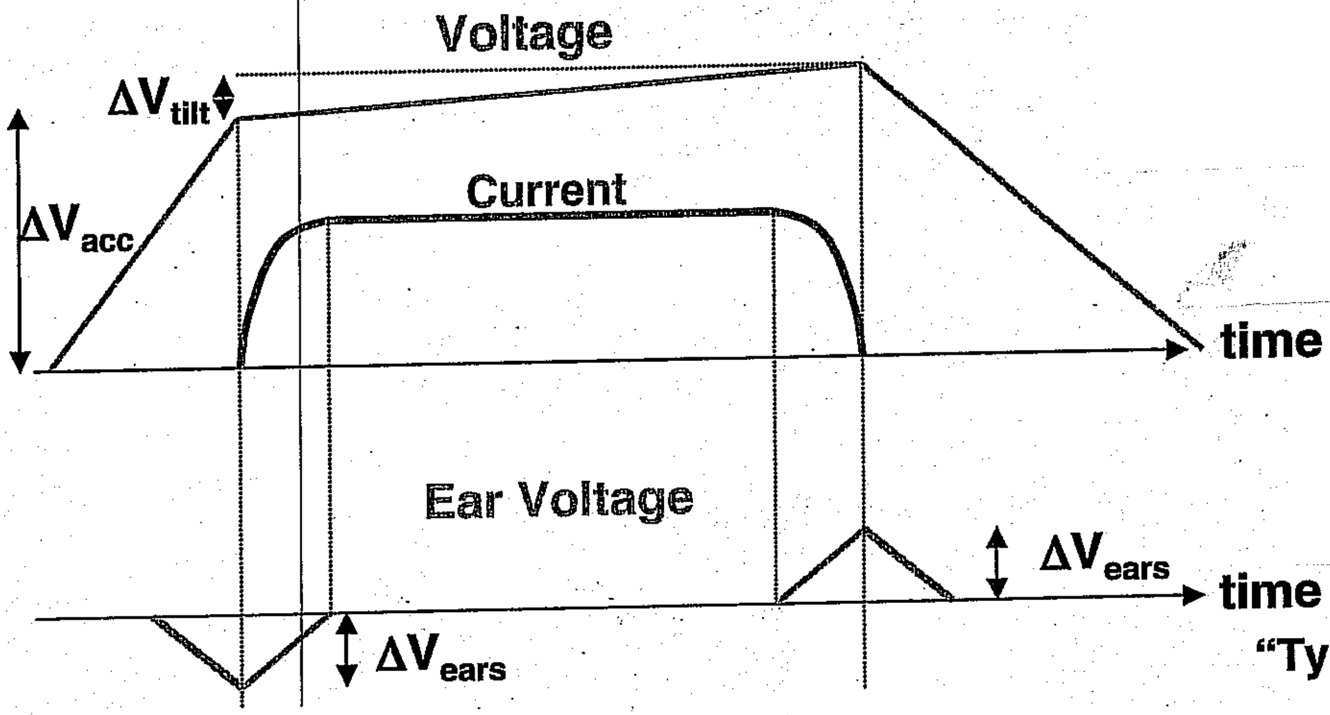

"Typical" numbers:

$\Delta V_{tilt} \sim$ 1 kV
$\Delta V_{ears} \sim$ 14 kV
$\Delta V_{acc} \sim$ 100 kV

12

*

COORDINATE SYSTEM

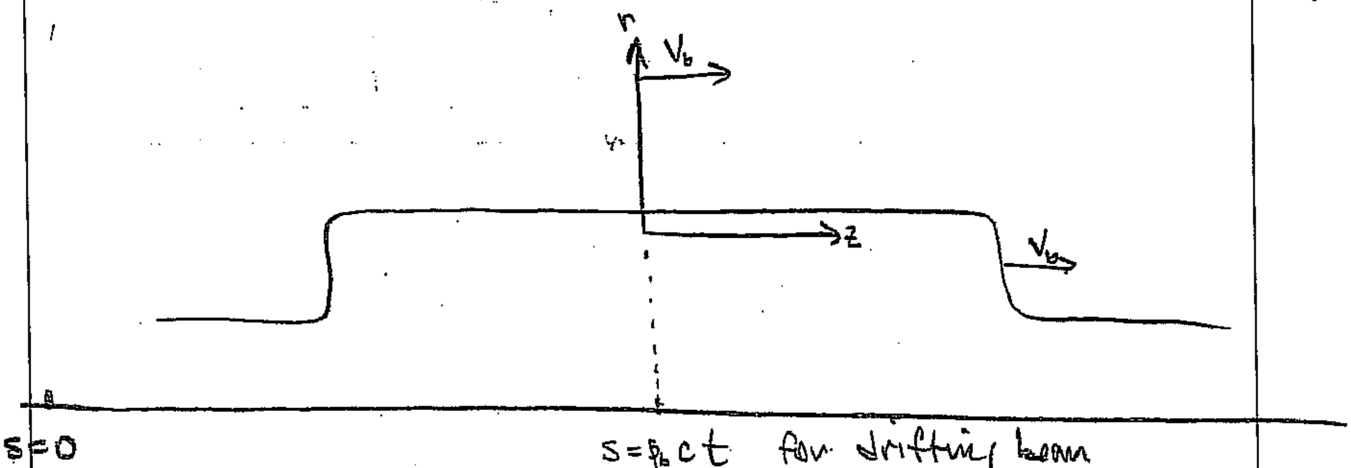

$s = \beta_b c t$ for drifting beam
= position of beam center in lab frame

$s \leftrightarrow t$ are related by $\beta_b c$ for drifting beam
z = longitudinal coordinate in beam frame ($z=0$ = beam center)
r = radial coordinate in beam frame (or lab frame).

(This class will assume non-relativistic dynamics)
These are ions with $\beta < 0.2$).

LONGITUDINAL PHYSICS OF LONG PULSES (BUNCH LENGTH >> r_{pipe})

"g-factor" model

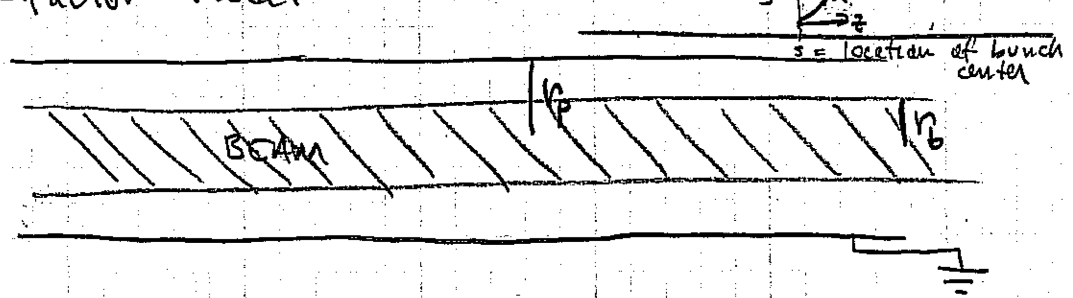

If $\dfrac{\partial^2\varphi}{\partial z^2} << \dfrac{1}{r}\left(\dfrac{\partial}{\partial r} r \dfrac{\partial\varphi}{\partial r}\right) \Rightarrow \dfrac{\partial\varphi}{\partial r} = \dfrac{-\lambda(r)}{2\pi\varepsilon_0 r}$

Let $\rho = \begin{cases} \rho_0 & 0<r<r_b \\ 0 & r_b<r<r_p \end{cases} \Rightarrow \lambda = \lambda_0\left(\dfrac{r}{r_b}\right)^2$

$$\varphi = \int \frac{\partial\varphi}{\partial r}dr = \begin{cases} \dfrac{\lambda}{2\pi\varepsilon_0}\left[\dfrac{1}{2}\left(1-\dfrac{r^2}{r_b^2}\right) + \ln\dfrac{r_p}{r_b}\right] & 0<r<r_b \\ \dfrac{\lambda}{2\pi\varepsilon_0}\ln\left(\dfrac{r_p}{r}\right) & r_b<r<r_p \end{cases}$$

$$\frac{\partial\phi}{\partial z} = \frac{1}{2\pi\varepsilon_0}\left[\frac{1}{2}\left(1-\frac{r^2}{r_b^2}\right) + \ln\frac{r_p}{r_b}\right]\frac{\partial\lambda}{\partial z} - \frac{1}{2\pi\varepsilon_0}\left[1-\frac{r^2}{r_b^2}\right]\frac{\lambda}{r_b}\frac{\partial r_b}{\partial z}$$

<u>If</u> $\rho = \text{const} \Rightarrow \dfrac{\lambda}{r_b^2} = \text{const} \quad \dfrac{\partial\lambda}{\partial z} = \dfrac{-2\lambda}{r_b}\dfrac{\partial r_b}{\partial z}$

$$\Rightarrow \frac{\partial\phi}{\partial z} = \frac{1}{2\pi\varepsilon_0}\ln\left(\frac{r_p}{r_b}\right)\frac{\partial\lambda}{\partial z}$$

$$E_z = \frac{-g}{4\pi\varepsilon_0}\frac{\partial\lambda}{\partial z}$$

where $g = 2\ln\left(\dfrac{r_p}{r_b}\right)$ [SPACE-CHARGE DOMINATED BEAM]

[Example of $\rho = \text{const}$. Magnetic Quad focusing $\dfrac{\lambda}{4\pi\varepsilon_0 V a} \simeq k_{\beta 0}^2 a \Rightarrow \rho \sim V k_{\beta 0}^2 \simeq \text{const}$]

(for space-charge dominated beam)

FOR EMITTANCE DOMINATED BEAMS:

RADIUS NOT DETERMINED BY λ

SO $\frac{\partial r_b}{\partial z} \simeq 0$

$$\left\langle \frac{\partial \phi}{\partial z} \right\rangle = \frac{1}{2\pi\varepsilon_0} \left[\frac{1}{2} \left(1 - \underbrace{\left\langle \frac{r^2}{r_b^2} \right\rangle}_{= 1/2} \right) + \ln \frac{r_p}{r_b} \right] \frac{\partial \lambda}{\partial z}$$

$$\Longrightarrow \quad g = 2 \ln \left(\frac{r_p}{r_b} \right) + \frac{1}{2}$$ (EMITTANCE DOMINATED BEAMS)

(SEE REISER, SECTION 6.3 FOR DISCUSSION ON g-factor).

Vlasov-equation for a drifting beam:

$$\frac{\partial f}{\partial s} + x'\frac{\partial f}{\partial x} + x''\frac{\partial f}{\partial x'} + y'\frac{\partial f}{\partial y} + y''\frac{\partial f}{\partial y'} + z'\frac{\partial f}{\partial z} + z''\frac{\partial f}{\partial z'} = 0$$

Let $\tilde{f}(z,z',s) \equiv \iiiint f \, dx\, dx'\, dy\, dy'$

INTEGRATING VLASOV EQUATION: If $z'' \neq f(x,x',y,y')$:

$$\Rightarrow \frac{\partial \tilde{f}}{\partial s} + \iiint x' \underbrace{\int \frac{\partial f}{\partial x} dx}_{= f\big|_{-\infty}^{\infty} = 0} dx'\, dy\, dy' + \cdots \; z'\frac{\partial \tilde{f}}{\partial z} + z''\frac{\partial \tilde{f}}{\partial z'} = 0$$

$$\Rightarrow \boxed{\frac{\partial \tilde{f}}{\partial s} + z'\frac{\partial \tilde{f}}{\partial z} + z''\frac{\partial \tilde{f}}{\partial z'} = 0}$$ 1 D Vlasov

Now let $\lambda \equiv q\int \tilde{f}\, dz'$; $\lambda \overline{z'} = \int \tilde{f} z'\, dz'$; $\lambda \overline{z'^2} \equiv \int \tilde{f} z'^2 dz'$

Also, let $\Delta z'^2 \equiv \overline{z'^2} - (\overline{z'})^2$

FLUID EQUATIONS

INTEGRATING 1 D. VLASOV OVER z':

$$\boxed{\frac{\partial \lambda}{\partial s} + \frac{\partial}{\partial z}(\lambda \overline{z'}) = 0}$$ (CONTINUITY EQUATION)

MULTIPLYING BY z' & INTEGRATING VLASOV OR z':

$$\frac{\partial}{\partial s}\lambda \overline{z'} + \frac{\partial}{\partial z}\lambda \overline{z'^2} - \lambda \overline{z''} = 0$$

DIVIDING BY λ, USING CONTINUITY EQUATION & DEFINITION OF $\Delta z'^2$:

$$\boxed{\underbrace{\frac{\partial \overline{z'}}{\partial s} + \overline{z'}\frac{\partial}{\partial z}\overline{z'}}_{\text{INERTIAL}} + \underbrace{\frac{1}{\lambda}\frac{\partial}{\partial z}(\lambda \Delta z'^2)}_{\text{PRESSURE TERM}} = \underbrace{\overline{z''}}_{\text{FORCE}}}$$ (MOMENTUM EQUATION)

Combining g-factor model with fluid equations

$$\frac{\partial \lambda}{\partial s} + \frac{\partial}{\partial z}(\lambda \bar{z}') = 0$$

$$\frac{\partial \bar{z}'}{\partial s} + \bar{z}' \frac{\partial \bar{z}'}{\partial z} + \underbrace{\frac{1}{\lambda}\frac{\partial}{\partial z}(\lambda \Delta z'^2)}_{\text{PRESSURE TERM}} = \underbrace{\frac{-gq}{4\pi\epsilon_0 m V_0^2}\frac{\partial \lambda}{\partial z}}_{\text{SPACE CHARGE TERM}}$$

WHEN PRESSURE TERM << SPACE CHARGE TERM,

(& LET $C_s^2 \equiv \frac{qg\lambda_0}{4\pi\epsilon_0 m}$ = "(SPACE CHARGE WAVE SPEED)^2"

$$\Longrightarrow \boxed{\begin{aligned} &\frac{\partial \lambda}{\partial s} + \lambda \frac{\partial \bar{z}'}{\partial z} + \bar{z}' \frac{\partial \lambda}{\partial z} = 0 \\ \& \quad &\frac{\partial \bar{z}'}{\partial s} + \bar{z}' \frac{\partial \bar{z}'}{\partial z} + \frac{C_s^2}{\lambda_0 V_0^2}\frac{\partial \lambda}{\partial z} = 0 \end{aligned}} \qquad (g1)$$

LINEARIZING g1

LET $\lambda = \lambda_0 + \lambda_1 \qquad \bar{z}' = \bar{z}_0' + \bar{z}_1'$

EQUILIBRIUM λ_0 = CONSTANT

$\bar{z}_0' = 0$

LINEARIZING

$$\frac{\partial \lambda_1}{\partial s} + \lambda_0 \frac{\partial \bar{z}_1'}{\partial z} = 0 \qquad (g2a)$$

$$\frac{\partial \bar{z}_1'}{\partial s} + \frac{C_s^2}{\lambda_0 V_0^2}\frac{\partial \lambda_1}{\partial z} = 0 \qquad (g2b)$$

TAKING $\frac{\partial}{\partial s}$ of (g2a) & $\frac{\partial}{\partial z}$ of g2b and combining:

$$\Longrightarrow \boxed{\frac{\partial^2 \lambda_1}{\partial s^2} - \frac{C_s^2}{V_0^2}\frac{\partial^2 \lambda_1}{\partial z^2} = 0 \quad \Longrightarrow \text{WAVE EQUATION}}$$

SOLVING WAVE EQUATION

$$\frac{\partial^2 \lambda_1}{\partial s^2} - \frac{c_s^2}{V_0^2}\frac{\partial^2 \lambda_1}{\partial z^2} = 0$$

Let $\lambda_1 = \tilde{\lambda}_1 \exp\left[\frac{i\omega}{V_0}s \pm ikz\right]$

$$-\frac{\omega^2}{V_0^2} + \frac{k^2 c_s^2}{V_0^2} = 0 \quad \Rightarrow \quad \omega = c_s k$$

$\Rightarrow$ PHASE & GROUP VELOCITY OF WAVES $= c_s$
(in beam frame)

GENERAL SOLUTION

$$\lambda_1 = \lambda_0 f_+[u_+] + \lambda_0 f_-[u_-]$$

where $u_+ = z + \frac{c_s s}{V_0} + C_0$ & $u_- = z - \frac{c_s s}{V_0} + C_0$

& $f_+[u]$ & $f_-[u]$ are any functions of the argument.
& C_0 is an arbitrary constant

$$\overline{z_1'} = \frac{c_s}{V_0}\left[-f_+[u_+] + f_-[u_-]\right]$$

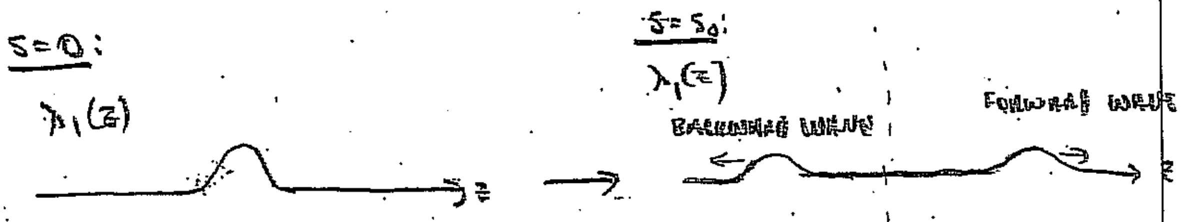

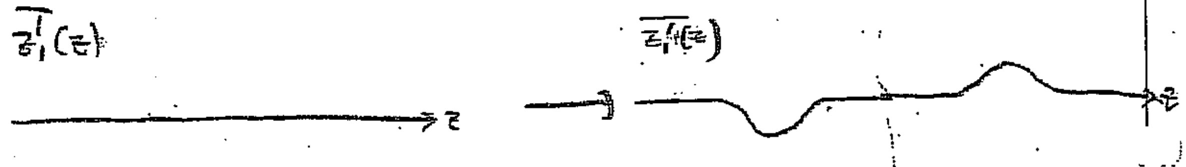

(18)

BEAM ENDS & RAREFACTION WAVES

(FALTENS & LEE, J. APP. PHYS. 61, 5219) (Also Landau & Lifshitz, Fluid Mechanics):

SUPPOSE YOU START WITH A PULSE THAT ENDS WITH A STEP FUNCTION IN λ. WHAT HAPPENS TO THE END?

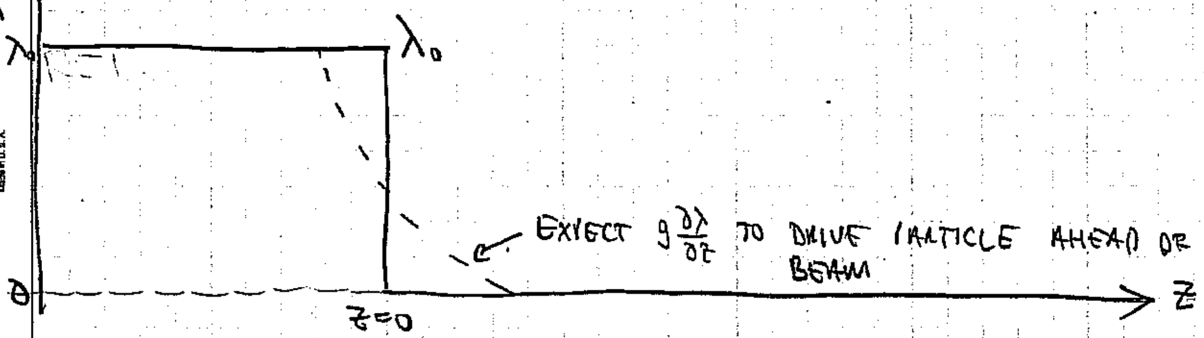

TO ANALYZE: RETURN TO <u>NON-LINEAR</u> FLUID EQUATIONS (SINCE $\delta\lambda \sim \lambda_0$) (g1):

$$\frac{\partial\lambda}{\partial s} + \lambda\frac{\partial\overline{z'}}{\partial z} + \overline{z'}\frac{\partial\lambda}{\partial z} = 0 \qquad \text{(CONTINUITY)}$$

$$\frac{\partial\overline{z'}}{\partial s} + \overline{z'}\frac{\partial\overline{z'}}{\partial z} + \frac{C_s^2}{\lambda_0 V_0^2}\frac{\partial\lambda}{\partial z} = 0 \qquad \text{(momentum)}$$

1ST IT IS CONVENIENT TO DEFINE: $\Lambda \equiv \lambda/\lambda_0$

$$V \equiv \frac{V_0}{C_s}\overline{z'}$$

$$\left(C_s^2 \equiv \frac{q}{m}\frac{g\lambda_0}{4\pi\epsilon_0}\right) \qquad \zeta \equiv \frac{V_0}{C_s}z$$

$$\Rightarrow \quad \frac{\partial\Lambda}{\partial s} + \Lambda\frac{\partial V}{\partial \zeta} + V\frac{\partial\Lambda}{\partial\zeta} = 0 \qquad \text{(CONTINUITY)}$$

$$\frac{\partial V}{\partial s} + V\frac{\partial V}{\partial\zeta} + \frac{\partial\Lambda}{\partial\zeta} = 0 \qquad \text{(momentum)} \qquad (r1)$$

TRY A SIMILARITY SOLUTION: $\Lambda = \Lambda(x)$ & $V = V(x)$

WHERE $x = \frac{z}{s} = \left(\frac{V_0 z}{c_s s}\right)$

$$\frac{\partial x}{\partial s} = -\frac{x}{s} \qquad \frac{\partial x}{\partial z} = \frac{x}{z}$$

$$\frac{\partial \Lambda}{\partial s} = -\frac{d\Lambda}{dx}\frac{x}{s} \qquad \frac{\partial \Lambda}{\partial z} = \frac{d\Lambda}{dx}\frac{x}{z} \qquad \frac{\partial V}{\partial s} = -\frac{dV}{dx}\frac{x}{s} \qquad \frac{\partial V}{\partial z} = \frac{dV}{dx}\frac{x}{z}$$

$$\left[-\frac{d\Lambda}{dx}\frac{x}{s} + \Lambda\frac{dV}{dx}\frac{x}{z} + V\frac{d\Lambda}{dx}\frac{x}{z}\right] = 0 \qquad \text{(CONTINUITY)}$$

$$\left[-\frac{dV}{dx}\frac{x}{s} + V\frac{dV}{dx}\frac{x}{z} + \frac{d\Lambda}{dx}\frac{x}{z}\right] = 0 \qquad \text{(momentum)}$$

MULTIPLY BY z/s & gather terms):

$$\Rightarrow \begin{bmatrix} V-x & \Lambda \\ 1 & V-x \end{bmatrix}\begin{bmatrix} d\Lambda/dx \\ dV/dx \end{bmatrix} = 0$$

FOR NON-TRIVIAL SOLUTION DETERMINANT MUST VANISH:

$$\boxed{\Lambda = [V-x]^2}$$

$$\Rightarrow \frac{d\Lambda}{dx} = 2[V-x]\left[\frac{dV}{dx} - 1\right] \quad \& \quad \frac{d\Lambda}{dx} = -[V-x]\frac{dV}{dx}$$

$$\Rightarrow -\frac{dV}{dx} = 2\frac{dV}{dx} - 2 \quad \Rightarrow \frac{dV}{dx} = \frac{2}{3}$$

$$\Rightarrow \boxed{\begin{aligned} V &= \tfrac{2}{3}x + C \\ \Lambda &= \left[-\tfrac{1}{3}x + C\right]^2 \end{aligned}}$$

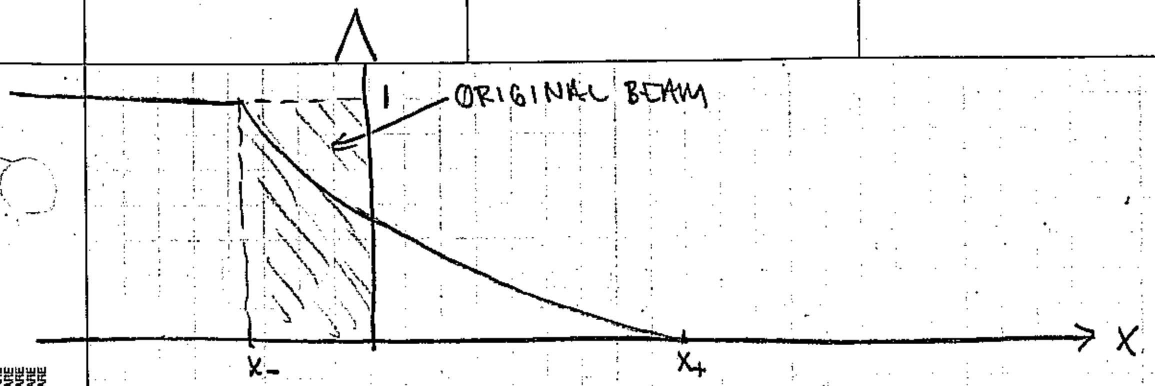

At x_+: $\Lambda = 0 \Rightarrow C = \frac{1}{3}X \qquad X_+ = 3C$

At x_-: $\Lambda = 1 \Rightarrow C = \frac{1}{3}X + 1 \Rightarrow X_- = 3C-3$

MASS CONSERVATION $\Rightarrow 1(-X_-) = -(3C-3) = \int_{3C-3}^{3C} \left[C - \frac{1}{3}x\right]^2 dx = -3\,\frac{\left[C-\frac{1}{3}x\right]^3}{3}\Bigg|_{3C-3}^{3C}$

$-(3C-3) = 1$

$\Rightarrow \boxed{C = \frac{2}{3}} \Rightarrow \begin{array}{l} X_- = -1 \\ X_+ = 2 \end{array}$

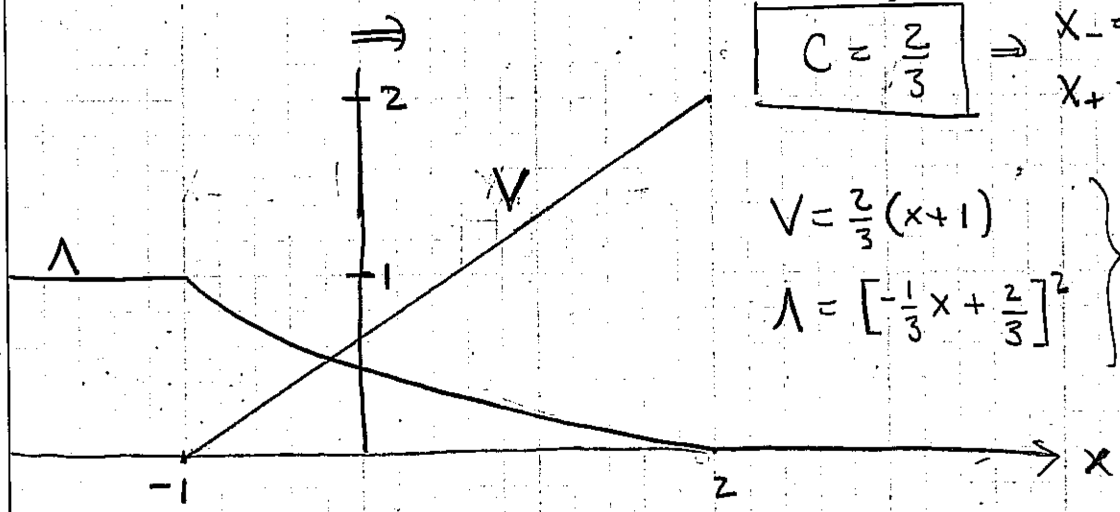

$$\left.\begin{array}{l} V = \frac{2}{3}(x+1) \\ \Lambda = \left[-\frac{1}{3}x + \frac{2}{3}\right]^2 \end{array}\right\} \text{for } -1 < x < 2$$

RECALL $X = \frac{V_0 z}{C_s S}$ SO $x = 2 \Rightarrow z = 2C_s\left(\frac{S}{V_0}\right)$

$x = -1 \Rightarrow z = -C_s\left(\frac{S}{V_0}\right)$

SO BEAM END EXPANDS AT TWICE SPACE-CHARGE WAVE SPEED & RAREFACTION WAVE PROPAGATES INWARD AT THE SPACE-CHARGE WAVE SPEED.

SNAPSHOTS OF λ/λ_0 VS z AT VARIOUS s

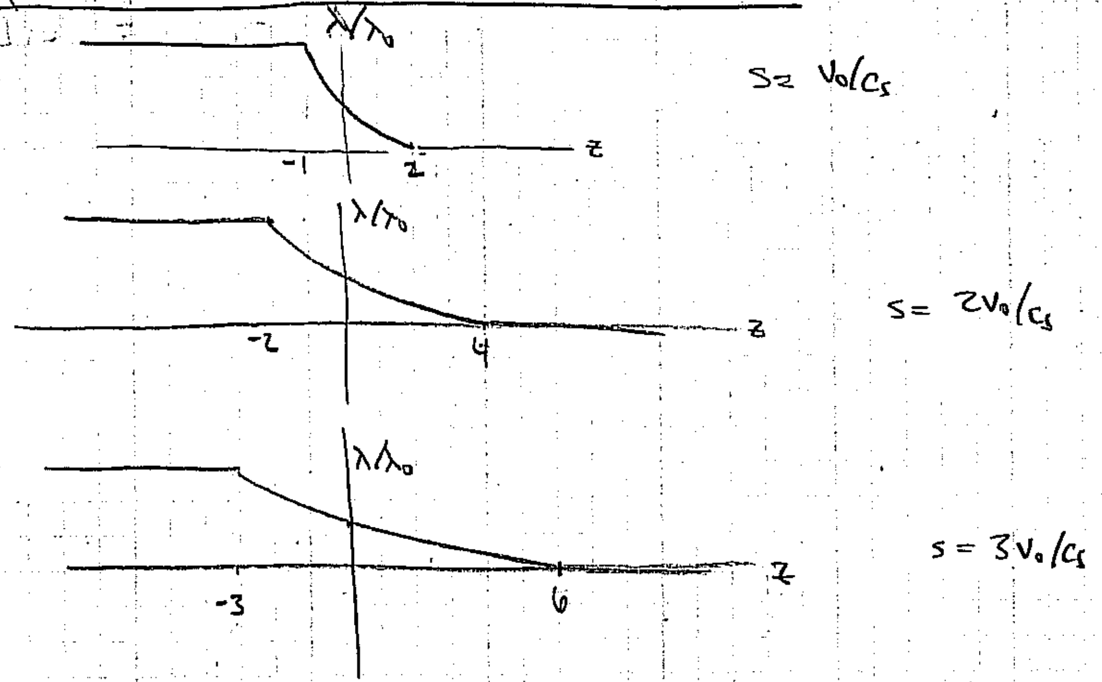

HOW DOES ONE PREVENT "END EROSION"?

APPLY EAR PULSES AT END OF BEAM:

$$V \sim E_z = \frac{-g}{4\pi\epsilon_0}\frac{\partial\lambda}{\partial z}$$

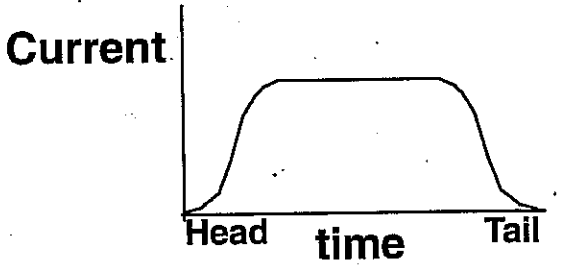

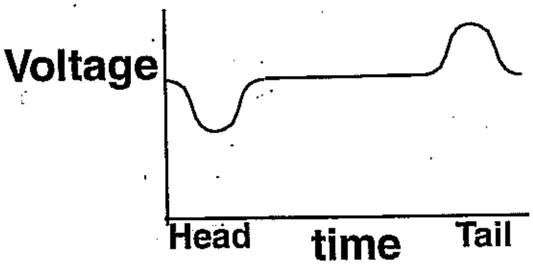

22

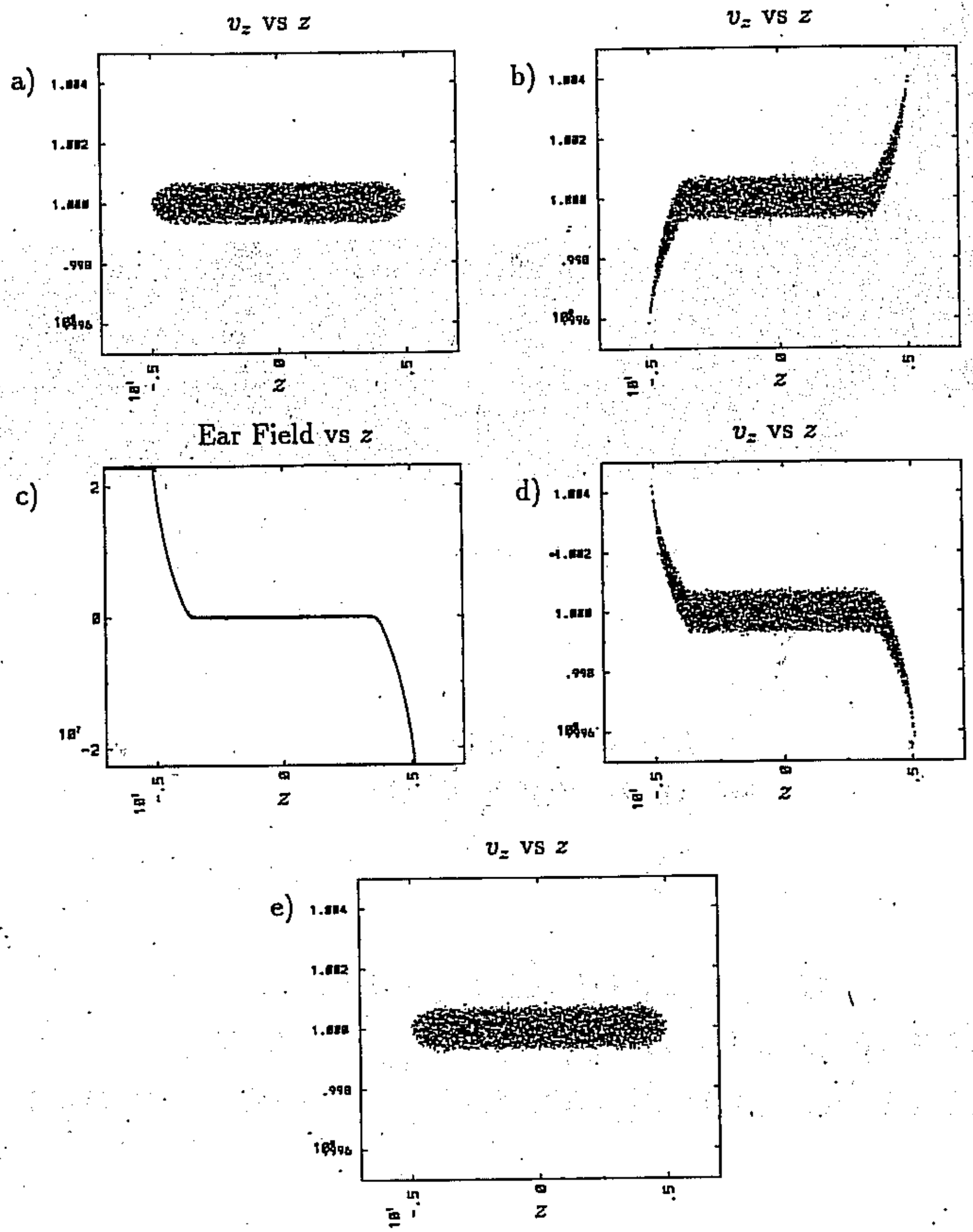

Figure 6.4: One cycle of intermittently-applied ears. (a) Initial phase space (b) Beam expands (c) Ear Field is applied (d) Beam is compressed (e) Beam expands back to its initial state

from D. Callahan Miller
PhD thesis, U.C. Davis, 1994.

John Barnard
Steven Lund
USPAS
June 2008

Injectors and longitudinal physics -- III

1. Longitudinal cooling from acceleration
2. Longitudinal instability
3. Bunch compression
4. Neuffer distribution

LONGITUDINAL COOLING

1. DURING INJECTION BEAM UNDERGOES LARGE LONGITUDINAL EXPANSION
2. $T_{\perp 0} = T_{\parallel 0}$ AT SOURCE, BUT $T_\perp \neq T_\parallel$ AFTER ACCELERATION
3. IMPLICATIONS FOR BEAM STABILITY AND EMITTANCE EVOLUTION

CONSIDER 1 D DIODE:

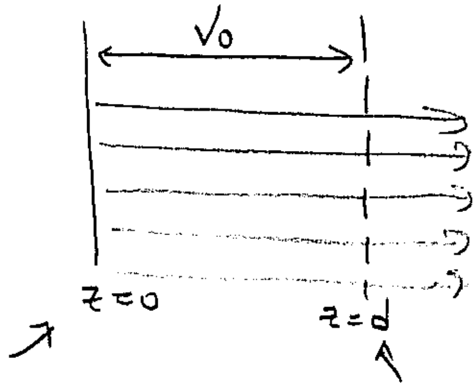

AT SOURCE

$$E_0 = \frac{p_{z0}^2}{2m}$$

$$\Delta E_{\parallel 0} \equiv \frac{\langle p_{z0}^2 \rangle}{2m} = \frac{1}{2} kT_{\parallel 0}$$

AT END OF DIODE

$$E_f = qV_0 + \frac{p_{z0}^2}{2m} = \frac{p_{zf}^2}{2m}$$

$$\Delta E_{\parallel f} = \Delta E_{\parallel 0} \neq \frac{1}{2} kT_f$$

SINCE $E_\parallel = \dfrac{p_z^2}{2m} \Rightarrow \Delta E_\parallel = \dfrac{2 p_z \Delta p_z}{2m}$

$$\frac{\Delta E}{E} = \frac{2 \Delta p_z}{p_z}$$

$$\frac{1}{2} kT_f \cong \frac{\Delta p_{zf}^2}{2m} = \left(\frac{p_{zf} \Delta E_f}{2E_f} \right)^2 \frac{1}{2m} = \frac{\Delta E_f^2}{4E_f} = \frac{kT_0}{2} \left[\frac{1}{2} \frac{kT_0}{qV_0} \right]$$

$$\Rightarrow \boxed{kT_f = \frac{1}{2} kT_0 \left[\frac{kT_0}{qV_0} \right]}$$

$$kT_f = \frac{1}{2} kT_0 \underbrace{\left[\frac{kT_0}{qV_0}\right]}_{\ll 1}$$

EXAMPLE $1000^\circ C \Leftrightarrow 0.1\ eV$

FOR $V_0 = 1\ MeV$

$kT_0 = 0.1\ eV$

$kT_f = 5. \times 10^{-9}\ eV$

$\boxed{\text{HOW CAN } kT_f \ll kT_0 \text{ BUT } \Delta E_f = \Delta E_0 ?}$

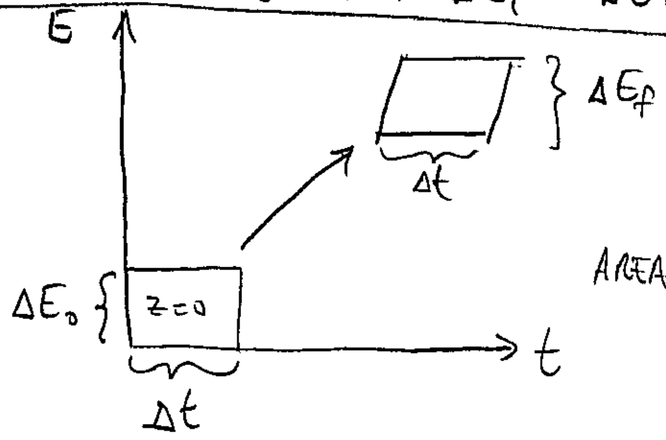

AREA IS CONSERVED

(PULSE DURATION STAYS THE SAME.)

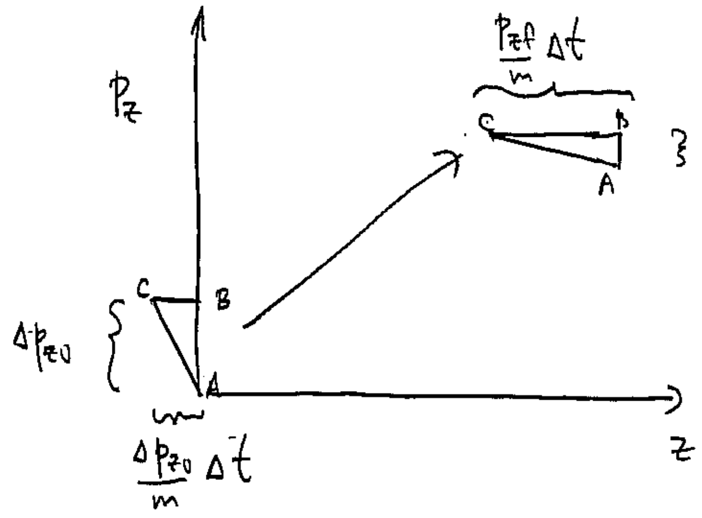

(BUNCH LENGTH GROWS)

AREA IS CONSERVED

$$\frac{1}{2}\frac{\Delta p_{z0}^2}{m}\Delta t = \frac{1}{2}\Delta p_{zf}\left(\frac{p_{zf}}{m}\right)\Delta t$$

$$\Rightarrow \Delta p_{zf} = \frac{\Delta p_{z0}^2}{p_{zf}}$$

$$\Rightarrow kT_f = \frac{1}{2} kT_0 \left(\frac{kT_0}{qV_0}\right)$$

CHANGE IN NOTATION

(4)

NOTE: $\overline{z'} \equiv \left\langle \frac{dz}{ds} \right\rangle$; $s \equiv v_0 t$

Let $u = \left\langle \frac{dz}{dt} \right\rangle$; then $u = v_0 \overline{z'}$

= fluid velocity in comoving frame

So

$$\frac{\partial \lambda}{\partial s} + \frac{\partial}{\partial z}(\lambda \overline{z'}) = 0 \quad \Rightarrow \quad \boxed{\frac{\partial \lambda}{\partial t} + \frac{\partial}{\partial z}(\lambda u) = 0}$$

$$\& \quad \frac{\partial \overline{z'}}{\partial s} + \overline{z'} \frac{\partial}{\partial z} \overline{z'} + \frac{1}{\lambda} \frac{\partial}{\partial z}(\lambda \Delta z'^2) = \overline{z''}$$

$$\Rightarrow \frac{\partial u}{\partial t} + u \frac{\partial u}{\partial z} + \frac{1}{\lambda} \frac{\partial}{\partial z}\left(\lambda \left[\langle v_z^2 \rangle - u^2\right]\right) = \overline{\ddot{z}} ,$$

Since $p_z = m \int_{-\infty}^{\infty} n [v_z^2 - u^2] \, d v_z$ where $n = \frac{\lambda}{\pi r_b^2}$

$$\Rightarrow \boxed{\frac{\partial u}{\partial t} + u \frac{\partial u}{\partial z} + \frac{\pi r_b^2}{m \lambda} \frac{\partial}{\partial z} p_z = \overline{\ddot{z}}} \qquad \text{where } \ddot{z} = \frac{d^2 z}{dt^2} = \frac{F_z}{m}$$

JOHN BARNARD & STEVEN LUND
USPAS JANUARY 2004 ⑥

"LONGITUDINAL" OR "RESISTIVE WALL" INSTABILITY

Let us return to the 1-D FLUID EQUATIONS

SEE REISER 6.3.2.
CALLAHAN-MILLER, PH.D. DISSERTATION U.C. DAVIS, 1994

$$\frac{\partial \lambda}{\partial t} + \frac{\partial}{\partial z}\lambda u = 0$$

$$\frac{\partial u}{\partial t} + u\frac{\partial u}{\partial z} + \underbrace{\frac{1}{\rho}\frac{\partial p_z}{\partial z}}_{\text{IGNORE AGAIN}} = \frac{-g q}{4\pi\epsilon_0 m v_0^2}\frac{\partial \lambda}{\partial z} + \underbrace{\frac{qE_z}{m}}_{\text{EXTERNALLY GENERATED}}$$

AS BEAM PASSES CONDUCTING SURFACE IMAGE CHARGE AND CURRENT INTERACTS WITH BEAM. HIGHLY GEOMETRY DEPENDENT.

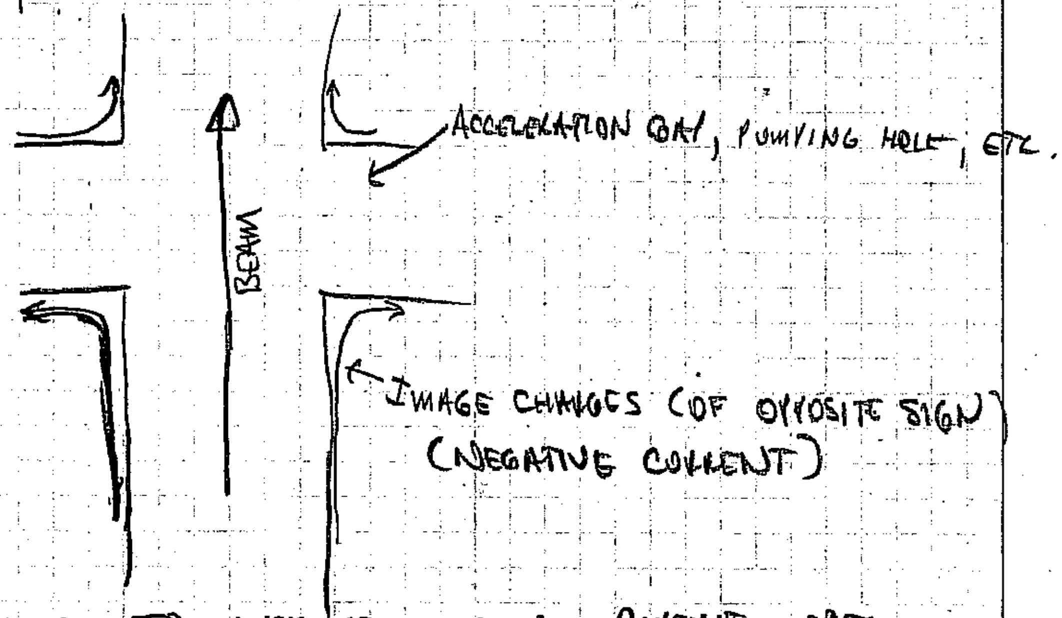

CAN BE CALCULATED APPROXIMATELY USING CIRCUIT MODEL.

RESISTIVITY IN WALL, AND COMPLICATED ELECTRON FLOW PATTERNS CREATE A RETARDING ELECTRIC FIELD ON BEAM.

MODEL OF IMPEDANCE (IN LONG WAVELENGTH REGIME)

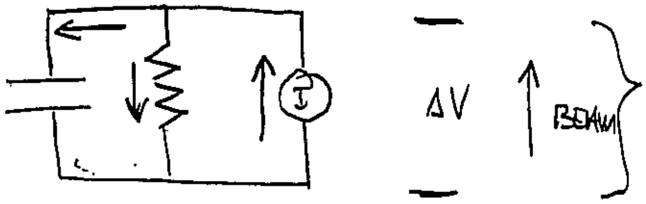

ONE MODULE OF MANY, EACH SEPARATED BY DISTANCE L

$$I = C\frac{d\Delta V}{dt} + \frac{\Delta V}{R} \qquad I = [CL]\frac{d\Delta V/L}{dt} + \frac{\Delta V/L}{R/L}$$

$$E = -\frac{\Delta V}{L} \qquad C^{+} = CL \qquad R^{*} = \frac{R}{L}$$

LET $I = I_0 + I_1 e^{-i\omega t}$ $\qquad E = E_0 + E_1 e^{-i\omega t}$

$$I_1 = i\omega C^{+} E_1 - \frac{E_1}{R^{*}}$$

$$\Rightarrow E_1 = \frac{-R^{*}}{1 - i\omega C^{+}R^{*}} I_1 \qquad Z^{*} \equiv -\frac{E_1}{I_1} = \frac{R^{*}}{1 - i\omega C^{+}R^{*}}$$

RETURNING TO THE 1D FLUID EQUATIONS

$$\frac{\partial \lambda}{\partial t} + \frac{\partial}{\partial z}\lambda v = 0 \qquad \frac{\partial u}{\partial t} + u\frac{\partial u}{\partial z} = \frac{-qg}{4\pi\epsilon_0 m}\frac{\partial \lambda}{\partial z} + \frac{qE_z}{m}$$

Let $\lambda = \lambda_0 + \lambda_1 \exp[i(kz - \omega t)]$

$\qquad u = v_0 + u_1 \exp[i(kz - \omega t)]$

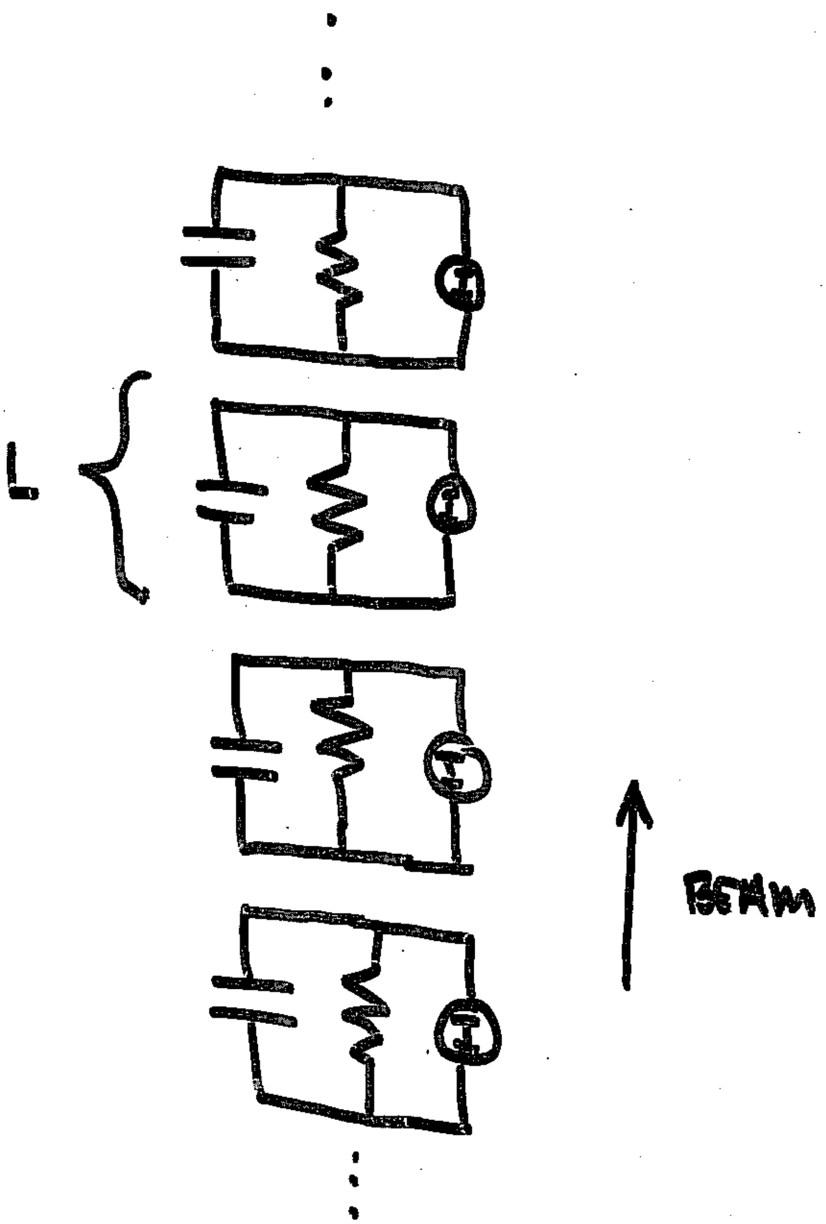

CONTINUOUS LIMIT:

$R^* = R/L$ Resistance per unit length

$C^* = CL$ C^{-1} per unit length

$E = \dfrac{\Delta V}{L}$ Average electric field

(7)

$$-i\omega\lambda_1 + ik\lambda_0 u_1 + ikV_0\lambda_1 = 0$$

$$-i\omega u_1 + ikV_0 u_1 + \underbrace{\frac{ikgq\,\lambda_1}{4\pi\epsilon_0 m_i}}_{=\frac{ikc_s^2}{\lambda_0}\lambda_1} + \frac{q}{m} Z^* \underbrace{(\lambda_0 V_1 + V_0\lambda_1)}_{=I_1} = 0$$

$$\begin{bmatrix} \omega - kV_0 & -k\lambda_0 \\ -\frac{c_s^2 k}{\lambda_0} + \frac{iq}{m} Z^* V_0 & \omega - kV_0 + \frac{iq}{m} Z^* \lambda_0 \end{bmatrix} \begin{bmatrix} \lambda_1 \\ u_1 \end{bmatrix} = 0$$

THE DETERMINANT OF THE ABOVE MATRIX MUST VANISH:

$$(\omega - kV_0)^2 + \frac{iq}{m} Z^* \lambda_0(\omega - kV_0) - c_s^2 k^2 + \frac{iq}{m} Z^* \lambda_0 V_0 k = 0$$

$$\boxed{(\omega - kV_0)^2 - c_s^2 k^2 + \frac{iq Z^* \lambda_0 \omega}{m} = 0} \quad \text{(LAB FRAME)}$$

Using a Galilean transformation, in the beam frame:

$$\omega' = \omega - kV_0 \qquad \text{' denotes beam frame}$$

$$k' = k$$

$$\boxed{\omega'^2 - c_s^2 k'^2 + \frac{iq Z^*(\omega')\lambda_0(\omega' + k'V_0)}{m} = 0} \quad \text{(BEAM FRAME)}$$

NOTE $Z^*(\omega') = Z^*(\omega = \omega' + k'V_0)$

8

CASE I PURE RESISTIVE IMPEDANCE $Z^* = R^*$ (REAL)

$$\omega'^2 = \pm c_s k' \sqrt{1 - iR^* \frac{q\lambda_0}{m} \frac{(\omega' + k'V_0)}{c_s^2 k'^2}}$$

Using $c_s^2 = \frac{gq\lambda_0}{4\pi\epsilon_0 m}$ & $\frac{\omega'}{k'} \sim c_s << V_0$

$$\omega' = \pm c_s k' \sqrt{1 - iR^* \left(\frac{4\pi\epsilon_0}{g}\right) \frac{V_0}{k'}}$$

$$\simeq \pm\left[c_s k' - i \frac{c_s V_0}{2}\left(\frac{4\pi\epsilon_0}{g}\right) R^*\right]$$

Since $\lambda_1, E_1 \sim \exp\left[i(k'z' - \omega' t')\right]$

Choosing "+" ($\mathrm{Re}\,\omega > 0$) $\Rightarrow$ $z' = c_s t$ line of const phase $\Rightarrow$ Forward propagating

($\mathrm{Im}\,\omega' < 0$) $\Rightarrow$ $\lambda_1 \sim \exp\left[-\frac{c_s V_0}{2}\left(\frac{4\pi\epsilon_0}{g}\right) R^* t\right]$ $\Rightarrow$ DECAYING PERTURBATION

CHOOSING "−"

($\mathrm{Re}\,\omega' < 0$) $\Rightarrow$ $z' = -c_s t'$ is line of constant phase

$\Rightarrow$ BACKWARD PROPAGATING

$$\Rightarrow \lambda_1 \sim \exp\left[\underbrace{+\frac{c_s V_0}{2}\left(\frac{4\pi\epsilon_0}{g}\right) R^*}_{G} t\right]$$

INSTABILITY!

$$\lambda_1 \simeq \lambda_{10} \exp[G]$$

(9b)

$$G = \left[\frac{C_s V_0}{2} \left(\frac{4\pi\epsilon_0}{g} \right) R^* t \right] =$$ LOGARITHMIC GAIN OF INSTABILITY $$= \ln\left(\frac{\lambda_{1\,final}}{\lambda_{initial}} \right)$$

Now $t_{max} = \left\{ \min \left\{ \begin{array}{l} l_b / C_s \\ t_{residence} \end{array} \right. \right.$

l_b / C_s: TRANSIT TIME FOR PERTURBATION TO TRAVEL FROM HEAD TO TAIL

$t_{residence}$: RESIDENCE TIME WITHIN ACCELERATOR

If upper condition holds

$$G \sim \frac{V_0^2}{2} \left(\frac{4\pi\epsilon_0}{g} \right) R^* \Delta t$$

If lower condition holds

$$G \sim \sqrt{\lambda}$$

$E = QV$ (10)

$$I \sim \frac{6\ \mathrm{MJ}}{4\ \mathrm{GeV}\ 200\ \mathrm{ns}} \sim \frac{QV}{V\Delta t}$$

EXAMPLE:

$$\sim 7.5\ \mathrm{kA}$$

FOR MATCHED BEAM IMPEDANCE

$$R^* = \frac{dV/ds}{I} \sim \frac{10^6\ \mathrm{V/m}}{10\ \mathrm{kA}} \sim 100\ \Omega/\mathrm{m}$$

$V_0 \sim 0.2c$

$\Delta t \sim 200\ \mathrm{ns}$

$$G \sim \frac{V_0^2}{2}\left(\frac{4\pi\varepsilon_0}{g}\right) R^* \Delta t$$

~ 3.6

(AN EARLY CONCERN FOR HEAVY ION FUSION).

$R^* = 100\,\Omega/m$

(11)

FOR ALL SIMULATIONS (p 11–15)

$V_0 = c/3$

$I = 3\,kA$

$l_b = 10\,m$

$\frac{r_b}{r_p} = 0.4$

$kT_\perp = kT_\parallel = 10\,keV$

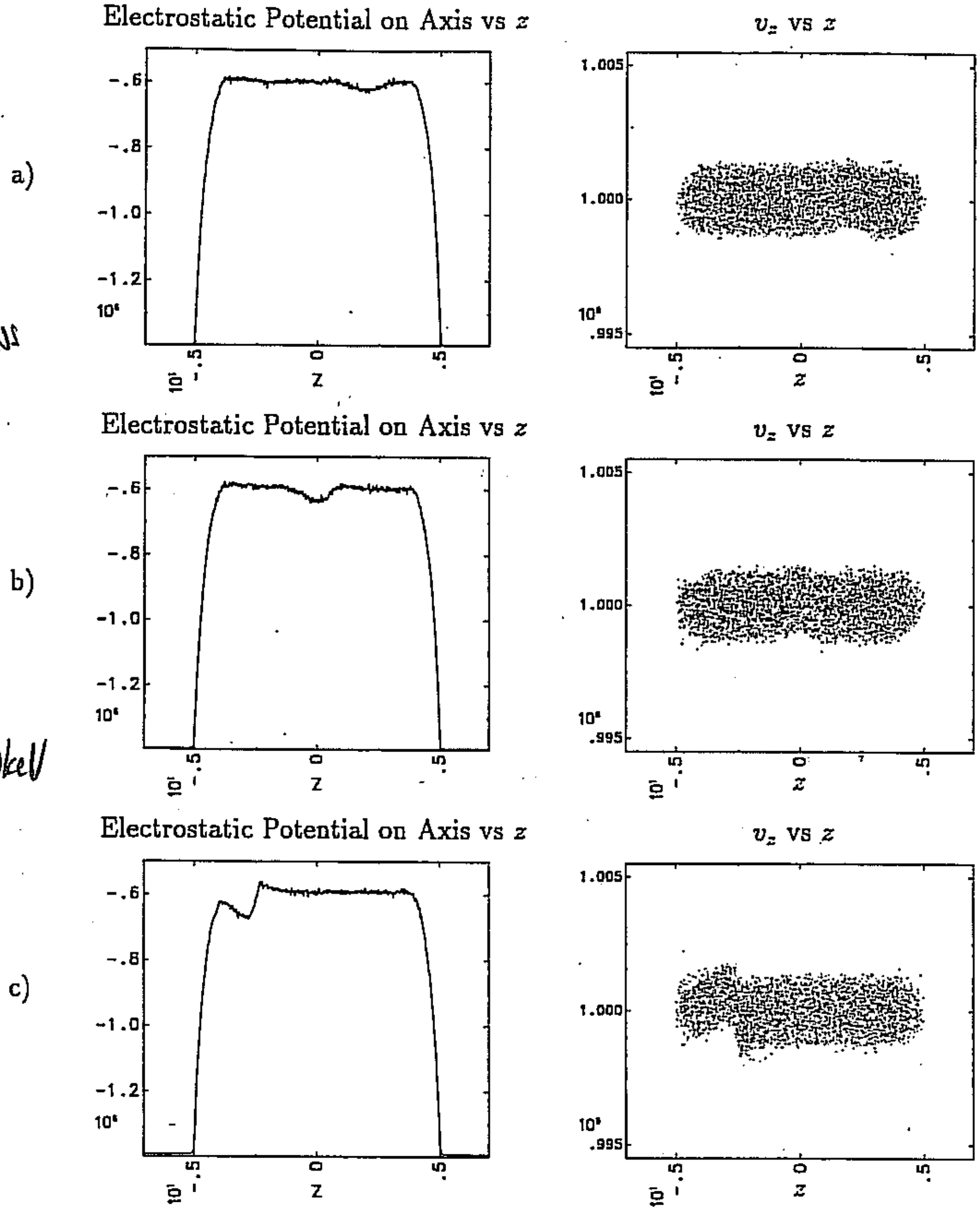

Figure 4.2: A simulation with 100 Ω/m resistance shows moderate growth. (a) 6.6 μs, (b) 10.9 μs, (c) 17.5 μs

from D.A. Callahan Miller, Ph.D. Thesis
U.C. Davis, 1994

$R^* = 100\ \Omega/m$ (12)

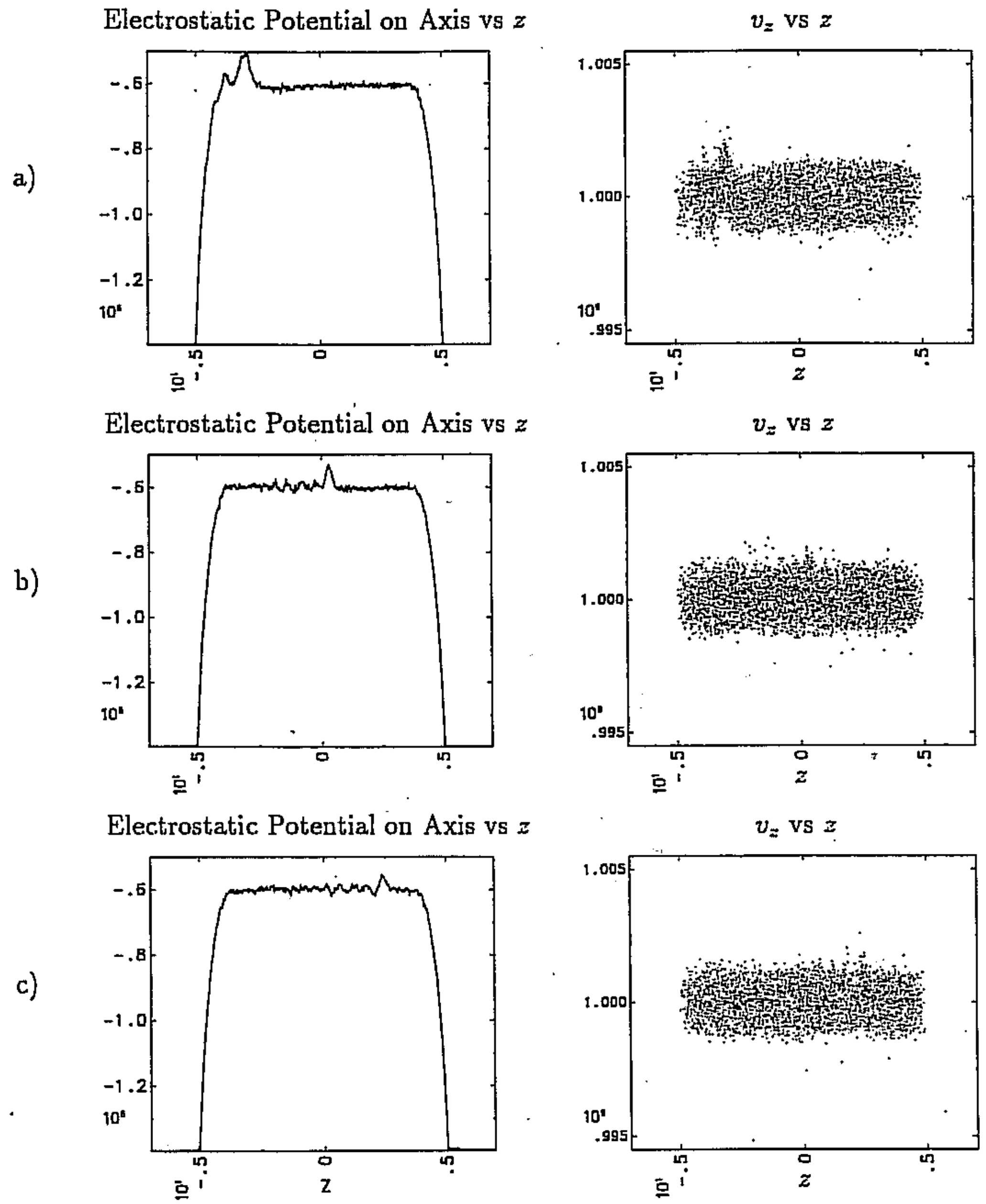

Figure 4.3: The perturbation reflects off the beam end and decays as it travels forward. (a) 28.4 μs, (b) 35.0 μs, (c) 39.4 μs

from D.A. Callahan Miller, Ph.D. Thesis
U.C. Davis, 1994
(FORWARD WAVE)

(13)

$R^* = 200\Omega/m$

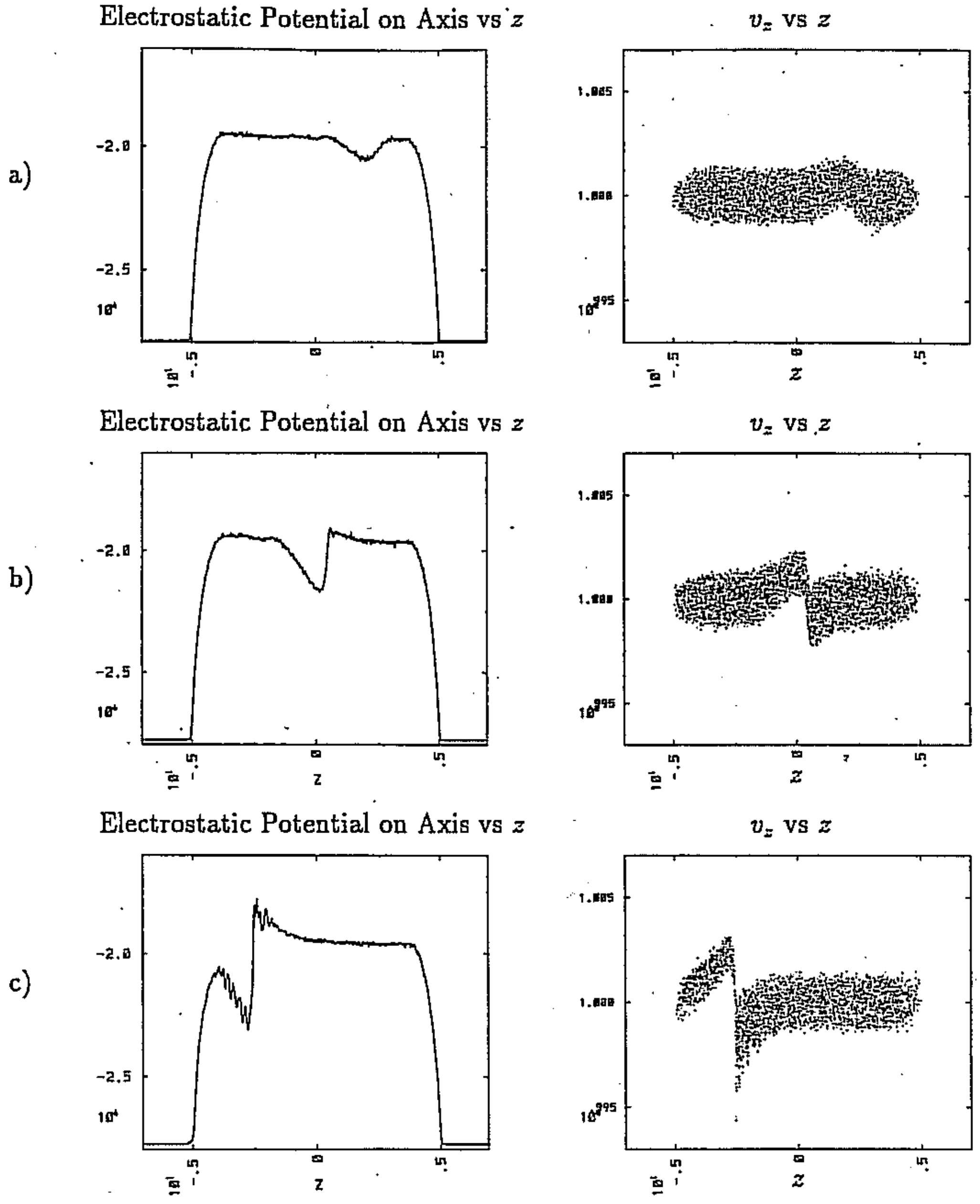

Figure 4.1: A simulation with 200 Ω/m resistance shows large amounts of growth. (a) 6.6 μs, (b) 10.9 μs, (c) 17.5 μs

from D. A. Callahan Miller, Ph. D. Thesis
U.C. Davis, 1994

(10)

CASE II RESISTIVE + CAPACITIVE IMPEDANCE

$$Z^* = \frac{R^*}{1 - i\omega C^+ R^*} = \frac{R^* + i\omega C^+ R^{*2}}{1 + \omega^2 C^{+2} R^{*2}}$$

GOING BACK TO PAGE 7:

IN LAB FRAME:

$$(\omega - kv_0)^2 - c_s^2 k^2 + \frac{iqR^* \lambda_0 \omega}{m(1 + \omega^2 C^{+2} R^{*2})} - \frac{q\omega^2 C^+ R^{*2} \lambda_0}{m(1 + \omega^2 C^{+2} R^{*2})} = 0$$

$$(\omega - kv_0)^2 - c_s^2 k^2 - \frac{4\pi\epsilon_0}{g} \frac{\omega^2 C R^{*2} c_s^2}{(1 + \omega^2 C^2 R^{*2})} + \frac{i4\pi\epsilon_0 c_s^2 R^* \omega}{g(1 + \omega^2 C^2 R^{*2})}$$

IN BEAM FRAME:

$$\omega'^2 - c_s^2 k^2 - \frac{4\pi\epsilon_0}{g} \frac{(\omega' + k'v_0)^2 C R^{*2} c_s^2}{(1 + (\omega' + k'v_0)^2 C^2 R^2)} + \frac{i4\pi\epsilon_0 c_s^2 R_*^2 (\omega' + k'v_0)}{g(1 + \omega^2 C^2 R^{*2})}$$

So if one takes limit $C \to \infty$ the final two terms tend to zero. Thus capacitance has reduced the instability growth rate.

$RC^* = 2 \times 10^{-8}$ s
$R^* = 100\Omega/m$

15

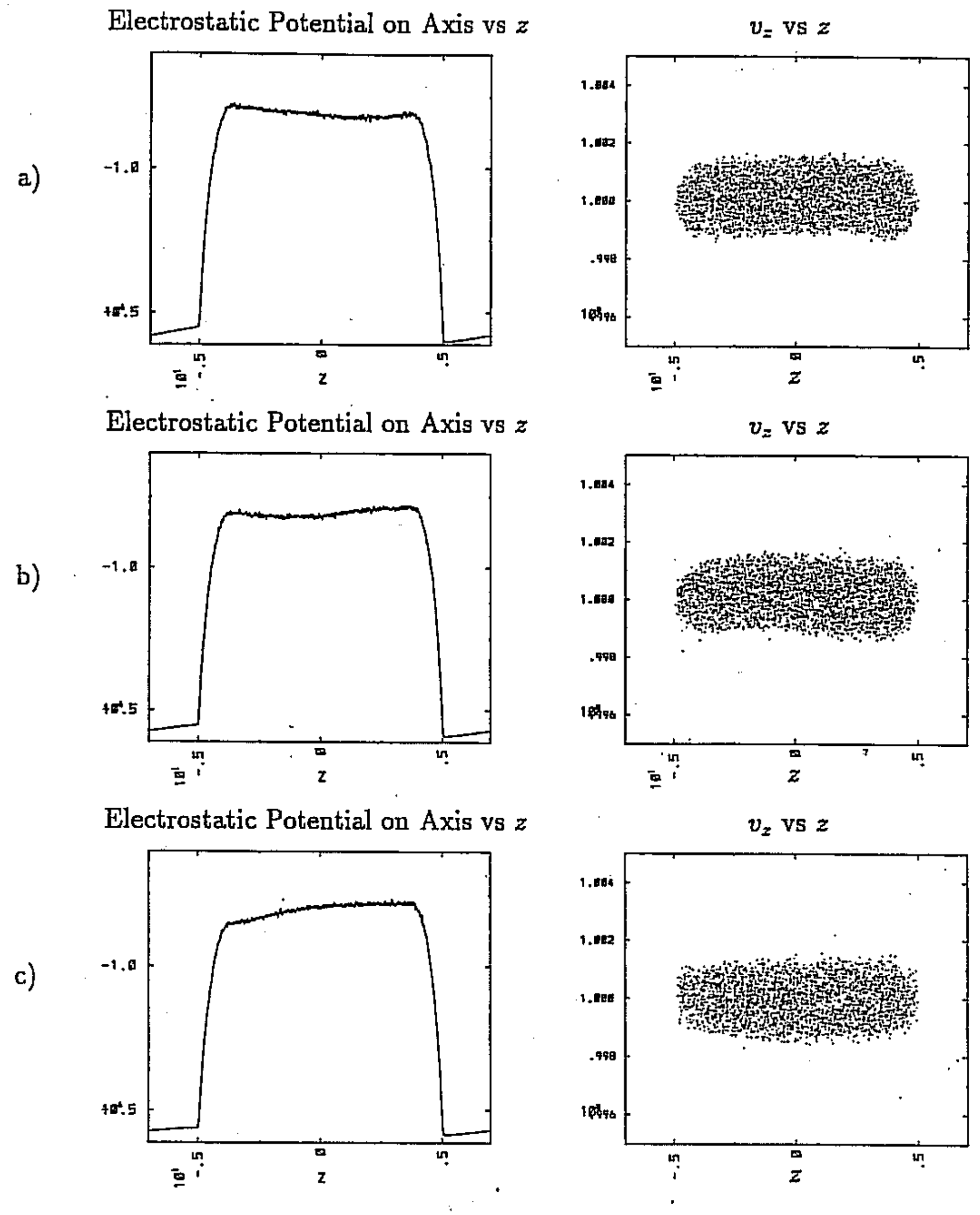

Figure 4.6: When capacitance is added to the system, a larger perturbation is launched, but little growth occurs (a) 6.6 μs, (b) 10.9 μs, (c) 17.5 μs

from D.A. Callahan Miller, Ph.D. Thesis,
U.C. Davis, 1994

Summary of Longitudinal Instability

"Resistive Wall" or "Longitudinal" Instability has potential to degrade longitudinal emittance in high current accelerators.

However, capacitance (e.g. from accelerating gaps) decreases growth can mitigate instability,

Not Discussed:

1. Longitudinal temperature damps instability (c.f. Reiser 6.3.3)

2. Feedback has been provided to control instability if needed

WARNERD & LUND (17)

DRIFT COMPRESSION

OBJECTS:

APPLY A HEAD-TO-TAIL VELOCITY TILT TO INCREASE CURRENT BY DECREASING PULSE DURATION

DURING COMPRESSION "EARS" ARE NOT REQUIRED

AT END OF DRIFT COMPRESSION, VELOCITY "TILT" SHOULD BE MINIMIZED, SO THAT CHROMATIC ABERRATIONS IN FINAL FOCUS ARE MINIMIZED.

18

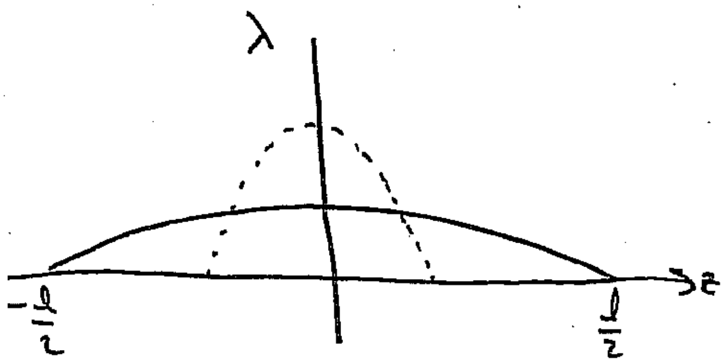

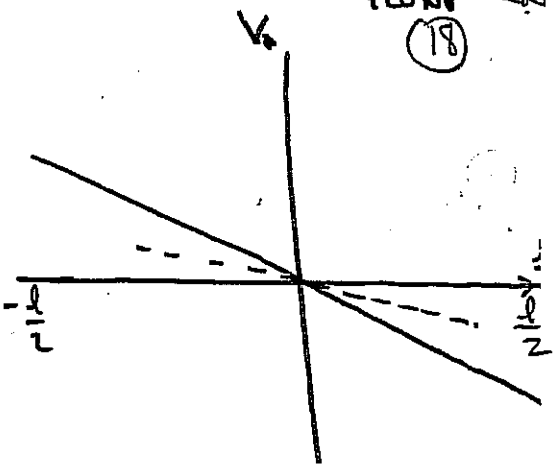

$$\frac{\partial \lambda}{\partial t} + \frac{\partial}{\partial z} \lambda v = 0$$ CONTINUITY EQUATION

$$\frac{\partial v}{\partial t} + v \frac{\partial v}{\partial z} = \frac{-q g}{m\, 4\pi\epsilon_0} \frac{\partial \lambda}{\partial z}$$ MOMENTUM EQUATION

LET $$\lambda = \lambda_0(t)\left(1 - \frac{4z^2}{l^2(t)}\right)$$ ← PARABOLIC LINE CHARGE PROFILE

$$V = -\Delta V(t) \frac{z}{l(t)}$$ ← LINEAR VELOCITY PROFILE

① MASS conservation:

$$Q_c = \int_{-l/2}^{l/2} \lambda \, dz = \lambda_0 \int_{-\frac{l}{2}}^{l/2} \left(1 - \frac{4z^2}{l^2}\right) dz = \frac{2}{3} \lambda_0 l = \text{constant}$$

(but $\lambda_0 = \lambda_0(t)$ & $l = l(t)$)

CALCULATING PARTIAL DERIVATIVES:

BARNARD & LUND

(19)

$$\frac{\partial\lambda}{\partial t} = \dot{\lambda}_0\left(1-\frac{4z^2}{l^2}\right) + 2\lambda_0\left(\frac{4z^2}{l^3}\right)\dot{l}$$

$$\frac{\partial\lambda}{\partial z} = \frac{-8z}{l^2}\lambda_0$$

$$\frac{\partial V}{\partial t} = -\Delta\dot{V}\left(\frac{z}{l}\right) + \frac{\Delta V\, z}{l^2}\dot{l}$$

$$\frac{\partial V}{\partial z} = -\frac{\Delta V}{l}$$

FROM DEFINITION OF ΔV & l:

$\Delta V = -\dot{l}$

(2) CONTINUITY EQUATION $\Rightarrow \left(1-\frac{4z^2}{l^2}\right)\left(\dot{\lambda}_0 - \frac{\Delta V\lambda_0}{l}\right) = 0$

(3) MOMENTUM EQUATION $\Rightarrow \left(\frac{z}{l}\right)\left[-\Delta\dot{V} + \frac{\dot{l}\Delta V}{l} + \frac{\Delta V^2}{l} + \frac{8qg}{m4\pi\epsilon_0}\frac{\lambda_0}{l}\right] = 0$

$$(1)\ \&\ (2) \Rightarrow \frac{\dot{\lambda}_0}{\lambda_0} = \frac{\Delta V}{l} = \frac{-\dot{l}}{l} \qquad (4)$$

$$(3)\ \&\ (4) \Rightarrow \boxed{\ddot{l} - \frac{12qg}{4\pi\epsilon_0 m}\frac{Q_c}{l^2} = 0}$$

where $Q_c = \frac{2}{3}\lambda_0 l = \text{const.}$

$\equiv$ CHARGE IN BUNCH (NOT PERVEANCE)

LONGITUDINAL "ENVELOPE" EQUATION (WITHOUT EMITTANCE)

BARNARD & LUND

(20)

MULTIPLY BY $\dot{l}$ & INTEGRATE:

$$\frac{\dot{l}^2}{2} + \frac{12gg}{4\pi\epsilon_0 m}\frac{Q_c}{l} = \cancel{\frac{\dot{l}_f^2}{2}}^{\to 0} + \frac{12gg}{4\pi\epsilon_0 m}\frac{Q_c}{l_f}$$

HERE SUBSCRIPT "f" = "final"

& SUBSCRIPT "o" = original or initial

$$\Rightarrow \quad \dot{l}_0 = \sqrt{\frac{16gg}{4\pi\epsilon_0 m}\lambda_f\left[1 - \frac{l_f}{l_0}\right]}$$

Now $Q_f = \dfrac{\lambda_f}{4\pi\epsilon_0 V_f}$ = FINAL PERVEANCE AT CENTER OF PARABOLIC PULSE

(NOTE $Q_c \equiv \frac{2}{3}\lambda_0 l$ = CHARGE

whereas $Q_F \equiv$ PERVEANCE (DIMENSIONLESS)

C = COMPRESSION RATIO $= \dfrac{l_0}{l_f}$

$\dfrac{\Delta V}{V_0}$ = velocity tilt $= \dfrac{|\dot{l}|}{V_0}$

$$\rightarrow \quad \boxed{\frac{\Delta V}{V} = \sqrt{8gQ_f\left[1 - \frac{1}{C}\right]}}$$

for $Q_f = 10^{-4}$

$g = 1.1$

$C = 20$

$\Rightarrow \dfrac{\Delta V}{V} = 0.029$

$$\boxed{\text{DRIFT LENGTH} \cong \frac{l}{\Delta V}V_0 = \frac{l}{\Delta V/V} = 345 \text{ m} \quad \text{for } l = 10 \text{ m}}$$

(21)

Vlasov - equation for a drifting beam:

$$\frac{\partial f}{\partial s} + x'\frac{\partial f}{\partial x} + x''\frac{\partial f}{\partial x'} + y'\frac{\partial f}{\partial y} + y''\frac{\partial f}{\partial y'} + z'\frac{\partial f}{\partial z} + z''\frac{\partial f}{\partial z'} = 0$$

Let $\tilde{f}(z,z',s) \equiv \iiiint f \, dx \, dx' \, dy \, dy'$

INTEGRATING VLASOV EQUATION: If $z'' \neq f(x,x',y,y')$:

$$\Rightarrow \frac{\partial \tilde{f}}{\partial s} + \iiint x' \underbrace{\int \frac{\partial f}{\partial x} dx}_{= f\big|_{-\infty}^{\infty} = 0} dx' \, dy \, dy' + \cdots \quad z'\frac{\partial \tilde{f}}{\partial z} + z''\frac{\partial \tilde{f}}{\partial z'} = 0$$

$$\Rightarrow \boxed{\frac{\partial \tilde{f}}{\partial s} + z'\frac{\partial \tilde{f}}{\partial z} + z''\frac{\partial \tilde{f}}{\partial z'} = 0} \quad \text{1 D Vlasov}$$

Now let $\lambda \equiv q\int \tilde{f} \, dz'$; $\lambda \overline{z'} = \int \tilde{f} z' dz'$; $\lambda \overline{z'^2} \equiv \int \tilde{f} z'^2 dz'$

Also, let $\Delta z'^2 \equiv \overline{z'^2} - (\overline{z'})^2$

FLUID EQUATIONS

INTEGRATING 1D VLASOV OVER z':

$$\boxed{\frac{\partial \lambda}{\partial s} + \frac{\partial}{\partial z}(\lambda \overline{z'}) = 0} \quad \text{(CONTINUITY EQUATION)}$$

MULTIPLYING BY z' & INTEGRATING VLASOV OR z':

$$\frac{\partial}{\partial s}\lambda \overline{z'} + \frac{\partial}{\partial z}\lambda \overline{z'^2} - \lambda \overline{z''} = 0$$

DIVIDING BY λ, USING CONTINUITY EQUATION & DEFINITION OF $\Delta z'^2$:

$$\boxed{\underbrace{\frac{\partial \overline{z'}}{\partial s} + \overline{z'}\frac{\partial}{\partial z}\overline{z'}}_{\text{INERTIAL}} + \underbrace{\frac{1}{\lambda}\frac{\partial}{\partial z}(\lambda \Delta z'^2)}_{\text{PRESSURE TERM}} = \underbrace{\overline{z''}}_{\text{FORCE}}} \quad \text{(MOMENTUM EQUATION)}$$

(22)

LONGITUDINAL ENVELOPE EQUATION

$$\frac{\partial \tilde{f}}{\partial s} + z' \frac{\partial \tilde{f}}{\partial z} + z'' \frac{\partial \tilde{f}}{\partial z'} = 0$$

Q_c = total charge in bunch

If $z'' = -K(s)z + \frac{qg}{4\pi\varepsilon_0 m v^2}\left(\frac{12 Q_c}{L^3}\right) z$

$$\Rightarrow \frac{\partial}{\partial s}\langle z^2\rangle = 2\langle z z'\rangle$$

$$\frac{\partial}{\partial s}\langle z z'\rangle = \langle z'^2\rangle + \frac{qg}{4\pi\varepsilon_0 m v^2}\left(\frac{12 Q_c}{L^3}\right)\langle z^2\rangle - K(s)\langle z^2\rangle$$

$$\frac{\partial}{\partial s}\langle z'^2\rangle = 2\left(\frac{qg}{4\pi\varepsilon_0 m v^2}\right)\left(\frac{12 Q_c}{L^3}\right)\langle z z'\rangle - 2K(s)\langle z z'\rangle$$

NOTE $\langle z^2\rangle = \frac{1}{Q_c}\int_{-\infty}^{\infty}\int_{-L/2}^{L/2} z^2 f(z,z')\,dz\,dz' = \frac{1}{20}L^2$

$$\varepsilon_z^2 = 25\left[\langle z^2\rangle\langle z'^2\rangle - \langle z z'\rangle^2\right]$$

$$\Rightarrow \frac{d^2 L}{ds^2} = \frac{16\,\varepsilon_z^2}{L^3} + \frac{12\, g q Q_c}{4\pi\varepsilon_0 m v^2 L^2} - K(s) L$$

Let $r_z = L/2$

$$\Rightarrow \boxed{\frac{d^2 r_z}{ds^2} = \frac{\varepsilon_z^2}{r_z^3} + \frac{3}{2}\frac{g q Q_c}{4\pi\varepsilon_0 m v^2}\frac{1}{r_z^2} - K(s) r_z}$$

SELF-CONSISTENT LONGITUDINAL DISTRIBUTION:

NEUFFER DISTRIBUTION — D. NEUFFER, PARTICLE ACCELERATORS, Vol 11, p 23 (1980)

RETURNING TO THE 1D VLASOV EQUATION:

$$\frac{\partial f}{\partial s} + z' \frac{\partial f}{\partial z} + z'' \frac{\partial f}{\partial z'} = 0$$

If $z'' = -A \frac{\partial \lambda}{\partial z} - K(s) z$

THEN,

$$f(z, z', s) = \frac{3N}{2\pi \varepsilon_z} \sqrt{1 - \frac{z^2}{r_z^2} - \frac{r_z^2 (z' - r_z' z / r_z)^2}{\varepsilon_z^2}}$$

for $-r_z < z < r_z$

& $\frac{r_z' z}{r_z} - \frac{\varepsilon_z}{r_z}\sqrt{1 - \frac{z^2}{r_z^2}} \leq z' \leq \frac{r_z' z}{r_z} + \frac{\varepsilon_z}{r_z}\sqrt{1 - \frac{z^2}{r_z^2}}$

is a solution to the 1D Vlasov equation.

HERE $\varepsilon_z^2 = 25 (\langle z^2\rangle\langle z'^2\rangle - \langle z z'\rangle^2] = \text{CONSTANT}$

N = total number of particles in bunch

r_z = hard edge of bunch

NOTE THAT $\lambda(z) = \frac{3}{4}\frac{N}{r_z}\left(1 - \frac{z^2}{r_z^2}\right) = \int_{-r_z}^{r_z} f(z, z', s)\, dz'$

$\Rightarrow \frac{\partial \lambda}{\partial z} \propto z \Rightarrow$ LINEAR SPACE CHARGE FIELD

Neuffer Distribution Function

$$f[z,z'] = \frac{3N}{2\pi\varepsilon_z}\sqrt{1-\frac{z^2}{r_z^2}-\frac{r_z^2(z'-r_z'z/r_z)^2}{\varepsilon_z^2}}$$

for:

$$-r_z \le z \le r_z$$

$$\frac{r_z'z}{r_z}-\frac{\varepsilon_z}{r_z}\sqrt{1-\frac{z^2}{r_z^2}} \le z' \le \frac{r_z'z}{r_z}+\frac{\varepsilon_z}{r_z}\sqrt{1-\frac{z^2}{r_z^2}}$$

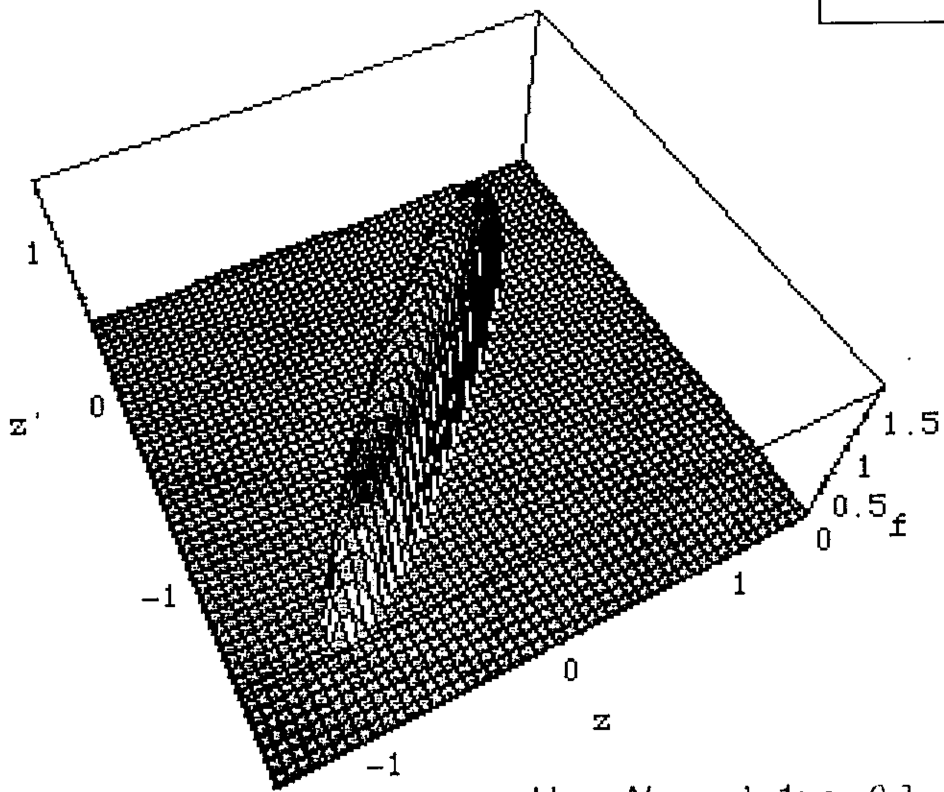

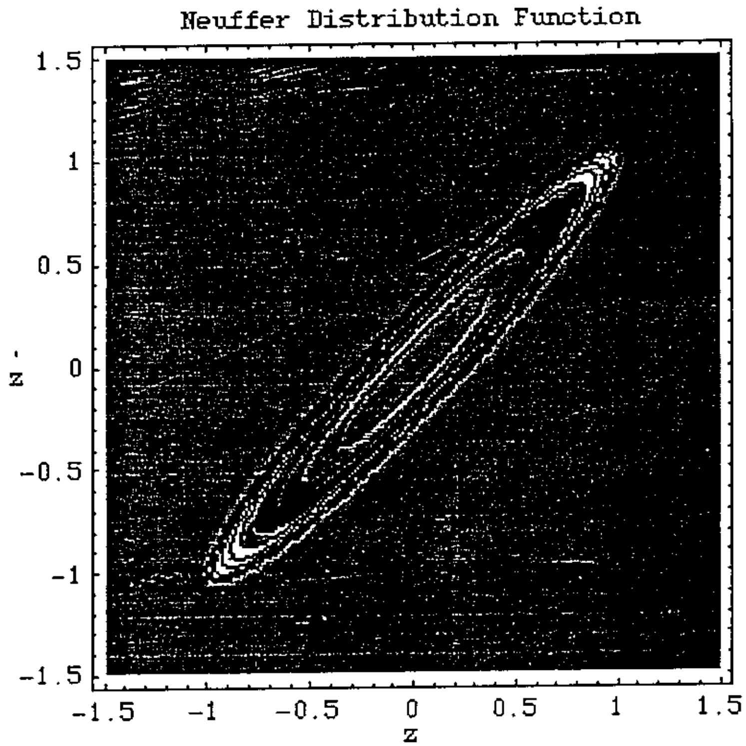

Here $N=r_z=r_z'=1$; $\varepsilon_z=0.3$

NOTE:

- DISTRIBUTION FUNCTION HAS ELLIPTICAL BOUNDARY IN z-z' PHASE SPACE
- $\pi \varepsilon_z$ IS AREA OF ELLIPSE AND K CONSTANT
- ANALOGOUS TO K-V DISTRIBUTION WITH LINEAR SPACE CHARGE FORCE AND SECOND ORDER ENVELOPE EQUATION TO DESCRIBE THE MOTION OF THE DISTRIBUTION:

$$\frac{d^2 r_z}{ds^2} = \frac{\varepsilon_z^2}{r_z^3} + \frac{3}{2}\frac{AN}{r_z^2} - K(s)\, r_z$$

NOTE ALSO THAT NEUFFER FUNCTION CAN BE USED FOR BUNCHED BEAMS IN WHICH $E_z \propto z$, AS IN A UNIFORM DENSITY ELLIPSOID.

Summary

1D VLASOV EQUATION

$$\frac{\partial \tilde{f}}{\partial s} + z' \frac{\partial \tilde{f}}{\partial z} + z'' \frac{\partial \tilde{f}}{\partial z'} = 0$$

& g-factor model

$$z'' = \frac{-g}{4\pi\epsilon_0 m V_z^2} \frac{\partial \lambda}{\partial z}$$

Leads to fluid equations:

$$\frac{\partial \lambda}{\partial s} + \frac{\partial}{\partial z}(\lambda \bar{z}') = 0$$

$$\frac{\partial \bar{z}'}{\partial s} + \bar{z}' \frac{\partial \bar{z}'}{\partial z} + \frac{1}{\lambda}\frac{\partial}{\partial z}(\lambda \Delta z'^2) + \frac{c_s^2}{\lambda_0 V_0^2}\frac{\partial \lambda}{\partial z} = 0$$

$\Rightarrow$ SPACE CHARGE WAVES

↳ LONGITUDINAL OR RESISTIVE WALL INSTABILITY

$\Rightarrow$ SPACE CHARGE RAREFACTION WAVES

$\Rightarrow$ PARABOLIC BUNCH COMPRESSION $\frac{\partial \lambda}{\partial z} \propto z$

VLASOV EQUATION ALSO $\Rightarrow$ ENVELOPE EQUATION

$$\frac{d^2 r_z}{ds^2} = \frac{\epsilon_z^2}{r_z^3} + \frac{3}{2}\frac{g q Q_c}{4\pi\epsilon_0 m v^2}\frac{1}{r_z^2} - K(s) r_z$$

KINETIC SOLUTION TO VLASOV EQUATION SATISFYING rms ENVELOPE EQUATION IS "NEUFFER DISTRIBUTION" (ANALOGOUS TO KV).

$$f(z,z') = \frac{3N}{2\pi\epsilon_z}\sqrt{1 - \frac{z^2}{r_z^2} - \frac{r_z^2 (z' - r_z' z/r_z)^2}{\epsilon_z^2}}$$

Transverse Centroid and Envelope Descriptions of Beam Evolution*

Steven M. Lund
Lawrence Livermore National Laboratory (LLNL)

Steven M. Lund and John J. Barnard
"Beam Physics with Intense Space-Charge"

US Particle Accelerator School

University of Maryland, held at Annapolis, MD
16-27 June, 2008
(Version 20080624)

* Research supported by the US Dept. of Energy at LLNL and LBNL under contract Nos. DE-AC52-07NA27344 and DE-AC02-05CH11231.

Transverse Centroid and Envelope Model: Outline

Comments:

- Some of this material related to J.J. Barnard lectures:
  - Transport limit discussions (Introduction)
  - Transverse envelope modes (Continuous Focusing Envelope Modes and Halo)
  - Longitudinal envelope evolution (Longitudinal Beam Physics III)
  - 3D Envelope Modes in a Bunched Beam (Cont. Focusing Envelope Modes and Halo)
- Specific topics will be covered in more detail here

Transverse Centroid and Envelope Model: Detailed Outline

Detailed Outline - 2

Detailed Outline - 3

10) Centroid and Envelope Descriptions via 1st Order Coupled Moment Equations

Formulation

Example Illustration -- Familiar KV Envelope Model

Contact Information

References

S1: Overview

Analyze transverse centroid and envelope properties of an unbunched $(\partial/\partial z = 0)$ beam

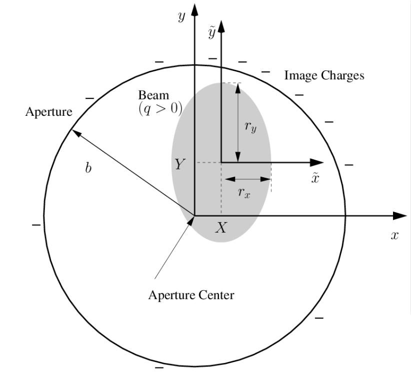

Transverse averages:

$$\langle \cdots \rangle_\perp \equiv \frac{\int d^2x_\perp \int d^2x'_\perp \; \cdots f_\perp}{\int d^2x_\perp \int d^2x'_\perp \; f_\perp}$$

Centroid:

$$\boxed{\begin{aligned} X &= \langle x \rangle_\perp \\ Y &= \langle y \rangle_\perp \end{aligned}}$$

x- and y-coordinates of beam center of mass

Envelope: (edge measure)

$$\boxed{\begin{aligned} r_x &= 2\sqrt{\langle (x - X)^2 \rangle_\perp} \\ r_y &= 2\sqrt{\langle (y - Y)^2 \rangle_\perp} \end{aligned}}$$

x- and y-principal axis radii of an elliptical beam envelope

- Apply to general f but base on uniform density f

Oscillations in the statistical beam centroid and envelope radii are the *lowest-order* collective responses of the beam

Centroid Oscillations: Associated with errors and are purposefully suppressed to the level possible

- Error Sources:
  - Beam distribution assymetries
  - Dipole bending terms from applied field optics
  - Imperfect mechanical alignment
- Exception: When the beam is kicked (insertion or extraction) into our out of a transport channel as is often done in rings

Envelope Oscillations: Can have two components in periodic focusing lattices

1) Matched Envelope: Periodic "flutter" synchronized to period of focusing lattice to yield net focusing

- Properly tuned flutter essential in Alternating Gradient quadrupole lattices

2) Mismatched Envelope: Excursions deviate from matched flutter motion and are seeded/driven by errors

Limiting maximum beam-edge excursions is desired for economical transport

- Reduces cost by Limiting material volume needed to transport an intense beam

Mismatched beams have larger envelope excursions and have more stability problems since mismatch adds another source of free energy that can drive statistical increases in particle amplitudes (see: J.J. Barnard lectures on Envelopes and Halo)

Example: FODO Quadrupole Transport Channel

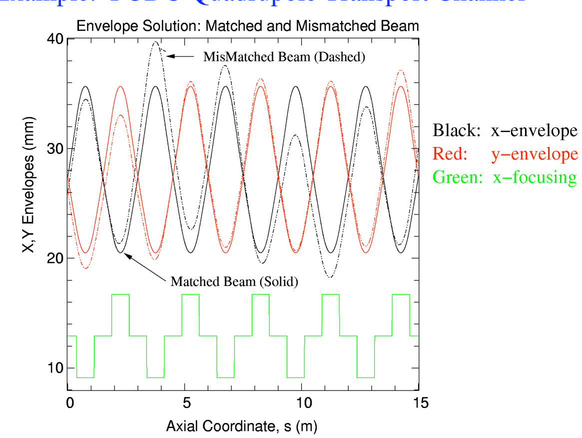

- Larger machine aperture is needed to confine a mismatched beam

Centroid and Envelope oscillations are the *most important collective modes* of an intense beam

- Force balances based on matched beam envelope equation predict scaling of transportable beam parameters
  - Used to design transport lattices
- Instabilities in beam centroid and/or envelope oscillations prevent reliable transport
  - Parameter locations of instability regions should be understood and avoided in machine design/operation

Although it is *necessary* to design to avoid envelope and centroid instabilities, it is not alone *sufficient* for effective machine operation

- Higher-order kinetic and fluid instabilities not expressed in the low-order envelope models can degrade beam quality and control and must also be evaluated
  - To be covered (see: S.M. Lund, lectures on Kinetic Stability)

S2: Derivation of Transverse Centroid and Envelope Equations of Motion

Analyze centroid and envelope properties of an unbunched $(\partial/\partial z = 0)$ beam

Transverse Statistical Averages:

Let N be the number of particles in a thin axial slice of the beam at axial coordinate s.

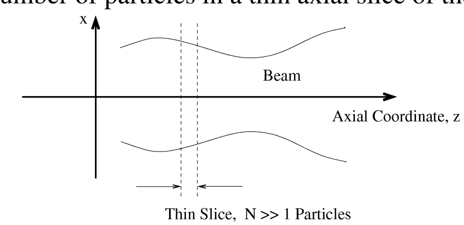

Equivalent averages can be defined in terms of the particles or the transverse Vlasov distribution function:

particles: $$\langle \cdots \rangle_\perp \equiv \frac{1}{N}\sum_{i=1}^{N}\Big|_{\text{slice}} \cdots$$

distribution: $$\langle \cdots \rangle_\perp \equiv \frac{\int d^2x_\perp \int d^2x'_\perp \cdots f_\perp}{\int d^2x_\perp \int d^2x'_\perp \; f_\perp}$$

- Averages can be generalized to include axial momentum spread

Transverse Particle Equations of Motion

Consistent with earlier analysis, take:

$$x'' + \frac{(\gamma_b\beta_b)'}{(\gamma_b\beta_b)}x' + \kappa_x x = -\frac{q}{m\gamma_b^3\beta_b^2c^2}\frac{\partial\phi}{\partial x}$$

$$y'' + \frac{(\gamma_b\beta_b)'}{(\gamma_b\beta_b)}y' + \kappa_y y = -\frac{q}{m\gamma_b^3\beta_b^2c^2}\frac{\partial\phi}{\partial y}$$

$$\nabla_\perp^2\phi = \left(\frac{\partial^2}{\partial x^2} + \frac{\partial^2}{\partial y^2}\right)\phi = -\frac{\rho}{\epsilon_0}$$

$$\rho = q\int d^2x'_\perp \; f_\perp \qquad \phi|_{\text{aperture}} = 0$$

Assume:

- Unbunched beam
- No axial momentum spread
- Linear applied focusing fields described by $\kappa_x, \; \kappa_y$
- Possible acceleration $\gamma_b\beta_b$ need not be constant

Various apertures are possible. Some simple examples:

Round Pipe

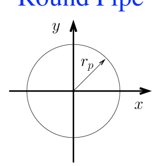

Linac magnetic quadrupoles, acceleration cells, ...

Elliptical Pipe

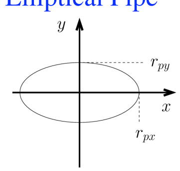

In rings with dispersion: in drifts, magnetic optics, ...

Hyperbolic Sections

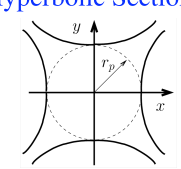

Electric quadrupoles

Review: Focusing lattices we will take in examples: Continuous and piecewise constant periodic solenoid and quadrupole doublet

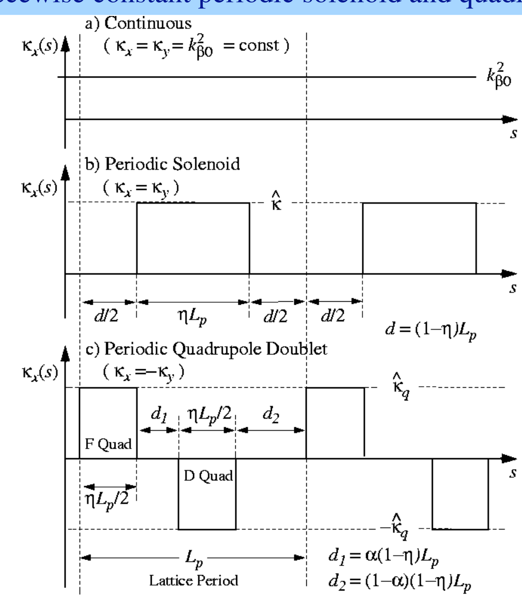

Lattice Period L_p

Occupancy η

$\eta \in [0, 1]$

Solenoid description carried out implicitly in Larmor frame

[see: S.M. Lund lectures on Transverse Particle Equations]

Syncopation Factor α

$$\alpha \in [0, \frac{1}{2}]$$

$$\alpha = \frac{1}{2} \Longrightarrow FODO$$

Distribution Assumptions

To lowest order, linearly focused intense beams are expected to be nearly uniform in density within the core of the beam out to an edge where the density falls rapidly to zero

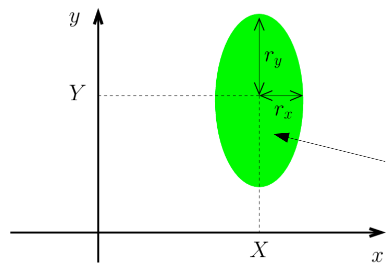

constant density in the beam:

$$\rho = \frac{\lambda}{\pi r_x r_y} = \text{const}$$

- Expected for near equilibrium structure for strong space-charge due to Debye screening (see: S.M. Lund, lectures on Transverse Equilibrium Distributions)
- Observed in simulations of stable non-equilibrium beams

$$\boxed{\begin{aligned}\rho(x,y) = q\int d^2x'_\perp\, f_\perp \simeq \begin{cases} \frac{\lambda}{\pi r_x r_y}, & (x-X)^2/r_x^2 + (y-Y)^2/r_y^2 < 1 \\ 0, & (x-X)^2/r_x^2 + (y-Y)^2/r_y^2 > 1\end{cases} \\ \lambda = q\int d^2x_\perp \int d^2x'_\perp\, f_\perp = \int d^2x\, \rho\end{aligned}}$$

Self-Field Calculation

Temporarily, we will consider an arbitrary beam charge distribution within an arbitrary aperture to formulate the problem.

Electrostatic field of a line charge in free-space

$$\boxed{\mathbf{E}_\perp = \frac{\lambda_0}{2\pi\epsilon_0}\frac{(\mathbf{x}_\perp - \tilde{\mathbf{x}})}{|\mathbf{x}_\perp - \tilde{\mathbf{x}}|^2}}$$

$\lambda_0 =$ line charge

$\mathbf{x}_\perp = \tilde{\mathbf{x}} =$ coordinate of charge

Resolve the field of the beam into direct (free space) and image terms:

$$\boxed{\mathbf{E}^s_\perp = -\frac{\partial\phi}{\partial\mathbf{x}_\perp} = \mathbf{E}^d_\perp + \mathbf{E}^i_\perp}$$

and superimpose free-space solutions for direct and image contributions

Direct Field

$$\mathbf{E}^d_\perp(\mathbf{x}_\perp) = \frac{1}{2\pi\epsilon_0}\int d^2\tilde{x}_\perp\,\frac{\rho(\tilde{\mathbf{x}}_\perp)(\mathbf{x}_\perp - \tilde{\mathbf{x}}_\perp)}{|\mathbf{x}_\perp - \tilde{\mathbf{x}}_\perp|^2}$$

$\rho(\mathbf{x}) =$ beam charge density

Image Field

$$\mathbf{E}^i_\perp(\mathbf{x}_\perp) = \frac{1}{2\pi\epsilon_0}\int d^2\tilde{x}_\perp\,\frac{\rho^i(\tilde{\mathbf{x}}_\perp)(\mathbf{x}_\perp - \tilde{\mathbf{x}}_\perp)}{|\mathbf{x}_\perp - \tilde{\mathbf{x}}_\perp|^2}$$

$\rho^i(\mathbf{x}) =$ beam imagecharge densityinduced on aperture

Direct Field:

The direct field solution for a uniform density beam in free-space was calculated for the KV equilibrium distribution

- see: S.M. Lund, lectures on Transverse Equilibrium Distributions

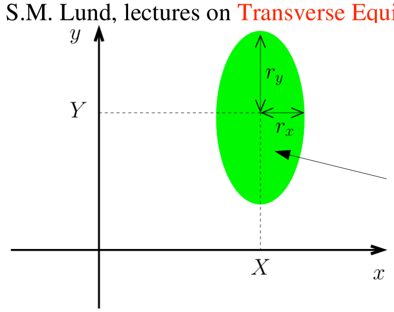

constant density in the beam:

$$\rho = \frac{\lambda}{\pi r_x r_y} = \text{const}$$

$$\boxed{\begin{aligned}E^d_x &= \frac{\lambda}{\pi\epsilon_0}\frac{x-X}{(r_x+r_y)r_x} \\ E^d_y &= \frac{\lambda}{\pi\epsilon_0}\frac{y-Y}{(r_x+r_y)r_y}\end{aligned}}$$

Expressions are valid only within the elliptical density beam -- where they will be applied in taking averages

Image Field:

Image structure depends on the aperture. Assume a round pipe (most common case) for simplicity.

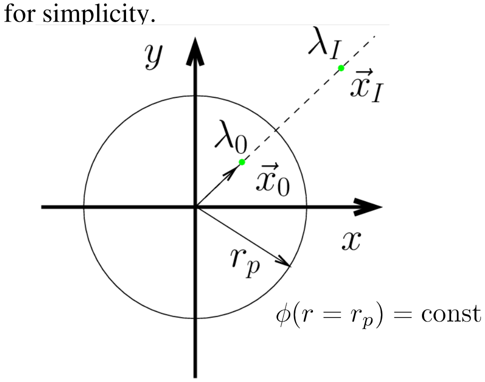

$\lambda_I = -\lambda_0$ image charge

$\mathbf{x}_I = \frac{r_p^2}{|\mathbf{x}_0|^2}\mathbf{x}_0$ image location

superimpose all images of beam:

$$\boxed{\mathbf{E}^i_\perp(\mathbf{x}_\perp) = -\frac{1}{2\pi\epsilon_0}\int_{\text{pipe}} d^2\tilde{x}_\perp\,\frac{\rho(\tilde{\mathbf{x}}_\perp)(\mathbf{x}_\perp - r_p^2\tilde{\mathbf{x}}_\perp/|\tilde{\mathbf{x}}_\perp|^2)}{|\mathbf{x}_\perp - r_p^2\tilde{\mathbf{x}}_\perp/|\tilde{\mathbf{x}}_\perp|^2|^2}}$$

- Difficult to calculate even for ρ corresponding to a uniform density beam

Examine limits of the image field to build intuition on the range of properties:

1) On-axis line charge: $\rho(\mathbf{x}_\perp) = \lambda \delta(\mathbf{x}_\perp - X\hat{\mathbf{x}})$

$$\boxed{\mathbf{E}^i_\perp(\hat{\mathbf{x}}_\perp = X\hat{\mathbf{x}}) = \frac{\lambda}{2\pi\epsilon_0 (r_p^2/X - X)}\hat{\mathbf{x}}}$$

- Generates nonlinear field at position of direct charge
- Field creates attractive force between direct and image charge

2) Centered, uniform density elliptical beam:

Expand using complex coordinates starting from the general image expression:

$$\underline{E}^i = E^i_y + iE^i_x = \sum_{n=2,4,\cdots}^{\infty} \underline{c}_n \underline{z}^{n-1} \qquad \underline{c}_n = \frac{i}{2\pi\epsilon_0}\int_{\text{pipe}} d^2x_\perp\, \rho(\mathbf{x}_\perp)\frac{(x-iy)^n}{r_p^{2n}}$$

$$\underline{z} = x + iy \qquad = \frac{i\lambda n!}{2\pi\epsilon_0 2^n (n/2+1)!(n/2)!}\left(\frac{r_x^2 - r_y^2}{r_p^4}\right)^{n/2}$$

$$i = \sqrt{-1}$$

The linear (n = 2) components of this expansion give:

$$\boxed{E^i_x = \frac{\lambda}{8\pi\epsilon_0}\frac{r_x^2 - r_y^2}{r_p^4}x, \qquad E^i_y = -\frac{\lambda}{8\pi\epsilon_0}\frac{r_x^2 - r_y^2}{r_p^4}y}$$

- Rapidly vanish (higher order terms more rapid) as beam becomes more round

3) Uniform density elliptical beam with a small displacement along the *x*-axis:

$$Y = 0 \qquad |X|/r_p \ll 1$$

Expand using complex coordinates starting from the general image expression:

- Use complex coordinates to simplify calculation

  E.P. Lee, E. Close, and L. Smith, Nuclear Instruments and Methods, 1126 (1987)

- Expressions become even more complicated with simultaneous *x*- and *y*-displacements and more complicated aperture geometries

Leading Order Image Fields

$$E^i_x = \frac{\lambda}{2\pi\epsilon_0 r_p^2}\left[f(x-X) + gX\right] + \Theta\left(\frac{X}{r_p}\right)^3$$

$$E^i_y = -\frac{\lambda}{2\pi\epsilon_0 r_p^2} fy + \Theta\left(\frac{X}{r_p}\right)^3$$

$$f = \frac{r_x^2 - r_y^2}{4r_p^2} + \frac{X^2}{r_p^2}\left[1 + \frac{3}{2}\left(\frac{r_x^2 - r_y^2}{r_p^2}\right) + \frac{3}{8}\left(\frac{r_x^2 - r_y^2}{r_p^2}\right)^2\right]$$

$$g = 1 + \frac{r_x^2 - r_y^2}{4r_p^2} + \frac{X^2}{r_p^2}\left[1 + \frac{3}{4}\left(\frac{r_x^2 - r_y^2}{r_p^2}\right) + \frac{1}{8}\left(\frac{r_x^2 - r_y^2}{r_p^2}\right)^2\right]$$

Comments on images:

- Sign is generally such that it will tend to increase beam displacements
  - Also (usually) weak linear focusing corrections for an elliptical beam
- Can be very difficult to calculate explicitly
  - Even for simple case of circular pipe
  - Special cases of simple geometry formulas can give idea on scaling
  - Generally suppress just by making the beam small relative to characteristic aperture dimensions and keeping the beam steered near-axis
- Depend strongly on the aperture geometry
  - Generally varies as a function of *s* in the machine aperture changes and/or beam symmetries evolve

Round Pipe

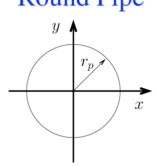

Elliptical Pipe

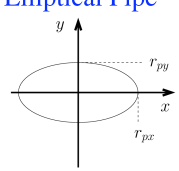

Hyperbolic Sections

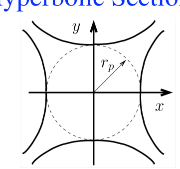

Coupled centroid and envelope equations of motion

Consistent with the assumed structure of the distribution (uniform density elliptical beam), denote:

Beam Centroid:

$$\boxed{X \equiv \langle x \rangle_\perp \qquad X' = \langle x' \rangle_\perp \\ Y \equiv \langle y \rangle_\perp \qquad Y' = \langle y' \rangle_\perp}$$

Coordinates with respect to centroid:

$$\boxed{\tilde{x} \equiv x - X \qquad \tilde{x}' = x' - X' \\ \tilde{y} \equiv y - Y \qquad \tilde{y}' = y' - Y'}$$

Envelope Edge Radii:

$$\boxed{r_x \equiv 2\sqrt{\langle \tilde{x}^2 \rangle_\perp} \qquad r'_x = \langle \tilde{x}\tilde{x}' \rangle_\perp / r_x \\ r_y \equiv 2\sqrt{\langle \tilde{y}^2 \rangle_\perp} \qquad r'_y = \langle \tilde{y}\tilde{y}' \rangle_\perp / r_y}$$

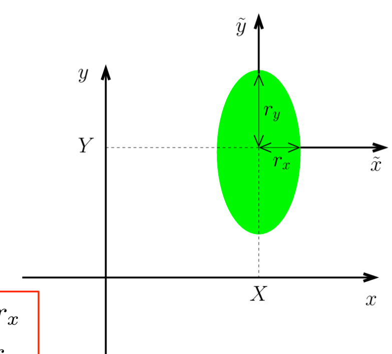

With the *assumed* uniform elliptical beam, all moments can be calculated in terms of: $X,\ Y \qquad r_x,\ r_y$

- Such truncations follow whenever the form of the distribution is "frozen"

Derive centroid equations: First use the self-field resolution for a uniform density beam, then the equations of motion for a particle within the beam are:

$$x'' + \frac{(\gamma_b\beta_b)'}{(\gamma_b\beta_b)}x' + \kappa_x x - \underbrace{\frac{2Q}{(r_x+r_y)r_x}(x-X)}_{\text{Direct Terms}} = \underbrace{\frac{q}{m\gamma_b^3\beta_b^2c^2}E_x^i}_{\text{Image Terms}}$$

$$y'' + \frac{(\gamma_b\beta_b)'}{(\gamma_b\beta_b)}y' + \kappa_y y - \frac{2Q}{(r_x+r_y)r_y}(y-Y) = \frac{q}{m\gamma_b^3\beta_b^2c^2}E_y^i$$

Perveance:

$$Q \equiv \frac{q\lambda}{2\pi\epsilon_0 m\gamma_b^3\beta_b^2c^2}$$ (not necessarily constant if beam accelerates)

average equations using: $\langle x'\rangle_\perp = \langle x\rangle'_\perp = X'$ etc., to obtain:

Centroid Equations:

$$X'' + \frac{(\gamma_b\beta_b)'}{(\gamma_b\beta_b)}X' + \kappa_x X = Q\left[\frac{2\pi\epsilon_0}{\lambda}\langle E_x^i\rangle_\perp\right]$$

$$Y'' + \frac{(\gamma_b\beta_b)'}{(\gamma_b\beta_b)}Y' + \kappa_y Y = Q\left[\frac{2\pi\epsilon_0}{\lambda}\langle E_y^i\rangle_\perp\right]$$

Note: the electric image field will cancel the coefficient $2\pi\epsilon_0/\lambda$

- $\langle E_x^i\rangle_\perp$ will generally depend on: $X,\ \ Y$ and $r_x,\ \ r_y$

To derive equations of motion for the envelope radii, first subtract the centroid equations from the particle equations of motion ($\tilde{x} \equiv x - X$) to obtain:

$$\tilde{x}'' + \frac{(\gamma_b\beta_b)'}{(\gamma_b\beta_b)}\tilde{x}' + \kappa_x\tilde{x} - \frac{2Q\tilde{x}}{(r_x+r_y)r_x} = \frac{q}{m\gamma_b^2\beta_b^2c^2}\left[E_x^i - \langle E_x^i\rangle_\perp\right]$$

$$\tilde{y}'' + \frac{(\gamma_b\beta_b)'}{(\gamma_b\beta_b)}\tilde{y}' + \kappa_y\tilde{y} - \frac{2Q\tilde{y}}{(r_x+r_y)r_x} = \frac{q}{m\gamma_b^2\beta_b^2c^2}\left[E_y^i - \langle E_y^i\rangle_\perp\right]$$

Differentiate the equation for the envelope radius (*y*-equations analogous):

$$r_x = 2\langle\tilde{x}^2\rangle_\perp^{1/2} \longrightarrow r'_x = \frac{2\langle\tilde{x}\tilde{x}'\rangle_\perp}{\langle\tilde{x}^2\rangle_\perp} = \frac{4\langle\tilde{x}\tilde{x}'\rangle_\perp}{r_x}$$

Define (motivated the KV equilibrium results) a statistical rms edge emittance:

$$\varepsilon_x \equiv 4\varepsilon_{x,\mathrm{rms}} \equiv 4\left[\langle\tilde{x}^2\rangle_\perp\langle\tilde{x}'^2\rangle_\perp - \langle\tilde{x}\tilde{x}'\rangle_\perp^2\right]^{1/2}$$

Differentiate the equation for r'_x again and use the emittance definition:

$$r''_x = 4\frac{\langle\tilde{x}\tilde{x}''\rangle_\perp}{r_x} + \frac{16[\langle\tilde{x}^2\rangle_\perp\langle\tilde{x}'^2\rangle_\perp - \langle\tilde{x}\tilde{x}'\rangle_\perp^2]}{r_x^3}$$

$$= 4\frac{\langle\tilde{x}\tilde{x}''\rangle_\perp}{r_x} + \frac{\varepsilon_x^2}{r_x^3}$$

and then employ the equations of motion to eliminate $\tilde{x}''$ in $\langle\tilde{x}\tilde{x}''\rangle_\perp$ to obtain:

Envelope Equations:

$$r''_x + \frac{(\gamma_b\beta_b)'}{(\gamma_b\beta_b)}r'_x + \kappa_x r_x - \frac{2Q}{r_x+r_y} - \frac{\varepsilon_x^2}{r_x^3} = 8Q\left[\frac{\pi\epsilon_0}{\lambda}\langle\tilde{x}E_x^i\rangle_\perp\right]$$

$$r''_y + \frac{(\gamma_b\beta_b)'}{(\gamma_b\beta_b)}r'_x + \kappa_y r_y - \frac{2Q}{r_x+r_y} - \frac{\varepsilon_y^2}{r_y^3} = 8Q\left[\frac{\pi\epsilon_0}{\lambda}\langle\tilde{y}E_y^i\rangle_\perp\right]$$

- $\langle\tilde{x}E_x^i\rangle_\perp$ will generally depend on: $X,\ \ Y$ and $r_x,\ \ r_y$

Comments on Centroid/Envelope equations:

- Centroid and envelope equations are coupled and must be solved simultaneously when image terms on the RHS cannot be neglected
- Image terms contain nonlinear terms that can be difficult to evaluate explicitly
  - Aperture geometry changes image correction
- The formulation is not self-consistent because a frozen form (uniform density) charge profile is assumed
  - Uniform density choice motivated by KV results and Debye screening see: S.M. Lund, lectures on Transverse Equilibrium Distributions
  - The assumed distribution form not evolving represents a fluid model closure

Comments on Centroid/Envelope equations (Continued):

- Constant (normalized when accelerating) emittances are generally assumed
  - See: S.M. Lund, lectures on Transverse Particle Equations

$\beta_b,\ \ \gamma_b,\ \ \lambda$ *s*-variation set by acceleration schedule

$$\begin{aligned}\varepsilon_{nx} &= \gamma_b\beta_b\varepsilon_x = \text{const}\\ \varepsilon_{ny} &= \gamma_b\beta_b\varepsilon_y = \text{const}\end{aligned} \longrightarrow \text{used to calculate } \varepsilon_x,\ \varepsilon_y$$

$$Q = \frac{q\lambda}{2\pi m\epsilon_0\gamma_b^3\beta_b^2c^2}$$

S3: Centroid Equations of Motion

Single Particle Limit: Oscillation and Stability Properties

Neglect image charge terms, then the centroid equation of motion becomes:

$$\boxed{\begin{aligned} X'' + \frac{(\gamma_b\beta_b)'}{(\gamma_b\beta_b)}X' + \kappa_x X = 0 \\ Y'' + \frac{(\gamma_b\beta_b)'}{(\gamma_b\beta_b)}Y' + \kappa_y Y = 0 \end{aligned}}$$

- Usual Hill's equation with generalized acceleration term
- Single particle form. Apply results from S.M. Lund lectures on Transverse Particle Equations: phase amplitude methods, Courant-Snyder invariants, and stability bounds, ...

Assume that applied lattice focusing is tuned for constant phase advances and/or that acceleration is weak and can be neglected. Then single particle stability results give immediately:

$$\boxed{\begin{aligned} \sigma_{0x} < 180^\circ \\ \sigma_{0y} < 180^\circ \end{aligned}}$$

centroid stability, 1st stability condition

/// Example: FODO channel centroid evolution

Mid-drift launch:

$X(0) = 1$ mm
$X'(0) = 1$ mrad

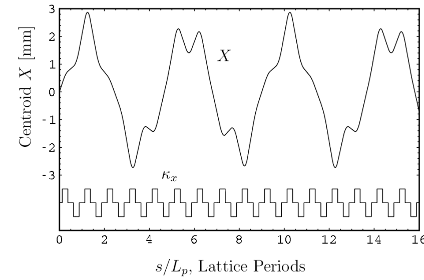

lattice/beam parameters:

$\beta_b = \text{const}$
$\sigma_{0x} = 80^\circ$
$L_p = 0.5$ m
$\eta = 0.5$

- Centroid exhibits expected characteristic stable betatron oscillations

///

Effect of Driving Errors

The reference orbit is ideally tuned for zero centroid excursions. But there will *always* be driving errors that can cause the centroid oscillations to accumulate with beam propagation distance:

$$\boxed{X'' + \frac{(\gamma_b\beta_b)'}{(\gamma_b\beta_b)}X' + \frac{G_n}{G_0}\kappa_q(s)X = \frac{G_n}{G_0}\kappa_q(s)\Delta_{xn}}$$

$\frac{G_n}{G_0} =$ nth quadrupole gradient error (unity for no error; s-varying)

$\Delta_{xn} =$ nth quadrupole transverse displacement error (s-varying)

/// Example: FODO channel centroid with quadrupole displacement errors

$\frac{G_n}{G_0} = 1$

$\Delta_{xn} = [-0.5, 0.5]$ mm (uniform dist)

same lattice as previous

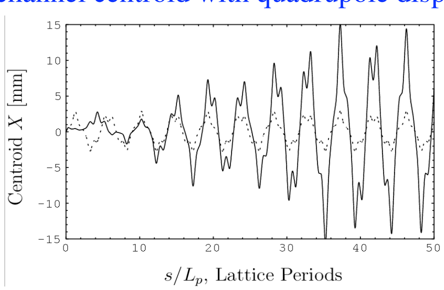

solid – with errors
dashed – no errors

///

Errors will result in a characteristic random walk increase in oscillation amplitude due to the (generally random) driving terms.

Control by:

- Synthesize small applied dipole fields to regularly steer the centroid back on-axis to the reference trajectory: X = 0 = Y, X' = 0 = Y'
- Fabricate and align focusing elements with higher precision
- Employ a sufficiently large aperture to contain the oscillations and limit detrimental nonlinear image charge effects

Economics dictates the optimal strategy

Effects of Image Charges

Model the beam as a displaced line-charge in a circular aperture. Then using the previously derived image charge field, the equations of motion reduce to:

$$\boxed{X'' + \frac{(\gamma_b\beta_b)'}{(\gamma_b\beta_b)}X' + \kappa_x X = \frac{QX}{r_p^2 - X^2}}$$

examine oscillation along *x*-axis

$$\frac{QX}{r_p^2 - X^2} \simeq \frac{Q}{r_p^2}X + \frac{Q}{r_p^4}X^3$$

linear correction

Nonlinear correction (smaller)

Example: FODO channel centroid with image charge corrections

$r_p = 30$ mm

$Q = 2 \times 10^{-4}$

same lattice as previous

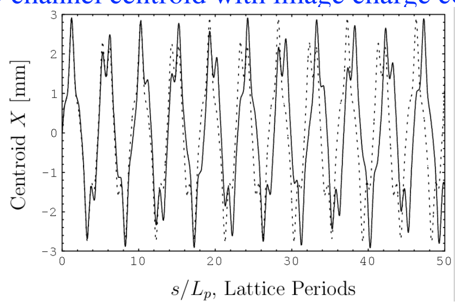

solid – with images

dashed – no images

Main effect of images appears to be an accumulated phase error of the centroid orbit since, generally the centroid error oscillations are not "matched" orbits. This will complicate extrapolations of errors over many lattice periods

Control by:

- Keeping centroid displacements X, Y small by correcting
- Make aperture (pipe radius) larger

General Comments:

- Images contributions to centroid excursions generally less problematic than misalignment errors in focusing elements

More detailed analyses show that the coupling of the envelope radii r_x, r_y to the centroid evolution in X, Y is often weak

- Fringe fields are more important for accurate calculation of centroid orbits since orbits are not part of a matched lattice
  - Nonideal orbits are poorly tuned to lattice and become more sensitive to the precise phase of impulses
- Over long path lengths many nonlinear terms can influence results
- Lattice errors are not often known so one must often analyze characteristic error distributions to see if centroids measured are consistent with expectations

S4: Envelope Equations of Motion

Overview: Reduce equations of motion for r_x, r_y

- Generally found that couplings to centroid coordinates X Y are weak
  - Centroid ideally zero
- Envelope eqns are most important in designing transverse focusing systems
  - Expresses average radial force balance (see following discussion)
  - Can be difficult to analyze analytically for scaling properties
  - "Systems" codes generally written using envelope equations, stability criteria, and practical engineering constraints
- Instabilities of the envelope equations in periodic focusing lattices must be avoided in machine operation
  - Instabilities are strong and real: not washed out with realistic distributions without frozen form
  - Represent lowest order "KV" modes of a full kinetic theory
- Previous derivation of envelope equations relied on Courant-Snyder invariants in linear applied and self-fields. Analysis shows that the same force balances result for a uniform elliptical beam with no image couplings.
  - Debye screening arguments suggest assumed uniform density model taken should be a good approximation for intense space-charge

KV/rms Envelope Equations: Properties of Terms

The envelope equation reflects low-order force balances:

$$r_x'' + \frac{(\gamma_b\beta_b)'}{(\gamma_b\beta_b)}r_x' + \kappa_x r_x - \frac{2Q}{r_x + r_y} - \frac{\varepsilon_x^2}{r_x^3} = 0$$

$$r_y'' + \frac{(\gamma_b\beta_b)'}{(\gamma_b\beta_b)}r_y' + \kappa_y r_y - \frac{2Q}{r_x + r_y} - \frac{\varepsilon_y^2}{r_y^3} = 0$$

	Applied Acceleration	Applied Focusing	Space-Charge Defocusing	Thermal Defocusing
Terms:	Lattice	Lattice	Perveance	Emittance

The "acceleration schedule" specifies both $\gamma_b\beta_b$ and λ then the equations are integrated with:

$$\boxed{\begin{aligned}\gamma_b\beta_b\varepsilon_x &= \text{const}\\ \gamma_b\beta_b\varepsilon_y &= \text{const}\end{aligned}}$$

normalized emittance conservation

$$\boxed{Q = \frac{q\lambda}{2\pi\epsilon_0 m\gamma_b^3\beta_b^2c^2}}$$

specified perveance

Reminder: It was shown for a coasting beam that the envelope equations remain valid for elliptic charge densities suggesting more general validity

[Sacherer, IEEE Trans. Nucl. Sci. 18, 1101 (1971), J.J. Barnard, Intro. Lectures]

For any beam with elliptic symmetry charge density in each transverse slice:

$$\boxed{\rho = \rho\left(\frac{x^2}{r_x^2} + \frac{y^2}{r_y^2}\right)}$$

Based on:

$$\langle x \frac{\partial \phi}{\partial x} \rangle_\perp = -\frac{\lambda}{4\pi\epsilon_0} \frac{r_x}{r_x + r_y}$$

see J.J. Barnard, Intro. Lectures

the KV envelope equations

$$\boxed{\begin{aligned} r_x''(s) + \kappa_x(s) r_x(s) - \frac{2Q}{r_x(s) + r_y(s)} - \frac{\varepsilon_x^2(s)}{r_x^3(s)} &= 0 \\ r_y''(s) + \kappa_y(s) r_y(s) - \frac{2Q}{r_x(s) + r_y(s)} - \frac{\varepsilon_y^2(s)}{r_y^3(s)} &= 0 \end{aligned}}$$

remain valid when (averages taken with the full distribution):

$$Q = \frac{q\lambda}{2\pi\epsilon_0 m \gamma_b^3 \beta_b^2 c^2} = \text{const} \qquad \lambda = q \int d^2x_\perp \, \rho = \text{const}$$

$$r_x = 2\langle x^2 \rangle_\perp^{1/2} \qquad \varepsilon_x = 4[\langle x^2 \rangle_\perp \langle x'^2 \rangle_\perp - \langle x x' \rangle_\perp^2]^{1/2}$$

$$r_y = 2\langle y^2 \rangle_\perp^{1/2} \qquad \varepsilon_y = 4[\langle y^2 \rangle_\perp \langle y'^2 \rangle_\perp - \langle y y' \rangle_\perp^2]^{1/2}$$

- Evolution changes often small in $\varepsilon_x, \ \varepsilon_y$

Properties of Envelope Equation Terms:

Applied Focusing: $\kappa_x r_x, \quad \kappa_y r_y$ and Acceleration: $\frac{(\gamma_b\beta_b)'}{(\gamma_b\beta_b)} r_x', \quad \frac{(\gamma_b\beta_b)'}{(\gamma_b\beta_b)} r_y'$

- Analogous to single particle orbit terms
- Contributions to beam envelope essentially the same as in single particle case
- Have strong s dependence, can be both focusing and defocusing
  - Act only in focusing elements and acceleration gaps

Perveance: $\frac{2Q}{r_x + r_y}$

- Acts continuously in s, always defocusing
- Becomes stronger (relatively to other terms) when the beam expands in cross-sectional area

Emittance: $\frac{\varepsilon_x^2}{r_x^3}$

- Acts continuously in s, always defocusing
- Becomes stronger (relatively to other terms) when the beam becomes small in cross-sectional area
- Scaling makes clear why it is necessary to inhibit emittance growth for applications where small spots are desired on target

As the beam expands, the perveance term will eventually dominate:

[see: S.M. Lund and B. Bukh, PRSTAB 7, 024801 (2004)]

Free expansion $(\kappa_x = \kappa_y = 0)$

Initial conditions:

$$r_x(s_i) = r_y(s_i) \qquad \frac{Q}{r_x(s_i)} = \frac{\varepsilon_x^2}{r_x^3(s_i)}$$

$$r_x'(s_i) = r_y'(s_i) = 0 \qquad Q = \frac{\varepsilon_x^2}{r_x^2(s_i)} = 10^{-3}$$

Cases:

Space-Charge Dominated: $\varepsilon_x = 0$

Emittance Dominated: $Q = 0$

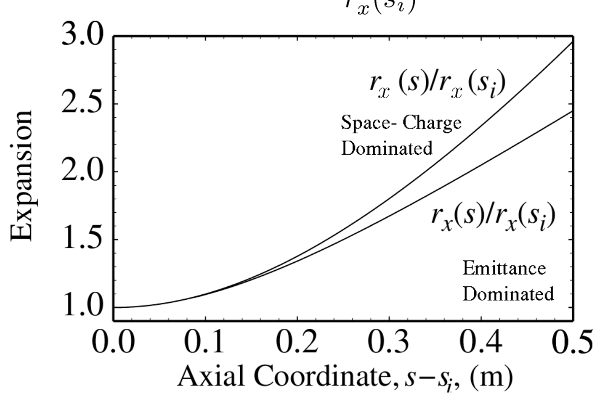

See PRSTAB article: solution is analytical in bounding limits shown

Parameters are chosen such that initial defocusing forces in two limits are equal

S5: Matched Envelope Solution:

Neglect acceleration $(\gamma_b\beta_b = \text{const})$ or use transformed variables:

$$\boxed{\begin{aligned} r_x''(s) + \kappa_x(s) r_x(s) - \frac{2Q}{r_x(s) + r_y(s)} - \frac{\varepsilon_x^2}{r_x^3(s)} &= 0 \\ r_y''(s) + \kappa_y(s) r_y(s) - \frac{2Q}{r_x(s) + r_y(s)} - \frac{\varepsilon_y^2}{r_y^3(s)} &= 0 \\ r_x(s + L_p) = r_x(s) \qquad & r_x(s) > 0 \\ r_y(s + L_p) = r_y(s) \qquad & r_y(s) > 0 \end{aligned}}$$

Matching involves finding specific initial conditions for the envelope to have the periodicity of the lattice:

Find Values of: $\boxed{\begin{matrix} r_x(s_i) & r_x'(s_i) \\ r_y(s_i) & r_y'(s_i) \end{matrix}}$ $\longrightarrow$ Such That: $\boxed{\begin{matrix} r_x(s_i + L_p) = r_x(s_i) & r_x'(s_i + L_p) = r_x'(s_i) \\ r_y(s_i + L_p) = r_y(s_i) & r_y'(s_i + L_p) = r_y'(s_i) \end{matrix}}$

- Typically constructed with numerical root finding from estimated/guessed values
  - Can be surprisingly difficult for complicated lattices and/or strong space-charge
- Iterative technique developed to numerically calculate without root finding

[S.M. Lund, S. Chilton and E.P. Lee, PRSTAB **9**, 064201 (2006)]

Typical Matched vs Mismatched solution for FODO channel:

Matched

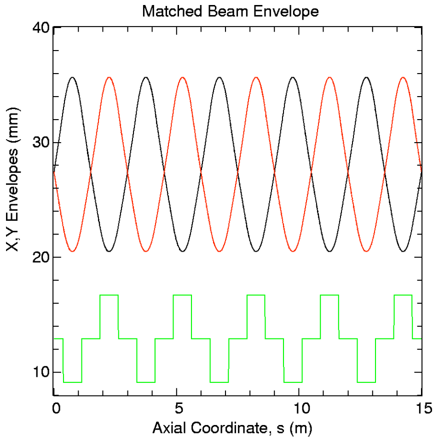

Mismatched

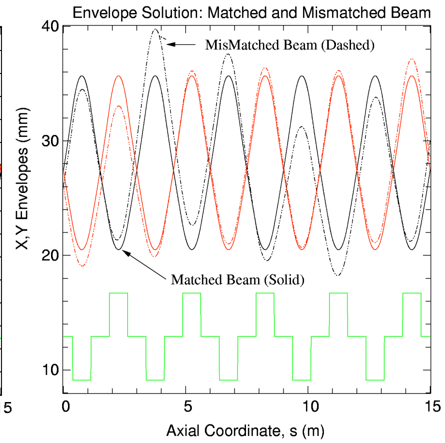

The matched beam is the most radially compact solution to the envelope equations rendering it highly important for beam transport

- Matching tends to exploit optics most efficiently to maintain confinement

The matched solution to the KV envelope equations reflects the symmetry of the focusing lattice and must in general be calculated numerically

$$\boxed{\begin{aligned} r_x(s+L_p) &= r_x(s) \\ r_y(s+L_p) &= r_y(s) \\ \varepsilon_x &= \varepsilon_y \end{aligned}}$$

<u>Parameters</u>

$L_p = 0.5$ m, $\sigma_0 = 80^\circ$, $\eta = 0.5$

$\varepsilon_x = 50$ mm-mrad

$\sigma/\sigma_0 = 0.2$

<u>Solenoidal Focusing</u>

$(Q = 6.6986 \times 10^{-4})$

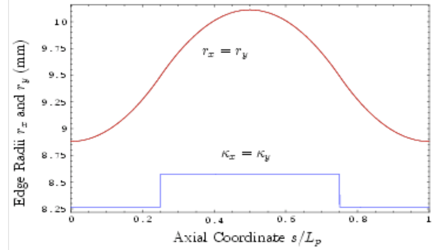

<u>FODO Quadrupole Focusing</u>

$(Q = 6.5614 \times 10^{-4})$

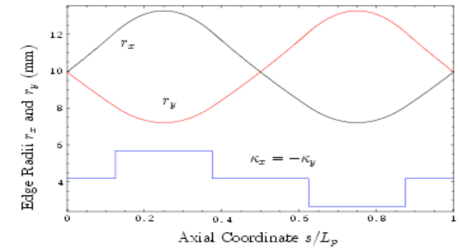

260

Symmetries of a matched beam are interpreted in terms of a local rms equivalent KV beam and moments/projections of the KV distribution

[see: S.M. Lund, lectures on Transverse Equilibrium Distributions]

Projection

x-y
area: $\pi r_x r_y \neq$ const

x-x'
area: $\pi\varepsilon_x =$ const
(CS Invariant)

y-y'
area: $\pi\varepsilon_y =$ const
(CS Invariant)

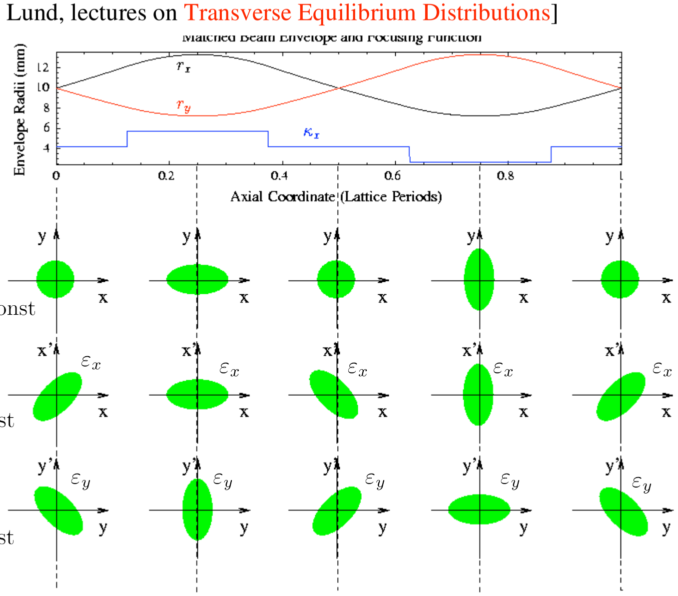

S6: Envelope Perturbations:

An extensive review article is available that both reviews/extends many aspects of envelope modes in periodic lattices covered in S6-S8: see S.M. Lund and B. Bukh, PRSTAB 024801 (2004) [henceforth denoted: PRSTAB Review]

In the envelope equations set:

Envelope Perturbations:

$$\begin{aligned} r_x(s) &= r_{xm}(s) + \delta r_x(s) \\ r_y(s) &= r_{ym}(s) + \delta r_y(s) \end{aligned}$$

Matched Envelope — Mismatch Perturbations

Driving Perturbations:

$$\begin{aligned} \kappa_x(s) &\rightarrow \kappa_x(s) + \delta\kappa_x(s) \\ \kappa_y(s) &\rightarrow \kappa_y(s) + \delta\kappa_y(s) \end{aligned} \quad \text{Focus}$$

$$Q \rightarrow Q + \delta Q(s) \quad \text{Perveance}$$

$$\begin{aligned} \varepsilon_x &\rightarrow \varepsilon_x + \delta\varepsilon_x(s) \\ \varepsilon_y &\rightarrow \varepsilon_y + \delta\varepsilon_y(s) \end{aligned} \quad \text{Emittance}$$

$$\begin{aligned} r_{xm}(s+L_p) &= r_{xm}(s) \qquad & r_{xm}(s) > 0 \\ r_{ym}(s+L_p) &= r_{ym}(s) \qquad & r_{ym}(s) > 0 \end{aligned}$$

$$\begin{aligned} r_{xm}(s) &\gg |\delta r_{xm}(s)| \\ r_{ym}(s) &\gg |\delta r_{ym}(s)| \end{aligned} \quad \longleftarrow$$

Amplitudes defined in terms of producing small envelope perturbations

- Driving terms and distribution errors drive envelope perturbations
  - Arise from many sources: focusing errors, lost particles, emittance growth, ...

The matched solution satisfies:

- Add subscript *m* to denote matched to distinguish from other solutions

$$r_x \to r_{xm} \qquad r_y \to r_{ym}$$

For matched beam envelope with periodicity of lattice

$$\boxed{\begin{aligned} &r''_{xm}(s) + \kappa_x(s) r_{xm}(s) - \frac{2Q}{r_{xm}(s)+r_{ym}(s)} - \frac{\varepsilon_x^2}{r_{xm}^3(s)} = 0 \\ &r''_{ym}(s) + \kappa_y(s) r_{ym}(s) - \frac{2Q}{r_{xm}(s)+r_{ym}(s)} - \frac{\varepsilon_y^2}{r_{ym}^3(s)} = 0 \\ &r_{xm}(s+L_p) = r_{xm}(s) \qquad r_{xm}(s) > 0 \\ &r_{ym}(s+L_p) = r_{ym}(s) \qquad r_{ym}(s) > 0 \end{aligned}}$$

Linearized Perturbed Envelope Equations:

- Neglect all terms of order δ^2 and higher: $(\delta r_x)^2, \quad \delta r_x \delta r_y, \ \delta Q \delta r_x, \ \cdots$

$$\boxed{\begin{aligned} &\delta r''_x + \kappa_x \delta r_x + \frac{2Q}{(r_{xm}+r_{ym})^2}(\delta r_x + \delta r_y) + \frac{3\varepsilon_x^2}{r_{xm}^4}\delta r_x \\ &\qquad = -r_{xm}\delta\kappa_x + \frac{2}{r_{xm}+r_{ym}}\delta Q + \frac{2\varepsilon_x^2}{r_{xm}^3}\delta\varepsilon_x \\ &\delta r''_y + \kappa_y \delta r_y + \frac{2Q}{(r_{xm}+r_{ym})^2}(\delta r_x + \delta r_y) + \frac{3\varepsilon_y^2}{r_{ym}^4}\delta r_y \\ &\qquad = -r_{ym}\delta\kappa_y + \frac{2}{r_{xm}+r_{ym}}\delta Q + \frac{2\varepsilon_y^2}{r_{ym}^3}\delta\varepsilon_y \end{aligned}}$$

Homogeneous Equations:

- Linearized envelope equations with driving terms set to zero

$$\boxed{\begin{aligned} &\delta r''_x + \kappa_x \delta r_x + \frac{2Q}{(r_{xm}+r_{ym})^2}(\delta r_x + \delta r_y) + \frac{3\varepsilon_x^2}{r_{xm}^4}\delta r_x = 0 \\ &\delta r''_y + \kappa_y \delta r_y + \frac{2Q}{(r_{xm}+r_{ym})^2}(\delta r_x + \delta r_y) + \frac{3\varepsilon_y^2}{r_{ym}^4}\delta r_y = 0 \end{aligned}}$$

Martix Form of the Linearized Perturbed Envelope Equations:

$$\boxed{\frac{d}{ds}\delta\mathbf{R} + \mathbf{K}\cdot\delta\mathbf{R} = \delta\mathbf{P}}$$

$$\delta\mathbf{R} \equiv \begin{pmatrix} \delta r_x \\ \delta r'_x \\ \delta r_y \\ \delta r'_y \end{pmatrix}$$ Coordinate vector

$$\mathbf{K} \equiv \begin{pmatrix} 0 & -1 & 0 & 0 \\ k_{xm} & 0 & k_{0m} & 0 \\ 0 & 0 & 0 & -1 \\ k_{0m} & 0 & k_{ym} & 0 \end{pmatrix}$$

Coefficient matrix

$$k_{0m} = \frac{2Q}{(r_{xm}+r_{ym})^2}$$

$$k_{jm} = \kappa_j + 3\frac{\varepsilon_j^2}{r_{jm}^4} + k_{0m} \qquad j = x, \ y$$

Has periodicity of the lattice period

$$\delta\mathbf{P} \equiv \begin{pmatrix} 0 \\ -\delta\kappa_x + 2\frac{\delta Q}{r_{xm}+r_{ym}} + 2\frac{\varepsilon_x\delta\varepsilon_x}{r_{xm}^3} \\ 0 \\ -\delta\kappa_y + 2\frac{\delta Q}{r_{xm}+r_{ym}} + 2\frac{\varepsilon_y\delta\varepsilon_y}{r_{ym}^3} \end{pmatrix}$$ Driving perturbation vector

Expand solution into homogeneous and particular parts:

$$\delta\mathbf{R} = \delta\mathbf{R}_h + \delta\mathbf{R}_p$$

$\delta\mathbf{R}_h =$ homogeneous solution

$\delta\mathbf{R}_p =$ particular solution

$$\frac{d}{ds}\delta\mathbf{R}_h + \mathbf{K}\cdot\delta\mathbf{R}_h = 0 \qquad \frac{d}{ds}\delta\mathbf{R}_p + \mathbf{K}\cdot\delta\mathbf{R}_p = \delta\mathbf{P}$$

Homogeneous Solution: Normal Modes

- Describes normal mode oscillations
- Original analysis by Struckmeier and Reiser [Part. Accel. **14**, 227 (1984)]

Particular Solution: Driven Modes

- Describes action of driving terms
- Characterize in terms of projections on homogeneous response (on normal modes)

Homogeneous solution expressible as a map:

$$\boxed{\begin{aligned} \delta\mathbf{R}(s) &= \mathbf{M}_e(s|s_i)\cdot\delta\mathbf{R}(s_i) \\ \delta\mathbf{R}(s) &= (\delta r_x, \delta r'_x, \delta r_y, \delta r'_y) \\ \mathbf{M}_e(s|s_i) &= \ 4\times 4 \text{ transfer map} \end{aligned}}$$

Now 4x4 system, but analogous to the 2x2 analysis of Hill's equation via transfer matrices: see S.M. Lund lectures on Transverse Particle Equations

Eigenvalues and eigenvectors of map through one period characterize normal modes and stability properties:

$$\boxed{\mathbf{M}_e(s_i + L_p|s_i)\cdot\mathbf{E}_n(s_i) = \lambda_n\mathbf{E}_n(s_i)}$$

Stability

$$\boxed{\lambda_n = \gamma_n e^{i\sigma_n} \quad \begin{aligned} &\sigma_n \to \text{mode phase advance (real)} \\ &\gamma_n \to \text{mode growth/damp factor (real)} \end{aligned}}$$

Mode Expansion/Launching

$$\boxed{\begin{aligned} \delta\mathbf{R}(s_i) &= \sum_{n=1}^{4}\alpha_n\mathbf{E}_n(s_i) \\ \alpha_n &= \text{const (complex)} \end{aligned}}$$

Eigenvalue/Eigenvector Symmetry Classes:

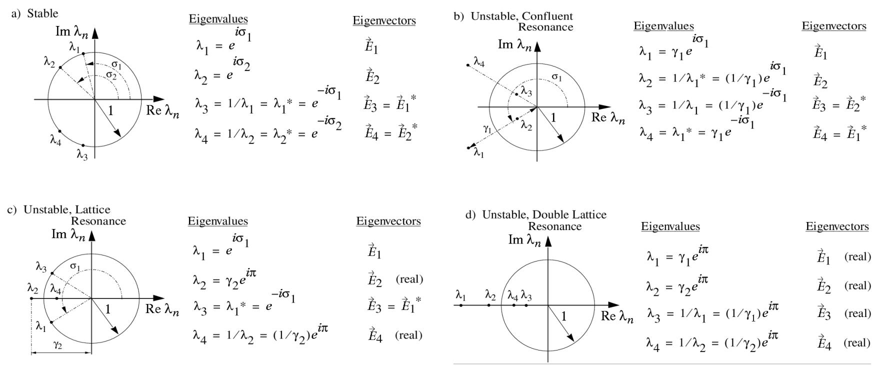

Symmetry classes of eigenvalues/eigenvectors:

- Determine normal mode symmetries
- See A. Dragt, Lectures on Nonlinear Orbit Dynamics, in Physics of High Energy Particle Accelerators, (AIP Conf. Proc. No. 87, 1982, p. 147)
- Envelope mode symmetries discussed fully in PRSTAB review
- Caution: Textbook by Reiser makes errors in mode symmetries and mislabels/identifies dispersion characteristics

Pure mode launching conditions:

Launching conditions for distinct normal modes corresponding to the eigenvalue classes illustrated:

$$A_\ell = \text{mode amplitude (real)} \qquad \ell = \text{ mode index}$$
$$\psi_\ell = \text{mode launch phase (real)}$$

Case	Mode	Launching Condition	Lattice Period Advance
(a) Stable	1 - Stable Osc.	$\delta\mathbf{R}_1 = A_1 e^{i\psi_1}\mathbf{E}_1 + \text{C.C.}$	$\mathbf{M}_e\delta\mathbf{R}_1(\psi_1) = \delta\mathbf{R}_1(\psi_1+\sigma_1)$
	2 - Stable Osc.	$\delta\mathbf{R}_2 = A_2 e^{i\psi_2}\mathbf{E}_2 + \text{C.C.}$	$\mathbf{M}_e\delta\mathbf{R}_2(\psi_2) = \delta\mathbf{R}_2(\psi_2+\sigma_2)$
(b) Unstable Confluent Res.	1 - Exp. Growth	$\delta\mathbf{R}_1 = A_1 e^{i\psi_1}\mathbf{E}_1 + \text{C.C.}$	$\mathbf{M}_e\delta\mathbf{R}_1(\psi_1) = \gamma_1\delta\mathbf{R}_1(\psi_1+\sigma_1)$
	2 - Exp. Damping	$\delta\mathbf{R}_2 = A_2 e^{i\psi_2}\mathbf{E}_2 + \text{C.C.}$	$\mathbf{M}_e\delta\mathbf{R}_2(\psi_2) = (1/\gamma_1)\delta\mathbf{R}_2(\psi_2+\sigma_1)$
(c) Unstable Lattice Res.	1 - Stable Osc.	$\delta\mathbf{R}_1 = A_1 e^{i\psi_1}\mathbf{E}_1 + \text{C.C.}$	$\mathbf{M}_e\delta\mathbf{R}_1(\psi_1) = \delta\mathbf{R}_1(\psi_1+\sigma_1)$
	2 - Exp. Growth	$\delta\mathbf{R}_2 = A_2\mathbf{E}_2$	$\mathbf{M}_e\delta\mathbf{R}_2 = -\gamma_2\delta\mathbf{R}_2$
	3 - Exp. Damping	$\delta\mathbf{R}_3 = A_3\mathbf{E}_4$	$\mathbf{M}_e\delta\mathbf{R}_3 = -(1/\gamma_2)\delta\mathbf{R}_3$
(d) Unstable Double Lattice Resonance	1 - Exp. Growth	$\delta\mathbf{R}_1 = A_1\mathbf{E}_1$	$\mathbf{M}_e\delta\mathbf{R}_1 = -\gamma_1\delta\mathbf{R}_1$
	2 - Exp. Growth	$\delta\mathbf{R}_2 = A_2\mathbf{E}_2$	$\mathbf{M}_e\delta\mathbf{R}_2 = -\gamma_2\delta\mathbf{R}_2$
	3 - Exp. Damping	$\delta\mathbf{R}_3 = A_3\mathbf{E}_3$	$\mathbf{M}_e\delta\mathbf{R}_3 = -(1/\gamma_1)\delta\mathbf{R}_3$
	4 - Exp. Damping	$\delta\mathbf{R}_4 = A_4\mathbf{E}_4$	$\mathbf{M}_e\delta\mathbf{R}_4 = -(1/\gamma_2)\delta\mathbf{R}_4$

$$\delta\mathbf{R}_\ell \equiv \delta\mathbf{R}_\ell(s_i) \qquad \mathbf{E}_\ell \equiv \mathbf{E}_\ell(s_i) \qquad \mathbf{M}_e \equiv \mathbf{M}_e(s_i + L_p|s_i)$$

$$\delta\mathbf{R}(s) = \begin{cases} A_1[\mathbf{E}_1(s)e^{i\psi_1(s)} + \mathbf{E}_1^*(s)e^{-i\psi_1(s)}] + A_2[\mathbf{E}_2(s)e^{i\psi_2(s)} + \mathbf{E}_2^*(s)e^{-i\psi_2(s)}], & \text{cases (a) and (b)} \\ A_1[\mathbf{E}_1(s)e^{i\psi_1(s)} + \mathbf{E}_1^*(s)e^{-i\psi_1(s)}] + A_2\mathbf{E}_2(s) + A_3\mathbf{E}_4(s), & \text{case (c)} \\ A_1\mathbf{E}_1(s) + A_2\mathbf{E}_2(s) + A_3\mathbf{E}_3(s) + A_4\mathbf{E}_4(s), & \text{case (d)} \end{cases}$$

Decoupled Modes

In a continuous or periodic solenoidal focusing channel

$$\kappa_x(s) = \kappa_y(s) = \kappa(s)$$

with a round matched-beam solution

$$\varepsilon_x = \varepsilon_y \equiv \varepsilon = \text{const}$$
$$r_{xm}(s) = r_{ym}(s) \equiv r_m(s)$$

envelope perturbations are simply decoupled with:

Breathing Mode: $$\delta r_+ \equiv \frac{\delta r_x + \delta r_y}{2}$$

Quadrupole Mode: $$\delta r_- \equiv \frac{\delta r_x - \delta r_y}{2}$$

The resulting decoupled envelope equations are:

Breathing Mode:

$$\delta r_+'' + \kappa\delta r_+ + \frac{2Q}{r_m^2}\delta r_+ + \frac{3\varepsilon^2}{r_m^4}\delta r_+ = -r_m\left(\frac{\delta\kappa_x + \delta\kappa_y}{2}\right) + \frac{1}{r_m}\delta Q + \frac{2\varepsilon^2}{r_m^3}\left(\frac{\delta\varepsilon_x + \delta\varepsilon_y}{2}\right)$$

Quadrupole Mode:

$$\delta r_-'' + \kappa\delta r_- + \frac{3\varepsilon^2}{r_m^4}\delta r_- = -r_m\left(\frac{\delta\kappa_x - \delta\kappa_y}{2}\right) + \frac{2\varepsilon^2}{r_m^3}\left(\frac{\delta\varepsilon_x - \delta\varepsilon_y}{2}\right)$$

Graphical interpretation of mode symmetries:

Breathing Mode:

$$\delta r_+ = \frac{\delta r_x + \delta r_y}{2}$$

Quadrupole Mode:

$$\delta r_- = \frac{\delta r_x - \delta r_y}{2}$$

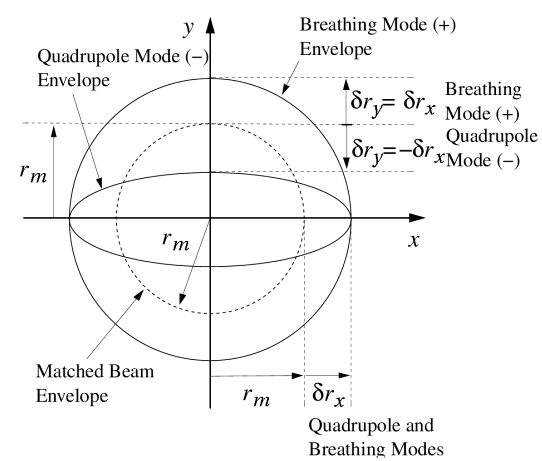

Decoupled Mode Properties:

Space charge terms ~ Q only directly expressed in equation for $\delta r_+(s)$

- Indirectly present in both equations from matched envelope $r_m(s)$

Homogeneous Solution:

- Restoring term for $\delta r_+(s)$ larger than for $\delta r_-(s)$
  - Breathing mode should oscillate faster than the quadrupole mode

Particular Solution:

- Misbalances in focusing and emittance driving terms can project onto either mode
  - nonzero perturbed $\kappa_x(s) + \kappa_y(s)$ and $\varepsilon_x(s) + \varepsilon_y(s)$ project onto breathing mode
  - nonzero perturbed $\kappa_x(s) - \kappa_y(s)$ and $\varepsilon_x(s) - \varepsilon_y(s)$ project onto quadrupole mode
- Perveance driving perturbations project *only* on breathing mode

Previous symmetry classes greatly reduce for decoupled modes:

Previous homogeneous 4x4 solution map:

$$\delta\mathbf{R}(s) = \mathbf{M}_e(s|s_i)\cdot\delta\mathbf{R}(s_i)$$
$$\delta\mathbf{R}(s) = (\delta r_x, \delta r'_x, \delta r_y, \delta r'_y)$$
$$\mathbf{M}_e(s|s_i) = \ 4\times 4 \text{ transfer map}$$

reduces to two independent 2x2 maps with greatly simplified symmetries:

$$\boxed{\begin{aligned}&\delta\mathbf{R} \equiv (\delta r_+, \delta r'_+, \delta r_-, \delta r'_-)\\ &\mathbf{M}_e(s_i+L_p|s_i) = \begin{bmatrix}\mathbf{M}_+(s_i+L_p|s_i) & 0\\ 0 & \mathbf{M}_-(s_i+L_p|s_i)\end{bmatrix}\end{aligned}}$$

with corresponding eigenvalue problems:

$$\boxed{\mathbf{M}_\pm(s_i+L_p|s_i)\cdot\mathbf{E}_n(s_i) = \lambda_\pm\mathbf{E}_n(s_i)}$$

Many familiar results from analysis of Hills equation (see: S.M. Lund lectures on Transverse Particle Equations) can be immediately applied to the decoupled case, for example:

$$\frac{1}{2}|\mathrm{Tr}\ \mathbf{M}_\pm(s_i+L_p|s_i)| < 1 \longrightarrow \text{mode stability}$$

Eigenvalue symmetries and launching conditions simplify for decoupled modes

Eigenvalue Symmetry 1:

Stable

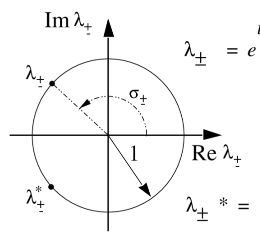

$\lambda_\pm = e^{i\sigma_\pm}$

$\lambda_\pm{}^* = 1/\lambda_\pm = e^{-i\sigma_\pm}$

Eigenvalue Symmetry 2:

Unstable, Lattice Resonance

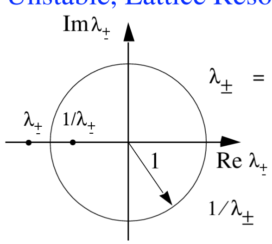

$\lambda_\pm = \gamma_\pm e^{-i\pi}$

$1/\lambda_\pm = (1/\gamma_\pm)e^{-i\pi}$

Launching Condition / Projections

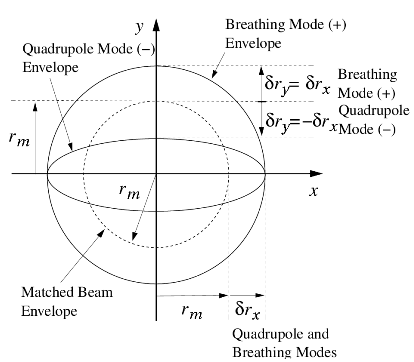

General Mode Limits

Using phase-amplitude analysis can show for any linear focusing lattice:

1) Phase advance of any normal mode satisfies the zero space-charge limit:

$$\boxed{\lim_{Q\to 0}\sigma_\ell = 2\sigma_0}$$

2) Pure normal modes evolve with a quadratic phase-space (Courant-Snyder) invariant in the normal coordinates of the mode

Simply expressed for decoupled modes with $\kappa_x = \kappa_y, \ \ \varepsilon_x = \varepsilon_y$

$$\boxed{\left[\frac{\delta r_\pm(s)}{w_\pm(s)}\right]^2 + [w'_\pm(s)\delta r_\pm(s) - w_\pm(s)\delta r'_\pm(s)]^2 = \text{const}}$$

where

$$w''_+ + \kappa w_+ + \frac{2Q}{r_m^2}w_+ + \frac{3\varepsilon^2}{r_m^4}w_+ - \frac{1}{w_+^3} = 0$$
$$w''_- + \kappa w_- + \frac{3\varepsilon^2}{r_m^4}w_- - \frac{1}{w_-^3} = 0$$
$$w_\pm(s+L_p) = w_\pm(s)$$

Analogous results for coupled modes [See Edwards and Teng, IEEE Trans Nuc. Sci. **20**, 885 (1973)]

- More complex expression due to coupling

S7: Envelope Modes in Continuous Focusing

Focusing:

$$\kappa_x(s) = \kappa_y(s) = k_{\beta 0}^2 = \left(\frac{\sigma_0}{L_p}\right)^2 = \text{const}$$

Matched beam:

symmetric beam:

$$\varepsilon_x = \varepsilon_y = \varepsilon = \text{const}$$
$$r_{xm}(s) = r_{ym}(s) = r_m = \text{const}$$

matched envelope:

$$k_{\beta 0}^2 r_m - \frac{Q}{r_m} - \frac{\varepsilon^2}{r_m^3} = 0$$

depressed phase advance:

$$\sigma = \sqrt{\sigma_0^2 - \frac{Q}{(r_m/L_p)^2}} = \frac{\varepsilon L_p}{r_m^2}$$

one parameter needed for scaled solution:

$$\frac{k_{\beta 0}^2 \varepsilon^2}{Q^2} = \frac{\sigma_0^2 \varepsilon^2}{Q^2 L_p^2} = \frac{(\sigma/\sigma_0)^2}{[1-(\sigma/\sigma_0)^2]^2}$$

Decoupled Modes:

$$\delta r_\pm(s) = \frac{\delta r_x(s) \pm \delta r_y(s)}{2}$$

Envelope equations of motion become:

$$L_p^2 \frac{d^2}{ds^2}\left(\frac{\delta r_+}{r_m}\right) + \sigma_+^2 \left(\frac{\delta r_+}{r_m}\right) = -\frac{\sigma_0^2}{2}\left(\frac{\delta\kappa_x}{k_{\beta 0}^2} + \frac{\delta\kappa_y}{k_{\beta 0}^2}\right) + (\sigma_0^2 - \sigma^2)\frac{\delta Q}{Q} + \sigma^2\left(\frac{\delta\varepsilon_x}{\varepsilon} + \frac{\delta\varepsilon_y}{\varepsilon}\right)$$

$$L_p^2 \frac{d^2}{ds^2}\left(\frac{\delta r_-}{r_m}\right) + \sigma_-^2 \left(\frac{\delta r_-}{r_m}\right) = -\frac{\sigma_0^2}{2}\left(\frac{\delta\kappa_x}{k_{\beta 0}^2} - \frac{\delta\kappa_y}{k_{\beta 0}^2}\right) + \sigma^2\left(\frac{\delta\varepsilon_x}{\varepsilon} - \frac{\delta\varepsilon_y}{\varepsilon}\right)$$

$\sigma_+ \equiv \sqrt{2\sigma_0^2 + 2\sigma^2}$ "breathing" mode phase advance

$\sigma_- \equiv \sqrt{\sigma_0^2 + 3\sigma^2}$ "quadrupole" mode phase advance

Homogeneous equations for normal modes:

$$\frac{d^2}{ds^2}\delta r_\pm + \left(\frac{\sigma_\pm}{L_p}\right)^2 \delta r_\pm = 0$$

- Simple harmonic oscillator equation

Homogeneous Solution (normal modes):

$$\delta r_\pm(s) = \delta r_\pm(s_i)\cos\left(\sigma_\pm \frac{s-s_i}{L_p}\right) + \frac{\delta r'_\pm(s_i)}{\sigma_\pm/L_p}\sin\left(\sigma_\pm \frac{s-s_i}{L_p}\right)$$

$\delta r_\pm(s_i), \quad \delta r'_\pm(s_i)$ mode initial conditions

Properties of continuous focusing homogeneous solution: Normal Modes

Mode Phase Advances

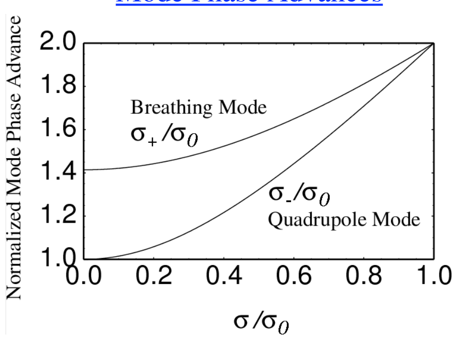

Mode Projections

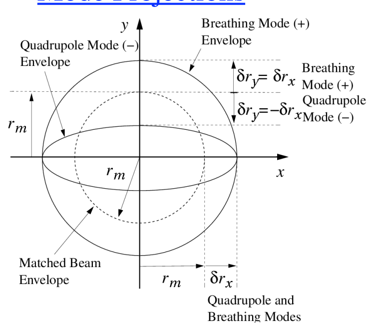

Breathing Mode: $\delta r_+ \equiv \dfrac{\delta r_x + \delta r_y}{2}$

Quadrupole Mode: $\delta r_- \equiv \dfrac{\delta r_x - \delta r_y}{2}$

Particular Solution (driving perturbations):

Green's function form of solution derived using projections onto normal modes see PRSTAB Review

$$\frac{\delta r_\pm(s)}{r_m} = \frac{1}{L_p^2}\int_{s_i}^{s} d\tilde{s}\; G_\pm(s,\tilde{s})\delta p_\pm(\tilde{s})$$

$$\delta p_+(s) = -\frac{\sigma_0^2}{2}\left[\frac{\delta\kappa_x(s)}{k_{\beta 0}^2} + \frac{\delta\kappa_y(s)}{k_{\beta 0}^2}\right] + (\sigma_0^2 - \sigma^2)\frac{\delta Q(s)}{Q} + \sigma^2\left[\frac{\delta\varepsilon_x(s)}{\varepsilon} + \frac{\delta\varepsilon_y(s)}{\varepsilon}\right]$$

$$\delta p_-(s) = -\frac{\sigma_0^2}{2}\left[\frac{\delta\kappa_x(s)}{k_{\beta 0}^2} - \frac{\delta\kappa_y(s)}{k_{\beta 0}^2}\right] + \sigma^2\left[\frac{\delta\varepsilon_x(s)}{\varepsilon} - \frac{\delta\varepsilon_y(s)}{\varepsilon}\right]$$

$$G_\pm(s,\tilde{s}) = \frac{1}{\sigma_\pm/L_p}\sin\left(\sigma_\pm \frac{s-\tilde{s}}{L_p}\right)$$

Green's function solution is *fully general*. Insight gained from simplified solutions for specific classes of driving perturbations:

- Adiabatic
- Sudden

covered here

- Ramped
- Harmonic

covered in PRSTAB Review article

Continuous Focusing – adiabatic particular solution

For driving perturbations $\delta p_+(s)$ and $\delta p_-(s)$ slow on quadrupole mode (slower mode) wavelength ~ $2\pi L_p/\sigma_-$ the solution is:

$$\frac{\delta r_+(s)}{r_m} = \frac{\delta p_+(s)}{\sigma_+^2}$$
$$= -\underbrace{\left[\frac{1}{2}\frac{1}{1+(\sigma/\sigma_0)^2}\right]}_{\text{Focusing}}\frac{1}{2}\left(\frac{\delta\kappa_x(s)}{k_{\beta 0}^2}+\frac{\delta\kappa_y(s)}{k_{\beta 0}^2}\right) + \underbrace{\left[\frac{1}{2}\frac{1-(\sigma/\sigma_0)^2}{1+(\sigma/\sigma_0)^2}\right]}_{\text{Perveance}}\frac{\delta Q(s)}{Q}$$
$$+ \underbrace{\left[\frac{(\sigma/\sigma_0)^2}{1+(\sigma/\sigma_0)^2}\right]}_{\text{Emittance}}\frac{1}{2}\left(\frac{\delta\varepsilon_x(s)}{\varepsilon}+\frac{\delta\varepsilon_y(s)}{\varepsilon}\right),$$

$$\frac{\delta r_-(s)}{r_m} = \frac{\delta p_-(s)}{\sigma_-^2}$$
$$= -\underbrace{\left[\frac{1}{1+3(\sigma/\sigma_0)^2}\right]}_{\text{Focusing}}\frac{1}{2}\left(\frac{\delta\kappa_x(s)}{k_{\beta 0}^2}-\frac{\delta\kappa_y(s)}{k_{\beta 0}^2}\right)$$
$$+ \underbrace{\left[\frac{2(\sigma/\sigma_0)^2}{1+3(\sigma/\sigma_0)^2}\right]}_{\text{Emittance}}\frac{1}{2}\left(\frac{\delta\varepsilon_x(s)}{\varepsilon}-\frac{\delta\varepsilon_y(s)}{\varepsilon}\right).$$

Coefficients of adiabatic terms in square brackets"[ ]"

Continuous Focusing – adiabatic solution coefficients

a) $\delta r_+ = (\delta r_x + \delta r_y)/2$ Breathing Mode Projection

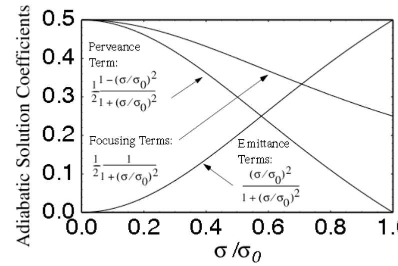

b) $\delta r_- = (\delta r_x - \delta r_y)/2$ Quadrupole Mode Projection

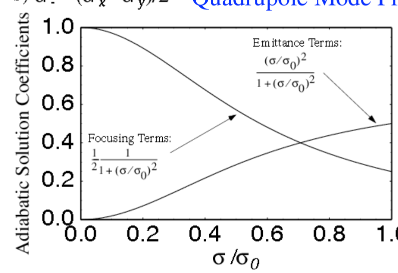

Relative strength of:

- Space-Charge (Perveance)
- Applied Focusing
- Emittance

terms vary with space-charge depression (σ/σ_0) for both breathing and quadrupole mode projections

Plots allow one to read off the relative importance of various contributions to beam mismatch as a function of space-charge strength

Continuous Focusing – sudden particular solution

For step function driving perturbations of form:

$$\boxed{\delta p_\pm(s) = \widehat{\delta p_\pm}\Theta(s-s_p)}$$

$s = s_p =$ axial coordinate perturbation applied

Hat quantities are constant amplitudes

with amplitudes:

$$\widehat{\delta p_+} = -\frac{\sigma_0^2}{2}\left[\frac{\widehat{\delta\kappa_x}}{k_{\beta 0}^2}+\frac{\widehat{\delta\kappa_y}}{k_{\beta 0}^2}\right] + (\sigma_0^2-\sigma^2)\frac{\widehat{\delta Q}}{Q} + \sigma^2\left[\frac{\widehat{\delta\varepsilon_x}}{\varepsilon}+\frac{\widehat{\delta\varepsilon_y}}{\varepsilon}\right] = \text{const}$$

$$\widehat{\delta p_-} = -\frac{\sigma_0^2}{2}\left[\frac{\widehat{\delta\kappa_x}}{k_{\beta 0}^2}-\frac{\widehat{\delta\kappa_y}}{k_{\beta 0}^2}\right] + \sigma^2\left[\frac{\widehat{\delta\varepsilon_x}}{\varepsilon}-\frac{\widehat{\delta\varepsilon_y}}{\varepsilon}\right] = \text{const}$$

The solution is given by the substitution in the expression for the adiabatic solution:

$$\boxed{\delta p_\pm(s) \to \widehat{\delta p_\pm}\left[1-\cos\left(\sigma_\pm\frac{s-s_p}{L_p}\right)\right]\Theta(s-s_p)}$$

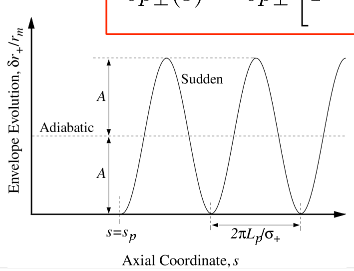

For the same amplitude of total driving perturbations, sudden perturbations result in 2x the envelope excursion that adiabatic perturbations produce.

S8: Envelope Modes in Periodic Focusing Channels

Overview

- Much more complicated the continuous limit results
  - Lattice can couple to oscillations and destabilize the system
  - Broad parametric instability bands can result
- Instability bands calculated will exclude wide ranges of parameter space from machine operation
  - Exclusion region depends on focusing type
  - Will find that alternating gradient quadrupole focusing tends to have more instability than high occupancy solenoidal focusing due to larger envelope flutter driving stronger, broader instability
- Results in this section are calculated numerically and summarized parametrically to illustrate the full range of mode characteristics
  - Results presented in terms of phase advances and normalized space-charge strength to allow broad applicability
  - Coupled 4x4 eigenvalue problem and mode symmetries identified in S6 are solved numerically and analytical limits are verified
- More information on results presented can be found in the PRSTAB Review

Solenoidal Focusing – Matched Envelope Solution

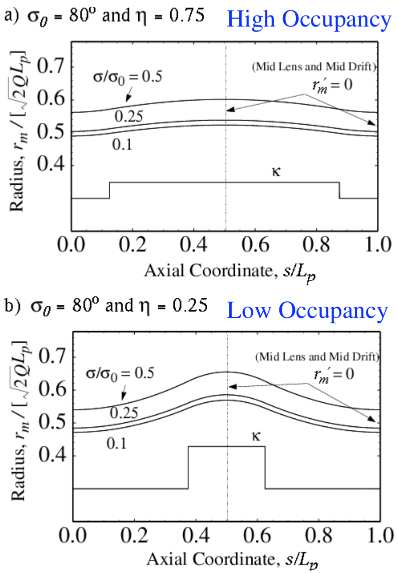

Focusing:

$$\kappa_x(s) = \kappa_y(s) = \kappa(s)$$

$$\kappa(s + L_p) = \kappa(s)$$

Matched Beam:

$$\varepsilon_x = \varepsilon_y = \varepsilon = \text{const}$$

$$r_{xm}(s) = r_{ym}(s) = r_m(s)$$

$$r_m(s + L_p) = r_m(s)$$

Comments:

- Envelope flutter a strong function of occupancy η
- Space-charge expands envelope but does not strongly modify periodic flutter

Using a transfer matrix approach on undepressed single-particle orbits set the strength of the focusing function for specified undepressed particle phase advance by solving:

- See: S.M. Lund, lectures on Transverse Particle Equations

Solenoidal Focusing - piecewise constant focusing lattice

$$\boxed{\cos\sigma_0 = \cos(2\Theta) - \frac{1-\eta}{\eta}\Theta\sin(2\Theta) \qquad \Theta \equiv \frac{\sqrt{\hat{\kappa}}L_p}{2}}$$

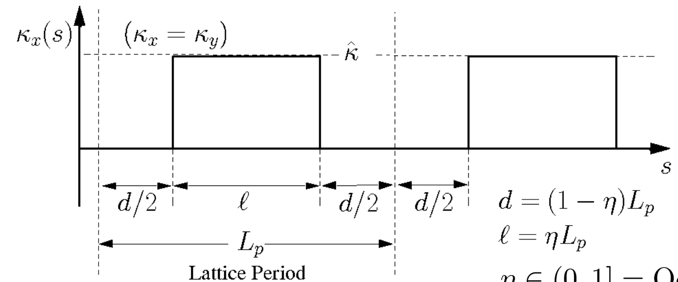

$d = (1-\eta)L_p$

$\ell = \eta L_p$

$\eta \in (0, 1] = \text{Occupancy}$

Solenoidal Focusing – parametric plots of breathing and quadrupole envelope mode phase advances two values of undepressed phase advance

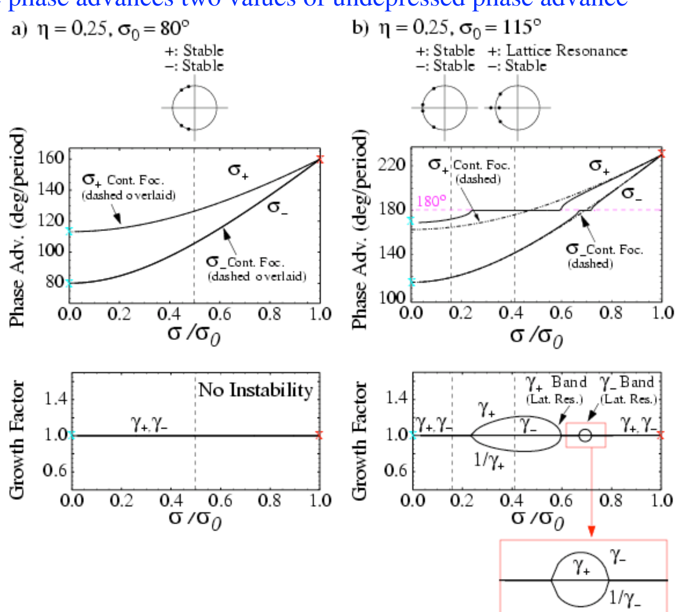

Solenoidal Focusing – mode instability bands become wider and stronger for smaller occupancy

$$\eta = \begin{cases} 0.75 & \text{(Blue)} \\ 0.25 & \text{(Green)} \\ 0.10 & \text{(Red)} \end{cases} \qquad \sigma_0 = 115^\circ$$

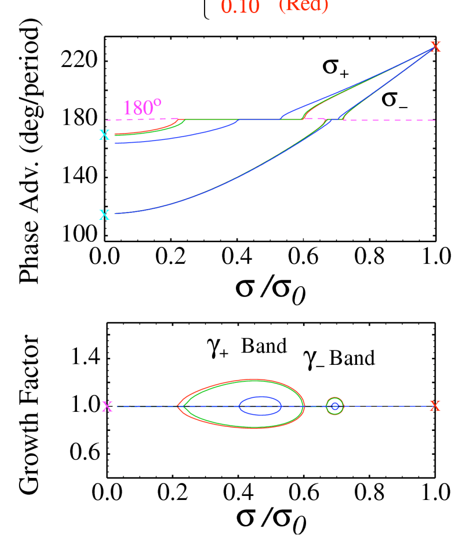

Comments:

- Phase advance in instability band 180 deg.
- Significant deviations from continuous model even outside the band of instability when space-charge strong
- Instability band becomes stronger for low occupancy

Solenoidal Focusing – broad ranges of parametric instability are found for the breathing and quadrupole bands that must be avoided in machine operation

$\eta = 0.75$ $\quad\quad$ $\eta = 0.25$

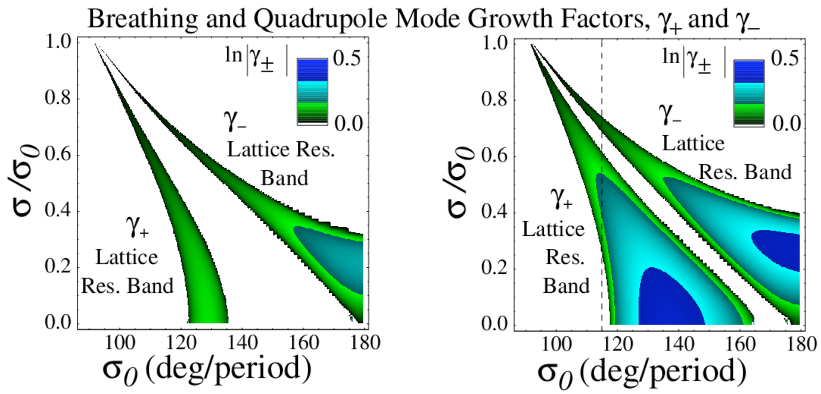

Solenoidal Focusing – parametric mode properties of band oscillations

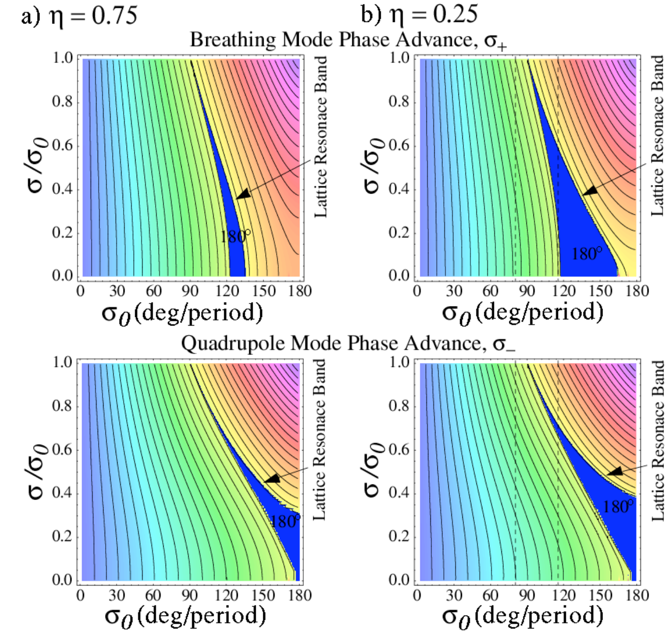

Quadrupole Doublet Focusing – Matched Envelope Solution

FODO and Syncopated Lattices

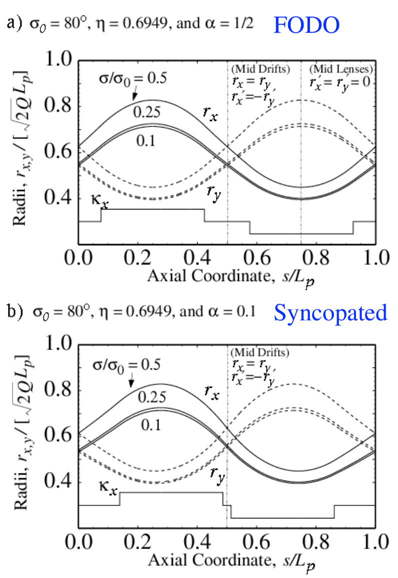

Focusing:

$$\kappa_x(s) = -\kappa_y(s) = \kappa(s)$$

$$\kappa(s + L_p) = \kappa(s)$$

Matched Beam:

$$\varepsilon_x = \varepsilon_y = \varepsilon = \text{const}$$

$$r_{xm}(s + L_p) = r_{xm}(s)$$

$$r_{ym}(s + L_p) = r_{ym}(s)$$

Comments:

- Envelope flutter a *weak* function of occupancy η
- Syncopation factors $\alpha \neq 1/2$ reduce envelope symmetry and can drive more instabilities
- Space-charge expands envelope

Using a transfer matrix approach on undepressed single-particle orbits set the strength of the focusing function for specified undepressed particle phase advance by solving:

See: S.M. Lund, lectures on Transverse Particle Equations

Quadrupole Doublet Focusing - piecewise constant focusing lattice

$$\cos\sigma_0 = \cos\Theta\cosh\Theta + \frac{1-\eta}{\eta}\theta(\cos\Theta\sinh\Theta - \sin\Theta\cosh\Theta) - 2\alpha(1-\alpha)\frac{(1-\eta)^2}{\eta^2}\Theta^2\sin\Theta\sinh\Theta \qquad \Theta \equiv \frac{\sqrt{|\hat{\kappa}|}L_p}{2}$$

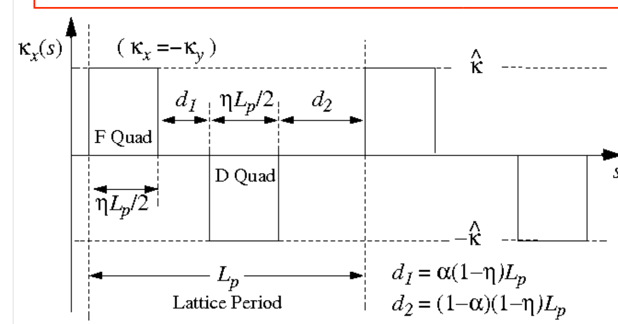

$\eta \in (0, 1]$ Occupancy

$\alpha \in [0, 1/2]$ Syncopation Factor

$\alpha = 1/2 \rightarrow$ FODO

Quadrupole Focusing – parametric plots of breathing and quadrupole envelope mode phase advances two values of undepressed phase advance

a) $\eta = 0.6949,\ \alpha = 0.1,\ \sigma_0 = 80^o$ FODO

b) $\eta = 0.6949,\ \alpha = 0.1,\ \sigma_0 = 115^o$ Syncopated

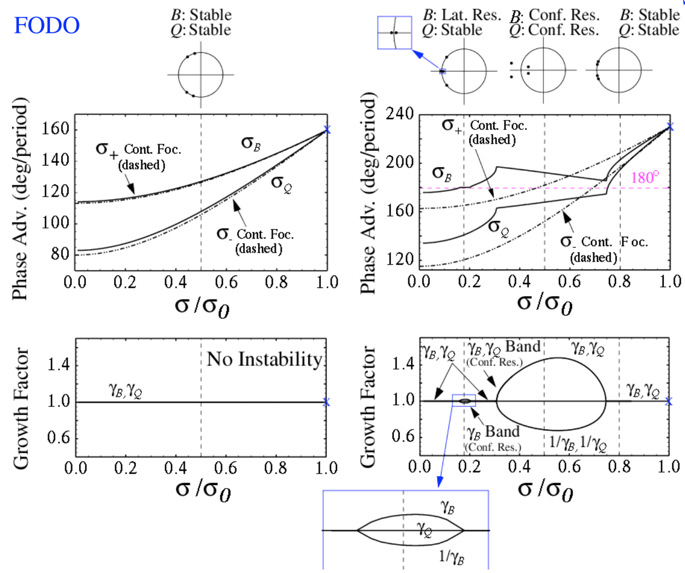

Quadrupole Focusing – mode instability bands vary little/strongly with occupancy for FODO/syncopated lattices

a) $\alpha = 1/2$ (FODO), $\sigma_0 = 115^o$ FODO

b) $\alpha = 0.1,\ \sigma_0 = 115^o$ Syncopated

$\eta = \begin{cases} 0.90 & \text{(Blue)} \\ 0.6949 & \text{(Black)} \\ 0.25 & \text{(Green)} \\ 0.10 & \text{(Red)} \end{cases}$

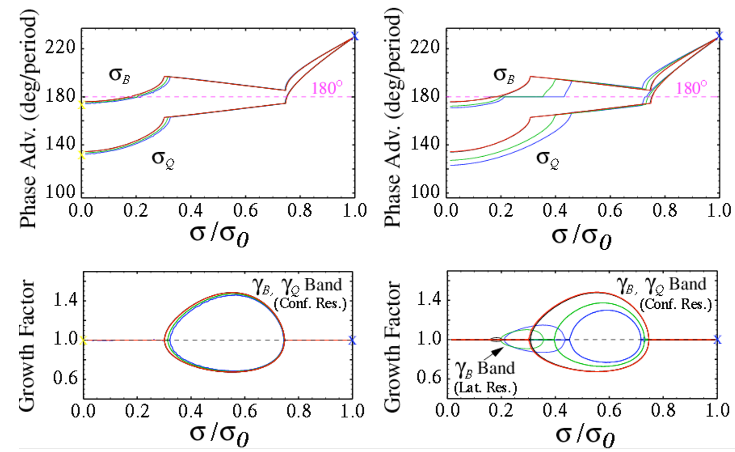

Quadrupole Focusing – broad ranges of parametric instability are found for the breathing and quadrupole bands that must be avoided in machine operation

FODO Lattice $\eta = 0.6949,\ \alpha = 1/2$

Syncopated Lattice $\eta = 0.6949,\ \alpha = 0.1$

Breathing and Quadrupole Mode Growth Factors, γ_B and γ_Q

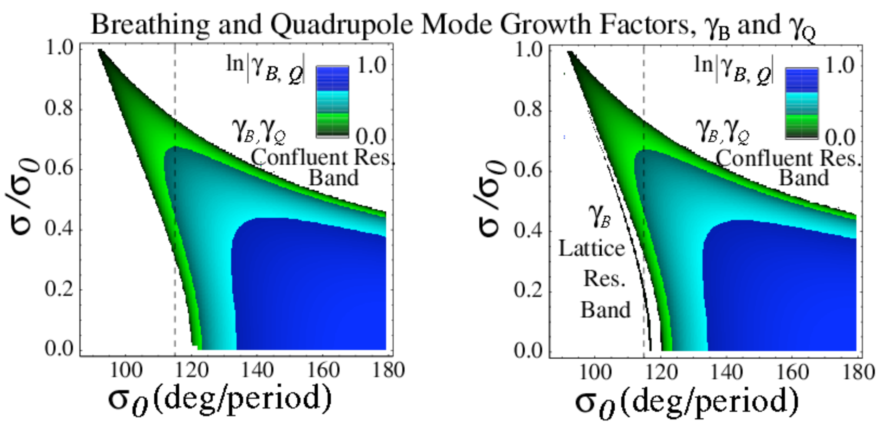

Quadrupole Focusing – parametric mode properties of band oscillations

a) $\eta = 0.6949,\ \alpha = 1/2$ FODO

b) $\eta = 0.6949,\ \alpha = 0.1$ Syncopated

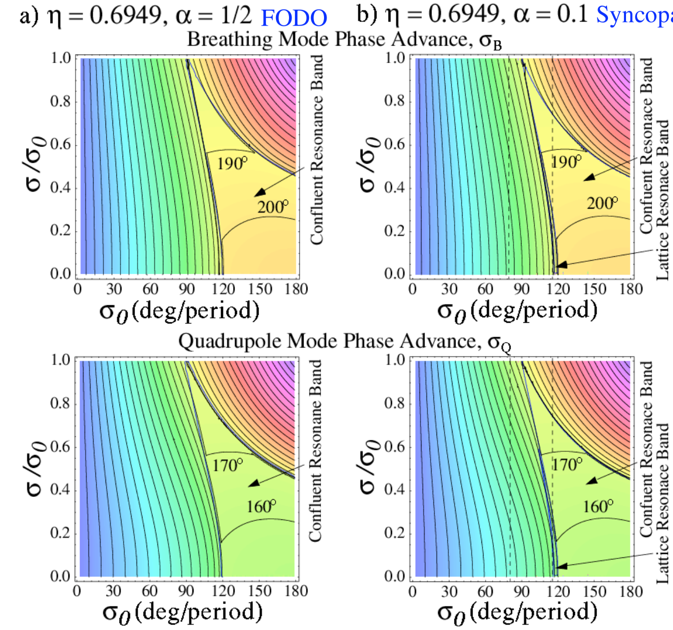

Quadrupole Focusing – mode structure varies strongly with mode phase and the location in the lattice (FODO example)

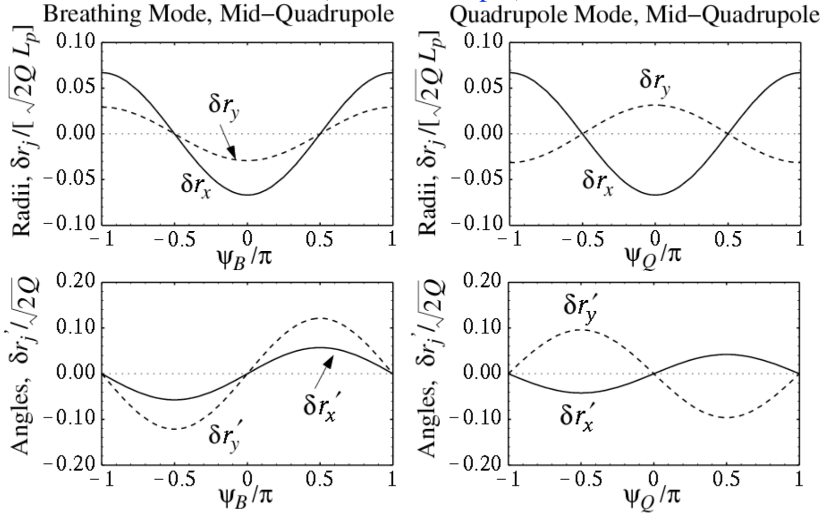

$\delta r_x \neq \delta r_y$
generally not exact
breathing symmetry

$\delta r_x \neq -\delta r_y$
generally not exact
quadrupole symmetry

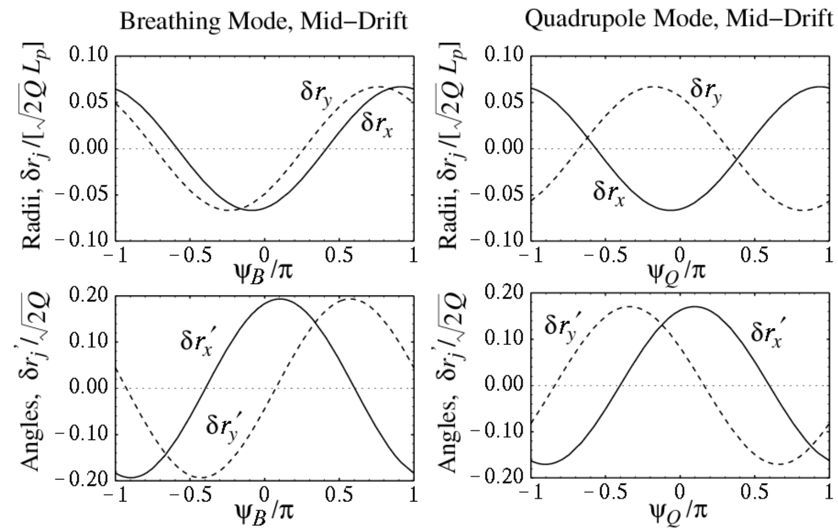

$\delta r_x \neq \delta r_y$
generally not exact
breathing symmetry

$\delta r_x \neq -\delta r_y$
generally not exact
quadrupole symmetry

Summary: Envelope band instabilities and growth rates for periodic solenoidal and quadrupole doublet focusing lattices

Envelope Mode Instability Growth Rates

Solenoid (η = 0.25) Quadrupole FODO (η = 0.70)

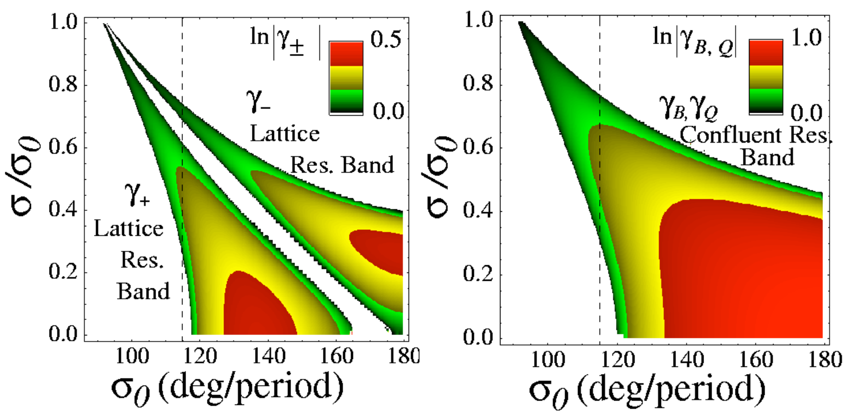

[S.M. Lund and B. Bukh, PRSTAB 024801 (2004)]

S9: Transport Limit Scaling Based on Envelope Models

See Handwritten Notes from 2006 USPAS

- Will attempt to convert to slides in future versions of the class

S8: Centroid and Envelope Descriptions via 1st Order Coupled Moment Equations

When constructing centroid and moment models, it can be efficient to simply write moments, differentiate them, and then apply the equation of motion. Generally, this results in lower order moments coupling to higher order ones and an infinite chain of equations. But the hierarchy can be truncated by:

- Assuming a fixed functional form of the distribution in terms of moments
- Neglecting coupling to higher order terms

Resulting first order moment equations can be expressed in terms of a closed set of moments and advanced in *s* or *t* using simple (ODE based) numerical codes. This approach can prove simpler to include effects where invariants are not easily extracted to reduce the form of the equations (as when solving the KV envelope equations in the usual form).

Examples of effects that might be more readily analyzed:

- Skew coupling in quadrupoles
- Chromatic effects in final focus
- Dispersion in bends

See: references at end of notes
J.J. Barnard, lecture on Heavy-Ion Fusion and Final Focusing

Resulting form of coupled moment equations:

$$\boxed{\frac{d}{ds}\mathbf{M} = \mathbf{F}(\mathbf{M})}$$

$\mathbf{M}$ = vector of moments, generally infinite

$\mathbf{F}$ = vector function of $\mathbf{M}$, generally nonlinear

- System advanced from a specified initial condition (initial value of $\mathbf{M}$)

Transverse moment definition:

$$\boxed{\langle \cdots \rangle_\perp \equiv \frac{\int d^2x_\perp \int d^2x'_\perp \cdots f_\perp}{\int d^2x_\perp \int d^2x'_\perp f_\perp}}$$

Can be generalized if other variables such as off momentum are included in f

Differentiate moments and apply equations of motion:

$$\frac{d}{ds}\langle \cdots \rangle_\perp \equiv \frac{\int d^2x_\perp \int d^2x'_\perp \left[\frac{d}{ds}\cdots\right] f_\perp}{\int d^2x_\perp \int d^2x'_\perp f_\perp}$$

+ apply equations of motion to simplify $\frac{d}{ds}\cdots$

When simplifying the results, if the distribution form is frozen in terms of moments (Example: assume uniform density elliptical beam) then we use constructs like:

$$n = \int d^2x'_\perp \, f_\perp \;= n(\mathbf{M})$$

to simplify the resulting equations and express the RHS in terms of elements of $\mathbf{M}$

1st order moments:

$\mathbf{X}_\perp = \langle \mathbf{x}_\perp \rangle_\perp$ Centroid coordinate

$\mathbf{X}'_\perp = \langle \mathbf{x}'_\perp \rangle_\perp$ Centroid angle

+ possible others if more variables. Example

$\Delta = \langle \frac{\delta p_s}{p_s} \rangle = \langle \delta \rangle$ Centroid off-momentum

$\vdots$ $\vdots$

2nd order moments:

It is typically convenient to subtract centroid from higher-order moments

$$\begin{aligned} \tilde{x} &\equiv x - X & \tilde{x}' &\equiv x' - X' \\ \tilde{y} &\equiv y - Y & \tilde{y}' &\equiv y' - Y' \\ \tilde{\delta} &\equiv \delta - \Delta \end{aligned}$$

x-moments	*y*-moments	*x-y* cross moments	dispersive moments
$\langle \tilde{x}^2 \rangle_\perp$	$\langle \tilde{y}^2 \rangle_\perp$	$\langle \tilde{x}\tilde{y} \rangle_\perp$	$\langle \tilde{x}\tilde{\delta} \rangle, \ \langle \tilde{y}\tilde{\delta} \rangle$
$\langle \tilde{x}\tilde{x}' \rangle_\perp$	$\langle \tilde{y}\tilde{y}' \rangle_\perp$	$\langle \tilde{x}'\tilde{y} \rangle_\perp, \ \langle \tilde{x}\tilde{y}' \rangle_\perp$	$\langle \tilde{x}'\tilde{\delta} \rangle, \ \langle \tilde{y}'\tilde{\delta} \rangle$
$\langle \tilde{x}'^2 \rangle_\perp$	$\langle \tilde{y}'^2 \rangle_\perp$	$\langle \tilde{x}'\tilde{y}' \rangle_\perp$	$\langle \tilde{\delta}^2 \rangle$

3rd order moments: Analogous to 2nd order case, but more for each order

$$\langle \tilde{x}^3 \rangle_\perp, \ \langle \tilde{x}^2\tilde{y} \rangle_\perp, \ \cdots$$

Many quantities of physical interest are expressed in transport can then be expressed in terms of moments calculated when the equations are numerically advanced in s and their evolutions plotted to understand behavior

- Many quantities of physical interest are expressible in terms of 1st and 2nd order moments

Example moments often projected:

Statistical beam size:
(rms edge measure)

$$r_x = 2\langle \tilde{x}^2 \rangle_\perp^{1/2}$$
$$r_y = 2\langle \tilde{y}^2 \rangle_\perp^{1/2}$$

Statistical emittances:
(rms edge measure)

$$\varepsilon_x = 4\left[\langle \tilde{x}^2 \rangle_\perp \langle \tilde{x}'^2 \rangle_\perp - \langle \tilde{x}\tilde{x}' \rangle_\perp^2\right]^{1/2}$$
$$\varepsilon_y = 4\left[\langle \tilde{y}^2 \rangle_\perp \langle \tilde{y}'^2 \rangle_\perp - \langle \tilde{y}\tilde{y}' \rangle_\perp^2\right]^{1/2}$$

Kinetic longitudinal temperature:
(rms measure)

$$T_s = \text{const} \times \langle \tilde{\delta}^2 \rangle$$

Illustrate approach with the familiar KV model

Truncation assumption: unbunched uniform density elliptical beam in free space

- $\delta = 0$, no axial velocity spread
- All cross moments zero, i.e. $\langle \tilde{x}\tilde{y} \rangle_\perp = 0$

$$\frac{d}{ds}\langle x \rangle_\perp = \langle x' \rangle_\perp \qquad \frac{d}{ds}\langle x^2 \rangle_\perp = 2\langle xx' \rangle_\perp$$
$$\frac{d}{ds}\langle x' \rangle_\perp = \langle x'' \rangle_\perp \qquad \frac{d}{ds}\langle x'^2 \rangle_\perp = 2\langle x'x'' \rangle_\perp$$
$$\vdots \qquad\qquad \vdots$$

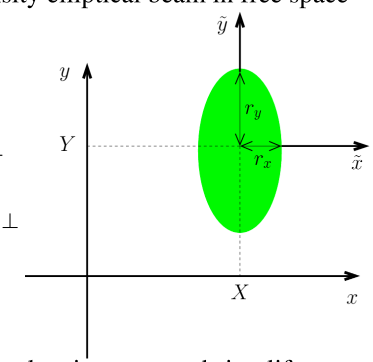

Use particle equations of motion within beam, neglect images, and simplify

- Apply equations in S2 with $\mathbf{E}^i_\perp = 0$

$$x'' + \frac{(\gamma_b\beta_b)'}{(\gamma_b\beta_b)}x' + \kappa_x x - \frac{2Q}{(r_x+r_y)r_x}(x - \langle x \rangle_\perp) = 0$$
$$y'' + \frac{(\gamma_b\beta_b)'}{(\gamma_b\beta_b)}y' + \kappa_y y - \frac{2Q}{(r_x+r_y)r_y}(y - \langle y \rangle_\perp) = 0$$

Resulting system of 1st and 2nd order moments

1st order moments:

$$\frac{d}{ds}\begin{bmatrix} \langle x \rangle_\perp \\ \langle x' \rangle_\perp \\ \langle y \rangle_\perp \\ \langle y' \rangle_\perp \end{bmatrix} = \begin{bmatrix} \langle x' \rangle_\perp \\ -\kappa_x(s)\langle x \rangle_\perp \\ \langle y' \rangle_\perp \\ -\kappa_y(s)\langle y \rangle_\perp \end{bmatrix}$$

2nd order moments:

$$\frac{d}{ds}\begin{bmatrix} \langle \tilde{x}^2 \rangle_\perp \\ \langle \tilde{x}\tilde{x}' \rangle_\perp \\ \langle \tilde{x}'^2 \rangle_\perp \\ \langle \tilde{y}^2 \rangle_\perp \\ \langle \tilde{y}\tilde{y}' \rangle_\perp \\ \langle \tilde{y}'^2 \rangle_\perp \end{bmatrix} = \begin{bmatrix} 2\langle \tilde{x}\tilde{x}' \rangle_\perp \\ \langle \tilde{x}'^2 \rangle_\perp - \kappa_x(s)\langle \tilde{x}^2 \rangle_\perp + \frac{Q\langle \tilde{x}'^2 \rangle_\perp}{[4\langle \tilde{x}^2 \rangle_\perp^{1/2}(\langle \tilde{x}^2 \rangle_\perp^{1/2} + \langle \tilde{y}^2 \rangle_\perp^{1/2})]} \\ -2\kappa_x(s)\langle \tilde{x}\tilde{x}' \rangle_\perp + \frac{2Q\langle \tilde{x}\tilde{x}' \rangle_\perp}{[4\langle \tilde{x}^2 \rangle_\perp^{1/2}(\langle \tilde{x}^2 \rangle_\perp^{1/2} + \langle \tilde{y}^2 \rangle_\perp^{1/2})]} \\ 2\langle \tilde{y}\tilde{y}' \rangle_\perp \\ \langle \tilde{y}'^2 \rangle_\perp - \kappa_y(s)\langle \tilde{y}^2 \rangle_\perp + \frac{Q\langle \tilde{y}'^2 \rangle_\perp}{[4\langle \tilde{y}^2 \rangle_\perp^{1/2}(\langle \tilde{x}^2 \rangle_\perp^{1/2} + \langle \tilde{y}^2 \rangle_\perp^{1/2})]} \\ -2\kappa_y(s)\langle \tilde{y}\tilde{y}' \rangle_\perp + \frac{2Q\langle \tilde{y}\tilde{y}' \rangle_\perp}{[4\langle \tilde{y}^2 \rangle_\perp^{1/2}(\langle \tilde{x}^2 \rangle_\perp^{1/2} + \langle \tilde{y}^2 \rangle_\perp^{1/2})]} \end{bmatrix}$$

- Express 1st and 2nd order moments separately in this case since uncoupled
- Form truncates due to frozen distribution form: all moments on LHS on RHS
- Integrate from initial moments values of s and project out desired quantities

Using 2nd order moment equations we can show that

$$\frac{d}{ds}\varepsilon_x^2 = 0 = \frac{d}{ds}\varepsilon_y^2$$

$$\Longrightarrow \quad \begin{aligned} \varepsilon_x^2 &= 16\left[\langle x^2 \rangle_\perp \langle x'^2 \rangle_\perp - \langle xx' \rangle_\perp^2\right] = \text{const} \\ \varepsilon_y^2 &= 16\left[\langle y^2 \rangle_\perp \langle y'^2 \rangle_\perp - \langle yy' \rangle_\perp^2\right] = \text{const} \end{aligned}$$

Using this, the 2nd order moment equations can be equivalently expressed in the standard KV envelope form:

$$\frac{dr_x}{ds} = r_x' \; ; \qquad \frac{d}{ds}r_x' + \kappa_x r_x - \frac{2Q}{r_x + r_y} - \frac{\varepsilon_x^2}{r_x^3} = 0$$
$$\frac{dr_y}{ds} = r_y' \; ; \qquad \frac{d}{ds}r_y' + \kappa_y r_y - \frac{2Q}{r_x + r_y} - \frac{\varepsilon_y^2}{r_y^3} = 0$$

- Moment form fully consistent with usual KV model .... as it must be
- Moment form generally easier to put in additional effects that would violate the usual emittance invariants

Relative advantages of the use of coupled matrix form versus reduced equations can depend on the problem/situation

Coupled Matrix Equations

$$\frac{d}{ds}\mathbf{M} = \mathbf{F}$$

M = Moment Vector
F = Force Vector

- Easy to formulate
  - Straightforward to incorporate additional effects
- Natural fit to numerical routine
  - Easy to code

Reduced Equations

$$X'' + \kappa_x X = 0$$

$$r_x'' + \kappa_x r_x - \frac{2Q}{r_x + r_y} - \frac{\varepsilon_x^2}{r_x^3} = 0$$

etc.

Reduction based on identifying invariants such as $\varepsilon_x^2 = 16\left[\langle \tilde{x}^2\rangle_\perp \langle \tilde{x}'^2\rangle_\perp - \langle \tilde{x}\tilde{x}'\rangle_\perp^2\right]$ helps understand solutions

- Compact expressions

These slides will be corrected and expanded for reference and any future editions of the US Particle Accelerator School class:
Beam Physics with Intense Space Charge, by J.J. Barnard and S.M. Lund

Corrections and suggestions are welcome. Contact:

Steven M. Lund
Lawrence Berkeley National Laboratory
BLDG 47 R 0112
1 Cyclotron Road
Berkeley, CA 94720-8201

SMLund@lbl.gov
(510) 486 – 6936

References: For more information see:

Image charge couplings:

E.P. Lee, E. Close, and L. Smith, Nuc. Inst. And Methods, 1126 (1987)

Seminal work on envelope modes:

J. Struckmeier and M. Reiser, *Theoretical Studies of Envelope Oscillations and Instabilities of Mismatched Intense Charged-Particle Beams in Periodic Focusing Channels*, Part. Accel. **14,** 227 (1984)

M. Reiser, *Theory and Design of Charged Particle Beams* (John Wiley, 1994, 2008)

Extensive review on envelope instabilities:

S.M. Lund and B. Bukh, *Stability Properties of the KV Envelope Equations Describing Intense Ion Beam Transport,* PRSTAB **7** 024801 (2004)

Efficient, Fail-Safe Generation of Matched Envelope Solutions:

S.M. Lund and S.H. Chilton, and E.P. Lee, *Efficient Computation of Matched Solutions of the KV Envelope Equations,* PRSTAB **9** 064201 (2006)

KV results:

F. Sacherer, *Transverse Space-Charge Effects in Circular Accelerators*, Univ. of California Berkeley, Ph.D Thesis (1968)

I. Kaphinskij and V. Vladimirskij, in *Proc. Of the Int. Conf. On High Energy Accel. and Instrumentation* (CERN Scientific Info. Service, Geneva, 1959) p. 274

Symmetries and phase-amplitude methods:

A. Dragt, *Lectures on Nonlinear Orbit Dynamics* in *Physics of High Energy Particle Accelerators,* (American Institute of Physics, 1982), AIP Conf. Proc. No. 87, p. 147

E. D. Courant and H. S. Snyder, *Theory of the Alternating-Gradient Synchrotron*, Annals of Physics **3**, 1 (1958)

Analytical analysis of matched envelope solutions and transport scaling:

E. P. Lee, *Precision matched solution of the coupled beam envelope equations for a periodic quadrupole lattice with space-charge*, Phys. Plasmas 9, 4301 (2005)

O.A. Anderson, *Accurate Iterative Analytic Solution of the KV Envelope Equations for a Matched Beam*, PRSTAB, **10** 034202 (2006)

Coupled Moment Formulations of Centroid and Envelope Evolution:

J.J. Barnard, H.D. Shay, S.S. Yu, A. Friedman, and D.P. Grote, *Emittance Growth in Heavy-Ion Recirculators*, 1992 PAC Proceedings, Ontario, Canada, p. 229

J.J. Barnard, J. Miller, I. Haber, *Emittance Growth in Displaced Space Charge Dominated Beams with Energy Spread*, 1993 PAC Proceedings, Washington, p. 3612 (1993)

J.J. Barnard, *Emittance Growth from Rotated Quadrupoles in Heavy Ion Accelerators,* 1995 PAC Proceedings, Dallas, p. 3241 (1995)

R.A. Kishek, J.J. Barnard, and D.P. Grote, *Effects of Quadrupole Rotations on the Transport of Space-Charge-Dominated Beams: Theory and Simulations Comparing Linacs with Circular Machines*, 1999 PAC Proceedings, New York, TUP119, p. 1761 (1999)

J.J. Barnard, R.O. Bangerter, E. Henestroza, I.D. Kaganovich, E.P. Lee, B.G. Logan, W.R. Meier, D. Rose, P. Santhanam, W.M. Sharp, D.R. Welch, and S.S. Yu, *A Final Focus Model for Heavy Ion Fusion System Codes*, NIMA **544** 243-254 (2005).

J.J. Barnard and B. Losic, *Envelope Modes of Beams with Angular Momentum*, Proc. 20th LINAC Conf., Monterey, MOE12 (2000)

J.J. Barnard and S.M. Lund
USPAS, June 2008

§9 Transport Limit Scaling Based on the Matched Beam Envelope Equations for Periodic Focusing Channels

The scaling of the maximum beam current, or equivalently, the maximum perveance Q that can be transported at a given energy with a specified focusing technology and lattice is of critical importance in designing optimal transport and acceleration channels. Needed equations can be derived from approximate analytical solutions to the matched beam envelope equations for a given lattice. Alternatively, numerical solutions of the envelope equations can be evaluated. But analytical solutions are preferable to understand scaling and enable rapid evaluation of design tradeoffs.

As a practical matter, equations derived must be applied to regimes where technology is feasible.

- Magnet Field Limits
- Electron breakdown
- Vacuum

⋮

Transport limits are inextricably linked to technology. Moreover, higher order stability constraints etc. must also be respected. Treatments of these topics are beyond the scope of this class. Here we present simplified treatments to highlight issues and methods.

First review an example sketched by J.J. Barnard in the Intro. lectures.

Transport Limits of a Periodic FODO Quadrupole Transport Channel

$$r_{xm}'' + \frac{(\gamma_b\beta_b)'}{(\gamma_b\beta_b)} r_{xm}' + \kappa_x r_{xm} - \frac{2Q}{r_{xm}+r_{ym}} - \frac{\varepsilon_x^2}{r_{xm}^3} = 0$$

$$r_{ym}'' + \frac{(\gamma_b\beta_b)'}{(\gamma_b\beta_b)} r_{ym}' - \kappa_x r_{ym} - \frac{2Q}{r_{xm}+r_{ym}} - \frac{\varepsilon_y^2}{r_{ym}^3} = 0$$

$$r_{xm}(s+L_p) = r_{xm}(s) \quad ; \quad r_{ym}(s+L_p) = r_{ym}(s)$$

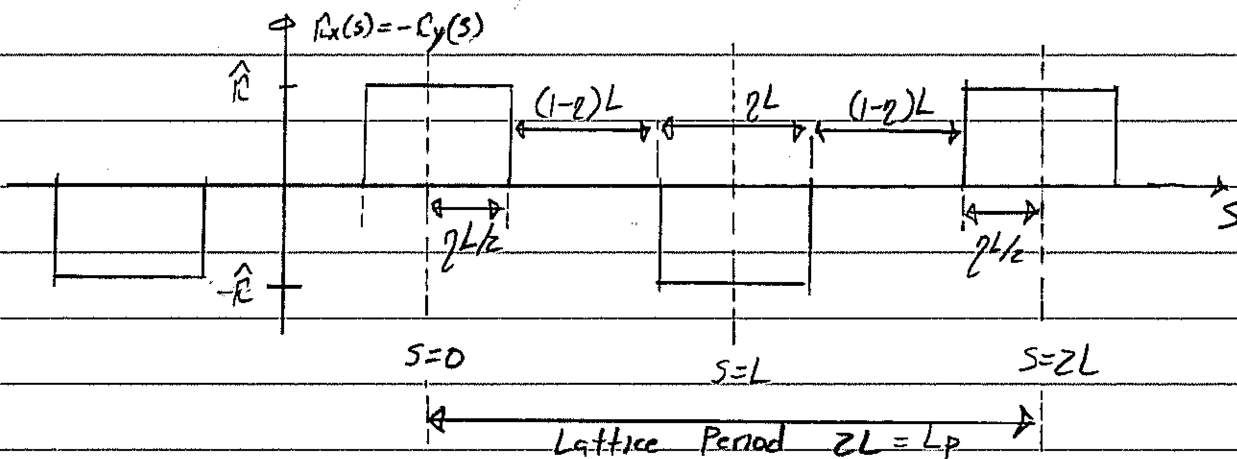

L = Half-Period $\qquad L = L_p/2$

η = Quadrupole "occupancy" $\qquad 0 < \eta \leq 1$

κ = Focus strength $\qquad \kappa = \begin{cases} \dfrac{qE_x'(s)}{m\gamma_b\beta_b^2c^2} \; ; & \text{Electric} \\ \dfrac{qB_y'(s)}{m\gamma_b\beta_b c} \; ; & \text{Magnetic} \end{cases}$

Expand $\kappa_x(s)$ as a Fourier Series:

$$\boxed{\begin{aligned} \kappa_x(s) &= \sum_{n=1}^{\infty} \kappa_n \cos\left(\frac{n\pi s}{L}\right) \\ \kappa_n &= \frac{1}{L}\int_0^{2L} \kappa_x(s)\cos\left(\frac{n\pi s}{L}\right) = \frac{2\hat{\kappa}}{n\pi}\left[1-(-1)^n\right]\sin\left(\frac{n\pi\eta}{2}\right) \end{aligned}}$$

And expand the periodic matched beam envelope by:

$$r_{xm} = r_b\left[1 + \Delta\cos\left(\frac{\pi s}{L}\right)\right] + \sum_{n=2}^{\infty}\Delta_{xn}\cos\left(\frac{n\pi s}{L}\right)$$

$$r_{ym} = r_b\left[1 - \Delta\cos\left(\frac{\pi s}{L}\right)\right] + \sum_{n=2}^{\infty}\Delta_{yn}\cos\left(\frac{n\pi s}{L}\right)$$

$r_b = \text{const} =$ avg. beam radius.

$|\Delta| = \text{const} \ll 1$

$\Delta_{\substack{x\\y}n}$ constants with $|\Delta_{\substack{x\\y}n}| \ll |\Delta|$

Take:

- $(\gamma_b\beta_b)' = 0 \quad\Rightarrow$ coasting beam
- $\varepsilon_x = \varepsilon_y = \varepsilon \quad\Rightarrow$ isotropic beam

and insert these expansions in the envelope equations.

Neglect:

- All terms $\mathcal{O}(\Delta^2)$ and higher
- Fast oscillation terms $\sim \cos\left(\frac{n\pi s}{L}\right)$ with $n \geq 2$.

to obtain two independent constraint equations:

Avg (const):
$$\frac{2\Delta\hat{\kappa}}{\pi} r_b \sin\left(\frac{\pi\eta}{2}\right) - \frac{Q}{r_b} - \frac{\varepsilon^2}{r_b^3} = 0$$

Fundamental $\propto \cos\left(\frac{\pi s}{L}\right)$:
$$-\Delta\left(\frac{\pi}{L}\right)^2 r_b + \frac{4\hat{\kappa}r_b}{\pi}\sin\left(\frac{\pi\eta}{2}\right) + \frac{3\Delta\varepsilon^2}{r_b^3} = 0$$

These equations can be solved to express the maximum beam edge excursion as

$$\boxed{\mathrm{Max}[r_{xm}] = \mathrm{Max}[r_{ym}] \simeq r_b(1+|\Delta|) = r_b\left\{1 + \frac{4|\hat{\kappa}|L^2}{\pi^3}\frac{\sin\left(\frac{\pi\eta}{2}\right)}{\left(1 - \frac{3L^2\varepsilon^2}{\pi^2 r_b^4}\right)}\right\}}$$

and the beam Perveance as:

$$\boxed{Q = \frac{2}{\pi^2}\left[\frac{\sin\left(\frac{\pi\eta}{2}\right)}{\left(\frac{\pi\eta}{2}\right)}\right]^2 \frac{\eta^2\hat{\kappa}^2L^2r_b^2}{\left(1-\frac{3L^2\varepsilon^2}{\pi^2 r_b^4}\right)} - \frac{\varepsilon^2}{r_b^2}}$$

Design Strategy:

1) Choose a lattice period $2L$, quadrupole occupancy η, and clear machine "pipe" radius r_p consistent with focusing technology employed.
2) Choose the largest possible focus strength $\hat{\kappa}$ (quadrupole current or voltage excitation) for beam energy with undepressed particle phase advance:

$$\boxed{\sigma_0 \lesssim 80^\circ/\text{period}, \quad \text{"Tiefenback Limit"}}$$

- Larger phase advances correspond to stronger focus and smaller beam cross-sectional area for given values of Q, ε.

- Weaker phase advance suppresses various particle, envelope, and collective instabilities for reliable transport: [Ref: M.G. Tiefenback, "Space-Charge Limits on the Transport of Ion Beams," U.C. Berkeley Ph.D Thesis, 1986 LBL-22465

3) Choose a suitable beam-edge to aperture clearance factor:

$$\boxed{\begin{gathered} r_p = \mathrm{Max}[r_{xm}] + \Delta_p \\ \Delta_p = \text{Clearance.} \end{gathered}}$$

to allow for misalignments, limit scraping of halo particles outside the beam core, reduce image charges, gas propagation times from the aperture to the beam, and other nonideal effects.

4) Evaluate choices made using higher-order theory, numerical simulations etc.. Iterate choices made to reoptimize when evaluating cost.

Effective application of this formulation requires extensive practical knowledge:

- Nonideal effects: collective instabilities, halo, electron and gas interactions (species contamination),....
- Technology limits: Voltage breakdown, vacuum, superconducting magnets,....

In practice, for intense beam transport, the emittance terms $\varepsilon_x, \varepsilon_y$ can often be neglected for the purpose of obtaining simpler scaling relations that are more easily understood.

$$\lim_{\varepsilon_x \to 0} \delta_x = 0$$

$$\lim_{\varepsilon_y \to 0} \delta_y = 0$$

$\Rightarrow$ Full space charge depression

In this limit $Q \to Q_{max}$, the maximum transportable perveance.

For our previous example for FODO quadrupoles, the $\varepsilon \to 0$ limit obtains:

$$\lim_{\varepsilon \to 0} \mathrm{Max}[r_{xm}] = r_b \left\{ 1 + \frac{4|\hat{\kappa}| L^2}{\pi^3} \sin\left(\frac{\pi}{2}\eta\right) \right\}$$

$$\lim_{\varepsilon \to 0} Q = Q_{max} = \frac{2}{\pi^2} \left[\frac{\sin\left(\frac{\pi}{2}\eta\right)^2}{\left(\frac{\pi}{2}\eta\right)} \right] \eta^2 \hat{\kappa}^2 L^2 r_b^2$$

S. M. Lund 71

Unfortunately, the method introduced before are inadequate for lattices with lesser degrees of symmetry such as syncopated quadrupole doublet lattices. However, methods introduced by Lee [E. P. Lee, Physics of Plasmas 9, 4301 (2002)], can be applied in this situation and also obtain more accurate results. It is beyond the scope of this class to carry out derivations with these methods, but we summarize results derived.

Quadrupole Doublet Lattice

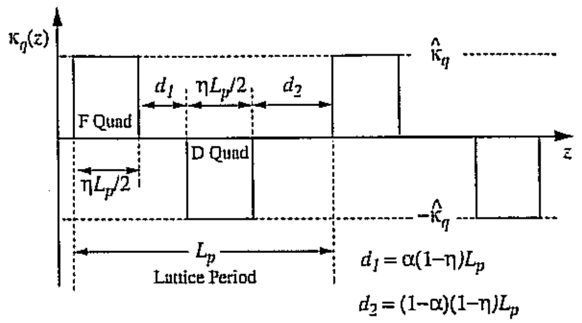

Denote:

Avg Radius: $\overline{r_m} = \int_0^{L_p} \frac{ds}{L_p} r_{xm}(s) = \int_0^{L_p} \frac{ds}{L_p} r_{ym}(s)$

Max Excursion in period: $\text{Max}[r_m] \equiv \text{Max}[r_{xm}, r_{ym}]$

Phase Advance

S.M. Lund 8/

$$\cos\sigma_0 = 1 - \frac{(\eta\widehat{\kappa_q}L_p^2)^2}{32}\left[\left(1-\frac{2}{3}\eta\right) - 4\left(\alpha-\frac{1}{2}\right)^2(1-\eta)^2\right].$$

For $\sigma_0 = 80^\circ$

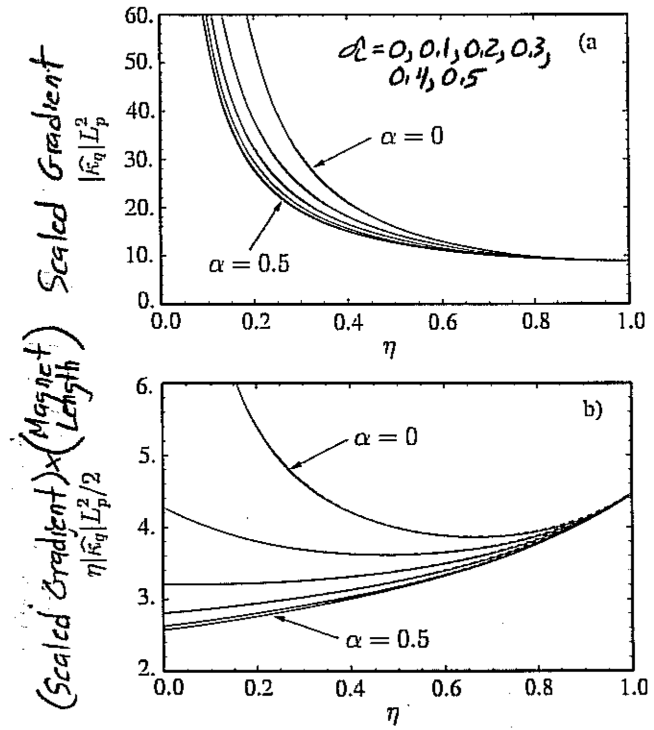

Envelope Flutter

$$\frac{\mathrm{Max}[r_m]}{\overline{r_m}} - 1 = \frac{(1-\cos\sigma_0)^{1/2}(1-\eta/2)[1-4(\alpha-1/2)^2(1-\eta)^2]}{2^{3/2}\left[(1-2\eta/3)-4(\alpha-1/2)^2(1-\eta)^2\right]^{1/2}}.$$

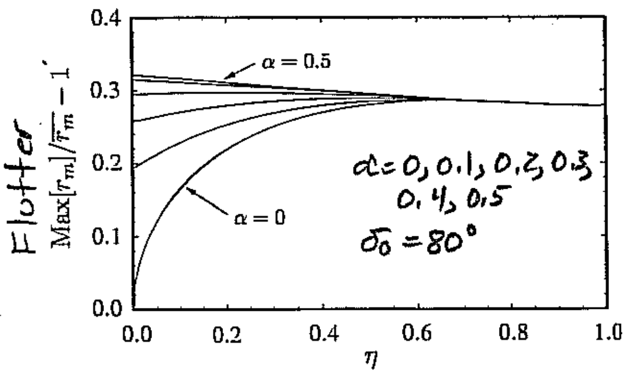

Relations Connecting Max Transportable Perveance Q_{max} and Lattice Parameters

$$
\begin{aligned}
Q_{\max} &= \frac{(1-\cos\sigma_0)^{1/2}}{2^{3/2}} \frac{\eta[(1-2\eta/3)-4(\alpha-1/2)^2(1-\eta)^2]^{1/2}}{(\mathrm{Max}[r_m]/\overline{r_m})^2} |\widehat{\kappa_q}|\, \mathrm{Max}[r_m]^2 \\
&= \frac{(1-\cos\sigma_0)^{1/2}}{2^{3/2}} \frac{\eta[(1-2\eta/3)-4(\alpha-1/2)^2(1-\eta)^2]^{1/2}}{\left\{1+\frac{(1-\cos\sigma_0)^{1/2}(1-\eta/2)[1-4(\alpha-1/2)^2(1-\eta)^2]}{2^{3/2}[(1-2\eta/3)-4(\alpha-1/2)^2(1-\eta)^2]^{1/2}}\right\}^2} |\widehat{\kappa_q}|\, \mathrm{Max}[r_m]^2 .
\end{aligned}
$$

$$
\begin{aligned}
\frac{\mathrm{Max}[r_m]}{L_p} &= \sqrt{\frac{Q_{\max}}{2(1-\cos\sigma_0)}} \left(\frac{\mathrm{Max}[r_m]}{\overline{r_m}}\right) \\
&= \sqrt{\frac{Q_{\max}}{2(1-\cos\sigma_0)}} \left\{1+\frac{(1-\cos\sigma_0)^{1/2}(1-\eta/2)[1-4(\alpha-1/2)^2(1-\eta)^2]}{2^{3/2}\,[(1-2\eta/3)-4(\alpha-1/2)^2(1-\eta)^2]^{1/2}}\right\},
\end{aligned}
$$

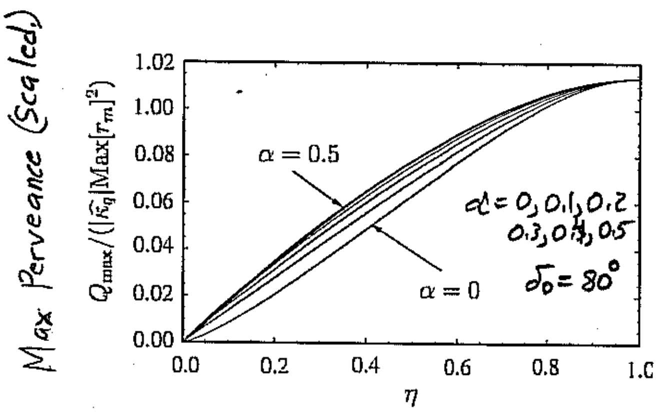

Derivation and aplication of scaling relations can be complicated. They are often applied in systems codes to generate plots that can be interpreted more readily.

John Barnard
Steven Lund
USPAS
June 2008

Mismatched Beams and Beam Halo

Envelope modes of beams in continuous focusing

Envelope modes of bunched beams in continuous focusing

Halos from mismatched beams

SMOOTH FOCUSING ENVELOPE MODES

- If $\frac{d}{ds}\gamma\beta = 0$ & $K(s) = k_{\beta 0}^2 =$ constant & $\epsilon_x = \epsilon_y$

$$\Rightarrow \quad r_x'' + k_{\beta 0}^2 r_x - \frac{2Q}{r_x + r_y} - \frac{\epsilon^2}{r_x^3} = 0$$

$$r_y'' + k_{\beta 0}^2 r_y - \frac{2Q}{r_x + r_y} - \frac{\epsilon^2}{r_y^3} = 0 \qquad (s1)$$

THE EQUILIBRIUM OCCURS WHEN $r_x'' = r_y'' = 0$
& $r_x = r_y = r_b$

$$\Rightarrow \quad k_{\beta 0}^2 r_b - \frac{Q}{r_b} - \frac{\epsilon^2}{r_b^3} = 0$$

THIS IS EASILY SOLVED FOR r_b:

$$r_b = \frac{Q^{1/2}}{k_{\beta 0}}\left[\frac{1}{2} + \frac{1}{2}\sqrt{1 + 4k_{\beta 0}^2\epsilon^2/Q^2}\right]^{1/2} \rightarrow \begin{cases} \dfrac{Q^{1/2}}{k_{\beta 0}}; & \dfrac{2k_{\beta 0}\epsilon}{Q} \ll 1 \\[2ex] \dfrac{\epsilon^{1/2}}{k_{\beta 0}^{1/2}}; & \dfrac{2k_{\beta 0}\epsilon}{Q} \gg 1 \end{cases}$$

Let $\quad r_x = r_b + \xi(s)$

$\quad\quad\;\; r_y = r_b + \eta(s)$

BARNARD (3)

LINEARIZING (S1)

$$(S1) \Rightarrow 0 = \xi'' + k_{\beta 0}^2 (r_b + \xi) - \frac{2Q}{2r_b}\left(1 - \frac{\xi}{2r_b} - \frac{\eta}{2r_b}\right) - \frac{\epsilon^2}{r_b^3}\left(1 - \frac{3\xi}{r_b}\right),$$

$$\& \quad 0 = \eta'' + k_{\beta 0}^2 (r_b + \eta) - \frac{2Q}{2r_b}\left(1 - \frac{\xi}{2r_b} - \frac{\eta}{2r_b}\right) - \frac{\epsilon^2}{r_b^3}\left(1 - \frac{3\eta}{r_b}\right)$$

SUBTRACTING THE EQUILIBRIUM:

$$\xi'' + \left(k_{\beta 0}^2 + \frac{Q}{2r_b^2} + \frac{3\epsilon^2}{r_b^4}\right)\xi + \frac{Q}{2r_b^2}\eta = 0$$

$$\eta'' + \left(k_{\beta 0}^2 + \frac{Q}{2r_b^2} + \frac{3\epsilon^2}{r_b^4}\right)\eta + \frac{Q}{2r_b^2}\xi = 0$$

USING $\quad k_\beta^2 = k_{\beta 0}^2 - \frac{Q}{r_b^2} = \frac{\epsilon^2}{r_b^4}$

$$\Rightarrow \quad \xi'' + \left(\tfrac{3}{2}k_{\beta 0}^2 + \tfrac{5}{2}k_\beta^2\right)\xi + \left(\tfrac{1}{2}k_{\beta 0}^2 - \tfrac{1}{2}k_\beta^2\right)\eta = 0 \qquad (A)$$

$$\eta'' + \left(\tfrac{3}{2}k_{\beta 0}^2 + \tfrac{5}{2}k_\beta^2\right)\eta + \left(\tfrac{1}{2}k_{\beta 0}^2 - \tfrac{1}{2}k_\beta^2\right)\xi = 0 \qquad (B)$$

LET $\chi_1 = \xi - \eta$ SUBTRACTING (B) FROM (A):

$$\chi_1'' + k_1^2 \chi_1 = 0$$

where $k_1^2 = \left(\tfrac{3}{2}k_{\beta 0}^2 + \tfrac{5}{2}k_\beta^2 - \tfrac{1}{2}k_{\beta 0}^2 + \tfrac{1}{2}k_\beta^2\right) = k_{\beta 0}^2 + 3k_\beta^2$

LET $\chi_2 = \xi + \eta$ ADDING (A) & (B):

$$\chi_2'' + k_2^2 \chi_2 = 0$$

where $k_2^2 = \left(\tfrac{3}{2}k_{\beta 0}^2 + \tfrac{5}{2}k_\beta^2 + \tfrac{1}{2}k_{\beta 0}^2 - \tfrac{1}{2}k_\beta^2\right) = 2k_{\beta 0}^2 + 2k_\beta^2$

(3.5)

Letting $\xi = \xi_0 e^{ik_1 s}$ $\eta = \eta_0 e^{ik_1 s}$ where $k_1^2 = k_{p0}^2 + 3k_p^2$

(A) $\Rightarrow$

$$-(k_{p0}^2 + 3k_p^2)\xi_0 + \left(\tfrac{3}{2}k_{p0}^2 + \tfrac{5}{2}k_p^2\right)\xi_0 + \left(\tfrac{1}{2}k_{p0}^2 - \tfrac{1}{2}k_p^2\right)\eta_0 = 0$$

$$\Rightarrow \quad \tfrac{1}{2}(k_{p0}^2 - k_p^2)\left[\xi_0 + \eta_0\right] = 0 \qquad (A')$$

(B) $$-(k_{p0}^2 + 3k_p^2)\eta_0 + \left(\tfrac{3}{2}k_{p0}^2 + \tfrac{5}{2}k_p^2\right)\eta_0 + \left(\tfrac{1}{2}k_{p0}^2 - \tfrac{1}{2}k_p^2\right)\xi_0 = 0$$

$$\Rightarrow \quad \tfrac{1}{2}(k_{p0}^2 - k_p^2)\left[\xi_0 + \eta_0\right] = 0 \qquad (B')$$

SIMILARLY FOR $\xi = \xi_0 e^{ik_2 s}$ and $\eta = \eta_0 e^{ik_2 s}$

(A) $\Rightarrow$

$$-(2k_{p0}^2 + 2k_p^2)\xi_0 + \left(\tfrac{3}{2}k_{p0}^2 + \tfrac{5}{2}k_p^2\right)\xi_0 + \left(\tfrac{1}{2}k_{p0}^2 - \tfrac{1}{2}k_p^2\right)\eta_0 = 0$$

$$\Rightarrow \quad \tfrac{1}{2}(k_{p0}^2 - k_p^2)\left[-\xi_0 + \eta_0\right] = 0 \qquad (A'')$$

(B) $\Rightarrow$

$$-(2k_{p0}^2 + 2k_p^2)\eta_0 + \left(\tfrac{3}{2}k_{p0}^2 + \tfrac{5}{2}k_p^2\right)\eta_0 + \left(\tfrac{1}{2}k_{p0}^2 - \tfrac{1}{2}k_p^2\right)\xi_0 = 0$$

$$\tfrac{1}{2}(k_{p0}^2 - k_{p0}^2)\left[-\eta_0 + \xi_0\right] = 0 \qquad (B'')$$

THE SOLUTIONS ARE:

$$y_1 \sim e^{ik_1 s} \Rightarrow \xi \,\&\, \eta \sim e^{ik_1 s}$$

EQUATIONS (A') & (B') CAN BE WRITTEN

$$\begin{pmatrix} 1 & 1 \\ 1 & 1 \end{pmatrix}\begin{pmatrix} \xi \\ \eta \end{pmatrix} = 0 \Rightarrow \xi = -\eta \Rightarrow \text{"QUADRUPOLE MODE"}$$

FOR $y_2 \sim e^{ik_2 s}$ THE MATRIX EQUATIONS (A'') & (B'') BECOME:

$$\begin{pmatrix} -1 & 1 \\ 1 & -1 \end{pmatrix}\begin{pmatrix} \xi \\ \eta \end{pmatrix} = 0 \Rightarrow \xi = \eta \Rightarrow \text{"BREATHING MODE"}$$

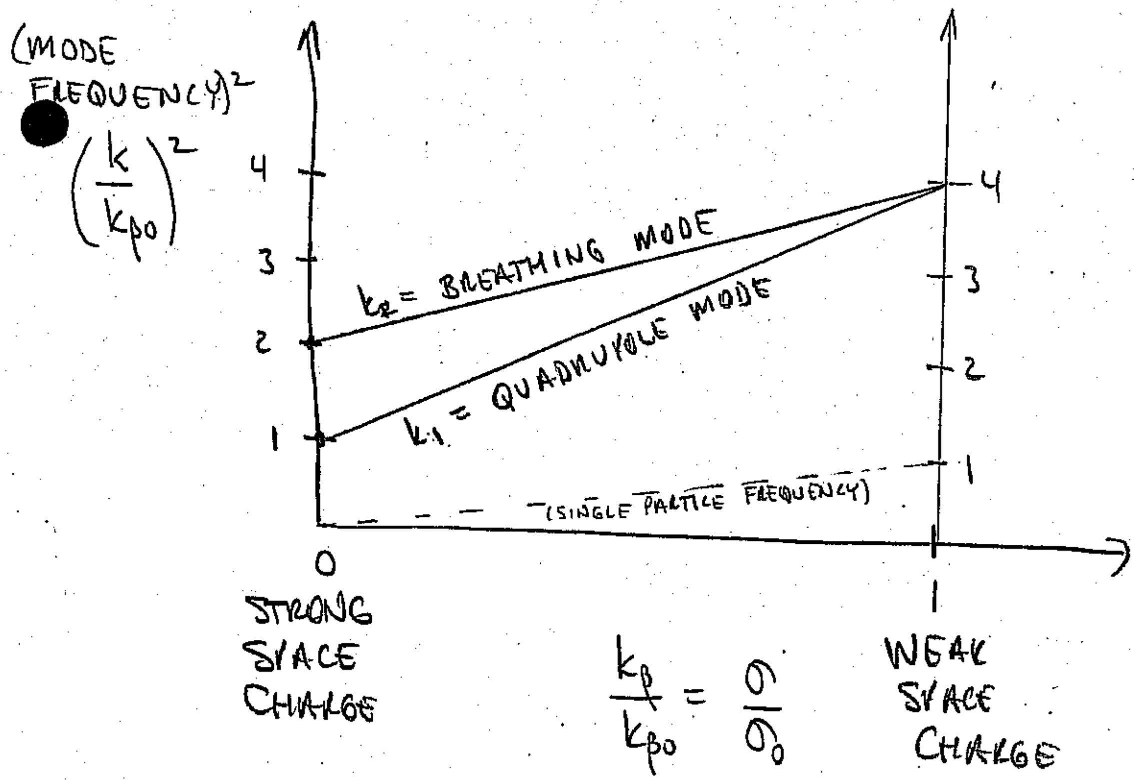

$$k_1^2 = k_{\beta 0}^2 + 3k_\beta^2 \qquad k_2^2 = 2k_{\beta 0}^2 + 2k_\beta^2 \quad \leftarrow \text{MODE FREQUENCY}$$

$$k_\beta^2 = k_{\beta 0}^2 - \frac{Q}{r_b^2} \quad \leftarrow \text{SINGLE PARTI FREQUENCY}$$

Smooth focusing: breathing mode and quadrupole mode

Breathing mode:

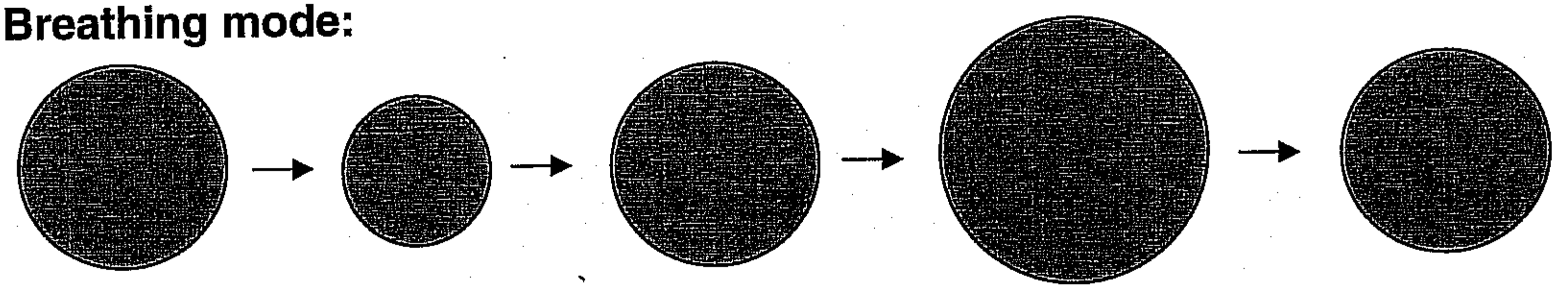

Quadrupole mode:

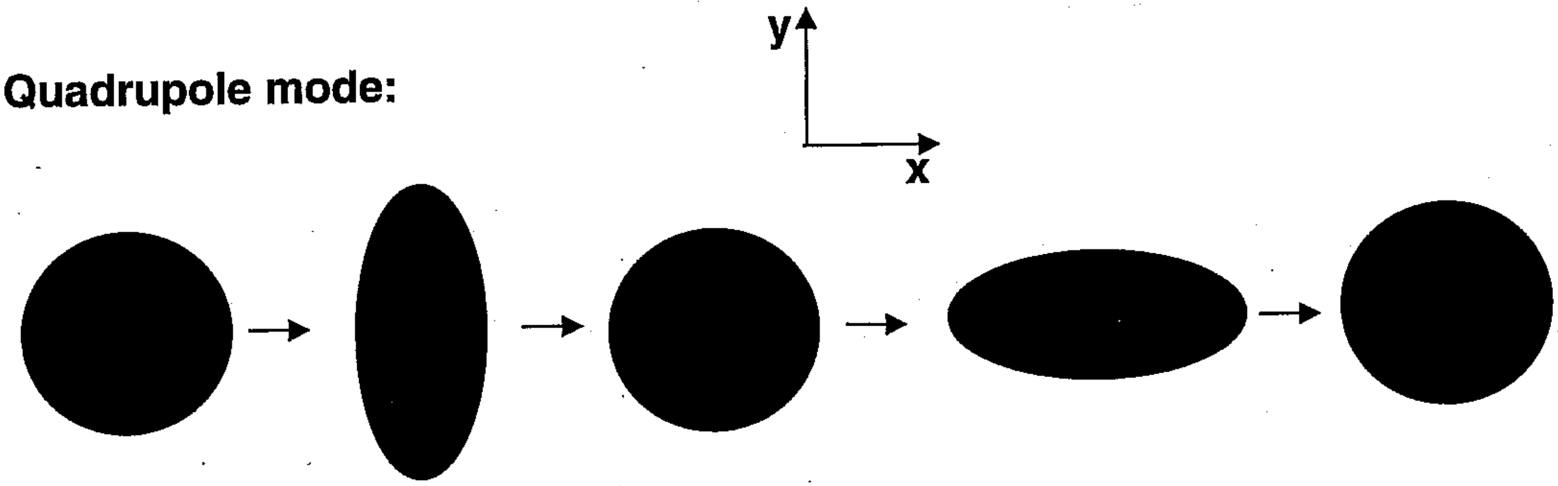

Note that in the quadrupole mode the beam area is nearly constant, whereas in the breathing mode, density increases increasing restoring force; hence breathing mode has the higher frequency of the two modes.

BARNARD 5

JOHN BARNARD
& STEVEN LUND
USPAS
JANUARY 2004

III. ENVELOPE MODES OF BUNCHED BEAMS

IN CONTINUOUS FOCUSING CHANNELS

Total field seen by particle is sum of rf and spacecharge

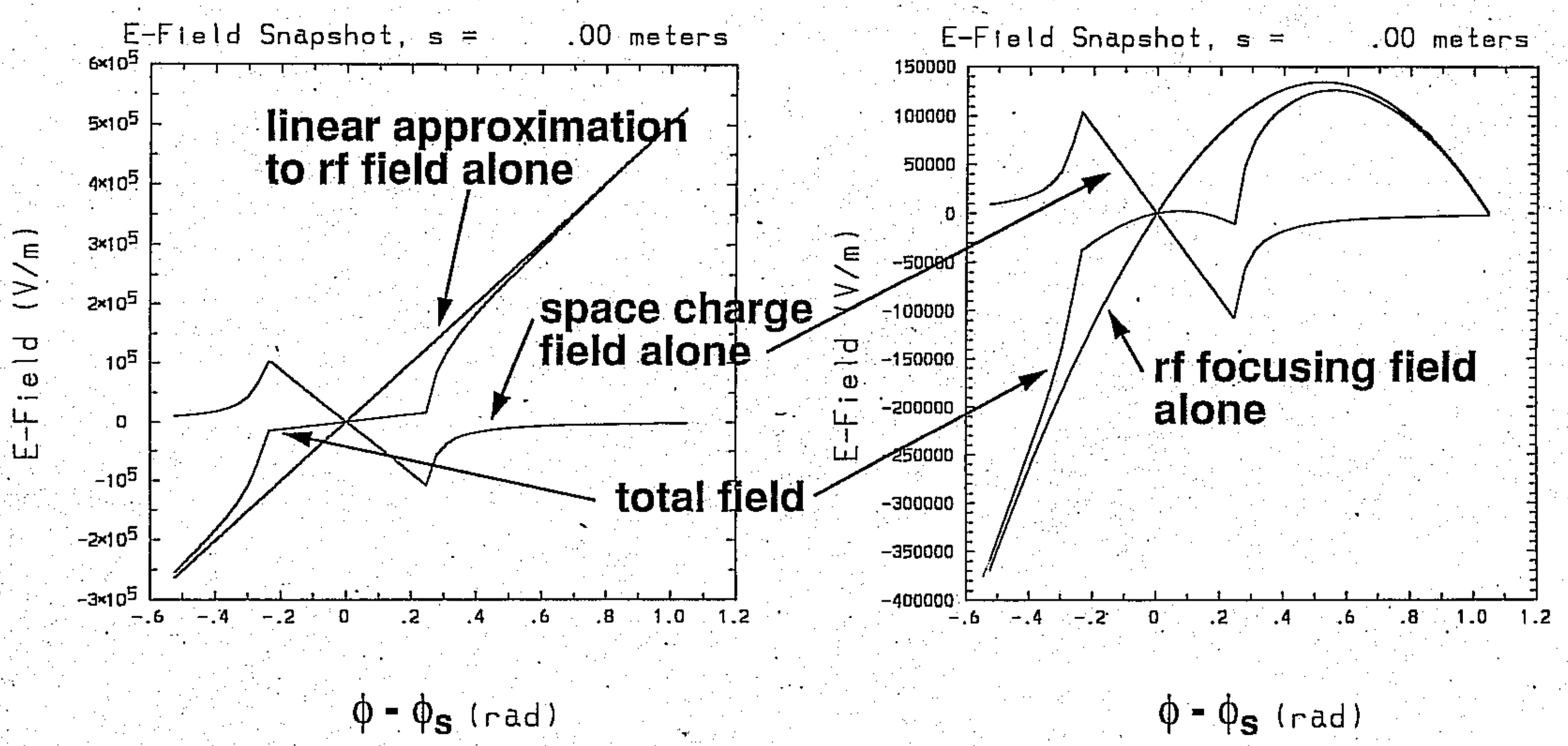

here $\phi - \phi_s = -\ (2\pi/\beta_s\lambda)\ \Delta z$, where $\beta_s c$ is the longitudinal velocity of the synchronous particle and $\lambda = c/\nu$ is the rf vacuum wavelength

7

SPACE-CHARGE FIELD OF BUNCHED BEAMS

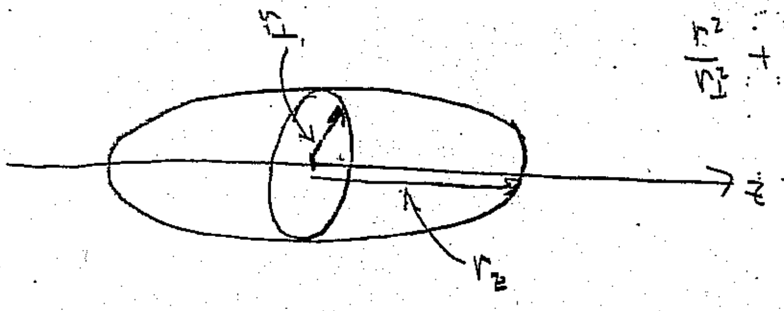

$$\frac{r^2}{r_\perp^2} + \frac{z^2}{r_z^2} = 1$$

BOUNDARY OF ELLIPSOID

THE POTENTIAL OF A UNIFORM DENSITY BUNCH IN FREE SPACE (A MACLAURIN SPHEROID) IS GIVEN BY:

(cf. Landau & Lifshitz, Classical Theory of Fields, p. 297)

$$\varphi = \frac{\rho}{4\epsilon_0}\left(\alpha_\perp r^2 + \alpha_\parallel z^2 - \delta\right)$$

where $$\alpha_\perp = r_\perp^2 r_z \int_0^\infty \frac{ds}{(r_\perp^2 + s)\,\Delta}$$

$$\alpha_\parallel = r_\perp^2 r_z \int_0^\infty \frac{ds}{(r_z^2 + s)\,\Delta}$$

$$\delta = r_\perp^2 r_z \int_0^\infty \frac{ds}{\Delta}$$

where $$\Delta^2 = (r_\perp^2 + s)^2 (r_z^2 + s)$$

FOR NON-RELATIVISTIC BEAM:

$$E_z = -\frac{\partial \varphi}{\partial z} = f\,\frac{\rho}{\epsilon_0}\, z$$

$$E_r = -\frac{\partial \varphi}{\partial r} = \frac{(1-f)}{2}\,\frac{\rho}{\epsilon_0}\, r$$

$$f = f(\alpha) = \begin{cases} \dfrac{\alpha^2}{1-\alpha^2}\left[\dfrac{1}{\sqrt{1-\alpha^2}}\tanh^{-1}\sqrt{1-\alpha^2} - 1\right] & \alpha < 1 \\ \dfrac{1}{3} & \alpha = 1 \\ \dfrac{\alpha^2}{\alpha^2-1}\left[1 - \dfrac{1}{\sqrt{\alpha^2-1}}\tan^{-1}\sqrt{\alpha^2-1}\right] & \alpha > 1 \end{cases} \qquad \alpha \equiv \frac{r_\perp}{r_z}$$

(9)

FOR RELATIVISTIC BEAM

(cf. Lund & Barnard 1997) PAC97 Conf. Proceedings, Vancouver

$$\frac{d^2 \underline{x}_\perp}{ds^2} = \frac{F_\perp}{\gamma_s \beta_s^2 mc^2} \qquad F_{\perp s} = \frac{-q}{\gamma_s^2}\frac{\partial\phi}{\partial \underline{x}_\perp} = \frac{q\rho}{2\gamma_s^2\epsilon_0}\left[1 - f(\alpha)\right]\underline{x}_\perp$$

$$\frac{d^2 \Delta z}{ds^2} = \frac{F_z}{\gamma_s^3 \beta_s^2 mc^2} \qquad F_{zs} = \frac{-q}{\gamma_s^2}\frac{\partial\phi}{\partial z} = \frac{q\rho}{\epsilon_0} f(\alpha)\Delta z$$

$$\alpha = \frac{r_\perp}{\gamma r_z} \qquad \left[\alpha = \frac{r_\perp}{(r_z \text{ in comoving frame})}\right]$$

COMBINING FOCUSING + SELF FIELDS

$$\frac{d^2}{ds^2}\Delta z = -k_{s0}^2 \Delta z + \frac{q\rho f(\alpha)}{\gamma_s^3 \beta_s^2 mc^2 \epsilon_0}\Delta z \qquad \text{(LINEAR rf)}$$

$$\frac{d^2}{ds^2}\underline{x}_\perp = -k_{\beta 0}^2 \underline{x}_\perp + \frac{q\rho\left[1 - f(\alpha)\right]}{2\gamma_s^3 \beta_s^2 mc^2 \epsilon_0}\underline{x}_\perp$$

$$\rho = \frac{3 I \lambda_{rf}}{4\pi r_\perp^2 r_z c} \qquad \text{where } \lambda_{rf} = \frac{2\pi c}{\omega}$$

Envelope Equations for an Unaccelerated Ellipsoidal Beam Bunch with Uniform Space-Charge

$$\boxed{\begin{aligned} \frac{d^2 r_\perp}{ds^2} + k_{\beta 0}^2 r_\perp - \frac{K_{3D}[1-f(\alpha)]}{2 r_\perp r_z} - \frac{\epsilon_x^2}{r_\perp^3} = 0 \\ \frac{d^2 r_z}{ds^2} + f_{nl}(\zeta)\, k_{s0}^2 r_z - \frac{K_{3D} f(\alpha)}{r_\perp^2} - \frac{\epsilon_z^2}{r_z^3} = 0 \end{aligned}}$$

$\alpha = \frac{r_\perp}{\gamma r_z}$

$f_{nl}(\zeta) = (15/\zeta^5)[(3-\zeta^2)\sin\zeta - 3\zeta\cos\zeta]$ Let $\zeta = (2\pi/\beta_s\lambda) r_z$

$k_{\beta 0}^2$	Undepressed Transverse Betatron Wavenumber-Squared
k_{s0}^2	Undepressed Longitudinal Synchrotron Wavenumber-Squared
$K_{3D} = 3qI\cancel{\lambda}/4\pi\epsilon_0\gamma_s^3\beta_s^3 mc^3$	3D Space-Charge Parameter (dimension of length)
$\epsilon_x^2 = 25[\langle x^2\rangle\langle x'^2\rangle - \langle xx'\rangle^2]$	3D Bunched Beam Transverse Emittance-Squared
$\epsilon_z^2 = 25[\langle \Delta z^2\rangle\langle \Delta z'^2\rangle - \langle \Delta z\Delta z'\rangle^2]$	3D Bunched Beam Longitudinal Emittance-Squared
f_{nl}	Accounts for Nonlinear rf Focusing, $f_{nl}(\zeta) \to 1$ when $\zeta \to 0$

- Envelope equations couple the transverse and longitudinal single-particle motion
- Bunch acceleration results in additional terms
- Linear rf envelope equations presented in Wangler, "Intro. to Linear Accelerators"

$\lambda_{rf} = \frac{2\pi c}{\omega}$ = rf vacuum wavelength

Envelope Equations will be used to:

- Calculate equilibrium values of the envelope widths r_z and $r_\perp$
- Calculate properties of mismatch eigenmodes
  - Mode wavenumber
  - Relative amplitude of transverse and longitudinal mismatch

$I \equiv \frac{qN_e}{\lambda_{rf}}$ = average current

$K_{3D} = \frac{3}{2} Q \lambda_{rf}$

10

(11)

BARNARD 21

Perturbed Envelope Equations
Yield Linear Eigenmode for a Mismatched Ellipsoidal Beam Bunch

Assume small-amplitude perturbations ($|\delta r_\perp|/r_{\perp 0} \ll 1$ and $|\delta r_z|/r_{z0} \ll 1$):

$$\boxed{\begin{aligned} r_\perp &= r_{\perp 0} + \delta r_\perp \exp(iks) \\ r_z &= r_{z0} + \delta r_z \exp(iks) \end{aligned}}$$

SEE
BARNARD & LUND
LUND & BARNARD
PAC 97, VANCOUVER
CONF. PROCEEDINGS

To obtain coupled linear mode equations:

$$\boxed{\begin{pmatrix} -k^2 + K_{11} & K_{12} \\ K_{21} & -k^2 + K_{22} \end{pmatrix} \begin{pmatrix} \delta r_\perp / r_{\perp 0} \\ \delta r_z / r_{z0} \end{pmatrix} = 0}$$

$$K_{11} = 4k_\beta^2 - \frac{K_{3D}}{r_{\perp 0}^2 r_{z0}} \left[1 - f(\alpha) - \frac{\alpha}{2}\frac{df(\alpha)}{d\alpha}\right]_{r_\perp = r_{\perp 0}, r_z = r_{z0}}$$

$$K_{22} = 4k_{s0}^2 \left[f_{nl}(\zeta) + \frac{\zeta}{4}\frac{df_{nl}(\zeta)}{d\zeta}\right]_{r_\perp = r_{\perp 0}, r_z = r_{z0}} - \frac{3K_{3D}}{r_{\perp 0}^2 r_{z0}} \left[f(\alpha) - \frac{\alpha}{3}\frac{df(\alpha)}{d\alpha}\right]_{r_\perp = r_{\perp 0}, r_z = r_{z0}}$$

$$K_{12} = \frac{K_{3D}}{2r_{\perp 0}^2 r_{z0}} \left[1 - f(\alpha) - \alpha\frac{df(\alpha)}{d\alpha}\right]_{r_\perp = r_{\perp 0}, r_z = r_{z0}}$$

$$K_{21} = \frac{K_{3D}}{r_{\perp 0}^2 r_{z0}} \left[2f(\alpha) - \alpha\frac{df(\alpha)}{d\alpha}\right]_{r_\perp = r_{\perp 0}, r_z = r_{z0}}$$

Solution of the quartic dispersion relation characterizes the envelope mismatch modes

Spatial Frequencies:

High Frequency Mode : $\quad k^2 = k_H^2 = \frac{1}{2}(K_{11} + K_{22}) + \frac{1}{2}\sqrt{(K_{11} - K_{22})^2 + 4K_{12}K_{21}}$

Low Frequency Mode : $\quad k^2 = k_L^2 = \frac{1}{2}(K_{11} + K_{22}) - \frac{1}{2}\sqrt{(K_{11} - K_{22})^2 + 4K_{12}K_{21}}$

Relative Amplitude of Transverse and Longitudinal Oscillations:

$$\frac{\delta r_\perp / r_{\perp 0}}{\delta r_z / r_{z0}} = \frac{K_{12}}{k^2 - K_{11}}$$

Envelope equations yield equilibrium beam parameters and eigenfrequencies and modes of mismatched beam

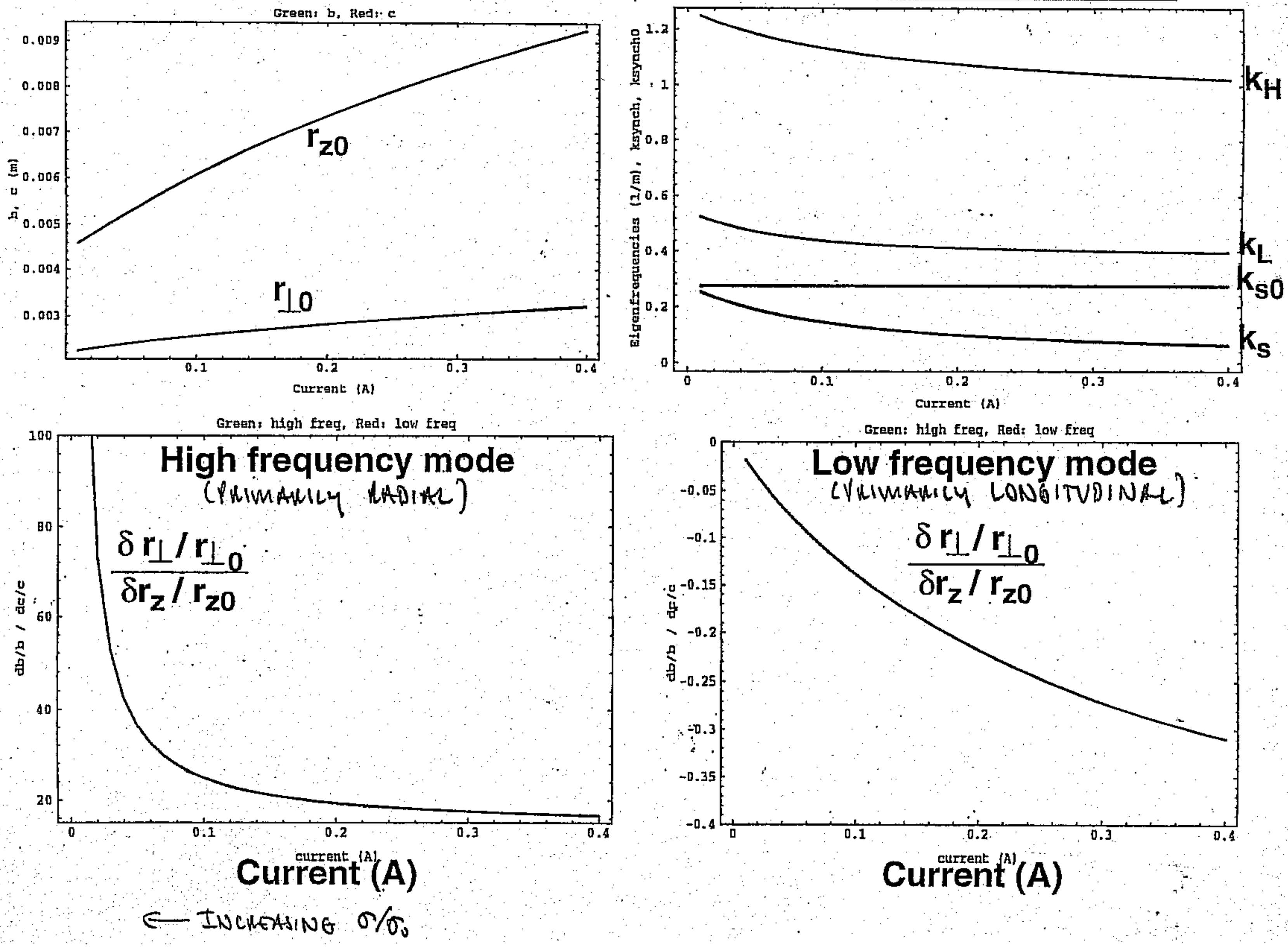

BARNARD 22

(12)

(13)

JOHN BARNARD
& STEVEN LUND
USPAS JANUARY 2004

III HALOS

1. WHAT IS HALO? WHY DO WE CARE?
2. QUALITATIVE PICTURE OF HALO FORMATION:
   MISMATCHES RESONANTLY DRIVE PARTICLES TO LARGE AMPLITUDE
3. CORE/PARTICLE MODELS
4. AMPLITUDE/PHASE ANALYSIS

BEAMHALO 24

FROM
"BEAM LOSS & BEAM HALO STUDIES"
ROBERT RYNE, 1995

FULLY SELF-CONSISTENT
PIC CODE RESULTS

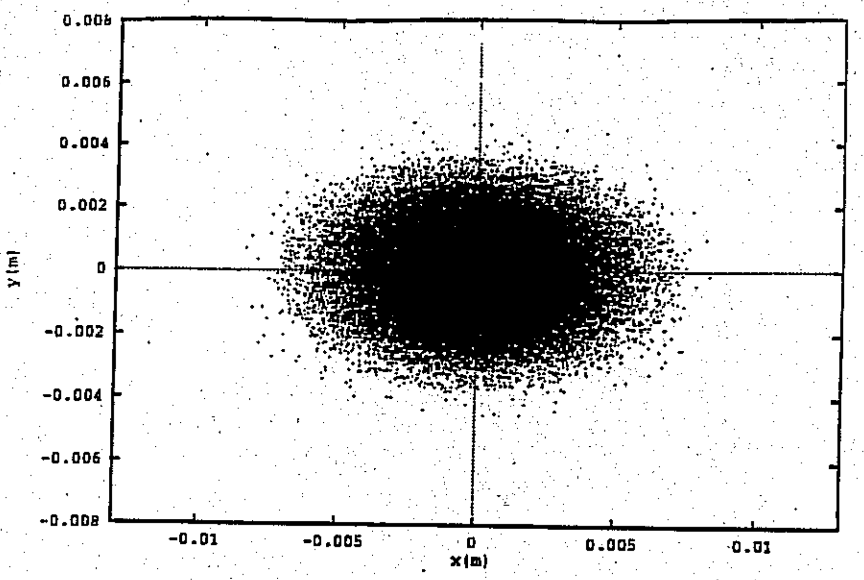

MATCHED
BEAM

Figure 5: Beam halo after 22 focusing periods in a FODO channel. The initial distribution is an *rms* matched Gaussian beam. ($\sigma_0 = 70\,\text{deg}$, $\sigma = 35\,\text{deg}$)

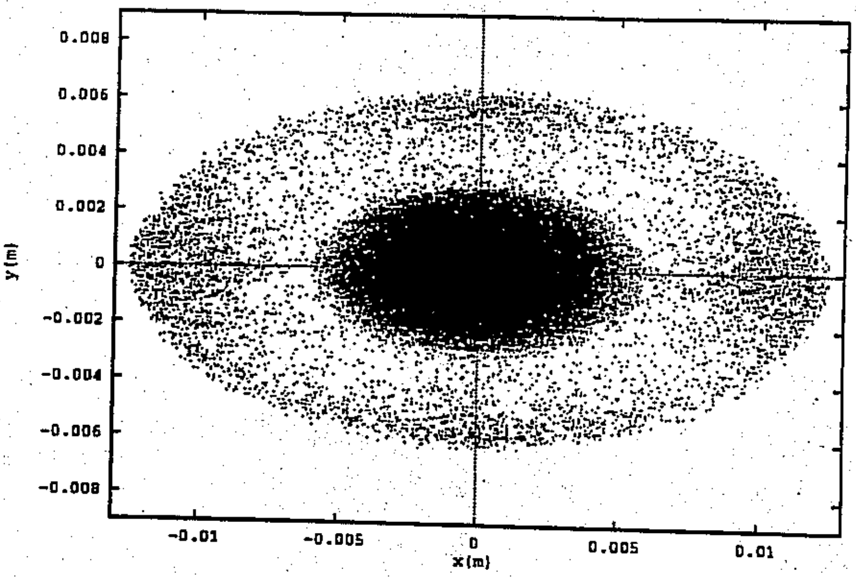

MISMATCHED
BEAM

Figure 6: Beam halo after 22 focusing periods in a FODO channel. The initial distribution is an *rms* mismatched Gaussian beam. ($\sigma_0 = 70\,\text{deg}$, $\sigma = 35\,\text{deg}$)

WHY DO WE CARE?

1). BEAM LOSS OF HIGH ENERGY PARTICLES

$\Rightarrow$ ACCELERATOR ACTIVATION

EXAMPLE: FOR THE 1 GeV, 100 mA ACCELERATOR PRODUCTION OF TRITIUM (APT) PARAMETERS

1 nA/m OF BEAM LOSS ALLOWED FOR "HANDS ON" MAINTENANCE (FOR $E \gtrsim 1$ GeV)

$\left(\frac{1\,nA}{m} \times 1000\,m \Rightarrow 10^{-6}\,A \text{ loss allowed}\right)$

$\Rightarrow \frac{10^{-6}\,A}{0.1\,A} \Rightarrow 10^{-5}$ fractional beam loss allowed!!

2). BEAM LOSS ON WALLS

$\Rightarrow$ ELECTRON / GAS EMISSION FROM WALLS

FOR LONG PULSE OR DC MACHINES, OR STORAGE RINGS, WHERE ELECTRONS CAN BE DRAWN INTO BEAM AND ACCUMULATION $\Rightarrow$ INSTABILITIES AND NON-LINEAR FIELDS COULD DESTROY BEAM EMITTANCE OR EVEN DISRUPT BEAM.

3). INCREASE IN EMITTANCE

MAY REDUCE FOCUSABILITY FOR APPLICATIONS REQUIRING A SMALL BEAM SPOT.

WHAT IS THE BASIC PHYSICS?

RECALL DISPERSION RELATION FOR ENVELOPE MODES:

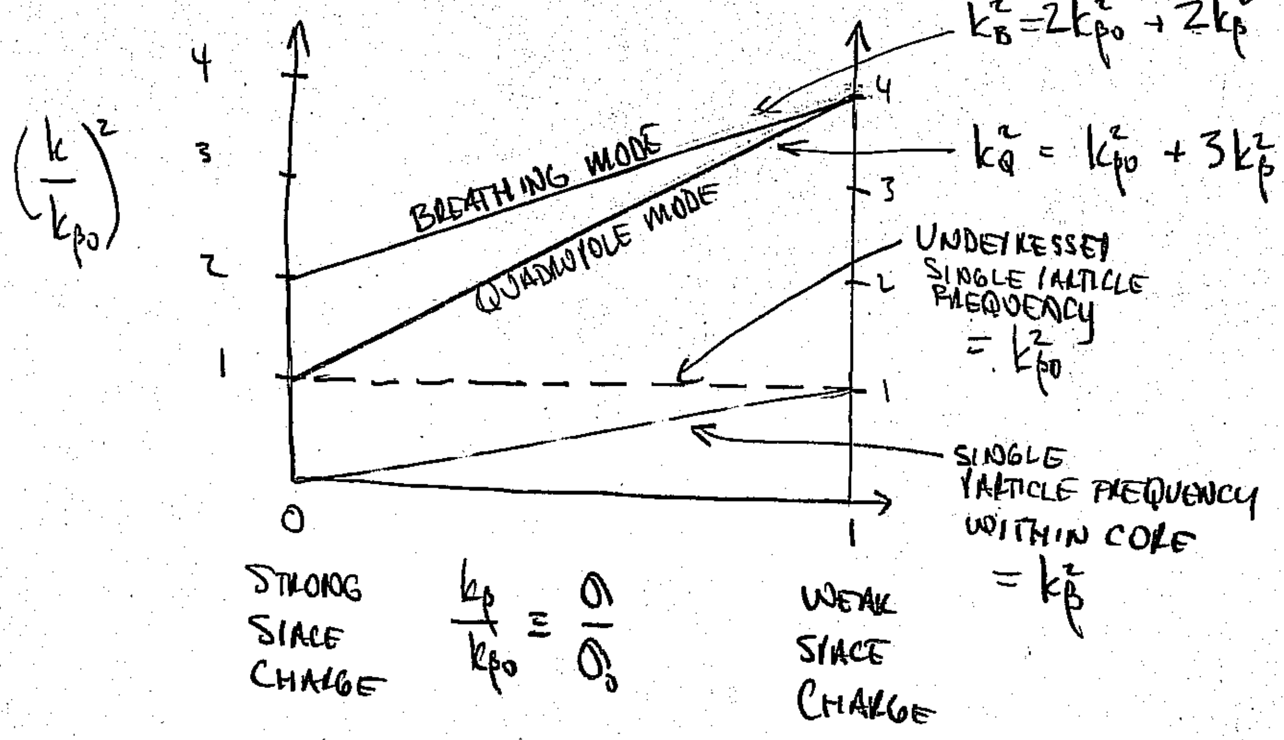

CONSIDER DIAGRAM FOR $\frac{k_B}{2}$ AND $\frac{k_Q}{2}$:

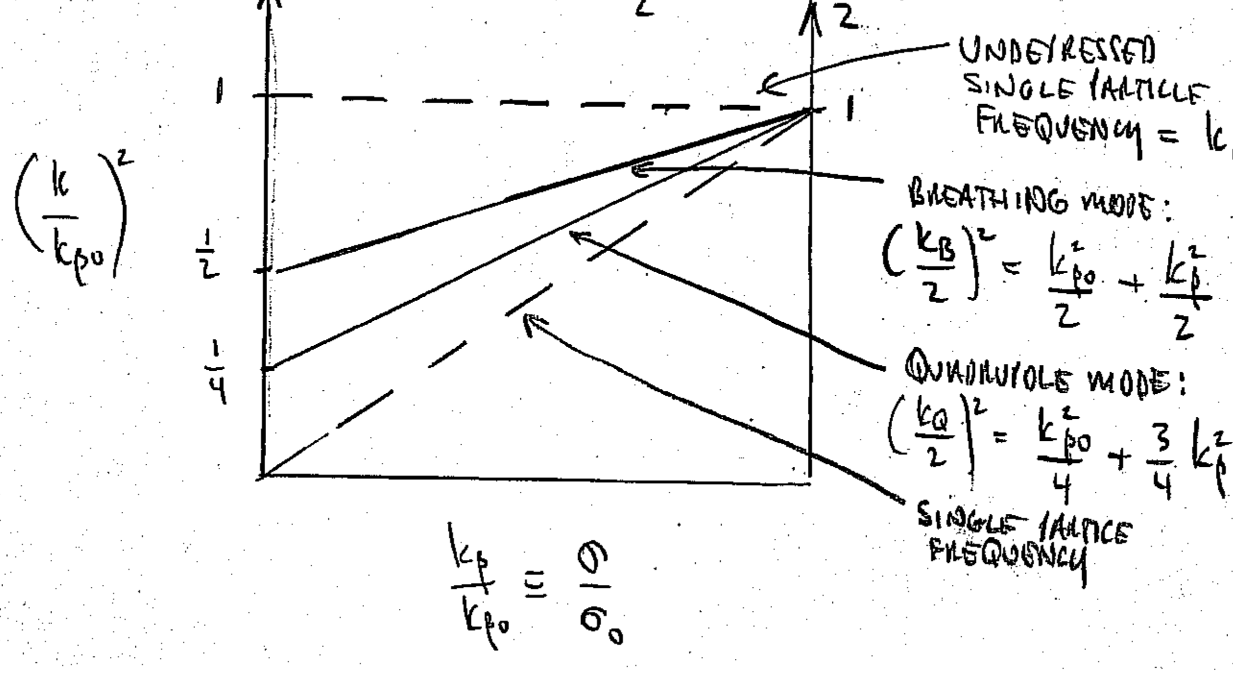

PARTICLES IN ORBITS FAR FROM CORE OSCILLATE AT FREQUENCY $k_{\beta 0}$, WHEREAS THOSE WITHIN CORE OSCILLATE AT FREQUENCY k_β.

AT INTERMEDIATE RADII, PARTICLE FREQUENCY = ENVELOPE FREQUENCY / 2

⇒ POSSIBILITY OF RESONANCE

⇒ MISMATCHES (EXCITATION OF ENVELOPE MODES) TOGETHER WITH COMMENSURATE PARTICLE FREQUENCY AND ENVELOPE HALF-FREQUENCY ARE THE SOURCE OF HALO.

SUGGESTS USING A <u>CORE / TEST PARTICLE</u> MODE TO EXPLORE THESE EFFECTS (O'CONNEL, WANGLER, JAMESON, RYNE, ...)

ASSUME KV ENVELOPE, OSCILLATING AT A MODE FREQUENCY.

USE KNOWN ANALYTIC FORMULAS INTERIOR AND EXTERIOR TO BEAM.

FOR EXAMPLE, FOR CIRCULAR BEAM

$$x'' = \begin{cases} -\left[k_{\beta 0}^2 - \frac{Q}{r_b^2}\right] x & \text{for } r < r_b \\ -\left[k_{\beta 0}^2 - \frac{Q}{r^2}\right] x & \text{for } r > r_b \end{cases}$$

Similarly for y.

$$r_b = r_{b0} + \delta r_b \cos(k_B s + \phi)$$

BREATHING MODE k_B

DISTRIBUTE TEST PARTICLES IN PHASE SPACE AND FOLLOW EVOLUTION OF ORBITS. ALLOWS PHYSICS STUDIES, WHICH CAN BE FOLLOWED UP WITH SELF-CONSISTENT PIC RUNS.

NOTE THAT THE SAME TYPE OF RESONANCES OCCUR LONGITUDINALLY, IN BUNCHED BEAMS.

BETATRON FREQUENCY → SYNCHROTRON FREQUENCY

$$k_{\beta 0} \rightarrow k_{s0}$$

$$k_\beta \rightarrow k_s \quad \text{(DEPRESSED SYNCHROTRON FREQUENCY)}$$

BREATHING MODE $\quad k_B \rightarrow k_L$ LOW FREQUENCY MODE

RESONANCE CONDITION

$$k_\beta < \frac{k_B}{2} < k_{\beta 0} \longrightarrow k_s < \frac{k_L}{2} < k_{s0}$$

ADDITIONAL COMPLICATION:

INTRINSIC NON-LINEARITY OF rf BUCKET

FROM Tom Wangler
Los Alamos National Lab

(20)

Stroboscopic Map (The Peanut Diagram)

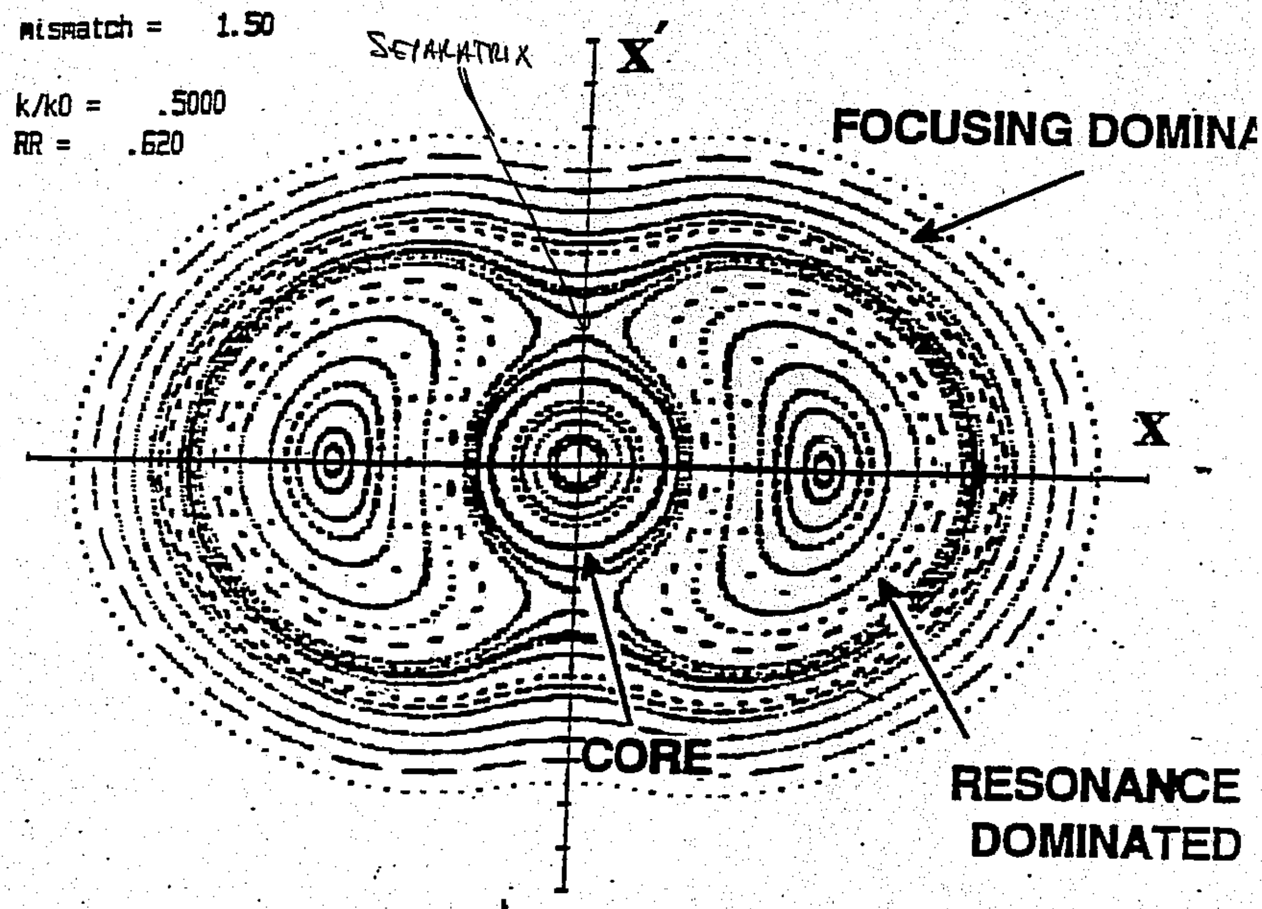

- Accumulate Many Snapshots of Phase Space Taken at Minimum Amplitude of Core Oscillation. (OR ANY PARTICULAR PHASE)
- Follow an Array of Particles to Obtain a "Trajectory Field".
- Regular Trajectories Appear as Smooth Curves.
- Chaotic Trajectories Appear as Stochastic Scatter.
- INITIAL POSITIONS OF PARTICLES IN PHASE SPACE WERE EQUALLY SPACED ALONG X & X′ AXES.

Orbits of resonant particles have amplitudes which are highly varying compared to non-resonant particles

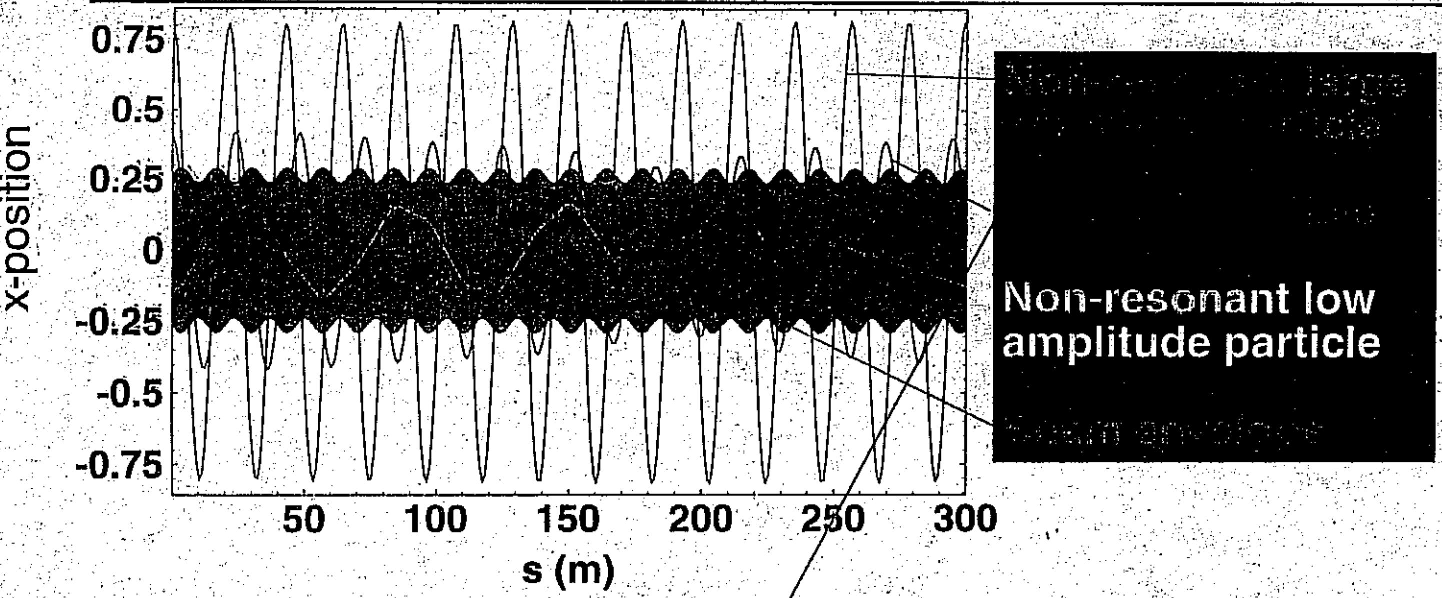

Oscillation frequency

$< k_{\beta 0}$ UNDEPRESSED BETATRON (PARTICLE OUTSIDE CORE)

$\sim k_{env}/2$ BREATHING MODE/2 $\approx k_{B}/2$

$\sim k_{\beta}$ DEPRESSED BETATRON (PARTICLE IN CORE)

k_{B} – BREATHING MODE

Poincare plot strobes phase space each envelope oscillation

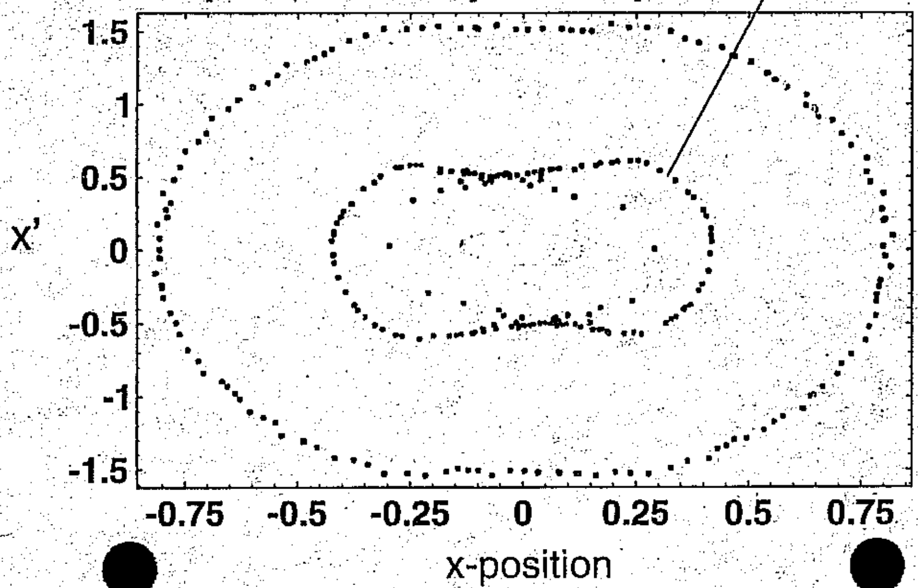

Note that resonant particle undergoes 11 oscillation periods, half of the 22 periods of the envelope. (The two non-resonant particles undergo 14 and 5 oscillation periods.)

Non-resonant large and small amplitude particles have regular orbits whereas resonant particles have varying amplitudes

(21)

Changing Poincare phase rotates diagram as expected

$k_L s = 0$

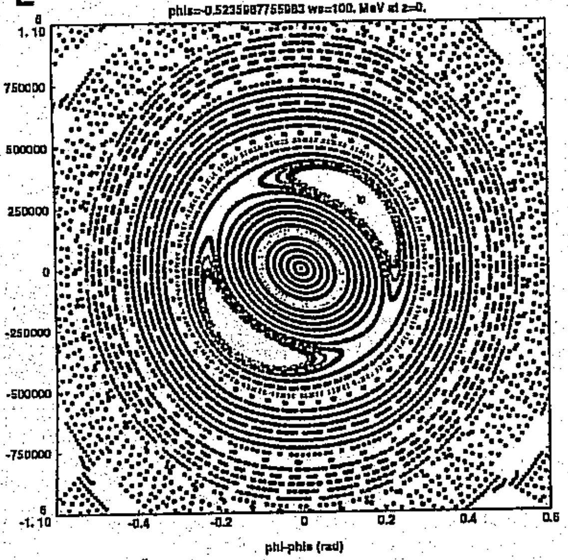

$k_L s = \pi/6$

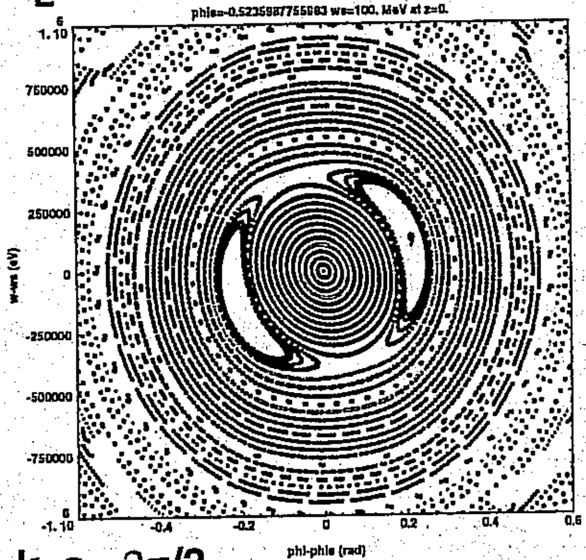

$k_L s = \pi/3$

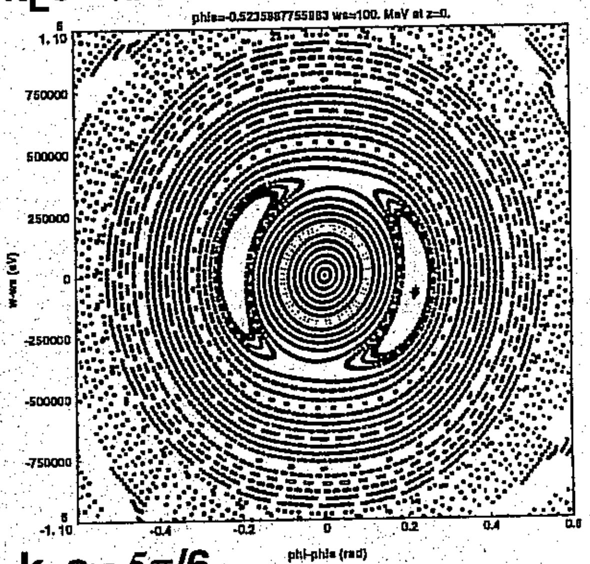

$k_L s = \pi/2$

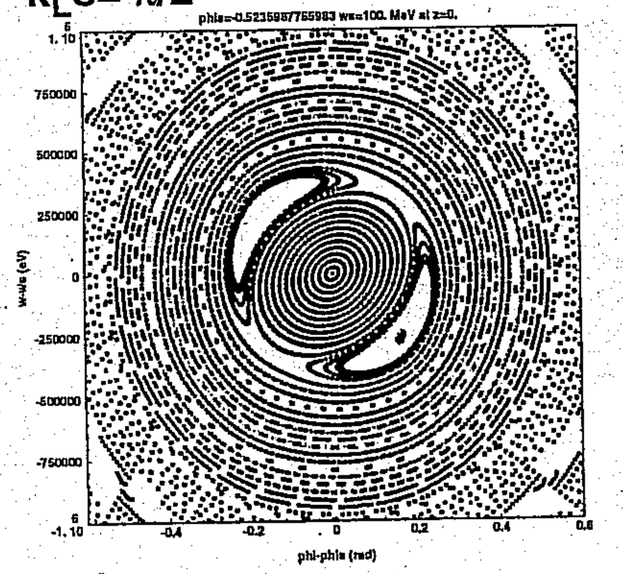

$k_L s = 2\pi/3$

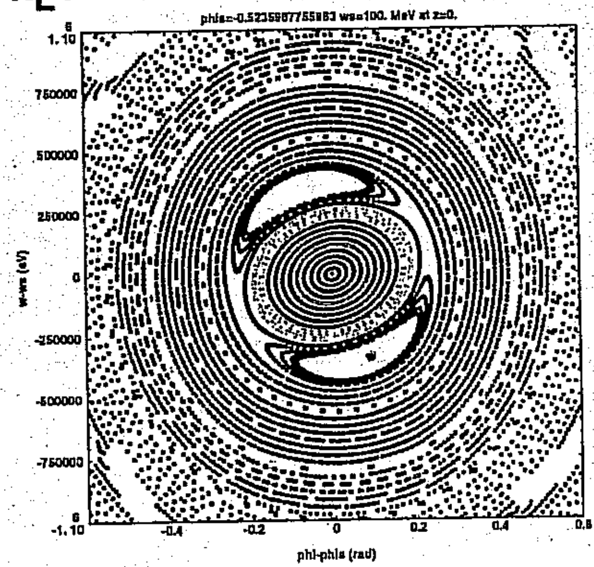

$k_L s = 5\pi/6$

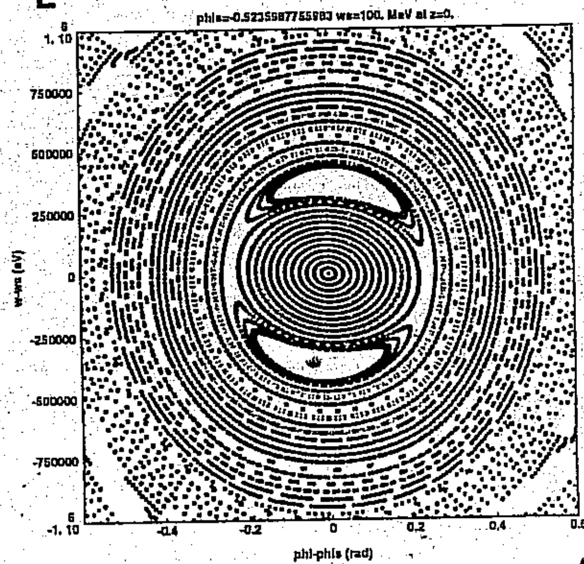

22

(CHANGING $k_L s$ by π ROTATES POINCARE PLOT BY π.)

$k_b^2/k_0^2 = 3 + \eta^2$ for the spherical bunch.

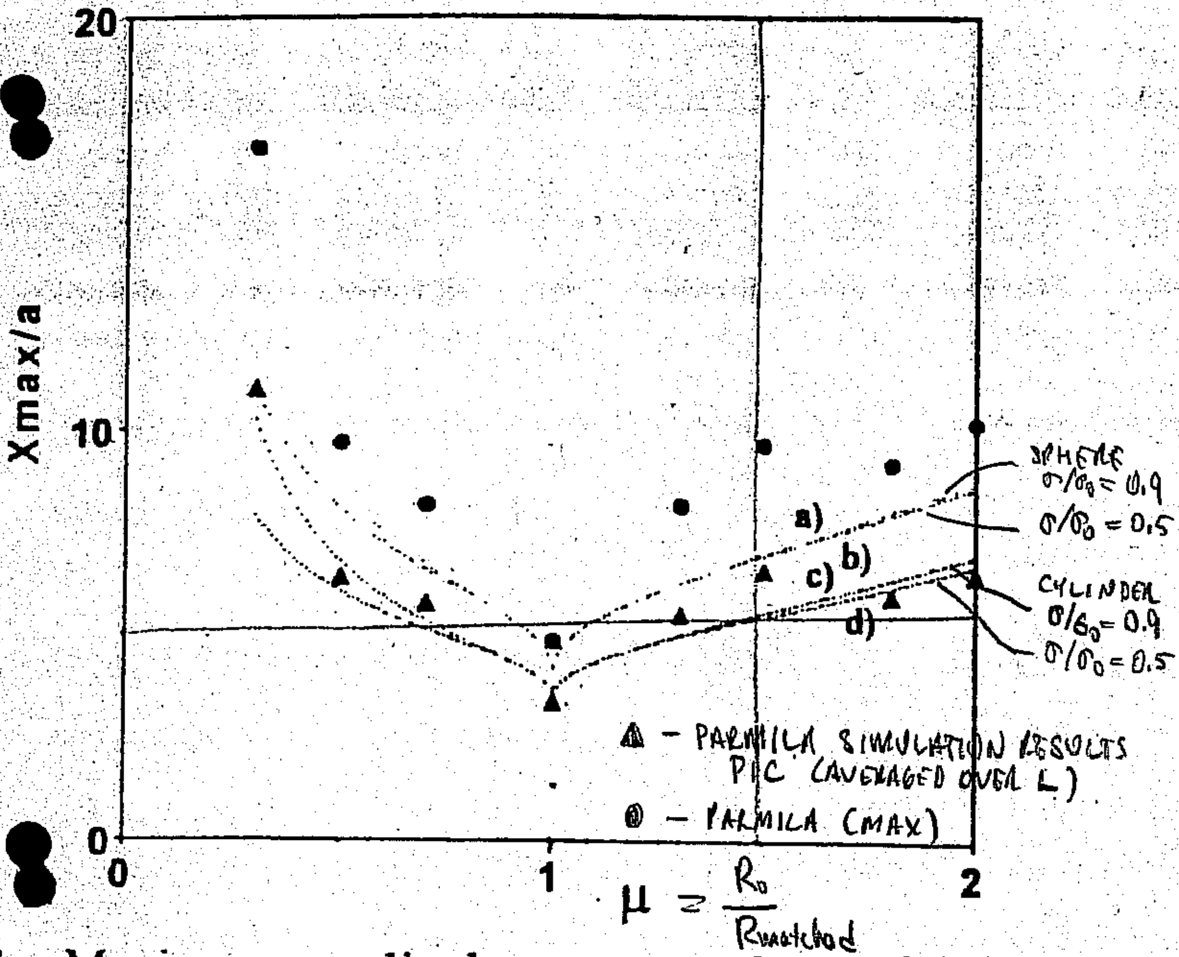

3. Maximum amplitudes versus μ for particles in the nance regions for the cylinder, and sphere models: a) re, $\eta = 0.9$, b) sphere, $\eta = 0.5$, c) cylinder, $\eta = 0.9$, and d) nder, $\eta = 0.5$. The triangles represent the smoothed MILA simulation results for comparison with the els, and the dots represent the maximum amplitudes ding quadrupole flutter.

a real linac, additional effects that are not included in the cle-core model, must be accounted for, such as beam-ope flutter associated with a quadrupole focusing system, eration, and the influence of other modes of the atched beam. We have conducted a test of the predictions he particle-core model, by carrying out PARMILA ations, using an r-z space-charge mesh with individual t 10^5 particles ...

note that t mesh to ens simulations

Work du that beam r the new lin mainly resp models to m formed. Th and one fo limited to a the strengt predictions bounds of th a linac. Sin produce sm consistent w that the brea the halo. To as well as p keeping ε sm can contribu beam-residu However, th than beam m

The author Gluckstern a

* Work supp

(24)

FROM WANGLER et al
XVIII Int'l LINAC CONF.
GENEVA, SWITZERLAND,
AUG. 26-30, 1996

WANGLER'S CORE/TEST PARTICLE RESULTS

$$\frac{X_{max}}{\langle x^2 \rangle^{1/2}} = A + B\left|\ln \mu\right| \qquad \mu = \left(\frac{r_{bi}}{r_{bo}}\right) = \frac{\text{INITIAL BEAM RADIUS}}{\text{MATCHED BEAM RADIUS}}$$

FOR

	σ/σ_0	A	B
CYLINDER	0.5	3.97	3.83
CYLINDER	0.9	3.91	4.25
SPHERE	0.5	4.87	5.30
SPHERE	0.9	4.81	5.56

Numerical Validation of 1D particle-core model

- Maximum beam size in large scale simulations found to be in excellent agreement with "peanut diagram" of particle-core model

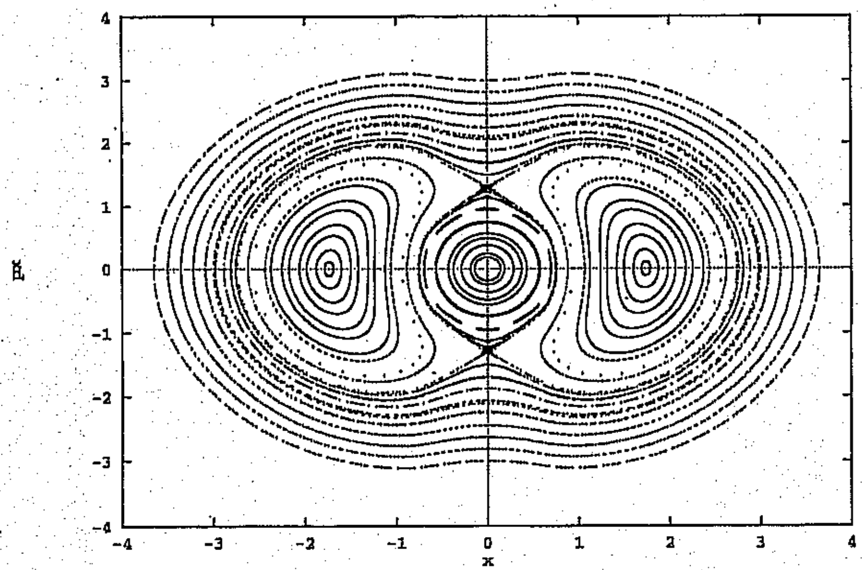

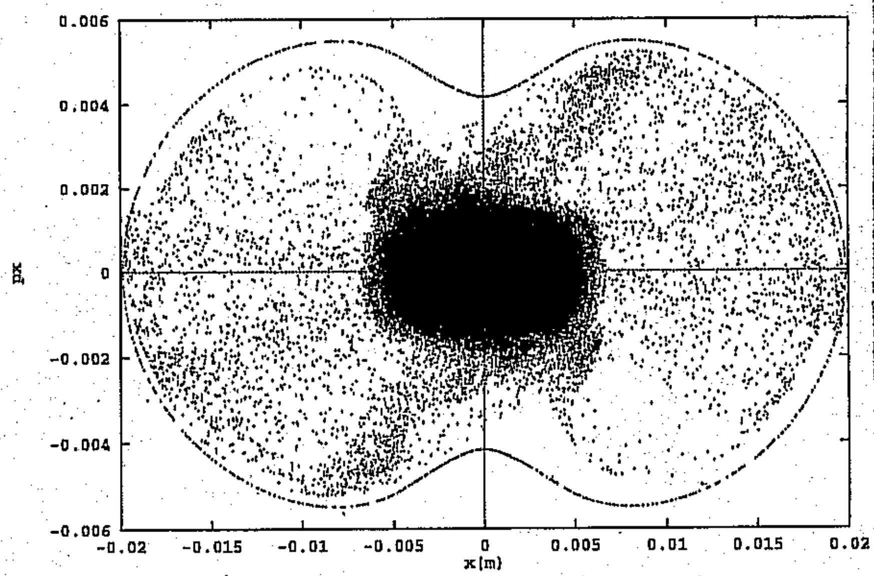

10

25

Longitudinal Particle-Core Model w/ RF Nonlinearity

- Core-Test-Particle (CTP) code
  exhibits asymmetry in peanut diagram also observed in simulations with HALO3D PIC code
- 200 mA simulation:

CTP test particles

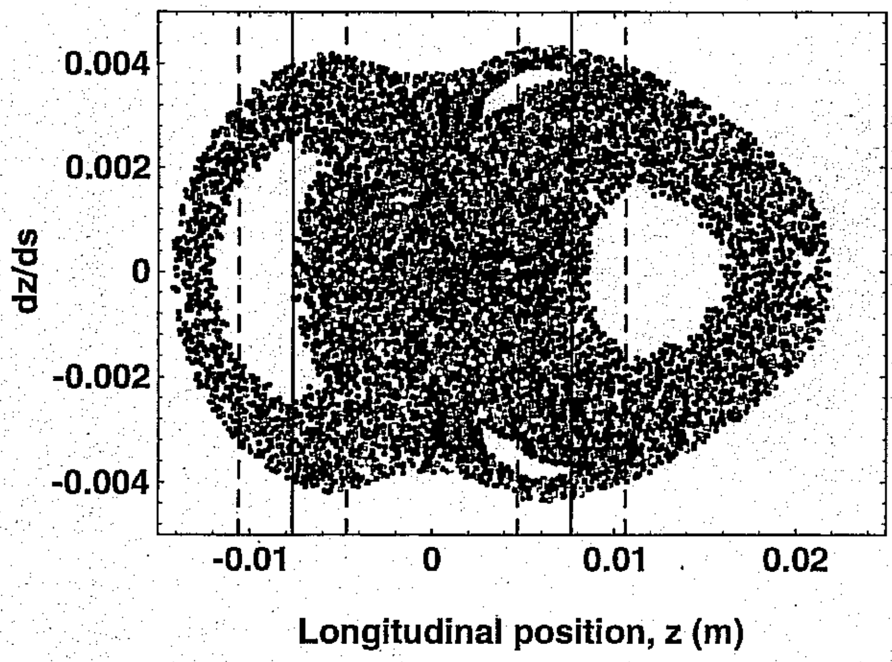

HALO3D beam particles

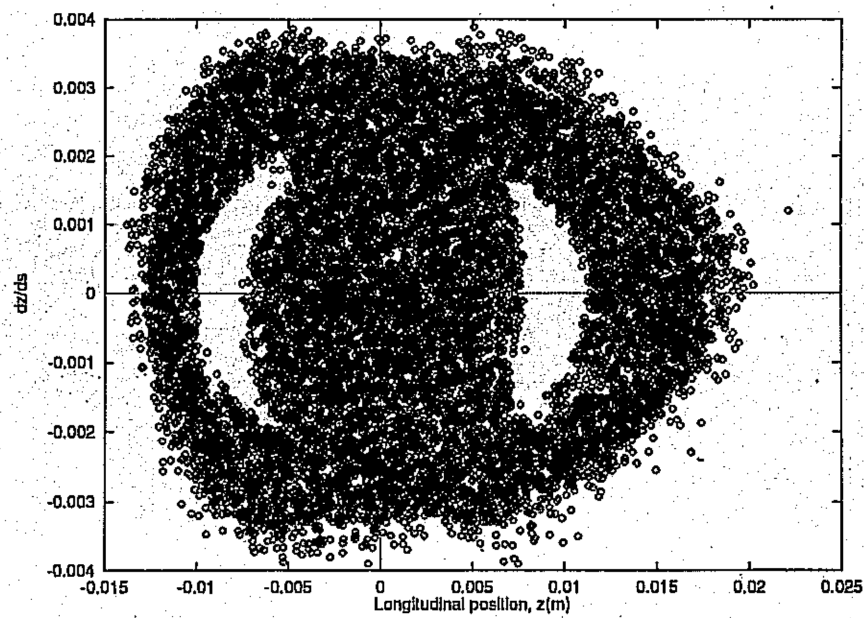

11

26

Longitudinal Particle-Core Model w/ RF Nonlinearity

- Absence of $k_L/2$ resonance (and associated halo) predicted by CTP analysis confirmed in HALO3D simulations
- 5 mA simulation:

CTP test particles

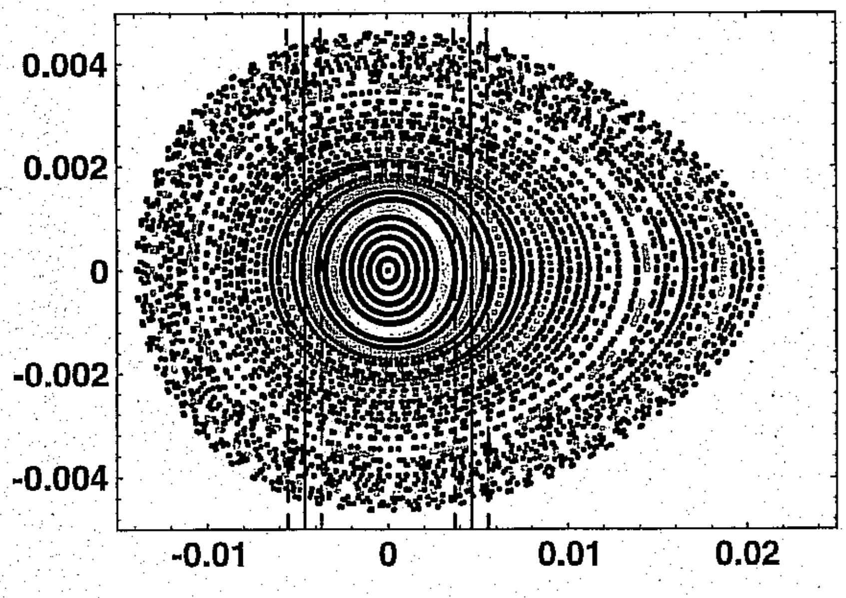

HALO3D test particles

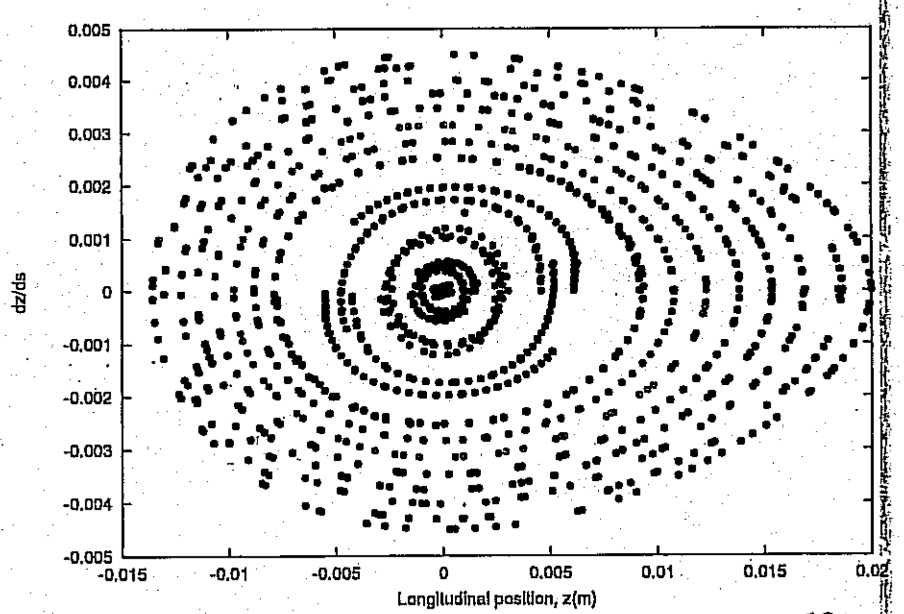

(27)

Model w/out RF Nonlinearity

- $k_L/2$ resonance present in 5 mA CTP run when nonlinearity is turned off. Also observed in HALO3D.

CTP test particles

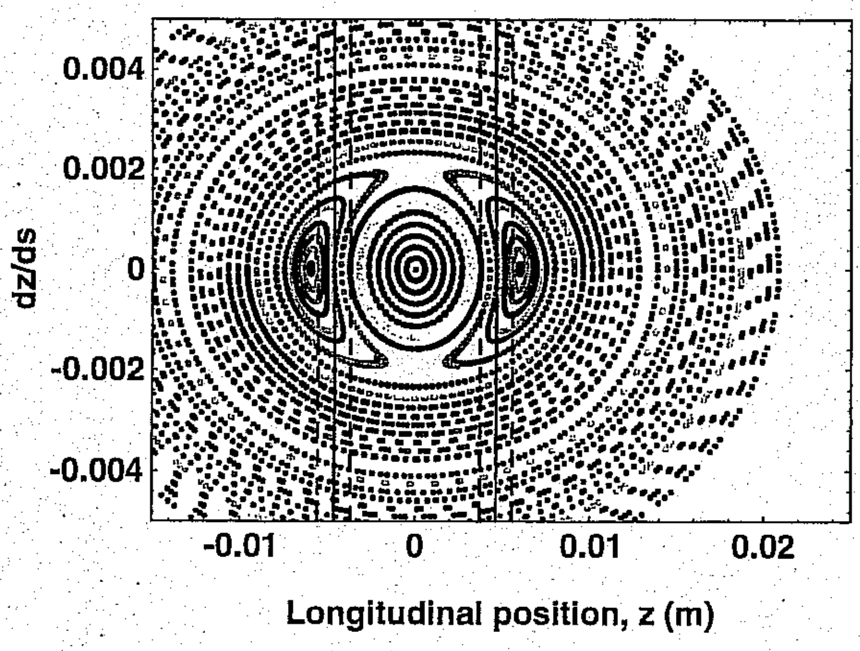

HALO3D test particles

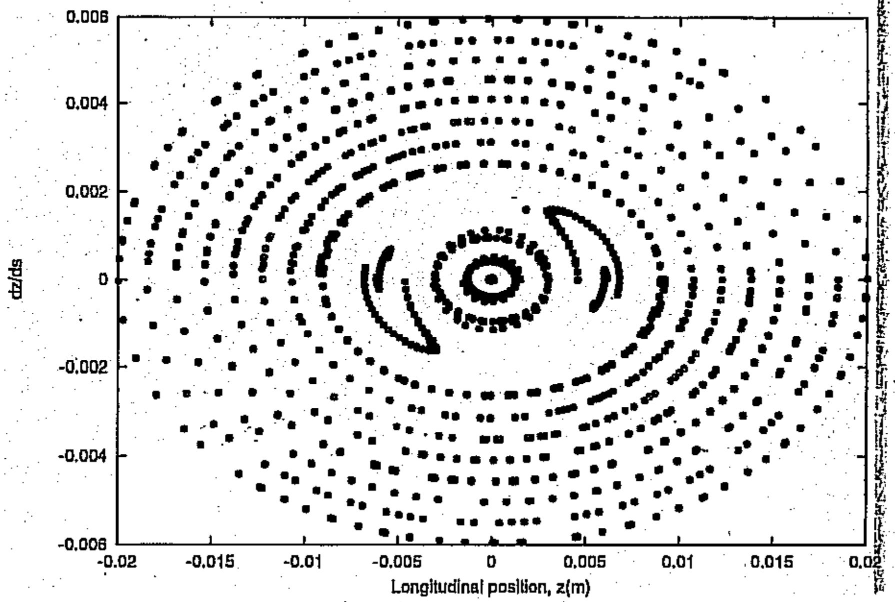

13

Numerically determined frequency and amplitude of particle oscillations: non-linear rf focusing

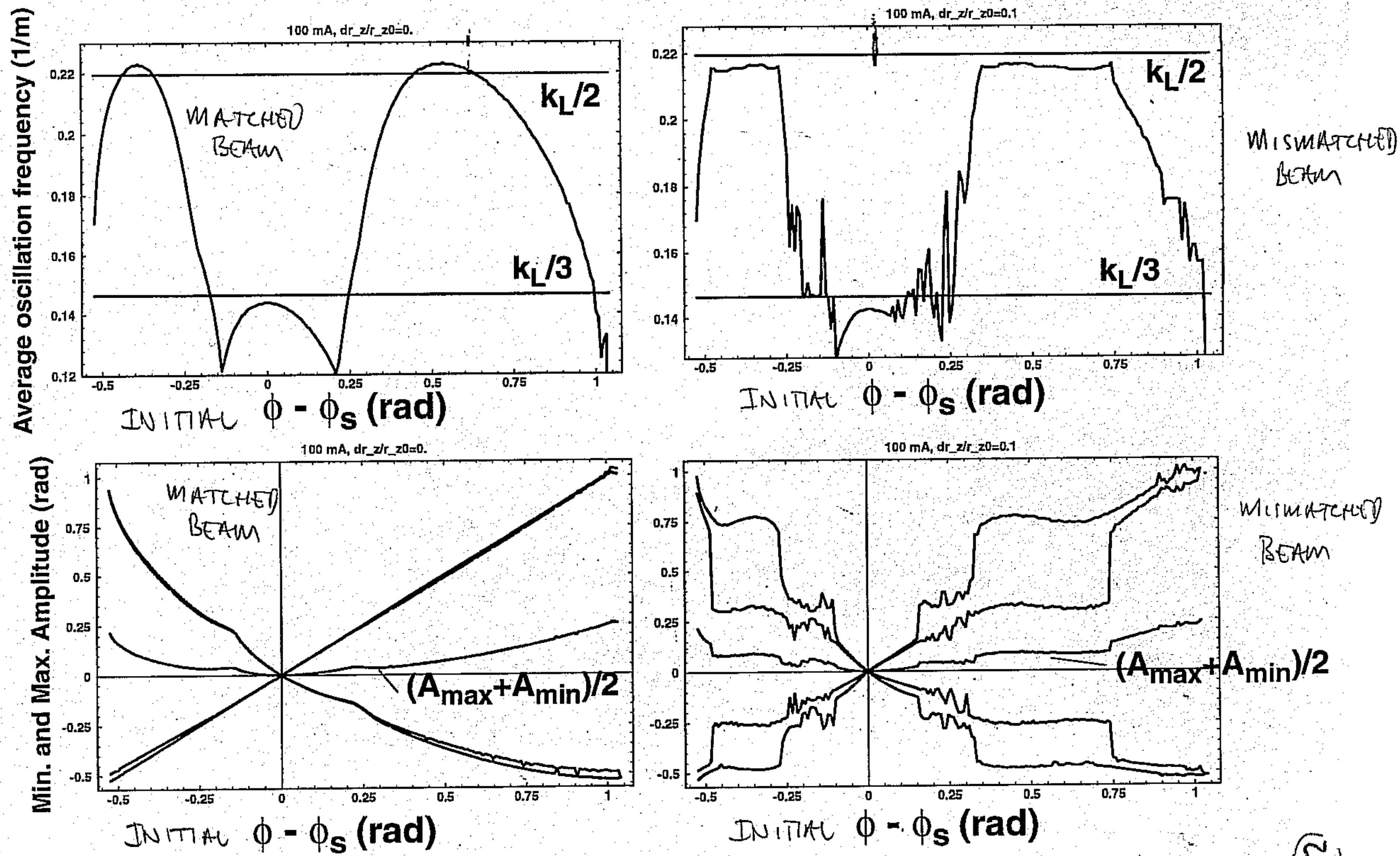

62

For non-linear rf, $k_L/2$ resonance occurs only over a range of current

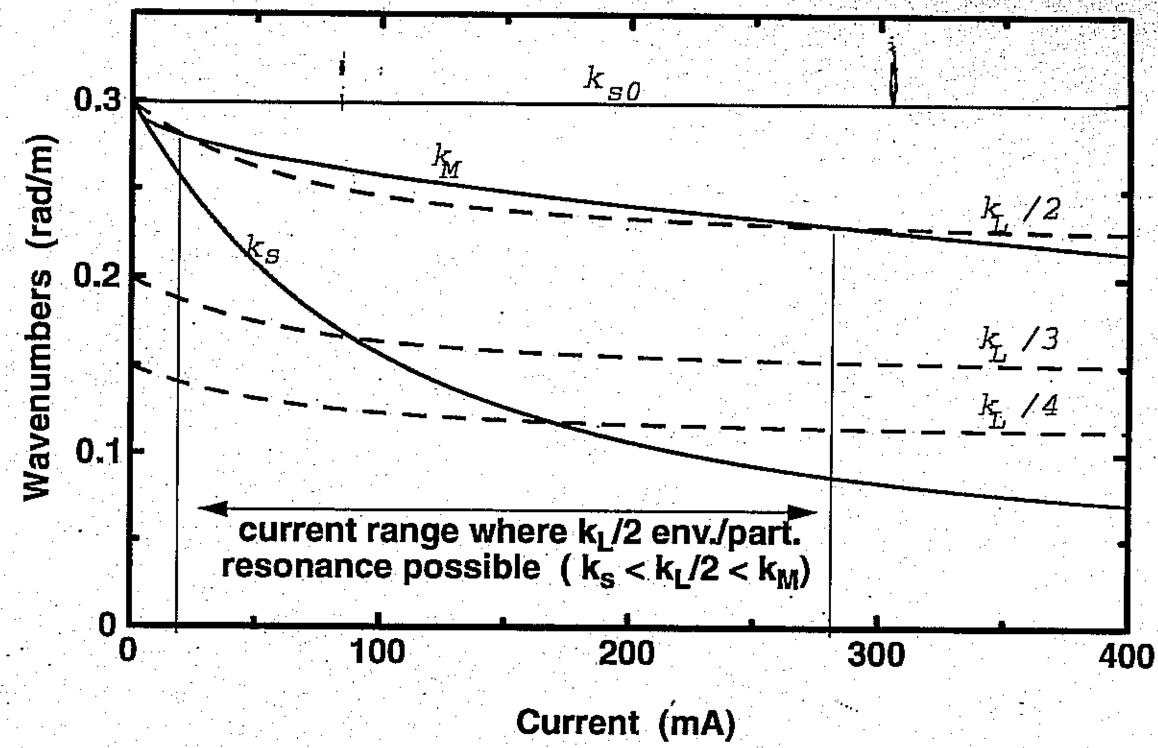

k_{s0} = single particle frequency

k_s = space-charge depressed synchrotron frequency

k_M = maximum particle oscillation frequency

k_L = longitudinal envelope oscillation frequency

30

(31)

Amplitude Phase Analysis

Gluckstern, Phys. Rev. Letters 73, 1247 1994

$$x'' + k_{\beta 0}^2 x = \begin{cases} \dfrac{Q}{r_b^2} x & \text{for } r < r_b \\ \dfrac{Q}{r^2} x & \text{for } r > r_b \end{cases}$$

Assume $r_b = r_{b0} + \epsilon \cos(k_B s)$

$$x'' + k_\beta^2 x = \overbrace{-\frac{Q}{r_{b0}^2} x \left(1 - \frac{r_{b0}^2}{r^2}\right) H(r - r_{b0})}^{\text{EXTERIOR}} + \overbrace{\frac{2\epsilon Q}{r_{b0}^2} x \cos k_B s \, H(r_{b0} - r)}^{\text{INTERIOR}}$$

NON-LINEAR TERM MAKES AMPLITUDE DEPENDENT FREQUENCY

ARISING SOLEY FROM ENVELOPE PERTURBATION; ALLOWS TRANSFER FROM CORE

$$H(x) = \begin{cases} 1 & x > 0 \\ 0 & x < 0 \end{cases}$$

$$k_\beta^2 \equiv k_{\beta 0}^2 - \frac{Q}{r_{b0}^2}$$

GLUCKSTERN TREATED GENERAL CASE OF ARBITRARY ANGULAR MOMENTUM. FOR ILLUSTRATION HERE I SET ANG. MOM = 0. $\Rightarrow x = r$

Use Phase Amplitude Method

$$\frac{x}{r_{b0}} \equiv A(s) \sin \psi(s) \qquad \psi \equiv k_\beta s + \alpha(s)$$

$$\frac{x'}{r_{b0}} \equiv k_\beta A(s) \cos \psi(s)$$

$k_\beta s$: Oscillation at depressed phase advance

$\alpha(s)$: SLOWLY CHANGING PHASE

Let $\quad x'' + k_\beta^2 x = f(x, s)$

$$= f(A, \psi, k_B s)$$

Note

$$\left.\begin{aligned} \frac{x'}{r_{b0}} &= A' \sin\psi + (k_\beta + \alpha') A \cos\psi \\ &= k_\beta A \cos\psi \end{aligned}\right\} \Rightarrow A' \sin\psi + \alpha' A \cos\psi = 0$$

$\frac{d}{ds}A$ & $\frac{d}{ds}\alpha$ CAN BE EXPRESSED IN TERMS OF f

$$x'' = k_p r_{bo} A' \cos\psi - k_p r_{bo} A \sin\psi \underbrace{(k_p + \alpha')}_{\psi'}$$

$$+ k_p^2 x = k_p^2 r_{bo} A \sin\psi$$

$$x'' + k_p^2 x = k_p r_{bo} A' \cos\psi - k_p r_{bo} A \sin\psi \, \alpha' = f(x, s)$$

ALSO $$A' \sin\psi + A \cos\psi \, \alpha' = 0$$

$$\begin{bmatrix} k_p r_{bo} \cos\psi & -k_p r_{bo} \sin\psi \\ \sin\psi & A \cos\psi \end{bmatrix} \begin{bmatrix} A' \\ \alpha' \end{bmatrix} = \begin{bmatrix} f \\ 0 \end{bmatrix}$$

INVERTING MATRIX:

$$\begin{bmatrix} A' \\ \alpha' \end{bmatrix} = \frac{1}{A k_p r_{bo}} \begin{bmatrix} A \cos\psi & k_p r_{bo} \sin\psi \\ -\sin\psi & k_p r_{bo} \cos\psi \end{bmatrix} \begin{bmatrix} f \\ 0 \end{bmatrix}$$

$$A' = \frac{\cos\psi}{k_p r_{bo}} f$$

$$\alpha' = \frac{-\sin\psi}{k_p r_{bo} A} f$$

USING THESE DEFINITIONS THE EQUATION OF MOTION CAN BE EXPRESSED AS:

$$A' = \frac{1}{k_\beta r_{\beta o}} f(A, \psi, k_B s)\cos\psi$$

$$\alpha' = \frac{-1}{k_\beta A r_{bo}} f(A, \psi, k_B s)\sin\psi$$

At resonance we expect $2k_\beta - k_B \sim 0$,
so define $\Psi = 2\psi - k_B s = (2k_\beta - k_B)s + 2\alpha$

$$\Rightarrow \Psi' = (2k_\beta - k_B) + 2\alpha'$$

ELIMINATE $k_B s$ in $f(A, \psi, k_B s)$ using

$$k_B s = 2\psi - \Psi$$

AVERAGE OVER ALL NON-RESONANT FREQUENCY COMPONENTS, FOR RESONANT PARTICLE EQUATIONS OF MOTION:

$$A_r' = \frac{1}{k_\beta r_{bo}} \int_{-\pi}^{\pi} \frac{d\psi}{2\pi} f(A_r, \Psi_r, \psi)\cos\psi$$

$$\alpha_r' = \frac{-1}{r_{bo} k_\beta A_r} \int_{-\pi}^{\pi} \frac{d\psi}{2\pi} f(A_r, \Psi_r, \psi)\sin\psi$$

A_r & $\Psi_r = (2k_\beta - k_B)s + 2\alpha$ are held fixed during integration.

THE RESULT is

$$A_r' = F_1(A_r, \Psi_r)$$
$$\Psi_r' = (2k_\beta - k_B) + 2F_2(A_r, \Psi_r)$$

where F_1 & F_2 are explicit functions A_r & Ψ_r

Let $\omega = A_r^2$

$$\omega' = 2A_r A_r' = 2A_r F_1(A_r, \Psi_r) = 2\omega^{1/2} F_1(\omega^{1/2}, \Psi_r)$$
$$\Psi' = (2k_\beta - k_B) + 2F_2(A_r, \Psi_r)$$

ω & Ψ are conjugate variables, and the resonant particle equation of motion can be derived from an s-independent Hamiltonian H as:

$$\omega' = \frac{\partial H}{\partial \Psi} \qquad \Psi' = -\frac{\partial H}{\partial \omega}$$

GLUCKSTEIN FOUND A CONSTANT OF THE MOTION $H_r(\omega, \Psi)$ which satisfies Hamilton's EQUATIONS.

RESONANT PARTICLE WOULD STAY ON LINES OF CONSTANT H.

(35)

GLUCKSTERN'S SIMPLIFIED EXAMPLE

$$x'' + k_\beta^2 x = -\frac{Q}{r_{b0}^4} x^3 + \frac{2\epsilon Q}{r_{b0}^2} x \cos k_B s$$

NON-LINEAR FORCE

OSCILLATING CORE

THIS example:

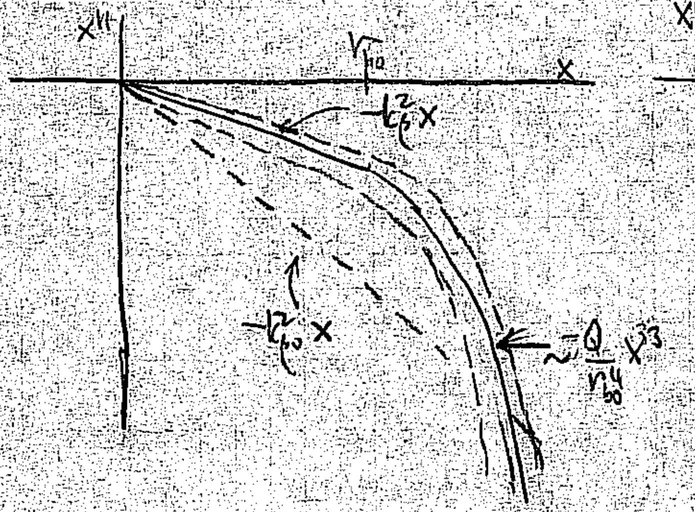

ACTUAL MODEL OF BREATHING BEAM

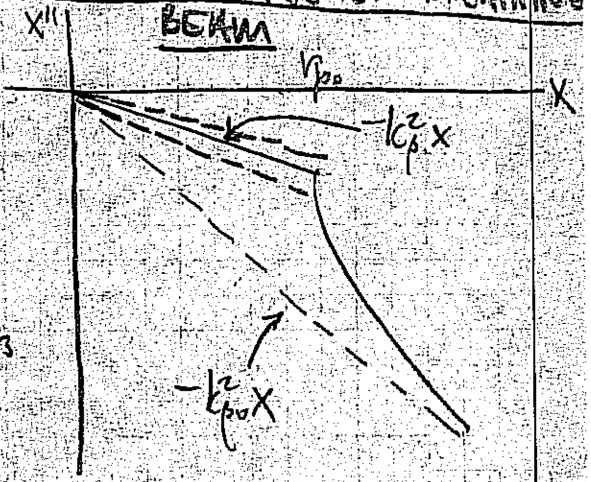

$$x'' + k_\beta^2 x = \frac{-Q}{r_{b0}^4} x^3 + \frac{2\epsilon Q}{r_{b0}^2} x \cos k_\beta s$$

$$= f(x, s)$$

$$= \frac{-Q}{r_{b0}} A^3 \sin^3\psi + \frac{2\epsilon Q}{r_{b0}} A \sin\psi \cos k_\beta s$$

(when $\frac{x}{r_{b0}} = A\sin\psi$ & $\frac{x'}{r_{b0}} = k_\beta A\cos\psi$)

$$\Rightarrow A' = \frac{\cos\psi}{k_\beta r_{b0}} f = \frac{-Q}{k_\beta r_{b0}^2} A^3 \sin^3\psi\cos\psi + \frac{\epsilon Q}{k_\beta r_{b0}^2} A \sin 2\psi \cos k_\beta s$$

$$\alpha' = \frac{-\sin\psi}{k_\beta r_{b0} A} f = \frac{Q}{k_\beta r_{b0}^2} A^2 \sin^4\psi + \frac{2\epsilon Q}{k_\beta r_{b0}^2} \sin^2\psi \cos k_\beta s$$

Using $\Psi \equiv 2\psi - k_\beta s \Rightarrow \cos k_\beta s = \cos[2\psi - \Psi]$

$$= \cos[2\psi]\cos[\Psi] + \sin[2\psi]\sin[\Psi]$$

TRIG IDENTITIES:

$$\sin 2\psi \cos k_\beta s = \frac{1}{2}\sin\Psi - \frac{1}{2}\cos 4\psi \sin\Psi + \frac{1}{2}\sin 4\psi \cos\Psi$$

$$\sin^4\psi = \frac{3}{8} - \frac{1}{2}\cos 2\psi - \frac{1}{8}\cos 4\psi$$

$$\sin^2\psi \cos k_\beta s = \cos\Psi\left[-\frac{1}{4} + \frac{1}{2}\cos 2\psi - \frac{1}{4}\cos 4\psi\right] + \sin\Psi\left[\frac{1}{2}\sin 2\psi - \frac{1}{4}\sin 4\psi\right]$$

$$\sin^3\psi\cos\psi = \frac{1}{4}\sin 2\psi - \frac{1}{8}\sin 4\psi$$

$$\Rightarrow \quad A_r' = \frac{\epsilon Q}{2k_p r_{b0}^2} A_r \sin \Psi_r$$

$$\Psi_r' = (2k_p - k_B) + 2\alpha_r'$$

$$= (2k_p - k_B) + \frac{3Q}{4k_p r_{b0}^2} A_r^2 + \frac{\epsilon Q}{k_p r_{b0}^2} \cos \Psi$$

DEFINE $w = A_r^2$

$$w' = 2A_r A_r' = \frac{\epsilon Q}{k_p r_{b0}^2} w \sin \Psi_r$$

$$\Psi_r' = (2k_p - k_B) + \frac{3Q}{4k_p r_{b0}^2} w + \frac{\epsilon Q}{k_p r_{b0}^2} \cos \Psi$$

A Hamiltonian can be found satisfying Hamilton's equations:

$$H = (2k_p - k_B) w + \frac{3}{8} \frac{Q}{k_p r_{b0}^2} w^2 + \frac{\epsilon Q}{k_p r_{b0}^2} w \cos \Psi$$

THIS CAN BE EXPRESSED AS:

$$\epsilon \cos \Psi = \Delta - \frac{3}{8} w - \frac{C}{w}$$

where C is determined by initial conditions and:

$$\Delta = k_p (k_B - 2k_p) r_{b0}^2 / Q$$

(NOTE: $k_B^2 = 4k_p^2 + 2Q/r_{b0}^2$ for breathing mode).

. (2.4)) and solv-

$\cos pz]$, (2.5)

$z]$. (2.6)

oscillatory terms
number $2q - p$

(2.7)

$\cos\Psi$, (2.8)

of this resonant
al of the motion

, (2.9)

and where the
he initial values
ape equation we
breathing mode,

, (2.10)

d by the space

Guided by the parametrization of the x and
separately, the amplitude-phase parametrizati
two-dimensional oscillation is written as

$$s = \frac{w^2 + L^2}{2w} - \frac{w^2 - L^2}{2w}\cos(2qz + \gamma).$$

Here w and γ are slowly varying amplitude
parameters which would be constant if the rig
Eq. (2.11) vanished. We now write

$$s' = q\,\frac{w^2 - L^2}{w}\sin(2qz + \gamma)$$

and use Eq. (2.11) and the required connectio
w' and γ' implied by Eq. (2.13) to obtain explic
sions for w' and γ'. We then average over osci

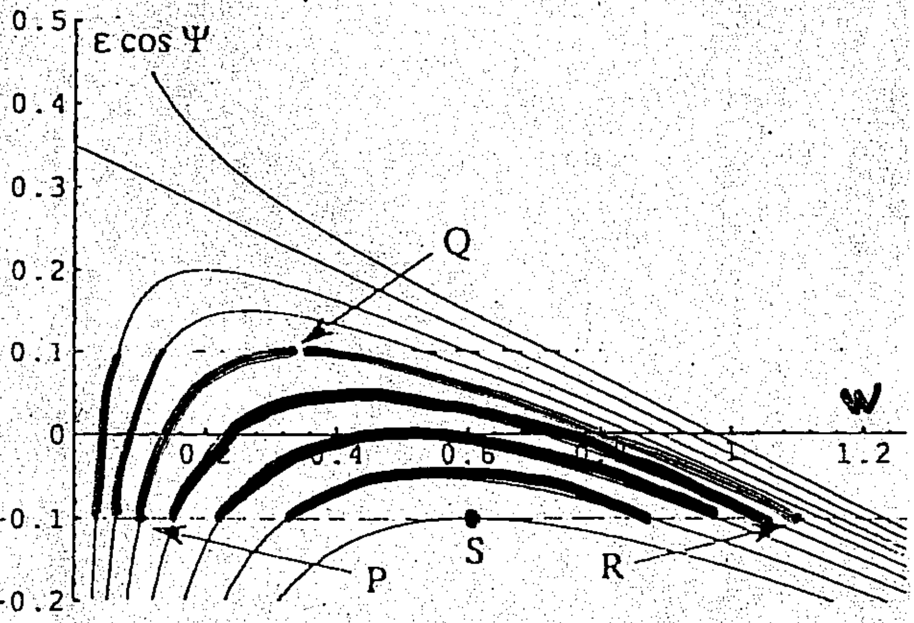

FIG. 1. Plot of $\epsilon\cos\Psi$ vs w for the simplified n
$\Delta = 0.35$.

39

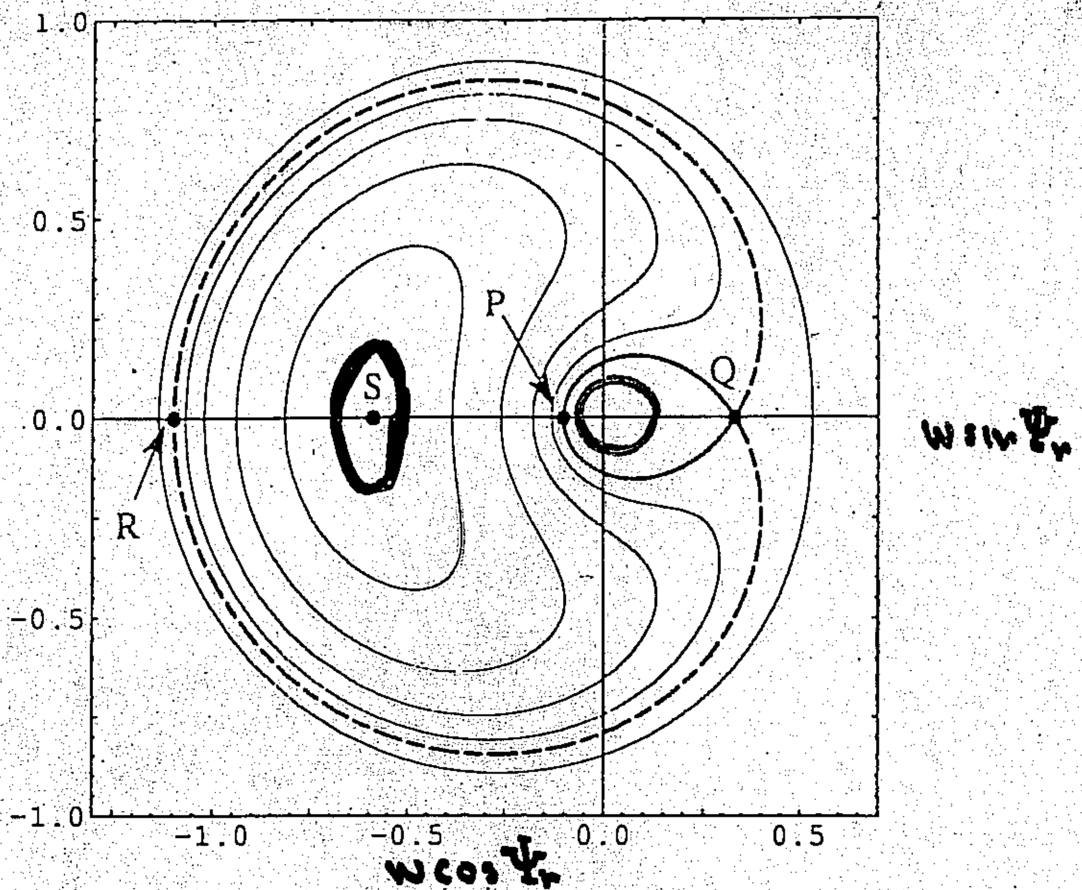

FIG. 2. Polar plot of w vs Ψ for the trajectories corresponding to the parametric resonance using $\Delta = 0.35$, $\epsilon = 0.1$, and the simplified model.

all wave numbers except $2q - p$, being careful to include the step functions as we obtain these averages. The final equations for w' and Ψ' [$\Psi = (2q - p)z + \gamma$] are similar to Eqs. (2.7) and (2.8) and again lead to an integral of the motion, which now is

$$g(1 - h)\epsilon \cos\Psi = f\Delta - t - C, \qquad (2.14)$$

where $f(w) = (w^2 + L^2)/2w$, $g(w) = (w^2 - L^2)/2w$. Here

(40)

(2.15)

Also

(2.16)

The arc-
quadrant.
ependence
ession for
; Eq. (2.6)

fect when
rough the
$\Delta = 0.35$
ry similar
Fig. 4 for
model in
cale for w
ning with
en by the

am.—The
to

Therefore the distribution in L for a K-V beam is unif
from $L = -1/2$ to $L = 1/2$ and vanishes for $|L| > 1/$

IV. Implications of the model.—Since the breat
K-V beam is a solution of the Vlasov equation, parti
within the core will continue to remain there, eve
the presence of the resonant interaction. If howe

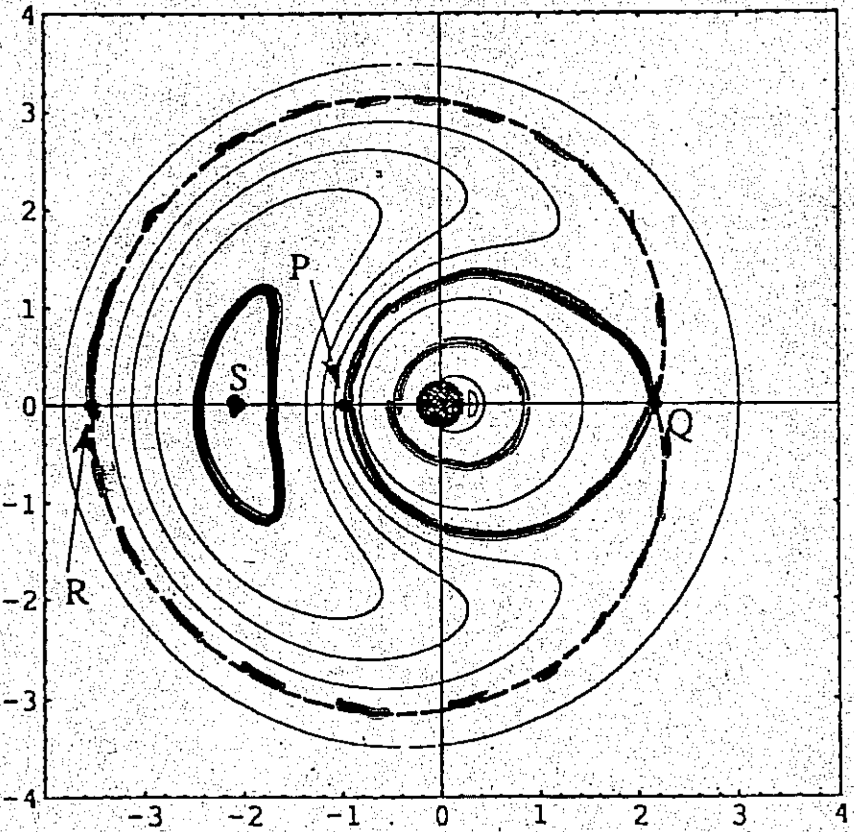

FIG. 4. Polar plot of w vs Ψ for the trajectories correspon
to the parametric resonance using $\Delta = 0.35$, $L = 0$, $\epsilon =$
and the exact model.

1

Bob Gluckstern
Univ. of Maryland.

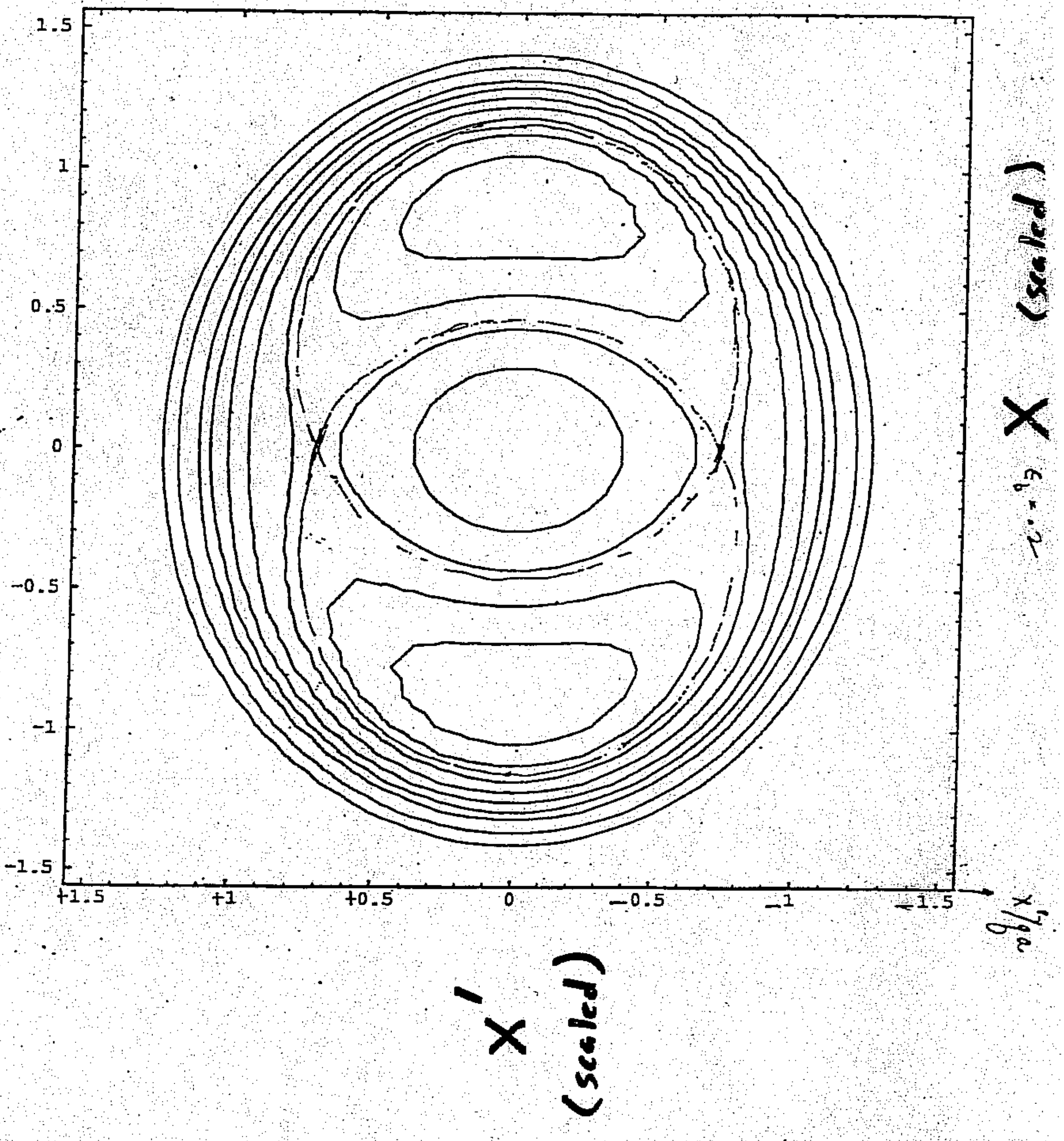

Fig 3.

FROM Tom Wangler
Los Alamos National Lab

Stroboscopic Map
(The Peanut Diagram)

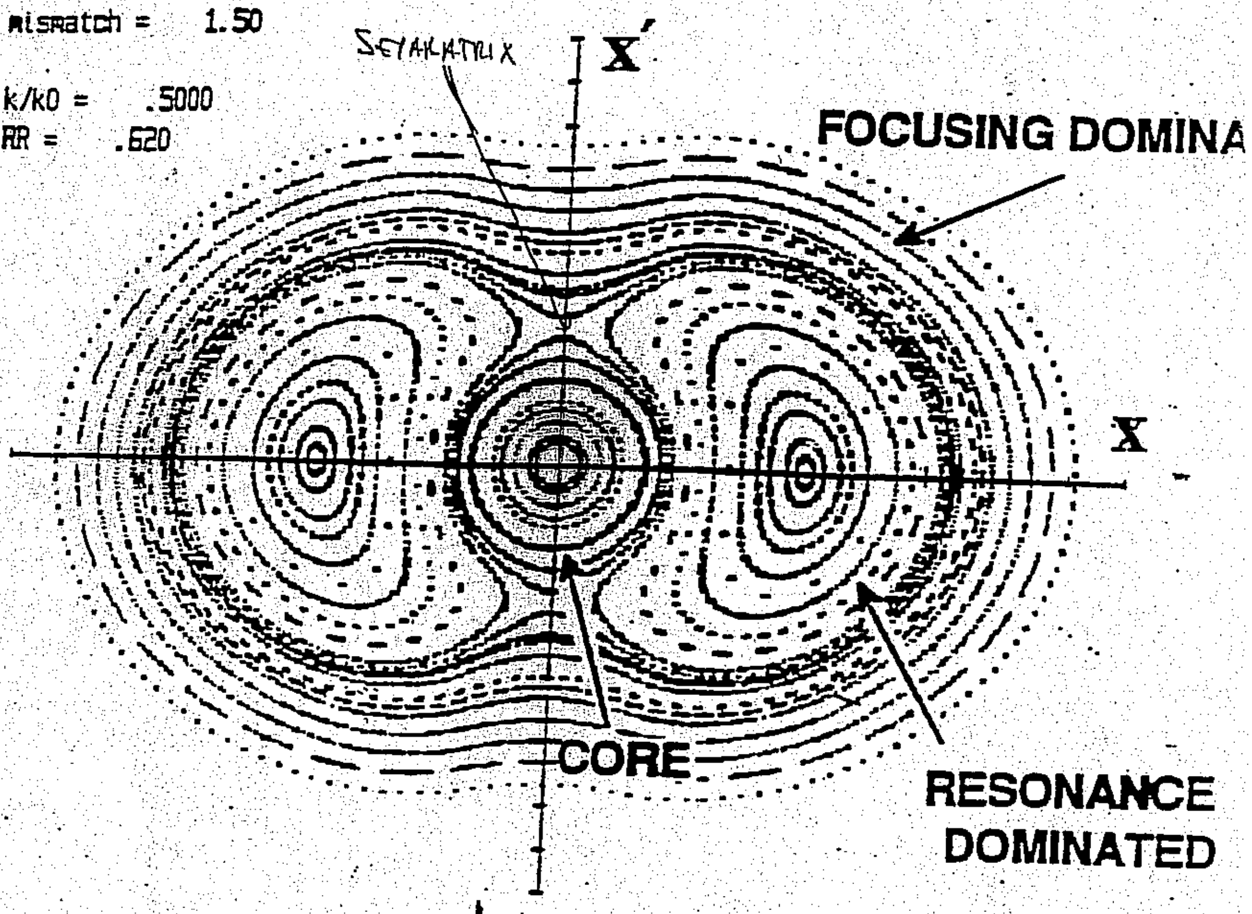

- Accumulate Many Snapshots of Phase Space Taken at Minimum Amplitude of Core Oscillation. (OR ANY PARTICULAR PHASE)
- Follow an Array of Particles to Obtain a "Trajectory Field".
- Regular Trajectories Appear as Smooth Curves.
- Chaotic Trajectories Appear as Stochastic Scatter.
- INITIAL POSITIONS OF PARTICLES IN PHASE SPACE WERE EQUALLY SPACED ALONG X & X' AXES.

(43)

Analytic Model for Halo Formation in High Current Ion Linacs

Robert L. Gluckstern
Physics Department, University of Maryland, College Park, Maryland 20742
(Received 8 March 1994)

We construct an azimuthally symmetric 2D model for halo formation in high current ion linacs. The driving term, a "breathing" oscillation caused by a transverse mismatch along the linac, leads to growth of ion amplitudes in the core through the parametric resonance. As the ion amplitude grows, its wave number increases, enhancing the resonance. This leads to the formation of a halo surrounding the core. We explore the dependence of this mechanism on the tune depression and the size of the mismatch. The model agrees well with simulations at Los Alamos, but does not yet include the effects of chaos observed in the simulations as the tune depression becomes severe.

PACS numbers: 41.85.−p, 29.17.+w, 29.27.Bd

I. Introduction.—High current, high duty factor ion linacs have become increasingly attractive in recent years. Among possible applications are heavy ion drivers for thermonuclear energy production, production of tritium, transmutation of radioactive wastes, and production of radioactive isotopes for medical use.

Obviously, it is desirable to accelerate the maximum possible current in such linacs. Much work has been done to explore the optimum transverse phase space distribution in such beams. In particular, the Kapchinsky-Vladimirsky (K-V) distribution [1] is simplest to analyze, since this projection into real space has a uniform density and therefore linear space charge forces. The stability of the K-V distribution has been analyzed and approximately confirmed by numerical simulations. Nevertheless it appears that, particularly at high currents, the K-V and other equilibrium distributions evolve to ones with rounded edges and tails. In many cases involving high peak current, the distribution spins off a cluster of particles in the form of a halo surrounding a dense core. This halo is seen in simulations as well as in actual linacs, such as LAMPF [2]. And efforts to remove the halo by collimation have been largely unsuccessful since the halos almost always regenerate.

It is clear that the halos will produce unacceptably high levels of radioactivity in high current, high duty factor linacs. For this reason considerable effort has recently been devoted to exploring their detailed structure and understanding the mechanism or mechanisms by which the halos are produced [3–6]. What has been learned is that halos are most likely to be produced at transition locations, such as where there are discontinuities in frequency, structure geometry, transverse focusing pattern, accelerating gradient and phase, etc.

In the present paper, we propose an analytic model for halo formation which appears to reproduce the main features seen in simulations and in actual linacs. In particular we consider a circular cw beam with a K-V core distribution and explore the motion of individual ions passing through the core. Since energy transfer between ions and the core can take place only if the core has a time dependent behavior, we consider the driving mechanism to be a "breathing" oscillation of the core. We then explore the resonant (parametric) interaction between the breathing core and the ions oscillating about and through the core. Of particular importance is the dependence of the frequency of each oscillating ion on its amplitude, which is related to the fraction of the oscillation for which the ion is within the core.

In spite of the fact that the actual distribution will have nonlinear fields, the use of a K-V distribution for the analysis leads us to a very likely mechanism for the development of the halo. In particular, the results provide an explanation for the low density region around the core which is surrounded by a somewhat higher density halo ring. This explanation will probably still apply for other self-consistent distributions.

II. Model.—We consider an azimuthally symmetric K-V core of radius a for which the equation of motion of an ion is

$$x'' + k^2 x = x \begin{Bmatrix} \kappa/a^2, & r \le a \\ \kappa/r^2, & r \ge a \end{Bmatrix}, \tag{2.1}$$

where the prime stands for d/dz, and k is the wave number of the transverse motion in the absence of space charge. The perveance of the beam, $\kappa = eI/2\pi\epsilon_0 m v^3$, is a dimensionless parameter proportional to the current I, where e, m, and v are the charge, mass, and ion velocity, and ϵ_0 is the permittivity of free space. The equation for y is identical to Eq. (2.1).

We now assume a core oscillation of wave number p of the form $a \to a(1 - \epsilon \cos pz)$ and expand a^{-2} in Eq. (2.1) to first order in ϵ, the relative oscillation amplitude. After some algebra, Eq. (2.1) can be written as

$$x'' + q^2 x = -\frac{\kappa}{a^2} x \left(1 - \frac{a^2}{r^2}\right) \Theta(r - a) + \frac{2\epsilon\kappa}{a^2} x \cos pz \, \Theta(a - r), \tag{2.2}$$

where $\Theta(u) = 1,0$ for $u > 0, u < 0$ and where $q = \sqrt{k^2 - \kappa/a^2}$ is the wave number of oscillations within the core.

0031-9007/94/73(9)/1247(4)$06.00

With the radial forces of Eq. (2.2), we see that the angular momentum $Lqa^2 = xy' - x'y = r^2\theta'$ is constant. The equation for radial motion then becomes

$$r'' + q^2\left(r - \frac{L^2a^4}{r^3}\right) = -\frac{\kappa}{a^2}r\left(1 - \frac{a^2}{r^2}\right)\Theta(r-a) + 2\frac{\epsilon\kappa}{a^2}r\cos pz\,\Theta(a-r). \tag{2.3}$$

The first term on the right makes the oscillation wave number depend on amplitude and the second allows for energy transfer between the core and the oscillating ion.

In order to understand the role of the different terms in Eq. (2.3), we construct a simplified model by setting $L = 0$ and invoking a pendulum model for the first term on the right side of Eq. (2.3) by replacing $r(1 - a^2/r^2)\Theta(r-a)$ by r^3/a^2, corresponding to the cubic nonlinear term for a pendulum. (However, its sign is opposite from the conventional pendulum since, in our model, the wave number *increases* with increasing amplitude.) In addition, we extend the driving term to all values of r. The simplified equation for x is therefore

$$x'' + q^2x = -\frac{\kappa}{a^2}\frac{x^3}{a^2} + 2\frac{\epsilon\kappa}{a^2}x\cos pz. \tag{2.4}$$

We now use the phase-amplitude method by writing $x/a = A\sin\psi$, $x'/a = qA\cos\psi$, where $\psi = qz + \alpha$, implying $A'\sin\psi + A\alpha'\cos\psi = 0$. Here A and α are taken to be the slowly varying amplitude and phase parameters of the ion oscillation. Substituting into Eq. (2.4) and solving for A' and α' we obtain

$$A' = -\frac{\kappa A}{qa^4}[A^2\sin^3\psi\cos\psi - \epsilon a^2\sin 2\psi\cos pz], \tag{2.5}$$

$$\alpha' = \frac{\kappa}{qa^4}[A^2\sin^4\psi - 2\epsilon a^2\sin^2\psi\cos pz]. \tag{2.6}$$

We now average over all rapidly varying oscillatory terms with the exception of the one with wave number $2q - p$ (the parametric resonance) and obtain

$$A' = \frac{\epsilon\kappa}{2qa^2}A\sin\Psi, \tag{2.7}$$

$$\Psi' = (2q - p) + \frac{3\kappa}{4qa^4}A^2 + \frac{\epsilon\kappa}{qa^2}\cos\Psi, \tag{2.8}$$

where $\Psi = (2q - p)z + 2\alpha$ is the phase of this resonant interaction. One then finds that an integral of the motion exists, enabling us to write [7]

$$\epsilon\cos\Psi = \Delta - \frac{3}{8}w - \frac{C}{w}, \tag{2.9}$$

where $w = A^2/a^2$, $\Delta = q(p - 2q)a^2/\kappa$, and where the integration constant C is determined by the initial values of w and 2α. By resorting to the envelope equation we can show that $p^2 = 4q^2 + 2\kappa/a^2$ for the breathing mode, so that

$$\Delta = \frac{1}{1 + \sqrt{(1 + k^2/q^2)/2}}, \tag{2.10}$$

where q/k is the tune depression caused by the space charge. In Fig. 1 we plot $\epsilon\cos\Psi$ vs w for $q/k = 0.412$, $\Delta = 0.35$, and various values of C. For $\epsilon = 0.1$, the polar plot of w vs Ψ is shown in Fig. 2. It is clear that Q is an unstable fixed point and that the origin and S are stable fixed points. Figure 2 is equivalent to a "second order stroboscopic plot" for integral values of $pz/2\pi$, and contains the main features of the resonant interaction. Specifically, all trajectories starting within the inner separatrix (thick solid curve) bounded by P and Q oscillate in stable orbits while any trajectory starting just outside will travel along the outer separatrix (thick dashed curve). For these particles, as the amplitude of motion grows the true oscillation wave number increases, enhancing the resonant term and *locking in* to the resonance. And the presence of a thin distribution of trajectories near the outer separatrix has the appearance of a halo in $x - y$ space at the radius corresponding to R in Figs. 1 and 2.

We now drop the simplified model and return to Eq. (2.3). Although the algebra is far more complicated we eventually obtain a more accurate version of Eq. (2.9) with a very similar set of curves to those in Figs. 1 and 2. First we rewrite Eq. (2.3) for the variable $s = r^2/a^2$, obtaining

$$s'' - \frac{(s')^2}{2s} + 2q^2\left(s - \frac{L^2}{s}\right) = -\frac{2\kappa}{a^2}(s-1)\Theta(s-1) + 4\frac{\epsilon\kappa}{a^2}s\cos pz\,\Theta(1-s). \tag{2.11}$$

Guided by the parametrization of the x and y motions separately, the amplitude-phase parametrization of the two-dimensional oscillation is written as

$$s = \frac{w^2 + L^2}{2w} - \frac{w^2 - L^2}{2w}\cos(2qz + \gamma). \tag{2.12}$$

Here w and γ are slowly varying amplitude and phase parameters which would be constant if the right side of Eq. (2.11) vanished. We now write

$$s' = q\frac{w^2 - L^2}{w}\sin(2qz + \gamma) \tag{2.13}$$

and use Eq. (2.11) and the required connection between w' and γ' implied by Eq. (2.13) to obtain explicit expressions for w' and γ'. We then average over oscillations at

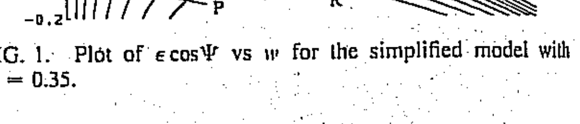

FIG. 1. Plot of $\epsilon\cos\Psi$ vs w for the simplified model with $\Delta = 0.35$.

(45)

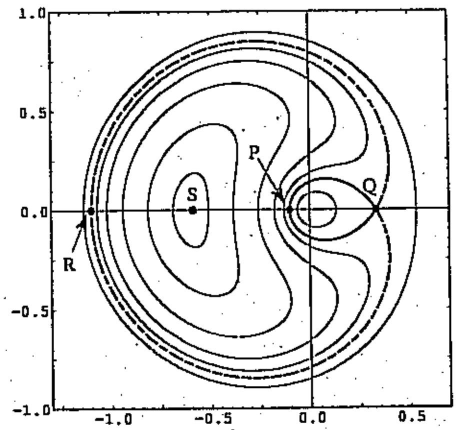

FIG. 2. Polar plot of w vs Ψ for the trajectories corresponding to the parametric resonance using $\Delta = 0.35$, $\epsilon = 0.1$, and the simplified model.

all wave numbers except $2q - p$, being careful to include the step functions as we obtain these averages. The final equations for w' and Ψ' [$\Psi = (2q - p)z + \gamma$] are similar to Eqs. (2.7) and (2.8) and again lead to an integral of the motion, which now is

$$g(1 - h)\epsilon \cos\Psi = f\Delta - t - C\,, \tag{2.14}$$

where $f(w) = (w^2 + L^2)/2w$, $g(w) = (w^2 - L^2)/2w$. Here

$$\pi h(w) = \tan^{-1}[\ell/(1 - f)] + \ell(1 - f)/2g^2 \tag{2.15}$$

for $w \geq 1$ and $\ell(w) = \sqrt{(w - 1)(w - L^2)/w}$. Also

$$t(w) = \frac{1}{\pi}\int_1^w \frac{dw}{wg}\left[(g^2 - f)\tan^{-1}\left(\frac{\ell}{1 - f}\right) + f\ell + L\tan^{-1}\left(\frac{2L\ell}{f - L^2}\right)\right], \tag{2.16}$$

for $w \geq 1$, and $h(w) = t(w) = 0$ for $w \leq 1$. The arctangents are taken to be in the first or second quadrant. The term in $b(w)$ comes from the amplitude dependence of the ion wave number. A more accurate expression for $b(w)$ can be obtained, if necessary, by solving Eq. (2.6) with $\epsilon = 0$.

Since the resonance will have its greatest effect when $L = 0$, corresponding to ion orbits which pass through the core center, we present a plot of $\epsilon \cos\Psi$ vs w for $\Delta = 0.35$ and $L = 0$ in Fig. 3. The pattern of curves is very similar to that in Fig. 1, and the w, Ψ polar plot in Fig. 4 for $\epsilon = 0.1$ has the same topology as for the simple model in Fig. 2, as is also the case for $L \neq 0$. But the scale for w is about 7 times larger, corresponding to a detuning with amplitude about 7 times smaller than that given by the 3/8 factor in Eq. (2.14).

III. Distribution of L in a symmetric K-V beam.—The distribution in L for a K-V beam is proportional to

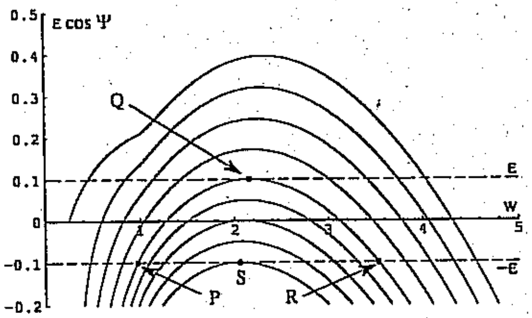

FIG. 3. Plot of $\epsilon \cos\Psi$ vs w for the exact model with $\Delta = 0.35$, $L = 0$.

$$f(L) \sim \int\int\int\int dx\,dy\,dx'\,dy'\,\delta\left(x^2 + y^2 + \frac{(x')^2}{q^2} + \frac{(y')^2}{q^2} - a^2\right)\delta(x'y - xy' - Lqa^2)\,. \tag{3.1}$$

We first do 45° rotations from the x/a, y'/qa space to the u, u' space and from the y/a, x'/qa space to the v, v' space and follow this by integrating over the polar angles in the uv' and vu' spaces. This leads to

$$f(L) \sim \int_0^\infty ds \int_0^\infty dt\,\delta(s + t - 1)\delta\left(\frac{s - t}{2} - L\right) = \begin{cases} 1, & 2|L| < 1 \\ 0, & 2|L| > 1 \end{cases}, \tag{3.2}$$

where $s = u^2 + (v')^2$ and $t = v^2 + (u')^2$ are both positive. Therefore the distribution in L for a K-V beam is uniform from $L = -1/2$ to $L = 1/2$ and vanishes for $|L| > 1/2$.

IV. Implications of the model.—Since the breathing K-V beam is a solution of the Vlasov equation, particles within the core will continue to remain there, even in the presence of the resonant interaction. If however,

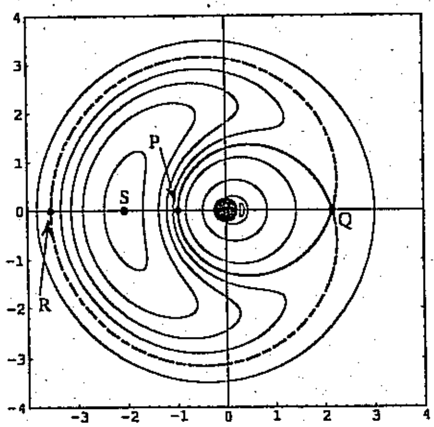

FIG. 4. Polar plot of w vs Ψ for the trajectories corresponding to the parametric resonance using $\Delta = 0.35$, $L = 0$, $\epsilon = 0.1$, and the exact model.

(46)

some other mechanism moves the particle outside the core, particularly to an oscillation amplitude exceeding that corresponding to the points P or Q in the figures, a halo will develop at a radius corresponding to point R in the figures. The most likely mechanism to do this is an instability associated with a nonlinear density perturbation. In addition, simulations show that chaotic motion develops near point Q in the figures for a large amplitude breathing mode at high current, enabling particles in the core to populate the halo.

V. Summary and discussion.—We considered a symmetric K-V beam undergoing a breathing mode and found that the parametric resonance ($2q = p$) is a vehicle for particles to leave the core of the beam and perform excursions to large amplitude, forming a distribution in real space in the form of a halo. In this calculation, we neglected the effect of high frequency terms, and the effect of other possible resonances and driving oscillations. Thus our model, which successfully describes a mechanism by which halos can and probably do form, is only an approximation to a much more complicated situation.

We have compared our predictions with some preliminary simulations performed for $L = 0$ by Wangler [8], and find that, for tune depressions from $q/k = 1$ to 0.6, the topology of the stroboscopic plot resembles Figs. 2 and 4 very closely. For tune depressions below 0.6, the stroboscopic plot shows the onset of chaotic behavior in an ever widening band near the inner separatrix as the tune depression deepens. Particles inside but near to the inner separatrix are then able to move outside the inner separatrix and participate more easily in the development of the halo.

Wangler's simulations using a K-V beam [8] confirm that core ions always remain within the inner separatrix. It is quite possible for core ions to lie outside the equivalent inner separatrix for nonuniform equilibrium charge density distributions. We therefore expect the halo mechanisms in the present model to apply to non-K-V beams as well. Lagniel's simulations [6] give similar results, showing the onset of chaos for high space charge as well as the similarity with the three-body astronomical problem.

Our present model is unable to describe either diffusion or chaos in the w, Ψ phase space. If we were to try to do so we would have to include the neglected high frequency terms, as well as resonances other than the one corresponding to the parametric resonance. Integrals of the motion corresponding to Eq. (2.14) would no longer be valid. Descriptions of the growth of halos including the effects of chaos and diffusion will require further analysis and/or extensive numerical simulations.

The author would like to thank Alex Dragt, Bob Jameson, Pierre Lapostolle, Ron Ruth, Rob, Ryne, Fred Skiff, and Tom Wangler for several helpful comments. He is also indebted to Dan Abell for performing the calculations leading to Figs. 1–4.

[1] See I.M. Kapchinsky, *Theory of Resonance Linear Accelerators* (Harford Academic Press, New York, 1985), p. 247ff.

[2] R.A. Jameson, Los Alamos Report No. LA-UR-93-1209 (unpublished). Jameson describes the early observations of emittance growth and halo production, with particular reference to LAMPF simulations and observations.

[3] M. Reiser, in Proceedings of the 1991 Particle Accelerator Conference, San Francisco, California, (unpublished), p. 2497.

[4] A. Cucchetti, M. Reiser, and T. Wangler, in Proceedings of the 1991 Particle Accelerator Conference (Ref. [3]), p. 251.

[5] J.S. O'Connell, T.P. Wangler, R.S. Mills, and K.R. Crandall, in Proceedings of the 1993 Particle Accelerator Conference, Washington, D.C. (unpublished), p. 3657.

[6] J.M. Lagniel, Nucl. Instrum. Methods Phys. Res., Sect. A 345, 46 (1994).

[7] This result can also be obtained using a contact transformation, followed by neglecting rapidly oscillating terms. In fact, the transformed Hamiltonian in the canonical variables w and Ψ is $H = (\kappa/qa^2)[w\epsilon\cos\Psi - \Delta w + 3w^2/8]$.

[8] Tom Wangler (private communication).

Transverse Kinetic Stability*

Steven M. Lund
Lawrence Livermore National Laboratory (LLNL)

Steven M. Lund and John J. Barnard
"Beam Physics with Intense Space-Charge"

US Particle Accelerator School

University of Maryland, held at Annapolis, MD
16-27 June, 2008
(Version 20080625)

* Research supported by the US Dept. of Energy at LLNL and LBNL under contract Nos. DE-AC52-07NA27344 and DE-AC02-05CH11231.

Transverse Kinetic Stability: Outline

Transverse Kinetic Stability: Detailed Outline

Detailed Outline - 2

Detailed Outline - 3

9) Uniform Density Beams and Extreme Energy States
- Variational Formulation
- Self-Field Energy Minimization

10) Collective Relaxation and rms Emittance Growth
- Conservation Constraints
- Relaxation Processes
- Emittance Growth Bounds from Space-Charge Nonuniformities

11) Halo Induced Mechanism of Higher Order Instability
- Halo Model for an Elliptical Beam
- Pumping Mechanism
- Stability Properties

12) Phase Mixing and Landau Damping in Beams
- (to be added, future editions)

Contact Information

References

S1: Overview: Machine Operating Points

Good transport of a single component beam with intense space-charge described by a Vlasov-Poisson type model requires:

1. Lowest Order:
   Stable single-particle centroid: $\sigma_0 < 180°$ see: Transverse Particle Eqns, Transverse Centroid and Env.
2. Next Order:
   Stable rms envelope: $\sigma_0, \; \sigma/\sigma_0$ both outside of envelope bands see: Transverse Centroid and Envelope Descriptions
3. Higher Order:
   "Stable" Vlasov description: To be covered these lectures

Transport of a relatively smooth initial beam distribution can fail or become "unstable" within the Vlasov model for several reasons:

- Collective modes internal to beam become unstable and grow
  - Large amplitudes can lead to statistical (rms) beam emittance growth
- Excessive halo generated
  - Increased statistical beam emittance and particle losses
- Combined processes above

Transport limits in periodic (FODO) quadrupole lattices that result from higher order processes have been measured in the SBTE experiment. These results had only limited theoretical understanding over 20+ years

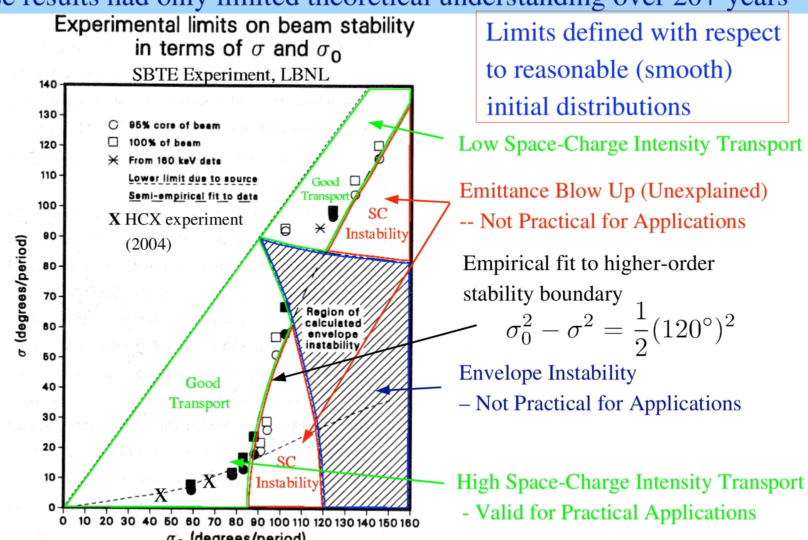

[M.G. Tiefenback, Ph.D Thesis, UC Berkeley (1986)]

Summary of beam stability with intense space-charge in a quadrupole transport lattice: centroid, envelope, and theory boundary based on higher order emittance growth/particle losses

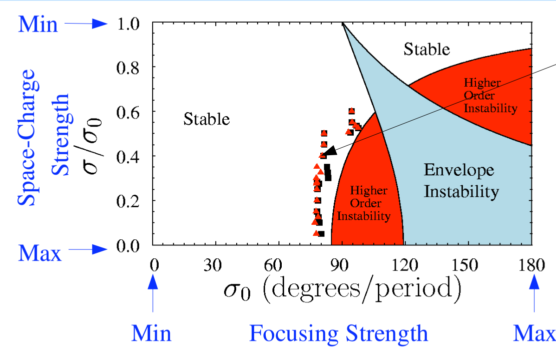

Theory stability boundary points

- Lund and Chawla, NIMA **561** 203 (2006)
- Lund, Barnard, Bukh, Chawla, and Chilton, NIMA **277** 173 (2007)

Recent theory analyzes AG transport limits without equilibria

- Suggests near core, chaotic halo resonances driven by matched beam envelope flutter can drive strong emittance growth and particle losses
- Results checked with fully self-consistent simulations

Analogous results (with less "instability") exist for solenoidal transport

S2: Overview:
Collective Modes and Transverse Kinetic Stability

In discussion of transverse beam physics we have focused on:

Equilibrium

- Used to estimate balance of space-charge and focusing forces
  - KV model for periodic focusing
  - Continuous focusing equilibria for qualitative guide on space-charge effects such as Debye screening and nonlinear equilibrium self-field effects

Centroid/Envelope Modes and Stability

- Lowest order collective oscillations of the beam
  - Analyzed assuming fixed internal form of the distribution
- Model only exactly correct for KV equilibrium distribution
  - Should hold in a leading-order sense for a wide variety of real beams
- Predictions of instability regions are well verified by experiment
  - Significantly restricts allowed system parameters for periodic focusing lattices

Example – Envelope Modes on a Round, Continuously Focused Beam

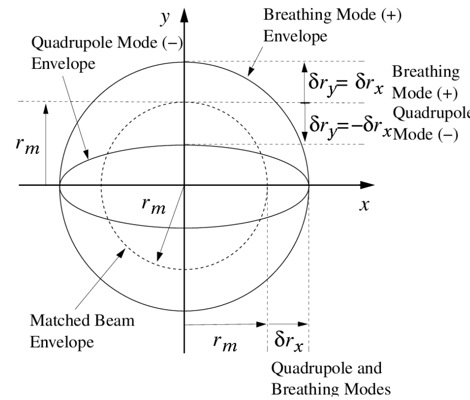

The analog of these modes in a periodic focusing lattice can be destabilized

- Constrains system parameters to avoid band (parametric) regions of instability

Reminder (lecture on *Centroid and Envelope Descriptions of Beams*): Instability bands of the KV envelope equation are well understood in periodic focusing channels

Envelope Mode Instability Growth Rates

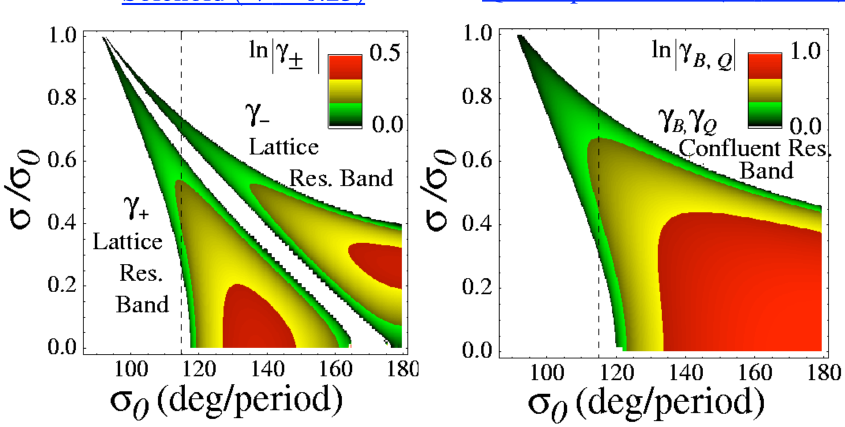

[S.M. Lund and B. Bukh, PRSTAB 024801 (2004)]

More instabilities are possible than can be described by statistical (moment/envelope) equations. Look at a more complete, Vlasov based kinetic theory including self-consistent space-charge:

Higher-order Collective (internal) Mode Stability

- Perturbations will generally drive nonlinear space-charge forces
- Evolution of such perturbations can change the beam rms emittance
- Many possible internal modes of oscillation should be possible
  - Frequencies can differ significantly from envelope modes
  - Creates more possibilities for resonant exchanges with a periodic focusing lattice and various beam characteristic responses opening many possibilities for system destabilization

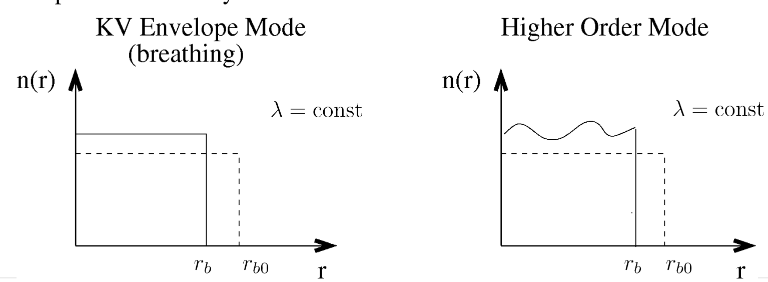

Plasma physics approach to beam physics:

Resolve:

$$f(\mathbf{x}_\perp, \mathbf{x}'_\perp, s) = f_\perp(\{C_i\}) + \delta f_\perp(\mathbf{x}_\perp, \mathbf{x}'_\perp, s)$$

equilibrium perturbation $f_\perp \gg |\delta f_\perp|$

and carry out equilibrium + stability analysis

Comments:

- Attraction is to parallel the impressive successes of plasma physics
  - Gain insight into preferred state of nature
- Beams are born off a source and may not be close to an equilibrium condition
  - Appropriate single particle constants of the motion unknown for periodic focusing lattices other than the KV distribution
- Intense beam self-fields and finite radial extent vastly complicate equilibrium description and analysis of perturbations

Review: Transverse Vlasov-Poisson Model: for a coasting, single species beam with electrostatic self-fields propagating in a linear focusing lattice:

$\mathbf{x}_\perp, \mathbf{x}'_\perp$ transverse particle coordinate, angle

$q, \quad m$ charge, mass

$\gamma_b, \quad \beta_b$ axial relativistic factors

$f_\perp(\mathbf{x}_\perp, \mathbf{x}'_\perp, s)$ single particle distribution

$H_\perp(\mathbf{x}_\perp, \mathbf{x}'_\perp, s)$ single particle Hamiltonian

Vlasov Equation (see J.J. Barnard, Introductory Lectures):

$$\frac{d}{ds} f_\perp = \frac{\partial f_\perp}{\partial s} + \frac{d\mathbf{x}_\perp}{ds} \cdot \frac{\partial f_\perp}{\partial \mathbf{x}_\perp} + \frac{d\mathbf{x}'_\perp}{ds} \cdot \frac{\partial f_\perp}{\partial \mathbf{x}'_\perp} = 0$$

Particle Equations of Motion:

$$\frac{d}{ds}\mathbf{x}_\perp = \frac{\partial H_\perp}{\partial \mathbf{x}'_\perp} \qquad \frac{d}{ds}\mathbf{x}'_\perp = -\frac{\partial H_\perp}{\partial \mathbf{x}_\perp}$$

Hamiltonian (see: S.M. Lund, lectures on Transverse Equilibrium Distributions):

$$H_\perp = \frac{1}{2}\mathbf{x}'^{\,2}_\perp + \frac{1}{2}\kappa_x(s)x^2 + \frac{1}{2}\kappa_y(s)y^2 + \frac{q}{m\gamma_b^3\beta_b^2c^2}\phi$$

Poisson Equation:

$$\left(\frac{\partial^2}{\partial x^2} + \frac{\partial^2}{\partial y^2}\right)\phi = -\frac{q}{\epsilon_0}\int d^2\mathbf{x}'_\perp \, f_\perp$$

+ boundary conditions on ϕ

Review: Focusing lattices, continuous and periodic (simple piecewise constant):

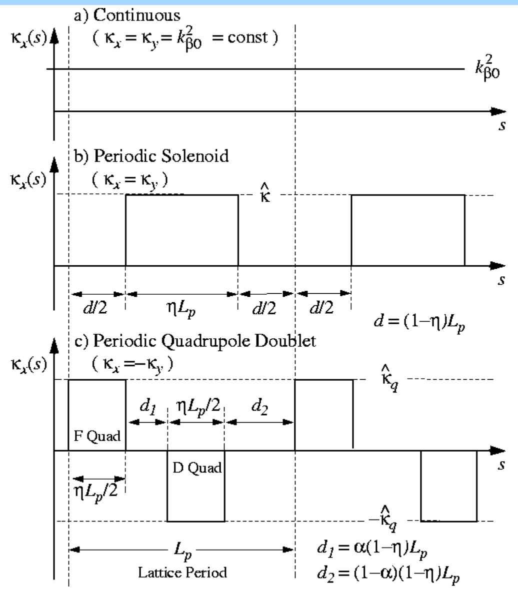

Lattice Period L_p

Occupancy η

$\eta \in [0, 1]$

Solenoid description carried out implicitly in Larmor frame [see: S.M. Lund, lectures on Transverse Particle Equations]

Syncopation Factor α

$$\alpha \in [0, \frac{1}{2}]$$

$$\alpha = \frac{1}{2} \implies FODO$$

Continuous Focusing: $\kappa_x = \kappa_y = k_{\beta 0}^2 = \text{const}$

$$\boxed{H_\perp = \frac{1}{2}\mathbf{x}'^{\,2}_\perp + \frac{1}{2}k_{\beta 0}^2\mathbf{x}_\perp^2 + \frac{q}{m\gamma_b^3\beta_b^2c^2}\phi}$$

Solenoidal Focusing (in Larmor frame variables): $\kappa_x = \kappa_y = \kappa(s)$

$$H_\perp = \frac{1}{2}\mathbf{x}'^{\,2}_\perp + \frac{1}{2}\kappa\mathbf{x}_\perp^2 + \frac{q}{m\gamma_b^3\beta_b^2c^2}\phi$$

Quadrupole Focusing: $\kappa_x = -\kappa_y = \kappa_q(s)$

$$H_\perp = \frac{1}{2}\mathbf{x}'^{\,2}_\perp + \frac{1}{2}\kappa_q x^2 - \frac{1}{2}\kappa_q y^2 + \frac{q}{m\gamma_b^3\beta_b^2c^2}\phi$$

We will concentrate on the continuous focusing model in these lectures

- Kinetic theory is notoriously complicated even in this (simple) case
- By analogy with envelope mode results expect that kinetic theory of periodic focusing systems to have more instabilities
- As in equilibrium analysis the continuous model can give simplified insight on a range of relevant kinetic stability considerations

S3: Linearized Vlasov Equation

Because of the complexity of kinetic theory, we will limit discussion to a simple continuous focusing model Vlasov-Poisson system for a coasting beam within a round pipe

$$\frac{df_\perp}{ds} = \left\{ \frac{\partial}{\partial s} + \mathbf{x}'_\perp \cdot \frac{\partial}{\partial \mathbf{x}_\perp} - \left(k_{\beta 0}^2 \mathbf{x}_\perp + \frac{q}{m\gamma_b^3\beta_b^2c^2}\frac{\partial \phi}{\partial \mathbf{x}_\perp} \right) \cdot \frac{\partial}{\partial \mathbf{x}'_\perp} \right\} f_\perp(\mathbf{x}_\perp, \mathbf{x}'_\perp, s) = 0$$

$$\nabla_\perp^2 \phi(\mathbf{x}_\perp, s) = -\frac{q}{\epsilon_0}\int d^2x'_\perp \; f_\perp(\mathbf{x}_\perp, \mathbf{x}_\perp, s)$$

$$\phi(|\mathbf{x}_\perp| = r_p, s) = \text{const}$$

Then expand the distribution and field as:

$$\begin{aligned} f_\perp &= \boxed{f_0(H_0)} + \boxed{\delta f_\perp} \\ \phi &= \boxed{\phi_0} \quad\; + \boxed{\delta\phi} \end{aligned}$$

equilibrium perturbation

Comment:
The Poisson equation connects $f_\perp$ nd ϕ so, $\delta f_\perp$ and $\delta\phi$ cannot be independently specified.
We quantify the connection shortly.

At present, there is *no assumption* that the perturbations are small.

The equilibrium satisfies:
(see: S.M. Lund, lectures on Transverse Equilibrium Distributions)

$$H_0 = \frac{1}{2}\mathbf{x}'^{\,2}_\perp + \frac{1}{2}k_{\beta 0}^2\mathbf{x}_\perp^2 + \frac{q}{m\gamma_b^3\beta_b^2c^2}\phi_0$$

$$f_0(H_0) = \quad \text{any non-negative function}$$

$$\frac{1}{r}\frac{\partial}{\partial r}\left(r\frac{\partial \phi_0}{\partial r}\right) = -\frac{q}{\epsilon_0}\int d^2x'_\perp \; f_0(H_0)$$

The unperturbed distribution must then satisfy the equilibrium Vlasov equation:

$$\left\{ \frac{\partial}{\partial s} + \mathbf{x}'_\perp \cdot \frac{\partial}{\partial \mathbf{x}_\perp} - \left(k_{\beta 0}^2 \mathbf{x}_\perp + \frac{q}{m\gamma_b^3\beta_b^2c^2}\frac{\partial \phi_0}{\partial \mathbf{x}_\perp} \right) \cdot \frac{\partial}{\partial \mathbf{x}'_\perp} \right\} f_0(H_0) = 0$$

Because the Poisson equation is linear:

$$\nabla_\perp^2 \delta\phi(\mathbf{x}_\perp, s) = -\frac{q}{\epsilon_0}\int d^2x'_\perp \; \delta f_\perp(\mathbf{x}_\perp, \mathbf{x}_\perp, s)$$

$$\delta\phi(|\mathbf{x}_\perp| = r_p, s) = \text{const}$$

Insert the perturbations in Vlasov's equation and expand terms:

$$\overbrace{\left\{ \frac{\partial}{\partial s} + \mathbf{x}'_\perp \cdot \frac{\partial}{\partial \mathbf{x}_\perp} - \left(k_{\beta 0}^2 \mathbf{x}_\perp + \frac{q}{m\gamma_b^3\beta_b^2c^2}\frac{\partial \phi_0}{\partial \mathbf{x}_\perp} \right) \cdot \frac{\partial}{\partial \mathbf{x}'_\perp} \right\} f_0(H_0)}^{0} \quad \text{equilibrium term}$$

$$+ \left\{ \frac{\partial}{\partial s} + \mathbf{x}'_\perp \cdot \frac{\partial}{\partial \mathbf{x}_\perp} - \left(k_{\beta 0}^2 \mathbf{x}_\perp + \frac{q}{m\gamma_b^3\beta_b^2c^2}\frac{\partial \phi_0}{\partial \mathbf{x}_\perp} \right) \cdot \frac{\partial}{\partial \mathbf{x}'_\perp} \right\} \delta f_\perp \quad \begin{array}{l}\text{equilibrium characteristics} \\ \text{of perturbed distribution}\end{array}$$

$$= \underbrace{\frac{q}{m\gamma_b^3\beta_b^2c^2}\frac{\partial \delta\phi}{\partial \mathbf{x}_\perp} \cdot \frac{\partial}{\partial \mathbf{x}'_\perp} f_0(H_0)}_{\text{perturbed field linear correction term}} + \underbrace{\frac{q}{m\gamma_b^3\beta_b^2c^2}\frac{\partial \delta\phi}{\partial \mathbf{x}_\perp} \cdot \frac{\partial}{\partial \mathbf{x}'_\perp}\delta f_\perp}_{\text{nonlinear term}}$$

Take the perturbations to be small-amplitude:

$$\begin{aligned} f_0(H_0) &\gg |\delta f_\perp| \\ \phi_0 &\gg \delta\phi \end{aligned}$$

<--- follows automatically from distribution/Poisson Eqn

and neglect the nonlinear terms to obtain the linearized Vlasov-Poisson system:

$$\left\{ \frac{\partial}{\partial s} + \mathbf{x}'_\perp \cdot \frac{\partial}{\partial \mathbf{x}_\perp} - \left(k_{\beta 0}^2 \mathbf{x}_\perp + \frac{q}{m\gamma_b^3\beta_b^2c^2}\frac{\partial \phi_0}{\partial \mathbf{x}_\perp} \right) \cdot \frac{\partial}{\partial \mathbf{x}'_\perp} \right\} \delta f_\perp(\mathbf{x}_\perp, \mathbf{x}'_\perp, s)$$

$$= \frac{q}{m\gamma_b^3\beta_b^2c^2}\frac{\partial \delta\phi(\mathbf{x}_\perp, s)}{\partial \mathbf{x}_\perp} \cdot \frac{\partial}{\partial \mathbf{x}'_\perp} f_0(H_0)$$

$$\nabla_\perp^2 \delta\phi(\mathbf{x}_\perp, s) = -\frac{q}{\epsilon_0}\int d^2x'_\perp \; \delta f_\perp(\mathbf{x}_\perp, \mathbf{x}_\perp, s) \qquad \delta\phi(|\mathbf{x}_\perp| = r_p, s) = \text{const}$$

Solution of the Linearized Vlasov Equation, the method of characteristics

The linearized Vlasov equation is a integral-partial differential equation system

- Highly nontrivial to solve
- Method of characteristics can be employed to simplify analysis due to the structure of the equation

Note that the equilibrium Vlasov equation is:

$$\left\{ \frac{\partial}{\partial s} + \mathbf{x}'_\perp \cdot \frac{\partial}{\partial \mathbf{x}_\perp} - \left(k_{\beta 0}^2 \mathbf{x}_\perp + \frac{q}{m\gamma_b^3\beta_b^2c^2}\frac{\partial \phi_0}{\partial \mathbf{x}_\perp} \right) \cdot \frac{\partial}{\partial \mathbf{x}'_\perp} \right\} f_0 = 0$$

$$\left.\frac{d}{ds}\right|_{\text{eq. orbit}} f_0 = 0$$

Interpret:

$$\left\{ \frac{\partial}{\partial s} + \mathbf{x}'_\perp \cdot \frac{\partial}{\partial \mathbf{x}_\perp} - \left(k_{\beta 0}^2 \mathbf{x}_\perp + \frac{q}{m\gamma_b^3\beta_b^2c^2}\frac{\partial \phi_0}{\partial \mathbf{x}_\perp} \right) \cdot \frac{\partial}{\partial \mathbf{x}'_\perp} \right\} = \left.\frac{d}{ds}\right|_{\text{eq. orbit}}$$

as a total derivative evaluated along an equilibrium particle orbit. This suggests employing the method of characteristics.

Method of Characteristics:

Equilibrium orbit:

$$\boxed{\begin{aligned} &\frac{d}{d\tilde{s}}\mathbf{x}_\perp(\tilde{s}) = \mathbf{x}'_\perp(\tilde{s}) \\ &\frac{d}{d\tilde{s}}\mathbf{x}'_\perp(\tilde{s}) = -k_{\beta 0}^2\mathbf{x}_\perp(\tilde{s}) - \frac{q}{m\gamma_b^3\beta_b^2c^2}\frac{\partial\phi_0(\mathbf{x}_\perp(\tilde{s}))}{\partial\mathbf{x}_\perp(\tilde{s})} \end{aligned}}$$

"Initial" conditions of characteristic orbit:

$$\boxed{\begin{aligned} \mathbf{x}_\perp(\tilde{s}=s) &= \mathbf{x}_\perp \\ \mathbf{x}'_\perp(\tilde{s}=s) &= \mathbf{x}'_\perp \end{aligned}}$$

Then the linearized Vlasov equation can be expressed as:

$$\frac{d}{d\tilde{s}}\delta f_\perp(\mathbf{x}_\perp(\tilde{s}),\mathbf{x}'_\perp(\tilde{s}),\tilde{s}) = \frac{q}{m\gamma_b^3\beta_b^2c^2}\frac{\partial\delta\phi(\mathbf{x}_\perp(\tilde{s}))}{\partial\mathbf{x}_\perp(\tilde{s})}\cdot\frac{\partial}{\partial\mathbf{x}'_\perp}f_0(H_0(\mathbf{x}_\perp(\tilde{s}),\mathbf{x}'_\perp(\tilde{s})))$$

This is a total derivative and can be integrated:

- To analyze instabilities assume growing perturbations that grow in s
- Neglect initial conditions at $\tilde{s}\to-\infty$ and integrate

$$\boxed{\begin{aligned} &\delta f_\perp(\mathbf{x}_\perp,\mathbf{x}'_\perp,s) = \frac{q}{m\gamma_b^3\beta_b^2c^2}\int_{-\infty}^{s}d\tilde{s}\,\frac{\partial\delta\phi(\mathbf{x}_\perp(\tilde{s}))}{\partial\mathbf{x}_\perp(\tilde{s})}\cdot\frac{\partial}{\partial\mathbf{x}'_\perp}f_0(H_0(\mathbf{x}_\perp(\tilde{s}),\mathbf{x}'_\perp(\tilde{s}))) \\ &\nabla_\perp^2\delta\phi(\mathbf{x}_\perp,s) = -\frac{q}{\epsilon_0}\int d^2x'_\perp\;\delta f_\perp(\mathbf{x}_\perp,\mathbf{x}_\perp,s) \\ &\delta\phi(|\mathbf{x}_\perp| = r_p,s) = \text{const} \end{aligned}}$$

Gives the self-consistent evolution of the perturbations

- Similar statement for nonlinear perturbations (Homework problem)

Effectively restates the Poisson equation as a differential-integral equation that is solved to understand the evolution of perturbations

- Simpler to work with but still *very* complicated

S4: Collective Modes on a KV Equilibrium Beam

Unfortunately, calculation of normal modes is generally complicated even in continuous focusing. Nevertheless, the normal modes of the KV distribution can be analytically calculated and give insight on the expected collective response of a beam with intense space-charge.

Review: Continuous Focusing KV Equilibrium

$$\boxed{f_\perp(H_\perp) = \frac{\hat{n}}{2\pi}\delta\left(H_\perp - \frac{\varepsilon^2}{2r_b^2}\right)}$$

$$r_b = \left(\frac{Q+\sqrt{4k_{\beta0}^2\varepsilon^2+Q^2}}{2k_{\beta0}^2}\right)^{1/2} = \text{const}$$

$k_{\beta 0} =$ Undepressed betatron wavenumber
$r_b =$ Beam edge radius
$\hat{n} =$ Beam number density
$Q =$ Dimensionless perveance
$\varepsilon =$ rms edge emittance

Further comments on the KV equilibrium: Distribution Structure

Equilibrium distribution:

$$\boxed{f_\perp \sim \delta[\text{Courant-Snyder invariants}]}$$

Forms a highly singular hyper-shell in 4D phase-space

Schematic:

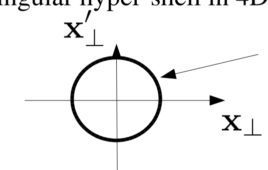

- Singular distribution has large "Free-Energy" to drive many instabilities
  - Low order envelope modes are physical and highly important (see: S.M. Lund, lectures on Centroid and Envelope Descriptions of Beams)
- Perturbative analysis shows strong collective instabilities
  - Hofmann, Laslett, Smith, and Haber, Part. Accel. **13**, 145 (1983)
  - Higher order instabilities (collective modes) have unphysical aspects due to (delta-function) structure of distribution and must be applied with care (see following lecture material)
  - Instabilities can cause problems if the KV distribution is employed as an initial beam state in self-consistent simulations

A full kinetic stability analysis of the KV equilibrium distribution is complicated and uncovers many strong instabilities

[I. Hofmann, J.L. Laslett, L. Smith, and I. Haber, Particle Accel. 13, 145 (1983); R. Gluckstern, Proc. 1970 Proton Linac Conf., Batavia 811 (1971)]

Expand Vlasov's equation to linear order with:

$$\boxed{f_\perp \rightarrow f_\perp(\text{ C.S. Invariant}) \; + \; \delta f_\perp}$$

$f_\perp(\text{C.S. Invariant})$ = equilibrium

$\delta f_\perp$ = perturbation

Solve the Poisson equation:

$$\nabla_\perp^2 \delta\phi = -\frac{q}{\epsilon_0}\int d^2x' \; \delta f_\perp$$

using truncated polynomials for $\delta\phi$ internal to the beam to represent a "normal mode" with pure harmonic variation, i.e., $\delta\phi \sim \text{func}(x,y)e^{-iks}$

$k = \text{const}$

$i = \sqrt{-1}$

$$\delta\phi = \sum_{m=0}^{n} A_m^{(0)}(s)x^{n-m}y^m + \sum_{m=0}^{n-2} A_m^{(1)}(s)x^{n-m-2}y^m + \cdots$$

$n = 2, 3, 4, \cdots$ "order" of mode

m can be restricted to even or odd terms

- Truncated polynomials can meet all boundary conditions
- Eigenvalues of a Floquet form transfer matrix analyzed for stability properties
  - Lowest order results reproduce KV envelope instabilities
  - Higher order results manifest many strong instabilities

Higher order kinetic instabilities of the KV equilibrium are strong and cover a wide parameter range for periodic focusing lattices

Example: FODO Quadrupole Stability

4th order ($n = 4$) even mode

[Hofmann et. al, Particle Accel. **13**, 145 (1983)]

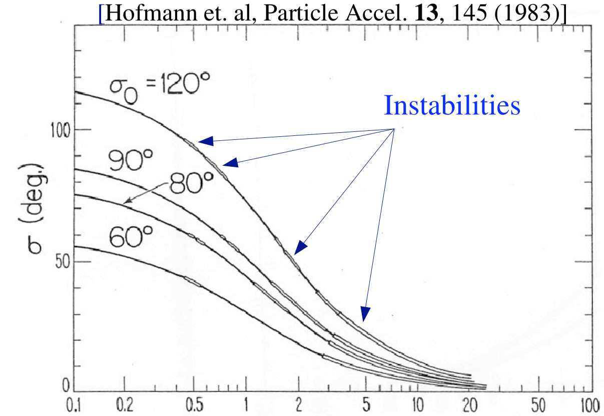

$\sigma/\sigma_0 \rightarrow 1$ (undepressed) --> Q' (space-charge parameter) increasing space-charge --> $\sigma/\sigma_0 \rightarrow 0$ (fully depressed)

The continuous focusing limit can be analyzed to better understand properties of internal modes on a KV beam (1)

[S. Lund and R. Davidson, Physics of Plasmas **5**, 3028 (1998): see Appendix B, C]

Continuous focusing, symmetric beam:

$$\kappa_x(s) = \kappa_y(s) = k_{\beta 0}^2 = \text{const}$$

$$\varepsilon_x = \varepsilon_y \equiv \varepsilon \qquad r_x = r_y \equiv r_b$$

Mode eigenfunction (2*n* "order" in the sense of Hoffman et. al.):

$$\delta\phi_n = \begin{cases} \frac{A_n}{2}\left[P_{n-1}\left(1 - 2\frac{r^2}{r_b^2}\right) + P_n\left(1 - 2\frac{r^2}{r_b^2}\right)\right], & 0 \le r \le r_b \\ 0, & r_b < r \end{cases}$$

$n = 1, 2, 3, \cdots$ $\quad A_n = \text{const}$ $\quad P_n(x) =$ nth order Legendre polynomial

Potential

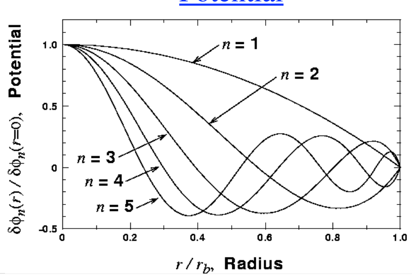

Density ($\delta n_n = \epsilon_0 \nabla_\perp^2 \delta\phi_n / q$)

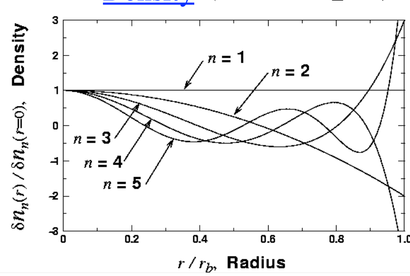

The continuous focusing limit can be analyzed to better understand properties of internal modes on a KV beam (2)

Mode dispersion relation for e^{-iks} variations:

$$2n + \frac{1 - \sigma/\sigma_0}{(\sigma/\sigma_0)^2}\left[B_{n-1}\left(\frac{k/k_{\beta 0}}{\sigma/\sigma_0}\right) - B_n\left(\frac{k/k_{\beta 0}}{\sigma/\sigma_0}\right)\right] = 0$$

where:

$$B_j(\alpha) \equiv \begin{cases} 1, & j = 0 \\ \frac{(\alpha/2)^2 - 0^2}{(\alpha/2)^2 - 1^2}\frac{(\alpha/2)^2 - 2^2}{(\alpha/2)^2 - 3^2}\cdots\frac{(\alpha/2)^2 - (j-1)^2}{(\alpha/2)^2 - j^2} & j = 1, 3, 5, \cdots \\ \frac{(\alpha/2)^2 - 1^2}{(\alpha/2)^2 - 2^2}\frac{(\alpha/2)^2 - 3^3}{(\alpha/2)^2 - 4^2}\cdots\frac{(\alpha/2)^2 - (j-1)^2}{(\alpha/2)^2 - j^2} & j = 2, 4, 6, \cdots \end{cases}$$

- Eigenfunction structure suggestive of wave perturbations often observed internal to the beam in simulations for a variety of beam distributions
- n distinct branches for 2*n* order (real coefficient) polynomial dispersion relation
- Some range of σ/σ_0 will be unstable for all $n > 1$
  - Instability exists for some n for $\sigma/\sigma_0 < 0.3985$
  - Growth rates are strong

Continuous focusing limit dispersion relation results for KV beam stability

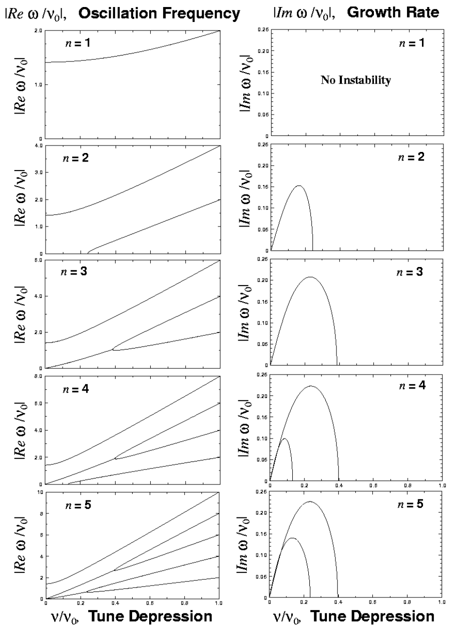

Notation Change:

$k/k_{\beta 0} \equiv \omega/\nu_0$

$\sigma/\sigma_0 \equiv \nu/\nu_0$

[S. Lund and R. Davidson, Physics of Plasmas **5**, 3028 (1998): see Appendix B, C]

For continuous focusing, fluid theory shows that some branches of the KV dispersion relation *are* physical

[S. Lund and R. Davidson, Physics of Plasmas **5**, 3028 (1998)]

Fluid theory:
- KV equilibrium distribution is reasonable in fluid theory
  - No singularities
  - Flat density and parabolic radial temperature profiles
- Theory truncated by assuming zero heat flow

Mode eigenfunctions:

Exactly the same as derived under kinetic theory!

Mode dispersion relation:

$$\boxed{\frac{k}{k_{\beta 0}} = \sqrt{2 + 2\left(\frac{\sigma}{\sigma_0}\right)^2 (2n^2 - 1)} \qquad n = 1,\ 2,\ 3,\ \cdots}$$

- Single, stable branch
  - Agrees well with high frequency branch from kinetic theory

Results show that aspects of higher-order KV internal modes are physical!

Continuous focusing limit dispersion relation results for KV beam stability

n = 1, envelope mode curves overlap

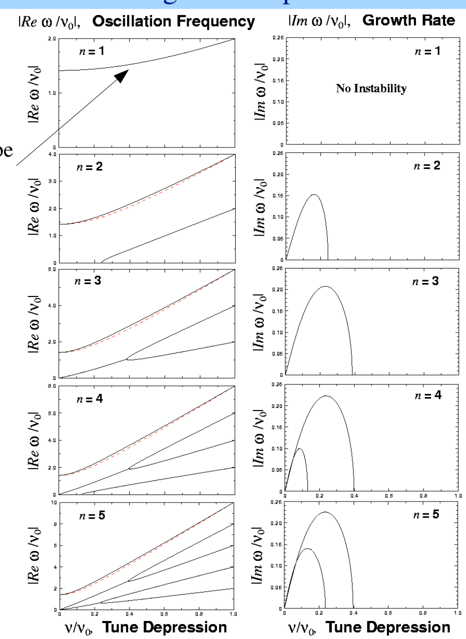

Notation Change:

$k/k_{\beta 0} \equiv \omega/\nu_0$

$\sigma/\sigma_0 \equiv \nu/\nu_0$

Red: Fluid Theory (no instability)

Black: Kinetic Theory (unstable branches)

[S. Lund and R. Davidson, Physics of Plasmas **5**, 3028 (1998)]

S5: Global Conservation Constraints

Apply for any initial distribution, equilibrium or not.
- Strongly constrain nonlinear evolution of the system.
- Valid even with a beam pipe provided that particles are not lost from the system and that symmetries are respected.
- Useful to bound perturbations, but yields no information on evolution timescales.

1) Generalized Entropy

$$\boxed{\begin{aligned} U_G &= \int d^2x_\perp \int d^2x'_\perp\ G(f_\perp) \ = \text{const} \\ G(f_\perp) &= \text{Any diffrentiable functions satisfying } G(f_\perp \to 0) = 0 \end{aligned}}$$

- Applies to all Vlasov evolutions.

// Examples

Line-charge: $G(f_\perp) = q f_\perp \longrightarrow \boxed{\lambda = q \int d^2x \int d^2x'\ f_\perp \ = \text{const}}$

Entropy: $G(f_\perp) = -\frac{f_\perp}{A} \ln\left(\frac{f_\perp}{f_0}\right)$ $\quad A,\ f_0$ constants

$$\longrightarrow \boxed{\mathcal{S} = -\int \frac{d^2x}{A} \int d^2x'\ f_\perp \ln\left(\frac{f_\perp}{f_0}\right) \ = \text{const}}$$

//

2) Transverse Energy in continuous focusing

$$\boxed{U_\mathcal{E} = \int d^2x'_\perp \int d^2x_\perp \left\{ \frac{1}{2}\mathbf{x}'^2_\perp + \frac{1}{2}k^2_{\beta 0}\mathbf{x}^2_\perp \right\} f_\perp + \int d^2x_\perp \frac{\epsilon_0 |\nabla_\perp \phi|^2}{2m\gamma_b^3\beta_b^2c^2} = \text{const}}$$

Here,

$$\int d^2x'_\perp \int d^2x_\perp \frac{1}{2}\mathbf{x}'^2_\perp f_\perp$$ ~ Kinetic Energy

$$\int d^2x'_\perp \int d^2x_\perp \frac{1}{2}k^2_{\beta 0}\mathbf{x}^2_\perp f_\perp$$ ~ Potential Energy of applied focusing forces

$$\int d^2x_\perp \frac{\epsilon_0 |\nabla_\perp \phi|^2}{2m\gamma_b^3\beta_b^2c^2}$$ ~ Self-Field Energy

- Does not hold when focusing forces vary in *s*
  - Can still be approximately valid for rms matched beams where energy will regularly pump into and out of the beam
- Self field energy term diverges in radially unbounded systems (no aperture)
  - Still useful if an appropriate infinite constant is subtracted (to regularize)

Comments on system energy form:

$$U_\mathcal{E} = \int d^2x'_\perp \int d^2x_\perp \left\{ \frac{1}{2}\mathbf{x}'^2_\perp + \frac{1}{2}k^2_{\beta 0}\mathbf{x}^2_\perp \right\} f_\perp + \int d^2x_\perp \frac{\epsilon_0 |\nabla_\perp \phi|^2}{2m\gamma_b^3\beta_b^2c^2} = \text{const}$$

Analyze the energy term:

zero for grounded aperture in finite system

$$\int d^2x_\perp \frac{\epsilon_0 |\nabla_\perp\phi|^2}{2} = \cancel{\int d^2x_\perp \frac{1}{2}\nabla_\perp \cdot (\phi\nabla_\perp\phi)} - \int d^2x_\perp \frac{1}{2}\phi\nabla^2_\perp\phi$$

or infinite constant in free space

Employ the Poisson equation:

$$\nabla^2_\perp \phi = -\frac{q}{\epsilon_0}\int d^2x'_\perp f_\perp$$

$$\longrightarrow \int d^2x_\perp \frac{\epsilon_0|\nabla_\perp\phi|^2}{2} = \int d^2x_\perp \int d^2x'_\perp \frac{q}{2\epsilon_0}\phi f_\perp$$

Giving:

$$\boxed{U_\mathcal{E} = \int d^2x'_\perp \int d^2x_\perp \left\{ \frac{1}{2}\mathbf{x}'^2_\perp + \frac{1}{2}k^2_{\beta 0}\mathbf{x}^2_\perp + \frac{1}{2}\frac{q\phi}{m\gamma_b^3\beta_b^2c^2} \right\} f_\perp = \text{const}}$$

symmetry factor

- Note the relation to the system Hamiltonian with a symmetry factor to not double count particle contributions

$$H_\perp = \frac{1}{2}\mathbf{x}'^{\,2}_\perp + \frac{1}{2}k^2_{\beta 0}\mathbf{x}^2_\perp + \frac{q}{m\gamma_b^3\beta_b^2c^2}\phi$$

Comments on self-field energy divergences:

In unbounded (free space) systems, far from the beam the field must look like a line charge:

$$-\frac{\partial\phi}{\partial r} \sim \frac{\lambda}{2\pi\epsilon_0 r} \qquad r > r_{\text{large}}$$

Resolve the total field energy into a finite (near) term and a divergent term:

$$\underbrace{\int d^2x_\perp \frac{\epsilon_0|\nabla_\perp\phi|^2}{2}}_{\text{total}} = \underbrace{\int_{r\le r_{\text{large}}} d^2x_\perp \frac{\epsilon_0|\nabla_\perp\phi|^2}{2}}_{\text{finite term}} + \underbrace{\frac{\lambda^2}{4\pi\epsilon_0}\int_{r_{\text{large}}}^{\infty} dr\frac{1}{r}}_{\text{logarithmically divergent term}}$$

- This divergence can be subtracted out to thereby regularized the system energy
  - Renders energy constraint useful for application to equilibria in radially unbounded systems such as thermal equilibrium

3) Angular Momentum

$$\boxed{U_\theta = \int d^2x_\perp \int d^2x'_\perp \, (yx' - x'y) f_\perp = \text{const}}$$

- Focusing and beam pipe (if present) must be axisymmetric
  - Useful for solenoidal magnetic focusing
  - Does not apply to alternating gradient quadrupole focusing since such systems do not have the required axisymmetry

4) Axial Momentum

$$\boxed{U_z = \int d^2x_\perp \int d^2x'_\perp \, m\gamma_b\beta_b c \, f_\perp = \text{const}}$$

- Trivial in present model, but useful when equations of motion are generalized to allow for a spread in axial momentum

Comments on applications of the global conservation constraints:

Global invariants strongly constrain the nonlinear evolution of the system
- Only evolutions consistent with Vlasov's equation are physical
- Constraints consistent with the model can bound kinematically accessible evolutions

Application of the invariants does not require (difficult to derive) normal mode descriptions
- But cannot, by itself, provide information on evolution timescales

Use of global constraints to bound perturbations has appeal since distributions in real machines may be far from an equilibrium. Used to:
- Derive sufficient conditions for stability
- Bound particle losses [O'Neil, Phys. Fluids **23**, 2216 (1980)]
- Bound changes of system moments (for example the rms emittance) under assumed relaxation processes

S6: Kinetic Stability Theorem for continuous focusing equilibria

[Fowler, J. Math Phys. **4,** 559 (1963); Gardner, Phys. Fluids **6**, 839 (1963); R. Davidson, Physics of Nonneutral Plasmas, Addison-Wesley (1990)]

Resolve:

$$f_\perp = f_0(H_0) + \delta f_\perp$$

$f_0(H_0) =$ Equilibrium (subscript 0) distribution

$\delta f_\perp =$ Perturbation about equilibrium

Employ generalized entropy and transverse energy global constraints (S5):

$$U_G = \int d^2x_\perp \int d^2x'_\perp \; G(f_\perp) \; = \text{const}$$

$$U_{\mathcal{E}} = \int d^2x'_\perp \int d^2x_\perp \left\{ \frac{1}{2}\mathbf{x}'^2_\perp + \frac{1}{2}k^2_{\beta 0}\mathbf{x}^2_\perp \right\} f_\perp \; + \; \int d^2x_\perp \frac{\epsilon_0 |\nabla_\perp \phi|^2}{2m\gamma_b^3\beta_b^2c^2} \; = \text{const}$$

Apply to equilibrium and full distribution to form an effective "free-energy":

$$\Delta U_G = U_G - U_{G0} = \text{const} \qquad \Delta U_{\mathcal{E}} = U_{\mathcal{E}} - U_{\mathcal{E}0} = \text{const}$$

$$\boxed{\begin{aligned} F &= \Delta U_{\mathcal{E}} - \Delta U_G \\ &= \int d^2x'_\perp \int d^2x_\perp \left\{ \frac{1}{2}\mathbf{x}'^2_\perp + \frac{1}{2}k^2_{\beta 0}\mathbf{x}^2_\perp \right\} \delta f_\perp \; + \; \int d^2x_\perp \frac{\epsilon_0 |\nabla_\perp \phi|^2}{2m\gamma_b^3\beta_b^2c^2} \\ &\quad + \int d^2x_\perp \int d^2x'_\perp \, [G(f_\perp) - G(f_0)] \; = \text{const} \end{aligned}}$$

The perturbed potential satisfies:

$$\delta\phi \equiv \phi - \phi_0 \qquad \nabla^2_\perp \delta\phi = -\frac{q}{\epsilon_0}\int d^2x'_\perp \; \delta f_\perp$$

Take $|\delta f_\perp| \ll f_0$ and Taylor expand to 2nd order

$$G(f_0 + \delta f_\perp) = G(f_0) + \frac{dG(f_0)}{df_0}\delta f_\perp + \frac{d^2G(f_0)}{df_0^2}\frac{(\delta f_\perp)^2}{2} + \Theta(\delta^3)$$

Without loss of generality, choose:

$$\frac{dG(f_0)}{df_0} = -H_0 = -\left(\frac{1}{2}\mathbf{x}'^2_\perp + \frac{1}{2}k^2_{\beta 0}\mathbf{x}^2_\perp + \frac{q\phi}{m\gamma_b^2\beta_b^2c^2} \right)$$

- This choice can *always* be realized

Then

$$\frac{d^2G(f_0)}{df_0^2} = -\frac{\partial H_0}{\partial f_0} = \frac{-1}{\partial f_0(H_0)/\partial H_0}$$

Some steps (few lines using partial integration) yields:

$$\boxed{F = \int d^2x_\perp \left\{ \frac{\epsilon_0 |\nabla_\perp \delta\phi|^2}{2m\gamma_b^3\beta_b^2c^2} - \int d^2x'_\perp \frac{(\delta f_\perp)^2}{\partial f_0(H_0)/\partial H_0} \right\} + \Theta(\delta^3) \; = \; \text{const}}$$

- If $\partial f_0(H_0)/\partial H_0 < 0$ then F is a sum of two positive definite terms and perturbations are bounded by F = const.

$$\boxed{F = \int d^2x_\perp \left\{ \frac{|\nabla_\perp \delta\phi|^2}{2m\gamma_b^3\beta_b^2c^2} - \int d^2x'_\perp \frac{(\delta f_\perp)^2}{\partial f_0(H_0)/\partial H_0} \right\} \; = \text{const}}$$

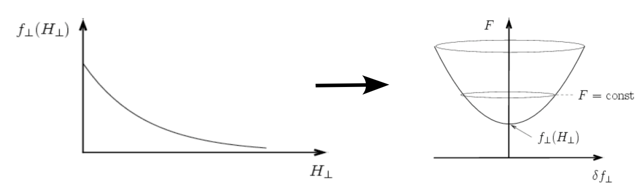

Value of F set by initial perturbations and concavity bounds excursions

Drop zero subscripts in stability statement:

Kinetic Stability Theorem

If $f_\perp(H_\perp)$ is a monotonic decreasing function of $H_\perp$ with $\partial f_\perp(H_\perp)/\partial H_\perp < 0$ then the equilibrium defined by $f_\perp(H_\perp)$ is stable to arbitrary small-amplitude perturbations.

- Is a sufficient condition for stability
  - Equilibria that violate the theorem may or may not be stable
- Mean value theorem can be used to generalize conclusions for arbitrary amplitude
  - R. Davidson proof

// Example Applications of Kinetic Stability Theorem

KV Equilibrium:

$$f_\perp(H_\perp) = \frac{\hat{n}}{2\pi}\delta(H_\perp - H_{\perp b})$$

$\partial f_\perp/\partial H_\perp$ changes sign
inconclusive stability by theorem

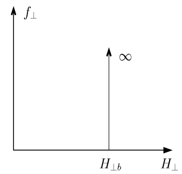

- Full normal mode analysis in Kinetic theory shows strong instabilities when space-charge becomes strong
- Not surprising, delta function represents a highly inverted population in phase-space with "free-energy" to drive instabilities

Waterbag Equilibrium:

$$f_\perp(H_\perp) = f_0\Theta(H_{\perp b} - H_\perp)$$
$$\partial f_\perp/\partial H_\perp = f_0\delta(H_\perp - H_{\perp b}) \leq 0$$

monotonic decreasing, stable by theorem

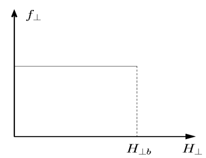

Thermal Equilibrium:

$$f_\perp(H_\perp) = f_0\exp(-\beta H_\perp),$$
$$\partial f_\perp/\partial H_\perp = -f_0\beta\exp(-\beta H_\perp) \leq 0$$

monotonic decreasing, stable by theorem

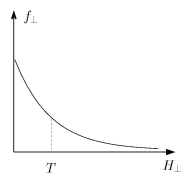

//

Add material to discuss combined application of the density inversion theorem and the kinetic stability theorem

- Monotonic decreasing radial density profile n(r) gives monotonic decreasing distribution f(H)
- Stability of radial density profiles follows for continuous focusing
- Extent this can be generalized to periodic focusing?

S7: rms Emittance Growth and Nonlinear Forces

Fundamental theme of beam physics is to minimize statistical beam emittance growth in transport to preserve focusability on target

Return to the full transverse beam model with:

$$x'' + \kappa_x x = -\frac{q}{m\gamma_b^3\beta_b^2c^2}\frac{\partial\phi}{\partial x} \quad + \quad \text{Applied Nonlinear Field Terms}$$

and express as:

$$\boxed{\begin{aligned} &x''(s) + \kappa_x(s)x(s) = f_x^L(s)x(s) + F_x^{NL}(x,y,s) \\ &f_x^L(s) = \text{Linear Space-Charge Coefficient} \\ &F_x^{NL}(x,y,s) = \text{Nonlinear Forces + Linear Skew Coupled Forces} \\ &\qquad\qquad\qquad (\text{Applied and Space-Charge}) \end{aligned}}$$

// Examples:

$$f_x^L(s) = \frac{Q}{r_b(s)}$$

Self-field forces within an axisymmetric (mismatched) KV beam core in a continuous focusing model

$$F_x^{NL}(x,y,s) = \text{Im}\left[b_3\left(\frac{x+iy}{r_p}\right)^2\right]$$

Electric (with normal and skew components) sextupole optic based on multipole expansions (see: lectures on Particle Equations of Motion) //

From the definition of the statistical (rms) emittance:

$$\varepsilon_x \equiv 4[\langle x^2\rangle_\perp\langle x'^2\rangle_\perp - \langle xx'\rangle_\perp^2]^{1/2}$$

Differentiate the squared emittance and apply the chain rule:

$$\begin{aligned}\frac{d}{ds}\varepsilon_x^2 &\equiv 32[\langle xx'\rangle_\perp\langle x'^2\rangle_\perp + \langle x^2\rangle_\perp\langle x'x''\rangle_\perp - \langle xx'\rangle_\perp\langle x'^2\rangle_\perp - \langle xx'\rangle_\perp\langle xx''\rangle_\perp] \\ &= 32[\langle x^2\rangle_\perp\langle x'x''\rangle_\perp - \langle xx'\rangle_\perp\langle xx''\rangle_\perp]\end{aligned}$$

Insert the equations of motion:

$$x'' + \kappa_x x = f_x^L x + F_x^{NL}$$

The linear terms cancel to show *for any beam distribution* that:

$$\boxed{\frac{d}{ds}\varepsilon_x^2 = 32\left[\langle x^2\rangle_\perp\langle x'F_x^{NL}\rangle_\perp - \langle xx'\rangle_\perp\langle xF_x^{NL}\rangle_\perp\right]}$$

Implications of:

$$\boxed{\frac{d}{ds}\varepsilon_x^2 = 32\left[\langle x^2\rangle_\perp \langle x' F_x^{NL}\rangle_\perp - \langle xx'\rangle_\perp \langle x F_x^{NL}\rangle_\perp\right]}$$

- Emittance evolution/growth is driven by nonlinear or skew coupling forces
  - Nonlinear terms can result from applied or space-charge fields
  - More detailed analysis shows that skew coupled forces cause *x*-*y* plane transfer oscillations but there is still a 4D quadratic invariant
- Minimize nonlinear forces to preserve emittance and maintain focusability
- This result (essentially) has already been demonstrated in the problem sets for the Introductory Lectures

If the beam is accelerating, the equations of motion become:

$$x'' + \frac{(\gamma_b\beta_b)'}{(\gamma_b\beta_b)}x' + \kappa_x x = f_x^L x + F_x^{NL}$$

and this result can be generalized (see homework problems) using the normalized emittance:

$$\boxed{\begin{aligned}&\varepsilon_{nx} \equiv \gamma_b\beta_b\varepsilon_x \\ &\frac{d}{ds}\varepsilon_{nx}^2 = 32(\gamma_b\beta_b)^2\left[\langle x^2\rangle_\perp \langle x' F_x^{NL}\rangle_\perp - \langle xx'\rangle_\perp \langle x F_x^{NL}\rangle_\perp\right]\end{aligned}}$$

S8: rms Emittance Growth and Nonlinear Space-Charge Forces

[Wangler et. al, IEEE Trans. Nuc. Sci. 32, 2196 (1985), Reiser, *Charged Particle Beams*, (1994)]

In continuous focusing all nonlinear force terms are from space-charge, giving:

$$\boxed{\frac{d}{ds}\varepsilon_x^2 = -\frac{32q}{m\gamma_b^3\beta_b^2c^2}\left[\langle x^2\rangle_\perp \langle x'\frac{\partial\phi}{\partial x}\rangle_\perp - \langle xx'\rangle_\perp \langle x\frac{\partial\phi}{\partial x}\rangle_\perp\right]}$$

For any axisymmetric beam it can be shown that:

$$\langle x\frac{\partial\phi}{\partial x}\rangle_\perp = \frac{1}{2}\langle\frac{\partial\phi}{\partial r}\rangle_\perp = -\frac{\lambda}{8\pi\epsilon_0}$$

$$\langle x'\frac{\partial\phi}{\partial x}\rangle_\perp = \frac{1}{2}\langle r'\frac{\partial\phi}{\partial x}\rangle_\perp = \frac{1}{8\pi\epsilon_0\lambda}\frac{dW}{ds}$$

$$W = \frac{\epsilon_0}{2}\int d^2x\, |\nabla_\perp\phi|^2$$

= self-field energy (per unit axial length)

For any axisymmetric beam it can also be shown that:

$$\langle xx'\rangle_\perp = \frac{1}{2}\langle rr'\rangle_\perp = -\frac{\langle x^2\rangle_\perp}{\lambda^2}\frac{dW_u}{ds}$$

W_u = W for an rms equivalent uniform density beam

These results give (Wangler, Lapostolle):

$$\boxed{\frac{d}{ds}\varepsilon_x^2 = -4Q\langle x^2\rangle_\perp \frac{d}{ds}\left(\frac{W-W_u}{\lambda^2}\right)}$$

$$\boxed{\frac{d}{ds}\varepsilon_x^2 = -8Q\langle x^2\rangle_\perp \frac{d}{ds}\left(\frac{W-W_u}{\lambda^2}\right)}$$

- Applies to both radially bounded and radially infinite systems
- Result does not require an equilibrium for validity – only axisymmetry
- For a beam with s-variation, this result suggests that *only* the (mismatched) KV equilibrium can subsequently evolve with no change in rms emittance
- Result can be partially generalizable [J. Struckmeier and I. Hofmann, Part. Accel. **39**, 219 (1992)] to an unbunched elliptical beam
  - Result may have implications to existence/nonexistence of nonuniform density Vlasov equilibria in periodic focusing channels

If the rms beam radius does not change much in the beam evolution:

$$r_b^2 = 2\langle x^2\rangle_\perp \simeq \text{const}$$

Then the equation can be trivially integrated to show that:

$$\boxed{\begin{aligned}&\Delta_{fi}(\varepsilon_x^2) = -4Qr_b^2\Delta_{fi}\left(\frac{W-W_u}{\lambda^2}\right) \\ &\Delta_{fi}(\cdots) \equiv \text{Final State Value – Initial State Value}\end{aligned}}$$

Consider the rms envelope equation to better understand what is required for $r_b^2 = \text{const}$

$$r_b'' + k_{\beta0}^2 r_b - \frac{Q}{r_b} - \frac{\varepsilon^2}{r_b^3} = 0$$

- Valid in an rms equivalent sense with $\varepsilon \neq \text{const}$ for a non-KV beam

If the emittance term is small relative to the perveance term and the intial beam starts out as matched we can approximate the equation as

$$k_{\beta0}^2 r_b - \frac{Q}{r_b} - \frac{\varepsilon^2}{r_b^3} = 0$$

and it is reasonable to expect the beam radius to remain nearly constant under modest changes in emittance. This ordering must be checked after estimating the emittance change based the final to initial state energy differences. See S9 and S10 analysis for a better understanding on how this can be valid.

S9: Uniform Density Beams and Extreme Energy States

Construct minima of the self-field energy per unit axial length:

$$\boxed{W = \frac{\epsilon_0}{2}\int d^2x_\perp \, |\nabla_\perp \phi|^2}$$

subject to: $\lambda = \text{const}$ ... fixed line-charge

$r_b = \sqrt{2\langle r^2\rangle_\perp} = \text{const}$ ... fixed rms equivalent beam radius

Using the method of Lagrange multipliers, vary (Helmholtz free energy):

$$F = W - \mu(\lambda/q)\langle r^2\rangle_\perp = \int d^2x_\perp \left\{\epsilon_0 \frac{|\nabla_\perp \phi|^2}{2} - \mu r^2 n\right\} \qquad \mu = \text{const}$$

and require that variations satisfy the Poisson equation and conserve charge

$$\nabla_\perp^2 \delta\phi = -\frac{q}{\epsilon_0}\delta n \qquad \delta\phi|_{\text{boundary}} = 0 \qquad \int d^2x_\perp \, \delta n = 0$$

Then variations *terminate* at 2nd order giving:

$$\delta F = -\int d^2x_\perp \, \{\mu r^2 + \text{const}\}\,\delta n + \epsilon_0 \int d^2x_\perp \nabla_\perp\phi \cdot \nabla_\perp \delta\phi + \frac{\epsilon_0}{2}\int d^2x_\perp |\nabla_\perp \delta\phi|^2$$

Integrating the 2nd term by parts and employing the Poisson equation then gives:

$$\boxed{\delta F = \int d^2x_\perp \, \{q\phi - \mu r^2 - \text{const}\}\,\delta n \; + \; \frac{\epsilon_0}{2}\int d^2x_\perp |\nabla_\perp \delta\phi|^2}$$

For an extremum, the first order term must vanish, giving *within the beam*:

$$q\phi = \mu r^2 + \text{const}$$

From Poisson's equation:

$$\frac{1}{r}\left(r\frac{\partial\phi}{\partial r}\right)\phi = \text{const}$$

This is the density of a uniform, axisymmetric beam, which implies that a uniform density axisymmetric beam results in an extremum. This extremum is also a global maximum since all variations about it (2nd term of boxed equation above) are positive definite.

Result:

At fixed line charge and rms radius, a uniform density beam minimizes the electrostatic self-field energy

The result:

At fixed line charge and rms radius, a uniform density beam minimizes the electrostatic self-field energy

combined with Wangler's Theorem:

$$\boxed{\frac{d}{ds}\varepsilon_x^2 = -Q\langle x^2\rangle_\perp \frac{d}{ds}\left(\frac{W - W_u}{\lambda^2}\right)}$$

shows that:

- Self-field energy changes from beam nonuniformity drives emittance evolution
- Expect the following trends in an evolving beam density profile
  - *Nonuniform* density => *more* *uniform* density <=> local emittance *growth*
  - *Uniform* density => *more nonuniform* density <=> local emittance *reduction*
- Should attempt to maintain beam density uniformity to preserve beam emittance and focusability

Results can be partially generalized to 2D elliptical beams

[J. Struckmeier and I. Hofmann, Part Accel. **39**, 219 (1992)]

S10: Collective Relaxation and rms Emittance Growth

The space-charge profile of intense beams can be born highly nonuniform out of nonideal (real) injectors or become nonuniform due to a variety of (error) processes. Also, low-order envelope matching of the beam may be incorrect due to focusing and/or distribution errors.

How much emittance growth and changes in other characteristic parameters may be induced by relaxation of characteristic perturbations?

- Employ Global Conservation Constraints of system to bound possible changes
- Assume full relaxation to a final, uniform density state for simplicity

What is the mechanism for the assumed relaxation?

- Collective modes launched by errors will have a broad spectrum
  - Phase mixing can smooth nonuniformities – mode frequencies incommensurate
- Nonlinear interactions, Landau damping, interaction with external errors, ...
- Certain errors more/less likely to relax:
  - Internal wave perturbations expected to relax due to many interactions
  - Envelope mismatch will not (coherent mode) unless amplitudes are very large producing copious halo and nonlinear interactions

Example: Relaxation of nonlinear space-charge waves

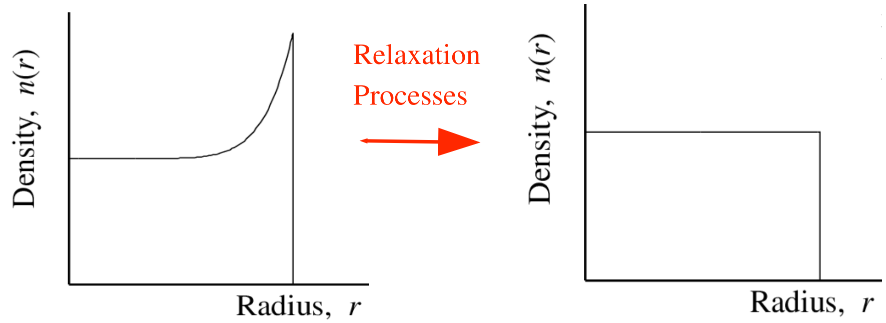

Reference: High resolution self-consistent PIC simulations shown in class

- Continuous focusing and a more realistic FODO transport lattice
  - Relaxation more complete in real lattice due to a richer frequency spectrum
- Relaxations surprisingly rapid: few undepressed betatron wavelengths observed in simulations

SM Lund, USPAS, June 2008 Transverse Kinetic Stability 53

Initial Nonuniform Beam Parameterization

$$n(r) = \begin{cases} \hat{n}\left[1 + \frac{1-h}{h}\left(\frac{r}{r_e}\right)^p\right], & 0 \leq r \leq r_e \\ 0, & r_e < r \leq r_p \end{cases}$$

$h =$ hollowing parameter $= n(r=0)/n(r=r_e)$

$p =$ radial index

$r_e =$ edge radius

$$\lambda = \int d^2x_\perp \, n = \pi q \hat{n} r_e^2 \left[\frac{(ph+2)}{(p+2)h}\right] \qquad r_b = 2\langle x^2\rangle_\perp^{1/2} = \sqrt{\frac{(p+2)(ph+4)}{(p+4)(ph+2)}}\, r_e$$

Normalize profiles to compare common rms radius (r_b) and total charge (λ)

Hollowed Initial Density

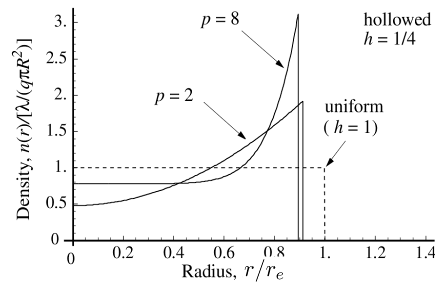

Peaked Initial Density

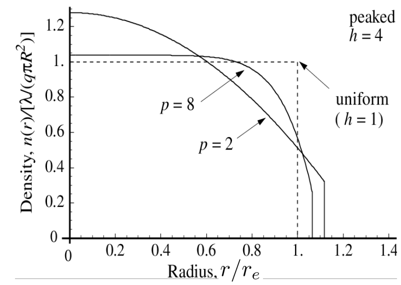

- Analogous definitions are made for the radial temperature profile of the beam

SM Lund, USPAS, June 2008 Transverse Kinetic Stability 54

Example Simulation, Initial Nonuniform Beam

$\sigma/\sigma_0 = 0.2$ Initial density: h=1/4, p=8 Initial Temp: h = infinity, p=2

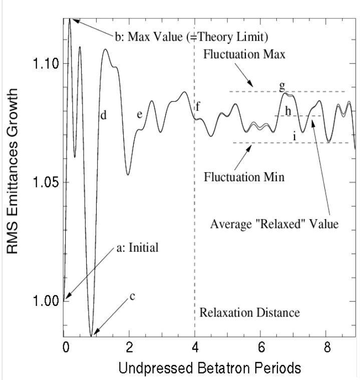

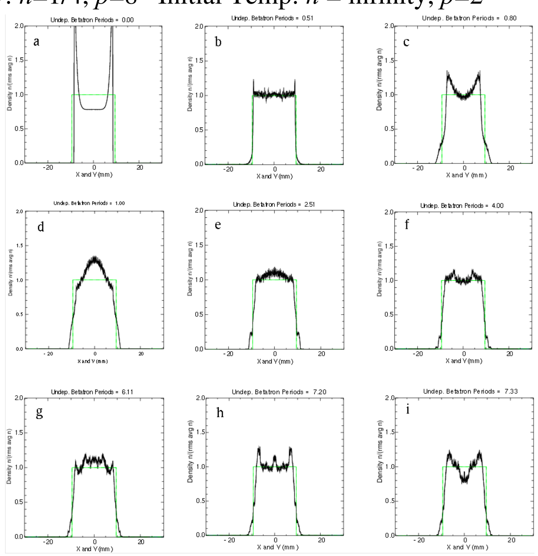

Show movie of evolution

[Lund, Grote, and Davidson, Nuc. Instr. Meth. A 544, 472 (2005)]

SM Lund, USPAS, June 2008 Transverse Kinetic Stability 55

Simulation results for a broad range of strong space-charge

Initial beam					Relaxed and transient beam		
σ_i/σ_0	Density		Temperature		Emittance growth		Undep. betatron periods to relax
	h	p	h	p	Theory	Simulation	
0.1	0.25	4	1	arb.	1.57	1.42 (1.57, 1.31–1.52)	3.5
			∞	2		1.45 (1.57, 1.38–1.52)	3.0
			0.5			1.41 (1.57, 1.30–1.52)	3.0
	0.25	8	1	arb.	1.43	1.33 (1.43, 1.28–1.38)	3.5
			∞	2		1.35 (1.43, 1.30–1.40)	4.5
			0.5			1.32 (1.43, 1.26–1.38)	4.0
0.20	0.25	4	1	arb.	1.17	1.11 (1.16, 1.09–1.13)	4.5
			∞	2		1.12 (1.16, 1.10–1.13)	3.0
			0.5			1.11 (1.16, 1.09–1.13)	4.0
	0.25	8	1	arb.	1.12	1.08 (1.12, 1.06–1.09)	5.5
			∞	2		1.08 (1.12, 1.07–1.09)	4.0
			0.5			1.08 (1.12, 1.06–1.09)	4.5

Theory results based on conservation of system charge and energy used to calculate the change in rms edge radius between initial (i) and final (f) matched beam states

$$\frac{(r_{bf}/r_{bi})^2 - 1}{1 - (\sigma_i/\sigma_0)^2} + \frac{p(1-h)[4+p+(3+p)h]}{(p+2)(p+4)(2+ph)^2} - \ln\left[\sqrt{\frac{(p+2)(ph+4)}{(p+4)(ph+2)}}\frac{r_{bf}}{r_{bi}}\right] = 0$$

Ratios of final to initial emittance are then obtainable from the matched envelope eqns:

$$\frac{\varepsilon_{xf}}{\varepsilon_{xi}} = \frac{r_{bf}}{r_{bi}}\sqrt{\frac{(r_{bf}/r_{bi})^2 - [1-(\sigma_i/\sigma_0)^2]}{(\sigma_i/\sigma_0)^2}}$$

SM Lund, USPAS, June 2008 Transverse Kinetic Stability 56

Theory estimates from global conservation constraints work well. What changes if the beam relaxes to a smooth thermal equilibrium instead? -- Very little change

Step 1:
Peaked to uniform

Step 2:
Uniform to Thermal

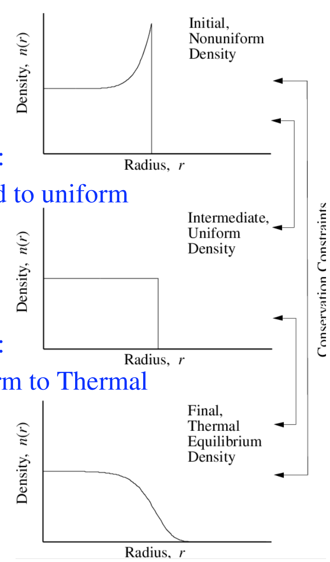

Regard as a two-step relaxation and apply conservation steps between each step

Essentially no rms changes in 2nd step!

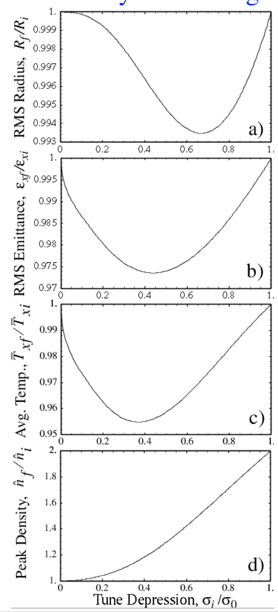

Lund, Barnard, and Miller, PAC 1995, p. 3278

S11: Halo Induced Mechanism of Higher Order Instability

In periodic focusing with alternating gradient quadrupole focusing (most common case), it has been observed in simulations and the laboratory that good transport in terms of little lost particles or emittance growth is obtained when the applied focusing strength satisfies:

$$\boxed{\sigma_0 \lesssim 85^\circ} \qquad \text{little dependence on} \quad \sigma/\sigma_0$$

It has been a 40+ year unsolved problem by what primary mechanism this limit comes about. It was long thought that collective modes coupled to the lattice were responsible. However:

- Modes carry little free energy (see S10) to drive strong emittance growth
- Particle losses and strong halo observed when stability criterion is violated
- Collective internal modes likely also pumped but hard to explain with KV

Recent progress helps clarify how this limit comes about via a strong halo-like resonance mechanism affecting near edge particles

- Does *not* require an equilibrium core beam

Self consistent Vlasov stability simulations were carried out to better quantify characteristics of instability

- 2D *x-y* slice simulations advanced in *s*
- Initial distributions: semi-Gaussian, a smooth equilibrium-like, and KV
- Carried out using the WARP PIC code

More Details:
Lund and Chawla, "Space-charge transport limits of ion beams in periodic quadrupole focusing channels," *Nuc. Instr. Meth. A* **561**, 203 (2006)

Parametric PIC simulations of quadrupole transport agree with experimental observations and show that large rms emittance growth can occur rapidly

Parameters: $\sigma_0 = 110^\circ$, $\sigma/\sigma_0 = 0.2$ $(L_p = 0.5 \text{ m}, \eta = 0.5)$
for initial semi-Gaussian distribution

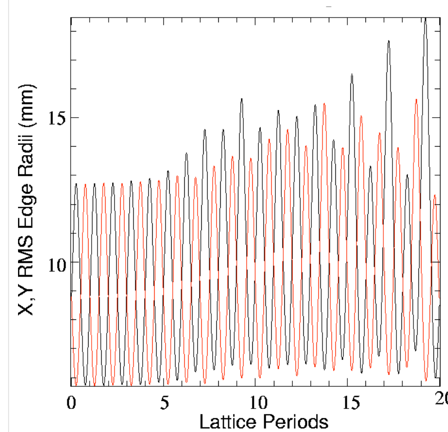

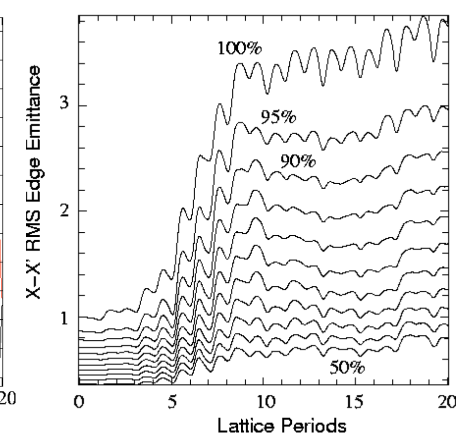

Higher $\sigma_0 \lesssim 85^\circ$ makes the onset of emittance growth larger and more rapid

Simulations suggest that transport limits observed are relatively insensitive to the structure of the initial distribution

Parameters: $\sigma_0 = 110°$, $\sigma/\sigma_0 = 0.2$ ($L_p = 0.5$ m, $\eta = 0.5$)

- Wide class of initial distributions probed – little difference in *x-y* plane averages which help average over initial phase choices associated with launching conditions
- Growth becomes larger and faster with increasing σ_0

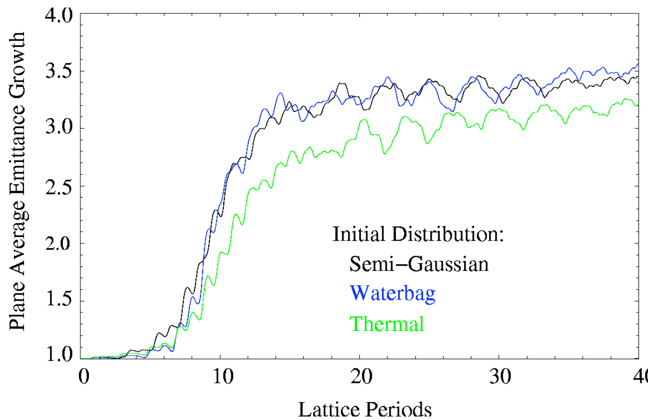

An essential feature is that particles evolve outside the core of the beam

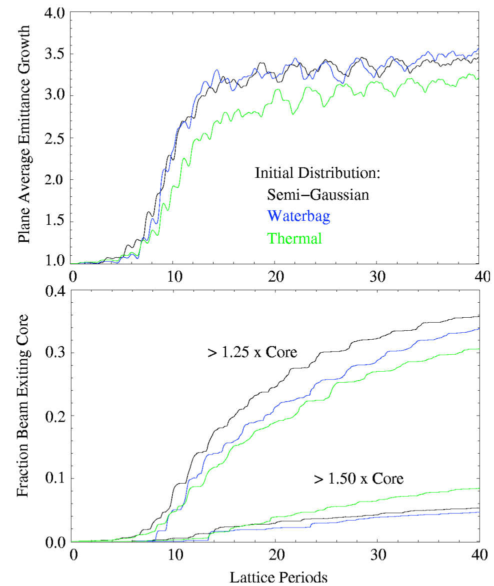

Take an instantaneous, rms equivalent measure of the core of the beam and "tag" particles that evolve outside the core:

$$r_x = 2\langle x^2 \rangle_\perp^{1/2}$$

$$r_y = 2\langle y^2 \rangle_\perp^{1/2}$$

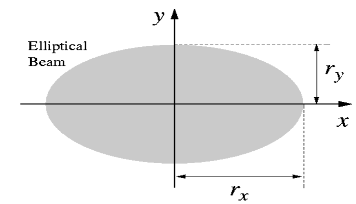

Poincare plots generated from different initial distributions agree qualitatively in areas of strong instability and show large oscillation amplitude particle are halo like with resonant structure

Lattice period Poincare strobe

$\sigma_0 = 110° \quad \sigma/\sigma_0 = 0.2$

Semi-Gaussian

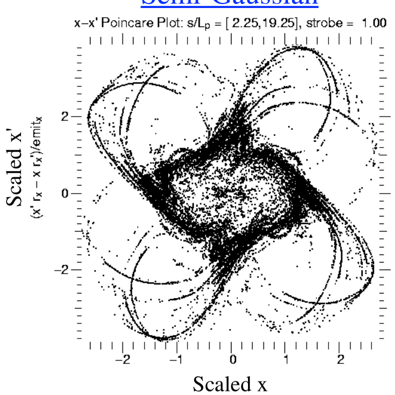

Thermal Equilibrium

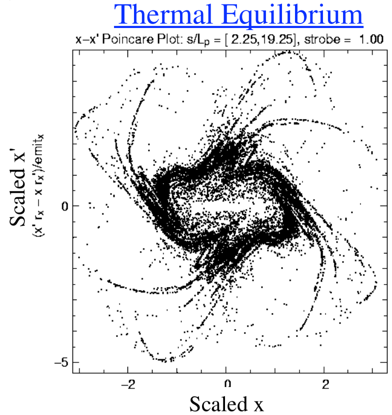

- Particles evolving along *x*-axis particles accumulated to generate clearer picture
  - Including off axis particles does *not* change basic conclusions

Extensive simulations were carried out to better understand the parametric nature of the emittance growth

- All simulations carried out 6 undepressed betatron periods
  - Enough to resolve transition boundary: transition growth can be larger if run longer
- Strong growth regions of initial distributions all similar (threshold can vary)
  - Irregular grid contouring with ~200 points (dots) to thoroughly probe possible instabilities

initial semi-Gaussian

- Initial thermal equilibrium almost identical

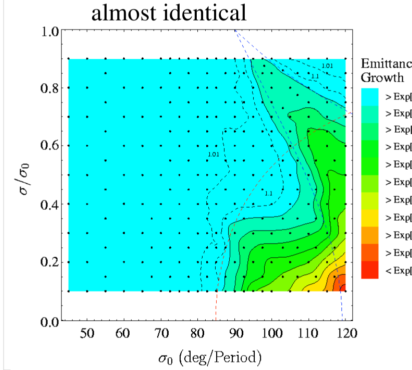

initial Waterbag Pseudo-Equilibrium

- Initial KV similar but does not excite envelope band

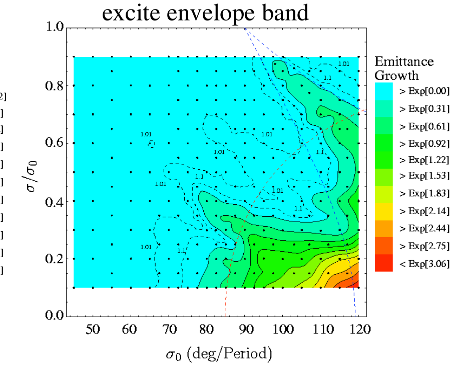

Core-Particle Model --- Transverse particle equations of motion for a test particle moving inside and outside a uniform density elliptical beam envelope

$$\boxed{\begin{aligned} x'' + \kappa_x x &= \frac{2QF_x}{(r_x + r_y)r_x} x \\ y'' + \kappa_y y &= \frac{2QF_y}{(r_x + r_y)r_y} y \end{aligned}}$$

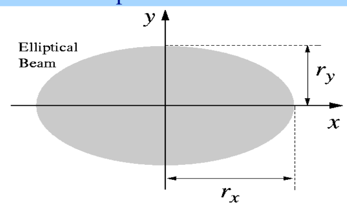

$$Q = \frac{q\lambda}{2\pi\epsilon_0 m\gamma_b^2\beta_b^2 c^2}$$ ..... dimensionless perveance

Where: inside the beam

$F_x = 1$

$F_y = 1$

outside the beam:

$$F_x = (r_x + r_y)\frac{r_x}{x} Re[\tilde{S}]$$

$$F_y = -(r_x + r_y)\frac{r_y}{y} Im[\tilde{S}]$$

with

$$\tilde{S} \equiv \frac{\tilde{z}}{r_x^2 - r_y^2}\left[1 - \sqrt{1 - \frac{(r_x^2 - r_y^2)}{\tilde{z}^2}}\right]$$

$$= \frac{1}{2\tilde{z}}\left[1 + \frac{1}{2}\frac{r_x^2 - r_y^2}{\tilde{z}^2} + \frac{1}{8}\frac{(r_x^2 - r_y^2)^2}{\tilde{z}^4} + \cdots\right]$$

$$\tilde{z} = x + iy$$

$$i = \sqrt{-1}$$

Particles oscillating radially outside the beam envelope will experience oscillating nonlinear forces that vary with space-charge intensity and can drive resonances

Continuous Focusing Axisymmetric Beam Radial Force

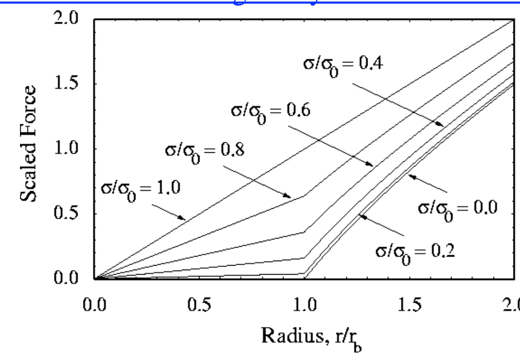

- Nonlinear force transition at beam edge larger for strong space-charge
- Edge oscillations of matched beam enhance nonlinear effects acting on particles moving outside the envelope
- In AG focusing envelope oscillation amplitude scales strongly with

Core-particle simulations: Poincare plots illustrate resonances associated with higher-order halo production near the beam edge for FODO quadrupole transport

- High order resonances near the core are strongly expressed
- Resonances stronger for higher σ_0 and stronger space-charge
- Can overlap and break-up (strong chaotic transition) allowing particles launched *near the core* to rapidly increase in oscillation amplitude

Lattice Period Poincare Strobe, particles launched [1.1,1.2] times core radius

Stable $\sigma_0 = 95°, \quad \sigma/\sigma_0 = 0.67$

Unstable $\sigma_0 = 110°, \quad \sigma/\sigma_0 = 0.1$

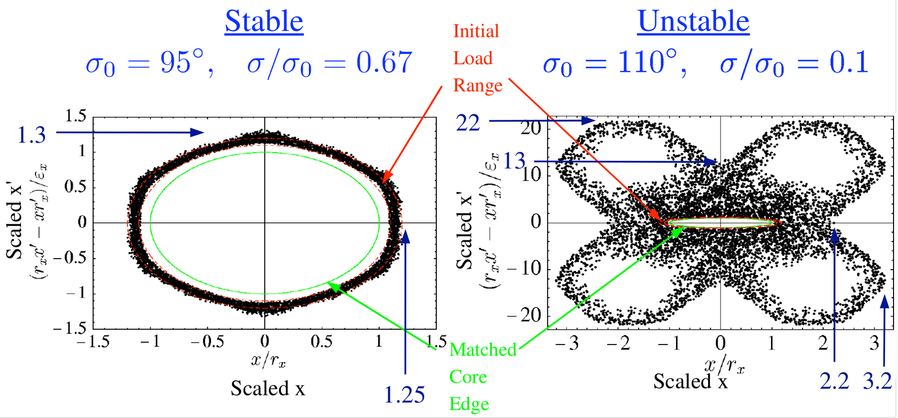

Core-particle simulations: Amplitude pumping of characteristic "unstable" phase-space structures is typically rapid and saturates whereas stable cases experience little or no growth

$\sigma_0 = 60°, \quad \sigma/\sigma_0 = 0.1$

$\sigma_0 = 110°, \quad \sigma/\sigma_0 = 0.1$

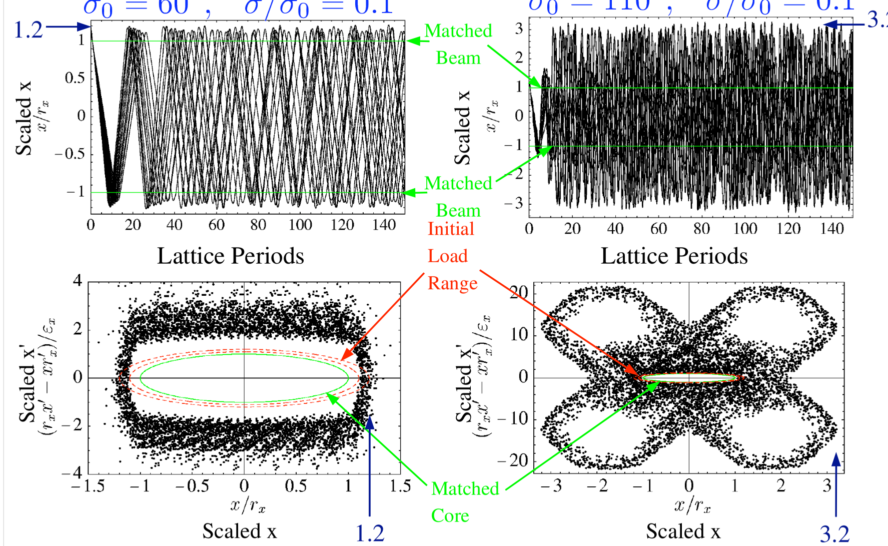

Core particle simulations: Stability boundary data from a "halo" stability criterion agree with experimental data for quadrupole transport limits

- Start at a point (σ_0, σ) deep within the stable region
- While increasing σ_0 vary σ to find a point (if it exists) where initial launch groups [1.05, 1.10] outside the matched beam envelope are pumped to max amplitudes of 1.5 times the matched envelope
  - Boundary position relatively insensitive to specific group and amplitude growth choices

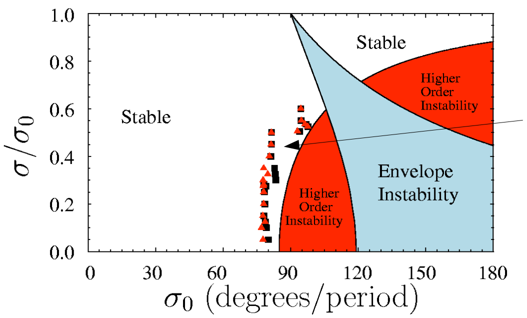

Stability boundary points for two slightly different amplitudes (triangles, squares)

Other halo analyses of transport limits conclude overly restrictive limits:
[Lagniel, Nuc. Instr. Meth. A **345**, 405 (1994)]

Contours of maximum particle amplitudes obtained in the core particle model are strongly suggestive of trends observed in self-consistent simulation and experimental data

Max amplitudes achieved for particles launched [1.05,1.1] times the core radius:
- Variation with small changes in launch position small

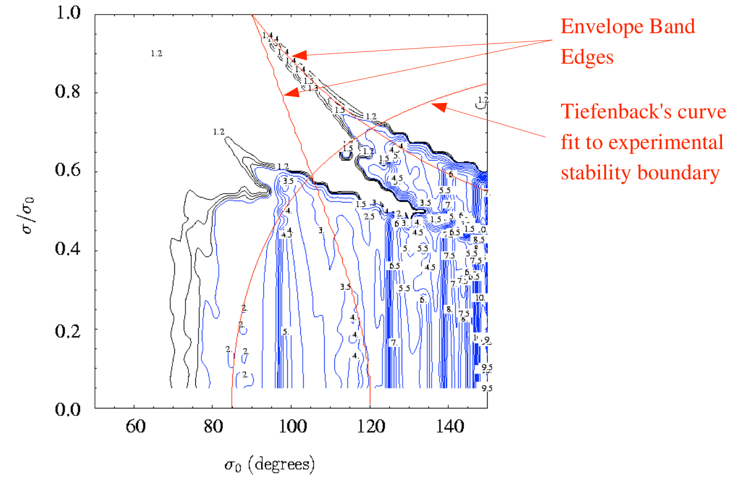

Conclusions

High-order space-charge related emittance growth has long been observed in intense beam transport in quadrupole focusing channels with $\sigma_0 \gtrsim 85^\circ$:
- SBTE Experiment at LBNL [M.G. Tiefenback, Ph.D Thesis, UC Berkeley (1986)]
- Simulations

A core-particle model has been developed that suggests observed transport limits result from a halo like mechanism:
- Near edge particles feel strong, rapidly oscillating nonlinear forces when moving just outside the matched beam envelope
- Drives a strongly chaotic resonance chain that limits at large amplitude resulting in a distorted beam and large statistical rms emittance growth
- Lack of core equilibrium provides a natural pump of significant numbers of particles outside the statistical beam edge and increase in oscillation amplitude

Instability mechanism expected to explain other features
- Stronger with envelope mismatch: consistent with observation that mismatched beams more unstable
- Weaker for focusing without much envelope fluctuation: high occupancy solenoids

More Details:

Lund and Chawla, *Space-charge transport limits of ion beams in periodic quadrupole focusing channels*, *Nuc. Instr. Meth. A* **561**, 203 (2006)

Lund, Barnard, Bukh, Chawla, and Chilton, *A core-particle model for periodically focused ion beams with intense space-charge*, *Nuc. Instr. Meth. A* **577**, 173 (2006)

Lund, Kikuchi, and Davidson, *Generation of intial kinetic distributions for simulation of long-pulse charged particle beams with high space-charge intensity*, submitted to PRSTAB

S12: Phase Mixing and Landau Damping in Beams

To be covered in future editions of class notes
- Likely inadequate time in lectures

These slides will be corrected and expanded for reference and any future editions of the US Particle Accelerator School class: *Beam Physics with Intense Space Charge*, by J.J. Barnard and S.M. Lund

Corrections and suggestions are welcome. Contact:

Steven M. Lund
Lawrence Berkeley National Laboratory
BLDG 47 R 0112
1 Cyclotron Road
Berkeley, CA 94720-8201

SMLund@lbl.gov
(510) 486 – 6936

References: For more information see:

M. Reiser, *Theory and Design of Charged Particle Beams*, Wiley (1994)

R. Davidson, *Theory of Nonneutral Plasmas*, Addison-Wesley (1989)

R. Davidson and H. Qin, Physics of Intense Charged Particle Beams in High Energy Accelerators, World Scientific (2001)

F. Sacherer, *Transverse Space-Charge Effects in Circular Accelerators*, Univ. of California Berkeley, Ph.D Thesis (1968)

S. Lund and B. Bukh, Review Article: *Stability Properties of the Transverse Envelope Equations Describing Intense Beam Transport*, PRST-Accel. and Beams 7, 024801 (2004)

S. Lund and R. Davidson, *Warm Fluid Description of Intense Beam Equilibrium and Electrostatic Stability Properties*, Phys. Plasmas 5, 3028 (1998)

D. Nicholson, *Introduction to Plasma Theory*, Wiley (1983)

References (2)

Lund and Chawla, *Space-charge transport limits of ion beams in periodic quadrupole focusing channels*, Nuc. Instr. Meth. A **561**, 203 (2006)

Lund, Barnard, Bukh, Chawla, and Chilton, *A core-particle model for periodically focused ion beams with intense space-charge*, Nuc. Instr. Meth. A **577**, 173 (2006)

J.J Barnard and S.M. Lund
USPAS, June 2008

1

S4 Collective Modes on a KV Equilibrium Beam

Here we take a KV equilibrium distribution with

$$\boxed{f_0(H_0) = \frac{\hat{n}}{2\pi}\,\delta\left[H_0 - \frac{\varepsilon_x^2}{2r_b^2}\right]}$$

$\hat{n}$ = constant density of KV equilibrium
ε_x^2 = x-emittance.
r_b = equilibrium beam radius.

$$k_{\beta 0}^2 r_b - \frac{Q}{r_b} - \frac{\varepsilon_x^2}{r_b^3} = 0$$

$$H_0 = \frac{1}{2}\vec{x}_\perp'^2 + \frac{k_{\beta 0}^2}{2}\vec{x}_\perp^2 + \frac{q\phi_0}{m\gamma_b^3\beta_b^2c^2}$$

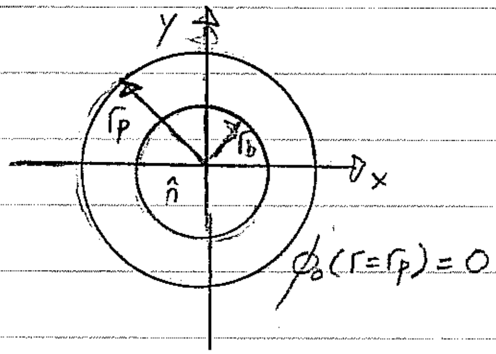

and assume small-amplitude axisymmetric $(\partial/\partial\theta=0)$ perturbations with normal mode form:

$$\boxed{\begin{aligned}\delta f(\vec{x}_\perp,\vec{x}_\perp',s) &= \delta f(r,\vec{x}_\perp',k)\,e^{-iks}\\ \delta\phi(\vec{x}_\perp,s) &= \delta\phi(r,k)\,e^{-iks}\end{aligned}}$$

k = const (mode eigenfrequency)

The equilibrium characteristics in the core of the KV beam can be expressed as:

$$\boxed{\begin{aligned}
r^2(\tilde{s}) &= r^2\cos^2[k_\beta(\tilde{s}-s)] + \frac{r r'}{k_\beta}\cos\psi \sin[2k_\beta(\tilde{s}-s)] \\
&\quad + \frac{r'^2}{k_\beta^2}\sin^2[k_\beta(\tilde{s}-s)] \\
x(\tilde{s}=s) &= r\cos\theta \quad ; \quad x'(\tilde{s}=s) = r'\cos\theta_p \\
y(\tilde{s}=s) &= r\sin\theta \quad ; \quad y'(\tilde{s}=s) = r'\sin\theta_p \\
\psi &\equiv \theta - \theta_p \\
k_\beta &= \left(k_{\beta 0}^2 - \frac{Q}{r_b^2}\right)^{1/2} = \frac{\varepsilon_x}{r_b^2} \quad \text{Depressed } \beta\text{-tron wavenumber of particle oscillations}
\end{aligned}}$$

These results can be inserted into the characteristic equation

$$\delta f(\vec{x}_\perp, \vec{x}_\perp', s) = \frac{q}{m\gamma_b^3\beta_b^2 c^2}\int_{-\infty}^{s} d\tilde{s}\; \frac{\partial \delta\phi(\vec{x}_\perp(\tilde{s}))}{\partial \vec{x}_\perp(\tilde{s})} \cdot \frac{\partial}{\partial \vec{x}_\perp'(\tilde{s})} f_0\left(H_0\left(\vec{x}_\perp(\tilde{s}), \vec{x}_\perp'(\tilde{s})\right)\right)$$

to derive an expression for $\delta f(r, \vec{x}_\perp')$. This expression can then be inserted into the Poisson equation

$$\frac{1}{r}\frac{\partial}{\partial r}\left(r\frac{\partial \delta\phi(r)}{\partial r}\right) = \frac{-q}{\epsilon_0}\int d^2x'\, \delta f(r, \vec{x}_\perp')$$

to derive a linear eigenvalue equation for $\delta\phi(r)$:

A significant amount of manipulation obtains the following form for the eigenvalue equation:

$$\left(\frac{\partial^2}{\partial r^2} + \frac{1}{r}\frac{\partial}{\partial r}\right)\delta\phi(r) = \frac{\hat{\omega}_p^2}{\gamma_b \beta_b^2 c^2}\,\Theta(r_b - r)\,\frac{1}{r_\perp'}\frac{\partial}{\partial r_\perp'} I_{orb}(r, r_\perp', k)\Big|_{r_\perp'^2 = \frac{\varepsilon_x^2}{r_b^2}\left(1-\frac{r^2}{r_b^2}\right)} \quad (1)$$

$$+ \frac{\hat{\omega}_p^2/(\gamma_b \beta_b^2 c^2)}{\varepsilon_x^2/r_b^2}\,\delta(r - r_b)\left[\delta\phi + I_{orb}(r, r_\perp', k)\right]_{r_\perp'=0} \quad (2)$$

Subject to: $\delta\phi(r = r_b) = 0$, $\hat{\omega}_p^2 = \frac{q^2\hat{n}}{\varepsilon_0 m}$ = Plasma Freq. Squared.

where:

$$\Theta(r_b - r) \equiv \begin{cases} 1 & r_b > r \\ 0 & r_b < r \end{cases} \quad \text{Heaviside Step function}$$

$$I_{orb}(r, r_\perp', k) = ik\int_{-\pi}^{\pi}\frac{d\psi}{2\pi}\int_{-\infty}^{s} d\tilde{s}\;\delta\phi(r(\tilde{s}), k)\, e^{-ik(\tilde{s}-s)}$$

Orbit integral.

Note:

- Term (1) $\propto \Theta(r_b - r)$ is a body-wave perturbation existing only in the core $(r < r_b)$ of the equilibrium beam.
- Term (2) $\propto \delta(r - r_b)$ is a surface-wave perturbation existing only at the edge $(r = r_b)$ of the equilibrium beam.
- The orbit integral $I_{orb}(r, r', k)$ depends on both $\delta\phi$ and the eigenfrequency k.

The Poisson equation has become a linear integro-differential eigenvalue equation fixing the mode perturbed potential $\delta\phi$ and eigenfrequency k.

This eigenvalue equation is difficult, but it has been solved analytically

- A finite polynomial in r^2 expansion of $\delta\phi$ for $r<r_b$ can satisfy the equation (terms truncate)
- Expansions are inserted into the characteristic integrals and coefficients are identified power-by-power in r^2 and assembled.

Solution (after much analysis)

Eigenfunction:

$$\boxed{\delta\phi_n(r) = \begin{cases} \frac{A_n}{2}\left[P_{n-1}(1-2r^2/r_b^2) + P_n(1-2r^2/r_b^2)\right] ; & 0 \le r < r_b \\ 0 ; & r_b < r \le r_p \end{cases}}$$

$n = 1, 2, 3, \ldots$ radial mode index

$A_n = \text{const.}$ linear mode amplitude.

$P_n(x)$ n'th order Legendre Polynomial

Dispersion Relation:

Each n-labeled eigenfunction has 2n (degenerate) "eigenfrequencies" k satisfying an nth degree polynomial in k^2 dispersion relation.

$$\boxed{2n + \frac{1-(\sigma/\sigma_0)^2}{(\sigma/\sigma_0)^2}\left[B_{n-1}\left(\frac{k/k_{\beta 0}}{\sigma/\sigma_0}\right) - B_n\left(\frac{k/k_{\beta 0}}{\sigma/\sigma_0}\right)\right] = 0}$$

where: $\frac{\sigma}{\sigma_0} \equiv \frac{k_\beta}{k_{\beta 0}} = \frac{(k_{\beta 0}^2 - Q/r_b^2)^{1/2}}{k_{\beta 0}}$

and

$$\boxed{B_n(\alpha) \equiv \begin{cases} 1 & n=0 \\ \frac{[(\alpha/2)^2-0^2]}{[(\alpha/2)^2-1^2]}\cdot\frac{[(\alpha/2)^2-2^2]}{[(\alpha/2)^2-3^2]}\cdots\cdots\frac{[(\alpha/2)^2-(n-1)^2]}{[(\alpha/2)^2-n^2]} & n=1,3,5,\ldots \\ \frac{[(\alpha/2)^2-1^2]}{[(\alpha/2)^2-2^2]}\cdot\frac{[(\alpha/2)^2-3^2]}{[(\alpha/2)^2-4^2]}\cdots\cdots\frac{[(\alpha/2)^2-(n-1)^2]}{[(\alpha/2)^2-n^2]} & n=2,4,6,\ldots \end{cases}}$$

Properties:

Radial Eigenfunction:

- Vanishes outside the equilibrium beam edge ($r > r_b$).
- Has $n-1$ nodes with $\delta\phi = 0$ within the equilibrium beam ($r < r_b$).
- Each n labeled eigenfunction has $2n$ distinct frequencies

Corresponding perturbed density can be calculated from Poisson's equation:

$$\boxed{\begin{aligned} \delta n_n &= \delta n_n(r) e^{-i\omega s} \\ \delta n_n(r) &= -\frac{\varepsilon_0}{q}\frac{1}{r}\frac{\partial}{\partial r}\left(r\frac{\partial \delta\phi_n}{\partial r}\right) \end{aligned}}$$

- Find that the perturbed density of the mode is more larger near the outer ($r \lesssim r_b$) edge of the beam for larger n.

Eigenfunction Form

Mode number n	$\delta\phi_n / A_n$ (potential)	δn_n (density, scaled units)
1	$1-\tilde{r}^2$	1
2	$1-4\tilde{r}^2+3\tilde{r}^4$	$4(1-3\tilde{r}^2)$
3	$1-9\tilde{r}^2+18\tilde{r}^4-10\tilde{r}^6$	$9(1-8\tilde{r}^2+10\tilde{r}^4)$
4	$1-16\tilde{r}^2+60\tilde{r}^4-80\tilde{r}^6+35\tilde{r}^8$	$16(1-15\tilde{r}^2+45\tilde{r}^4-35\tilde{r}^6)$
⋮	⋮	⋮

$\tilde{r} \equiv r/r_b$

Radial Eigenfunction

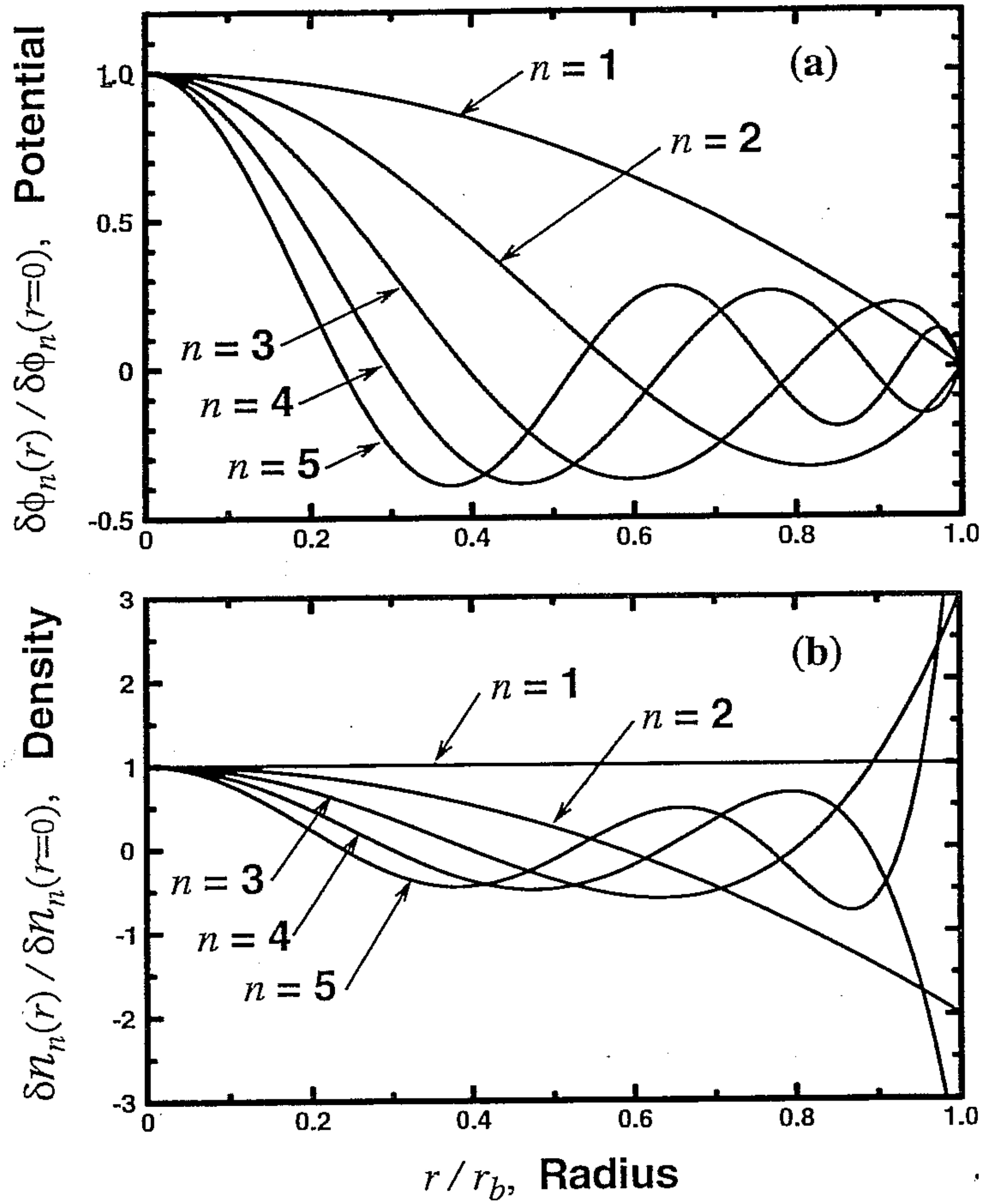

S. M. Lund

Perturbations should introduce no net charge into the system:

$$2\pi \int_0^{r_p} dr\, r\, \delta n(r) = 0$$

The $r < r_b$ component of the perturbations are not the only terms present. For the $r < r_b$ eigenfunctions calculated: $\int_0^{r_d} dr\, r\, \delta n_n(r) \neq 0$. A more detailed analysis shows that:

$$\boxed{\delta n_n(r) = \underbrace{\delta n_n(r)\Big|_{body} \Theta(r_b - r)}_{\substack{\text{body-wave} \\ \text{perturbation} \\ \text{in core of} \\ \text{equilibrium}}} + \underbrace{\delta n_n\Big|_{surface} \frac{r_b^2}{r}\delta(r - r_b)}_{\substack{\text{singular} \\ \text{Charge conserving} \\ \text{beam edge adjustment.} \\ \text{at } r = r_b}}}$$

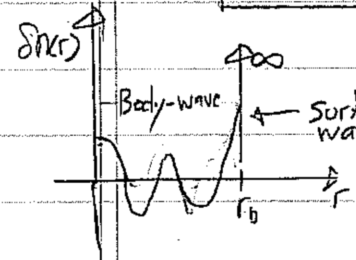

where:

$$\delta n_n\Big|_{body} = -\frac{\varepsilon_0}{q}\frac{1}{r}\frac{\partial}{\partial r}\left(r\frac{\partial \delta\phi_n}{\partial r}\right)$$

$$\delta n_n\Big|_{surface} = \text{const} \times (-1)^n n A_n$$

To linear order this is equivalent to:

$$\boxed{n(r) = \left[\hat{n} + \delta n_n(r)\Big|_{body}\right] \Theta\left[r_b + \delta r_b - r\right]}$$

$$\delta r_b = \text{const} \times (-1)^n n A_n$$ readjustment of beam edge radius.

Dispersion Relation

- Polynomial in k^2 $\Rightarrow$ $\pm k$ solutions and therefore there will be unstable growing perturbations if k is complex:

$$\delta\phi \sim \delta\phi_n(r)\, e^{-iks}$$

$$k = k_r \pm i k_I \qquad \begin{array}{l} k_r = \text{real part} \\ k_I = \text{imaginary part} \end{array}$$

For the unstable branch:

$$\delta\phi \sim \delta\phi_n(r)\, e^{-ik_r s} \cdot e^{|k_I| s} \Rightarrow \text{exponential growth.}$$

- k is a function of n and σ/σ_0 <u>only</u>.
  - $0 \le \sigma/\sigma_0 \le 1$

0: strongest possible space charge.

1: zero space-charge.

- <u>Instabilities will occur over a range of σ/σ_0 and will turn off for σ/σ_0 large enough</u> (weak space-charge).

KV beam is always stable for zero space-charge since orbits are stable.

<u>Dispersion Relations:</u>

<u>Mode number n</u>	<u>Dispersion relation</u>
1	$(k/k_{\beta 0})^2 - 2(1+\sigma^2/\sigma_0^2) = 0$
2	$(k/k_{\beta 0})^4 - 2(1+9\sigma^2/\sigma_0^2)(k/k_{\beta 0})^2 - 4(\sigma^2/\sigma_0^2)(1-17\sigma^2/\sigma_0^2) = 0$
⋮	⋮ Rapidly more complicated!

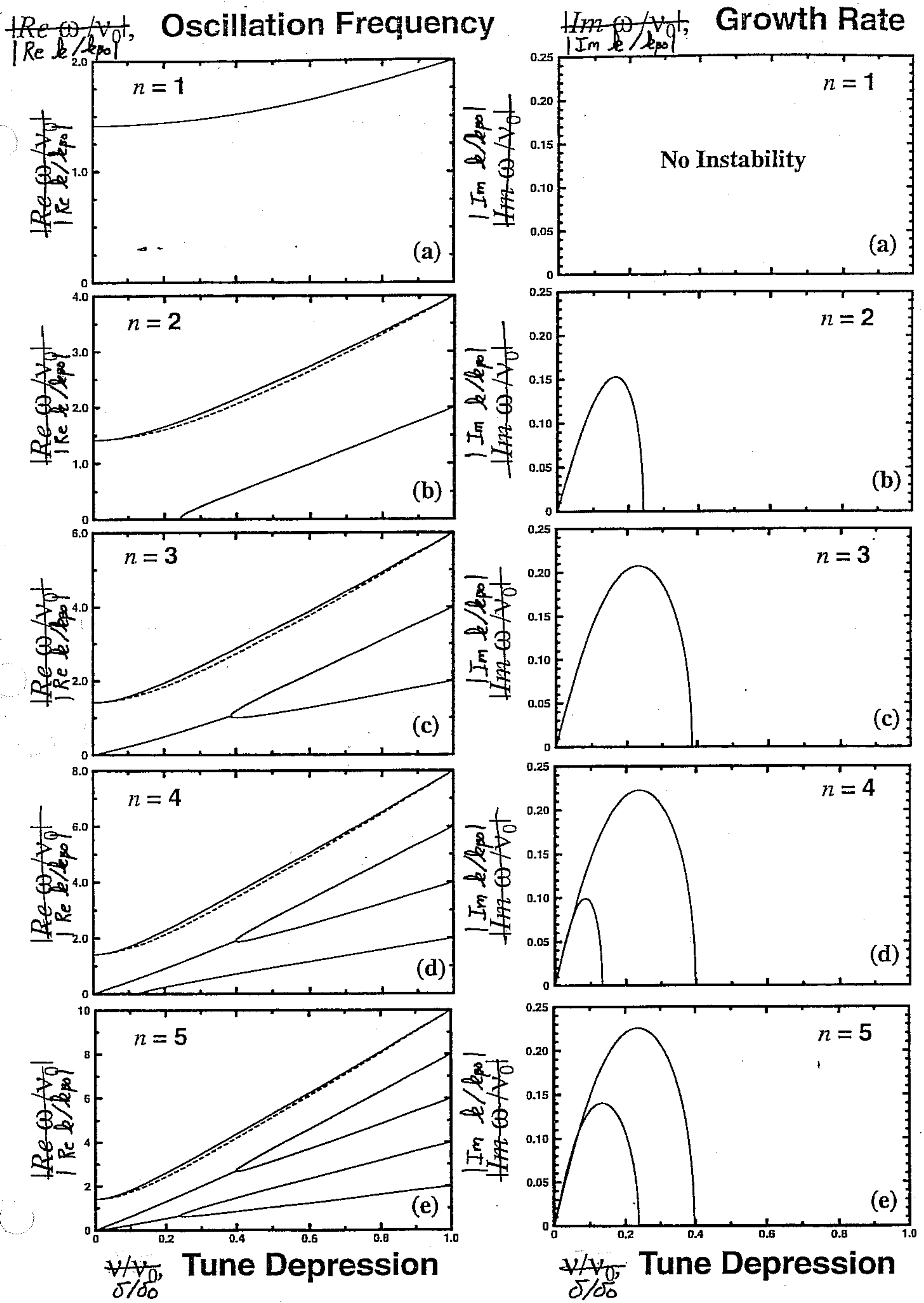

~~|Re ω/v0|~~, Oscillation Frequency
|Re k/kpo|
~~|Im ω/v0|~~, Growth Rate
|Im k/kpo|
n = 1
n = 2
n = 3
n = 4
n = 5
No Instability
(a)
(b)
(c)
(d)
(e)
~~ν/ν0~~, Tune Depression
δ/δo

Fig. 8

Example: $n = 1$, Envelope Mode

$$\delta\phi_1 = \begin{cases} A_1[1-(r/r_b)^2], & 0 \le r \le r_b, \\ 0, & r_b \le r \le r_p, \end{cases}$$

$$(k/k_{\beta 0})^2 = 2 + 2(\sigma/\sigma_0)^2$$

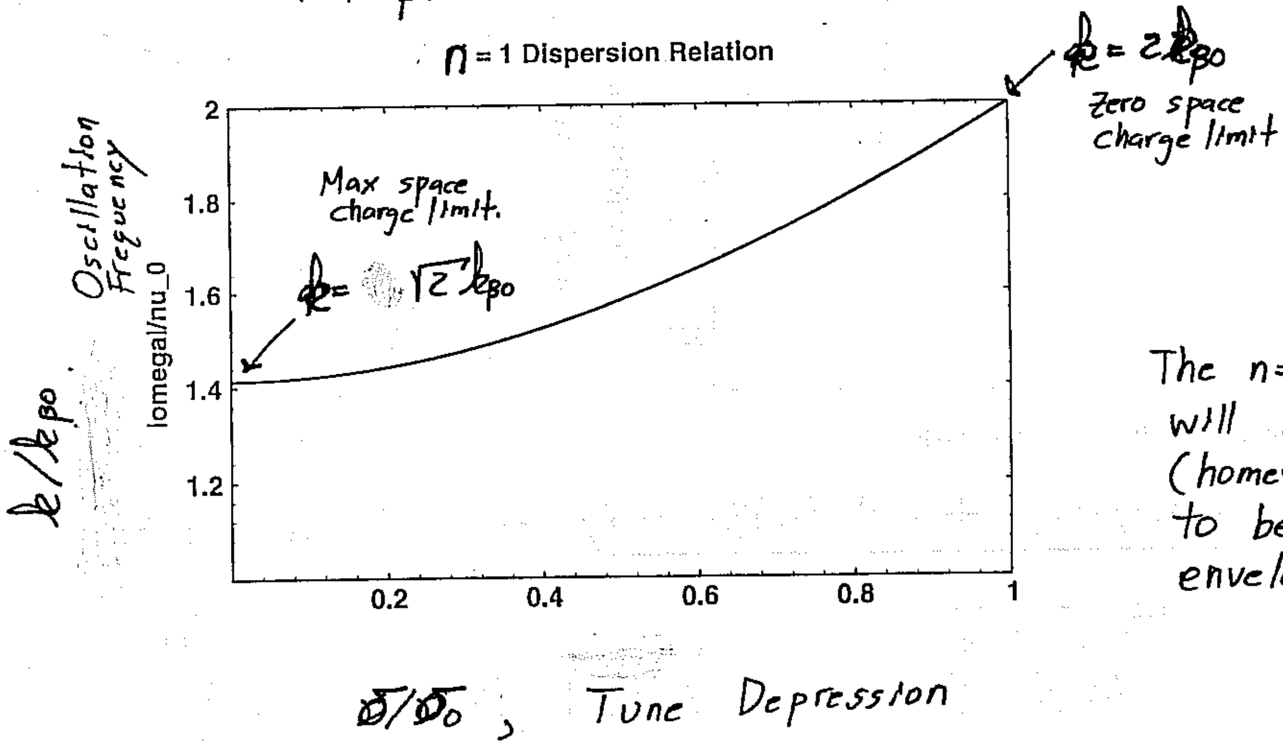

The n=1 mode will be shown (homework) to be the usual envelope mode

Oscillation Frequency

10/

Example: $n = 2$ Mode

$$\delta\phi_2 = \begin{cases} A_2[1 - 4(r/r_b)^2 + 3(r/r_b)^4], & 0 \le r \le r_b, \\ 0, & r_b \le r \le r_p, \end{cases}$$

$$(\omega/\nu_0)^2 = 1 + 9(\nu/\nu_0)^2 \pm \sqrt{1 + 22(\nu/\nu_0)^2 + 13(\nu/\nu_0)^4}$$

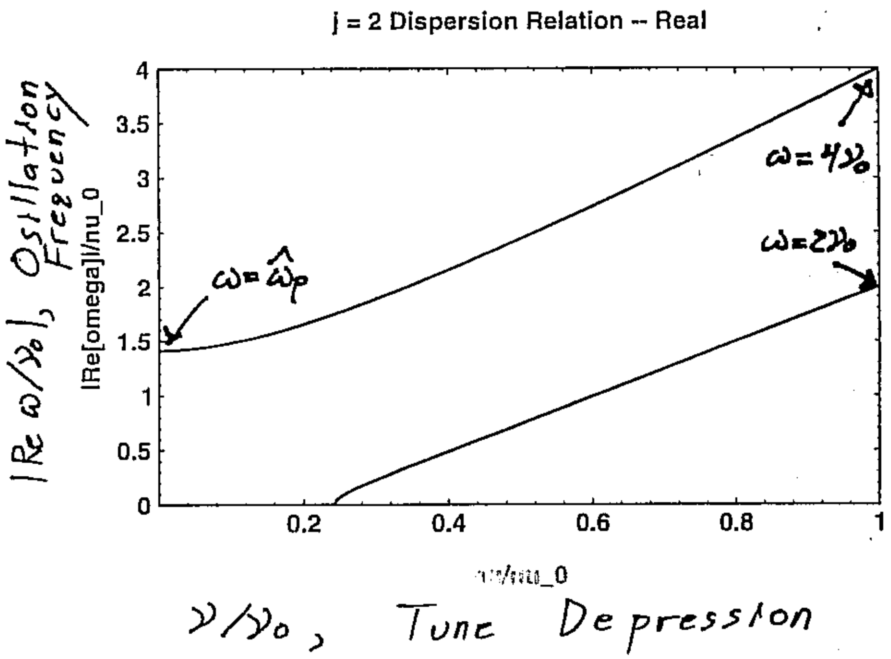

Oscillation Frequency

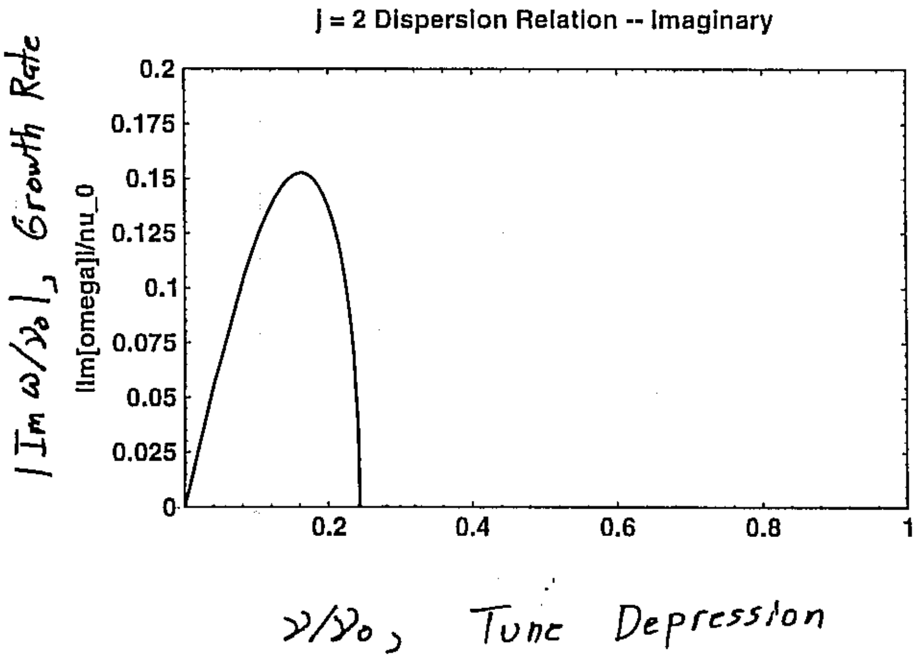

Growth Rate

Discussion:

As might be expected on physical grounds, the singular KV distribution drives numerous, strong, collective instabilities. This implies that the KV model is suspect since real beams are often transported where the KV model would predict strong instability. However:

- <u>Low-order KV features (envelope modes) are correct and well verified.</u>
- <u>Higher order collective modes</u> observed on intense beam cores often <u>look similiar</u> to the KV model predictions in density/potential etc, <u>but are not unstable.</u>

How is this situation resolved? A partial answer was suggested by a fluid model developed by Lund and Davidson. In this model:

- Density and tempeture profiles (i.e., low order features) of the KV model were preserved.
- The singular phase-space structures were eliminated.

A stability analysis obtained:

Mode Eigenfunction: $(r<r_b)$

$$\delta\phi_n = \frac{A_n}{2}\left[P_{n-1}\left(1-2\frac{r^2}{r_b^2}\right) + P_n\left(1-2\frac{r^2}{r_b^2}\right)\right]$$

Mode Dispersion Relation:

$$\left(\frac{k}{k_{\beta 0}}\right)^2 = 2 + 2\left(\frac{\sigma}{\sigma_0}\right)^2(2n^2-1)$$

$$n = 1, 2, 3, \ldots\ldots$$

Features of fluid model:

- Identical radial eigenfunction to the full kinetic theory
- Fluid mode dispersion relation predicts stability for all modes and closely tracks the (stable) high frequency branch of the KV dispersion relation for the full range of space charge strength $0 \leq \sigma/\sigma_0 \leq 1$
  - Fluid mode dispersion relation plotted dashed on KV mode plots.
  - The $n=1$ fluid envelope mode is identical to the KV envelope mode.

Since the fluid model reproduces the coarse macroscopic features of the KV model – which can be a good approximation at high space-charge intensities, this implies:

- KV model mode eigenfunctions should roughly model those of intense beams with smooth distributions.
- Oscillation frequencies may be close to the (stable) high frequency KV mode branch
  - May be other lower frequency branches that are also physical.
- Many high-order KV instabilities may be of little relevance to real beams.
  - Low order (envelope and maybe others) can be relevant.

The real issue for high intensity collective modes may not be higher order KV instabilities but if low-order collective modes can:

- Be driven unstable by periodic (s-varying) focusing structures in machine lattices, errors in rings, etc.
- Drive the production of beam halo, etc.

References:

Material on the kinetic stability of KV beams is found mostly in journals.

Original references

Gluckstern, Proc. 1970 Proton Linac Conference, Nat. Accel. Lab., pg. 811 – First KV mode analysis.

T.F. Wang and L. Smith, Part. Accel. 12, 247 (1982). – Simplified (closed form) mode eigenfunction and dispersion relation.

Interpretation of Branches, Mode Structure, KV Fluid Stability

S.M. Lund and R.C. Davidson, Physics of Plasmas 5, 3028 (1998). Detailed analysis of eigenfunctions, dispersion relations, etc. in appendices. Fluid mode analysis and interpretations of KV modes.

Other papers by Hoffmann, Gluckstern, and others. Hoffmann et. al. analyzed KV in periodic focusing lattices.

John Barnard
Steven Lund
USPAS
June 2008

Intrabeam collisions, gas and electron effects in intense beams

1. Beam/beam coulomb collisions
2. Beam/gas scattering
3. Charge changing processes
4. Gas pressure instability
5. Electron cloud processes
6. Electron-ion instability

Gas and electron effects

-Effects are quite different depending on q, m of species being accelerated

-Circular accelerators vs. Linacs
($t_{residence}$ ~ ms to days vs. 10's of μs)

-Long pulse vs. short pulse
(t_{pulse} ~ 10's of μs vs. 10's of ns)

3

HI^+ Heavy ion	Residual gas molecule	e^- electron

Processes:

1. Coulomb collisons (intra-beam)

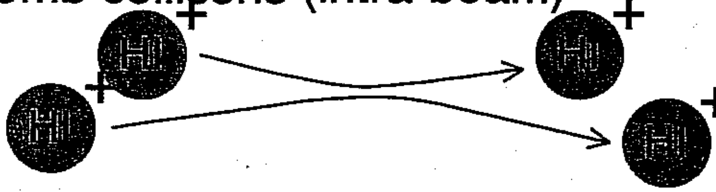

2. Coulomb collisions with residual gas

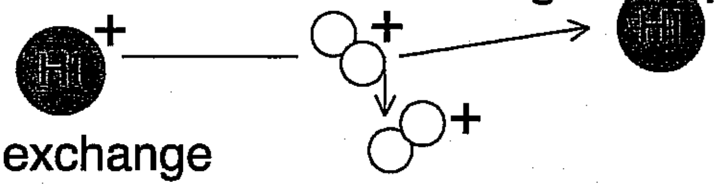

3. Charge exchange

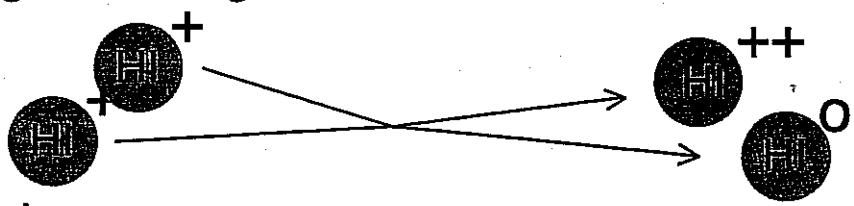

4. Stripping

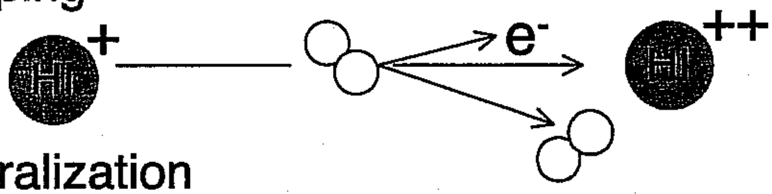

5. Neutralization

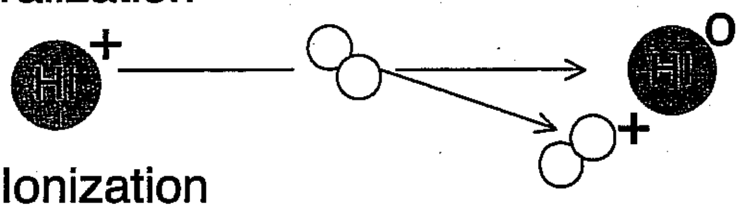

6. Gas Ionization

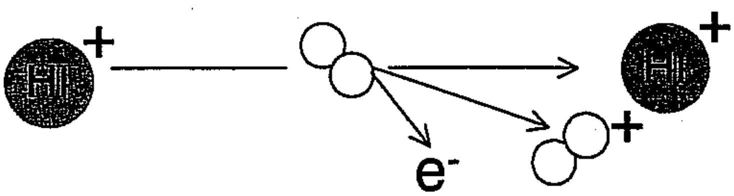

4

7. Wall interactions

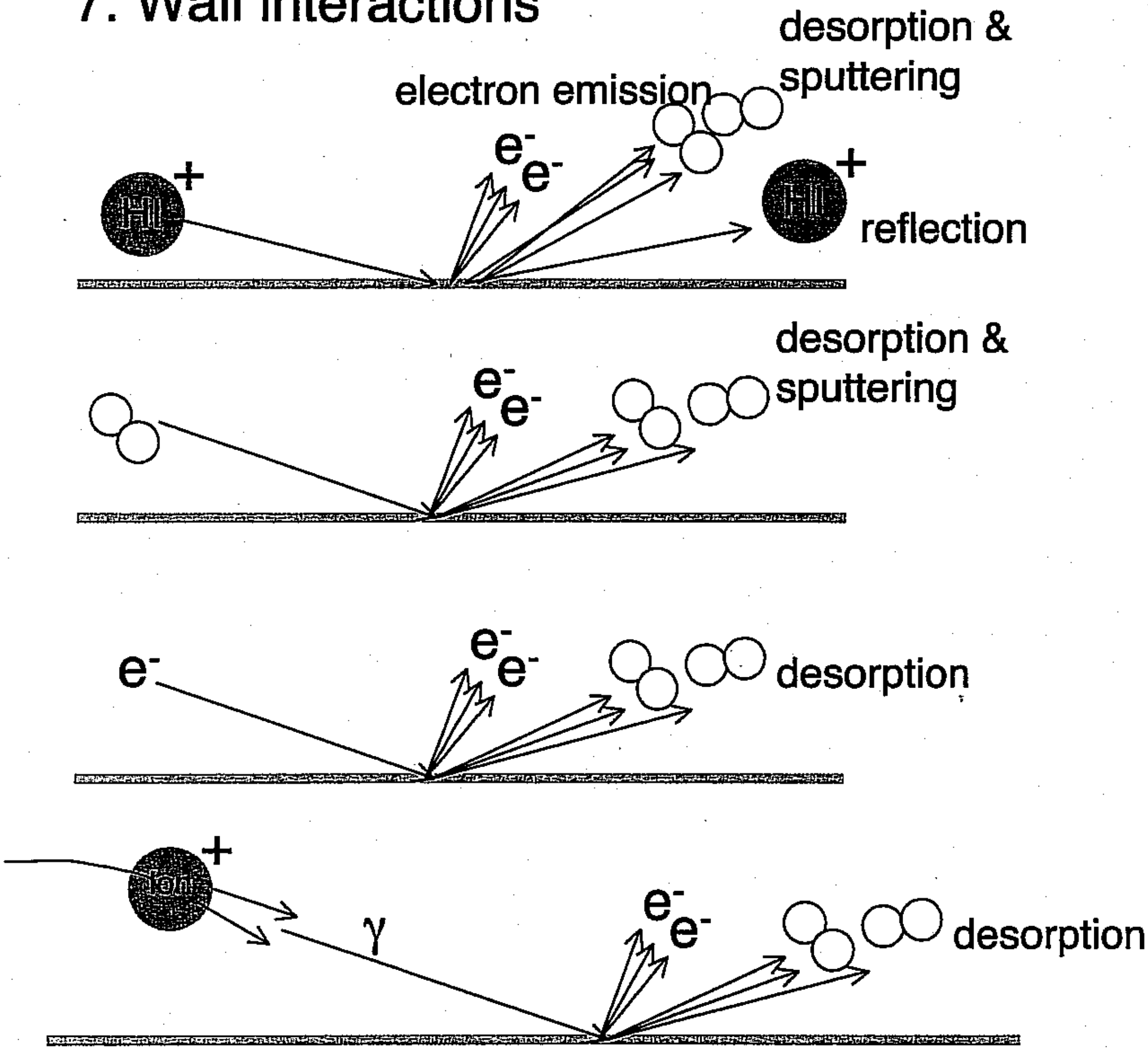

γ	synchrotron photon

1. COLLISIONS WITHIN BEAM REISER 6.4

CONSIDER EFFECTS OF COULOMB COLLISIONS IN A CONTINUOUS BEAM PROPAGATING THROUGH A SMOOTH FOCUSING CHANNEL WITH $T_{\perp 0} \neq T_{\parallel 0}$

(IF $T_{\perp 0} = T_{\parallel 0} \Rightarrow$ BEAM ALREADY RELAXED).

FROM ICHIMARU & ROSENBLUTH, PHYS FLUIDS 13, 2778, (1970):

$$\frac{dT_\perp}{dt} = -\frac{1}{2}\frac{dT_\parallel}{dt} = \frac{-(T_\perp - T_\parallel)}{\tau}$$

(SINCE $T_x = T_y = T_\perp$, $T_\parallel$ CHANGES AT TWICE THE RATE OF $T_\perp$)
(SINCE $2k_B T_\perp + k_B T_\parallel = \text{const}$)

τ = RELAXATION TIME

$$= \frac{15\,(k_B T_{eff}/mc^2)^{3/2}(4\pi\epsilon_0)^2 m^2 c^3}{8\pi^{1/2} q^4 \ln\Lambda \; n} = \left(\frac{15\,\pi^{1/2}}{8\ln\Lambda}\right)\nu_c^{-1}$$

COULOMB COLLISION APPROXIMATE RATE FOR LARGE ANGLES (PAGE 9 OF INTRODUCTION NOTES)

$$\ln\Lambda = \begin{cases} \ln \dfrac{(\epsilon_0 k T_{eff})^{3/2}\, 12\pi}{q^3 n^{1/2}} & \text{for } \lambda_D < r_b \\[2ex] \ln \dfrac{12\pi\epsilon_0\, k T_{eff}\, r_b}{q^2} & \text{for } \lambda_D > r_b \end{cases}$$

$$T_{eff} = T_\perp \left[\frac{15}{4}\int_{-1}^{1} \frac{\mu^2(1-\mu^2)\,d\mu}{[(1-\mu^2) + \mu^2(T_\parallel/T_\perp)]^{3/2}}\right]^{-2/3}$$

T_{eff} is an appropriate average of $T_\perp$ & $T_\parallel$

$\frac{T_{eff}}{T_\perp}$

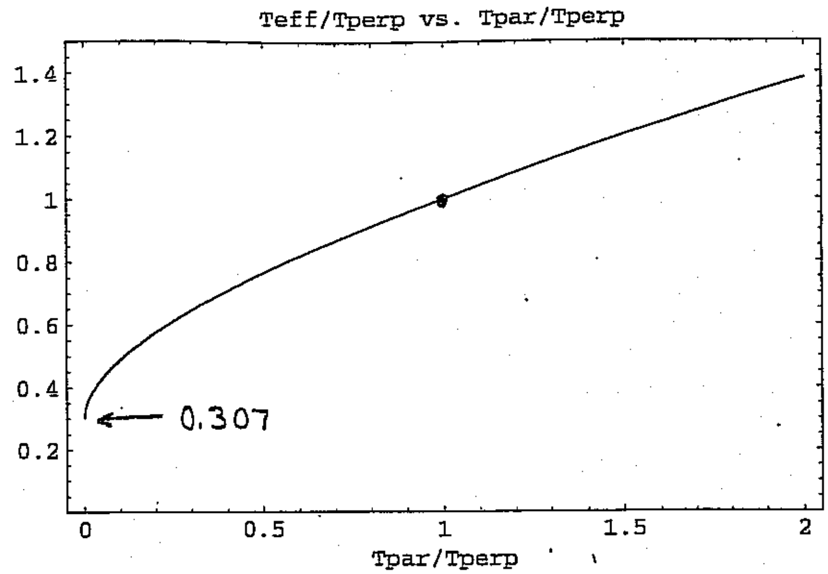

FOR $T_\parallel = 0$

$$T_\perp = \frac{2}{3} T_{\perp 0}\left(1 + \frac{1}{2} e^{-3t/\tau_{\rm eff}}\right), \qquad (6.156a)$$

(APPROXIMATE SOLUTIONS)

$$T_\parallel = \frac{2}{3} T_{\perp 0}\left(1 - e^{-3t/\tau_{\rm eff}}\right), \qquad (6.156b)$$

$\tau_{eff} = 0.42\,\tau_{eq}$

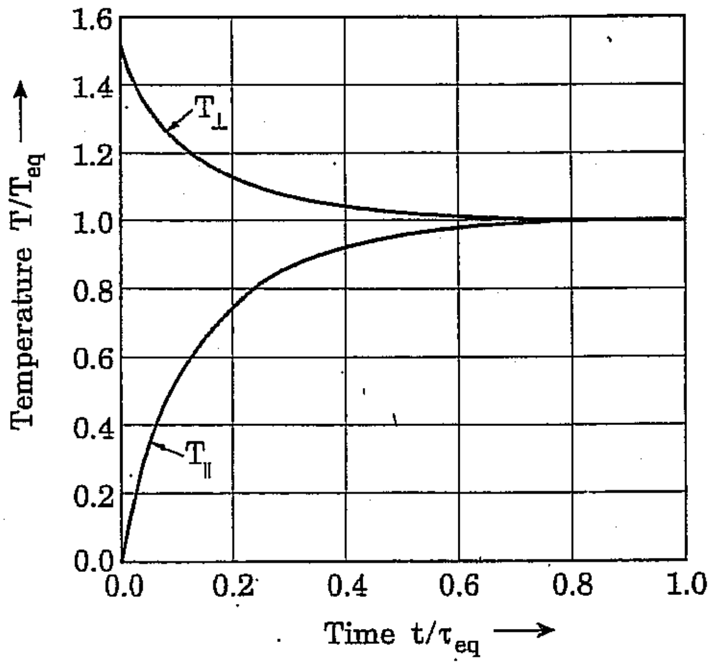

FROM REISER p.527

$\tau_{eq} = \tau(T_{eq})$

BOERSCH EFFECT

AREN'T COLLISIONS NEGLIGIBLE? (NOT ALWAYS)

PUTTING IN NUMBERS:

FOR IONS:

$$\tau_{eff} = 4.3\cdot 10^{-4}\,s\ \frac{(A^{1/2})}{Z^4}\left(\frac{kT_{eff}}{1\,eV}\right)^{3/2}\left(\frac{15}{\ln\Lambda}\right)\left(\frac{10^{10}\,cm^{-3}}{n}\right)$$

$$\ln\Lambda = \ln\left[\frac{1.5\cdot 10^5\ (kT/1eV)^{3/2}}{Z^3\ (n/10^{10}\,cm^{-3})}\right]$$

EXAMPLE: 2 MeV INJECTOR

$\tau_{eff} \simeq 8.8\cdot 10^{-4}\,s$ for $A = 39$, $kT_{eff} = 0.3\,eV$, $Z = 1$, $\ln\Lambda = 8.5$, $n = 10^{10}\ cm^{-3}$

$$t_{transit} \simeq \frac{2d}{v} \approx \frac{2\,(2m)}{(.01)\,3\cdot 10^8} = 1.3\ \mu s$$

So $\tau_{eff} >> t_{transit}$ $\Rightarrow$ collisions are rare BUT

$$T_{\substack{accel\\cool}} = \frac{1}{2}\left(\frac{kT_0}{qV}\right)kT_0 = 2.5\cdot 10^{-9}\ eV \quad \text{for } \begin{array}{l} kT_0 = 0.1\,eV \\ qV = 2\,MeV \end{array}$$

$$T_{\parallel\,collisions} \cong \frac{2}{3}T_{\perp 0}\left(1 - \exp\left(-3t/\tau_{eff}\right)\right) \simeq 2T_{\perp 0}\left(\frac{t_{transit}}{\tau_{eff}}\right) = .006\,eV$$

for $T_{\perp 0} = 1\,eV$

(8)

SO $T_{\perp}$ FROM "BOERSCH EFFECT"

>> $T_{\parallel}$ FROM LONGITUDINAL COOLING

100 SHEETS
U.S.A.

COULOMB COLLISIONS IN RESIDUAL GAS (REISER 6.4.3)

JACKSON CHAPTER 13

(RUTHERFORD SCATTERING)

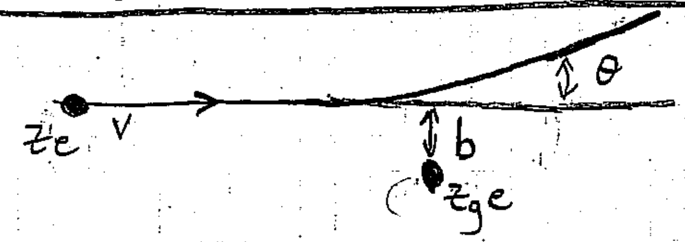

$$\frac{dp_x}{dt} = \frac{Z Z_g e^2}{4\pi\epsilon_0 r^2}\frac{b}{r} \Longrightarrow \Delta p = \int_{-\infty}^{\infty} \frac{dp_x}{dt}\frac{dt}{dz}\,dz$$

$$= \frac{Z Z_g e^2 b}{4\pi\epsilon_0 V}\underbrace{\int_{-\infty}^{\infty}\frac{dz}{(z^2+b^2)^{3/2}}}_{2/b^2}$$

$$= \frac{2 Z Z_g e^2}{4\pi\epsilon_0 V b}$$

$$\theta \cong \frac{\Delta p}{p} = \frac{2 Z Z_g e^2}{4\pi\epsilon_0 p V b} \Rightarrow \frac{db}{d\theta} \sim \frac{1}{\theta^2}$$

DIFFERENTIAL CROSS SECTION FOR SCATTERING WITH IMPACT PARAMETER b INTO SOLID ANGLE $d\Omega$ AT ANGLE θ SATISFIES

$$\underbrace{2\pi b\, db}_{\text{AREA}} = \frac{d\sigma}{d\Omega}\underbrace{2\pi \sin\theta\, d\theta}_{\text{SOLID ANGLE}}$$

$$\Rightarrow \frac{d\sigma}{d\Omega} = \frac{b}{\sin\theta}\left|\frac{db}{d\theta}\right| = \left(\frac{2 Z Z_g e^2}{4\pi\epsilon_0 p V}\right)^2 \frac{1}{\theta^4}$$

ELECTRON SCREENING PUTS CUTOFF AT SMALL θ (LARGE b) SO BETTER TO USE

$$\frac{d\sigma}{d\Omega} = \left(\frac{2 Z Z_g e^2}{4\pi\epsilon_0 p V}\right)^2 \frac{1}{(\theta^2+\theta_{min}^2)^2}$$

AVERAGE ANGLE SQUARED FOR A SINGLE SCATTERING IS:

$$\overline{\theta^2} = \frac{\int \theta^2 \frac{d\sigma}{d\Omega} 2\pi \sin\theta \, d\theta}{\int \frac{d\sigma}{d\Omega} 2\pi \sin\theta \, d\theta} \simeq \frac{\int_0^{\theta_{max}} \frac{\theta^3}{(\theta^2+\theta_{min}^2)^2} d\theta}{\int_0^{\theta_{max}} \frac{\theta}{(\theta^2+\theta_{min}^2)^2} d\theta}$$

$$\simeq 2\,\theta_{min}^2 \ln\left(\frac{\theta_{max}}{\theta_{min}}\right)$$

ASSUMES $\theta_{max}^2 \gg \theta_{min}^2$

& $\ln\left(\frac{\theta_{max}}{\theta_{min}}\right) \gg 1$

MULTIPLE COLLISIONS

AFTER TRAVERSING DISTANCE s, AND UNDERGOING N_s COLLISIONS, THE MEAN SQUARE ANGLE $\overline{\Theta^2}$

$$\left[\sigma_s = \pi\left(\frac{2 z Z_g e^2}{4\pi\epsilon_0 p v}\right)^2 \frac{1}{\theta_{min}^2}\right]$$

$$\overline{\Theta^2} = N_s\,\overline{\theta^2} = n_g \sigma_s s\,\overline{\theta^2}$$

$$= 16\pi n_g \left(\frac{z Z_g e^2}{4\pi\epsilon_0 m c^2 \gamma \beta^2}\right)^2 \ln\left(\frac{\theta_{max}}{\theta_{min}}\right) s$$

JACKSON ARGUES θ_{max} ARISES FROM DISTRIBUTED NATURE OF NUCLEUS (NOT POINT CHARGE) AND θ_{min} ARISES FROM SCREENING OF ELECTRONS OR UNCERTAINTY PRINCIPLE

$$\ln\frac{\theta_{max}}{\theta_{min}} \simeq \ln\left(204\, Z_g^{-1/3}\right)$$

$$\Delta\langle x'^2\rangle = \frac{1}{2}\,\overline{\Theta^2} \qquad \left[\text{since } \Delta\langle x'^2\rangle + \Delta\langle y'^2\rangle = \Delta\overline{\Theta^2}\right]$$

$$\epsilon = 4\sqrt{\langle x^2\rangle\langle x'^2\rangle - \langle xx'\rangle^2}$$

FOR A MATCHED BEAM

$$k_p^2\langle x^2\rangle = \langle x'^2\rangle \qquad \text{where } k_p = \text{depressed betatron wavenumber}$$

$$\Rightarrow \quad \epsilon = \frac{4\langle x'^2\rangle}{k_p}$$

$$\Delta\,\epsilon = \frac{4\;\Delta\langle x'^2\rangle}{k_p} = \frac{2\,\overline{\Theta^2}}{k_p}$$

$$\Rightarrow \boxed{\frac{d\epsilon}{ds} = \frac{32\pi}{k_p}\, n_g \left(\frac{Z Z_g e^2}{4\pi\epsilon_0 mc^2\gamma\beta^2}\right)^2 \ln\left(204\, Z_g^{-1/3}\right)}$$

IN TERMS OF NORMALIZED EMITTANCE:

$$\boxed{\frac{d\epsilon_N}{ds} = \frac{32\pi}{k_p}\, n_g \left(\frac{Z Z_g e^2}{4\pi\epsilon_0 mc^2}\right)^2 \frac{1}{\gamma\beta^3} \ln\left(204\, Z_g^{-1/3}\right)}$$

<u>Example:</u> $n_g = 10^{-7}$ torr $= 3.5\cdot 10^{9}\ \text{cm}^{-3} = 3.5\cdot 10^{15}\ \text{m}^{-3}$

$k_{p0} = 2.5\ \text{m}^{-1}$ $\quad k_p = 0.25\ \text{m}^{-1}$

$Z_g = 7$; $Z = 19$, $A = 39$, $\beta = 0.01$, $\epsilon_N = 1\cdot 10^{-6}$ m-rad

$\Rightarrow \frac{d\epsilon_N}{ds} = 3.7\cdot 10^{-11}\ \text{m}^{-1}$ $\Rightarrow$ Need 27 km to equal original emittance!

(But more important for rings & low mass!)

"PRESSURE "BUMPS" AND

BEAM LOSS FROM CHARGE CHANGING COLLISIONS

REFERENCE: WORKSHOP ON BEAM INDUCED PRESSURE RISE IN RINGS, BNL, Dec. 2003,

σ_s = STRIPPING CROSS SECTION

σ_{ce} = CHARGE EXCHANGE CROSS SECTION

σ_i = IONIZATION CROSS SECTION

V_{cm} = mean ion velocity in ion beam frame

(1) BEAM LOSS

$$\frac{dn_b}{dt} = -\sigma_s V_i n_b \bar{n} - \sigma_{ce} V_{cm} n_b^2 - \left.\frac{\partial n_b}{\partial t}\right|_{HALO}$$

(2) GAS EVOLUTION

$\bar{n}$ = average gas density

$$\frac{d}{dt}\bar{n} = \underbrace{\eta_G \sigma_i V_i n_b \bar{n}\left(\frac{V_{beam}}{V_{pipe}}\right)}_{\text{IONIZATION}} + \underbrace{\eta_{HI} \sigma_s V_i n_b \bar{n}\left(\frac{V_{beam}}{V_{pipe}}\right)}_{\text{STRIPPING}}$$

$$+ \underbrace{\eta_{HI} \sigma_{ce} V_{cm} n_b^2\left(\frac{V_{beam}}{V_{pipe}}\right)}_{\text{CHARGE EXCHANGE}} + \underbrace{q}_{\text{OUTGASSING}} - \underbrace{(S/A_p)\,\bar{n}}_{\text{PUMPING}}$$

V_{beam} = VOLUME OF BEAM; V_{pipe} = VOLUME OF PIPE

S = Effective linear pumping rate $[m^3 s^{-1}/m]$ $\quad A_p = \pi r_p^2$ = AREA OF PIPE

q = OUTGASSING rate $= \frac{2\pi r_p Q}{\pi r_p^2} = \frac{2Q}{r_p}$; $\quad Q = \frac{\#}{m^2 s}$

η_G = GAS MOLECULES DESORBED PER INCIDENT RESIDUAL GAS ION

η_{HI} = GAS MOLECULES DESORBED PER INCIDENT HEAVY ION STRIKING WALL

($V_{beam}/V_{pipe} \rightarrow \left(\frac{r_b^2}{r_{pipe}^2}\right) v_{rep}\, \Delta t_{beam}$ for a rep rated linac)

If we take $n_b \simeq$ constant

then we may express gas evolution equation as:

$$\frac{d\bar{n}}{dt} = \frac{\bar{n}}{\tau} + q_{eff}$$

with solution:

$$\bar{n} = (\bar{n}_0 + \tau q_{eff}) \exp[t/\tau] - \tau q_{eff}$$

HERE
$$\tau = \frac{1}{(\eta_g \sigma_i + \eta_{HI} \sigma_s)\left(\frac{V_{beam}}{V_{pipe}}\right) n_b V_i - S/A_p}$$

$$q_{eff} = q + \eta_{HI} \sigma_{CE} V_{cm} n_b^2 \left(\frac{V_{beam}}{V_{pipe}}\right)$$

EQUILIBRIUM REACHED IF $\tau < 0$ (i.e. pumping exceeds desorption).

$$\Rightarrow \bar{n} = -\tau q_{eff} = \frac{q + \eta_{HI} \sigma_{CE} V_{cm} n_b^2 (V_{beam}/V_{pipe})}{S/A_p - (\eta_g \sigma_i + \eta_{HI} \sigma_s)\left(\frac{V_{beam}}{V_{pipe}}\right) n_b V_i}$$

INSTABILITY IF

$$n_b V_i \geq \frac{\frac{S}{A_p}\left(\frac{V_{pipe}}{V_{beam}}\right)}{\eta_g \sigma_i + \eta_{HI} \sigma_s}$$

Instability first observed on the ISR proton storage ring, limiting current in rings in 1970's.

$$\text{If} \quad l_{beam} = l_{pipe}$$

INSTABILITY CRITERION MAY BE WRITTEN

$$I > \frac{zeS}{\eta_g \sigma_i + \eta_{HI} \sigma_s}$$

EXAMPLE: ISR

If $S = 100\ l\, s^{-1} m^{-1} = 0.1\ m^3 s^{-1} m^{-1}$

$\eta_g = 4$

$\sigma_i = 10^{-22}\ m^2 = 10^{-16}\ cm^2\ ;\ \sigma_s = 0$

$z = 1$ (protons)

$\Rightarrow I \leq 40$ Amperes

(PRESSURE RUNAWAYS WERE OBSERVED ON the ISR AT 14-18A, (BENVENUTI et al, IEEE Trans. on Nuc. Sci. NS-24, 1773, 1977)

SEE "BEAM INDUCED PRESSURE RISE IN RINGS"
13th ICFA BEAM DYNAMICS MINI WORKSHOP, BNL, Dec. 9-12, 2003.
WEBSITE: http://www.c-ad.bnl.gov/icfa

"ELECTRON CLOUD EFFECTS"

REFERENCE: CERN e-CLOUD WORKSHOP
http://wwwslap.cern.ch/collective/ecloud02/proceedings.html

BASIC IDEA

IN ION storage rings or collider rings:

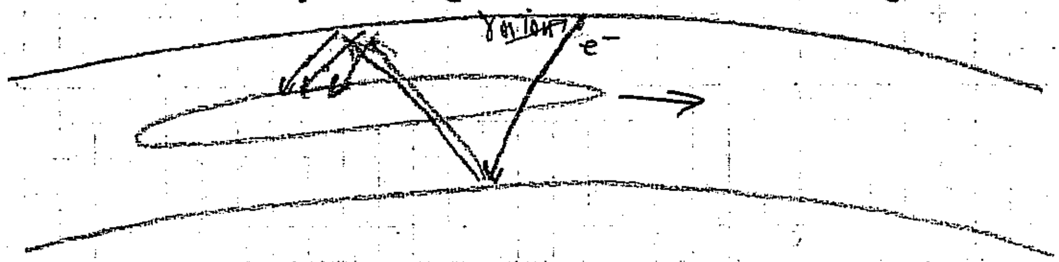

ELECTRONS ARE ATTRACTED TO POSITIVE POTENTIAL OF BEAM & ACCUMULATE

SOME SYMPTOMS:

1. BEAM LOSS & pressure rise
2. HIGH FREQUENCY CENTROID oscillations

SOME ACCELERATORS WHICH SHOW EVIDENCE OF e⁻ EFFECTS
1. LANL PSR
2. CERN PS & SPS
3. BNL RHIC

COULD LIMIT PLANNED/ UNDER CONSTRUCTION:
1. SNS ACCUMULATOR RING
2. LHC

cf. "Electron-cloud effects in High Intensity Proton Accelerators" J. Wei & R. Macek, CERN

BEAM INDUCED MULTIPACTING

a). MULTI-BUNCH

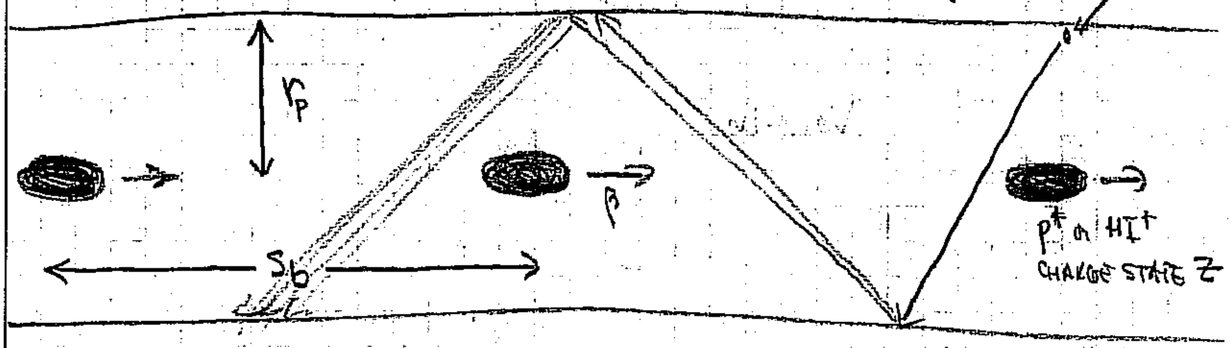

USING COULOMB COLLISION FORMULA FROM PAGE 9:

$$\Delta p_x \cong \frac{2 Z N_b e^2}{4\pi\epsilon_0 v r_p}$$

N_b = Number of ions of charge Z in bunch

$$\Delta E_e = m_e c^2\left[\sqrt{\frac{\Delta p_x^2}{m^2c^2}+1} - 1\right] = m_e c^2\left[\sqrt{\left(\frac{2 r_e Z N_b}{\beta r_p}\right)^2 + 1} - 1\right]$$

$$\cong 2 r_e^2 m_e c^2 \frac{Z^2 N_b^2}{\beta^2 r_p^2}$$

for $\Delta E_e \ll m_e c^2$ $\left(\text{or } \frac{2 r_e Z N_b}{\beta r_p} \ll 1\right)$

(where $r_e = \frac{e^2}{4\pi\epsilon_0 m_e c^2} \simeq 2.8\times10^{-15}\,\text{m}$)

DEFINE A MULTIPACTING PARAMETER $\mathcal{g}_m$

$$\mathcal{g}_m = \frac{\text{TIME FOR ELECTRON TO CROSS PIPE}}{\text{TIME BETWEEN BUNCHES}} = \frac{2 r_p}{s_b}\frac{\beta}{\beta_e}$$

$$\cong \frac{\beta^2 r_p^2}{Z N_b r_e s_b}$$

RESONANCE CONDITION:

$$\mathcal{g}_m = 1$$

s_b = distance between bunches

b). SINGLE-BUNCH BEAM-INDUCED MULTIPACTING

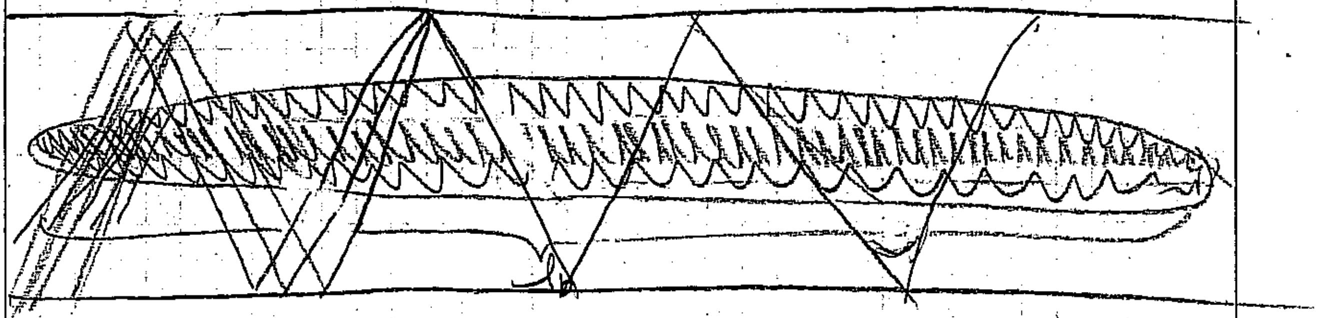

$$\varsigma_s = \frac{r_p}{l_b}\frac{\beta}{\beta_e} = \frac{\text{time for electrons to cross pipe}}{\text{passage time for half of the bunch}}$$

Recall:

$$\varphi = \begin{cases} \dfrac{\lambda}{2\pi\epsilon_0}\left[\dfrac{1}{2}\left(1-\dfrac{r^2}{r_b^2}\right)+\ln\dfrac{r_p}{r_b}\right] & 0<r<r_b \\ \dfrac{\lambda}{2\pi\epsilon_0}\left[\ln\dfrac{r_p}{r}\right] & r_b<r<r_p \end{cases}$$

$$\frac{1}{2}m_e v_e^2 + q\varphi \simeq \text{const} \simeq 0$$

$$\beta_e \sim \frac{1}{2}\sqrt{\frac{2q\varphi}{m_e c^2}} \sim \sqrt{\frac{N_0 Z e^2}{l_b 4\pi\epsilon_0 m_e c^2}} \sim \sqrt{\frac{Z r_e N_0}{l_b}}$$

(AVERAGE e^- VELOCITY)

$$\Rightarrow \varsigma_s = \frac{\beta r_p}{\sqrt{r_e l_b N_0 Z}}$$

THE ENERGY GAIN OF THE ELECTRON, RELIES ON THE DENSITY CHANGING OVER THE COURSE OF THE BUNCH.

$$\Delta E_e \sim \frac{m_e c^2}{2}\left[\frac{Z r_e N_0(s)}{l_b}\right] - \frac{m_e c^2}{2}\left[\frac{Z r_e N_0(s+\Delta s)}{l_b}\right]$$

$$\sim \frac{m_e c^2}{2}\left(\frac{\partial N_0}{\partial z}\Delta z\right)\left(\frac{Z r_e}{l_b}\right)$$

$$\Delta E_e \sim \frac{m_e c^2}{2}\left(\frac{\partial N_0}{\partial z}\Delta z\right)\left(\frac{Z r_e}{l_b}\right)$$

$$\Delta z = \frac{v_p}{v_e}\beta c = \beta r_p \sqrt{\frac{l_b}{Z r_e N_0}}\,; \qquad \frac{\partial N_0}{\partial z} \sim \frac{N_b}{l_b}$$

So $\Delta E_e \approx m_e c^2 \left(\frac{Z N_0 r_e}{l_b^3}\right)^{1/2} \beta r_p$

$\delta \leq 1 \Rightarrow$ Electron build up possible within bunch

WHAT IS STEADY STATE ELECTRON DENSITY?

Electrons can build up until E_r at pipe ~ 0.

$$\Rightarrow \lambda_e = \lambda_J$$

$$\pi r_p^2 n_e = \pi r_b^2 Z n_i$$

$$n_e = \left(\frac{r_b}{r_p}\right)^2 Z n_i$$

(19)

ELECTRON - ION INSTABILITY

(SEE ALSO R.C. DAVIDSON & H. Qin, Physics of Intense Charged Particle Beams in High Energy Accelerators, p 503 FOR KINETIC TREATMENT).

CONSIDER A UNIFORM DISTRIBUTION OF ELECTRONS (AT REST) WHICH HAS THE SAME RADIUS (OR SLIGHTLY SMALLER RADIUS) AS A UNIFORM DENSITY ION BEAM, THAT IS MOVING AT VELOCITY V_z (OUT OF THE PLANE OF THE PAPER).

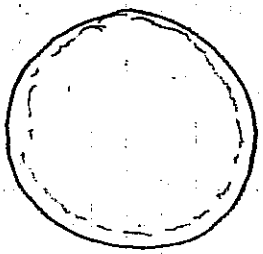

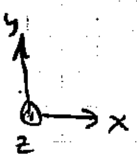

$$E_x = \frac{\lambda_i(r)}{2\pi\epsilon_0 r_0}\frac{(x-x_i)}{r} = \frac{\rho_i}{2\epsilon_0}(x-x_i)$$

THE EQUATION OF MOTION FOR THE CENTROID OF THE ELECTRONS IS OBTAINED FROM

$$m_e\ddot{x} = \frac{-e\rho_i}{2\epsilon_0}(x-x_i) + \frac{e\rho_e}{2\epsilon_0}(x-x_e)$$

or

$$\frac{d^2x_e}{dt^2} = -\frac{\omega_{pi}^2}{2}\left(\frac{m_i}{q}\frac{e}{m_e}\right)(x_e - x_i)$$

here $\omega_{pi}^2 = \frac{q^2 n_i}{\epsilon_0 m_i} = \frac{q\rho_i}{\epsilon_0 m_i}$

(THE CENTER OF oscillation for the electrons is the center of the ion beam).

x_e = centroid of electron beam

x_i = centroid of ion beam

THE EQUATION OF MOTION FOR THE CENTROID OF THE IONS IS GIVEN BY

$$\frac{d^2 x_i}{dt^2} = -\omega_{\beta 0}^2 x_i - \left[\frac{m_e N_e}{m_i N_i}\right]\left(\frac{\omega_{fi}^2}{2}\,\frac{m_i}{q}\,\frac{e}{m_e}\right)(x_i - x_e)$$

THE TOTAL MOMENTUM KICK TO EACH SPECIES MUST BE EQUAL & OPPOSITE

$$\Rightarrow \quad \frac{d^2 x_i}{dt^2} = -\omega_{\beta 0}^2 x_i - f\,\frac{\omega_{fi}^2}{2}(x_i - x_e)$$

HERE $f \equiv \dfrac{e N_e}{q N_i}$ = fractional neutralization

Now $\dfrac{d}{dt}$ = total derivative $= \dfrac{\partial}{\partial t} + v_z \dfrac{\partial}{\partial z}$

$\Rightarrow$ THE ION & ELECTRON EQUATIONS MAY BE WRITTEN

$$\left(\frac{\partial}{\partial t} + v_z \frac{\partial}{\partial z}\right)^2 x_i = -\omega_{\beta 0}^2 x_i - f\,\frac{\omega_{fi}^2}{2}(x_i - x_e)$$

$$\frac{\partial^2}{\partial t^2} x_e = -\frac{\omega_{pi}^2}{2}\left(\frac{m_i}{q}\,\frac{e}{m_i}\right)(x_e - x_i)$$

Now let $X_e = X_e \exp[i(\omega t - kz)]$; $\quad X_i = X_i \exp[i(\omega t - kz)]$

$$\Rightarrow (-\omega^2 + 2\omega k V_z - k^2 V_z^2) X_i = -\omega_{p0}^2 X_i - f \frac{\omega_{pi}^2}{2} (X_i - X_e)$$

$$-\omega^2 X_e = -\frac{\omega_{pi}^2}{2}\left(\frac{m_i}{m_e}\frac{e}{q}\right)(X_e - X_i)$$

$$\Rightarrow \left[(\omega - kV_z)^2 - \omega_{p0}^2 - f\frac{\omega_{pi}^2}{2}\right] X_i = -\frac{f\omega_{pi}^2}{2} X_e$$

$$\left[\omega^2 - \frac{\omega_{pi}^2}{2}\left(\frac{m_i}{m_e}\frac{e}{q}\right)\right] X_e = -\frac{\omega_{pi}^2}{2}\left(\frac{m_i}{m_e}\frac{e}{q}\right) X_i$$

Muliplying the above equations and dividing by $X_e X_i$, yields the dispersion relation:

$$\underbrace{\left[(\omega - kV_z)^2 - \omega_{p0}^2 - f\frac{\omega_{pi}^2}{2}\right]}_{\text{ION BETATRON FREQUENCY (INCREASED BY SPACE CHARGE OF ELECTRONS))}} \underbrace{\left[\omega^2 - \frac{\omega_{pi}^2}{2}\left(\frac{m_i}{m_e}\frac{e}{q}\right)\right]}_{\text{ELECTRON oscillating IN POTENTIAL WELL OF ION}} = \underbrace{+\frac{f\omega_{pi}^4}{4}\left(\frac{m_i}{m_e}\frac{e}{q}\right)}_{\text{COUPLING}}$$

So a beam with high spatial frequency undergoing betatron oscillations in the comoving frame, $\therefore kV_z - \omega \cong \sqrt{\omega_{p0}^2 + \frac{f\omega_{pi}^2}{2}}$ will resonate with electrons oscillating in the ion well if

$$\omega \cong \frac{\omega_{pi}}{\sqrt{2}}\sqrt{\frac{m_i e}{m_e q}}$$

Giving rise to instability!

From Davidson & Qin (22)
Physics of Intense Charged Particle Beams, 2001.

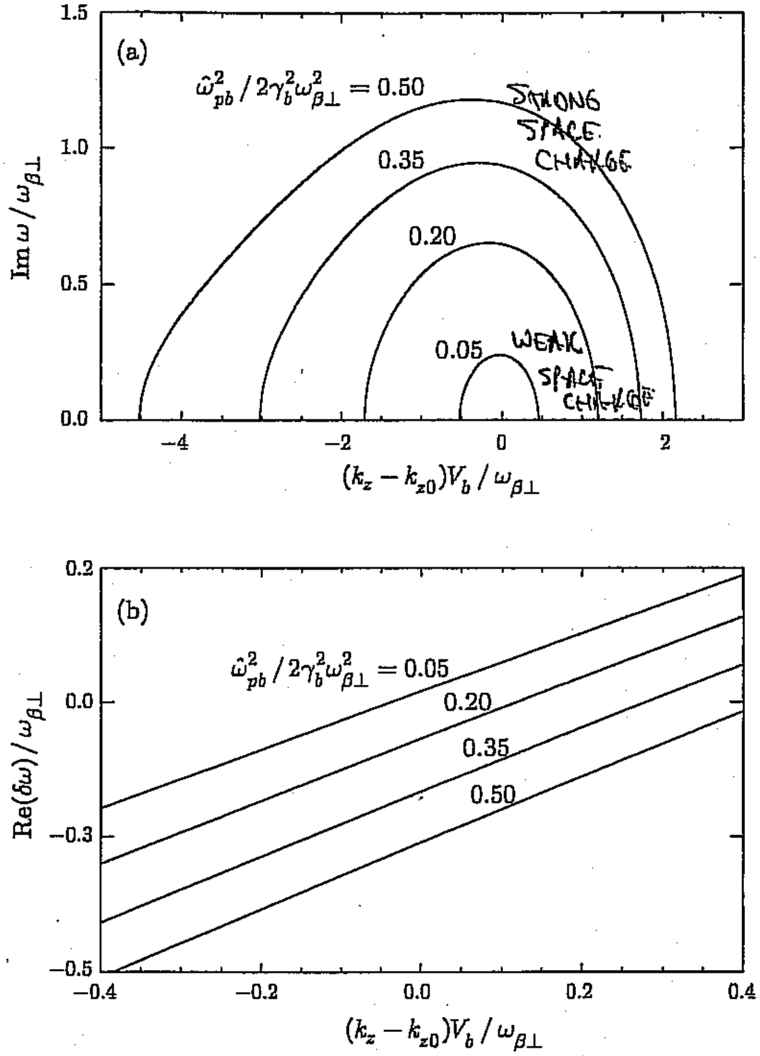

$\omega_{\beta\perp}^2 \equiv \omega_{\beta 0}^2$

$\frac{\hat{\omega}_{pb}^2}{2\gamma_b^2\omega_{\beta\perp}^2} = \left(1 - \frac{\nu^2}{\nu_0^2}\right)$

Figure 10.11. Plots of (a) normalized growth rate ($Im\omega/\omega_{\beta\perp}$), and (b) normalized real frequency $(Re\omega - \omega_e)/\omega_{\beta b}$ versus shifted axial wavenumber $(k_z - k_{z0})V_b/\omega_{\beta\perp}$ obtained from the dispersion relation (10.103) for the unstable branch with positive real frequency. System parameters correspond to $v_{T\|b} = 0 = v_{T\|e}$, $m_b/m_e = 1836$ (protons), $(\gamma_b - 1)m_bc^2 = 800$ MeV, $r_b/r_w = 0.5$, and $f = 0.1$. Curves are shown for several values of normalized beam intensity $\hat{\omega}_{pb}^2/2\gamma_b^2\omega_{\beta\perp}^2$ ranging from 0.05 to 0.5.

$k_{z0}V_z = \omega \mp \sqrt{\omega_{\beta 0}^2 + f\omega_i^2/2}$; $\omega = \frac{\omega_{pi}}{2}\sqrt{\frac{m_i e}{m_e q}}$

From DAVIDSON & QIN, 2001 (23)

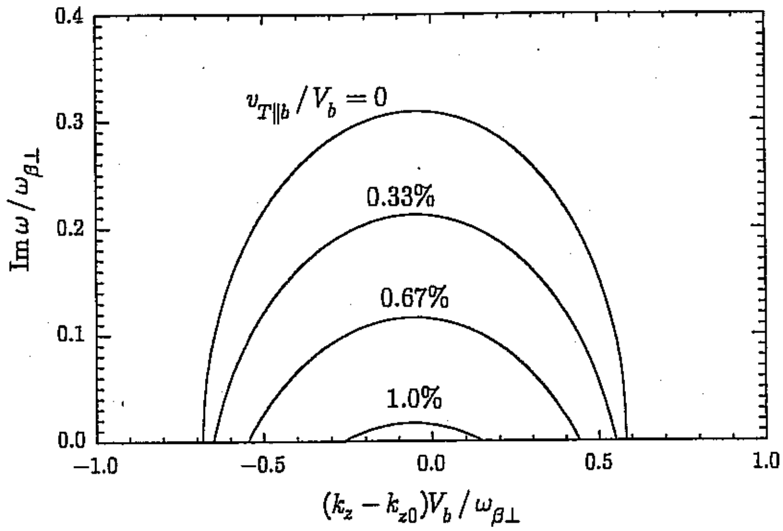

Figure 10.12. Plot of normalized growth rate ($Im\omega/\omega_{\beta\perp}$), and normalized real frequency $(Re\omega - \omega_e)/\omega_{\beta\perp}$ versus positive real frequency. System parameters correspond to $\hat{\omega}_{pb}^2/2\gamma_b^2\omega_{\beta\perp}^2 = 0.07$, $v_{T\|e} = v_{T\|b}$, $m_b/m_e = 1836$ (protons), $(\gamma_b - 1)m_bc^2 = 800$ MeV, $r_b/r_w = 0.5$, and $f = 0.1$. Curves are shown for several values of normalized ion thermal spread $v_{T\|b}/V_b$ ranging from 0 to 0.01.

velocity V_b [Eq. (10.105)], it is expected that Landau damping by parallel ion kinetic effects can have a strong stabilizing influence at modest values of $v_{T\|b}/V_b$. That this is indeed the case is evident from Fig. 10.12, which shows a substantial reduction in maximum growth rate and eradication of the instability over the instability bandwidth as $v_{T\|b}/V_b$ is increased from 0 to 0.01.

We now make use of the nonlinear particle perturbative simulation method [60, 61] described in Sec. 8.5 to illustrate several important properties of the two-stream instability in intense beam systems (Sec. 10.4.2).

(24)

PREVENTIVE MEASURES (from J. Wei & L. Macek, CERN electron cloud workshop 2003).

- SUPPRESS ELECTRON GENERATION
  - SURFACE TREATMENT OF THE VACUUM PIPE
  - KICKER MAGNETS IN GAPS
  - VACUUM PORTS SCREENED TO REDUCE E-field
  - CLEARING ELECTRODES
  - HIGH VACUUM
  - SOLENOIDS - TO REDUCE MULTIPACTING

25

Summary of Electron, Gas, Pressure, & Scattering Effects

1. Coulomb collisions within beam can transfer energy from $\perp$ to $\parallel$ and provide lower limit on $T_{\parallel}$, higher than from accelerative cooling.

2. Coulomb interactions with residual gas nuclei provide a source of emittance growth (but not important for higher mass and linac residence times).

3. Pressure instability from desorption of residual gas by stripped beam ions hitting wall or beam-ionized residual gas atoms, forced to wall by E-field of beam. Limits current in rings or high rep rate linac.

4. Electrons can cascade and reach a "quasi" equilibrium population of similar line charge to the ion beam. Electron-ion two stream instability is unstable, and can lead to transverse instability, similar to what is observed in some proton rings.

(1)

John Barnard
Steven Lund
USPAS
June 2008

An application of intense beams

1. Heavy-ion fusion
   - A. Requirements
   - B. Targets for ICF
   - C. Accelerator
   - D. Drift compression
   - E. Final focus
   - F. Experiments

Inertial Fusion Energy (IFE) power plants of the future will consist of four parts

Inertial fusion energy system:

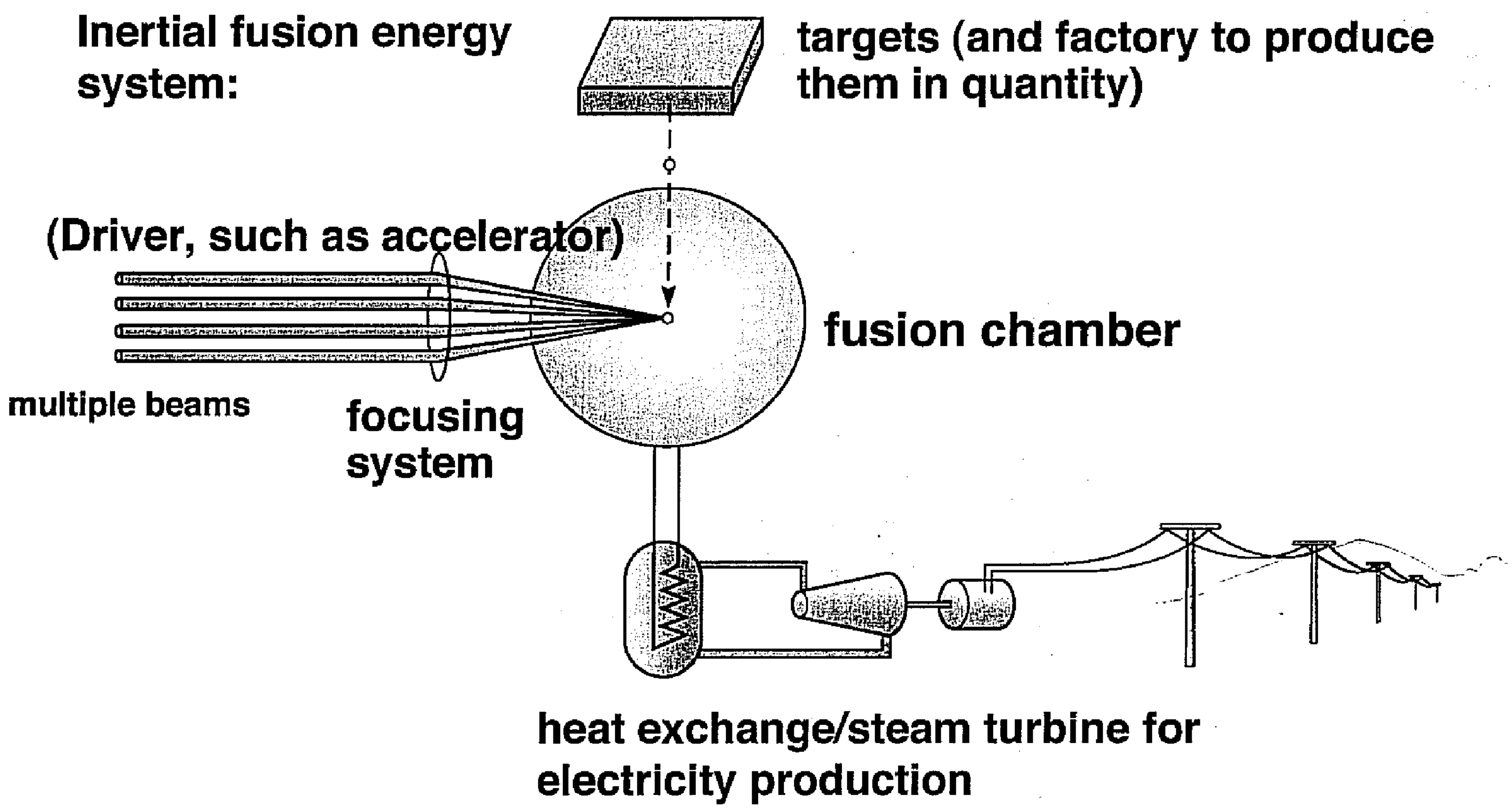

Heavy Ion Fusion provides an attractive approach to long term energy production

Fusion offers an inexaustible, long term solution to the problem of future energy supplies free from long-lived radioactive by-products and greenhouse CO_2.

Inertial Confinement Fusion (ICF) uses laser or particle beams to implode a target, raising the temperature and density of the fuel, creating the conditions necessary for the following reaction:

$$D + T \rightarrow n\ (14.06\ \text{MeV}) + He^4\ (3.52\ \text{MeV})\ .$$

Heavy ion accelerators are a strong candidate for inertial fusion *energy production* (IFE) because of:

- High efficiency
- High repetition rate
- Survivability of final lens
- Favorable target illumination geometry

(3)

National Ignition Facility has 192 beams of 40-cm aperture arranged in four beam clusters

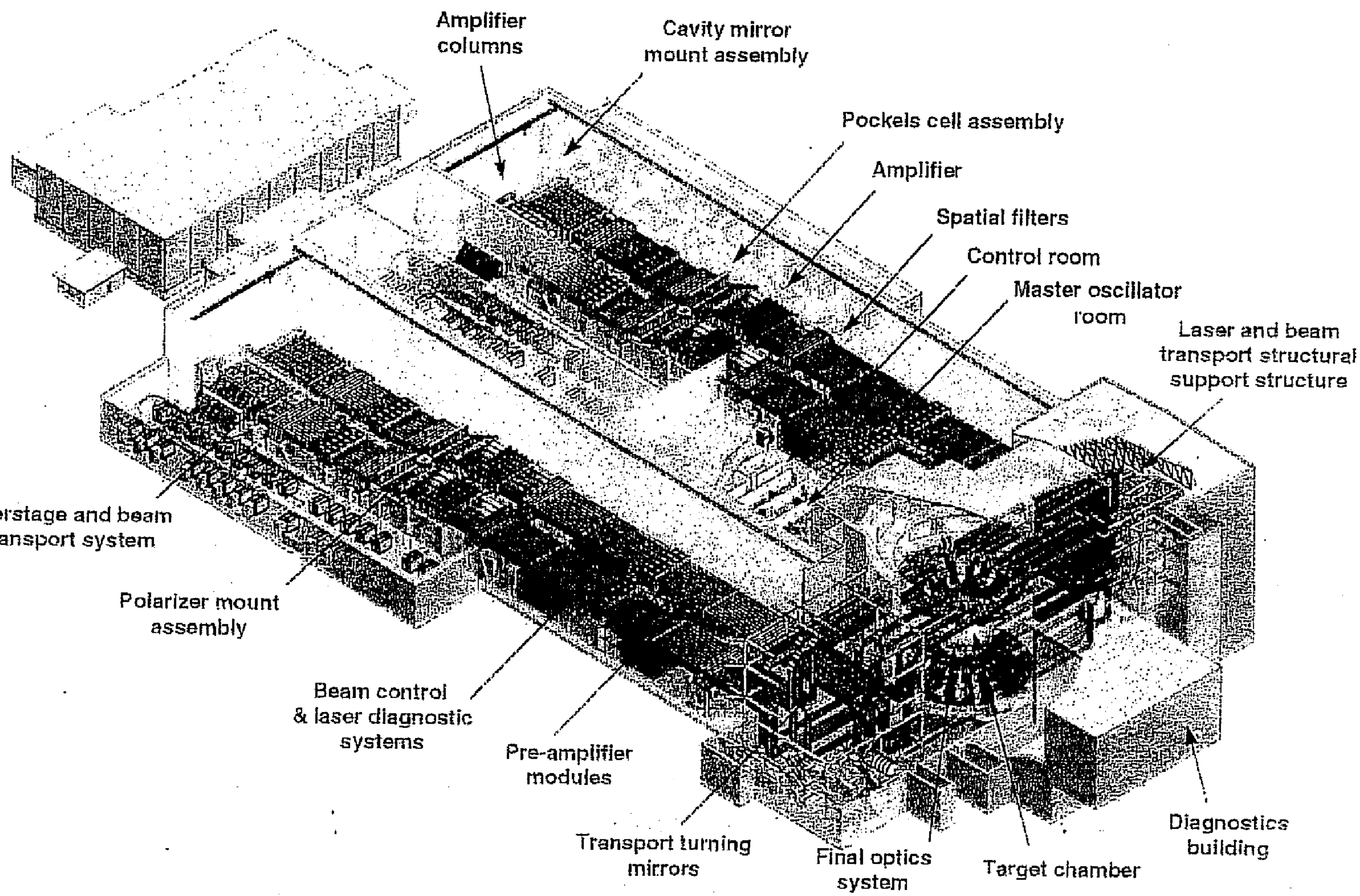

NIF illustrates many of the features of IFE development and will play a critical role in addressing IFE feasibility

40-00-0996-2100YA
03GAD/gbh

5/1/98
EMC/lca

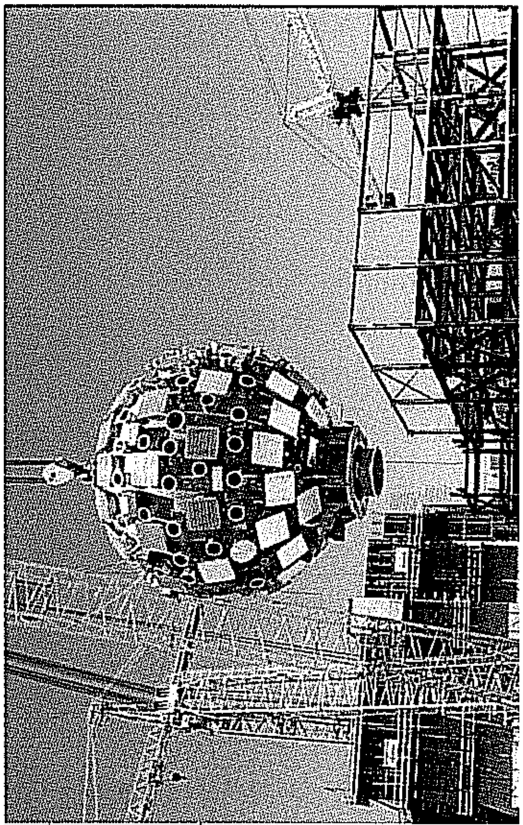
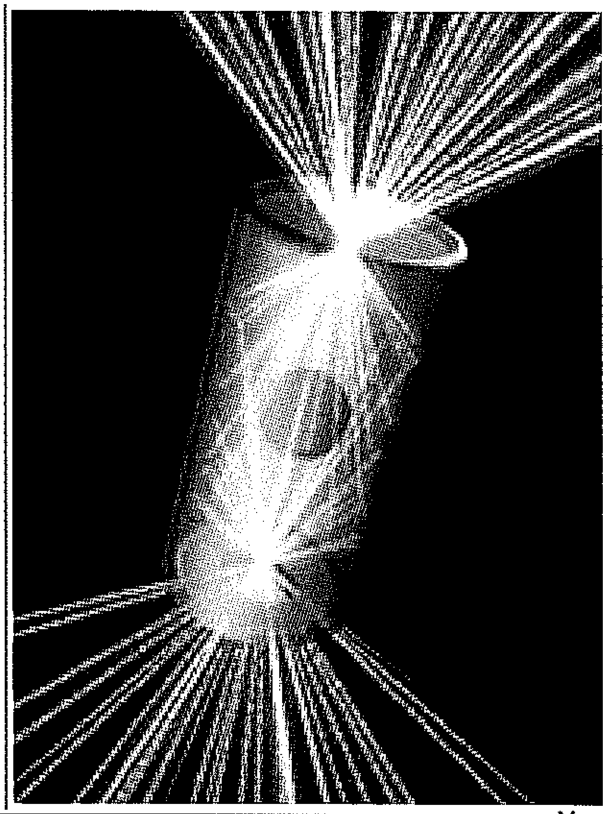
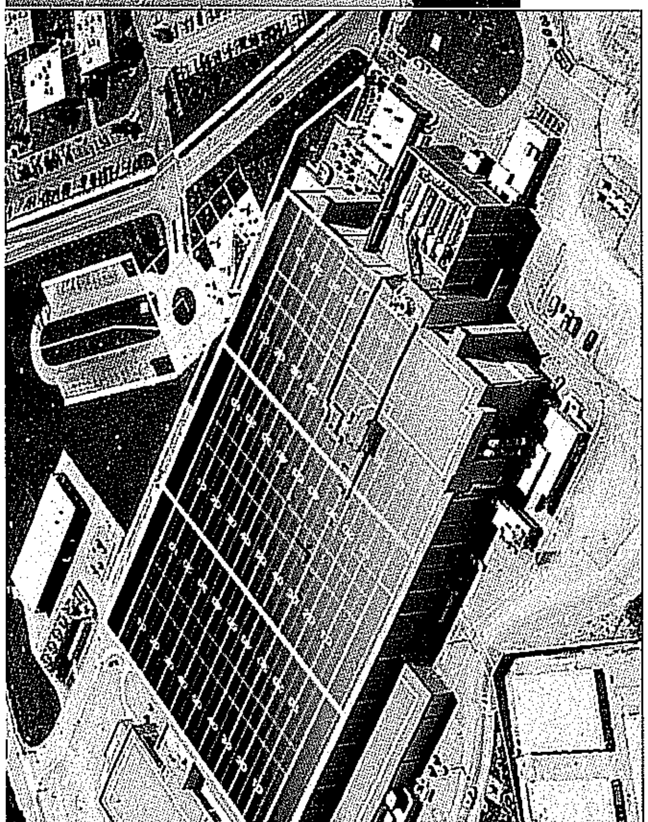
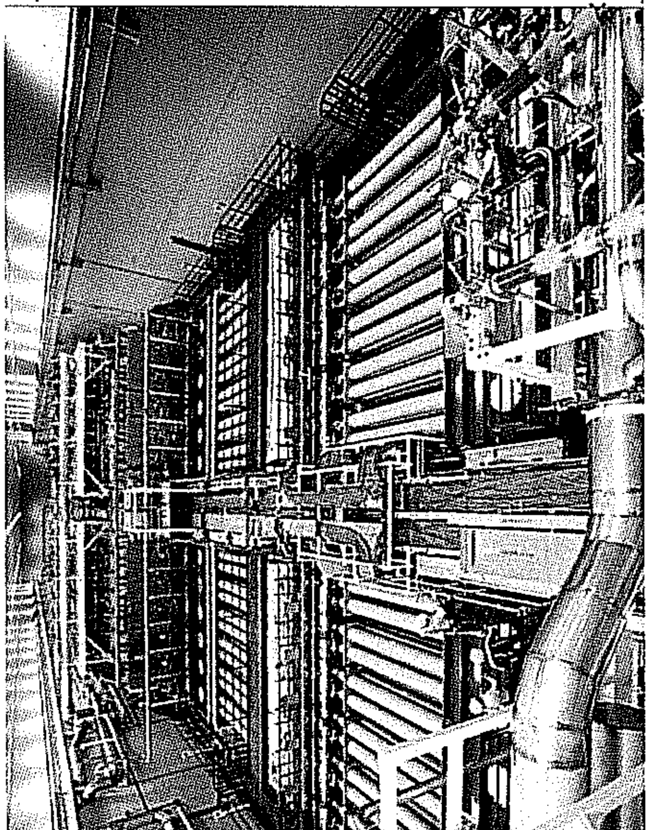

The two principal approaches to ICF are direct drive and indirect drive

Two types of targets:

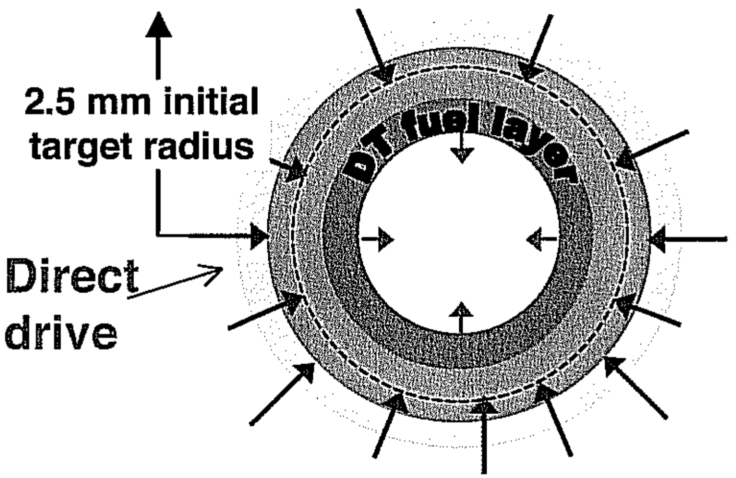

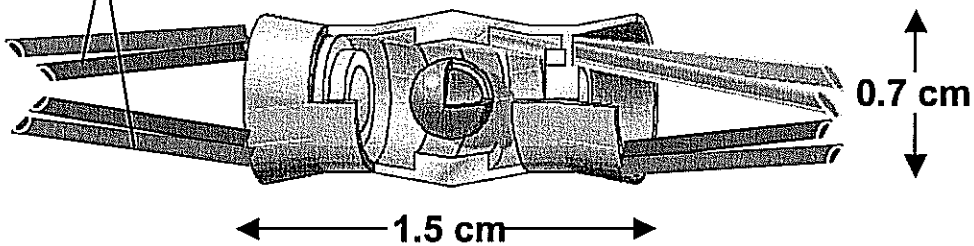

Direct drive advantages:

Higher coupling efficiency with potential for higher gain

Indirect drive advantages:

Relaxed beam uniformity (reduced hydro instability)

Significant commonality for lasers and ion beams

Significant simplification of chamber geometry

The two principal approaches to ICF are direct drive and indirect drive

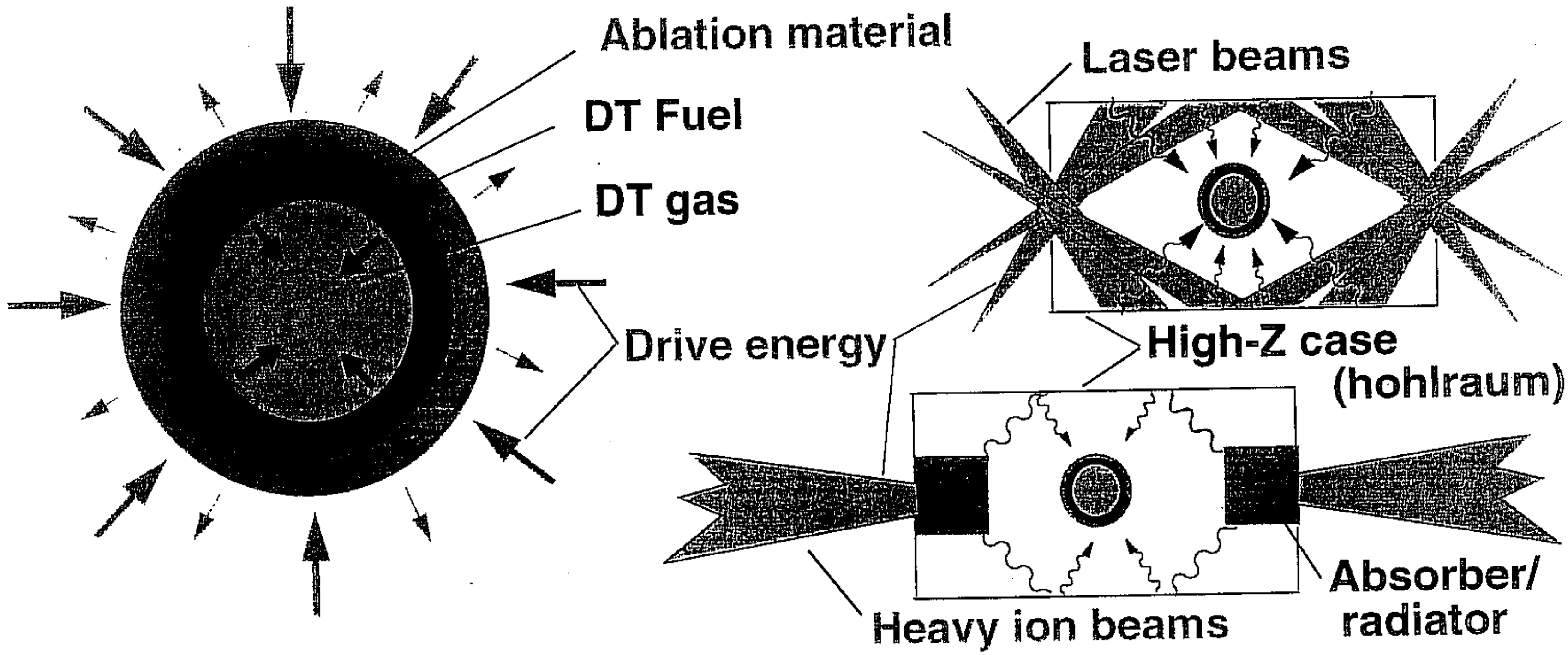

Direct drive:

Advantage:

Higher coupling efficiency (with potential for higher gain)

Indirect drive:

Advantages:

Relaxed beam uniformity (reduced hydro instability)
Significant commonality for lasers and ion beams
Significant simplification of chamber geometry

6

"FAST IGNITION" IS AN ALTERNATIVE TO "HOT SPOT" IGNITIO

- CAPSULE IS COMPRESSED ON LOW ADIABAT
- SECOND "IGNITOR" PULSE STARTS IGNITION PROCESS

<u>COMPRESSION PULSE</u> $E \sim 200\,kJ - 1\,MJ$

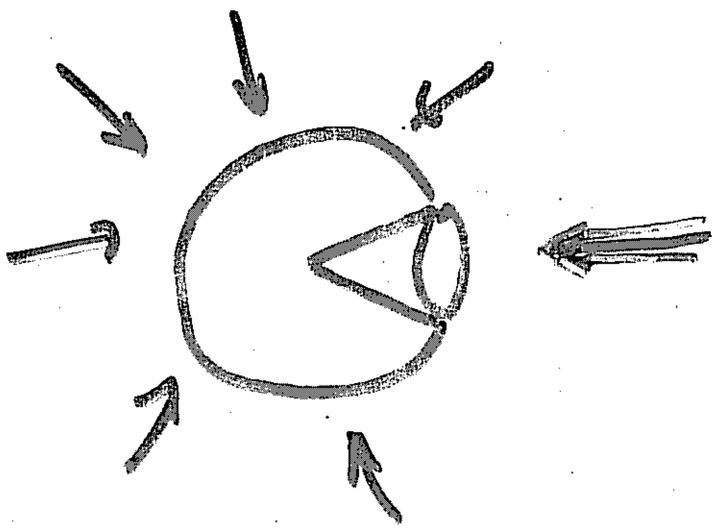

<u>IGNITOR PULSE</u> (CREATES ELECTRON OR ION BEAM)

$E \sim 20\,kJ$

$\tau \sim 20\,ps$

$r \sim 20\,\mu$

A "DISTRIBUTED RADIATOR" TARGET PRODUCES HIGH GAIN IN RADIATION-HYDRODYNAMIC SIMULATIONS

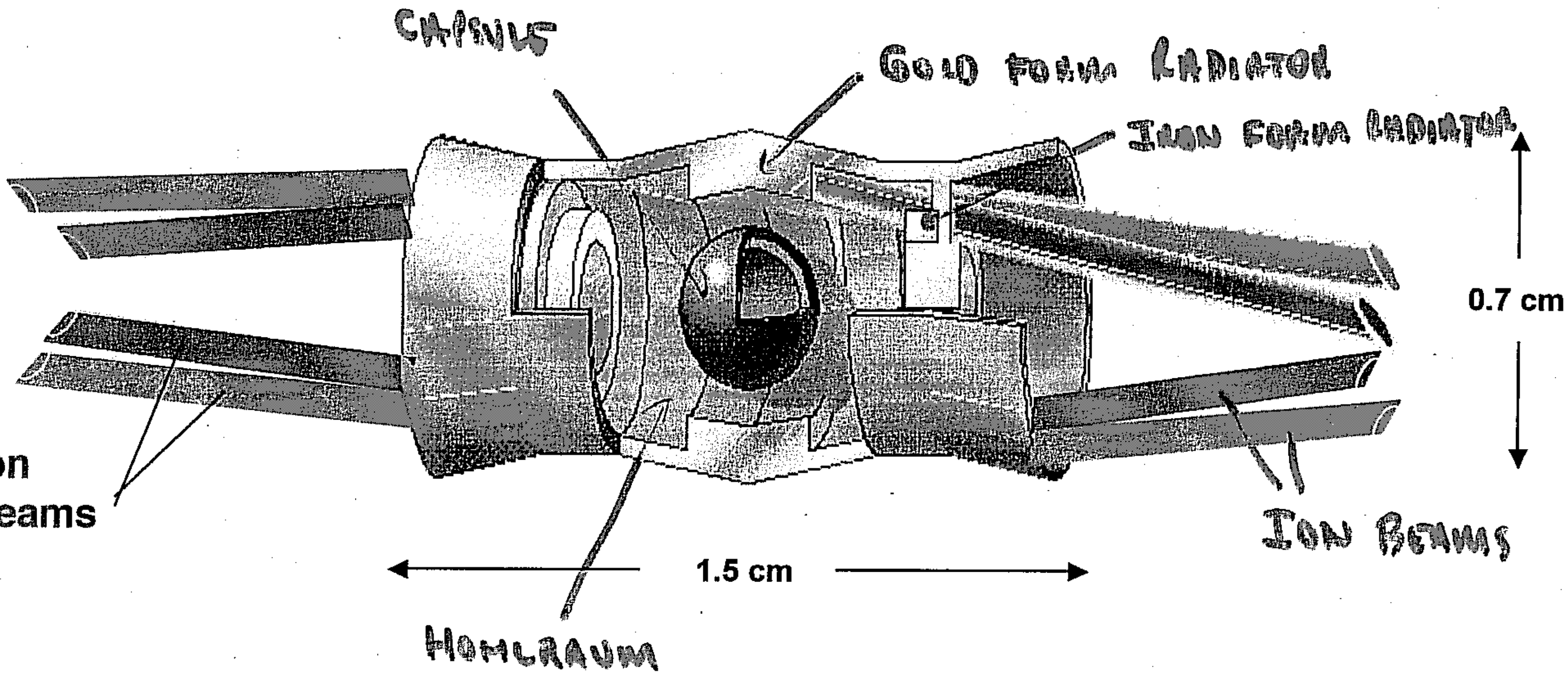

The Heavy Ion Fusion Science Virtual National Laboratory

Ion current profile and radiation temperature

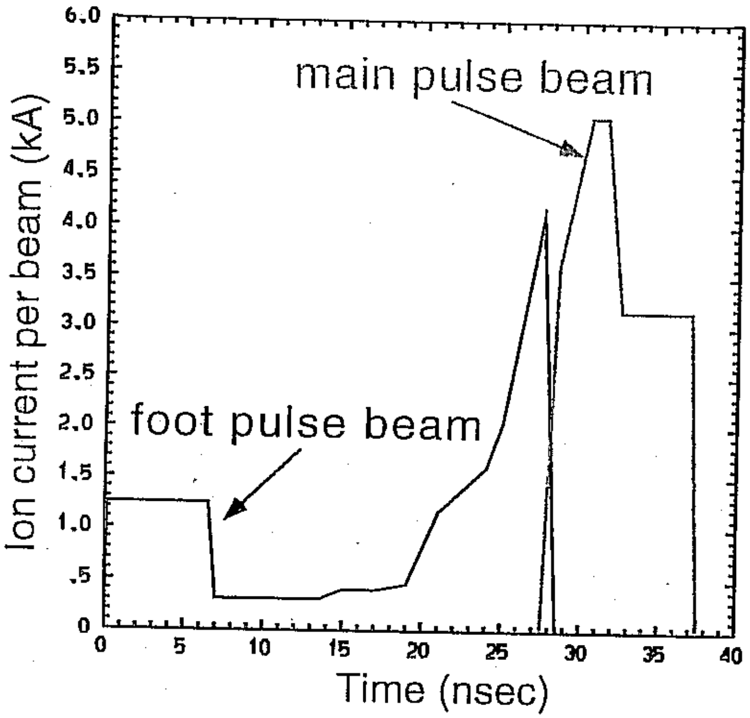

Current assumes 16 beams in foot pulse
32 beams in main pulse

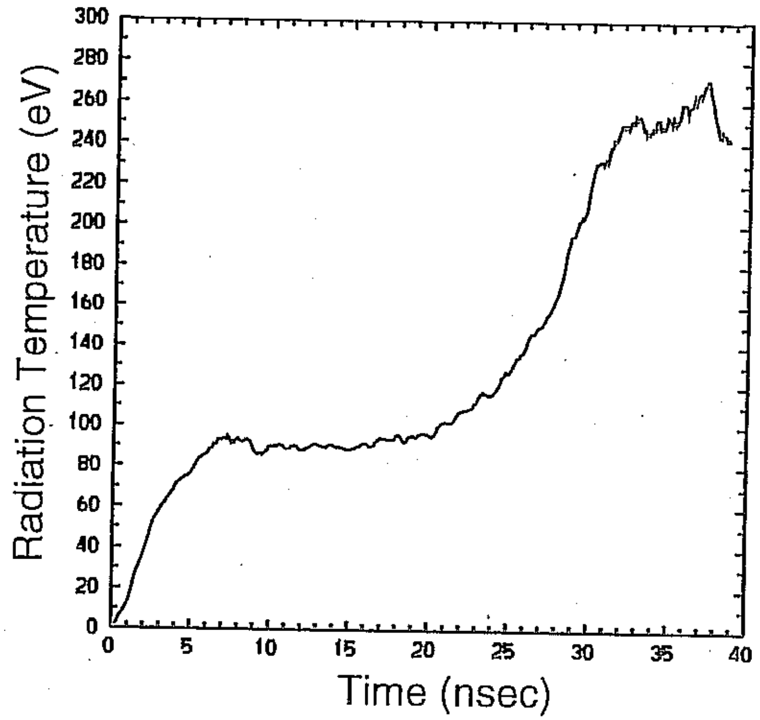

Callahan 11/97

Overlapping Gaussian, elliptical beams are focused at the end of the target

Each beam is an ellipse

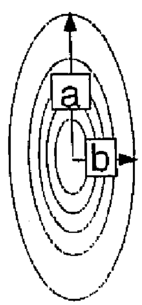

8 beams overlap in the foot pulse

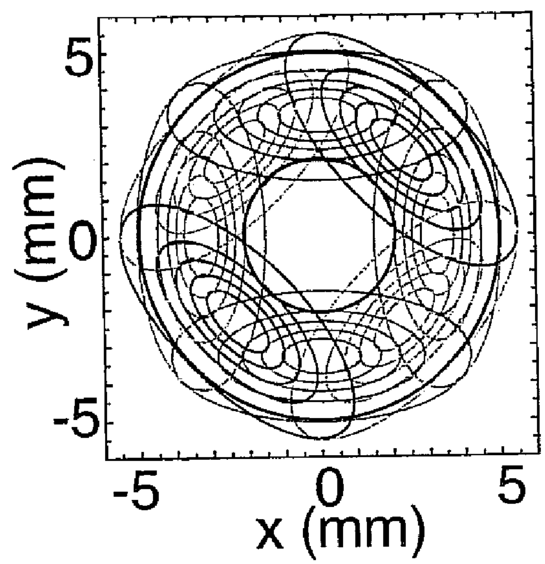

Sum of 8 foot pulse beams

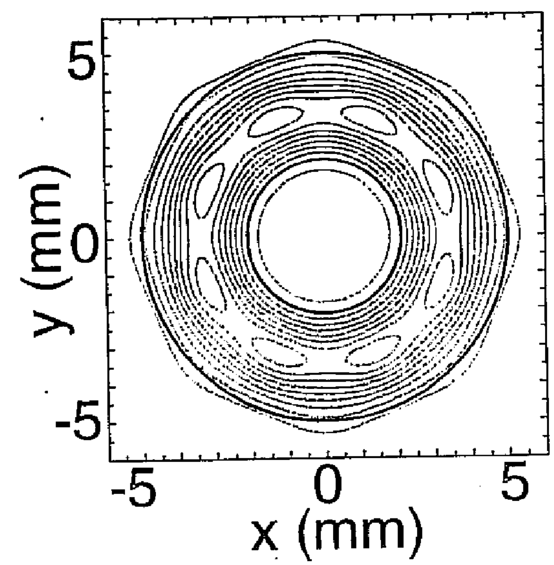

a = 4.15 mm
b = 1.8 mm
effective r=2.7 mm
95% of charge inside

Azimuthal asymmetry:
foot pulse: -1.6% in m=8
main pulse: 0.06% in m=16

Callahan 8/97

9

Berkeley Lab

Why Heavy Ions?

<u>Target requires</u>:

3.5 - 6 MJ in ~ 10 ns $\Rightarrow$ ~ 500 TW

Range ~ 0.02 - .2 g/cm^2

Range requirement $\rightarrow$ **Higher mass $\Leftrightarrow$ higher kinetic energy**

Power Requirement $\rightarrow$ **Current $\propto \frac{1}{\text{kinetic energy}}$**

Higher mass requires lower current (easier to focus).

4

10

Heavier Ions ⇒ Higher Kinetic Energy

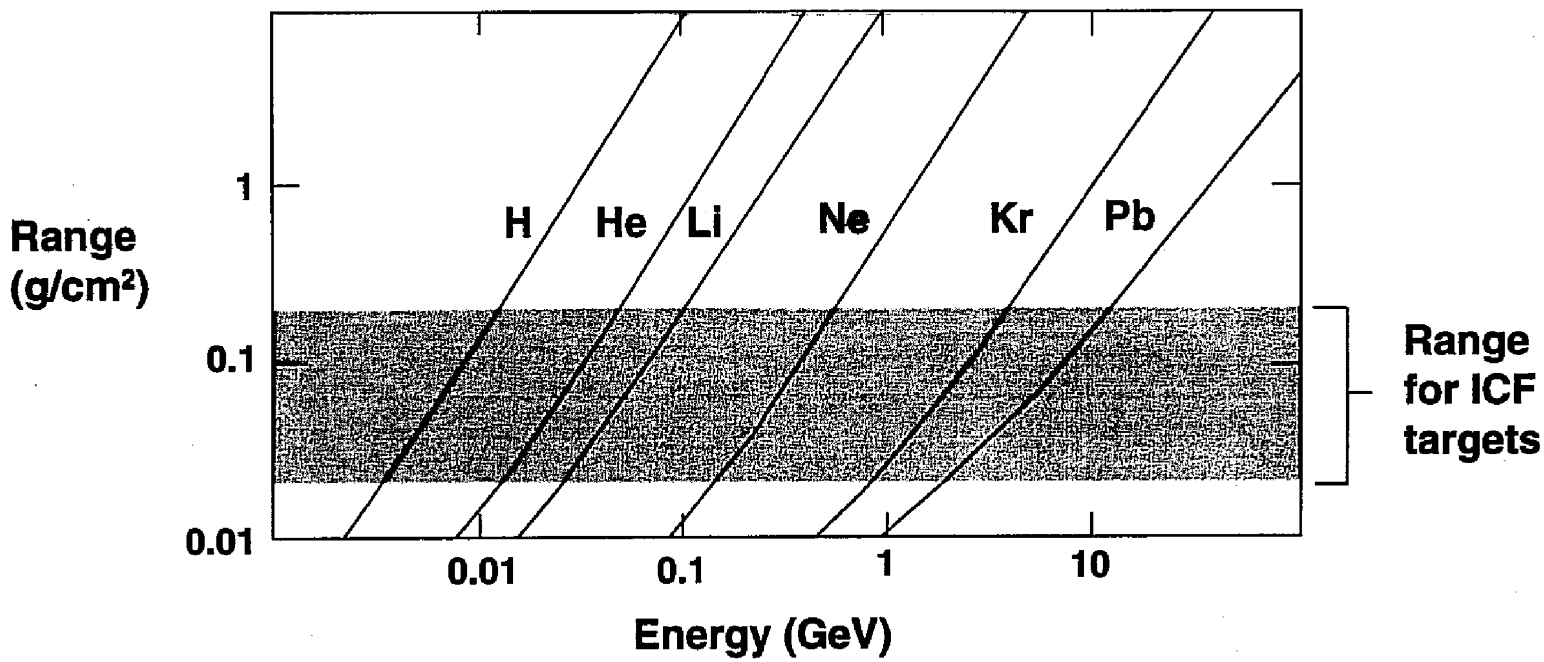

Targets require high power (kinetic energy x current).

- Light Ion Fusion requires high-current, unconventional accelerators (Sandia 1970s).
- Heavy Ion Fusion requires lower currents enabling the use of more conventional high energy accelerators (Maschke ~ 1974).

There are two principle methods of acceleration

1. r.f. acceleration

(Approach in Europe and Japan)

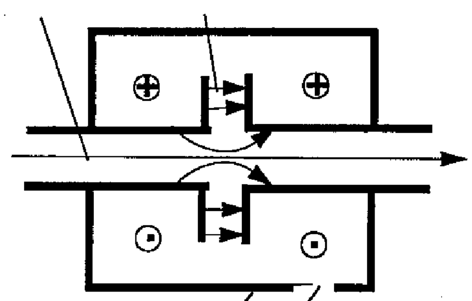

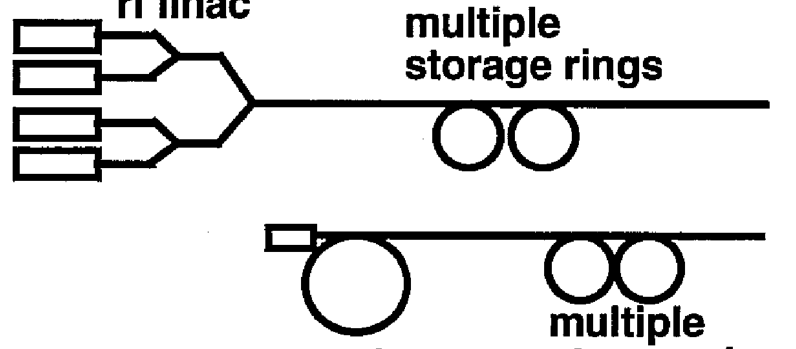

2. Induction acceleration

(U.S. approach)

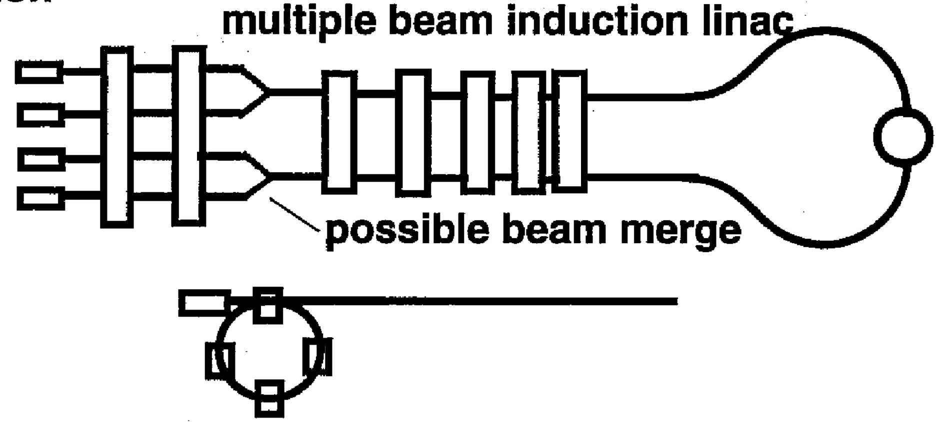

21

Induction acceleration for HIF consists of several subsystems and a variety of beam manipulations

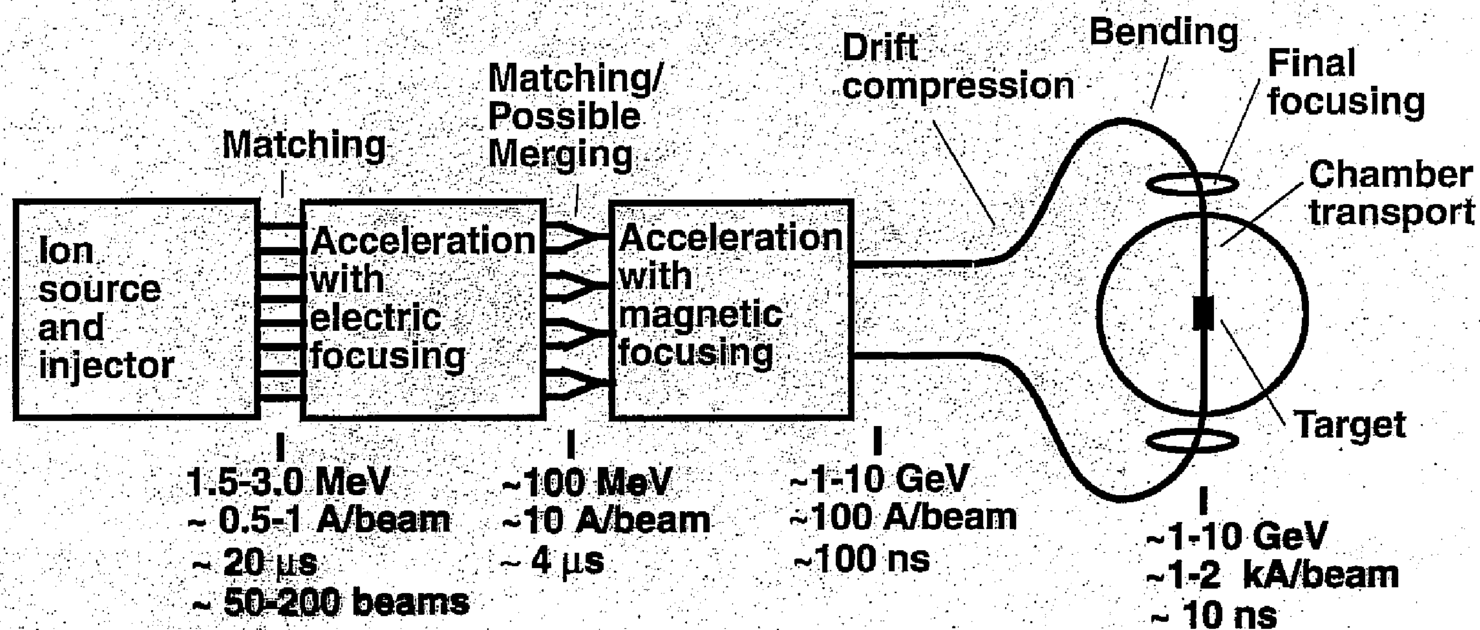

13

A Robust Point Design study established a baseline for a multiple-beam quadrupole induction linac HIF driver

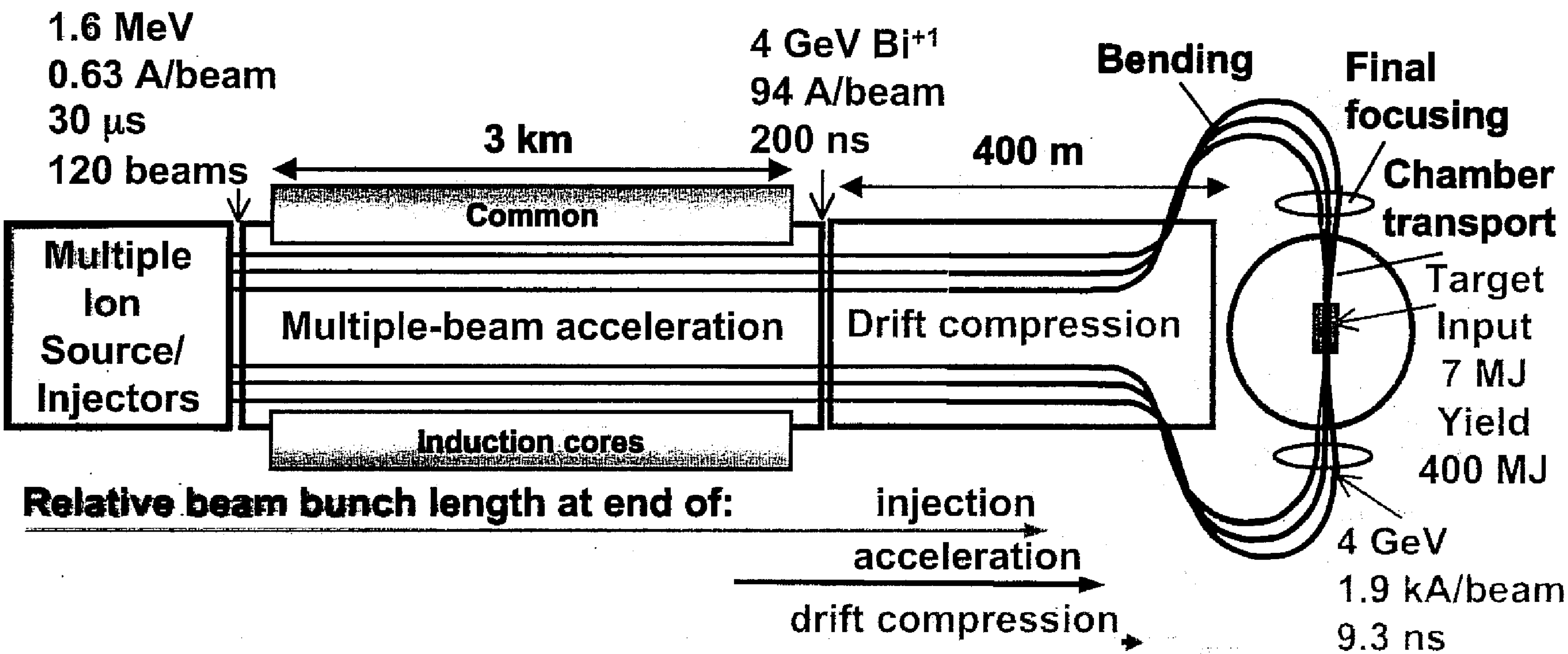

The Heavy Ion Fusion Virtual National Laboratory

A solenoid focus option leads to a low V, high current modular driver with advantageous development path

Pulse energy ~ 6.7 MJ

V~ 200-300 MV: T~ 2.5 GeV Xe^{+8} ions or T ~ 200 MeV for Ne^{+1}

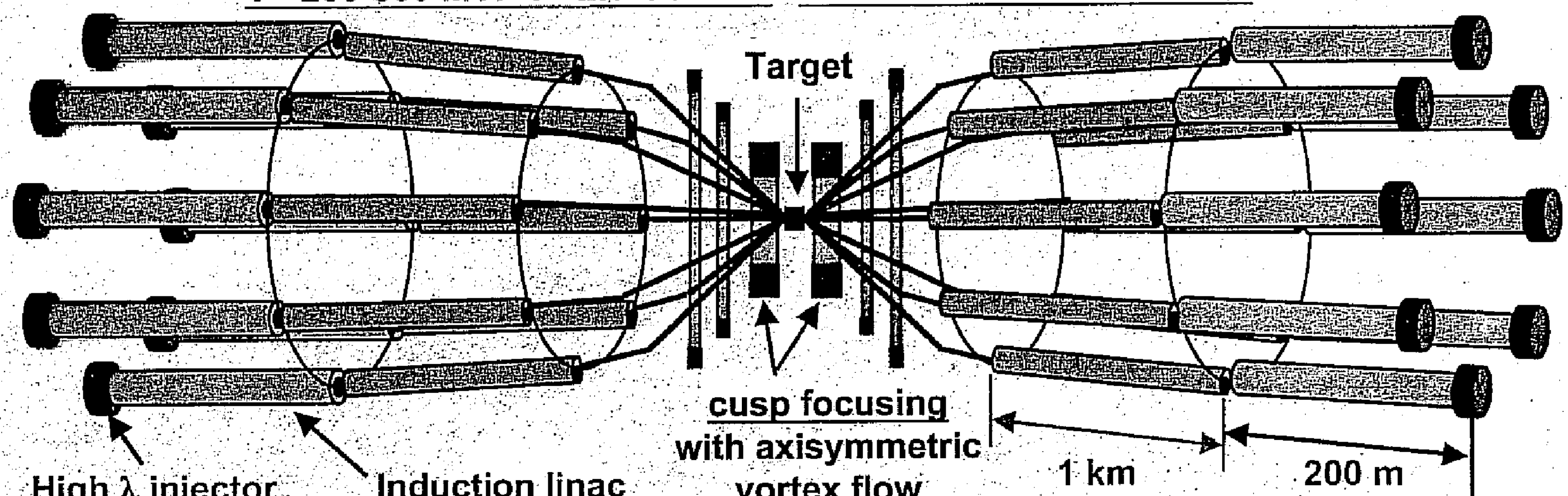

High λ injector

Merging beamlet source/injector

or

accel/decel injector

Induction linac

single beams

r_p ~ 15 cm

B_s ~ 9T

I ~ 6.7 kA

T ~ 2.5 GeV

Δt ~ 100 ns

double pulsed for foot and main pulses

cusp focusing with axisymmetric vortex flow

or

adiabatic plasma lense assisted pinch with cross-jet flow. liquid walls

Neutralized drift compression

Δv/v ~ 0.01

(no space charge stagnation)

The Heavy Ion Fusion Virtual National Laboratory

PPPL

Summary of Current Limits From Different Focusing Methods

Einzel Lens

$$Q_{max} \cong \frac{3\pi^2}{8}\left(\frac{q\phi_0}{m v_0^2}\right)^2\left(\frac{r_b}{L}\right)^2$$

Solenoids

$$Q_{max} = \left(\frac{\omega_c r_b}{2\gamma\beta c}\right)^2$$

Quadrupole Focusing

MAGNETIC

$$Q_{max} \cong \frac{\eta\Phi_0}{2\pi}\left(\frac{\sin\frac{\eta\pi}{2}}{\frac{\eta\pi}{2}}\right)\begin{bmatrix} \dfrac{B r_b}{[B\rho]}\left[\dfrac{r_b}{r_p}\right] \\ \dfrac{2qV_q}{\gamma m v_z^2}\left[\dfrac{r_b^2}{r_p^2}\right]\end{bmatrix}$$

Electric

For Non-Relativistic Beams

$$\lambda_{max} \propto \frac{\phi_0^2}{V} \qquad \lambda_{max} \propto \frac{q}{m} B^2 r_p^2 \qquad \lambda_{max} \propto \begin{cases} B_1 V^{1/2} r_p \\ V_q \end{cases}$$

NOTE
ϕ_0 = Voltage between Einzel lenses
V_q = Voltage on a quad relative to ground
V = particle energy / q

Major components of an induction linac

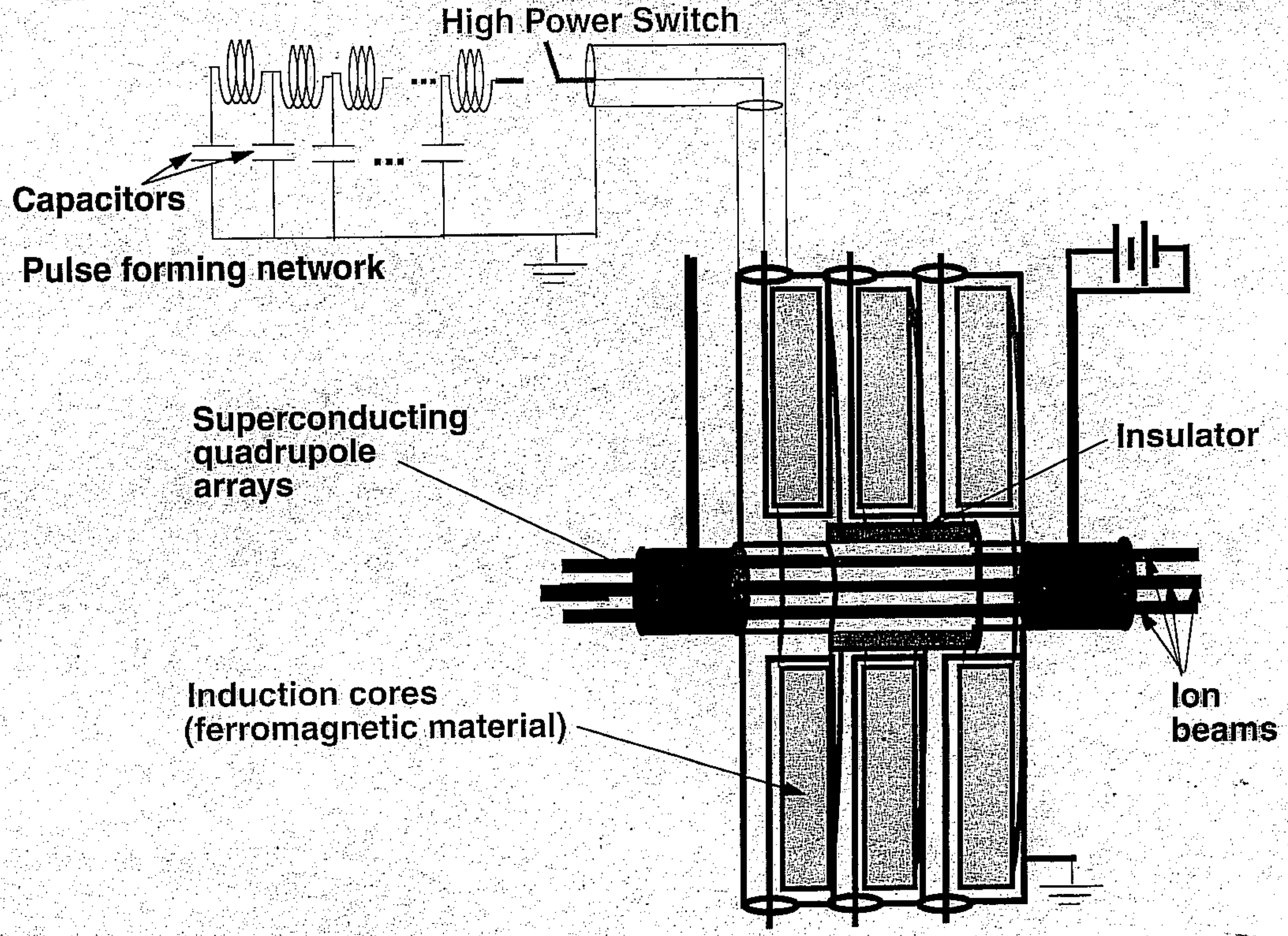

15

BERKELEY LAB

An Induction Core

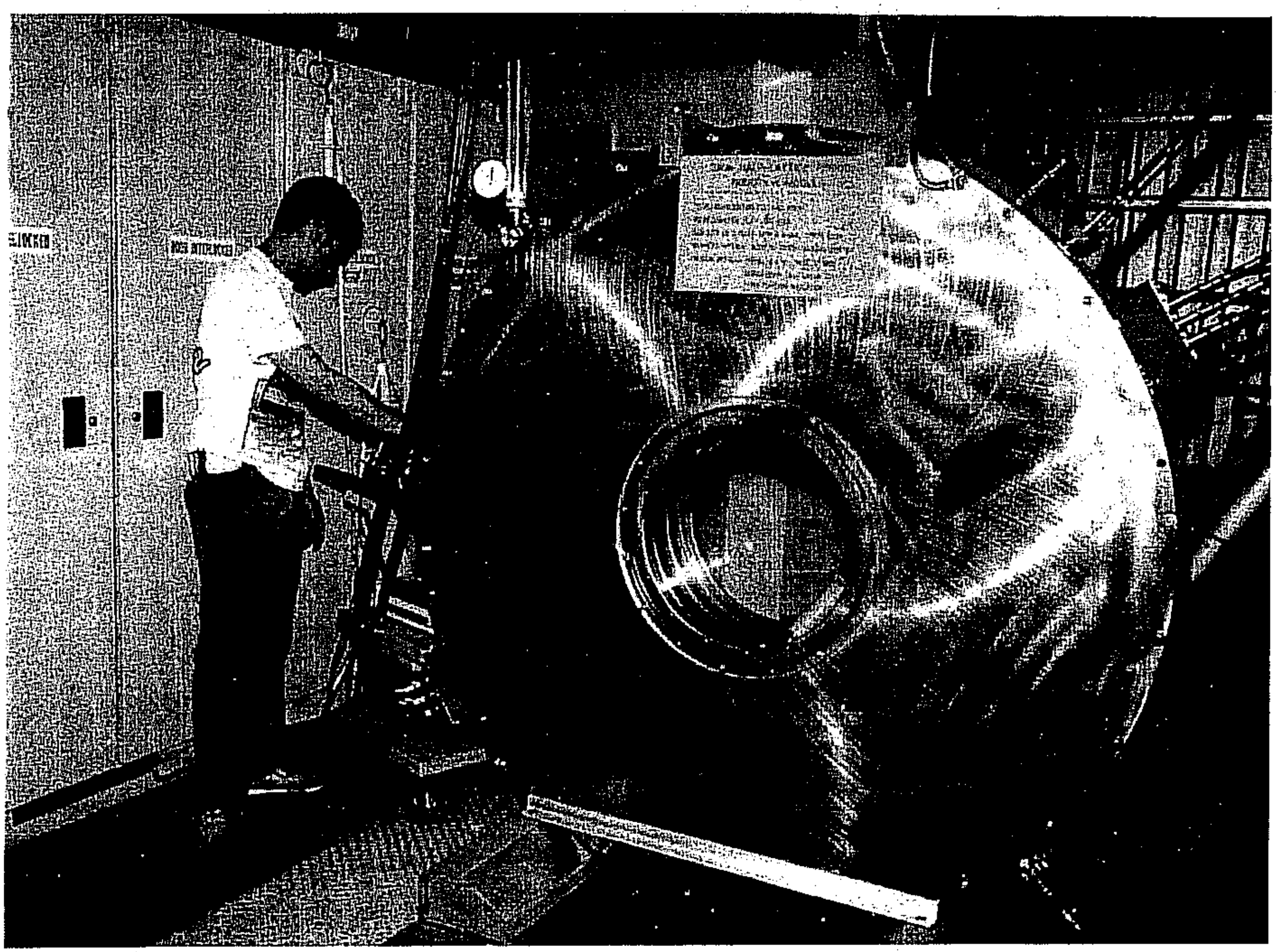

(16)

An array of small beamlets increases the total beam current through the core

From class:
$\frac{Q}{a} = \left(\frac{\omega_q^2}{4c^2}\right) a$
$\omega_q \cong \frac{\eta c^2 B'}{[B\rho]}$
$I \sim \beta^3 Q \sim a^2 B \beta^2 / r_p$
$Q \simeq \frac{\eta B' \sigma}{[B\rho]} \frac{a}{4}$

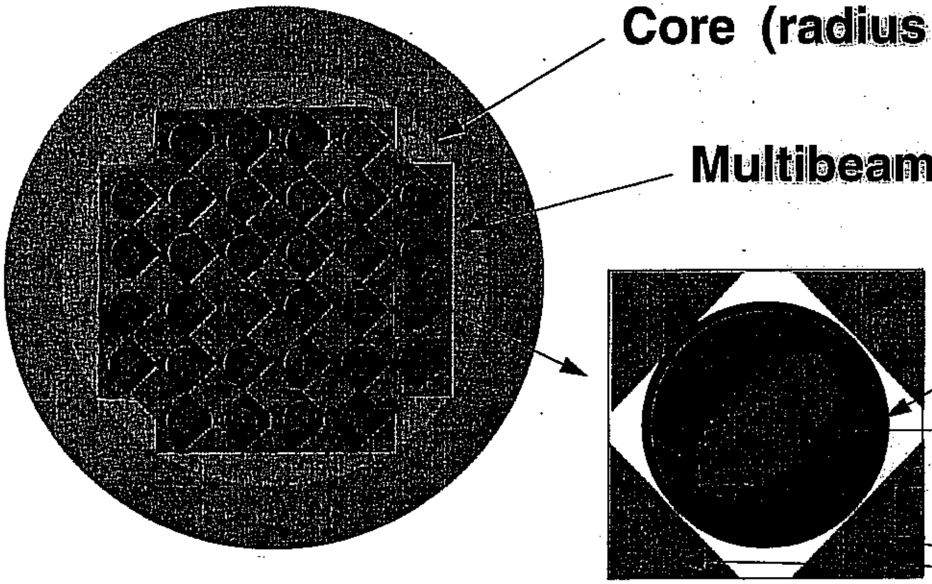

Current per beam = $I_b \sim a^2 B \beta^2 / r_p$

$r_p \sim a$ (until misalignments require minimum size--better: $r_p = c_1 a + c_2$)

so $I_b \sim a$; N_b = number of beams in array $\sim R^2_{core} / a^2$

Total current through core = $I_{tot} = N_b I_b \sim R^2_{core} / a$ (until misalignments dominate scaling)

17

A Typical driver has about 2000 individual modules

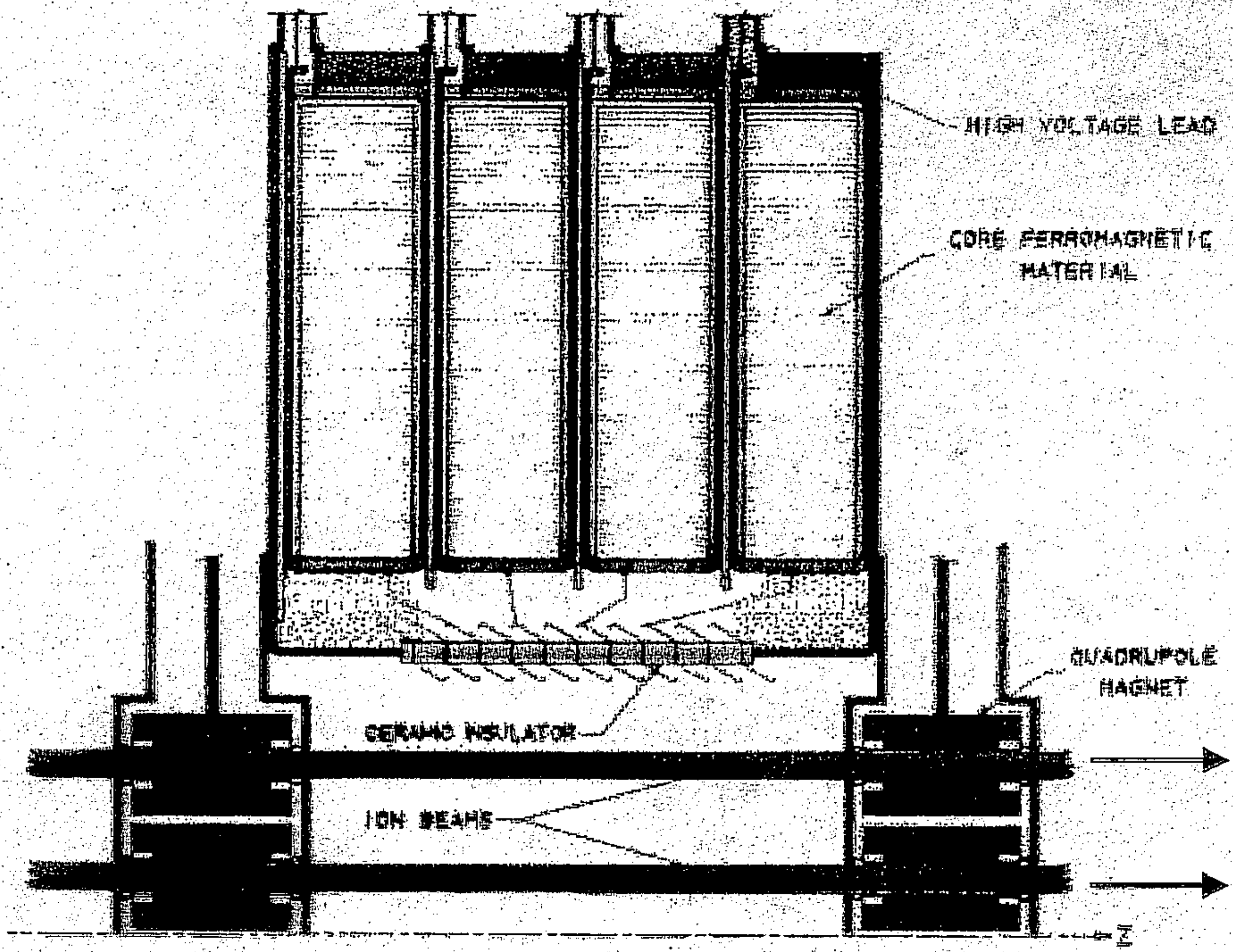

Focusability at the target is key scientific issue

Conditions of beam at target are set by hohlraum and implosion physics

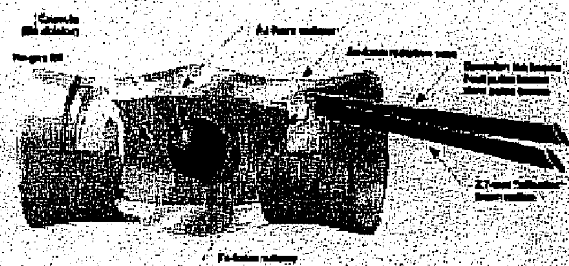

Energy in pulse: ~ 3 to 6 MJ

Duration of main pulse: ~ 8 to 10 ns

Duration of foot pulse: ~ 30 ns

Spot radius: ~ 1.5 to 3 mm

Transverse and longitudinal compression are required to meet target specifications.

y z

Length of beam just outside of injector ~25-50 m → **At target ~ 0.5 - 1 m**

y x

Radius of beam at source ~ 1-3 cm → **At target ~ 1.5-3 mm**

Compression factors of 10 to 50 in both longitudinal and transverse directions are required.

4

In an induction linac, certain limits constrain design

BERKELEY LAB

Phase advance per lattice period $\sigma_0 < \sim 85^{\circ}$ **(to avoid envelope/lattice instabilities & emittance growth).**

Space charge is limited by external focusing $K < (\sigma_0 a/2L)^2$ **where K is the perveance (proportional to line charge density over beam Voltage), a is the average beam radius and L is the half-lattice period.**

Velocity tilt $\Delta v/v <\sim 0.3$ for electrostatic quads **(larger for magnetic quads) to avoid mismatches at head and tail of beam, and to ensure tail radius within pipe and head σ_0 within limit)**

Volt-seconds per meter $(dV/ds)\, l/v_0 <\sim$ 1.5-2.0 V-s/m **(for "reasonable" core sizes)**

Voltage gradient $dV/ds <\sim$ 1-2 MV/m **(to avoid breakdown in gaps)**

19

Sources of non-linearity and mismatch are well defined

Berkeley Lab

Sources of non-linearities
- External focusing magnets
- Space-charge
- Multiple-beam effects

Sources of mismatch
- Accelerator imperfections
  - Quad strength and placement errors
  - Acceleration waveform errors
  - Bend strength errors
- Velocity tilt

Simulations give reliable and definitive tolerances on each source

20

Several potential instabilities have been investigated in HIF drivers

Temperature anisotropy instability

After acceleration $T_{||} << T_{\perp}$, internal beam modes are unstable; saturation occurs when $T_{||} \sim T_{\perp}/3$

Longitudinal resistive instability

Module impedance interacts with beam, amplifying space-charge waves that are backward propagating in beam frame

Beam break-up (BBU) instability

High frequency waves in induction module cavities interact transversely with beam

Beam-plasma instability

Beam interacts with residual gas in target chamber

All of these instabilities have known analytic linear growth rates, which constrain the accelerator design (to ensure minimal growth or benign saturation).

M. de Hoon studied a final current pulse that is flat with parabolic ends using the HERMES code

15 ns final pulse duration

The initial tilt on the beam is about 4% (compare to ~30% at the beginning of the accelerator)

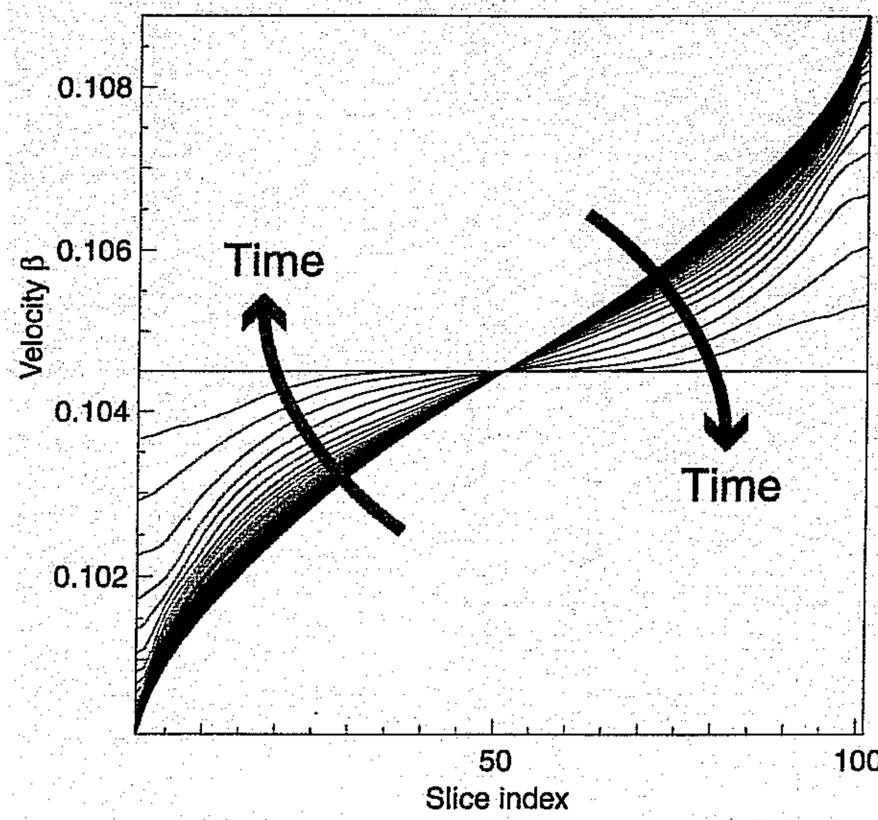

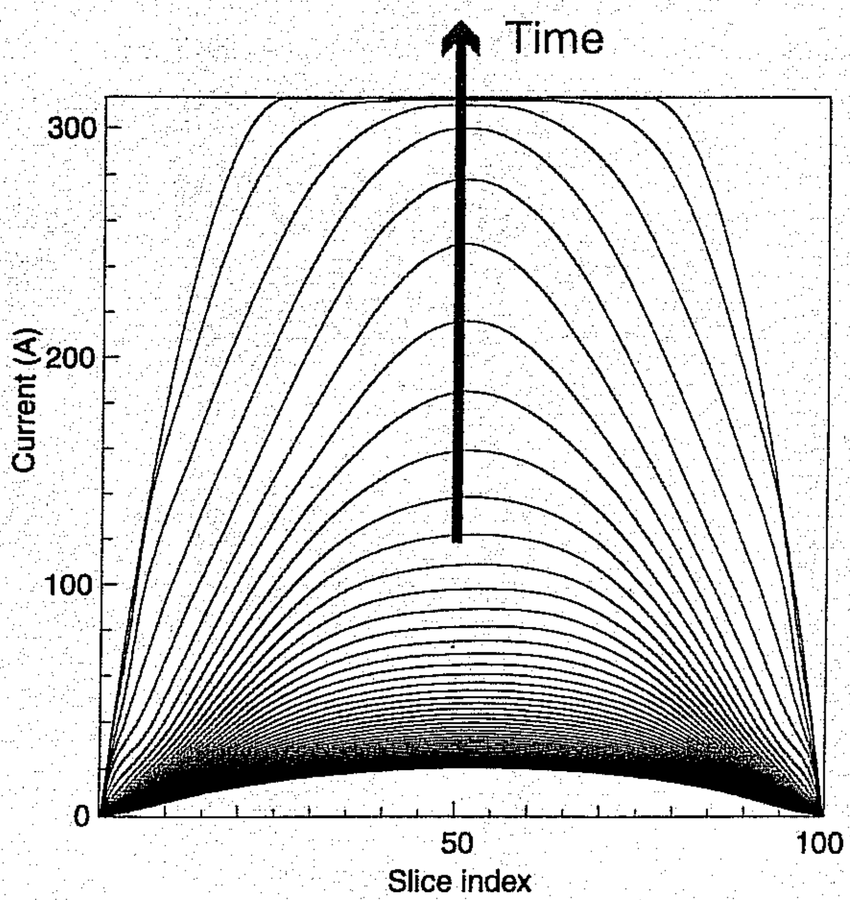

Although the final beam profile is flat, it is parabolic for most of the drift compression

(21)

Drift compression section is designed by running code first backwards from target, then forwards after rematching

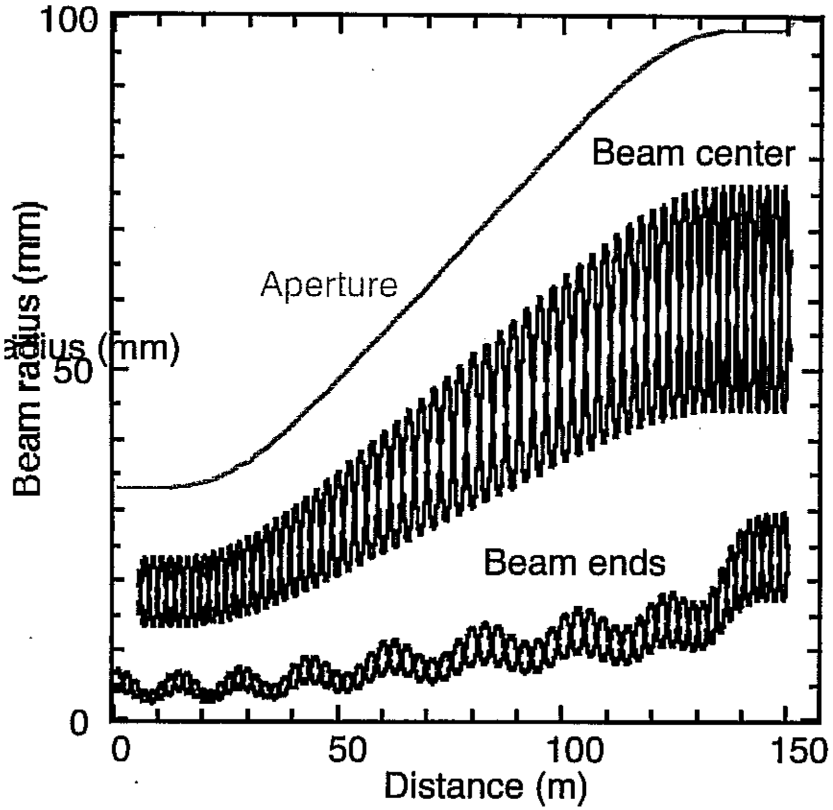

Begin with a desired 20ns, constant-energy pulse at end of compression, track backwards, design lattice for central slice; beam end becomes mismatched early on

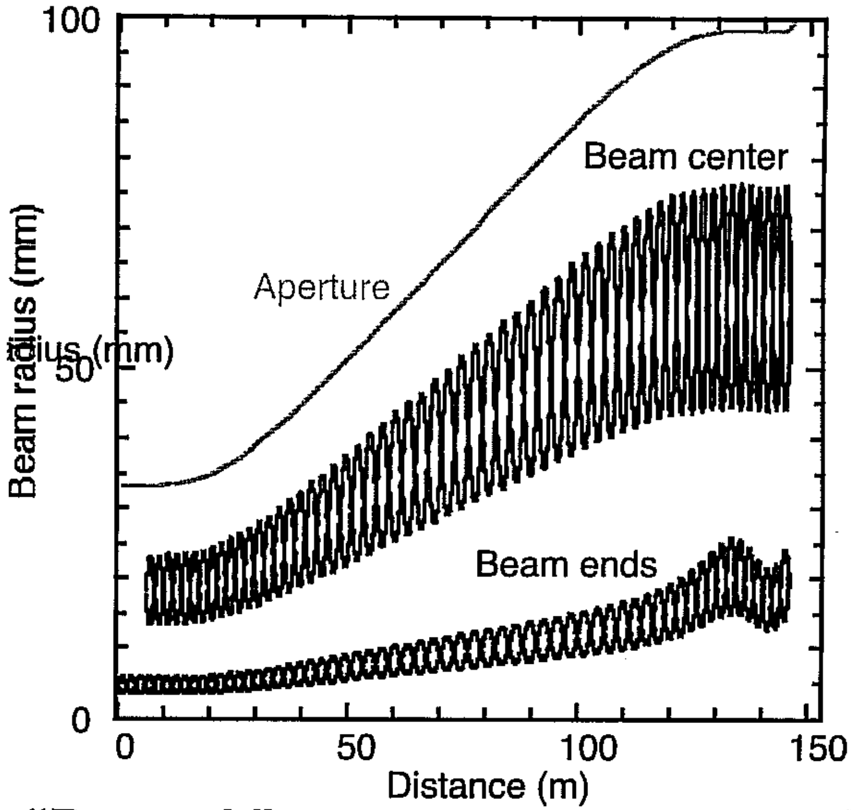

"Rematch" at entrance to compression section, by adjusting a,a',b,b'; then track forward

The HYLIFE-II Ion beam-driven power plant is shown with a two-end target, illustrated from two sides and a linear heavy-ion induction driver

The liquid wall protection including beam ports is provided by pumping molten salt (Flibe) through the chamber

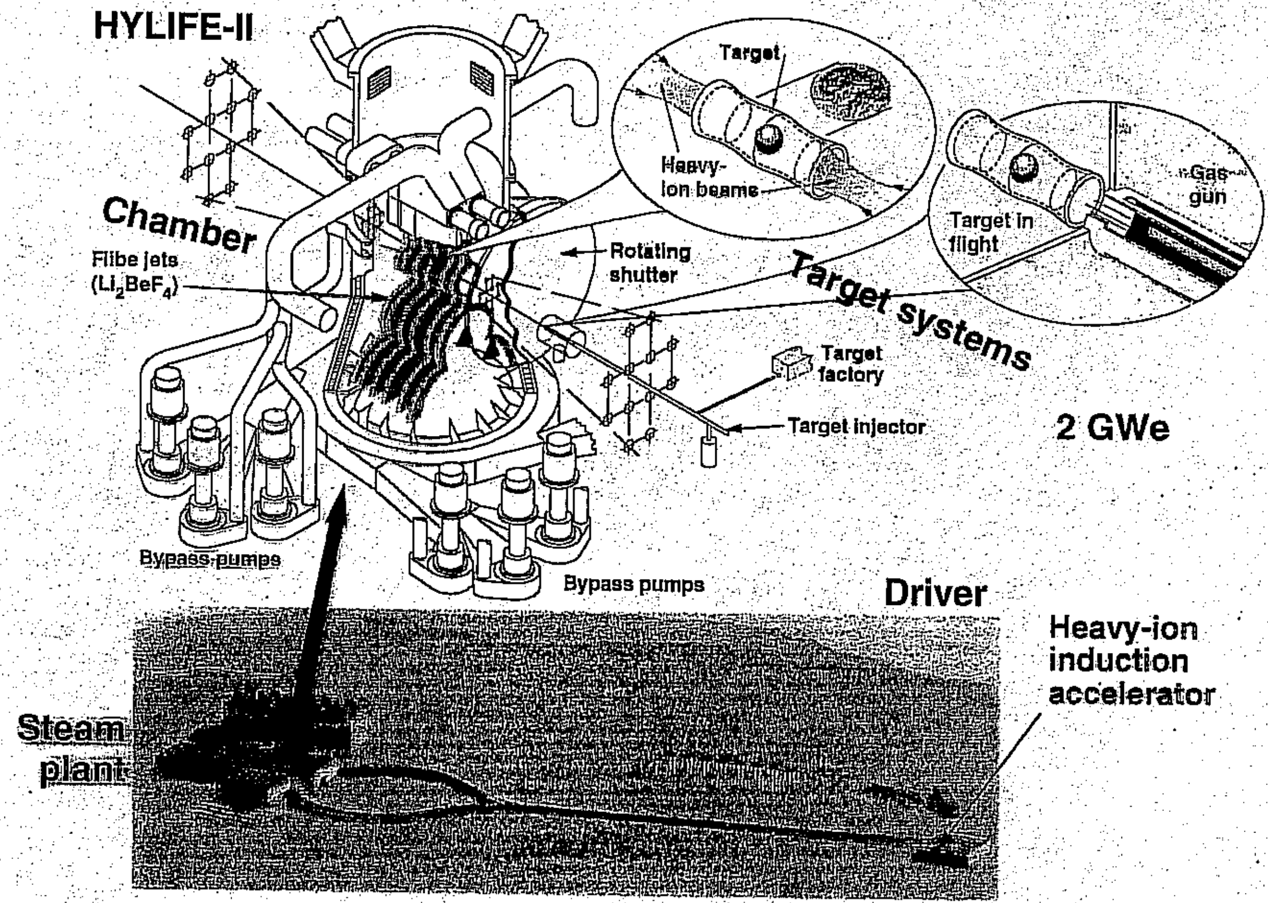

Liquid-jet protected fusion chambers for long lifetime, low cost, and low environmental impact

05-00-1194-3846U
16RWM/gbh

10/7/98

(26)

The First Wall Protected by Neutron-thick Molten Salt FLiBe,
FLiBe is a low Z salt ⇒ low activation ⇒ Green fusion energy

(One Half Cut Away)

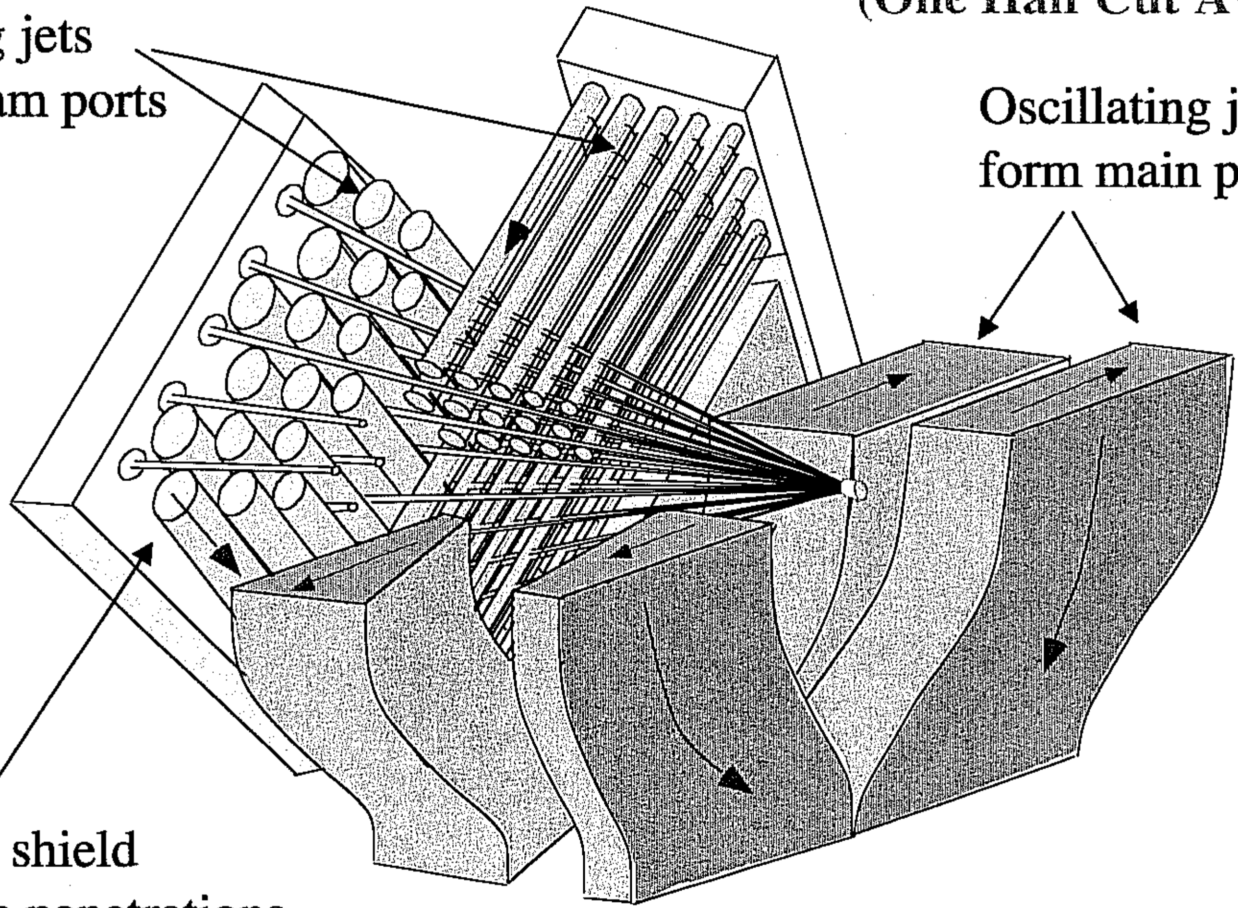

A number of final focus options are being considered for HIF applications

4 quad design

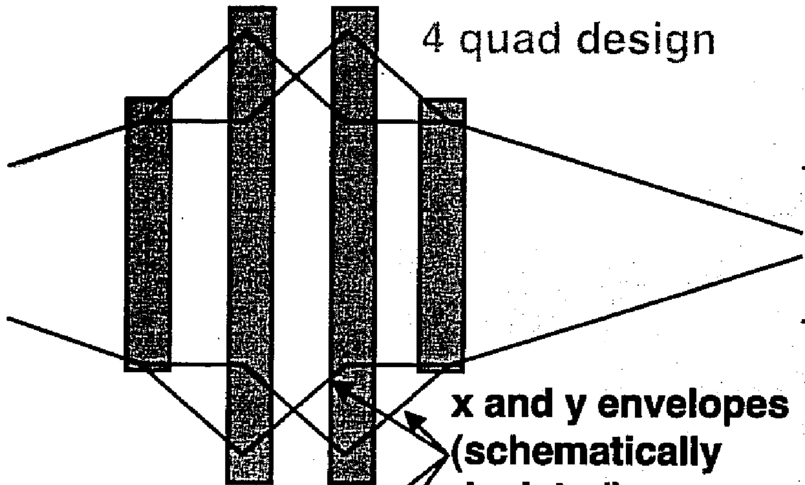

x and y envelopes (schematically depicted)

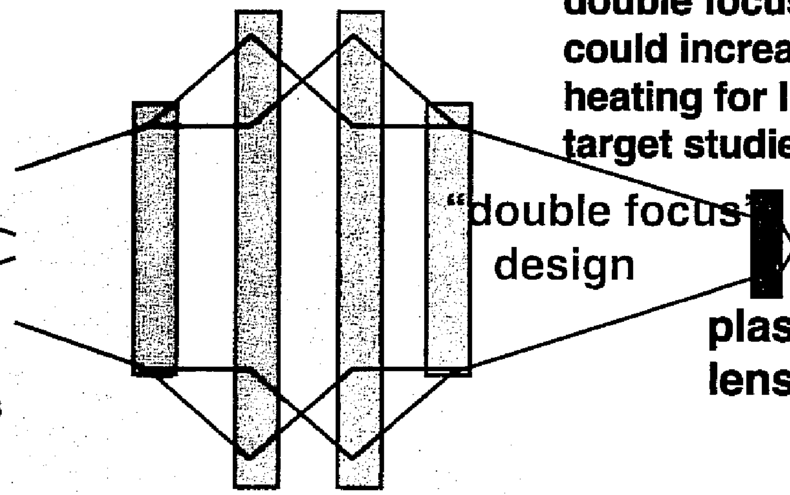

"double focus" design

double focus design could increase spot heating for IRE target studies

plasma lens

6 quad design

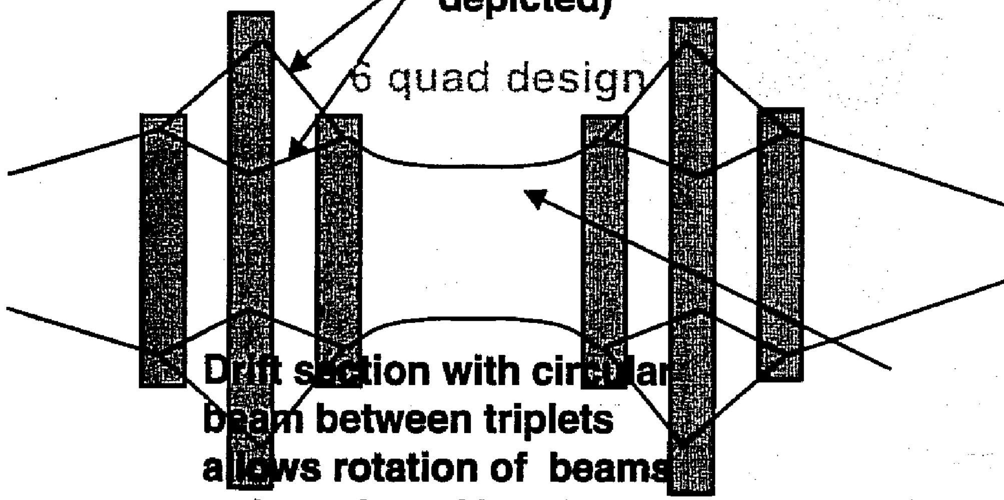

Drift section with circular beam between triplets allows rotation of beams or insertion of bend

Solenoid or cusp focusing is being considered for modul[ar] drivers:

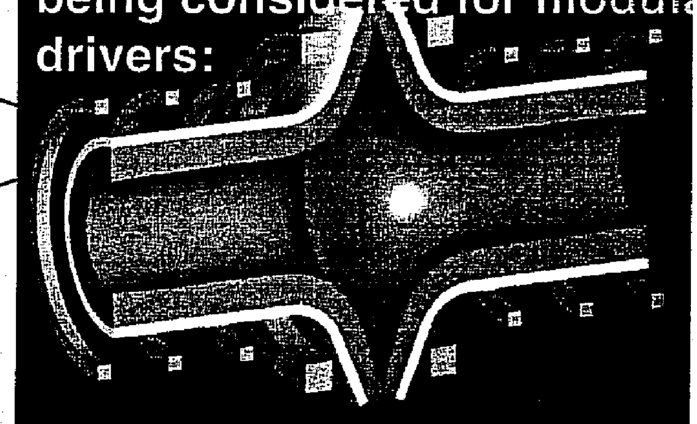

ESTIMATING SPOT SIZE

$$r_x'' + \frac{(\gamma_b \beta_b)'}{\gamma_b \beta_b} r_x + \kappa_x r_x - \frac{2Q}{r_x + r_y} - \frac{\epsilon_x^2}{r_x^3} = 0$$

$$r_y'' + \frac{(\gamma_b \beta_b)'}{\gamma_b \beta_b} r_y + \kappa_y r_y - \frac{2Q}{r_x + r_y} - \frac{\epsilon_y^2}{r_y^3} = 0$$

IN CHAMBER: NO EXTERNAL FOCUSING, NO ACCELERATION AND BEAM IS OFTEN CIRCULAR (BY DESIGN)

$\Rightarrow$ $\kappa_x = \kappa_y = (\gamma_b \beta_b)' = 0$ & $r_x = r_y = r_b$

$\Rightarrow$ ENVELOPE EQUATION IS:

$$r_b'' = \frac{Q}{r_b} + \frac{\epsilon^2}{r_b^3}$$

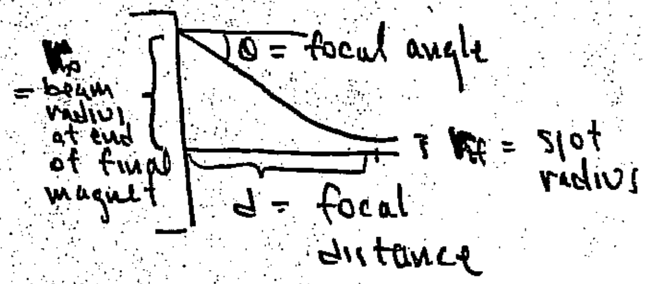

MULTIPLYING BY r_b' & INTEGRATING $\Rightarrow$

$$\frac{r_{bf}'^2}{2} - \frac{r_{bo}'^2}{2} = Q \ln \frac{r_{bf}}{r_{bo}} + \frac{\epsilon^2}{2 r_{bo}^2} - \frac{\epsilon^2}{2 r_{bf}^2}$$

Now $r_{bo}' \cong \theta$ $\qquad$ r_{bf} = spot radius $\qquad$ $r_{bf} << r_{bo}$

$r_{bf}' = 0$ $\qquad$ $r_{bo} \cong d\theta$

$$\Rightarrow \boxed{\theta^2 \cong 2Q \ln\left(\frac{\theta d}{r_{bf}}\right) + \frac{\epsilon^2}{r_{bf}^2}}$$

FOR EMITTANCE DOMINATED SPOT: $\quad r_{bf} = \dfrac{\epsilon}{\theta}$

"CHROMATIC ABERRATIONS" TEND TO BROADEN SPOT

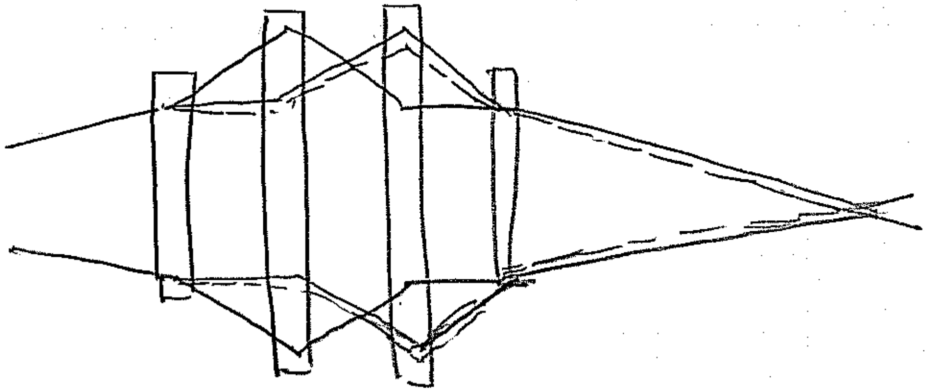

SINCE QUADRUPOLE MAGNET FOCUSING $\propto \frac{1}{V_z}$

(i.e. $x'' = \frac{qB'}{\gamma m v_z} x$) A SPREAD IN LONGITUDINAL VELOCITY GIVES RISE TO A BROADENING OF FINAL SPOT.

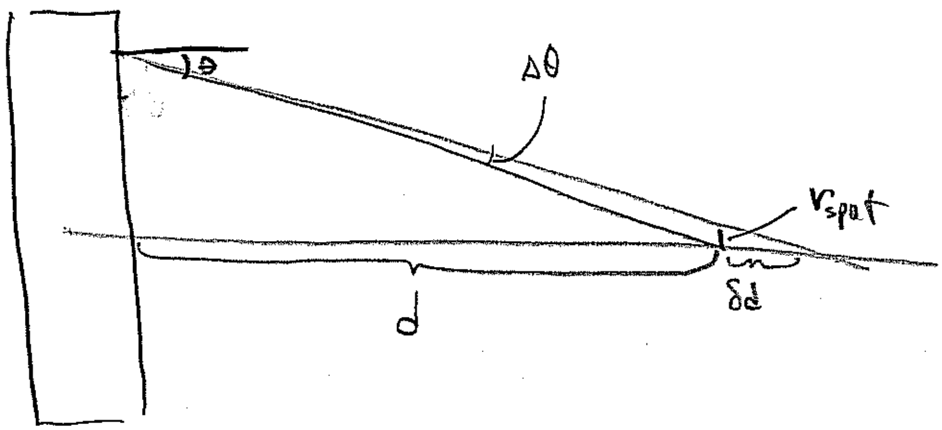

$$r_{spot} = \theta\,\delta d$$
$$= \theta \frac{dd}{d\theta}\frac{d\theta}{d\gamma}\,\delta\gamma$$
$$= \alpha\,\theta d\left(\frac{\delta p}{p}\right)$$

α = some constant depending on focal system

HEURISTICALLY THE CONTRIBUTION FROM CHROMATIC ABERRATIONS CAN BE WRITTEN

$$r^2_{chrom} = \alpha^2 d^2 \left(\frac{\delta\gamma}{\gamma}\right)^2 \theta^2$$

where α depends on system, typically 4-8

$$r^2_{spot} = r^2_{bf} + r^2_{chrom}$$

DETAILED SIMULATIONS OR MOMENT CODE RESULTS REQUIRED TO FIX α.

We constructed moment models to study chromatic effects (through 2nd order) in final focus system

$$\frac{dp_x}{dt} = q(E_x + v_z B_y - v_y B_z)$$

Expand through 2nd order in x', y', $k_{\beta 0}x$, $k_{\beta 0}y$, $\delta p/p$

$$x'' + \left(\frac{1}{\gamma v_{z0}}\frac{d}{dz}(\gamma v_z)\right)x' = \frac{qB'}{\gamma m v_{z0}}x\left(1-\frac{\delta p}{p}\right) + \frac{q\lambda}{4\pi\varepsilon_0 m v_{z0}^2}\frac{(x-\bar{x})(1-\frac{2\delta p}{p})}{(\Delta x^2 + [\Delta x^2 \Delta y^2]^{1/2})}$$

The equation of motions can be written (where $\delta = \delta p/p$**) :**

$$\boxed{x'' = K_{xx}x + K_{xx1}x\delta \qquad y'' = K_{yy}y + K_{yy1}y\delta}$$

Here:

$$K_{xx} = \frac{B'}{[B\rho]_0} + \frac{Q}{2(\Delta x^2 + [\Delta x^2 \Delta y^2]^{1/2})} \qquad K_{yy} = \frac{-B'}{[B\rho]_0} + \frac{Q}{2(\Delta y^2 + [\Delta x^2 \Delta y^2]^{1/2})}$$

$$K_{xx1} = -\left[\frac{B'}{[B\rho]_0} + \frac{2Q}{2(\Delta x^2 + [\Delta x^2 \Delta y^2]^{1/2})}\right] \qquad K_{yy1} = -\left[\frac{-B'}{[B\rho]_0} + \frac{2Q}{2(\Delta y^2 + [\Delta x^2 \Delta y^2]^{1/2})}\right]$$

B' = **quadrupole gradient;** $[B\rho]$ = **Ion rigidity** $= p/q$; Q = **perveance** $= \dfrac{q\lambda}{2\pi\varepsilon_0 \gamma_0^3 m v_{z0}^2}$

We take averages of 2nd, 3rd,… order quantities, forming infinite set of 1st order ode's

$$\frac{d}{ds}\langle x^2\rangle = 2\langle xx'\rangle$$

$$\frac{d}{ds}\langle xx'\rangle = \langle x'^2\rangle + \langle xx''\rangle$$

$$= \langle x'^2\rangle + K_{xx}\langle x^2\rangle + \underline{K_{xx1}\langle x^2\delta\rangle}$$

$$\frac{d}{ds}\langle x'^2\rangle = 2\langle x'x''\rangle$$

$$= 2K_{xx}\langle xx'\rangle + \underline{2K_{xx1}\langle xx'\delta\rangle}$$

$$\frac{d}{ds}\langle x^2\delta\rangle = 2\langle xx'\delta\rangle$$

$$\frac{d}{ds}\langle xx'\delta\rangle = \langle x'^2\delta\rangle + \langle xx''\delta\rangle$$

$$= \langle x'^2\delta\rangle + K_{xx}\langle x^2\delta\rangle + \underline{K_{xx1}\langle x^2\delta^2\rangle}$$

$$\frac{d}{ds}\langle x'^2\delta\rangle = 2\langle x'x''\delta\rangle$$

$$= 2K_{xx}\langle xx'\delta\rangle + \underline{2K_{xx1}\langle xx'\delta^2\rangle}$$

…

$$\frac{d}{ds}\langle x^2\delta^n\rangle = 2\langle xx'\delta^n\rangle$$

$$\frac{d}{ds}\langle xx'\delta^n\rangle = \langle x'^2\delta^n\rangle + \langle xx''\delta^n\rangle$$

$$= \langle x'^2\delta^n\rangle + K_{xx}\langle x^2\delta^n\rangle + \underline{K_{xx1}\langle x^2\delta^{n+1}\rangle}$$

$$\frac{d}{ds}\langle x'^2\delta^n\rangle = 2\langle x'x''\delta^n\rangle$$

$$= 2K_{xx}\langle xx'\delta^n\rangle + \underline{2K_{xx1}\langle xx'\delta^{n+1}\rangle}$$

=> term higher order by one

The Heavy Ion Fusion Virtual National Laboratory

Infinite set of equations can be truncated, but are reliable over only finite distances

Two equivalent methods of truncation have been employed:

1. $\langle x^2\delta^2\rangle \approx \langle x^2\rangle\langle\delta^2\rangle$ **and** $\langle xx'\delta^2\rangle \approx \langle xx'\rangle\langle\delta^2\rangle$ **; or**
2. **Noticing that** $\frac{1}{1+\delta} = 1-\delta+\delta^2+\ldots$ **and** $\frac{1}{1-\delta} = 1+\delta+\delta^2+\ldots$ **thus,**

$$\frac{1}{1-\delta}-\frac{1}{1+\delta} = 2\delta+2\delta^3+\ldots \quad \textbf{also} \quad \frac{\delta}{1+\delta} = 1-\frac{1}{1+\delta}$$

so that we may, to good approximation, write

$$\frac{d}{ds}\langle x^2\rangle = 2\langle xx'\rangle \qquad \frac{d}{ds}\langle xx'\rangle = \langle x'^2\rangle + K_{xx}\langle x^2\rangle + \frac{K_{xx1}}{2}\left[\left\langle\frac{x^2}{1-\delta}\right\rangle - \left\langle\frac{x^2}{1+\delta}\right\rangle\right] + O\left(x^2\delta^3\right)$$

$$\frac{d}{ds}\langle x'^2\rangle = 2K_{xx}\langle xx'\rangle + K_{xx1}\left[\left\langle\frac{xx'}{1-\delta}\right\rangle - \left\langle\frac{xx'}{1+\delta}\right\rangle\right] + O(xx'\delta^3)$$

$$\frac{d}{ds}\left\langle\frac{xx'}{1+\delta}\right\rangle = \left\langle\frac{x'^2}{1+\delta}\right\rangle + K_{xx}\left\langle\frac{x^2}{1+\delta}\right\rangle - K_{xx1}\left\langle\frac{x^2}{1+\delta}\right\rangle + K_{xx1}\langle x^2\rangle \qquad \frac{d}{ds}\left\langle\frac{x^2}{1+\delta}\right\rangle = 2\left\langle\frac{xx'}{1+\delta}\right\rangle$$

$$\frac{d}{ds}\left\langle\frac{x'^2}{1+\delta}\right\rangle = 2K_{xx}\left\langle\frac{xx'}{1+\delta}\right\rangle + 2K_{xx1}\langle xx'\rangle - 2K_{xx1}\left\langle\frac{xx'}{1+\delta}\right\rangle$$

Truncated set of equations forms closed set.

both methods give nearly identical results for $\langle\delta^2\rangle$ in the regime of interest; similar equations for $\langle x^2/(1-\delta)\rangle$, $\langle xx'/(1-\delta)\rangle$, $\langle x'^2/(1-\delta)\rangle$, and the same set for y; 18 equations total.

Comparison of moment equations with Particle-in-Cell (WARP[1]) simulations (1% velocity spread)

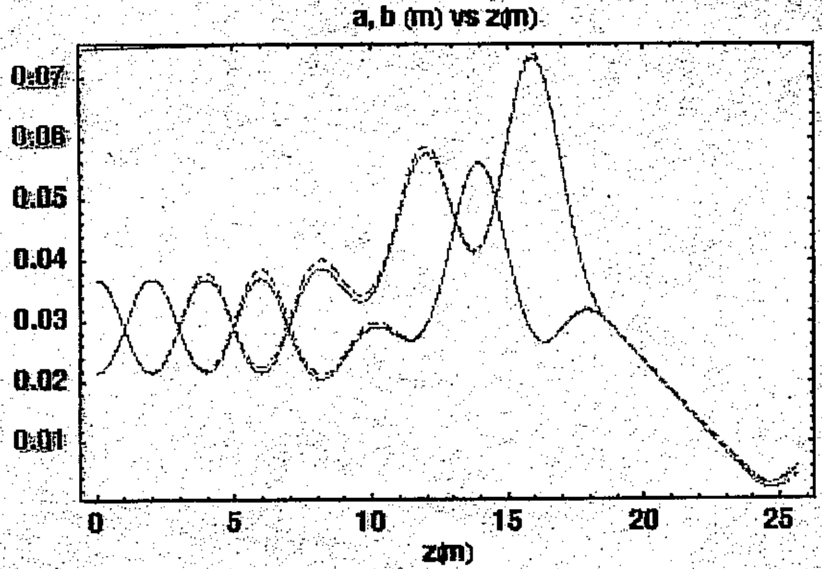

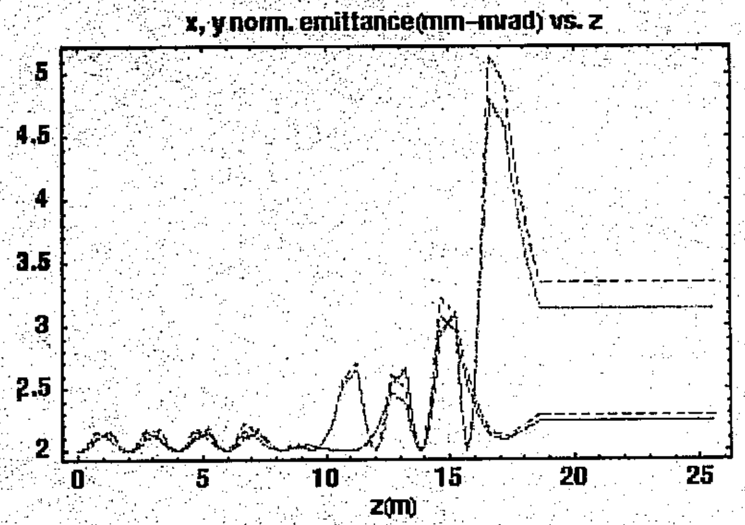

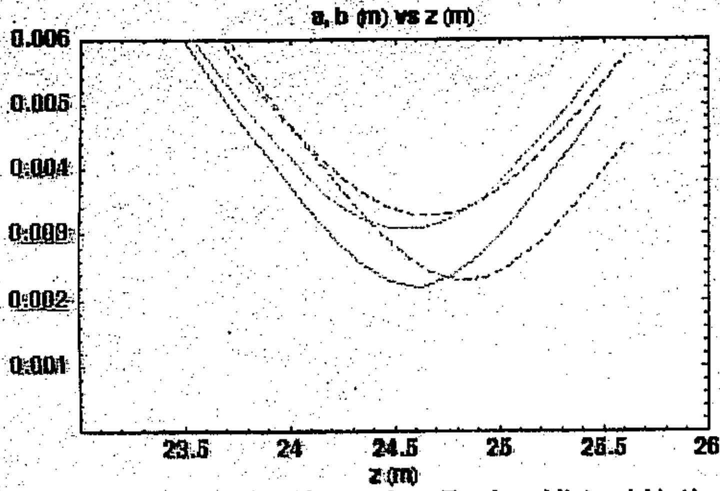

Particle simulations:
Dashed, red (x) and blue (y)
Initial distribution: KV

Moment calcluations:
Solid, magenta (x), and aqua (y)

The Heavy Ion Fusion Virtual National Laboratory

Comparison of moment equations with PIC simulations (WARP) -- no velocity spread

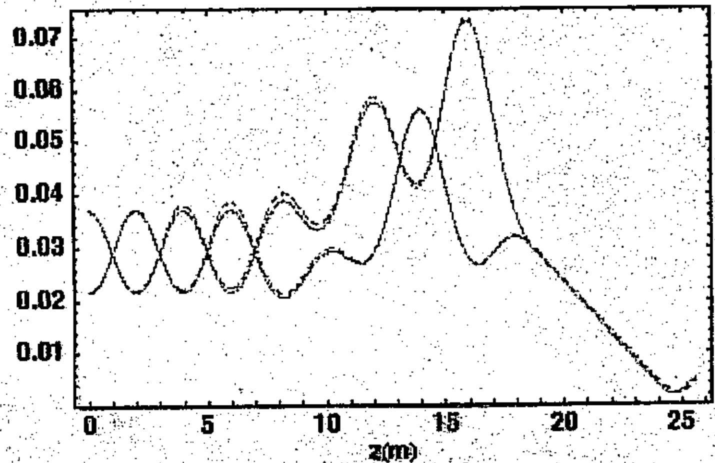

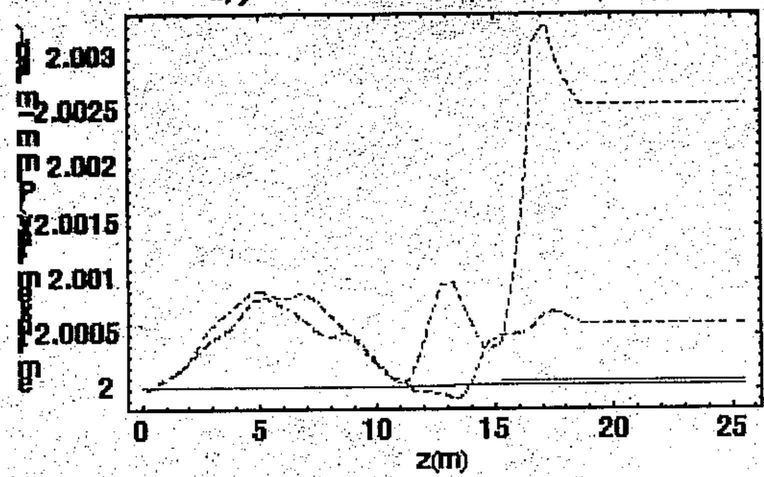

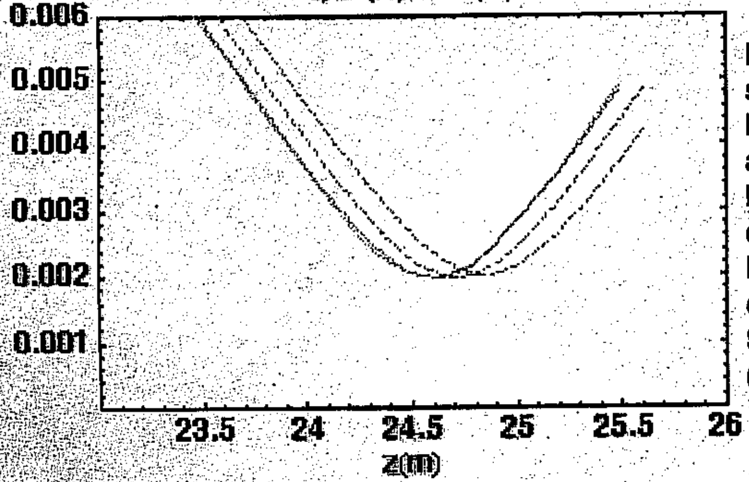

Particle simulations: Dashed, red (x) and blue (y)
Initial distribution: KV
Moment calcluations: Solid, magenta (x), and aqua (y)

Focusing strength B'/[Bρ] (1/m²) vs z

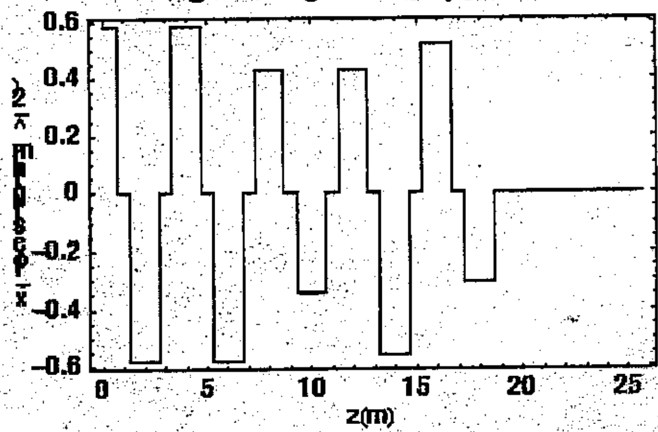

The HIFS VNL has two ongoing experiments, and a long range plan for HEDP studies and Heavy Ion Fusion

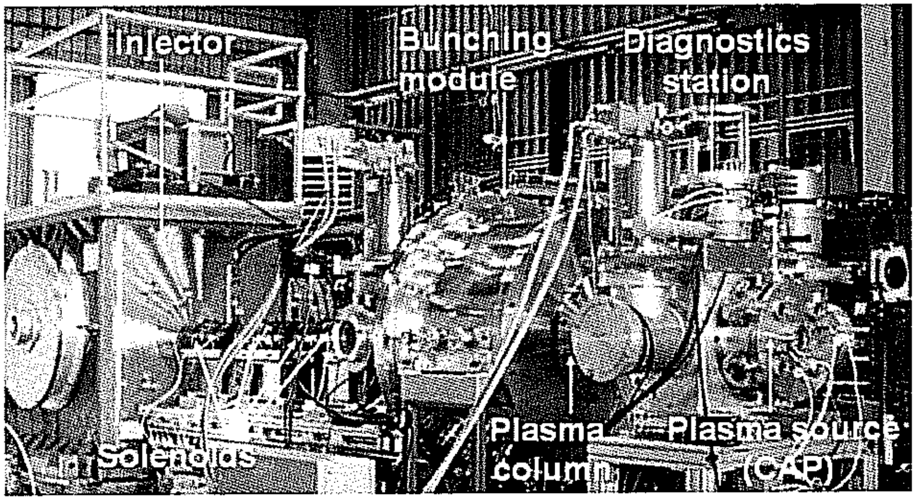

Today:

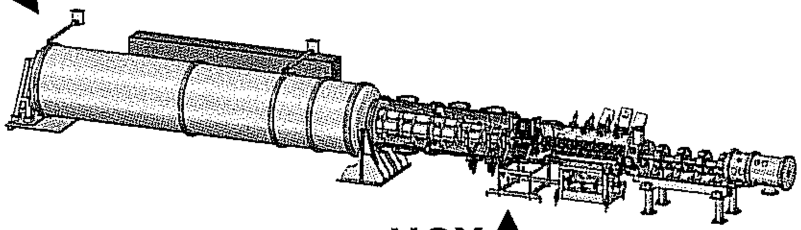

HCX

1.7 MeV, ~0.025 μC

NDCX I

0.4 MeV, 0.003 μC

Soon

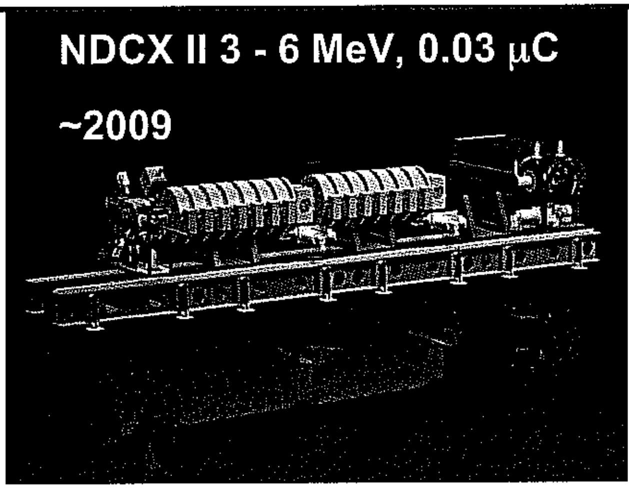

Future

IB-HEDPX (with CD0)
5 - 15 year goal
20 - 40 MeV, 0.3 - 1.0 μC
WDM User facility

10 kJ Machine for HIF
10 - 20 year goal
Target implosion physics

HIF/WDM beam science: neutralized focusing and drift compression are now being tested for use in WDM and HIF

Both techniques virtually eliminate the repulsive effects of space charge on transverse and longitudinal compression

Transverse compression (= focusing the beam to a small spot, raising the watts/cm^2): Recent VNL experiments, eg. scaled final focus experiment, (MacLaren et al 2002), NTX (Roy et al 2004), and current NDCX-1 have demonstrated benefits of neutralization by plasmas, also required for HIF.

Longitudinal compression (= raising the watts): WDM experiments require very short, intense pulses (<~ 1 ns) (shorter than needed for HIF). Neutralization allows high current/high power beams. Modular HIF concept also pushes limit of high current.

NDCX-1 has demonstrated > factor 70 pulse compression, and simultaneous transverse and longitudinal focusing

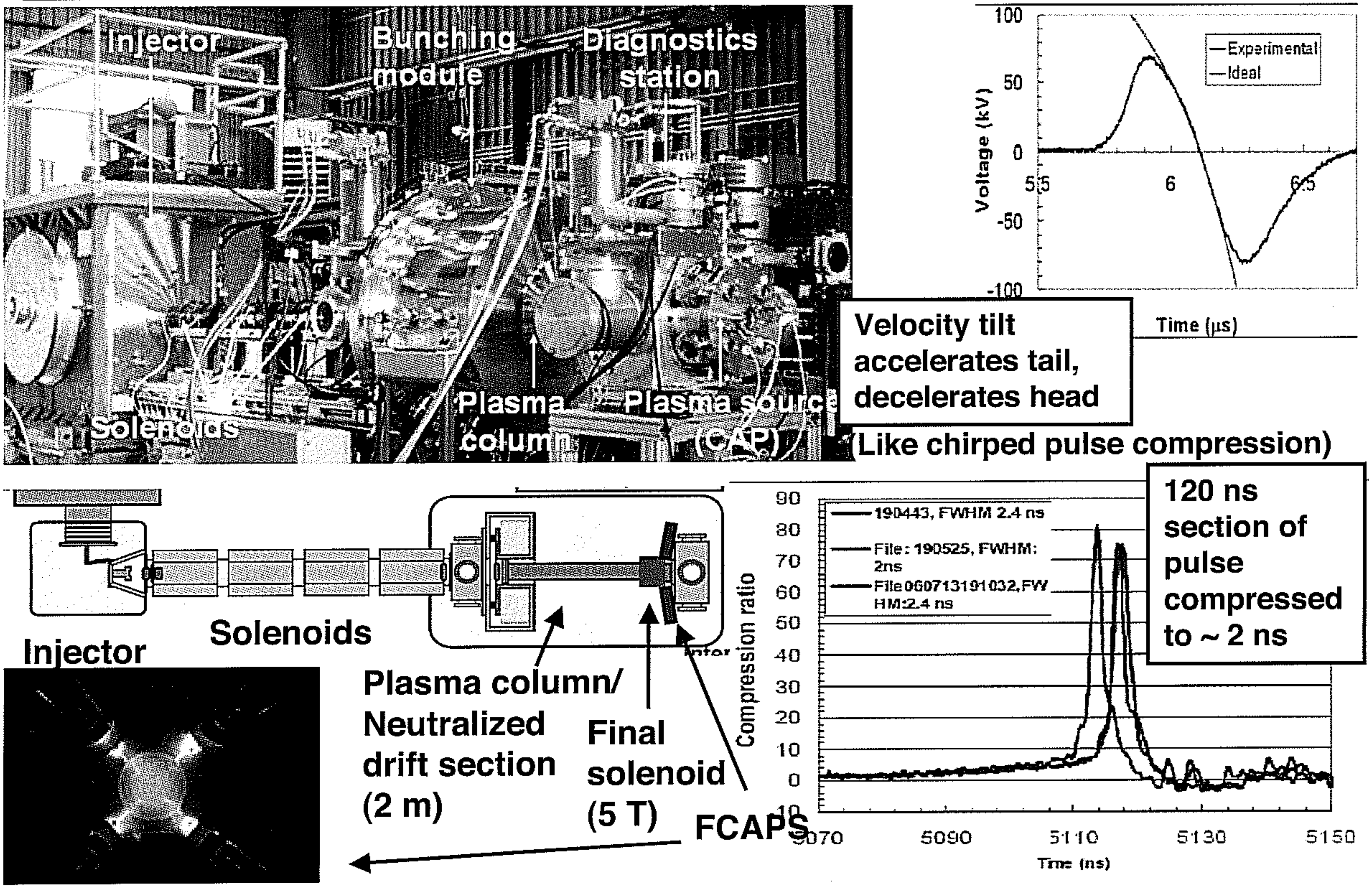

Artist's Conception of an HIF Power Plant on a few km^2 site

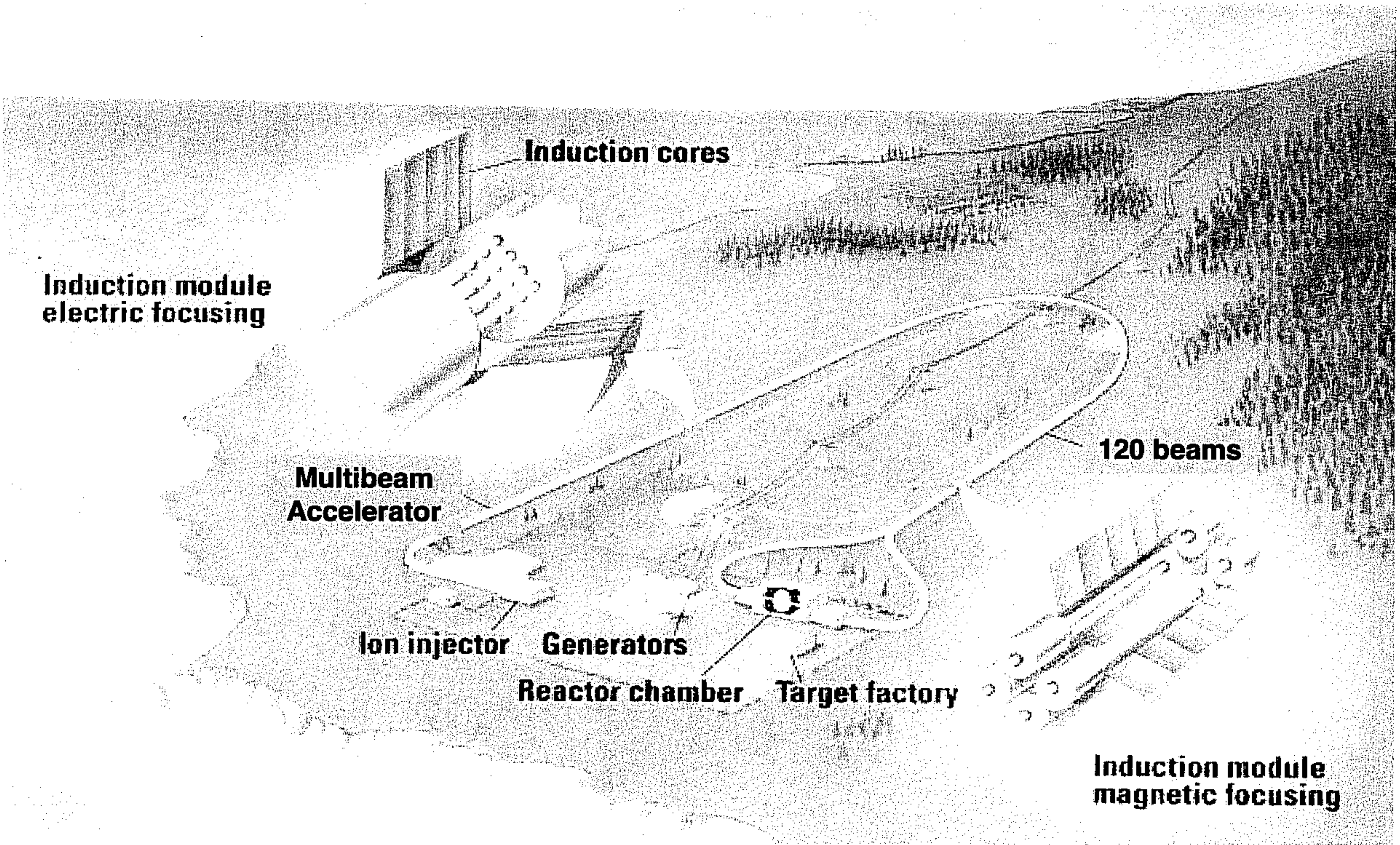

Simulation Techniques for Intense Beams*

Steven M. Lund
Lawrence Livermore National Laboratory (LLNL)

Steven M. Lund and John J. Barnard
"Beam Physics with Intense Space-Charge"

US Particle Accelerator School

University of Maryland, held at Annapolis, MD
16-27 June, 2008
(Version 20080622)

* Research supported by the US Dept. of Energy at LLNL and LBNL under contract Nos. DE-AC52-07NA27344 and DE-AC02-05CH11231.

Simulation Techniques for Intense Beams: Outline

Simulation Techniques for Intense Beams: Detailed Outline

Detailed Outline - 2

Detailed Outline - 3

S1: Why Numerical Simulation?

Builds intuition of intense beam physics
- "The purpose of computation is insight, not numbers"
  Richard Hamming, chief mathematician of the Manhattan Project and Turning Award recipient
- Advantages over laboratory experiments:
  - Full nonintrusive beam diagnostics are possible
  - Effects can be turned on and off

Allows analysis of more realistic situations than analytically tractable
- Realistic geometries
- Non-ideal distributions
- Combined effects
- Large amplitude (nonlinear) effects

Insight obtained can motivate analytical theories
- Suggest and test approximations and models to most simply express relevant effects

Why Numerical Simulation? (2)

Can quantify expected performance of specific machines
- Machines and facilities expensive – important to have high confidence that systems will work as intended

Computers and numerical methods/libraries are becoming more powerful
Enables both analysis of more realistic problems and/or better numerical convergence
- Bigger and faster hardware
  - Processor speed increasing
  - Parallel machine architectures
  - Greater memory
- More developed software
  - Improved numerical methods
  - Libraries of debugged code modules
  - Graphics and visualization tools

Why Numerical Simulation? (3)

Simulations are increasingly powerful and valuable in the analysis of intense beams, but should not be used to exclusion
- Parametric scaling is *very* important in machine design
  - Often it is hardest to understand what specific choices should be made in physical aperture sizes, etc.
  - Although scaling can be explored with simulation, analytical theory often best illustrates the trade-offs, sensitivities, and relevant combinations of parameters
- Concepts often fail due to limits of technology (e.g., fabrication tolerances, material failures, and unanticipated properties) and hence full laboratory testing is vital
  - Many understood classes of errors can be probed with simulation.
  - Unanticipated error sources are most dangerous
- Economic realities often severely limit what can be constructed
  - Simulating something unattainable may serve little purpose

Why Numerical Simulation? (4)

The highest understanding and confidence is achieved when results from analytic theory, numerical simulation, and experiment all converge

- Motivates model simplifications and identification of relevant sensitivities

Numerical simulation skills are highly sought in many areas of accelerator and beam physics

- Specialists readily employable
- Skills transfer easily to many fields of physics and engineering

Numerous programming languages are employed in numerical simulations of intense beams

- Most common today: Fortran, Fortran 90, C, C++, Java, ...
- Strengths and weaknesses depend on application, preferences, and history (legacy code)

Results are analyzed with a variety of graphics packages:

- Commonly used: NCAR, Gist, Gnuplot, IDL, Narcisse...
- Plot frames combine into movies
- Use can greatly simplify construction of beam visualization diagnostics

Why Numerical Simulation? (5)

A modern and flexible way to construct simulation packages is to link routines in fast, compiled code with an interactive interpreter such as:

- Examples: Python, Basis, Yorick, ...

Advantages of using interactive interpreters:

- Allows routines to be coded in mixed languages
  - Renders choice of programming languages less important
- Flexible reconfiguration of code modules possible to adapt for specific, unanticipated needs
  - Reduces need for recompilation and cumbersome structures for special uses
  - Aids cross-checking problems and debugging
- "Steering" of code during runs to address unanticipated side effects
- In the case of Python, facilitates modern, object-oriented structure

Why Numerical Simulation? (6)

Discussing particular programming languages and graphics packages is beyond the scope of this class. Here our goal is to survey numerical simulation methods employed without presenting details of specific implementations.

However, we will show examples based on the "WARP" particle-in-cell code developed for intense beam simulation at LLNL and LBNL

- WARP is so named since it works on a "warped" Cartesian mesh with bends
- WARP is a family of particle-in-cell code tools built around a common Python interpreter for flexible operation
- Optimized for the simulation of intense beams with self-consistent electrostatic space-charge forces
- Actively maintained and extended:
  - Diagnostics
  - E-cloud
  - Electromagnetic effects and dense plasmas

  ⋮

More on WARP later after discussion of methods, etc.

S2: Classes of Intense Beam Simulations
S2A: Overview

There are three distinct classes of modeling of intense ion beams applicable to numerical simulation

1) Particle methods (see: S2B)
2) Distribution methods (see: S2C)
3) Moment methods (see: S2D)

All of these draw heavily on methods developed for the simulation of neutral plasmas. The main differences are:

- Lack of overall charge neutrality
  - Single species typical, though electron + ion simulations are common too
- Directed motion of the beam along accelerator axis
- Applied field descriptions of the lattice
  - Optical focusing elements
  - Accelerating structures

We will review and contrast these methods before discussing specific numerical implementations

S2B: Particle Methods: Equations of Motion

Classical point particles are advanced with self-consistent interactions given by the Maxwell Equations

- Most general: If actual number of particles are used, this is approximately the physical beam
- Often intractable using real number of beam particles due to numerical work and problem size

Equations of motion (time domain, 3D, for generality)

ith particle:

$$\frac{d\mathbf{p}_i}{dt} = \mathbf{F}_i = q_i\left(\mathbf{E} + \frac{d\mathbf{x}_i}{dt}\times\mathbf{B}\right)$$

$$m_i\gamma_i\frac{d\mathbf{x}_i}{dt} = \mathbf{p}_i \quad ; \quad \gamma_i = \left[1 + \frac{\mathbf{p}_i^2}{(m_i c)^2}\right]^{1/2}$$

Initial conditions

$\mathbf{x}_i(t=0)$

$\mathbf{p}_i(t=0)$

Particle orbits $\mathbf{x}_i(t),\ \mathbf{p}_i(t)$ solved as a function of time

S2B: Particle Methods: Fields

Fields (electromagnetic in most general form)

Charge Density

$$\nabla\cdot\mathbf{E} = \frac{\rho}{\epsilon_0}$$

$$\nabla\times\mathbf{E} = -\frac{\partial\mathbf{B}}{\partial t}$$

Current Density

$$\nabla\cdot\mathbf{B} = 0$$

$$\nabla\times\mathbf{B} = \mu_0\mathbf{J} + \mu_0\epsilon_0\frac{\partial\mathbf{E}}{\partial t}$$

$$\rho(\mathbf{x},t) = \rho_{\text{ext}}(\mathbf{x},t) + \sum_i q_i\delta[\mathbf{x}-\mathbf{x}_i(t)]$$

external (applied)

particle beam

$$\mathbf{J}(\mathbf{x},t) = \mathbf{J}_{\text{ext}}(\mathbf{x},t) + \sum_i q_i\frac{d\mathbf{x}}{dt}\delta[\mathbf{x}-\mathbf{x}_i(t)]$$

+ boundary conditions on $\mathbf{E},\ \mathbf{B}$

S2C: Distribution Methods: Equations of Motion

Distribution Methods

- Based on reduced (statistical) continuum models of the beam
- Two classes: (microscopic) kinetic models and (macroscopic) fluid models
- Here, distribution means a function of continuum variables
- Use a 3D collision-less Vlasov model to illustrate concept
  Obtained from statistical averages of particle formulation

Example Kinetic Model: Vlasov Equation of Motion

$q_i = q\,;\ m_i = m\,;$ easy to generalize for multiple species (see later slide)

$$\left\{\frac{\partial}{\partial t} + \mathbf{v}\cdot\frac{\partial}{\partial x} + q\left(\mathbf{E} + \mathbf{v}\times\mathbf{B}\right)\right\} f(\mathbf{x},\mathbf{p},t) = 0$$

$$\mathbf{v} = \frac{\mathbf{p}}{\gamma m} = \frac{\mathbf{p}/m}{[1+\mathbf{p}^2/(mc)^2]^{1/2}}$$

Initial condition

$f(\mathbf{x},\mathbf{p},t=0)$

$f(\mathbf{x},\mathbf{p},t)$ evolved from t = 0

$\mathbf{x},\ \mathbf{p},\ t$ independent variables

S2C: Distribution Methods: Fields

Fields: Same as in particle methods but with $\rho,\ \mathbf{J}$ expressed in proper form for coupling to the distribution

Charge Density

$$\nabla\cdot\mathbf{E} = \frac{\rho}{\epsilon_0}$$

$$\nabla\times\mathbf{E} = -\frac{\partial\mathbf{B}}{\partial t}$$

Current Density

$$\nabla\cdot\mathbf{B} = 0$$

$$\nabla\times\mathbf{B} = \mu_0\mathbf{J} + \mu_0\epsilon_0\frac{\partial\mathbf{E}}{\partial t}$$

$$\rho(\mathbf{x},t) = \rho_{\text{ext}}(\mathbf{x},t) + q\int d^3p\, f(\mathbf{x},\mathbf{p},t)$$

external (applied)

beam

$$\mathbf{J}(\mathbf{x},t) = \mathbf{J}_{\text{ext}}(\mathbf{x},t) + q\int d^3p\ \mathbf{v} f(\mathbf{x},\mathbf{p},t)$$

+ boundary conditions on $\mathbf{E},\ \mathbf{B}$

S2C: Distribution Methods: Vlasov Equation

The Vlasov Equation is essentially a continuity equation for an incompressible "fluid" in 6D phase-space. To see this, note that

$$\frac{\partial}{\partial \mathbf{p}} \cdot \mathbf{v} \times \mathbf{B} = 0$$

The Vlasov Equation can be expressed as

$$\frac{\partial f}{\partial t} + \frac{\partial}{\partial \mathbf{x}} \cdot (\mathbf{v} f) + \frac{\partial}{\partial \mathbf{p}} \cdot (q[\mathbf{E} + \mathbf{v} \times \mathbf{B}] f) = 0$$

$$\Rightarrow \frac{\partial f}{\partial t} + \frac{\partial}{\partial \mathbf{x}} \cdot \left(\left.\frac{d\mathbf{x}}{dt}\right|_{\text{orbit}} f \right) + \frac{\partial}{\partial \mathbf{p}} \cdot \left(\left.\frac{d\mathbf{p}}{dt}\right|_{\text{orbit}} f \right) = 0$$

which is manifestly the form of a continuity equation in 6D phase-space, i.e., probability is not created or destroyed

S2C: Distribution Methods: Collision Corrections

The effect of collisions can be included by adding a collision operator:

$$\boxed{\left\{ \frac{\partial}{\partial t} + \mathbf{v} \cdot \frac{\partial}{\partial \mathbf{x}} + \frac{\partial}{\partial \mathbf{p}} \cdot (q[\mathbf{E} + \mathbf{v} \times \mathbf{B}]) \right\} f = \left.\frac{\partial f}{\partial t}\right|_{\text{coll}}}$$

For most applications in beam physics, $\left.\frac{\partial f}{\partial t}\right|_{\text{coll}}$ can be neglected.

- See: estimates in J.J. Barnard, Intro Lectures

For exceptional cases, specific forms of collisions terms can be found in Nicholson, *Intro to Plasma Theory*, Wiley 1983, and similar plasma physics texts

S2C: Distribution Methods: Comment on the PIC Method

The common Particle-in-Cell (PIC) method is *not* really a particle method, but rather a distribution method that uses a collection of smoothed "macro" particles to simulate Vlasov's Equation. This can understood roughly by noting that Vlasov's Equation can be interpreted as

$$\frac{d}{dt} f(\mathbf{x}, \mathbf{p}, t) = 0$$

Total derivative along a test particle's path

$\Longrightarrow$ Advance particles in a continuous field "fluid" to eliminate particle collisions

Important Point:

PIC is a method to solve Vlasov's Equation, *not* a discrete particle method

This will become clear after these lectures

S2C: Distribution Methods: Multispecies Generalizations

Subscript species with j. Then in the Vlasov equation replace:

$$f \longrightarrow f_j$$
$$m \longrightarrow m_j$$
$$q \longrightarrow q_j$$

and there is a separate Vlasov equation for each of the j species.

Replace the charge and current density couplings in the Maxwell Equations with and appropriate form to include charge and current contributions from all species:

$$\rho(\mathbf{x}, t) = \rho_{\text{ext}}(\mathbf{x}, t) + \sum_j q_j \int d^3p\, f_j(\mathbf{x}, \mathbf{p}, t)$$

$$\mathbf{J}(\mathbf{x}, t) = \mathbf{J}_{\text{ext}}(\mathbf{x}, t) + \sum_j q_j \int d^3p\, \mathbf{v} f_j(\mathbf{x}, \mathbf{p}, t)$$

Also, if collisions are included the collision operator should be generalized to include collisions between species as well as collisions of a species with itself

S2C: Fluid Models

Fluid Models

- Obtained from further averages of kinetic model
- Described in terms of "macroscopic" variables (density, flow velocity, pressure...) that vary in $\mathbf{x}$ and t
- Models must be closed (truncated) at some order via physically motivated assumptions (cold, negligible heat flow, ...)

Moments:

Density	$n:$	$n(\mathbf{x},t) = \int d^3p\; f(\mathbf{x},\mathbf{p},t)$
Flow velocity	$\mathbf{V}:$	$n\mathbf{V}(\mathbf{x},t) = \int d^3p\; \mathbf{v} f(\mathbf{x},\mathbf{p},t)$
Flow momentum	$\mathbf{P}:$	$n\mathbf{P}(\mathbf{x},t) = \int d^3p\; \mathbf{p} f(\mathbf{x},\mathbf{p},t)$
Pressure tensor	$\mathcal{P}_{ij}:$	$n\mathcal{P}_{ij}(\mathbf{x},t) = \int d^3p\; [p_i - P_i(\mathbf{x},t)] \times [v_j - V_j(\mathbf{x},t)] f(\mathbf{x},\mathbf{p},t)$
Higher rank objects	$\vdots$	$\vdots$

S2C: Fluid Models: Equations of Motion

Equations of Motion (Eulerian approach)

Continuity:

$$\frac{\partial n}{\partial t} + \frac{\partial}{\partial \mathbf{x}} \cdot [n\mathbf{V}] = 0$$

Force: ith component

$$n\left(\frac{\partial}{\partial t} + \mathbf{V}\cdot\frac{\partial}{\partial \mathbf{x}}\right) P_i + \sum_j \frac{\partial}{\partial x_j}\mathcal{P}_{ij} = qn[\mathbf{E} + \mathbf{V}\times\mathbf{B}]_i$$

Field:

Maxwell Equations with charge and current density coupling to fluid variables given by:

$$\rho(\mathbf{x},t) = \rho_{\rm ext}(\mathbf{x},t) + qn(\mathbf{x},t)$$
$$\mathbf{J}(\mathbf{x},t) = \mathbf{J}_{\rm ext}(\mathbf{x},t) + qn(\mathbf{x},t)\mathbf{V}(\mathbf{x},t)$$

S2C: Fluid Model: Multispecies Generalization

Subscript species with j. Then in the continuity, force, pressure, ... equations replace

Particle Properties	Moments
$m \longrightarrow m_j$	$n \longrightarrow n_j$
$q \longrightarrow q_j$	$\mathbf{V} \longrightarrow \mathbf{V}_j$
	$\vdots$

Replace the charge and current density couplings in the Maxwell Equations with

$$\rho(\mathbf{x},t) = \rho_{\rm ext}(\mathbf{x},t) + \sum_j q_j n_j(\mathbf{x},t)$$
$$\mathbf{J}(\mathbf{x},t) = \mathbf{J}_{\rm ext}(\mathbf{x},t) + \sum_j q_j n_j(\mathbf{x},t)\mathbf{V}_j(\mathbf{x},t)$$

S2C: Lagrangian Formulation of Distribution Methods

In kinetic and especially fluid models it can be convenient to adopt *Lagrangian* methods. For fluid models these can be distinguished as follows:

Eulerian Fluid Model:

Flow quantities are functions of space ($\mathbf{x}$) and and evolve in time (t)

- Example: density $n(\mathbf{x},t)$ and flow velocity $\mathbf{V}(\mathbf{x},t)$

Lagrangian Fluid Model:

Identify parts of evolution (flow) with objects (material elements) and follow the flow in time (t)

- Shape and position of elements must generally evolve to represent flow
- Example: envelope model edge radii $r_x(s),\ r_y(s)$

Many distribution methods for Vlasov's Equation are hybrid Lagrangian methods

- Macro particle "shapes" in PIC (Particle in Cell) method to be covered can be thought of as Lagrangian elements representing a Vlasov flow

S2C: Example Lagrangian Fluid Model

1D Lagrangian model of the longitudinal evolution of a cold beam
- Discretize fluid into longitudinal elements with boundaries
- Derive equations of motion for elements

Coordinates:
Charges:
Masses:
Velocities:

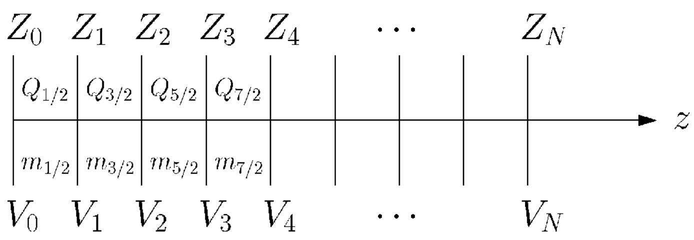

$z = Z_i$ slice boundaries

$\frac{dZ_i}{dt} = V_i$ velocities of slice boundaries

$Q_{i+1/2}$ fixed

$m_{i+1/2}$ fixed

$\frac{q}{m} = \text{const}$ for single species (set initial coordinates)

Example Lagrangian Fluid Model, Continued (2)

Solve the equations of motion

$$\frac{dZ_i(t)}{dt} = V_i(t)$$
$$\frac{dV_i(t)}{dt} = \frac{q}{m} E_z(Z_i, t)$$

for all the slice boundaries. Several methods might be used to calculate E_z:

1) Take "slices" to have some radial extent modeled by a perpendicular envelope etc. and deposit the $Q_{i+1/2}$ onto a grid and solve:

$$\nabla^2 \phi = -\frac{\rho}{\epsilon_0} \qquad E_z = -\frac{\partial \phi}{\partial z}$$

subject to $E_z \to 0$ as $|z| \to \infty$

2) Employ a "g-factor" model

$$E_z = -\frac{g}{4\pi\epsilon_0}\frac{\partial \lambda}{\partial z}$$

λ calculated from $Q_{i+1/2}$ and radial extent of the elements etc.

3) Pure 1D model using Gauss' Law

S2D: Moment Methods

Moment Methods
- Most reduced description of an intense beam
  - Often employed in lattice designs
- Beam represented by a finite (closed and truncated) set of moments that are advanced from initial values
  - Here by moments, we mean functions of a single variable *s* or *t*
- Such models are not generally self-consistent
  - Some special cases such as a stable transverse KV equilibrium distribution (see: S.M. Lund lectures on Transverse Equilibrium Distributions) are consistent with truncated moment description (rms envelope equation)
  - Typically derived from assumed distributions with self-similar evolution
- See: S.M. Lund lectures on Transverse Equilibrium Distributions for more details on moment methods

S2D: Moment Methods: 1st Order Moments

Many moment models exist. Illustrate with examples for transverse beam evolution

Moment definition:

$$\boxed{\langle \ldots \rangle_\perp \equiv \frac{\int d^2x_\perp \int d^2x'_\perp \ldots f}{\int d^2x_\perp \int d^2x'_\perp f}}$$

1st order moments:

$$\mathbf{X} = \langle \mathbf{x} \rangle_\perp \qquad \text{Centroid coordinate}$$
$$\mathbf{X}' = \langle \mathbf{x}' \rangle_\perp \qquad \text{Centroid angle}$$
$$\Delta = \left\langle \frac{\delta p_s}{p_s} \right\rangle_\perp \equiv \langle \delta \rangle_\perp \qquad \text{Off momentum}$$
$$\vdots \qquad \vdots$$

S2D: Moment Methods: 2nd and Higher Order Moments

2nd order moments:

x moments	y moments	x-y cross moments	dispersive moments
$\langle x^2 \rangle_\perp$	$\langle y^2 \rangle_\perp$	$\langle xy \rangle_\perp$	$\langle x\delta \rangle_\perp$, $\langle y\delta \rangle_\perp$
$\langle xx' \rangle_\perp$	$\langle yy' \rangle_\perp$	$\langle x'y \rangle_\perp$, $\langle xy' \rangle_\perp$	$\langle x'\delta \rangle_\perp$, $\langle y'\delta \rangle_\perp$
$\langle x'^2 \rangle_\perp$	$\langle y'^2 \rangle_\perp$	$\langle x'y' \rangle_\perp$	$\langle \delta^2 \rangle_\perp$

It is typically convenient to subtract centroid from higher-order moments

$$\tilde{x} \equiv x - X \qquad \tilde{x}' \equiv x' - X'$$
$$\tilde{y} \equiv y - Y \qquad \tilde{y}' \equiv y' - Y'$$

$$\langle \tilde{x}^2 \rangle_\perp = \langle (x-X)^2 \rangle_\perp = \langle x^2 \rangle_\perp - X^2, \text{ etc.}$$

3rd order moments: Analogous to 2nd order case, but more for each order

$$\langle x^3 \rangle_\perp , \langle x^2 y \rangle_\perp , \ldots$$

S2D: Moment Methods: Common 2nd Order Moments

Many quantities of physical interest are expressed in terms of moments

Statistical beam size: (rms edge measure)

$$r_x = 2 \langle \tilde{x}^2 \rangle_\perp^{1/2}$$
$$r_y = 2 \langle \tilde{y}^2 \rangle_\perp^{1/2}$$

Statistical emittances: (rms edge measure)

$$\varepsilon_x = 4 \left[\langle \tilde{x}^2 \rangle_\perp \langle \tilde{x}'^2 \rangle_\perp - \langle \tilde{x}\tilde{x}' \rangle_\perp^2 \right]^{1/2}$$
$$\varepsilon_y = 4 \left[\langle \tilde{y}^2 \rangle_\perp \langle \tilde{y}'^2 \rangle_\perp - \langle \tilde{y}\tilde{y}' \rangle_\perp^2 \right]^{1/2}$$

S2D: Moment Methods: Equations of Motion

Equations of Motion

- Can be expressed in terms of moments of combinations of moments that are of physical interest
- Moments are advanced from specified initial conditions

Form equations:

$$\frac{d}{ds}\mathbf{M} = \mathbf{F}(\mathbf{M})$$

M = vector of moments, generally infinite

F = vector function of **M**, generally nonlinear

Moment methods generally form an infinite chain of equations that do *not* truncate. To be useful the system must be truncated. Truncations are usually carried out by assuming a specific form of the distribution that can be described by a finite set of moments

- Self-similar evolution: form of distribution assumed not to change
  - Analytical solutions often employed
- Neglect of terms

A simple example will be employed to illustrate these points

S2D: Moment Methods: Example: Transverse Envelope Eqns.

Truncation assumption: unbunched uniform density elliptical beam in free space

- $\delta = 0$, no axial velocity spread
- All cross moments zero, i.e. $\langle \tilde{x}\tilde{y} \rangle_\perp = 0$

Centroid: $X = \langle x \rangle_\perp$, $Y = \langle y \rangle_\perp$

Envelope: $r_x = 2 \langle \tilde{x}^2 \rangle_\perp^{1/2}$, $r_y = 2 \langle \tilde{y}^2 \rangle_\perp^{1/2}$

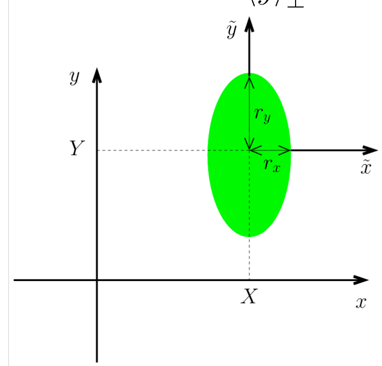

For: $\frac{\tilde{x}^2}{r_x^2} + \frac{\tilde{y}^2}{r_y^2} < 1$

$$E_{\tilde{x}} = \frac{\lambda}{\pi\epsilon_0} \frac{\tilde{x}}{(r_x + r_y) r_x}$$

$$E_{\tilde{y}} = \frac{\lambda}{\pi\epsilon_0} \frac{\tilde{y}}{(r_x + r_y) r_y}$$

$\lambda =$ line charge density

These results are employed to derive the moment equations of motion (See S.M. Lund lectures on Transverse Centroid and Envelope Models)

Example Continued (2) - Equations of Motion in Matrix Form

$$\frac{d}{ds}\begin{bmatrix} X \\ X' \\ Y \\ Y' \end{bmatrix} = \begin{bmatrix} X' \\ -\kappa_x(s)X \\ Y' \\ -\kappa_y(s)Y \end{bmatrix}$$

$$\frac{d}{ds}\begin{bmatrix} \langle \tilde{x}^2 \rangle_\perp \\ \langle \tilde{x}\tilde{x}' \rangle_\perp \\ \langle \tilde{x}'^2 \rangle_\perp \\ \langle \tilde{y}^2 \rangle_\perp \\ \langle \tilde{y}\tilde{y}' \rangle_\perp \\ \langle \tilde{y}'^2 \rangle_\perp \end{bmatrix} = \begin{bmatrix} 2\langle \tilde{x}\tilde{x}' \rangle_\perp \\ \langle \tilde{x}'^2 \rangle_\perp - \kappa_x(s)\langle \tilde{x}^2 \rangle_\perp + \frac{Q\langle \tilde{x}'^2 \rangle_\perp}{[4\langle \tilde{x}^2 \rangle_\perp^{1/2}(\langle \tilde{x}^2 \rangle_\perp^{1/2} + \langle \tilde{y}^2 \rangle_\perp^{1/2})]} \\ -2\kappa_x(s)\langle \tilde{x}\tilde{x}' \rangle_\perp + \frac{2Q\langle \tilde{x}\tilde{x}' \rangle_\perp}{[4\langle \tilde{x}^2 \rangle_\perp^{1/2}(\langle \tilde{x}^2 \rangle_\perp^{1/2} + \langle \tilde{y}^2 \rangle_\perp^{1/2})]} \\ 2\langle \tilde{y}\tilde{y}' \rangle_\perp \\ \langle \tilde{y}'^2 \rangle_\perp - \kappa_y(s)\langle \tilde{y}^2 \rangle_\perp + \frac{Q\langle \tilde{y}'^2 \rangle_\perp}{[4\langle \tilde{y}^2 \rangle_\perp^{1/2}(\langle \tilde{x}^2 \rangle_\perp^{1/2} + \langle \tilde{y}^2 \rangle_\perp^{1/2})]} \\ -2\kappa_y(s)\langle \tilde{y}\tilde{y}' \rangle_\perp + \frac{2Q\langle \tilde{y}\tilde{y}' \rangle_\perp}{[4\langle \tilde{y}^2 \rangle_\perp^{1/2}(\langle \tilde{x}^2 \rangle_\perp^{1/2} + \langle \tilde{y}^2 \rangle_\perp^{1/2})]} \end{bmatrix}$$

- Form truncates due to assumed distribution form
- Self-consistent with the KV distribution. See: S.M. Lund lectures on Transverse Equilibrium Distributions

Example Continued (3) - Reduced Form Equations of Motion

Using 2nd order moment equations we can show that

$$\frac{d}{ds}\varepsilon_x^2 = 0 = \frac{d}{ds}\varepsilon_y^2$$

$$\Longrightarrow \boxed{\begin{aligned} \varepsilon_x^2 &= 16\left[\langle x^2 \rangle_\perp \langle x'^2 \rangle_\perp - \langle xx' \rangle_\perp^2\right] = \text{const} \\ \varepsilon_y^2 &= 16\left[\langle y^2 \rangle_\perp \langle y'^2 \rangle_\perp - \langle yy' \rangle_\perp^2\right] = \text{const} \end{aligned}}$$

The 2nd order moment equations can be equivalently expressed as

$$\boxed{\begin{aligned} \frac{dr_x}{ds} &= r_x' \ ; \quad \frac{d}{ds}r_x' + \kappa_x r_x - \frac{2Q}{r_x + r_y} - \frac{\varepsilon_x^2}{r_x^3} = 0 \\ \frac{dr_y}{ds} &= r_y' \ ; \quad \frac{d}{ds}r_y' + \kappa_y r_y - \frac{2Q}{r_x + r_y} - \frac{\varepsilon_y^2}{r_y^3} = 0 \end{aligned}}$$

Example Continued (4) : Contrast Form of Matrix and Reduced Form Moment Equations

Relative advantages of the use of coupled matrix form versus reduced equations can depend on the problem/situation

Coupled Matrix Equations

$$\frac{d}{ds}\mathbf{M} = \mathbf{F}$$

M = Moment Vector

F = Force Vector

- Easy to formulate
  - Straightforward to incorporate additional effects
- Natural fit to numerical routine
  - Easy to code

Reduced Equations

$$X'' + \kappa_x X = 0$$

$$r_x'' + \kappa_x r_x - \frac{2Q}{r_x + r_y} - \frac{\varepsilon_x^2}{r_x^3} = 0$$

etc.

Reduction based on identifying invariants such as $\varepsilon_x^2 = 16\left[\langle \tilde{x}^2 \rangle_\perp \langle \tilde{x}'^2 \rangle_\perp - \langle \tilde{x}\tilde{x}' \rangle_\perp^2\right]$ helps understand solutions

- Compact expressions

S2E: Hybrid Methods

Beyond the three levels of modeling outlined earlier:

1) Particle methods
2) Distribution methods
3) Moment methods

there exist numerous "hybrid" methods that combine features of several methods.

Examples:

- Particle-in-Cell (PIC) models with shaped particles
- Gyro-kinetic models
  - Average over fast gyro motion in magnetic fields: common in plasma physics
- Delta-f models
  - Evolve perturbed distribution with marker particles

⋮

Hybrid Methods Continued (2)

General comments:

- Particle and distribution methods are appropriate for higher levels of detail
- Moment methods are used for rapid iteration of machine design
  - Moments also typically calculated as diagnostics in particle and distribution methods
- Even within one (e.g. particle) there are many levels of description:
  - Electromagnetic and electrostatic, with many field solution methods
  - 1D, 2D, 3D

  ⋮
- Employing a hierarchy of models with full diagnostics allows cross-checking (both in numerics and physics) and aids understanding
  - No single method is best in all cases

S3: Overview of Basic Numerical Methods
S3A: Discretizations

General approach is to discretize independent variables in each of the methods and solve for dependent variables which in some cases may be discretized as well

time (or s)

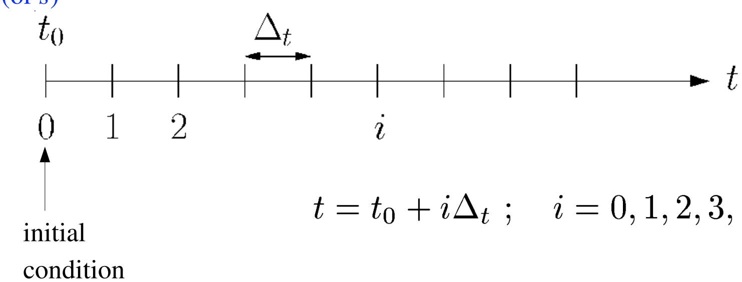

$$t = t_0 + i\Delta_t \; ; \quad i = 0, 1, 2, 3, \ldots$$

- Nonuniform meshes also possible
  - Can add resolution where needed
  - Increases complexity

In typical applications may apply these descriptions in a variety of ways

- Move a transverse thin slice of a beam...

Transverse Coordinate Discretization

Spatial Coordinates (transverse)

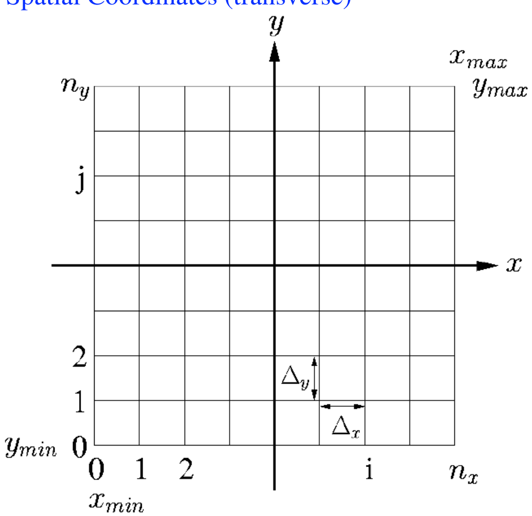

$$x_i = x_{min} + i\Delta_x$$
$$y_j = y_{min} + j\Delta_y$$

$$\Delta_x = (x_{max} - x_{min})/n_x$$
$$\Delta_y = (y_{max} - y_{min})/n_y$$

$$i = 0, 1, 2, ..., n_x$$
$$j = 0, 1, 2, ..., n_y$$

Analogous for 3D, momentum coordinates, etc.

Transverse Coordinate Discretization – Applications

In typical applications may apply these discretizations in a variety of ways:

Transverse Slice Simulation:

- Move a transverse thin "slice" of beam along the axial coordinate s of a reference particle

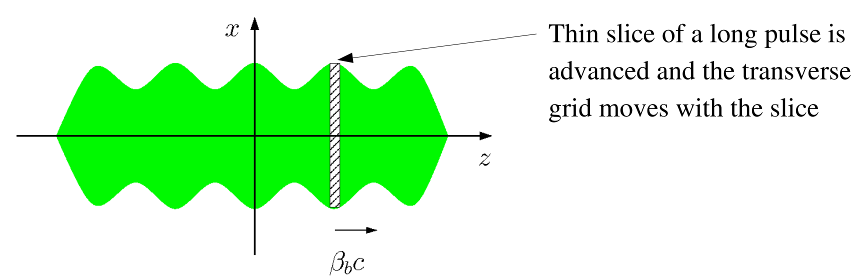

- Limitations:
  - This "unbunched" approximation is not always possible
  - 3D effect can matter, e.g. in short pulses and/or beams ends

Transverse Coordinate Discretization – Applications (2)

Steady State Simulation:

- Simulate the middle of a long pulse where a time stationary beam fills the grid

Example: Mid-Pulse Diode

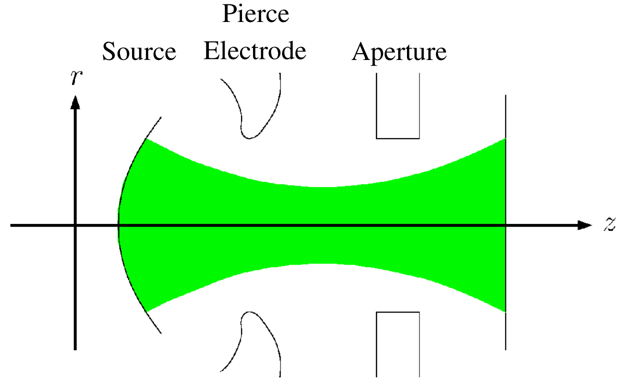

- Mesh is stationary, leading to limitations
  - Beam pulse always has ends: see J.J. Barnard lectures on Longitudinal Physics
  - Assumes that the mid-pulse in nearly time-independent in structure

Transverse Coordinate Discretization – Applications (3)

Full 3D Simulation

- Simulate a 3D beam with a moving mesh that follows a reference particle (possibly beam centroid).

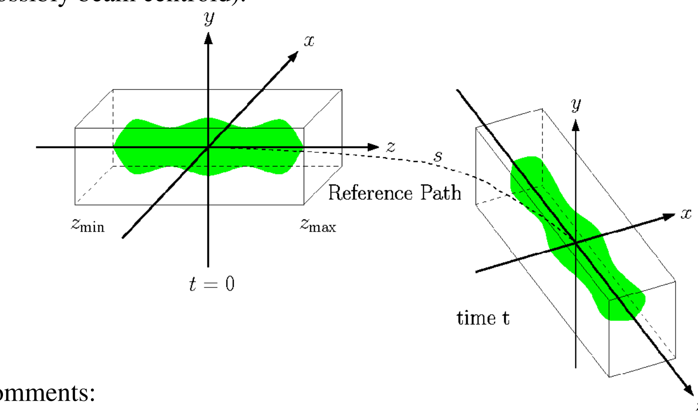

- Comments:
  - Most realistic level of modeling, but also most numerically intensive
  - Grid can be moved in discretized jumps so that applied fields maintain alignment with the grid

S3B: Discrete Numerical Operations

Let x represent a spatial coordinate and $f(x)$ some continuous function of x

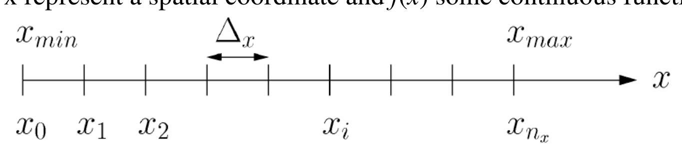

$$x_i = x_{min} + i\Delta_x; \quad \Delta_x = (x_{max} - x_{min})/n_x$$

$$i = 0, 1, 2, ..., n_x$$

Denote $f_i \equiv f(x_i)$, etc. and Taylor expand one grid point forward and backward about $x = x_i$

$$f_{i+1} = f_i + \left.\frac{\partial f}{\partial x}\right|_i \Delta_x + \frac{1}{2!}\left.\frac{\partial^2 f}{\partial x^2}\right|_i \Delta_x^2 + \frac{1}{3!}\left.\frac{\partial^3 f}{\partial x^3}\right|_i \Delta_x^3 + ...$$

$$f_{i-1} = f_i - \left.\frac{\partial f}{\partial x}\right|_i \Delta_x + \frac{1}{2!}\left.\frac{\partial^2 f}{\partial x^2}\right|_i \Delta_x^2 - \frac{1}{3!}\left.\frac{\partial^3 f}{\partial x^3}\right|_i \Delta_x^3 + ...$$

The same methodology can be applied to other spatial (*x, y,* etc.), axial (*s*), and temporal (*t*) coordinates

Discrete Numerical Operations: Derivatives

Simple, but inaccurate expressions for 1st order derivatives follow immediately from the forward and backward expansions

2 point: (non-centered)

Forward:
$$\boxed{\left.\frac{\partial f}{\partial x}\right|_i = \frac{f_{i+1} - f_i}{\Delta_x} + \mathcal{O}(\Delta_x)}$$

Backward:
$$\boxed{\left.\frac{\partial f}{\partial x}\right|_i = \frac{f_i - f_{i-1}}{\Delta_x} + \mathcal{O}(\Delta_x)}$$

A more accurate, centered discretization for a 1st order derivative is obtained by subtracting the two expansions.

3 point: (centered)

$$\boxed{\left.\frac{\partial f}{\partial x}\right|_i = \frac{f_{i+1} - f_{i-1}}{2\Delta_x} + \mathcal{O}(\Delta_x^2)}$$

- More accuracy generally will require the use of more function points

Discrete Numerical Operations: Derivatives (2)

The expansions can be relabeled (*i* -> *i*+1, etc.) and the resulting set of equations can be manipulated to obtain 5-point and other higher-order forms with higher accuracy:

5 point: (centered)
$$\boxed{\left.\frac{\partial f}{\partial x}\right|_i = \frac{f_{i-2} - 8f_{i-1} + 8f_{i+1} - f_{i+2}}{12\Delta_x} + \mathcal{O}(\Delta_x^4)}$$

Still higher order, and more accurate, forms are possible but rapidly become cumbersome and require more points.

Similar methods can be employed to obtain discretizations of higher order derivatives. For example,

3 point: (centered)
$$\boxed{\left.\frac{\partial^2 f}{\partial x^2}\right|_i = \frac{f_{i+1} - 2f_i + f_{i-1}}{\Delta_x^2} + \mathcal{O}(\Delta_x^2)}$$

Discrete Numerical Operations: Integrals/Quadrature

Take n_x even, then $\int_{x_{min}}^{x_{max}} d\tilde{x}\, f(\tilde{x})$ can be composed as sub-integrals of the form

$$\int_{x_{i-1}}^{x_{i+1}} d\tilde{x}\, f(\tilde{x})$$

Using a linear approximation (Trapezoidal Rule):

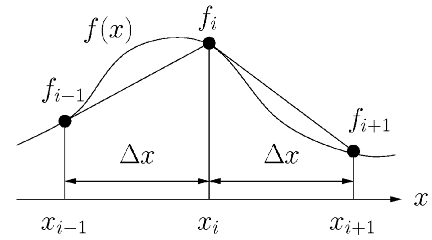

$$\boxed{\int_{x_{i-1}}^{x_{i+1}} dx\, f(x) = \frac{f_{i-1} + 2f_i + f_{i+1}}{2}\Delta_x + \mathcal{O}(\Delta_x^3)}$$

Discrete Numerical Operations: Integrals/Quadrature (2)

Better approximations can be found (e.g., Simpson's Rule) using Taylor series expansions and the previous discrete derivatives:

$$f(x) = f_i + \frac{f_{i+1} - f_{i-1}}{2\Delta_x}x + \frac{f_{i+1} - f_i + f_{i-1}}{\Delta_x^2}x^2 + \ldots$$

giving:

$$\boxed{\int_{x_{i-1}}^{x_{i+1}} dx\, f(x) = \frac{f_{i-1} + 4f_i + f_{i+1}}{3}\Delta_x + \mathcal{O}(\Delta_x^5)}$$

In the examples given, uniform grids have been employed and the formulas presented for derivatives and integrals are readily generalized to multiple dimensions.

Discrete Numerical Operations: Irregular Grids

Nonuniform grids can be used to effectively concentrate resolution where it is needed

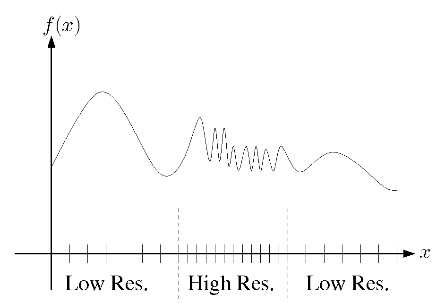

- Can be used most effectively when high resolution is needed only in limited regions and simulation domains are large
- Nonuniform grids make discretized formulas more complicated, particularly with respect to ordering errors
  - A simple example of nonuniform derivative calculation is included in the homework to illustrate methods

Discrete Numerical Operations: Axisymmetric Systems

To be added: Slide to discuss how to solve cylindrically symmetric problems pointing out origin problems. Suggest that it is often better to simply do in 2D *x-y* geometry and use conserved angular momentum.

S3C: Numerical Solution of Moment Methods – Time Advance

We now have the tools to numerically solve moment methods. The moment equations may always be written as an N-dimensional set of coupled 1st order ODEs (see: S2C and S.M. Lund lectures on Transverse Envelope Equations):

$$\mathbf{M} = \left(\langle x \rangle_\perp, \cdots, \langle x^2 \rangle_\perp, \cdots\right) \quad \text{N-dim vector of moments}$$

$$\frac{d\mathbf{M}}{ds} = \mathbf{F}(\mathbf{M}, s) \quad \text{vector equation of motion}$$

- Methods developed to advance moments can also be used for advances in particle and distribution methods

/// Example: Axisymmetric envelope equation for a continuously focused beam

$$\frac{d^2R}{ds^2} + k_{\beta 0}^2 R - \frac{Q}{R} - \frac{\varepsilon_x^2}{R^3} = 0 \qquad R = 2\sqrt{\langle x^2 \rangle_\perp}$$

$$\frac{d}{ds}\begin{bmatrix} R \\ R' \end{bmatrix} = \begin{bmatrix} R' \\ -k_{\beta 0}^2 R + \frac{Q}{R} + \frac{\varepsilon_x^2}{R^3} \end{bmatrix} \qquad k_{\beta 0}^2,\ Q,\ \varepsilon_x^2,\ \text{constants}$$

///

S3C: Numerical Solution of Moment Methods – Euler Advance

Euler's Method:

Apply the forward difference formula

$$\left.\frac{d\mathbf{M}}{ds}\right|_i = \frac{\mathbf{M}_{i+1} - \mathbf{M}_i}{\Delta_s} + \mathcal{O}(\Delta_s) = \mathbf{F}(\mathbf{M}_i, s_i)$$

Rearrange to obtain 1st order Euler advance:

$$\boxed{\mathbf{M}_{i+1} = \mathbf{M}_i + \mathbf{F}(\mathbf{M}_i, s_i)\Delta_s + \mathcal{O}(\Delta_s^2)}$$

- Moments advanced in discrete steps in s from initial values

Note that N_s steps will lead to a total error

$$\boxed{\text{error} \sim N_s \cdot \mathcal{O}(\Delta_s^2) \sim \frac{s_{max} - s_{min}}{\Delta_s}\mathcal{O}(\Delta_s^2) \sim \mathcal{O}(\Delta_s)}$$

- Error decreases only linearly with step size
- Numerical work for each step is only one evaluation of **F**

S3C: Numerical Solution of Moment Methods – Order Advance

Definition:

A discrete advance with error $\mathcal{O}(\Delta_s^n)$ is an (*n*-1)th order method

- Euler's method is a 1st order method
- Higher order methods are generally used for ODE's in moment methods
  – Cheap to evaluate **F**
- Low order methods are generally used for particle and distribution methods
  – Expensive to evaluate **F**

S3C: Numerical Solution of Moment Methods – Runge-Kutta Advance

Runge-Kutta Method:

Integrate from s_i to s_{i+1} :

$$\frac{d\mathbf{M}}{ds} = \mathbf{F}(\mathbf{M}, s)$$

$$\mathbf{M}_{i+1} = \mathbf{M}_i + \int_{s_i}^{s_{i+1}} ds\, \mathbf{F}(\mathbf{M}, s)$$

Approximate **F** with a Taylor expansion through the midpoint of the step, $s_{i=1/2}$

$$\mathbf{F}(\mathbf{M}, s) = \mathbf{F}(\mathbf{M}_{i+1/2}, s_{i+1/2}) + \left.\frac{\partial \mathbf{F}}{\partial s}\right|_{s_{i+1/2}} (s - s_{i-1/2}) \quad + \ldots$$

The linear term integrates to zero, leaving

$$\Rightarrow \mathbf{M}_{i+1} = \mathbf{M}_i + \mathbf{F}(\mathbf{M}_{i+1/2}, s_{i+1/2}) \cdot \Delta_s + \mathcal{O}(\Delta_s^3)$$

Runge-Kutta Advance (2)

Note: only need $\mathbf{M}_{i+1/2}$ to $\mathcal{O}(\Delta_s^2)$ for $\mathcal{O}(\Delta_s^3)$ accuracy
Apply Euler's method for the two-step procedure:

2nd Order Runge-Kutta Method:

Step 1: $\mathbf{K} = \mathbf{F}(\mathbf{M}_i, s_i)\Delta_s$

Step 2: $\mathbf{M}_{i+1} = \mathbf{M}_i + \mathbf{F}\left(\mathbf{M}_i + \frac{\mathbf{K}}{2}, s_i + \frac{\Delta_s}{2}\right)\Delta_s + \mathcal{O}(\Delta_s^3)$

- Requires two evaluations of **F** per advance
- 2nd order accurate in Δ_s

Higher order Runge-Kutta schemes are derived analogously from various quadrature formulas. Such formulas are found in standard numerical methods texts

- Typically, methods with error $\mathcal{O}(\Delta_s^{N+1})$ will require N evaluations of **F**

S3C: Numerical Solutions of Moment Methods

Many methods are employed to advance moments and particle orbits.

A general survey of these methods is beyond the scope of this lecture. But some general comments can be made:

- Many higher-order methods with adaptive step sizes exist that refine accuracy to specified tolerances and are optimized for specific classes of equations
- Choice of numerical method often relates to numerical work and stability considerations
- Certain methods can be formulated to exactly preserve relevant single-particle invariants
  - "Symplectic" methods preserve Hamiltonian structure of dynamics
- Accelerator problems can be demanding due to multiple frequency scales and long tracking times/distances
  - Hamiltonian dynamics; phase space volume does not decay

S3C: Numerical Solutions of Moment Methods – Numerical Stability

"Numerical Reversibility" test of stability:

In this method, the final value of an advance is used as an initial condition. Then the problem is run backwards to the original starting point and deviations from the initial conditions taken in the original advance are analyzed.

- Often a simple, but stringent test of accuracy
- Will ultimately fail due to roundoff errors and cases where there is a sensitive dependence on initial conditions
- Orbits can be wrong but qualitatively right. We will quantify this notion better later. So lack of full convergence does not necessarily mean that useless results will be obtained.

We will now briefly overview an application of moment equations, namely the KV envelope equations, to a practical high current transport lattice that was designed for Heavy Ion Fusion applications at Lawrence Berkeley National Laboratory.

S3C: Moment Equation Application: Perp. KV Envelope Eqns

Neglect image charges and nonlinear self-fields (emittance constant) to obtain moment equations for the evolution of the beam envelope radii

$$\frac{d^2 r_x}{ds^2} + \kappa_q r_x - \frac{2Q}{r_x + r_y} - \frac{\varepsilon_x^2}{r_x^3} = 0 \qquad r_x = 2\sqrt{\langle x^2 \rangle_\perp}$$

$$\frac{d^2 r_y}{ds^2} - \kappa_q r_y - \frac{2Q}{r_x + r_y} - \frac{\varepsilon_y^2}{r_y^3} = 0 \qquad r_y = 2\sqrt{\langle y^2 \rangle_\perp}$$

$$Q = \frac{qI}{2\pi\epsilon_0 m c^3 \gamma_b^3 \beta_b^3}$$

Dimensionless Perveance
measures space-charge strength

$$\varepsilon_x = 4\left[\langle x^2\rangle_\perp \langle x'^2\rangle_\perp - \langle x x'\rangle_\perp^2\right]^{1/2}$$

$$(\varepsilon_{xn} = \gamma_b \beta_b \varepsilon_x \text{ normalized})$$

RMS Edge Emittance
measures x-x' phase-space area
~(beam size)sqrt(thermal temp.)

The matched beam solution together with parametric constraints from engineering, higher-order theory, and simulations are used to design the lattice.

Application Example Continued (2) – Focusing Lattice

Take an alternating gradient FODO doublet lattice

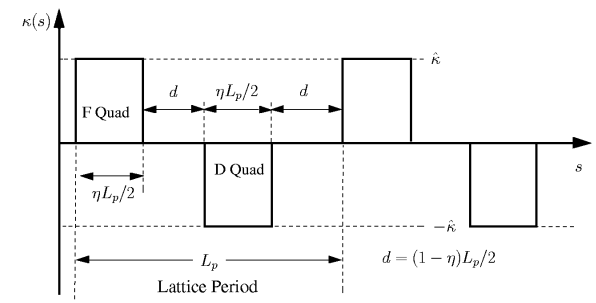

$$d = (1-\eta)\frac{L_p}{2} \qquad \eta = \text{Quadrupole Occupancy } (0 < \eta \le 1)$$

Focusing Strength

$$\hat{\kappa} = \begin{cases} \dfrac{1}{[B\rho]}\left|\dfrac{dB_x}{dy}\right|, & \text{Magnetic Quadrupole} \\ \dfrac{1}{[B\rho]\beta_b c}\left|\dfrac{dE_x}{dy}\right|, & \text{Electric Quadrupole} \end{cases}$$

Rigidity
$$[B\rho] = m\gamma_b\beta_b c/q$$

446

Application Example Contd. (3) – Matched Envelope Properties

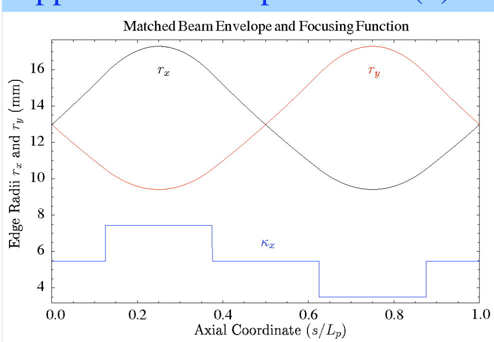

Ion
K⁺, E = 2 MeV
Current
I = 800 mA
Lattice
$L_p = 0.5\text{m}$
$\eta = 1/2$
$\sigma_0 = 80°/\text{Lattice Period}$

Envelope Properties:

1) Low Emittance Case: $\varepsilon_x = \varepsilon_y = 50$ mm-mrad; $\sigma = 9.42°/\text{Lattice Period}$

$\text{Max}[r_x] = \text{Max}[r_y] = 17.3$ mm $\text{Max}[r_x'] = -\text{Min}[r_y'] = 47.5$ mrad

$\text{Min}[r_x] = \text{Min}[r_y] = 9.41$ mm $\text{Max}[r_y'] = -\text{Min}[r_x'] = 47.5$ mrad

2) High Emittance Case: $\varepsilon_x = \varepsilon_y = 200$ mm-mrad; $\sigma = 32.13°/\text{Lattice Period}$

$\text{Max}[r_x] = \text{Max}[r_y] = 18.9$ mm $\text{Max}[r_x'] = -\text{Min}[r_y'] = 52.4$ mrad

$\text{Min}[r_x] = \text{Min}[r_y] = 10.1$ mm $\text{Max}[r_y'] = -\text{Min}[r_x'] = 52.4$ mrad

S4: Numerical Solution of Particle and Distribution Methods

S4A: Overview

Particle Methods – Generally not used at high space-charge intensity
Distribution Methods – Preferred (especially PIC) for high space-charge. We will motivate why now.

Why are direct particle methods are not a good choice for typical beams?

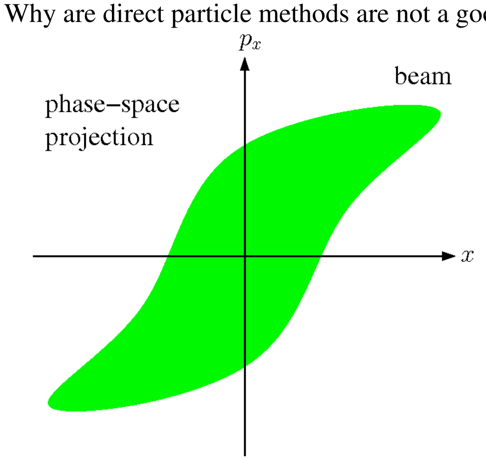

N particle coordinates
$\{\mathbf{x}_i, \mathbf{p}_i\}$

Physical beam (typical)
$N \sim 10^{10} - 10^{14}$ particles

Although larger problems are possible every year with more powerful computers, current processor speeds and memory limit us to
$N \lesssim 10^8$ particles

Numerical Solution of Particle and Distribution Methods (2)

Represent the beam by Lagrangian "macroparticles" advanced in time

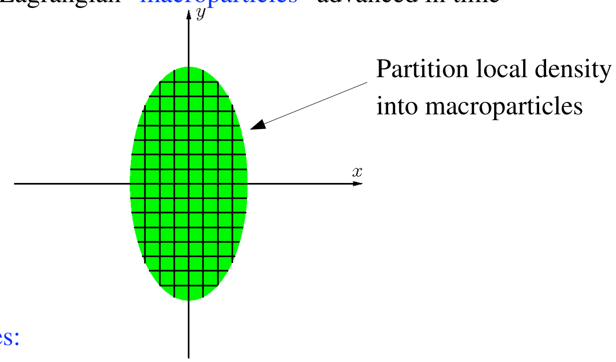

Macroparticle Properties:

- Same q/m ratio as real particle
  - Gives same single particle dynamics in the applied field
- More collisions due to macroparticles having more close approaches
  - Enhanced collisionality is unphysical
  - Controlled by smoothing the macroparticle interaction with the self-field. More on this later.

Numerical Solution of Particle and Distribution Methods (3)

Direct Vlasov as an example:

Discretize grid points $\{\boldsymbol{x}_i, \boldsymbol{p}_i\}$

Advance distribution $f(\boldsymbol{x},\boldsymbol{p},t)$ at discrete grid points in time

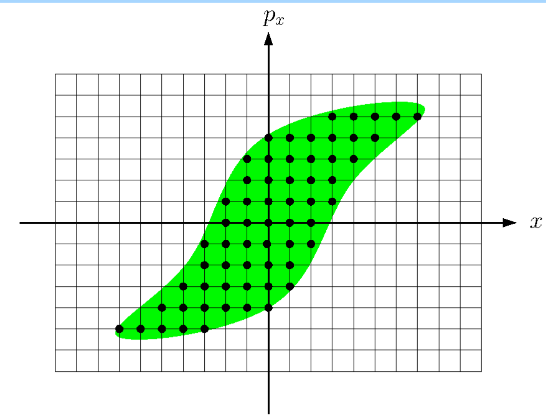

- Continuum distribution advanced on a discrete phase-space mesh
  - Extreme memory for high resolution. Example: for 4D x-p_x, y-p_y with 100 mesh points on each axis -> $100^4 = 10^8$ values to store in fast memory (RAM)
- Discretization errors can lead to aliasing and unphysical behavior (negative probability, etc.)

Numerical Solution of Particle and Distribution Methods (4)

Both particle and distribution methods can be broken up into two basic parts:

1) Moving particles or distribution evaluated at grid points through a finite time (or axial space) step
2) Calculation of beam self-fields consistently with the distribution of particles

In both methods, significant fractions of run time may *be devoted to diagnostics*

- Moment calculations can be computationally intensive and may be "gathered" frequently for evolution "histories"
- Phase space projections ("snapshot" in time)
- Fields (snapshot in time)

Diagnostics are also critical!

- Without appropriate diagnostics runs are useless, even if correct
- Must accumulate and analyze/present large amounts of data in an understandable format

Significant code development time may also be devoted to creating (loading) the initial distribution of particles to simulate

- Loading will usually only take a small fraction of total run time

S4B: Integration of Equations of Motion

Higher order methods require more storage and numerical work per time step

- Fieldsolves are expensive, especially in 3D, and several fieldsolves per step can be necessary for higher order accuracy

Therefore, low-order methods are typically used for self-consistent space-charge.
The "leapfrog" method is most common

- Only need to store prior position and velocity
- One fieldsolve per time step

Illustrate the leapfrog method for non-relativistic particle equations of motion:

- Develop methods for particles but can be applied to moments, distributions,...

$$m\frac{d\mathbf{v}}{dt} = \mathbf{F} = q(\mathbf{E} + \mathbf{v}\times\mathbf{B})$$
$$\frac{d\mathbf{x}}{dt} = \mathbf{v}$$

Leapfrog Method for Electric Forces

Leapfrog Method: for *velocity independent* (Electric) forces

Leapfrog Advance (time centered): Advance velocity and position out of phase

$$1) \quad m\frac{\mathbf{v}_{i+1/2} - \mathbf{v}_{i-1/2}}{\Delta_t} = \mathbf{F}_i \qquad \mathbf{F} = \mathbf{F}(\mathbf{x})$$

$$2) \quad \frac{\mathbf{x}_{i+1} - \mathbf{x}_i}{\Delta_t} = \mathbf{v}_{i+1/2}$$

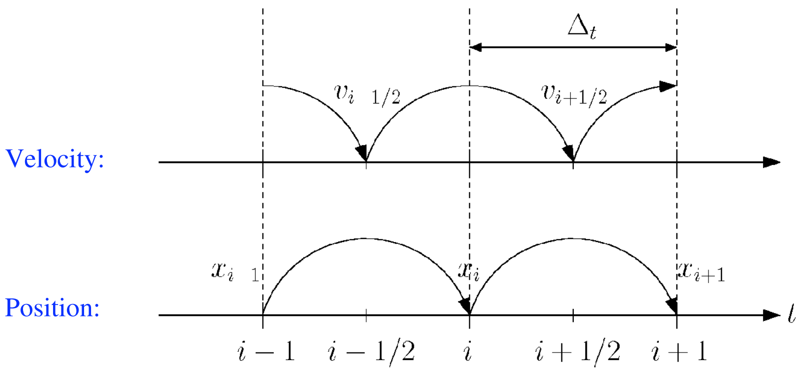

Leapfrog Method: Order

To analyze the properties of the leapfrog method it is convenient to write the map in an alternative form:

$$i \rightarrow i+1 \ : \ \begin{cases} \dfrac{\mathbf{x}_{i+1} - \mathbf{x}_i}{\Delta_t} = \mathbf{v}_{i+1/2} \\ \dfrac{\mathbf{x}_i - \mathbf{x}_{i-1}}{\Delta_t} = \mathbf{v}_{i-1/2} \end{cases}$$

Subtract the two equations above and apply the other leapfrog advance formula:

$$\Longrightarrow \quad m\frac{\mathbf{v}_{i+1/2} - \mathbf{v}_{i-1/2}}{\Delta_t} = \boxed{m\frac{\mathbf{x}_{i+1} - 2\mathbf{x}_i + \mathbf{x}_{i-1}}{\Delta_t^2} = \mathbf{F}_i}$$

Note correspondence of formula to discretized derivative:

$$\left.\frac{\partial^2 f}{\partial x^2}\right|_i = \frac{f_{i+1} - 2f_i + f_{i-1}}{\Delta_x^2} + \mathcal{O}(\Delta_x^2)$$

- $\mathbf{x}_{i+1}$ fixed from $\mathbf{x}_i, \ \mathbf{x}_{i-1}, \ \mathbf{F}_i$ to $\mathcal{O}(\Delta_t^4)$
- Leapfrog method is 2[nd] order accurate

Initial conditions must be desynchronized in leapfrog method

Leapfrog Method: Synchronization

Since **x** and **v** are not evaluated at the same time in the leapfrog method synchronization is necessary both to start the advance cycle and for diagnostics

- Initial conditions: typically, **v** is pushed back half a cycle

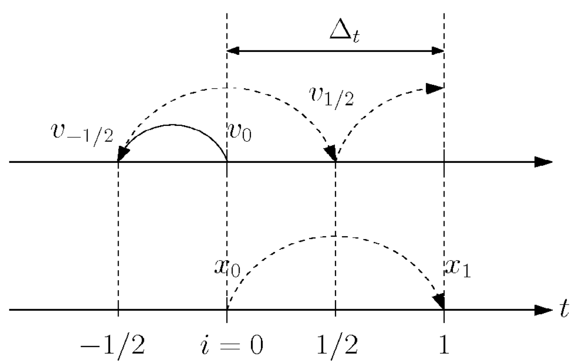

- When evaluating diagnostic quantities such as moments the particle coordinates and velocities should first be synchronized analogously to above

Leapfrog Method for Magnetic and Electric Forces -- The Boris Method

Velocity Dependent Forces

Another complication in the evolution ensues when the force has velocity dependence, as occurs with magnetic forces. This complication results because ***x*** and ***v*** are advanced out of phase in the leapfrog method

$$\boxed{\mathbf{F} = q\mathbf{E} + q\mathbf{v} \times \mathbf{B}}$$

velocity term

- Electric field **E** accelerates
- Magnetic field **B** bends particle trajectory without change in speed |**v**|

A commonly implemented time centered scheme for magnetic forces is the following 3-step "Boris" method:

J. Boris, in *Proceedings of the 4[th] Conference on the Numerical Simulation of Plasmas* (Naval Research Lab, Washington DC 1970)

The Boris Advance

Boris Advance: 3-step, time-centered

1) Half-step acceleration in electric field

$$\mathbf{v}^{(1)}_{i+1/2} = \mathbf{v}_{i-1/2} + \frac{q}{m}\mathbf{E}_i\frac{\Delta_t}{2}$$

2) Rotation in magnetic field. Here choose coordinates so that

$$\mathbf{B}_i = B_i\hat{z}\ ,\ \omega_{ci} = \frac{qB_i}{m}$$

$$\parallel \mathbf{B}_i\ :\qquad v^{(2)}_{z_{i+1/2}} = v^{(1)}_{z_{i+1/2}}$$

$$\perp \mathbf{B}_i\ :\qquad \begin{bmatrix} v^{(2)}_{z_{i+1/2}} \\ v^{(1)}_{z_{i+1/2}} \end{bmatrix} = \begin{bmatrix} \cos(\omega_{ci}\Delta_t) & \sin(\omega_{ci}\Delta_t) \\ -\sin(\omega_{ci}\Delta_t) & \cos(\omega_{ci}\Delta_t) \end{bmatrix} \begin{bmatrix} v^{(2)}_{z_{i+1/2}} \\ v^{(1)}_{z_{i+1/2}} \end{bmatrix}$$

3) Half-step acceleration in electric field

$$\mathbf{v}_{i+1/2} = \mathbf{v}^{(3)}_{i+1/2} = \mathbf{v}^{(2)}_{i+1/2} + \frac{q}{m}\mathbf{E}_i\frac{\Delta_t}{2}$$

Boris Advance Continued (2)

Complication: on startup, how does one generate the out-of-phase **x**, **v** advance from the initial conditions?

- Calculate **E**, **B** with initial conditions
- Move **v** backward half a time step
  - Rotate with **B** a half-step
  - Decelerate a half-step in **E**

Similar comments hold for synchronization of **x**, **v** for diagnostic accumulation

Now we will look at the numerical properties of the leapfrog advance cycle

- Only use a simple "electric" force example to illustrate issues

Leapfrog Advance: Errors and Numerical Stability

To better understand the leapfrog method consider the simple harmonic oscillator:

$$\boxed{\frac{d^2x}{dt^2} = -\omega^2 x,\ \omega = \text{const}} \implies \begin{aligned} x &= C_0\cos\omega t + C_1\sin\omega t \\ &= x_0\cos(\omega t + \psi_0) \end{aligned}$$

Discretized equation of motion

$$\boxed{\frac{x_{i+1} - 2x_i + x_{i-1}}{\Delta_t^2} = -\omega^2 x_i}$$

Exact solution

Try a solution of the form $\quad x_i = ce^{j\tilde{\omega} i\Delta_t},\ j \equiv \sqrt{-1}$

$$\Rightarrow e^{j\tilde{\omega}\Delta_t} - 2 + e^{-j\tilde{\omega}\Delta_t} = -\omega^2\Delta_t^2$$

$$2 - 2\cos(\tilde{\omega}\Delta_t) = \omega^2\Delta_t^2$$

$$\sin^2\left(\frac{\tilde{\omega}\Delta_t}{2}\right) = \frac{\omega^2\Delta_t^2}{4}$$

$$\Rightarrow \boxed{\sin\left(\frac{\tilde{\omega}\Delta_t}{2}\right) = \frac{\omega\Delta_t}{2}}$$

This has solutions for $\omega\Delta_t < 2$ and it is straightforward to show via expansion that for small $\omega\Delta_t$

$$\boxed{\begin{aligned}\omega\Delta_t = \tilde{\omega}\Delta_t + \frac{(\tilde{\omega}\Delta_t)^3}{24} \\ + \mathcal{O}\left[(\tilde{\omega}\Delta_t)^5\right]\end{aligned}}$$

Leapfrog Errors and Numerical Stability Continued (2)

It follows for the leapfrog method applied to a simple harmonic oscillator:

- For $\omega\Delta_t < 2$ the method is stable
- There is *no* amplitude error in the integration
- For $\omega\Delta_t \ll 1$ the phase error is

Actual phase: $\quad \psi \equiv \omega\Delta_t i$

Simulated phase: $\tilde{\psi} \equiv \tilde{\omega}\Delta_t i \approx \omega\Delta_t i + \frac{(\omega\Delta_t)^3}{24}i$

Error phase: $\quad \Delta\psi \equiv \tilde{\psi} - \psi \approx \frac{(\omega\Delta_t)^3}{24}i$

Note: i to get to a fixed time $\sim \Delta_t^{-1}$ and therefore phase errors decrease as $\mathcal{O}(\Delta_t^2)$

// Example: $\omega = 2\pi/\tau$

Time step	Steps for a π phase error
$\Delta_t = 0.1\tau$	$24\pi/(0.1\cdot 2\pi)^3 \approx 3\times 10^2$
$\Delta_t = 0.01\tau$	$24\pi/(0.01\cdot 2\pi)^3 \approx 3\times 10^5$

//

Leapfrog Errors and Numerical Stability Continued (3)

Contrast: Numerical and Actual Orbit: Simple Harmonic Oscillator

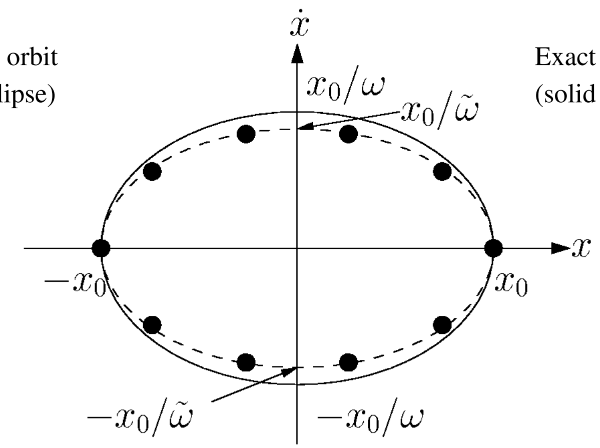

Emittance = (Phase Space Area)/π

Exact: $\varepsilon = x_0^2/\omega$

Numerical: $\tilde{\varepsilon} = x_0^2/\tilde{\omega}$

$$\frac{\tilde{\varepsilon}}{\varepsilon} \approx 1 - \frac{(\omega\Delta_t)^2}{24}$$

Leapfrog Errors and Numerical Stability Continued (4)

The numerical orbit conserves phase space area regardless of the number of steps taken! The slight differences between the numerical and actual orbits can be removed by rescaling the angular frequency to account for the discrete step

- More general analysis of the leapfrog method shows it has "symplectic" structure, meaning it preserves the Hamiltonian nature of the dynamics
- Symplectic methods are important for long tracking problems (typical in accelerators) to obtain the right orbit structure
  - Runge-Kutta methods are not symplectic and can result in artificial numerical damping in long tracking problems

Example: Contrast of Non-Symplectic and Symplectic Advances

Contrast: Numerical and Actual Orbit for a Simple Harmonic Oscillator

use scaled coordinates (max extents unity for analytical solution)

Symplectic Leapfrog Advance:

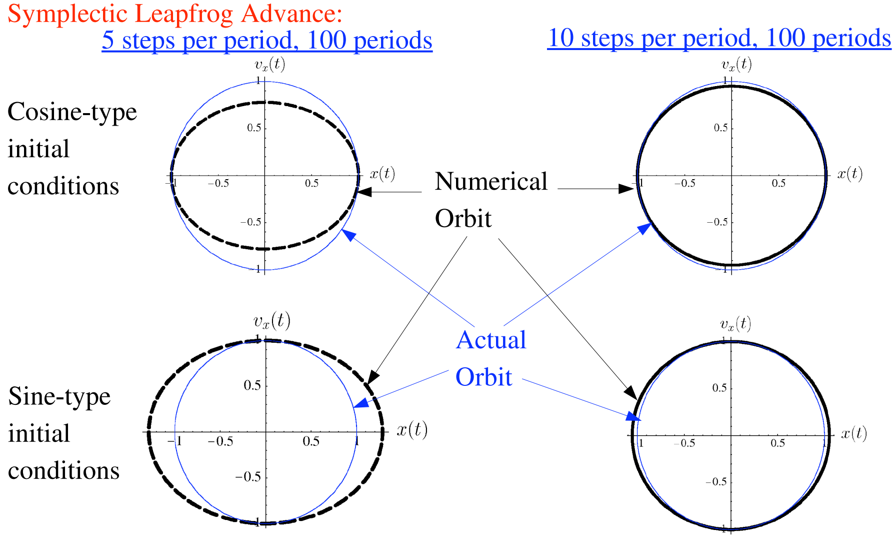

Example: Contrast of Non-Symplectic and Symplectic Advances (2)

Contrast: Numerical and Actual Orbit for a Simple Harmonic Oscillator

Non-Symplectic 2nd Order Runge-Kutta Advance: (see earlier notes on RK advance)

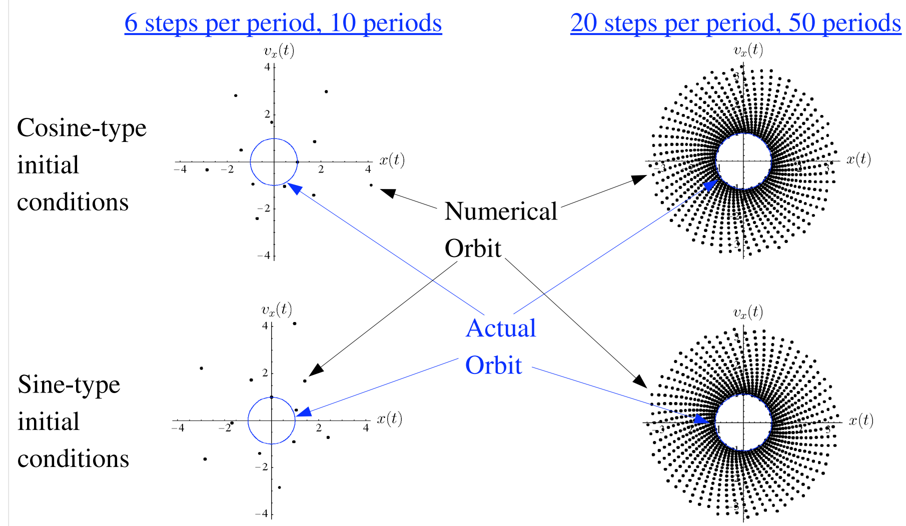

Example: Contrast of Non-Symplectic and Symplectic Advances (3)

Contrast: Numerical and Actual Orbit for a Simple Harmonic Oscillator

Non-Symplectic 4th Order Runge-Kutta Advance: (analog to notes on 2nd order RK adv)

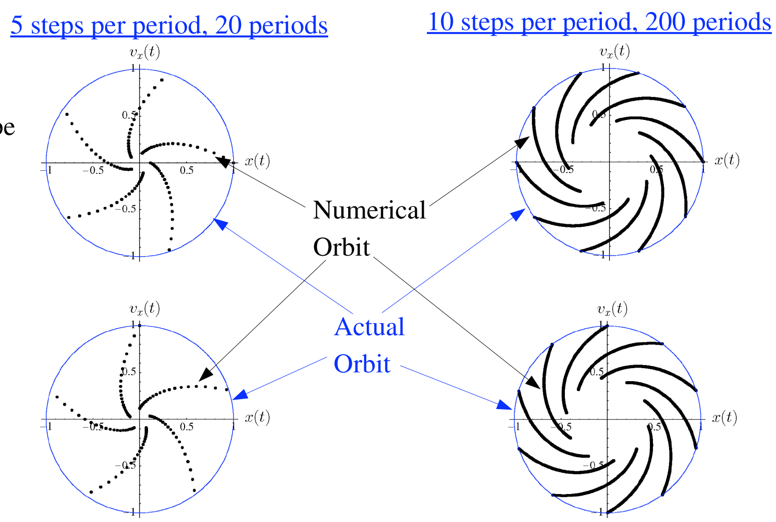

Example: Leapfrog Stability Applied to the Nonlinear Envelope Equation in a Continuous Focusing Lattice

For linear equations of motion, numerical stability requires:

$$\boxed{k\Delta_s < 2}$$

Here, k is the wave number of the phase advance of the quantity evolving under the linear force. The continuous focusing envelope equation is nonlinear:

$$\frac{d^2 r_x}{ds^2} + k_{\beta 0}^2 r_x - \frac{2Q}{r_x + r_y} - \frac{\varepsilon_x^2}{r_x^3} = 0$$

$$\frac{d^2 r_y}{ds^2} + k_{\beta 0}^2 r_y - \frac{2Q}{r_x + r_y} - \frac{\varepsilon_y^2}{r_y^3} = 0$$

Several wavenumbers k can be expressed in the envelope evolution:

$k_\beta = \sigma / L_p$ .... Depressed Particle Betatron Motion

$k_{\beta 0} = \sigma_0 / L_p$ .... Undepressed Particle Betatron Motion

$k_Q \equiv \sqrt{k_{\beta 0}^2 + 3k_\beta^2}$ .... Quadrupole Envelope Mode

$k_B \equiv \sqrt{2k_{\beta 0}^2 + 2k_\beta^2}$ .... Breathing Envelope Mode

Example: Leapfrog Stability and the Continuous Foc. Envelope Equation (2)

Expect that $k_{\beta 0}\Delta_s < 2$ for the fastest (largest k) component determines stability.

Numerical simulations for an initially matched envelope with: $\sigma/\sigma_0 = 1/2$

$k_\beta\Delta_s$	$k_{\beta 0}\Delta_s$	$k_Q\Delta_s$	$k_B\Delta_s$	Stable?
0.500	1.00	1.32	1.58	Yes
0.600	1.20	1.59	1.90	Yes
0.630	1.26	1.67	1.99	Yes
0.635	1.27	1.68	2.01	No
0.640	1.28	1.69	2.02	No

The highest k-mode, the breathing mode, appears to determine stability, i.e. $k_B\Delta_s < 2$ is the stability criterion. Other values of σ/σ_0 produce results in agreement with this conclusion.

Example: Leapfrog Stability and the Continuous Foc. Envelope Equation (3)

Numerical simulations an initially matched envelope with:$\sigma_0 = 80^\circ$, $\sigma/\sigma_0 = 1/2$

Note that numerical errors seed small amplitude mismatch and that the plot scale to the left is ~ 10^{-13}, corresponding to numerical errors.

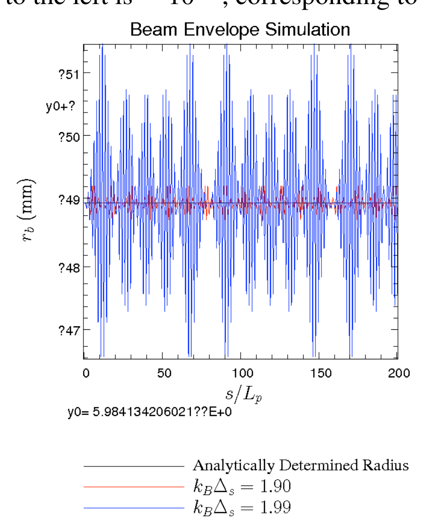

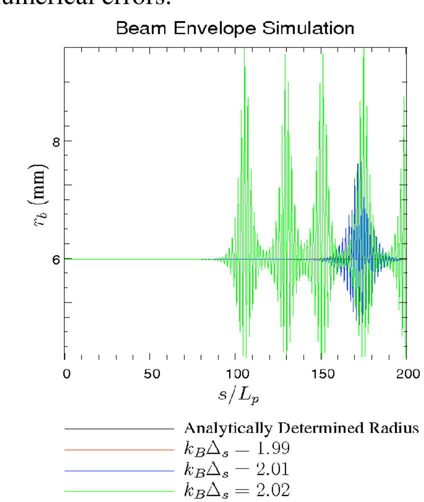

Comments of 2D and 3D Axisymmetric Particle Moves

To be added:

Comments on moving ring particles:
- 3D axisymmetry => particles rings, 3D axisymmetry => particles are infinite cylindrical shells.
- Angular momentum will be conserved for such particles (can rotate)
- Easier to do in many cases using x-y movers

S4C: Field Solution

The self-consistent calculation of beam-produced self-fields is vital to accurately simulate forces acting on particles in intense beams

$$\mathbf{F} = q(\mathbf{E} + \mathbf{v} \times \mathbf{B})$$

- Techniques outlined here are also applicable to distribution methods

Fields can be resolved into externally applied and self (beam generated) components

$$\boxed{\begin{aligned}\mathbf{E} &= \mathbf{E}_a + \mathbf{E}_s \\ \mathbf{B} &= \mathbf{B}_a + \mathbf{B}_s\end{aligned}}$$

$\mathbf{E}_a$, $\mathbf{B}_a$ applied fields generated by magnets and electrodes
- Sometimes calculated at high resolution in external codes and imported or specified via analytic formulas
- Sometimes calculated from code fieldsolve via applied charges and currents and boundary conditions

$\mathbf{E}_s$, $\mathbf{B}_s$ self fields generated by beam charges and currents
- At high beam intensities can be a large fraction (on average) of applied fields
- Important to calculate with realistic boundary conditions

Electrostatic Field Solution

For simplicity, we restrict analysis to electrostatic problems to illustrate methods:

$\mathbf{B} = \mathbf{B}_a$ $\quad$ $\mathbf{B}_a$ specified via another code or theory

$\mathbf{E} = \mathbf{E}_a + \mathbf{E}_s$ $\quad$ $\mathbf{E}_a$ due to biased electrodes and $\mathbf{E}_s$ due to beam space-charge

The Maxwell equations to be solved for $\mathbf{E}$ are

$$\boxed{\begin{aligned}\nabla \cdot \mathbf{E} &= \frac{\rho}{\epsilon_0} \qquad + \text{ boundary conditions on } \mathbf{E} \\ \nabla \times \mathbf{E} &= 0\end{aligned}}$$

$\nabla \times \mathbf{E} = 0$ implies that we can always take $\mathbf{E} = -\nabla\phi$ and so

$$\boxed{\begin{aligned}\nabla^2 \phi &= -\frac{\rho}{\epsilon_0} \qquad + \text{ boundary conditions on } \phi \\ \mathbf{E} &= -\nabla\phi\end{aligned}}$$

Electrostatic Field Solution: Typical Problem

As an example, it might be necessary to solve (2D) fields of a beam within an electric quadrupole assembly.

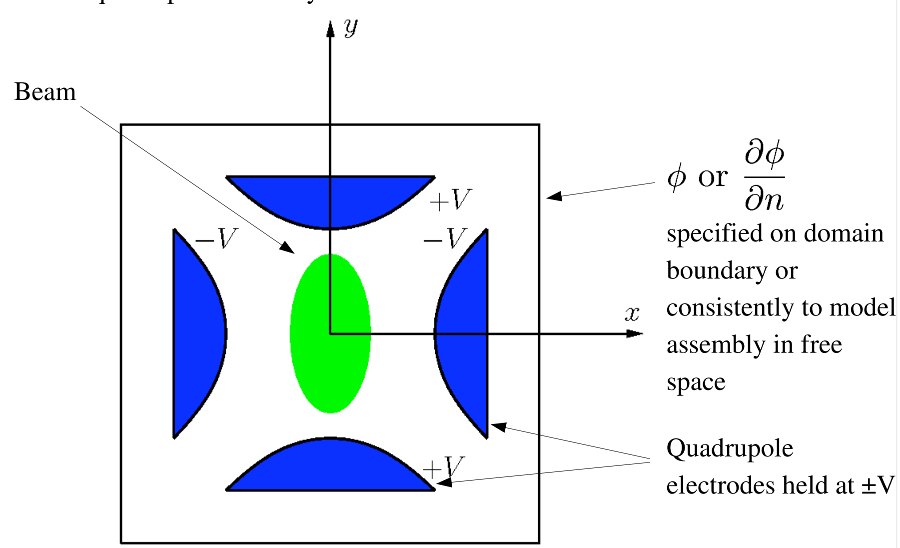

Electrostatic Field Solution by Green's Function

Formally, the solution to ϕ can be constructed with a Green's function, illustrated here with Dirichlet boundary conditions:

$$\nabla^2 G(\mathbf{x},\mathbf{x}') = -4\pi\delta(\mathbf{x}-\mathbf{x}')$$
$$G(\mathbf{x},\mathbf{x}')|_{\mathbf{x}'_b} = 0$$
$$\mathbf{x}'_b \equiv \mathbf{x}' \text{ on boundaries}$$

Definitions:
$$\frac{\partial}{\partial n} \equiv \hat{\mathbf{n}}\cdot\frac{\partial}{\partial \mathbf{x}}$$
$\hat{\mathbf{n}} \equiv$ Unit normal vector to boundary surface

This yields

$$\phi(\mathbf{x}) = \frac{1}{4\pi\epsilon_0}\int_V d^3x'\ \rho(\mathbf{x}')G(\mathbf{x},\mathbf{x}') - \frac{1}{4\pi}\oint_S d^2x'\ \phi(\mathbf{x}')\frac{\partial G(\mathbf{x},\mathbf{x}')}{\partial n'}$$

Self-field component $\equiv \phi_s$ | Applied field from electrode potentials $\equiv \phi_a$

$$\mathbf{E}_s = -\frac{\partial \phi_s}{\partial \mathbf{x}} \qquad \mathbf{E}_a = -\frac{\partial \phi_a}{\partial \mathbf{x}}$$

Electrostatic Field Solution by Green's Function (2)

Applied Field:

ϕ_a can be calculated in advance and need not be recalculated if transverse geometry does not change

- Can be analytical in simple situations

Self Field:

Let: $q_M,\ \mathbf{x}_i =$ Macro-particle charge and coordinate

$N_p =$ Macro-particle number

$$\phi_s = \frac{1}{4\pi\epsilon_0}\int d^3x'\ \rho(\mathbf{x}')G(\mathbf{x},\mathbf{x}') = \frac{q_M}{4\pi\epsilon_0}\sum_{i=1}^{N_p}\int d^3x'\ \delta(\mathbf{x}'-\mathbf{x}_i)G(\mathbf{x},\mathbf{x}')$$

$$\boxed{\phi_s = \frac{q_M}{4\pi\epsilon_0}\sum_{i=1}^{N_p} G(\mathbf{x},\mathbf{x}_i)}$$

Then the field at the ith macro-particle is (self-field term removed):

$$\boxed{\mathbf{E}_{si} = \left.\frac{\partial \phi_s}{\partial \mathbf{x}}\right|_{\mathbf{x}=\mathbf{x}_i} = \frac{q_M}{4\pi\epsilon_0}\sum_{\substack{j=1\\ j\neq i}}^{N_p}\left.\frac{\partial G(\mathbf{x},\mathbf{x}_j)}{\partial \mathbf{x}}\right|_{\mathbf{x}=\mathbf{x}_i}}$$

Electrostatic Field Solution by Green's Function (3)

The Green's Function expression for ϕ_a will, in general, be a numerically intensive expression to evaluate at *each* macroparticle

- $N_p(N_p - 1)$ terms to evaluate and G itself will in general be complicated and may require many costly numerical operations for each term, limiting N_p
- Small N_p for which this procedure is practical will result in a noisy field
  - Enhanced, unphysically high, close approaches (collisions) with poor statistics can change the physics
- Special "fast multipole" methods based on Green's functions can reduce the scaling to $\sim N_p$ or $\sim N_p ln(N_p)$.
  - Coefficient is large and smoothing is not easily implemented, often rendering such methods inferior to gridded methods to be covered shortly

// Example: Self fields in free space

$$G(\mathbf{x},\mathbf{x}') = \frac{1}{|\mathbf{x}-\mathbf{x}'|}\ ; \quad \mathbf{E}_{si} = \frac{q_M}{4\pi\epsilon_0}\sum_{\substack{j=1\\ j\neq i}}^{N_p}\frac{(\mathbf{x}_i-\mathbf{x}_j)}{|\mathbf{x}_i-\mathbf{x}_j|^3}$$ //

Field Solution on a Discrete Grid

An alternative procedure is needed to

1) Calculate fields efficiently by disretization of the Maxwell equations
2) Smooth interactions to compensate for limited particle numbers

Approach: Solve the Maxwell Equations on a discrete spatial grid and then smooth the interactions calculated from the gridded field.

Discretization: 2D uniform grid (1D and 3D analogous)

$$x_i = x_{min} + i\Delta_x \quad \Delta_x = (x_{max} - x_{min})/n_x \quad i = 0,1,2,...,n_x$$
$$y_j = y_{min} + j\Delta_y \quad \Delta_y = (y_{max} - y_{min})/n_y \quad j = 0,1,2,...,n_y$$

$$\left.\begin{aligned}\mathbf{E}_{ij} &= \mathbf{E}(x_i,y_j)\\ \phi_{ij} &= \phi(x_i,y_j)\\ \rho_{ij} &= \rho(x_i,y_j)\end{aligned}\right\}$$ Field components, potential, and charge are gridded

Comments:

- ρ_{ij} must be calculated from macro-particles, not necessarily on grid points
- Fields will ultimately be needed at marco-particle coordinates, not on grid

These issues will be covered later under "particle weighting"

Field Solution on a Discrete Grid: Example Problem, Beam in an Electric Quadrupole

Beam in an electric quadrupole lattice (2D)

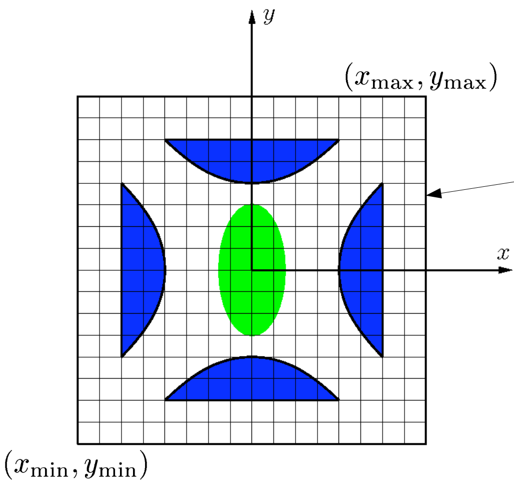

ϕ or $\dfrac{\partial \phi}{\partial n}$ specified on grid boundary and possibly on surfaces within the grid

Gridded Field Solution: Discretized Poisson Eqn.

For low order differencing, the Poisson Equation becomes

$$\frac{\phi_{i+1,\,j} - 2\phi_{i,\,j} + \phi_{i-1,\,j}}{\Delta_x^2} + \frac{\phi_{i,\,j+1} - 2\phi_{i,\,j} + \phi_{i,\,j-1}}{\Delta_y^2} = -\frac{\rho_{i,\,j}}{\epsilon_0}$$

with the gridded field components calculated as

$$E_{x_{ij}} = \frac{\phi_{i+1,\,j} - \phi_{i-1,\,j}}{2\Delta_x}$$
$$E_{y_{ij}} = \frac{\phi_{i,\,j+1} - \phi_{i,\,j-1}}{2\Delta_y}$$

Boundary conditions must also be incorporated as constraint equations

Dirichlet Conditions: ϕ specified on surfaces

Neumann Conditions: $\dfrac{\partial \phi}{\partial n}$ specified on surfaces

Gridded Field Solution: Discretized Dirichlet Boundary Cond

Dirichlet Conditions: ϕ specified on surface

Example: $\phi = V =$ const at right grid edge

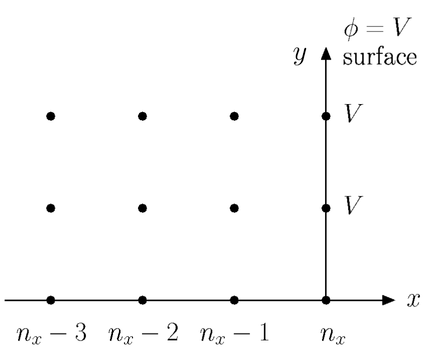

$\phi_{n_x,\,j} = V =$ const

For $i = n_x - 1$ cells

$$\frac{V - 2\phi_{n_x-1,\,j} + \phi_{n_x-2,\,j}}{\Delta_x^2} + \frac{\phi_{n_x-1,\,j+1} - 2\phi_{n_x-1,\,j} + \phi_{n_x-1,\,j-1}}{\Delta_y^2} = -\frac{\rho_{n_x-1,\,j}}{\epsilon_0}$$

Gridded Field Solution: Discretized Neumann Boundary Cond

Neumann Conditions: $\dfrac{\partial \phi}{\partial n}$ specified on surfaces

Example: $\dfrac{\partial \phi}{\partial n} = G =$ const at right grid edge

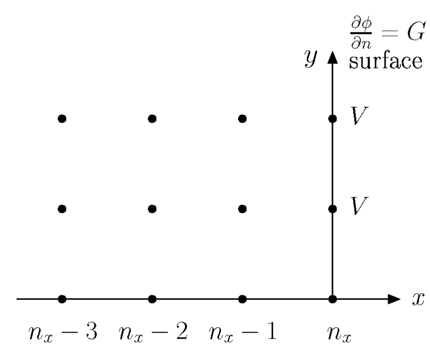

Use 1st order forward difference formula at surface

$$\frac{\phi_{n_x-1,\,j} - \phi_{n_x,\,j}}{\Delta_x} = G$$

Solution of Discretized Poisson Eqn -- Direct Matrix Method

The finite-differenced Poisson Equation and the boundary conditions can be expressed in matrix form as:

$$\boxed{\overline{\mathbf{M}} \cdot \mathbf{\Phi} = \mathbf{S}}$$

$\overline{\mathbf{M}} =$ Coefficients matrix from local finite differences. This matrix will be sparse, i.e., most elements will equal zero

$\mathbf{\Phi} =$ Vector of potentials at grid points

$\mathbf{S} =$ "Source" terms resulting from beam charge deposited on the grid (ρ_{ij}) and known potentials from boundary condition constraints

Formal solution found by matrix inversion:

$$\boxed{\mathbf{\Phi} = \overline{\mathbf{M}}^{-1} \cdot \mathbf{S}}$$

Direct inversion of $\overline{\mathbf{M}}^{-1}$ is not practical due to the large dimension of the problem

- $\overline{\mathbf{M}}$ will in general be sparse due to use of local, low-order finite differencing
- Many fast, numerically efficient inversion methods exist for sparse matrices
  - Specific method best used depends on type of differencing and BC's

Example Discretized Field Solution

To illustrate this procedure, consider a simple 1D example with Dirichlet BC's

$$\frac{d^2\phi}{dx^2} = -\frac{\rho}{\epsilon_0} \qquad \begin{array}{ll} \phi(x_l) = V_l & \text{left BC} \\ \phi(x_r) = V_r & \text{right BC} \end{array}$$

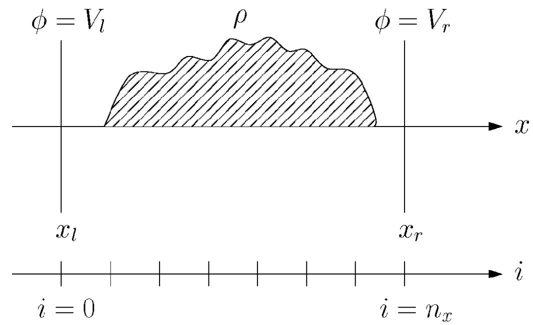

Discretize:

$$\frac{\phi_{i+1} - 2\phi_i + \phi_{i-1}}{\Delta x^2} = -\frac{\rho_i}{\epsilon_0}$$

$$\phi_0 = V_l$$
$$\phi_{n_x} = V_r$$

$$x_i = x_l + i\Delta_x, \quad \Delta_x = (x_r - x_l)/n_x; \quad i = 0, 1, 2, ..., n_x$$

Note: ρ_0 , ρ_{n_x} irrelevant

- Correspond to surface terms that fix boundary condition potentials

Example Discretized Field Solution (2)

The 1D discretized Poisson equation and boundary conditions can be expressed in matrix form as:

$$\begin{bmatrix} -2 & 1 & & & & & 0 \\ 1 & -2 & 1 & & & & \\ & 1 & -2 & 1 & & & \\ & & \ddots & \ddots & \ddots & & \\ & & & 1 & -2 & 1 & \\ & & & & 1 & -2 & 1 \\ 0 & & & & & 1 & -2 \end{bmatrix} \cdot \begin{bmatrix} \phi_1 \\ \phi_2 \\ \phi_3 \\ \vdots \\ \phi_{n_x-3} \\ \phi_{n_x-2} \\ \phi_{n_x-1} \end{bmatrix} = -\frac{\Delta_x^2}{\epsilon_0} \begin{bmatrix} \rho_1 + \frac{\epsilon_0}{\Delta_x^2} V_l \\ \rho_2 \\ \rho_3 \\ \vdots \\ \rho_{n_x-3} \\ \rho_{n_x-2} \\ \rho_{n_x-1} + \frac{\epsilon_0}{\Delta_x^2} V_r \end{bmatrix}$$

Matrix has tri-diagonal structure and can be rapidly inverted to find the ϕ_i

- Sparse matrices need not be stored in full (waste of memory)

S4: Particle Methods – Field Solution Methods on Grid

Many other methods exist to solve the discretized field equations. These methods fall into three broad classes:

1) Direct Matrix Methods

- Fast inversion of sparse matrix

2) Spectral Methods

- Fast Fourier Transform (FFT)
  - Periodic boundary conditions
  - Sine transform ($\phi = 0$ on grid boundary)
  - FFT + capacity matrix for arbitrary conductors
  - Free space boundary conditions

3) Relaxation Methods

- Successive over-relaxation (SOR)
  - General boundary conditions and structures
- Multigrid (good, fast, and accurate method for complicated boundaries)

Field Solution Methods on Grid Continued (2)

Sometimes methods in these three classes are combined. For example, one might employ spectral methods transversely and invert the tri-diagonal matrix longitudinally.

Other discretization procedures are also widely employed, giving rise to other classes of field solutions such as:

- Finite elements
- Variational
- Monte Carlo

Methods of field solution are central to the efficient numerical solution of intense beam problems. It is not possible to review them all here. But before discussing particle weighting, we will first overview the important spectral methods and FFT's

Spectral Methods and the FFT

The spectral approach combined with numerically efficient Fast Fourier Transforms (FFT's) is commonly used to efficiently solve the Poisson Equation on a discrete spatial grid

- Approach provides spectral information on fields that can be used to smooth the interactions
- Efficiency of method enabled progress in early simulations
  - Computers had very limited memory and speed
- Method remains important and can be augmented in various ways to implement needed boundary conditions
  - Simple to code with numerical libraries
  - Efficiency still important ... especially in 3D geometries

Spectral Method: Discrete Fourier Transform

Illustrate in 1D for simplicity (multidimensional case analogous)

$$\boxed{\frac{d^2\phi}{dx^2} = -\frac{\rho}{\epsilon_0}}$$

Continuous Fourier Transforms (Reminder)

$$\tilde{\phi}(k) = \int_{-\infty}^{\infty} dx\, e^{ikx}\phi(x) \qquad \tilde{\rho}(k) = \int_{-\infty}^{\infty} dx\, e^{ikx}\rho(x)$$

$$\phi(x) = \int_{-\infty}^{\infty} \frac{dk}{2\pi}\, e^{-ikx}\tilde{\phi}(k) \qquad \rho(x) = \int_{-\infty}^{\infty} \frac{dk}{2\pi}\, e^{-ikx}\tilde{\rho}(k)$$

Transform Poisson Equation: $k^2\tilde{\phi}(k) = \dfrac{\tilde{\rho}(k)}{\epsilon_0}$

$$\boxed{\phi(x) = \int_{-\infty}^{\infty} \frac{dk}{2\pi} e^{-ikx}\frac{\tilde{\rho}(k)}{\epsilon_0 k^2}}$$

Similar procedures work to calculate the field on a finite, discrete spatial grid

- Develop by analogy to continuous transforms

Discrete Fourier Transform (2)

Discretize the problem as follows:

$$x_j = x_{min} + j\Delta_x; \quad \Delta_x = \frac{x_{max} - x_{min}}{n_x}; \quad j = 0, 1, 2, ..., n_x$$

$n_x + 1$ grid points

$$\phi_j \equiv \phi(x_j)$$

n_x distinct values (periodic)

$$k_n \equiv \frac{2\pi n}{n_x \Delta_x} \qquad n = -\frac{n_x}{2}, ..., 0, ..., \frac{n_x}{2}$$

The discrete transform is the defined by analogy to the continuous transform by:

$$\tilde{\phi}(k_n) = \int_{-\infty}^{\infty} dx\, e^{ik_n x}\phi(x) \iff \begin{aligned} \tilde{\phi}_n &\equiv \Delta_x \sum_{j=0}^{n_x} e^{ik_n(x_j - x_{\min})}\phi_j \\ &= \Delta_x \sum_{j=0}^{n_x} \exp\left(\frac{i2\pi nj}{n_x}\right)\phi_j \end{aligned}$$

Discrete Fourier Transform (3)

$$\begin{array}{ccc} \underline{\text{Grid}} & & \underline{\text{Transform}} \\ \phi_j & \Longleftrightarrow & \tilde{\phi}_n \\ (n_x + 1 \text{ values}) & & (n_x + 1 \text{ complex values}) \end{array}$$

Note that $\tilde{\phi}_n$ is periodic in *n* with period n_x

$$\tilde{\phi}_{-n} = \tilde{\phi}_{n_x - n}$$

- Let $n = 0, 1, 2, ..., n_x$ so *n* and *j* have the same ranges

Then an inverse transform can be constructed *exactly*:

$$\boxed{\phi_j = \frac{1}{n_x \Delta_x} \sum_{n=0}^{n_x} \exp\left(-\frac{i2\pi nj}{n_x}\right) \tilde{\phi}_n}$$

- This exact inversion is proved in the problems by summing a geometric series

Spectral Methods: Aliasing

The discrete transform describes a periodic problem if indices are extended
- Discretization errors (aliasing) can occur

Figure to be edited:

$$\lim_{x \to \pm\infty} \phi(x) = 0$$

Plots will be replaced with real transforms based on a Gaussian distribution in future versions of the notes

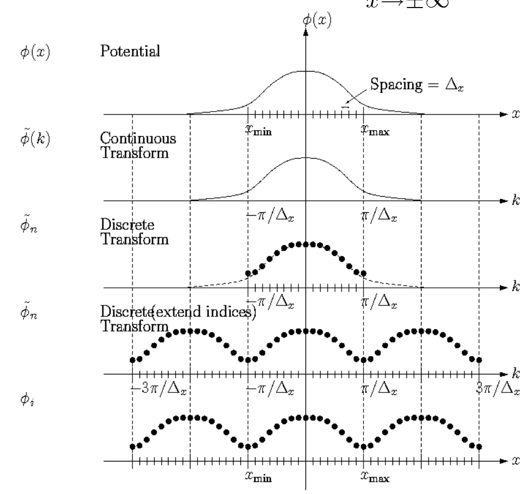

Discrete Transform Formulas

Application of the Discrete Fourier Transform to solve Poisson's Equation:

$$E_x = -\frac{d\phi}{dx} \quad \Longleftrightarrow \quad E_{xj} = -\frac{\phi_{j+1} - \phi_{j-1}}{2\Delta_x}$$

$$\frac{d^2\phi}{dx^2} = -\frac{\rho}{\epsilon_0} \quad \Longleftrightarrow \quad \frac{\phi_{j+1} - 2\phi_j + \phi_{j-1}}{\Delta_x^2} = -\frac{\rho}{\epsilon_0}$$

Applying the discrete transform yields:

$$\boxed{\tilde{E}_{xn} = i\kappa_n \tilde{\phi}_n \qquad \kappa_n = k_n \left[\frac{\sin(k_n \Delta_x)}{k_n \Delta_x}\right] \equiv k_n \text{dif}(k_n \Delta_x) \qquad k_n \equiv \frac{2\pi n}{(n_x+1)\Delta_x}}$$

Poisson's Equation becomes:

$$\boxed{\tilde{\phi}_n = \frac{\tilde{\rho}_n}{\epsilon_0 K_n^2} \; ; \quad K_n^2 \equiv k_n^2 \text{dif}^2(k_n \Delta_x/2) = k_n^2 \left[\frac{\sin(k_n \Delta_x/2)}{k_n \Delta_x/2}\right]^2}$$

Note: factors of K_n^2 need only be calculated once per simulation (store values)

Derivation of Discrete Transform Eqns.

/// Example Derivation of a formula for the discrete transformed E-field:

Discretized E-field $\quad E_{xj} = -\dfrac{\phi_{j+1} - \phi_{j-1}}{2\Delta_x}$

Transforms

$$\phi_j = \frac{1}{(n_x+1)\Delta_x} \sum_{n=0}^{n_x} \exp\left(-\frac{i2\pi nj}{n_x+1}\right) \tilde{\phi}_n$$

$$E_{xj} = \frac{1}{(n_x+1)\Delta_x} \sum_{n=0}^{n_x} \exp\left(-\frac{i2\pi nj}{n_x+1}\right) \tilde{E}_{xn}$$

Substitute transforms into difference formula:

$$2\Delta_x \sum_{n=0}^{n_x} \exp\left(-\frac{i2\pi nj}{n_x+1}\right) \tilde{E}_{xn}$$

$$= -\sum_{n=0}^{n_x} \exp\left(-\frac{i2\pi nj}{n_x+1}\right) \tilde{\phi}_n \left\{ \exp\left(-\frac{i2\pi n}{n_x+1}\right) - \exp\left(\frac{i2\pi n}{n_x+1}\right) \right\}$$

$$= \Delta_x \sum_{n=0}^{n_x} \exp\left(-\frac{i2\pi nj}{n_x+1}\right) \tilde{E}_{xn} = i \sum_{n=0}^{n_x} \exp\left(-\frac{i2\pi nj}{n_x+1}\right) \sin\left(\frac{2\pi n}{n_x+1}\right) \tilde{\phi}_n$$

$$\Delta_x \sum_{n=0}^{n_x} \exp\left(-\frac{i2\pi nj}{n_x+1}\right)\tilde{E}_{xn} = i\sum_{n=0}^{n_x}\exp\left(-\frac{i2\pi nj}{n_x+1}\right)\sin\left(\frac{2\pi n}{n_x+1}\right)\tilde{\phi}_n$$

This equation must hold true for each term in the sum proportional to $\exp\left(-\frac{i2\pi nj}{n_x+1}\right)$ to be valid for a general j.

$$\Rightarrow \tilde{E}_{xn} = \frac{i}{\Delta_x}\sin\left(\frac{2\pi n}{n_x+1}\right)\tilde{\phi}_n$$

$$k_n = \frac{2\pi n}{(n_x+1)\Delta_x}$$

$$\Rightarrow \boxed{\begin{aligned}\tilde{E}_{xn} &= ik_n\left[\frac{\sin(k_n\Delta_x)}{k_n\Delta_x}\right]\tilde{\phi}_n \\ &= ik_n \mathrm{dif}(k_n\Delta_x)\tilde{\phi}_n\end{aligned}}$$

///

Spectral Methods: Discrete Transform Field Solution

Typical discrete Fourier transform field solution (not optimized)

$$\boxed{\begin{array}{ccccccccc} & \text{Forward Transform} & & \text{Multiply} & & \text{Inverse Transform} & & \text{Finite Difference} & \\ \rho_j & \longrightarrow & \tilde{\rho}_n & \longrightarrow & \tilde{\phi}_n & \longrightarrow & \phi_j & \longrightarrow & E_{xj} \\ & \text{DFT} & & \cdot\dfrac{1}{K_n^2} & & \text{IDFT} & & & \end{array}}$$

- K_n^2 factors can be calculated once and stored to increase numerical efficiency

Discussion of Spectral Methods and the FFT

The Fast Fourier Transform (FFT) makes this procedure numerically efficient

- Discrete transform (no optimization), $\sim(n_x+1)^2$ complex operations
- FFT exploits symmetries to reduce needed operations to $\sim (n_x+1)ln(n_x+1)$
  - Huge savings for large n_x
- The needed symmetries exist only for certain numbers of grid points. In the simplest manifestations: $n_x + 1 = 2^p$, $p = 1, 2, 3, ...$
  - Reduced griding freedom
  - Other manifestations allow $n_x + 1 = 2^p$ and products of prime numbers for more possibilities

The FFT can be combined with other procedures such as capacity matrices to implement boundary conditions for interior conductors, etc.

- This allows rapid field solutions in complicated geometries when capacity matrix elements can be pre-calculated and stored

FFT is the fastest method for simple geometry

- Simple to code using typical numerical libraries for FFT's

S4D: Weighting: Depositing Particles on the Field Mesh and Interpolating Gridded Fields to Particles

We have outlined methods to solve the electrostatic Maxwell's equations on a discrete spatial grid. To complete the description we must:

- Specify how to deposit macro-particle charges and current onto the grid
- Specify how to interpolate fields on the spatial grid points to the macroparticle coordinates (not generally on the grid) to apply in the particle advance
- Smooth interactions resulting from the small number of macro-particles to reduce artificial collisions resulting from the use of an unphysically small number of macro-particles needed for rapid simulation

This is called the *particle weighting* problem

Weighting (2)

Particle weighting problem for electrostatic fields

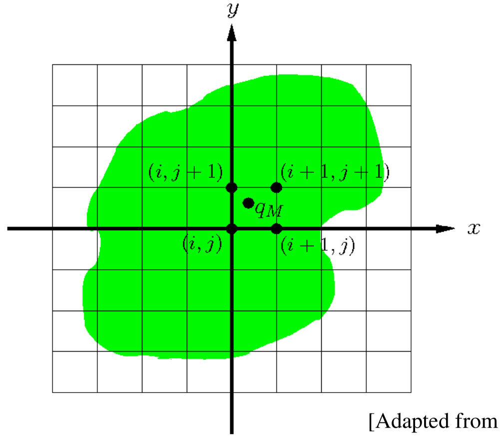

[Adapted from Birdsall and Langdon]

It is found that it is usually better to employ the same weighting schemes to deposit both the macro-particle charges and currents on the mesh and to extrapolate the fields at gridded points to the macro-particles

- Avoids unphysical self-forces where the particle accelerates itself

Weighting Methods

Many methods of particle weighting exist. They can be grouped into 4 categories:

1) Nearest Grid Point
2) Cloud in Cell (CIC)
  - Shaped particles
  - PIC method, linearly shaped particles
3) Multipole
  - Dipole, subtracted dipole, etc.
4) Higher order methods
  - Splines
  - ***k***-space cutoffs in discrete transforms
  - ⋮

Possible hybrid methods also exist. We will illustrate methods 1) and 2) for electrostatic problems. Descriptions of other methods can be found in the literature.

Weighting: Nearest Grid Point

1) Nearest Grid Point: Assign charges to the nearest grid cell

- Fast and simple: Show for 1D; 2D and 3D generalization straightforward
- Noisy

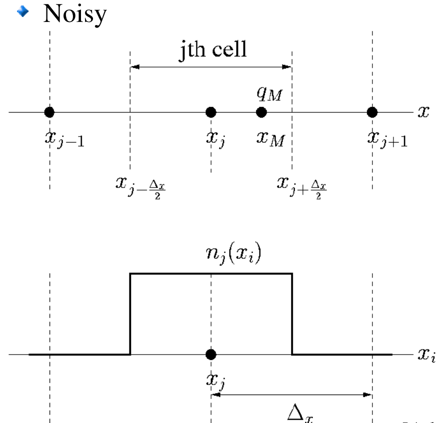

$q_M =$ Charge of macro-particle

$x_M =$ Coordinate of macro-particle

$x_j =$ Closest grid cell

Charge Deposition:

$$q_j = q_M$$

Field "Interpolation":

$$E_x|_{x=x_M} = E_{xj}$$

[Adapted from Birdsall and Langdon]

Comments:

- Currents can be interpolated to grid similarly for electromagnetic solving and/or diagnostics

Weighting : Cloud in Cell

2) Cloud in Cell: Shaped macro-particles pass freely through each other

- Smoother than Nearest Grid Point, but more numerical work
- For linear interpolation results in simple, commonly used "Particle in Cell" (PIC) method

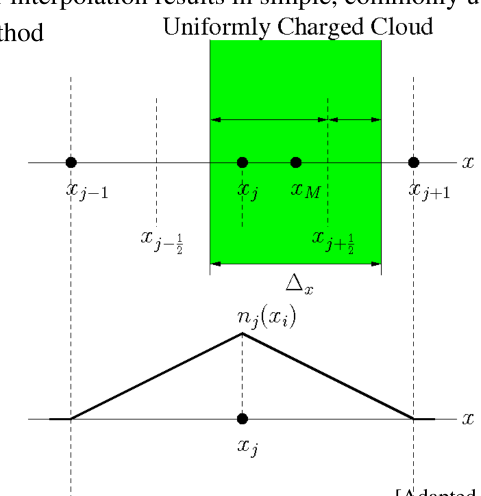

[Adapted from Birdsall and Langdon]

Cloud in Cell (2)

$$q_M \ , \ x_M = \text{Charge and coordinate of macro-particle}$$
$$x_j = \text{Closest grid cell}$$

Charge Deposition:

$$q_j = q_M \left[\frac{\Delta_x - (x_M - x_j)}{\Delta_x} \right] = q_M \frac{x_{j+1} - x_M}{\Delta_x}$$

$$q_{j+1} = q_M \left[\frac{x_M - x_j}{\Delta_x} \right]$$

Field Interpolation:

$$E_x|_{x=x_M} = \left[\frac{x_{j+1} - x_M}{\Delta_x} \right] E_j + \left[\frac{x_M - x_j}{\Delta_x} \right] E_{j+1}$$

Comments:

- Linear interpolation results in triangularly shaped particles
- Shape smooths interactions reducing collisionality
  - Vlasov evolution with limited number of shaped particles
- Simple shape is fast to calculate numerically
- Currents can be interpolated to grid similarly for electromagnetic solving and/or diagnostics

Weighting: Area Weighting

In a 2D cloud-in-cell system, weighting is accomplished using rectangular "area weighting" to nearest grid points

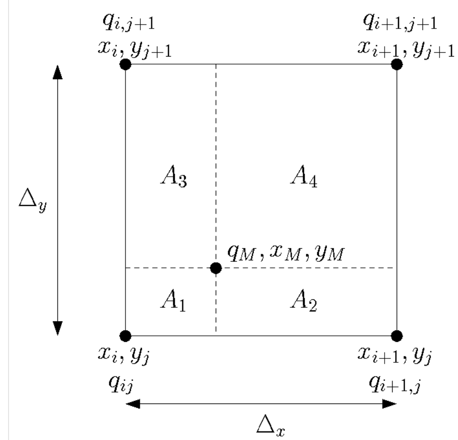

$$q_M = \text{Macro-particle charge}$$
$$(x_M, y_M) = \text{Macro-particle coordinates}$$

$$q_{ij} = \text{Mesh charges}$$

Area Weighting (2)

Charge Deposition:

$$q_{ij} = \left(1 - \frac{A_1}{\Delta_x \Delta_y}\right) q_M \qquad A_1 = (x_M - x_i)(y_M - y_j)$$

$$q_{i+1,j} = \left(1 - \frac{A_2}{\Delta_x \Delta_y}\right) q_M \qquad A_2 = (x_{i+1} - x_M)(y_M - y_j)$$

$$q_{i,j+1} = \left(1 - \frac{A_3}{\Delta_x \Delta_y}\right) q_M \qquad A_3 = (x_M - x_i)(y_{j+1} - y_M)$$

$$q_{i+1,j+1} = \left(1 - \frac{A_4}{\Delta_x \Delta_y}\right) q_M \qquad A_4 = (x_{i+1} - x_M)(y_{j+1} - y_M)$$

Field Interpolation:

$$\mathbf{E} = \frac{A_4}{\Delta_x \Delta_y} \mathbf{E}_{ij} + \frac{A_3}{\Delta_x \Delta_y} \mathbf{E}_{i+1,j} + \frac{A_2}{\Delta_x \Delta_y} \mathbf{E}_{i,j+1} + \frac{A_1}{\Delta_x \Delta_y} \mathbf{E}_{i+1,j+1}$$

Comments:

- Easily generalized to 3D using volumes
- Currents can be interpolated to grid similarly for electromagnetic solving and/or diagnostics

Higher Order Weighting: Splines

To be added: Slide on Splines to
illustrate what is meant by higher order methods
Make Points:
- Requires more numerical work and harder to code
- Some schemes can introduce neg probability problems
- Should evaluate against simpler low order methods using same computer power to see which method wins.

S4E: Computational Cycle for Particle-In-Cell Simulations

We now have (simplified) notions of the parts that make up a Particle-In-Cell (PIC) simulation of Vlasov beam evolution

1) Particle Moving
2) Field Solver on a discrete grid
3) Weighting of particle and fields to and from the grid

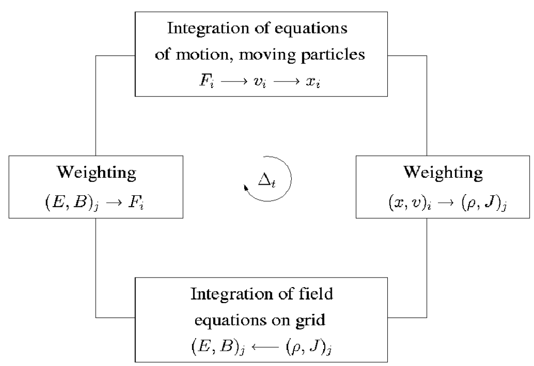

[Adapted from Birdsall and Langdon]

Computational Cycle for Particle-In-Cell Simulations Contd.

Comments:

- Diagnostics must also be accumulated for useful runs (see S5)
  - Particles (coordinates and velocities) and fields will need to be synchronized (common time) when diagnostics are accumulated
- Initial conditions must be set (particle load, see S6)
  - Particle and field variables may need appropriate de-synchronization to initialize advance

S5: Diagnostics

Diagnostics are *extremely* important. Without effective diagnostics even a correct and well converged simulation is useless. Diagnostics must be well formulated to display relevant quantities in a manner that increases physical understanding by highlighting important processes. This can be difficult since there can be a variety of issues and multiple effects taking place simultaneously.

Diagnostics can be grouped into two broad categories:

1) Snapshot Diagnostics
   - Examples: Particle distribution projections at a particular values of s or t
   - Data can be saved to generate plots after the run or just the needed plots can be generated during the run using linked graphics packages etc.

2) History Diagnostics
   - Examples: moments for the statistical beam centroid, envelope, and emittances
   - Data for history plots must be accumulated and saved over several simulation advance steps

See handwritten notes from USPAS 06 for remaining diagnostics slides

- Will be updated in future versions of the notes

S6: Initial Distributions and Particle Loading

To start the large particle or distribution simulations, the initial distribution function of the beam must be specified.

- For direct Vlasov simulations the distribution need simply be deposited on the phase-space grid

For PIC simulations, an appropriate distribution of macro-particle phase-space coordinates must be generated or "loaded" to represent the Vlasov distribution

Discussion:

In realistic accelerators, focusing elements are *s*-varying. In such situations there are no known smooth equilibrium distributions.

- The KV distribution is an exact equilibrium for linear focusing fields, but has unphysical (singular) structure in 4-dimensional transverse phase-space

Moreover, it is unclear in most cases if the beam is even best thought of as an equilibrium distribution as is typical in plasma physics. In accelerators, the beam in generally injected from a source and may only reside in the machine (especially for a linac) for a small number of characteristic oscillation periods and may not fully relax to an equilibrium like state within the machine.

Initial Distributions: Source-to-Target Simulations

The lack of known, physically reasonable equilibria and the fact that the beams are injected from a source motivates so-called "source-to-target" simulations where particles are simulated off the source and tracked to the target. Such first principles simulations are most realistic if carried out with the actual focusing fields, accelerating waveforms, alignment errors, etc. Source-to-target simulations are highly valuable to measure expected machine performance.

However, ideal source-to-target simulations can rarely be carried out due to:

- Source is often incompletely described
  - Example: important alignment and material errors may not be known
- Source may contain physics not adequately in imperfectly modeled
  - Example: plasma injectors with complicated material physics, etc.
- Computer limitations:
  - Memory required and simulation time
  - Convergence and accuracies
  - Limits of numerical methods applied

    Ex: singular description needed for Child-Langmuir model of space-charge limited injection

Initial Distributions: Types of Specified Loads

Due to the practical difficulty of always carrying out simulations off the source, two alternative methods are commonly applied:

1) Load an idealized initial distribution
   - Specify at some specific time
   - Based on physically reasonable theory assumptions
2) Load experimentally measured distribution
   - Construct/synthesize a distribution based on experimental measurements

Discussion:

The 2nd option of generating a distribution from experimental measurements, unfortunately, often has practical difficulties:

- Real diagnostics often are far from ideal 6D snapshots of beam phase-space
  - Distribution must be reconstructed from partial data
  - Typically many assumptions must be made in the synthesis process
- Process of measuring the beam can itself change the beam
- It can sometimes be helpful to understand processes and limitations starting from cleaner, more idealized initial beam states

Discussion Continued:

Because of the practical difficulties of loading a distribution based exclusively on experimental measurements, idealized distributions are often loaded:

- Employ distributions based on reasonable, physical ansatzes
- Use limited experimental measures to initialize:
  - Energy, current, rms equivalent beam sizes and emittances
- Simpler initial state can often aid insight:
  - Fewer simultaneous processes can allow one to more clearly understand how limits arise
  - Seed perturbations of relevance when analyzing resonance effects, instabilities, halo, etc.

A significant complication is that there are no known exact smooth equilibrium distribution functions valid for periodic focusing channels:

- Approximate theories valid for low phase advances may exist Davidson, Struckmeier, and others

Formulate a simple approximate procedure to load an initial distribution that reflects features one would expect of an equilibrium

Initial Distributions Based on Continuous Focusing Equilibria

Simple psudo-equilibrium initial distribution:

- Use rms equivalent measures to specify the beam
  - Natural set of parameters for accelerator applications
- Map rms equivalent beam to a smooth, continuous focused matched beam
  - Use smooth core models that are stable in continuous focusing:
    - Waterbag Equilibrium
    - Parabolic Equilibrium
    - Thermal Equilibrium
    - ⋮

    } See Notes on: *Transverse Equilibrium Distributions*
- Transform continuous focused beam for rms equivalency with original beam specification
  - Use KV transforms to preserve uniform beam Courant-Snyder invariants

Procedure will apply to any s-varying focusing channel

- Focusing channel need not be periodic
- Beam can be initially rms equivalent matched or mismatched if launched in a periodic transport channel
- Can apply to both 2D transverse and 3D beams

Procedure for Initial Distribution Specification

Assume focusing lattice is given:

$$\boxed{\kappa_x(s), \quad \kappa_y(s) \quad \text{specified}}$$

Strength usually set by specifying undepressed phase advances $\sigma_{0x}, \quad \sigma_{0y}$

Step 1:

For each particle (3D) or slice (2D) specify 2nd order rms properties at axial coordinate s

Envelope coordinates/angles:

$$r_x(s) = 2\langle x^2\rangle_\perp^{1/2} \qquad r'_x(s) = 2\langle xx'\rangle_\perp / \langle x^2\rangle_\perp^{1/2}$$
$$r_y(s) = 2\langle y^2\rangle_\perp^{1/2} \qquad r'_y(s) = 2\langle yy'\rangle_\perp / \langle y^2\rangle_\perp^{1/2}$$

Emittance:

$$\varepsilon_x(s) = 4[\langle x^2\rangle_\perp \langle x'^2\rangle_\perp - \langle xx'\rangle_\perp^2]^{1/2}$$
$$\varepsilon_y(s) = 4[\langle y^2\rangle_\perp \langle y'^2\rangle_\perp - \langle yy'\rangle_\perp^2]^{1/2}$$

Perveance:

$$Q = \frac{q\lambda(s)}{2\pi\epsilon_0 m\gamma_b^3(s)\beta_b^2(s)c^2}$$

Procedure for Initial Distribution Specification (2)

If the beam is rms matched, we take:

$$r''_x + \kappa_x r_x - \frac{2Q}{r_x + r_y} - \frac{\varepsilon_x^2}{r_x^3} = 0 \qquad \begin{aligned}\kappa_x(s+L_p) &= \kappa_x(s)\\ \kappa_y(s+L_p) &= \kappa_y(s)\end{aligned}$$

$$r''_y + \kappa_y r_y - \frac{2Q}{r_x + r_y} - \frac{\varepsilon_y^2}{r_y^3} = 0 \qquad \begin{aligned}r_x(s+L_p) &= r_x(s)\\ r_y(s+L_p) &= r_y(s)\end{aligned}$$

- Not necessary even for periodic lattices
  - Procedure applies to mismatched beams

Procedure for Initial Distribution Specification (3)

Step 2:

Define an rms matched, continuously focused beam in each transverse s-slice:

Continuous	s-Varying	
$r_b(s) =$	$\sqrt{r_x(s) r_y(s)}$	Envelope Radius
$\varepsilon_b(s) =$	$\sqrt{\varepsilon_x(s)\varepsilon_y(s)}$	Emittance
$Q(s) =$	$Q(s)$	Perveance

Define a (local) matched beam focusing strength in continuous focusing:

$$\cancel{r''_b} + k_{\beta 0}^2 r_b - \frac{Q}{r_b} - \frac{\varepsilon_b^2}{r_b^2} = 0$$

$$\boxed{k_{\beta 0}^2(s) = \frac{Q(s)}{r_b^2(s)} + \frac{\varepsilon_b^2(s)}{r_b^4(s)}}$$

Procedure for Initial Distribution Specification (4)

Step 3:

Specify an rms matched continuously focused equilibrium consistent with step 2:

Specify an equilibrium function:

$$\boxed{f_\perp(x, y, x', y') = f_\perp(H_\perp)} \qquad H_\perp = \frac{1}{2}\mathbf{x}_\perp'^2 + \frac{1}{2}k_{\beta 0}^2 \mathbf{x}_\perp^2 + \frac{q\phi}{m\gamma_b^3\beta_b^2 c^2}$$

and constrain parameters used to define the equilibrium function with:

$$\lambda = q\int d^2x \int d^2x'\ f_\perp(H_\perp) \qquad \text{Line Charge <--> Perveance}$$

$$r_b^2 = \frac{4\int d^2x\ \int d^2x'\ x^2 f_\perp(H_\perp)}{\int d^2x\ \int d^2x'\ f_\perp(H_\perp)} \qquad \text{rms edge radius}$$

$$\frac{\varepsilon_b^2}{r_b^2} = \frac{4\int d^2x\ \int d^2x'\ x'^2 f_\perp(H_\perp)}{\int d^2x\ \int d^2x'\ f_\perp(H_\perp)} \qquad \text{rms edge emittance}$$

- Constraint equations are generally highly nonlinear and must be solved numerically
  - Allows specification of beam with natural accelerations variables

Procedure for Initial Distribution Specification (5)

Load N particles in x,y,x',y' phase space consistent with continuous focusing equilibrium distribution $f_\perp(H_\perp)$

Step A (set particle coordinates):

Calculate beam radial number density *n*(*r*) by (generally numerically) solving the Poisson/stream equation and load particle *x*,*y* coordinates:

$$x = r\cos\theta$$

$$y = r\sin\theta$$

- Radial coordinates *r*: Set by transforming uniform deviates consistent with *n*(*r*)
- Azimuthal angles θ: Distribute randomly or space for low noise

Step B (set particle angles):

Evaluate $f_\perp(U, r)$ with $U = \sqrt{x'^2 + y'^2}$ at the particle *x, y* coordinates loaded in step A to calculate the angle probability distribution function and load *x', y'* coordinates:

$$x' = U\cos\xi$$

$$y' = U\sin\xi$$

- Radial coordinate *U*: Set by transforming uniform deviates consistent with $f_\perp(U, r)$
- Azimuthal coordinate ξ: Distribute randomly or space for low noise

Procedure for Initial Distribution Specification (6)

Step 4:

Transform continuous focused beam coordinates to rms equivalency in the system with s-varying focusing:

$$\boxed{\begin{aligned} x &= \frac{r_x}{r_b}x_i & y &= \frac{r_y}{r_b}y_i \\ x' &= \frac{\varepsilon_x}{\varepsilon_b}\frac{r_b}{r_x}x_i' + \frac{r_x'}{r_b}x_i & y' &= \frac{\varepsilon_y}{\varepsilon_b}\frac{r_b}{r_y}y_i' + \frac{r_y'}{r_b}y_i \end{aligned}}$$

Here, $\{x_i\},\ \{y_i\},\ \{x_i'\},\ \{y_i'\}$ are coordinates of the continuous equilibrium loaded

- Transform reflects structure of Courant-Snyder invariants

Comments on Procedure for Initial Distribution Specification

- Applies to both 2D transverse and 3D beams
- Easy to generalize procedure for beams with centroid offsets
- Generates a charge distribution with elliptical symmetry
  - Sacherer's results on rms equivalency apply
  - Distribution will reflect self-consistent Debye screening
- Equilibria are only pseudo-equilibria since transforms are not exact
  - Nonuniform space-charge results in errors
  - Transform consistent with preserved Courant-Snyder invariants for uniform density beams
  - Errors largest near the beam edge - expect only small errors for very strong space charge where Debye screening leads to a flat density profile with rapid fall-off at beam edge
- Many researchers have presented or employed aspects of the improved loading prescription presented here, including:

I. Hofmann, GSI	M. Reiser, U. Maryland	M. Ikigami, KEK
E. Startsev, PPPL	Y. Batygin, SLAC	

PIC simulations with the WARP code (see S9) were carried out to verify that the loading procedure results in less fluctuations and waves in self-consistent Vlasov evolutions from the load

Show evolutions from a matched load in a periodic FODO quadrupole transport lattice:

pseudo-thermal
semi-Gaussian (for contrast)

Find:

- Works well for $\sigma_0 \lesssim 85^\circ$
  - Should not work where beam is unstable and all distributions are expected to become unstable for $\sigma_0 >\sim 85^\circ$ see:

    Experiment: Tiefenback, Ph.D. Thesis, U.C. Berkeley (1986)
    Theory: Lund and Chawla, Proc. 2005 Part. Accel. Conf.

- Works better when matched envelope has less "flutter"
  - Solenoids: larger lattice occupancy η
  - Quadrupoles: smaller σ_0
  - Not surprising since less flutter" corresponds to being closer to continuous focusing

WARP PIC Simulation (see S9) Results – Pseudo Thermal Equilibrium

$$\sigma_0 = 70^\circ, \quad L_p = 0.5 \text{ m}, \quad \varepsilon_x = \varepsilon_y = 50 \text{ mm-mrad}$$

$\sigma/\sigma_0 = 0.2$

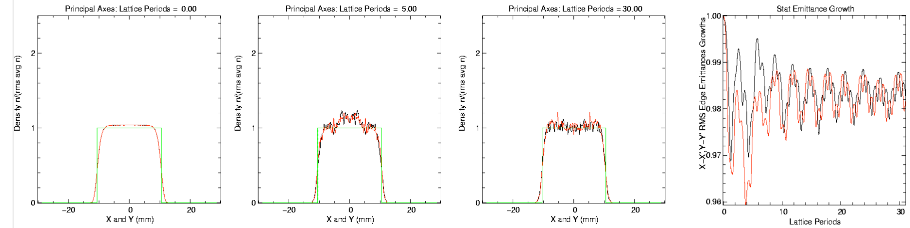

$\sigma/\sigma_0 = 0.7$

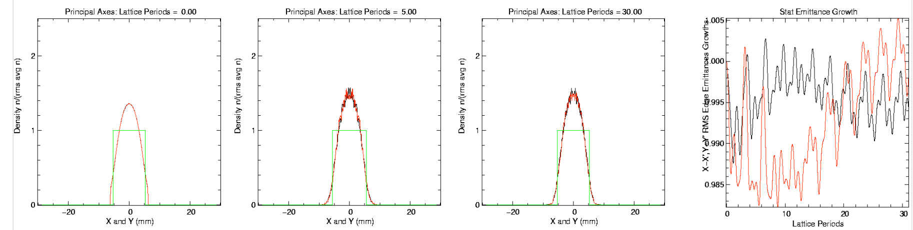

WARP PIC Simulation (see S9) Results – Semi-Gaussian (for contrast)

$$\sigma_0 = 70^\circ, \quad L_p = 0.5 \text{ m}, \quad \varepsilon_x = \varepsilon_y = 50 \text{ mm-mrad}$$

$\sigma/\sigma_0 = 0.2$

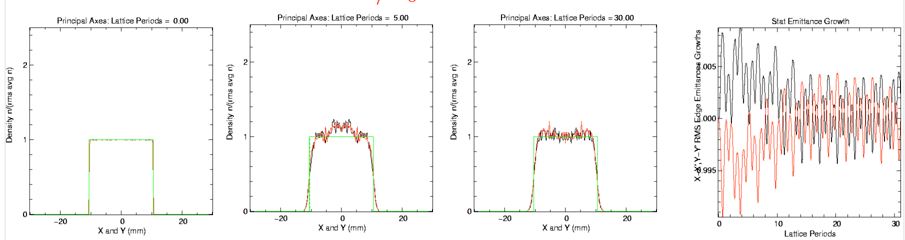

$\sigma/\sigma_0 = 0.7$

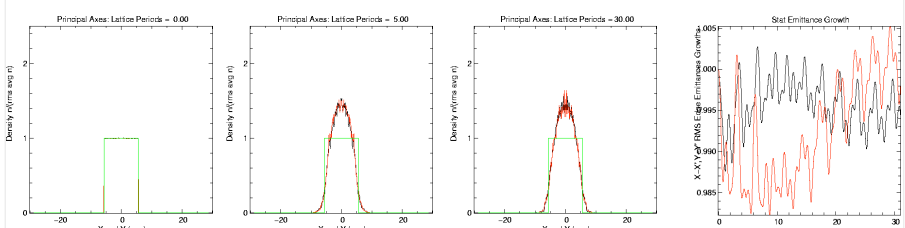

See handwritten notes from USPAS 06 for remaining distribution loading slides

- Will be updated in future versions of the notes

Initial Loads: The Semi-Gaussian Distribution

See handwritten notes from USPAS 06

- Will be updated in future versions of the notes

S7: Numerical Convergence

Numerical simulations must be checked for proper resolution and statistics to be confident that answers obtained are correct and physical:

Resolution of discretized quantities

- Time t or axial s step of advance
- Spatial grid of fieldsolve
- For direct Vlasov: the phase-space grid

Statistics for PIC

- Number of macroparticles used to represent Vlasov flow to control noise

Increased resolution and statistics generally require more computer resources (time and memory) to carry out the required simulation. It is usually desirable to carry out simulations with the minimum resources required to achieve correct, converged results that are being analyzed. Unfortunately, there are no set rules on adequate resolution and statistics. What is required generally depends on:

- What quantity is of interest
- How long an advance is required
- What numerical methods are being employed .....

General Guidance on Numerical Convergence Issues

Although it is not possible to give detailed rules on numerical convergence issues, useful general guidance can be given:

- Find results from similar problems using similar methods when possible
- Analyze quantities that are easy to interpret and provide good measures of convergence for the use of the simulation
  - Some moments like rms emittances:

$$\epsilon_x = 4\left[\langle \tilde{x}^2 \rangle_\perp \langle \tilde{x}'^2 \rangle_\perp - \langle \tilde{x}\tilde{x}' \rangle_\perp^2\right]^{1/2} \qquad \begin{aligned} \tilde{x} &\equiv x - \langle x \rangle_\perp \\ \tilde{x}' &\equiv x' - \langle x' \rangle_\perp \end{aligned}$$

  can provide relatively sensitive and easy to interpret measures of relative phase-space variations induced by numerical effects when plotted as overlaid time (or s) evolution "histories"
- Benchmark code against problems with known analytical solutions and properties
  - Apply a variety of numerical methods to judge which applies best
- Benchmark code against established, well verified simulation tools
  - Use different numerical methods expected to be more or less accurate

- Recheck convergence whenever runs differ significantly or when different quantities are analyzed
  - What is adequate for one problem/measure may not be for another
  - Ex: rms envelope evolution easier to converge than collective modes
- Although it is common to increase resolution and statistics till quantities do not vary, it is *also* useful to purposefully analyze poor convergence so characteristics of unphysical errors can be recognized
  - Learn characteristic signature of failures to resolve effects so subtle onset issues can be recognized more easily
- Expect to make *many* setup, debugging, and convergence test runs for each useful series of simulations carried out

See handwritten notes from USPAS 06 for remaining slides

- Will be updated in future versions of the notes

S8: Practical Considerations:
A: Overview

Intense beam simulation problems can be highly demanding on computer resources – particularly for realistic higher dimensional models. The problem size that can be simulated is dictated by computer resources available in fast memory and the run time required to complete the simulation

- Fast Memory (RAM)
- Wall Clock Run Time (Computer Speed)

Both of these can depend strongly on the architecture of computer system that the problem is run on:

- Serial Machine
- Parallel Machine

can strongly influence the size of the problem that can be simulated. We will present rough estimates of the computer memory required for simulations and provide some guidance on how the total simulation time can scale on various computer systems. The discussion is limited to PIC and direct Vlasov simulations.

S8B: Practical Considerations: Fast Memory

Fast computer memory (RAM) dictates how large a problem can be simulated

- If a problem will not fit into fast memory (RAM), computer performance will be severely compromised
- Writes to hard disks are slow

There are 3 main contributions to the problem size for typical PIC or direct Vlasov simulations:

1) Particle Phase Space Coordinates (PIC) or Discretized Distribution Function (Direct Vlasov)
2) Gridded Field
3) General Code Overhead

These three contributions to memory required are discussed in turn

Particle and field quantities are typically stored in double precision:

	Representation	Digits (Floating Point)	Bytes Memory
	Single Precision	8	4
Most problems	Double Precision	16	8

Estimates of Required Fast Memory

1) Particle Phase Space Coordinates (PIC):

B = bytes of floating point number (typically 8 for double precision)

N_p = number macro particles (0 for direct Vlasov)

D = dimension of variables characterizing particles

$$\boxed{\text{Memory} = B * N_p * D \text{ Bytes}}$$

The dimension D depends on the specific type of PIC simulation and methods employed

/// Common Examples of D:

3D PIC: $D = 7$

$x,\ y,\ z$

$p_x,\ p_y,\ p_z,\ \gamma^{-1}$

2D Transverse Slice PIC: $D = 5$

$x,\ y$

$p_x,\ p_y, \gamma^{-1}$ + p_z (D=6) some models

γ^{-1} is often included often to optimize the mover ///

Estimates of Required Fast Memory

1) Discretized Distribution Function (Direct Vlasov):

B = bytes of floating point number (typically 8 for double precision)

N_{pm} = number mesh points of grid describing the discretized particle phase space

$$\boxed{\text{Memory} = B * N_{pm} \quad \text{Bytes}}$$

The value of N_{pm} depends critically on the dimensionality of the phase space

// Examples of N_{pm} scaling for a uniform phase-space meshes:

Problem	Phase Space	N_{pm}	Scaling ($n_x = n_{p_x} \equiv n$ etc)
1D $\parallel$	$z - p_z$	$n_z n_{p_z}$	n^2
2D $\perp$ Slice	$x - p_x,\ y - p_y$	$n_x n_y n_{p_x} n_{p_y}$	n^4
2D Slice	$x - p_x,\ y - p_y,\ p_z$	$n_x n_y n_{p_x} n_{p_y} n_{p_z}$	n^5
3D	$x - p_x,\ y - p_y\ z - p_z$	$n_x n_y n_{p_x} n_{p_y}$	n^6

$$n_x = \text{number mesh points in } x \text{ etc.}$$

Rapid growth of N_{pm} with dimensionality severely limits tractability of problems

Memory required for a double precision (B = 8) uniform phase-space grid with 100 zone discretization per degree of freedom:

$$n_x = n_{p_x} \equiv n = 100 \ \text{ etc.}$$
$$\text{D} = \text{dimension of phase-space}$$

$$\text{Memory} = 8 * n^D \ \text{Bytes}$$

Problem	D	Memory (Bytes) (n = 100)
1D $\parallel$	2	$80 \times 10^3 \sim 80$ KB
2D $\perp$ Slice	4	$80 \times 10^6 \sim 80$ MB
2D Slice	5	$80 \times 10^9 \sim 80$ GB
3D	6	$8 \times 10^{12} \sim 8000$ GB

//

Rapidly increasing problem size with phase-space dimension D practically limits what can be simulated on direct Vlasov models with reasonable resolution *even on large parallel computers*:

- Irregular phase-space grids that place resolution where it is needed can partially alleviate scaling problem
- Optimal methods must also only grid minimal space exterior to the oscillating beam core in alternating gradient lattices

2) Gridded Field:

Required memory for a gridded field solve depends on the class of field solve (electrostatic, electromagnetic), mesh size, and numerical method employed. For a concrete illustration, consider *electrostatic* problems using a simple FFT field solve:

- Discrete Fourier Transform complex, but transform is of real functions. Proper optimization allows use of transforms using only real ϕ and ρ arrays
- Electric field is typically not stored and is calculated for each particle only where it is needed. Spatial grid location need not be stored.
  - Some methods store gridded E to optimize specific problems

N_{fm} = number mesh points of field spatial grid

$$\boxed{\text{Memory} = 2 * B * N_{fm} \quad \text{Bytes}}$$

Factor of 2 for: ρ, ϕ

Number of mesh points N_{fm} depends *strongly* on the dimensionality of the field solve and the structure of the mesh

- Generally more critical to optimize storage and efficiency (see next section) of fieldsolvers in higher dimensions

Examples for uniform meshes:

$$N_{fm} = n_z \qquad \text{1D (Longitudinal)}$$
$$= n_x n_y \qquad \text{2D (Transverse Slice)}$$
$$= n_x n_y n_z \qquad \text{3D}$$

$$n_x = \text{number mesh points in } x \text{ etc.}$$

3) General Code Overhead:

System memory is also used for:

- Scratch arrays for various numerical methods (fieldsolvers, movers, etc.)
- History accumulations of diagnostic moments
- Diagnostic routines
- Graphics packages, external libraries, etc.
  - Graphics packages can be large!

$$\text{Memory} = M_{overhead} \quad \text{Bytes}$$

Characteristic of packages used, size of code, and methods employed. But typical numbers can range 1 MB – 20 MBytes

Summary: Total Memory Required:

For illustrative example, add contributions for electrostatic PIC

PIC: $\quad \text{Tot Memory} = B * (N_p * D + 2 * N_{fm}) + M_{overhead}$ Bytes

Direct Valsov: $\quad \text{Tot Memory} = 2 * B * (N_{pm} + N_{fm}) + M_{overhead}$ Bytes

Reminder: Machine fast memory (RAM) capacity *should not be exceeded*

- Storing data on disk and cycling to RAM generally too slow!

S8C: Practical Considerations: Run Time

Run time can depend on many factors including:

- Type of problem
- Dimensionality of problem and number of particles and/or mesh points
- Numerical methods employed (particle moving, fieldsolve, ...)
- Moments and diagnostics accumulated
- Architecture/speed of computer system

It is not possible to give fully general guidance on estimating run times. However, to better characterize the time required, it can be useful to benchmark the code on the computer to be employed in terms of:

t_{step} = Time for an "ordinary" run step

Generally, parts of the code that more time is spent in should be more carefully optimized to minimize total run time. Care should generally be applied with:

- Particle mover
- Field solver
- Frequent diagnostics such as moments

Diagnostics, loaders, problem setup routines, etc. can often be coded with less care for optimization since they are only executed infrequently. However:

- Diagnostics often take a large amount of development time
  - Often better to code as simply as possible!

Software profiling tools can be useful to best understand where "bottlenecks" occur so effort on optimization can be appropriately directed for significant returns.

Dimenstionality plays a strong role in required run time

Some general guidance for electrostatic PIC Simulations:

1D: (Longitudinal typical)

Fieldsolve generally fast: small fraction of time compared to moving particles

- Green's function methods can be used (Gauss Law)

2D: (Transverse slice typical)

Fieldsolve typically a small fraction of time relative to moving particles if fast gridded methods are applied (like FFT based methods)

- Special boundary conditions can increase the fraction

Method	Numerical Work
FFT with Periodic BC	Small fraction of particle moving
FFT with Capacity Matrix	.
SOR	.
.	.
Green's Function	Dominates particle moving

3D:

Fieldsolve typically comparable in time or dominates time for particle moving even if fast, gridded methods are applied

- Fieldsolve efficiency of *critical* importance in 3D to optimize run time
- Whole classes can be taught just on methods of 3D electrostatic field solves for Poission's equation

Some general guidance for Direct Vlasov Simulations:

The rapid growth of the problem size with the phase space-dimension and available fast computer memory can severely limit problem sizes that can be simulated:

- Numerical work can be significant to advance the discretized distribution over characteristics
- Size of gridded field arrays can be very large leading to slow advances
  - Uniform mesh: D

The type of computer system employed can also strongly influence run time

- Processor Speed
- Memory Speed
  - RAM
  - Fast, optimized cache memory
- System Architecture (see next section)
  - Serial
  - Parallel
- Library Optimization
  - Especially for parallel machines

S8D: Practical Considerations: Machine Architectures

Problems may be simulated on:

1) Serial Machines
   - Single processor or an independently run processor on a multi-processor machine (example: most present multi-"core" processors)

2) Parallel Machine
   - Multi-processors coordinated to work as a large single processor
   - Usually employ independent memory for each processor making up the machine but sometimes uses shared memory among processors

Serial machines represent traditional computers (PCs workstations, etc), whereas parallel machines are generally less familiar.

Overview of parallel simulations:

In recent years parallel machines have significantly improved with libraries that allow more "natural" problem formulation with less effort and they are enabling significantly larger simulations to be carried out

- Several 100 million particles typically practical to simulate on large machines

Typical Parallel Machine Architecture

Beam problems may often be conveniently partitioned among processors in terms of axial slices. Schematic example (5 processors):

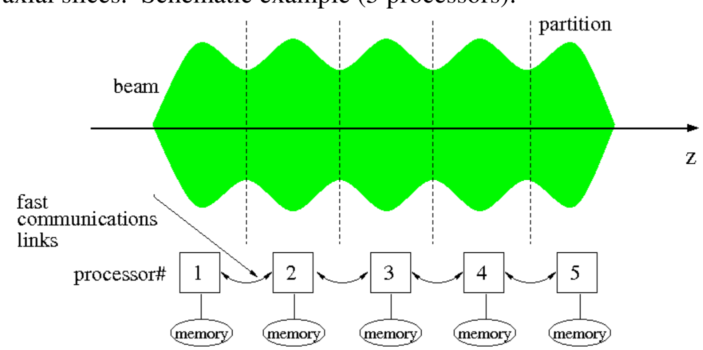

- Sharing of data at boundaries is necessary for fieldsolve
- Problems with axial velocity spread will generally require sorting of particles to maintain the load balance between processors
  - Processors should ideally all perform an equal amount of work since the slowest will dictate the total time of the advance step

Ideal parallelization will result in a linear speedup with processor number

- Actual speedup less due to:
  - Overhead in data transfers
  - Lack of ideal load balance causing processors to wait on the slowest one that the problem is partitioned among

$$\tau_{\text{step}} = \text{Time "ordinary" step in compuational cycle}$$
$$t_{\text{sim}} = \frac{\text{Simulation Time}}{\tau_{\text{step}}}$$

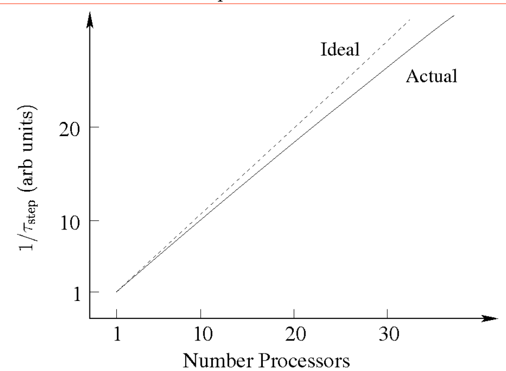

Even with the significant advances in problem size and speed promised by parallel computers, the solution of realistic 3D beam problems with direct (not gridded) fields remains far too large a problem to simulate with present coputer systems. Thus, for detailed simulations, we often push computer resources to the maximum extent possible.

- Better numerical algorithms
- Parallelization
- ....

S9: WARP Code Overview

See handwritten notes from USPAS 06 for remaining slides

- Will be updated in future versions of the notes

S10: Example Simulations

Examples to this point have mostly been simply formulated to illustrate concepts. Here, we present results from more complex simulations carried out in support of experiments, theory, and for machine design. Simulations highlighted include:

- Electrostatic Quadrupole Injector
- Multi-beamlet Injector
- Collective Mode Effects
- Detailed Transport Lattice Design
- Transport Limits in Periodic Quadrupole Focusing Channels
- Electron Cloud Effects for Ion Beam Transport

All these simulations, as well as many of the preceding illustrations in the lecture notes, were produced with the WARP code described in S9. Only select issues from the problems are highlighted.

Example: Electrostatic Quadrupole Injector

See handwritten notes from USPAS 06 for remaining slides

- Will be updated in future versions of the notes

These slides will be corrected and expanded for reference and any future editions of the US Particle Accelerator School class: *Beam Physics with Intense Space Charge*, by J.J. Barnard and S.M. Lund

Corrections and suggestions are welcome. Contact:

Steven M. Lund
Lawrence Berkeley National Laboratory
BLDG 47 R 0112
1 Cyclotron Road
Berkeley, CA 94720-8201

SMLund@lbl.gov
(510) 486 – 6936

Acknowledgments

Sven Chilton (UCB, LLNL) assisted in the development of part of these lecture notes and in generating some of the numerical examples and figures

Special thanks are deserved for Alex Friedman, Dave Grote, and Jean-Luc Vay of the Lawrence Livermore and Lawrence Berkeley National Laboratories for help with these notes and extensively educating the authors in simulation methods.

Rami Kishek (UMD) assisted teaching a version of this class and contributed to the notes. Irving Haber (UMD), Christine Celata (LBL), and Bill Fawley (LBL) helped educate the authors on various simulation methods.

Michiel de Hoon helped with an early version of the lectures and with example Lagrangian methods.

References: For more information see:

Numerical Methods

Forman S. Acton, *Numerical Methods that Work*, Harper and Row Publishers, New York (1970)

Steven E. Koonin, *Computational Physics*, Addison-Wesley Publishing Company (1986)

W. Press, B. Flannery, S. Teukolsky, W. Vetterling, *Numerical Recipes in C: The Art of Scientific Computing*, Cambridge University Press (1992).

Particle Methods

C.K. Birdsall and A.B. Langdon, *Plasma Physics via Computer Simulation*, McGraw-Hill Book Company (1985).

R.W. Hockney and J.W. Eastwood, *Computer Simulation using Particles*, Institute of Physics Publishing (1988).

US Particle Accelerator School 2008 S.M. Lund 28/

Simulation Techniques – Supplement.

§5 Diagnostics:

Depend on what is analyzed. Typical choices:

- Moments – statistical sums over the particle distribution (slices and full beam), often plotted as time histories as the beam evolves in the accelerator:

centroid: $x_c = \langle x \rangle_\perp$ ......

RMS Widths: Beam Size $r_x = 2\langle (x-x_c)^2 \rangle^{1/2}$, ... etc.

Emittance: $\varepsilon_x = 16\left[\langle (x-x_c)^2\rangle\langle (x'-x_c')^2\rangle - \langle (x-x_c)(x'-x_c')\rangle^2\right]^{1/2}$,

etc.

Here; $\langle \cdots \rangle_\perp = \frac{1}{N_s}\sum_i^{\text{slice}} \{\cdots\}_i$ .... etc.

Slice emittance "history"

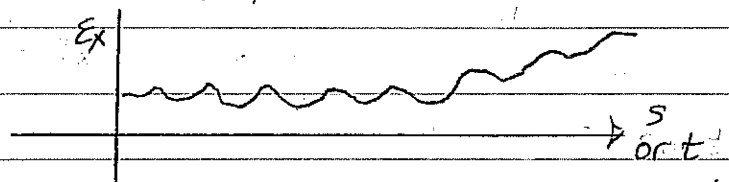

- Particle phase-space projections plotted as snapshots in time (x-x', y-y', x-y, x'-y', ...).

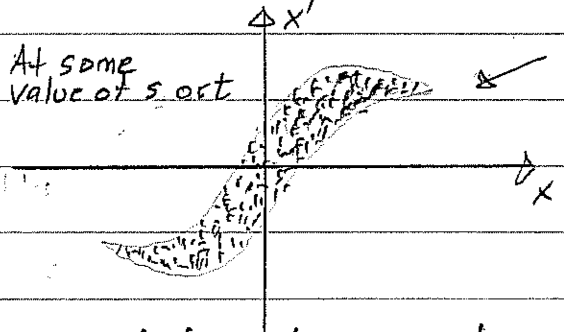

scatter plot of enough macro-particles to visualize the phase-volume and structure of the beam.

Plotting snapshots at periodic locations allows vizualization of the evolution of beam distortions:

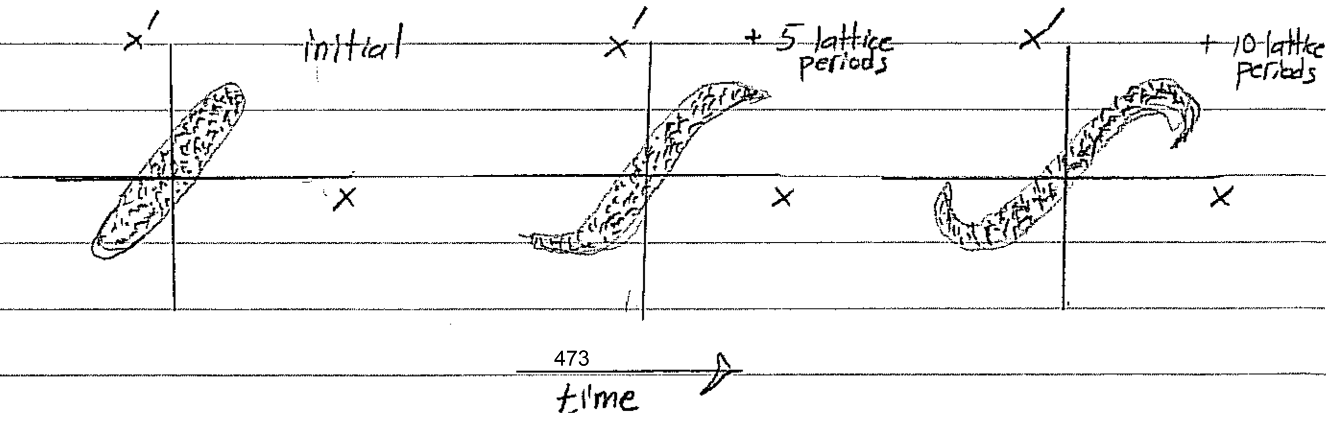

S.M. Lund #29

- Field Diagnostics:

Contours of self and applied fields illustrate field structure.

Examples:

1) Total potential contors of ϕ (self and applied) of an elliptical beam in an electric quadrupole formed by 4 biased rods.

same ϕ contours with beam particles plotted

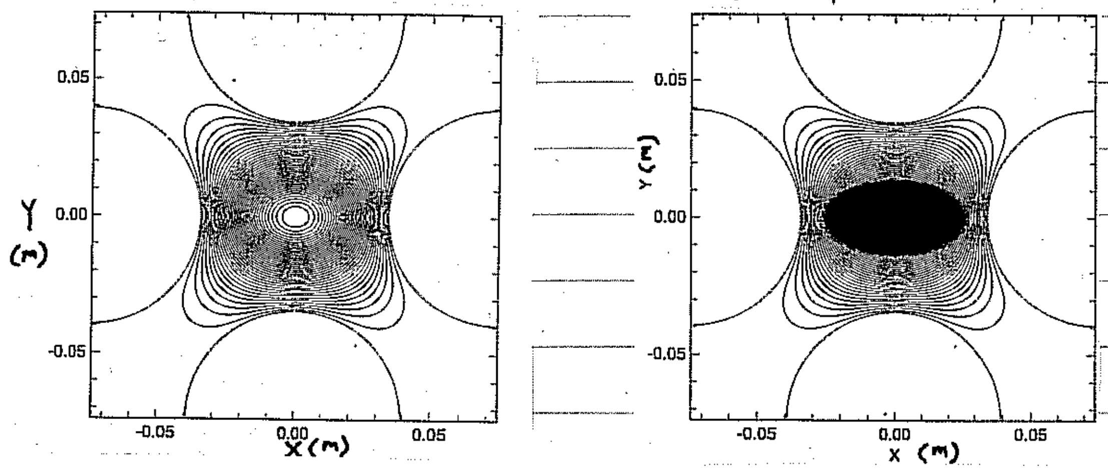

2) Applied Field   Scalar magnetic potential contours of a permanant magnet lense illustrate the structure of applied field nonlinearities:

8 Block Permanent Magnet Quadrupole.

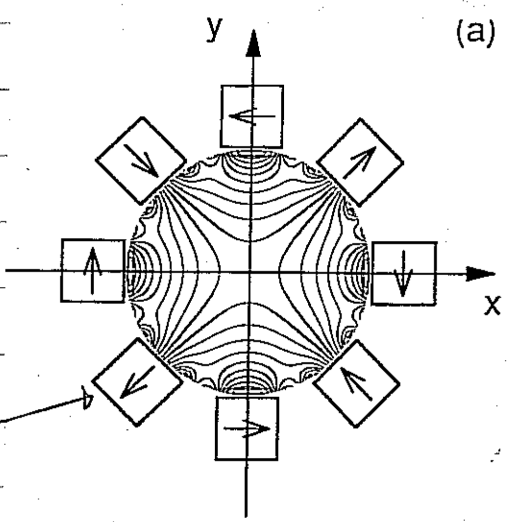

Note: contours deviate from hyperbolic near apeture edge.

Numerous other field diagnostics are possible:

- Field energy, multipole moments,

§6 Particle Loads

To start the simulation, one must specify and "load" the initial distribution function.

In realistic accelerators, focusing elements are s-varying. In such situations there are in general no known equilibrium distribution functions. Moreover, it is unclear in most cases if the beam is even best thought of as an equilibrium + perturbations as is typical in plasma physics. Rather, in accelerators, the beam is injected from a source and may only reside in the machine (especially a linac) for a small number of characteristic oscillation periods and may not fully relax to an equilibrium-like state. In such situations, so-called "source-to-target" simulations where the particles are simulated off the source and tracked to the target can be most realistic if carried out with realistic focusing fields, accelerating waveforms, alignment errors, etc.

Unfortunately, such idealized source-to-target simulations can rarely be carried out due to computer limitations.

- Memory limits
- Numerical convergance and accuracy ....

Two ways around this limitation:

1) Load experimentally measured distribution at some point in the machine and advance as an initial condition.
2) Load an idealized initial distribution.

The 1st option can have practical difficulties:

- Diagnostics often are far from an ideal 6D "snapshot" of the beam phase-space.
  - Much information typically lost.
- Process of measuring the beam can itself change the beam.

Most commonly, some experimental measures such as:

- rms beam sizes r_x, r_y, r_x', r_y'
- rms emittances $\varepsilon_x, \varepsilon_y$

are loaded in the form of idealized distributions.

It can be insightful to initialize the beam in a simplified manner

- Fewer simultaneous processes can allow one to more clearly see how limits arise.
- Seed perturbations of relevance when analyzing resonance effects, instabilities, halo, etc.

In these situations it is often useful to load a round, continuously focused distribution such as:

- Thermal Equilibrium
- Waterbag
- KV

and then transform the particle coordinates to "match" the local focusing structure of the lattice using a local KV envelope solution:

$$\frac{d^2}{ds^2} r_x(s) + \kappa_x(s) r_x(s) - \frac{2Q(s)}{r_x(s)+r_y(s)} - \frac{\varepsilon_x^2(s)}{r_x^3(s)} = 0$$

$$\frac{d^2}{ds^2} r_y(s) + \kappa_y(s) r_y(s) - \frac{2Q(s)}{r_x(s)+r_y(s)} - \frac{\varepsilon_y^2(s)}{r_y^3(s)} = 0$$

$\kappa_x(s), \kappa_y(s)$ = lattice focusing constants

$Q(s)$ = local perveance (specified)

$\varepsilon_x(s), \varepsilon_y(s)$ = local emittances (specified)

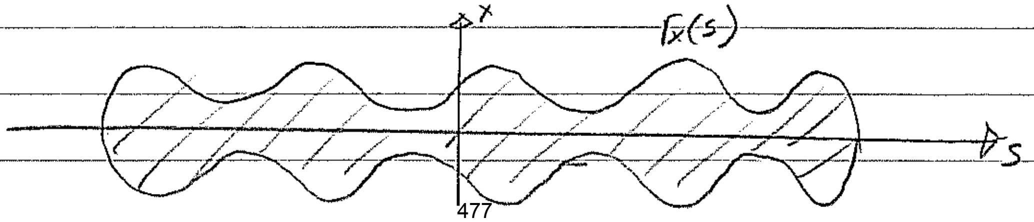

Procedure:

1st

Load in each $\perp$ slice round, continuous distribution:

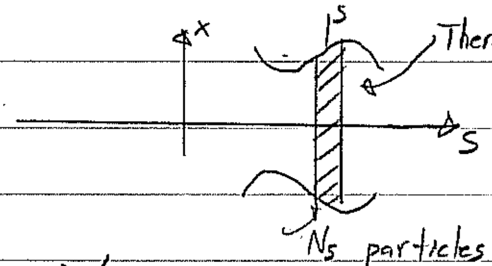

$$r_b = \sqrt{r_x r_y}$$
$$\varepsilon_b = \sqrt{\varepsilon_x \varepsilon_y}$$

$\Rightarrow$ $\vec{x}_i$, $\vec{x}_i'$ specified

2nd

Transform the spatial coordinates to match the elliptical envelope structure

$$x_i \longrightarrow \frac{r_x}{r_b} x_i$$

$$y_i \longrightarrow \frac{r_y}{r_b} y_i$$

3rd

Transform the local thermal velocity spreads to obtain the right average thermal force.

$$x_i' \longrightarrow \frac{\varepsilon_x}{\varepsilon_b} \frac{r_b}{r_x} x_i'$$

$$y_i' \longrightarrow \frac{\varepsilon_y}{\varepsilon_b} \frac{r_b}{r_y} y_i'$$

4th

Add the correct coherent velocity to match the needed envelope angle.

$$x_i' \longrightarrow x_i' + r_x' \frac{x_i}{r_x}$$

$$y_i' \longrightarrow y_i' + r_y' \frac{y_i}{r_y}$$

// Aside — The semi-Gaussian Distribution

It is not necessary to always load something based on a transformation of an equilibrium distribution to get a good quiescent load. Note that for high space-charge intensities:

- Beam space charge will be more or less uniform out to the edge, where the density will rapidly fall to zero.

- If the beam is injected off a uniform tempeture source or has relaxed, one expects roughly uniform thermal velocity spread across the cross-section of the beam.

This suggests the so-called "semi-Gaussian" load specified as follows:

- Uniform density within an elliptical beam envelope.

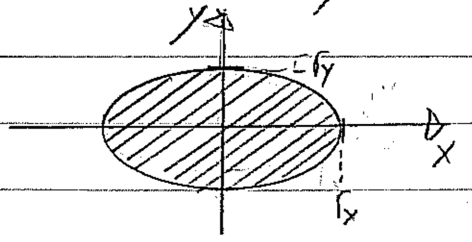

x_i, y_i uniformly distributed for $(x/r_x)^2 + (y/r_y)^2 \le 1$.

- Gaussian distributed thermal velocity spread with the correct coherent velocity to match the needed envelope angles

$$x_i' = r_x' \frac{x_i}{r_x} + \frac{\varepsilon_x}{2 r_x} \tilde{r}_{x_i}$$
$$y_i' = r_y' \frac{y_i}{r_y} + \frac{\varepsilon_y}{2 r_y} \tilde{r}_{y_i}$$

$\tilde{r}_{x,y}$ Gaussian distributed with unit variance $\left(\frac{1}{N_s} \sum_i^{\text{slice}} \tilde{r}_{x,y_i}^2 = 1 \right)$

The semi-Gaussian load results in "squared" initial x-x' and y-y' phase space projections:

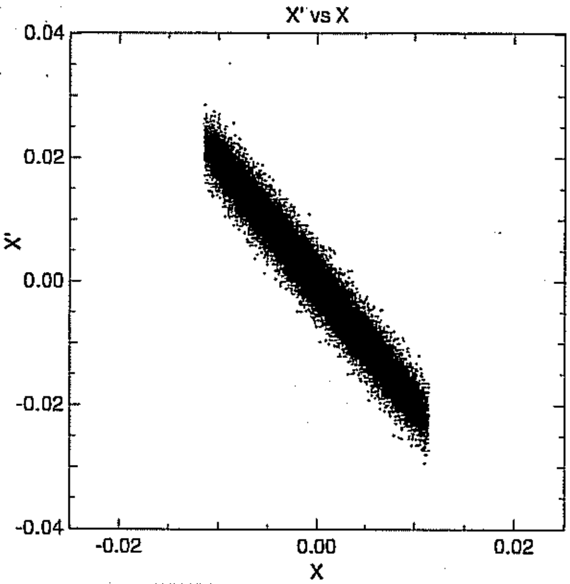

Initial load in a symmetric FODO AG Quadrupole transport lattice

The unphysical edges typically relax rapidly without perturbing the low order RMS structure of the beam (envelope match, emittance, etc.).

1 lattice period advance

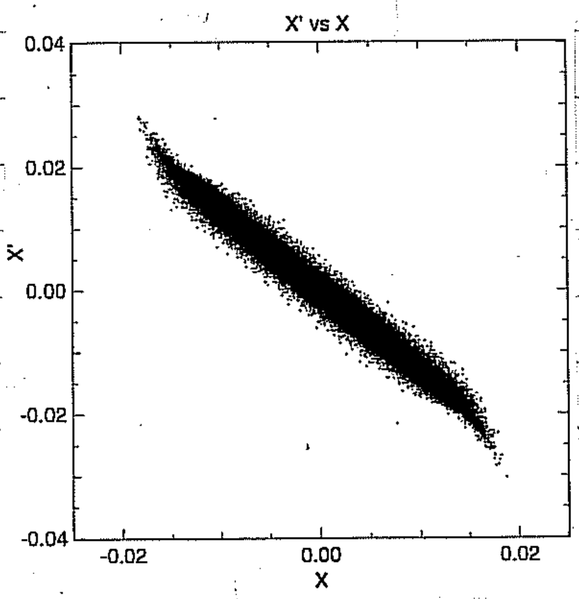

4 lattice period advance

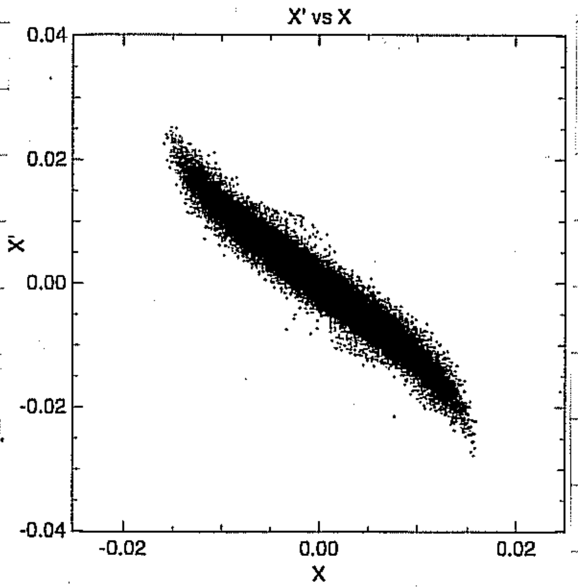

Numerous other loading techniques exist to address specific issues.

§7 Numerical Convergence

Numerical simulations must be checked for proper resolution and statistics to be confident that answers obtained are correct and physical.

Resolution on discritized quantities
- Time step in particle advance
- Spatial grid for fields

Statistics (number of macroparticles) to control noise.

More resolution and statistics require more computer time and memory. To be practical, one generally wishes to solve problems with the minimum resources required to achieve correct, converged answers. Unfortunately, there are no set rules on what resolution and statistics are required. This depends on what one is examining, how long the simulations are run, what numerical methods are employed, ...

Some general guidance:

- The statistical rms emittances:

$$\varepsilon_x = 4\left[\langle x^2\rangle_\perp \langle x'^2\rangle_\perp - \langle xx'\rangle_\perp^2\right]^{1/2}$$
$$\varepsilon_y = 4\left[\langle y^2\rangle_\perp \langle y'^2\rangle_\perp - \langle yy'\rangle_\perp^2\right]^{1/2}$$

often prove to be sensitive and easy to interpret measures of numerical differences when plotted as overlaid time histories.
  - picks up small phase space distortions induced by numerical errors.

general guidance continued ....

- To get started, find results from similar problems using similar methods.

- Benchmark code and methods against problems with known analytical solutions, established codes using both similar and different numerical methods, ...

- Recheck numerical convergence whenever runs differ significantly or when differing quantities are analyzed.

  - What is adequate for one measure of the beam (say image charge structure) may not be for another (say collective modes).

- Although it is common to increase resolution and statistics till relevant quantities do not vary, it is also useful to purposefully analyze poor resolution and statistics regimes so the characteristics of unphysical numerical errors can be recognized.

- Expect to make many setup, convergence, and debugging runs for each useful series of simulations carried out.

Specific Numerical Convergence Comments:

Time Resolution.

These comments are applicable to both spatial or time steps of the particle advance. We will frame estimates in terms of timesteps.

- Particle coordinates should not move through more than one cell in a single step. This is a standard "Courant" condition:

$$\boxed{\begin{aligned} v_x \Delta_t &< \Delta_x \\ v_y \Delta_t &< \Delta_y \\ v_z \Delta_t &< \Delta_z \end{aligned}}$$

for all particles.

- Enough steps should be taken to resolve variations in applied field structures.

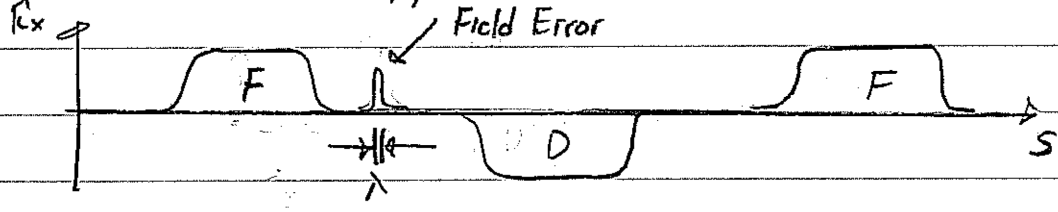

$$\boxed{v_s \Delta_t < \lambda}$$

; λ = shortest wavelength of field structures to be modeled

- Phase variations in collective waves (if of interest) should be resolved. For a leap-frog mover this requires:

ω = mode frequency component

$$\boxed{\frac{\omega_i \Delta_t}{2\pi} < \frac{1}{2}}$$

Spatial Resolution

For cold beams the beam edge can be sharp for most reasonable distribution functions:

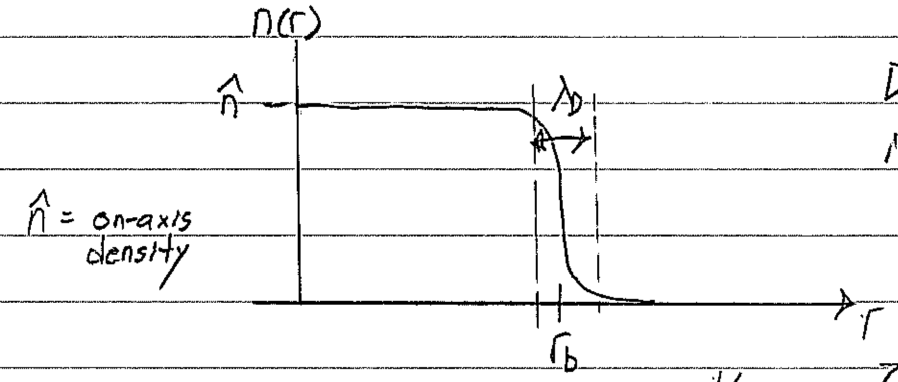

Density falls off in $\mathcal{O}(\lambda_D)$

Debye length: $\lambda_D = \dfrac{v_t}{\omega_p} = \left(\dfrac{\varepsilon_0 k_B T}{\hat{n} q^2}\right)^{1/2}$ $\qquad v_t = (k_B T/m)^{1/2}$, $\quad \omega_p = \left(\dfrac{q^2 \hat{n}}{\varepsilon_0 m}\right)^{1/2}$

$$r_b = \sim 5\lambda_D \rightarrow 30\lambda_D \quad \text{typical.}$$

To resolve edge physics, the mesh should have several cells across the rapid density variation near the edge of the beam.

$$\boxed{dx, dy < \frac{\lambda_{D x,y}}{2} \qquad \lambda_{D x,y} = \left(\frac{k_B T_{x,y}}{m}\right)^{1/2} \qquad T_{x,y} = \text{local kinetic temperature}}$$

The mesh should also resolve relevant spatial scales associated with processes of interest:

- If applied electrostatic fields are calculated from biased conductors, the mesh should resolve conductor structures or special corrections should be made.
- Self-field fluctuations induced by collective modes should be resolved.

Collective mode resolution: From Eigenfunctions to be presented later in the class:

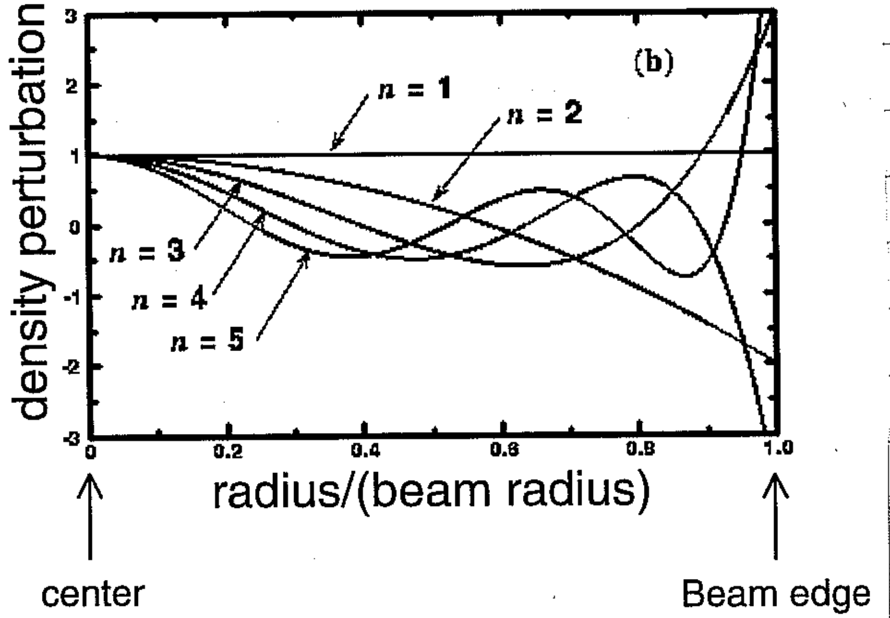

Collective mode density perturbations on a uniform density beam.

$\Rightarrow$ $dx, dy < \lambda$ ~ shortest characteristic wavelength of modes of interest.

Note that higher order modes (n larger) will become hard to resolve. Moreover, such perturbations also oscillate rapidly making time (s) stepsize resolution likewise difficult.

Statistics:

Collective effects typically require having a significant number of particles N_D within the characteristic screening radius characterized by the Debye length:

2D: $$N_D = \sum_i \int_{\substack{\text{circle} \\ |\vec{x}|<\lambda_D}} d^2x \; \delta^{(2)}(\vec{x}-\vec{x}_i) \gg 1$$

$\vec{x}_i$ = macro-particle coordinate.

3D: $$N_D = \sum_i \int_{\substack{\text{sphere} \\ |\vec{x}|<\lambda_D}} d^3x \; \delta^{(3)}(\vec{x}-\vec{x}_i) \gg 1$$

where:

$$\lambda_D = \frac{v_t}{\omega_p} = \left(\frac{\varepsilon_0 k_B T}{\hat{n} q^2}\right)^{1/2}$$

$$v_t = (k_B T/m)^{1/2}$$

$$\omega_p = \left(\frac{q^2 \hat{n}}{\varepsilon_0 m}\right)^{1/2}$$

$\sum_i \Rightarrow$ sum over all macro particles.

In simulations of higher order collective modes it may also be necessary to have a significant number of particles per cell on a mesh that resolves the relevant spatial variations of mode induced self-field fluctuations.

2D: $$N_{cell} = \sum_i \int_{cell} d^2x \; \delta^{(2)}(\vec{x}-\vec{x}_i) \gg 1$$

3D: $$N_{cell} = \sum_i \int_{cell} d^3x \; \delta^{(3)}(\vec{x}-\vec{x}_i) \gg 1$$

- Larger N_{cell} prevents local self-fields from being noise dominated.
- Larger N_{cell} leads to larger N_D, typically $N_D > N_{cell}$ since λ_D must be resolved on the grid.

Good statistics are <u>only</u> needed in the beam core with the possible exception of certain beam-halo problems and near the beam edge.

- Most beams will only occupy a fraction of the full grid.

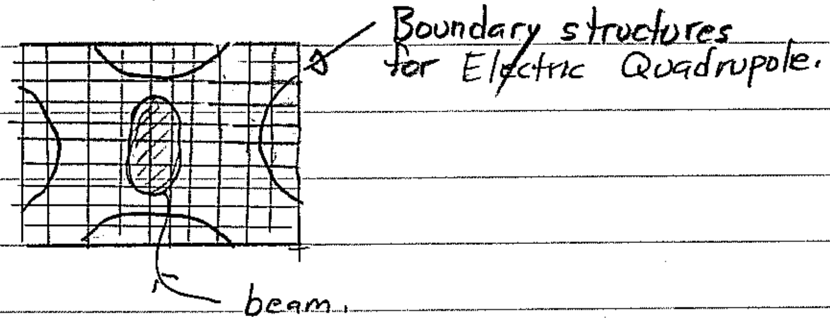

statistics should be evaluated in the cells that the beam occupies rather than average grid measures.

No comprehensive rules exist for how good the statistics must be. <u>Individual problems must be checked and verified.</u> Some general comments:

- What is adequate will typically depend on what is analyzed
  - Image fields may be resolved with few particles
  - Collective waves may take many particles if low noise (interpetable) diagnostic projections are needed.
- Longer runs generally require increased statistics
- Poor statistics result in unphysical collisionality that is often characterized by a linear rise in beam emittances with simulation time.

Classes of Particle Simulations.

How important is smoothing?

3D Beam: $N \sim 10^{10} - 10^{14}$ particles typical
Simulations: $N \lesssim 10^{8}$ practical (modern parallel computers) ; typical $10^3 - 10^6$

Each simulation particle may represent: $10^3 \rightarrow 10^{11}$ particles in the real beam for 3D simulations.

- Smoothing involved with particle weightings are key to obtaining physical answers. and limiting collisionality.

Is the situation really this bad?

- Lower dimensonal models typically simulated.

3D Model

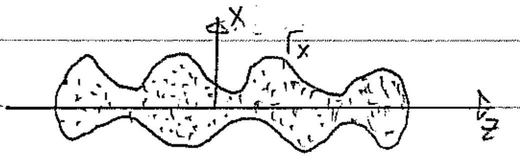

N point particles with smoothed interactions

Phase Space:

Physical Charge – point charges

$$\rho = \sum_i q\, \delta(x-x_i)\,\delta(y-y_i)\,\delta(z-z_i)$$

$\left.\begin{matrix} x, y, z \\ p_x, p_y, p_z \end{matrix}\right\}$ 6D

Smoothed charge

$$\rho = \sum_i q_M\, f(x-x_i, y-y_i, z-z_i)$$

q_M: Macro particle charge

f: smoothed shape function

2D ⊥ Thin Slice Model

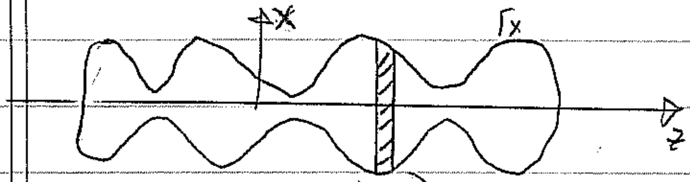

N line charges with smoothed interactions.

Thin slice
$\frac{\partial}{\partial z} << \nabla_\perp$

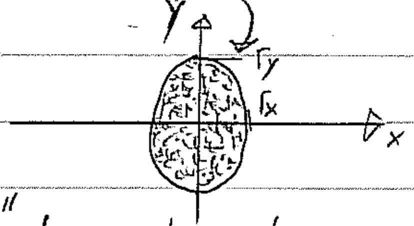

Phase Space:

$\left.\begin{matrix} x, y \\ p_x, p_y \end{matrix}\right\}$ 4D + possible 1D p_z

4D or 5D

"Physical" charge - line charges

$$\rho = \sum_i \lambda_p \delta(x-x_i)\delta(y-y_i)$$

Smoothed charge - λ_M : Macro particle line charge

$$\rho = \sum_i \lambda_M f(x-x_i, y-y_i)$$ f : smoothing function

The slice must be tracked in s with each particle moving the same increment in s with each step so that a slice maps to a slice.

- If p_z is included the velocity distribution must be assumed "frozen in".

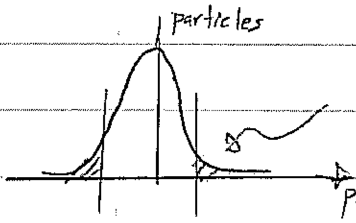

parts that would leave assumed replenished by particles from adjacent slices.

- Response to acceleration may be modeled with

- "Thick" slice models also possible with periodic boundary conditions, on the "slice" to try to recover some 3D effects of a long pulse in a periodic lattice.

2D r-z Model

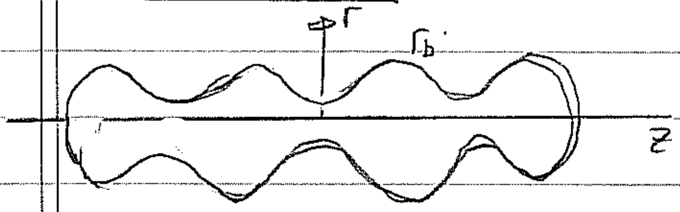

N charged Rings with smoothed interactions

$\partial/\partial\theta = 0$ Axisymmetric

Phase Space.

$\left.\begin{matrix} r, z \\ p_r, p_z \end{matrix}\right\}$ 4D + possible 1D p_θ (angular mom.)

4D or 5D.

physical charge - cylindrical rings

$$\rho = \sum_i \frac{Q_i}{2\pi} \frac{\delta(r-r_i)\delta(z-z_i)}{r_i}$$

smoothed charge

$$\rho = \sum_i \frac{Q_M}{2\pi} \frac{f(r-r_i, z-z_i)}{r_i}$$

Q_M : Macro particle charge
f : Smoothing function.

- Used to model solinoidal transport of an initial axisymmetric beam.
- Sometimes used to model AG beams with an approximately equivalent, s-dependant focusing force. $\vec{x}_\perp'' = k_{\beta 0}^2(s)\vec{x}_\perp + \ldots\ldots$

1D Axisymmetric Model

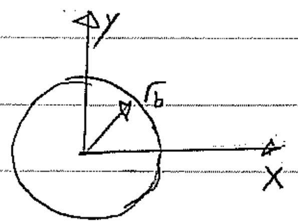

N charged cylinders with smoothed interactions

$\partial/\partial\theta = 0$

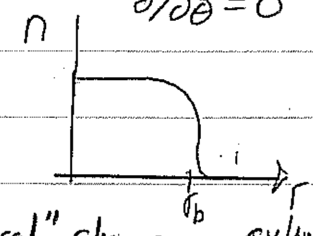

Phase - Space

$\left.\begin{matrix} r \\ p_r \end{matrix}\right\}$ 2D + possible p_θ, p_z

2D to 4D

"physical" charge - cylindrical sheets

$$\rho = \sum_i \frac{Q_i}{2\pi} \frac{\delta(r-r_i)}{r_i}$$

smoothed charge

$$\rho = \sum_i \frac{Q_M}{2\pi} \frac{f(r-r_i)}{r_i}$$

Q_M : Macro charge
f : Smoothing function

- Simple model for continuously focused, axisymmetric beams

1D Slab Model

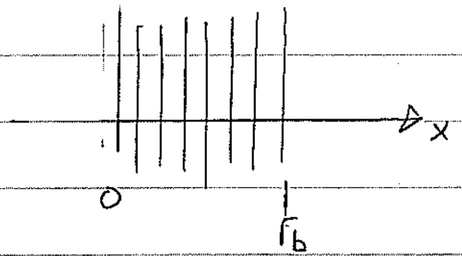

N charged slabs with smoothed interactions.

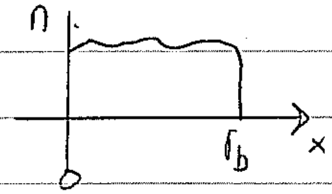

Phase-Space

$\left.\begin{array}{l} x \\ p_x \end{array}\right\}$ 2D + possible p_y, p_z

2D to 4D

"physical" charge - sheets

$$\rho = \sum_i \sigma\,\delta(x - x_i)$$

smoothed charge

$$\rho = \sum_i \sigma_M\, f(x - x_i)$$

σ_M: macro particle charge
f: smoothing function

- Most simple model, but slab geometry is least physical.

It is not immediately clear how such different models can in many cases represent qualitatively similar collective interactions since force laws can change form with dimension. For example, in free space, we find that:

Model	Free Space Field due to ith "particle"	
3D	$\vec{E} = \dfrac{q_i\,(\vec{x} - \vec{x}_i)}{4\pi\varepsilon_0\,\lvert\vec{x} - \vec{x}_i\rvert^3}$	
2D	$\vec{E} = \dfrac{\lambda_i\,(\vec{x} - \vec{x}_i)}{2\pi\varepsilon_0\,\lvert\vec{x} - \vec{x}_i\rvert^2}$	λ_i = line-charge "particle"
1D	$E_x = \dfrac{\sigma_i\,(x - x_i)}{2\varepsilon_0\,\lvert x - x_i\rvert}$	σ_i = sheet charge "particle"

The reason these radically different interactions can give similar physics is that the screening associated with collective interactions is found to be similar:

- Debye screening has similar characteristics in each dimension.

Showed 2D form, in class. Will show in final that the 3D scaling obtains the same Debye length definition.

$$\Rightarrow \quad \lambda_D = \frac{v_{thermal}}{\omega_p} = \left(\frac{\varepsilon_0 k_B T}{\hat{n} q^2}\right)^{1/2} \qquad v_t = (k_B T/m)^{1/2} \qquad \omega_p = \left(\frac{q^2 \hat{n}}{\varepsilon_0 m}\right)^{1/2}$$

- <u>It is much easier to have a significant number of particles within the characteristic screening distances for lower dimensional problems.</u>

  - Lower dimensional simulations can more easily resolve collective effects!
    (Sometimes people run 3D simulations for collective modes and present garbage answers due to resolution difficulties)

// Example

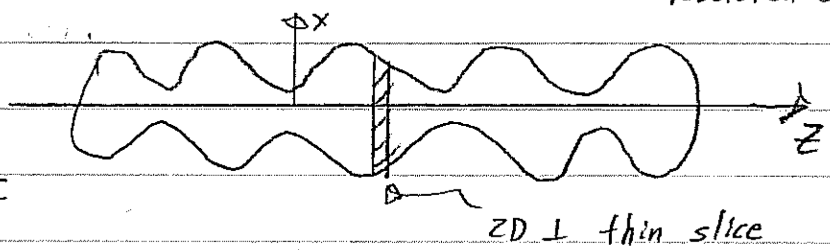

$q = Ze$ ions

$e = 1.6 \times 10^{-19}\ C$

$\lambda \sim 10^{-13} \rightarrow 10^{-7}\ C/m$ typical for intense beams

$$\frac{\#\ \text{particles}}{\text{cm}} = \frac{\lambda}{Ze \cdot 100} \sim \frac{10^4}{Z} \rightarrow \frac{10^{10}}{Z} \qquad q = Ze$$

charge state

- Smoothing still important in lower dimensions and real beam is 3D

//

89

S.M. Lund Class

WARP Code Overview

Electrostatic Multi-dimensional PIC Code

WARP3d – x, y, z, p_x, p_y, p_z
Moves in t

Many Fieldsolvers:
SOR, Multigrid, FFT,
FFT + Tridiag, FFT + Cap Ma

WARPxy – x, y, p_x, p_y, p_z
Moves in s

WARPrz – r, z, p_r, p_z, p_θ
Moves in t

WARPenv – envelope solver
used to seed / load PIC
r_x, r_y, r_x', r_y'
Advances in s

Hermes – Fluid ∥ + Gridded
Space Charge Field

- Common diagnostic tools built around gist graphics
- Run with python interpreter

Example Script
"ag-slice.py"

3D PIC simulations are being used to guide retrofits of an existing ESQ injector at LBL

1st principles, mid-pulse 3D simulations have been carried out to guide injector retrofits aimed at decreasing beam aberrations

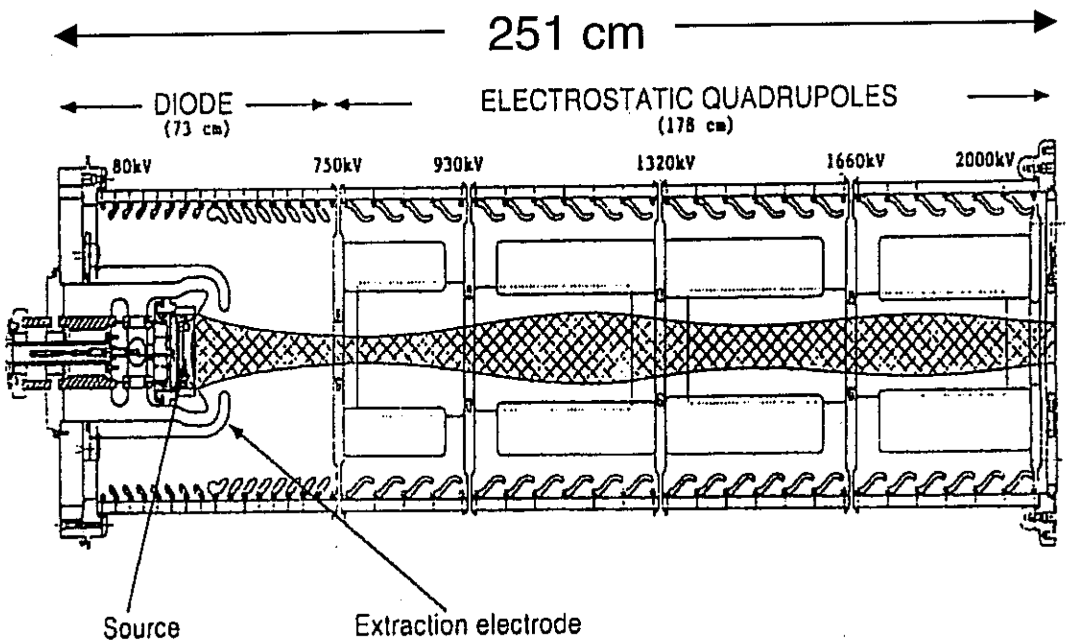

Multi-Shot Film Images of Beam at Injector Exit

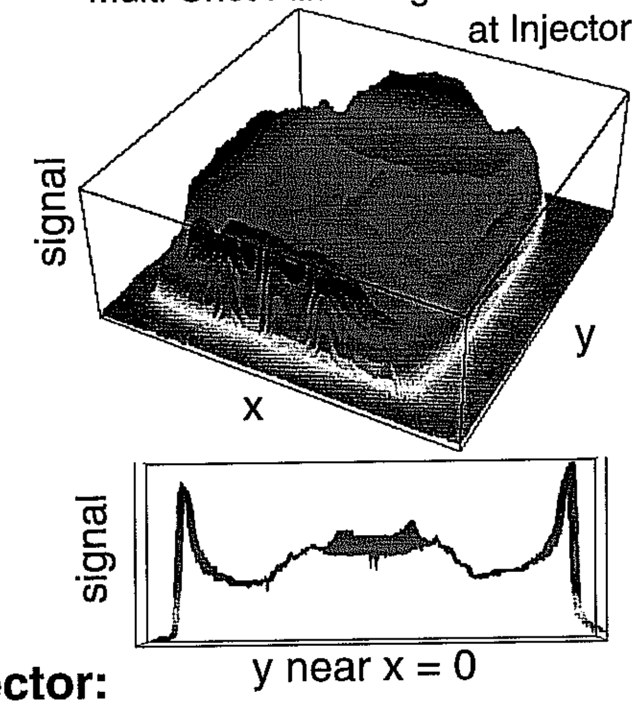

Parameters expected at exit of retrofitted injector:

Energy:	**E = 1.71 MeV**	
Current:	**I = 692 mA, K**	
Emittance:	$\varepsilon_n = 1.1\ \pi$ **mm-mrad**	**rms edge measure**
	$\sim 0.7\ \pi$ **mm-mrad**	**measure eliminating empty entrained space**
Envelope:	**r_x = 56.3 mm**	**r_x' = 53.8 mrad**
	r_y = 55.7 mm	**r_y' = -44.8 mrad**

HCX Injector: Simulations show distribution distortions in the retrofitted injector should be more modest

Mid-pulse distribution projections at exit plane of injector

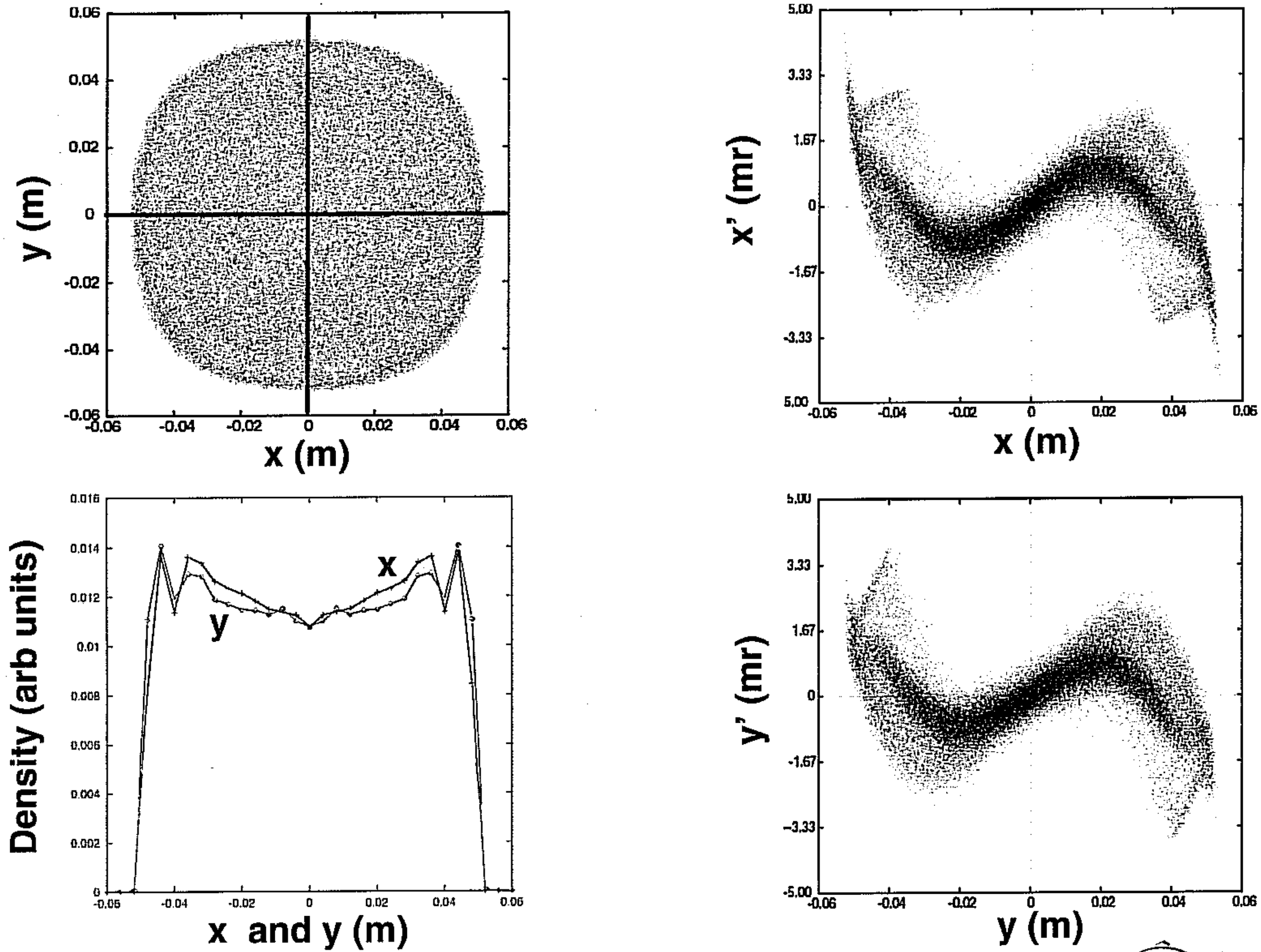

Overall convergence and divergence angles removed to illustrate distortions

S.M. Lund 55/

Simulations show how waveform rise-time determines beam head mismatch

Tuned 1d diode voltage waveform rise-time is 400 ns -- deviations from this lead to significant mismatch effects in the beam head and particle loss with resultant worries about breakdown, electron effects, etc.

Rise-time τ = 800 ns

beam head particle loss < 0.1%

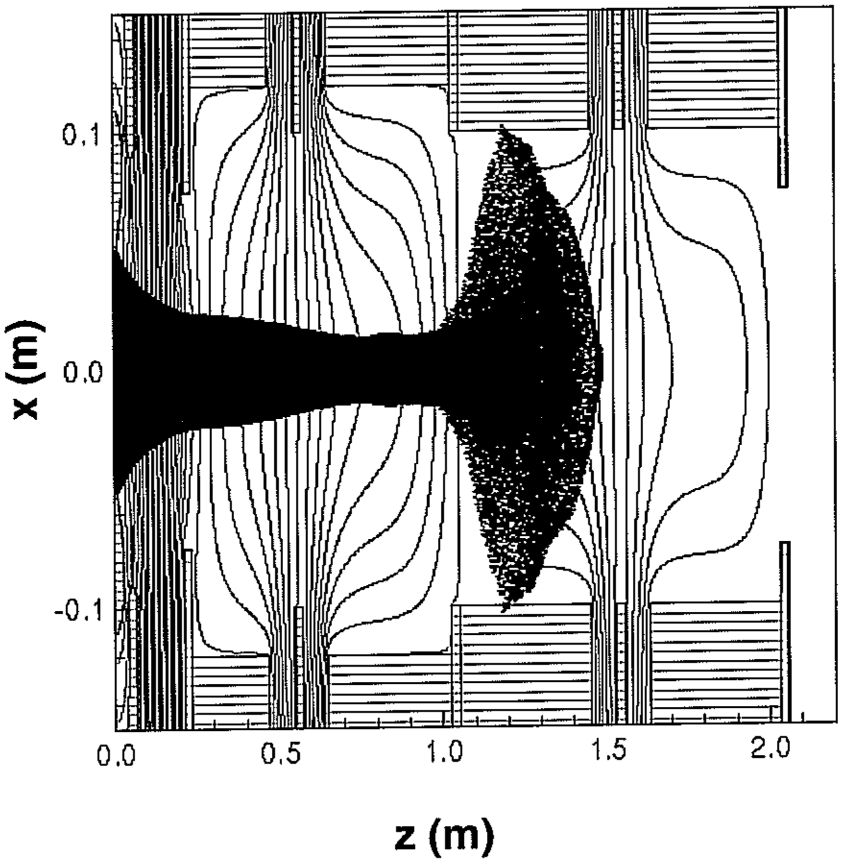

Rise-time τ = 400 ns

zero beam head particle loss

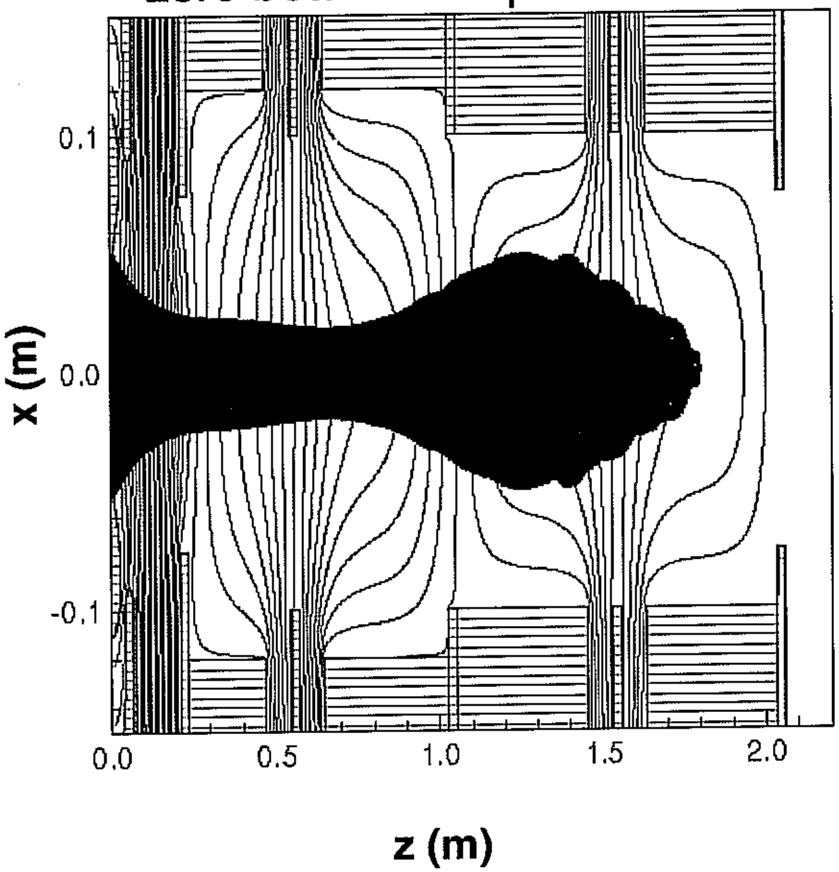

S.M. Lund 56/

Initial distribution distortions will launch a spectrum of collective mode perturbations that evolve

Kinetic and fluid theories have been employed to analyze perturbations on a uniform density intense-beam equilibrium [Lund and Davidson, Phys. Plasmas, 5 3028 (1998)]

Small Amplitude Perturbations (arbitrary units, kinetic and fluid theory)

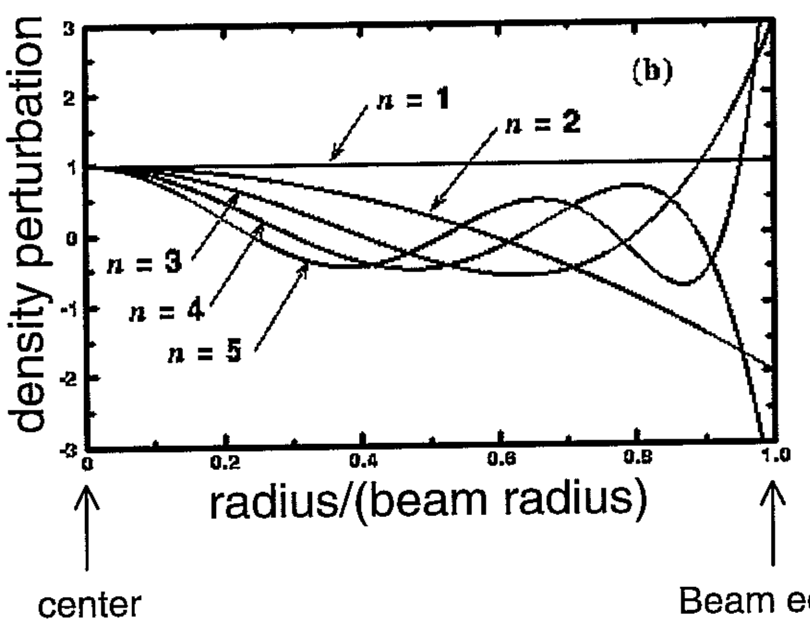

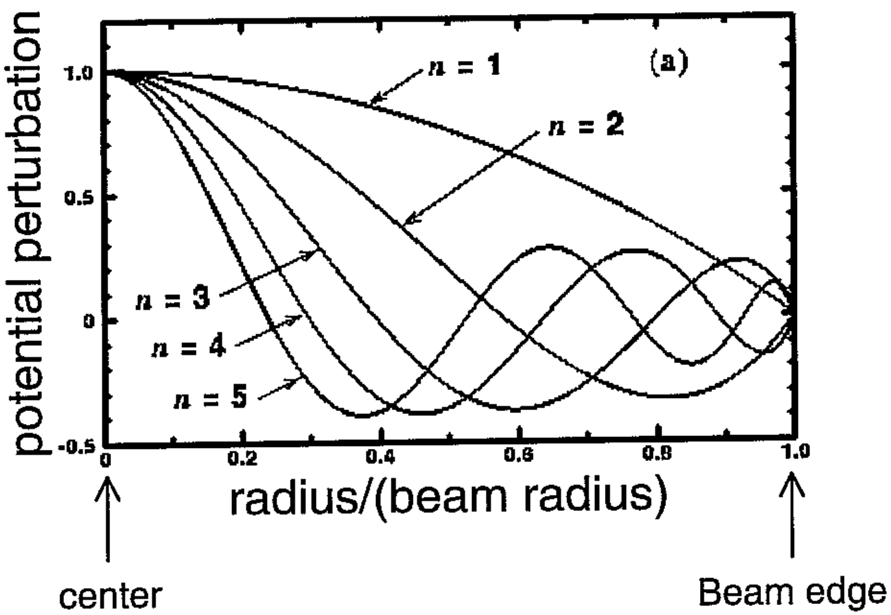

Mode Dispersion Relation (fast branch, from fluid theory)

$$\frac{\sigma_n}{\sigma_0} = \sqrt{2 + 2\left(\sigma/\sigma_0\right)^2 (2n^2 - 1)}$$

σ_n = mode phase advance

n = 1,2,3, ……

Example:
$\sigma_0 = 80^\circ$, $\sigma/\sigma_0 = 0.2$
$\sigma_1 = 115^\circ$, $\sigma_5 = 182^\circ$, ….

S.M. Lund 57/

Perturbations launched by initial distribution nonuniformities can phase-mix to a more uniform profile with increased emittance

Mode spectrum launched can undergo a rapid cascade, settling to a smaller amplitude and lower order distortion

- ❒ Approximate conservation constraints employed to bound emittance increases resulting from full relaxation to a uniform profile [Lund, Lee, and Barnard, Proc. Linac 2000, pg. 290]
- ❒ How will such evolutions influence the range and interpretation of measurements

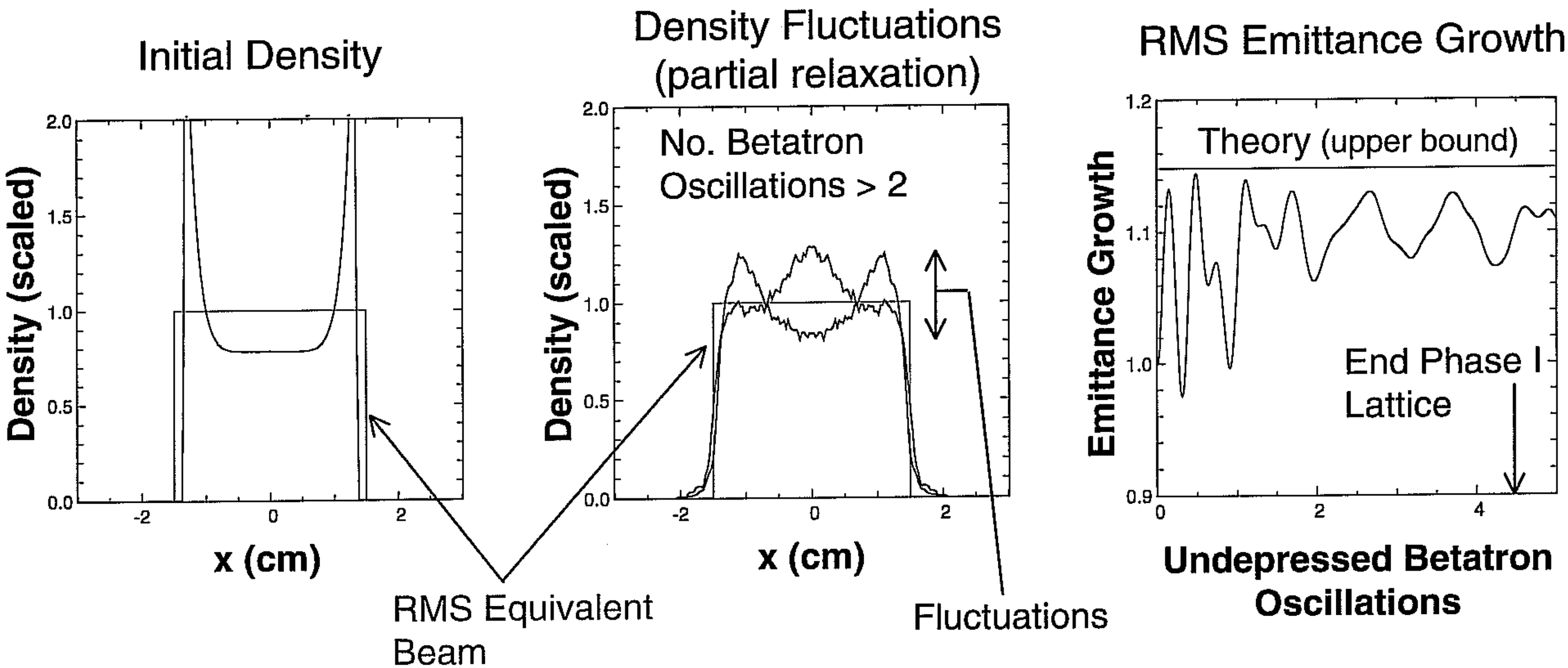

S.M. Lund 58/

Analytic theory has been used to parametrically bound emittance growth due to the relaxation of space-charge nonunifomities

Approximate conservation constraints can be employed to estimate maximal emittance increases resulting from the relaxation of an initial nonuniform density profile to a final, uniform profile [Lund, Lee, and Barnard, Proceedings Linac 2000, Monterey, CA, pg. 290]

Initial Density

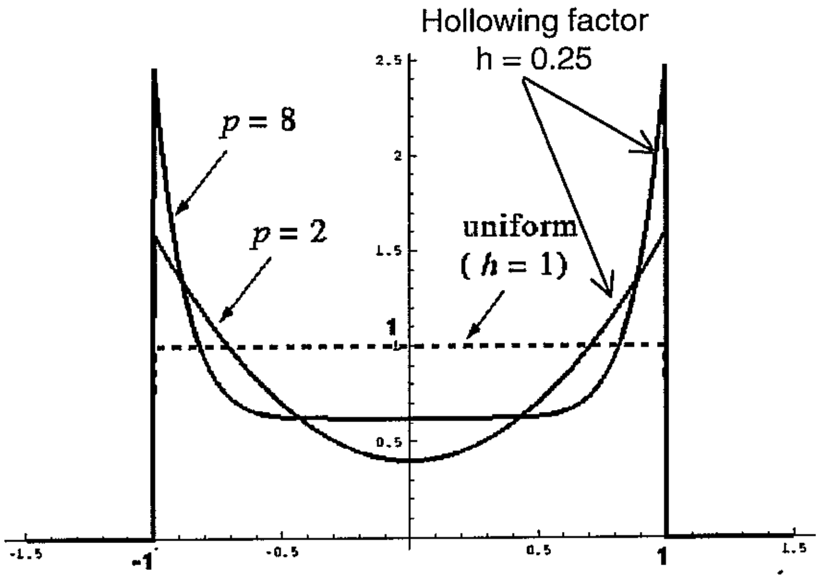

Normalized Radial Coordinate

hollowing ~ r^p

h = ratio min to max density

Emittance Growth on Relaxation

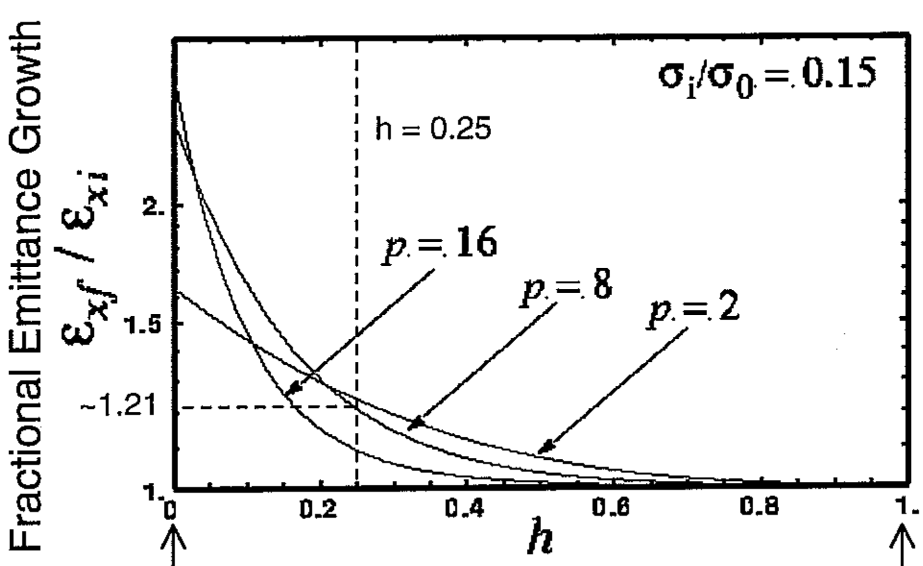

Initial Hollowing Parameter

Extremely Hollowed

Uniform

S.M. Lund 5/9/

HCX Phase II: A wide range of parametric simulations have been carried out with realistic magnetic transport lattices

A syncopated magnetic transport lattice of ~ 50 lattice periods has been designed

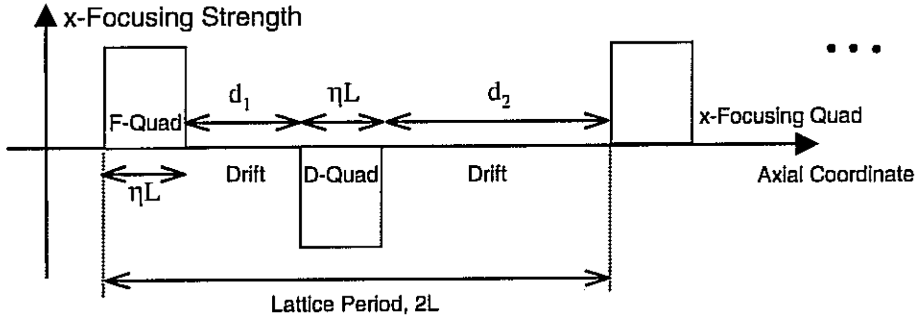

		HCX:
η = Quadrupole Occupancy	$(0 < \eta < 1)$	$\eta = 0.453$
α = Syncopation Factor	$(0 < \alpha < 1)$	$\alpha = 0.248$

Drifts:

$d_1 = \alpha(1-\eta)\eta L$

$d_2 = (1-\alpha)(1-\eta)\eta L$

Superconducting magnetic quadrupoles have been designed and prototyped

$r_p = 29.5$ mm	$B_q' = 104$ T/m (max)	$B_q \sim 6$ Tesla (wire)
$\ell = 136$ mm	$\ell_{eff} = 101$ mm	Integrated Field Error $< 15 \times 10^{-3}$

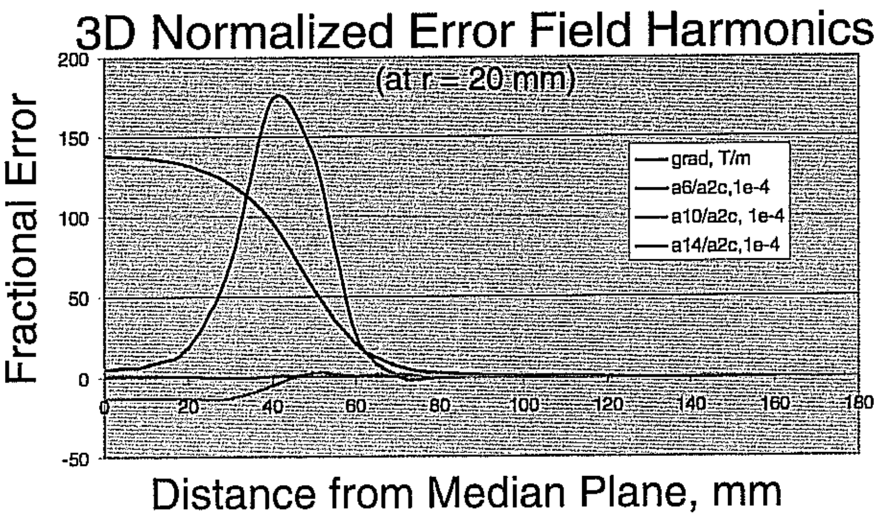

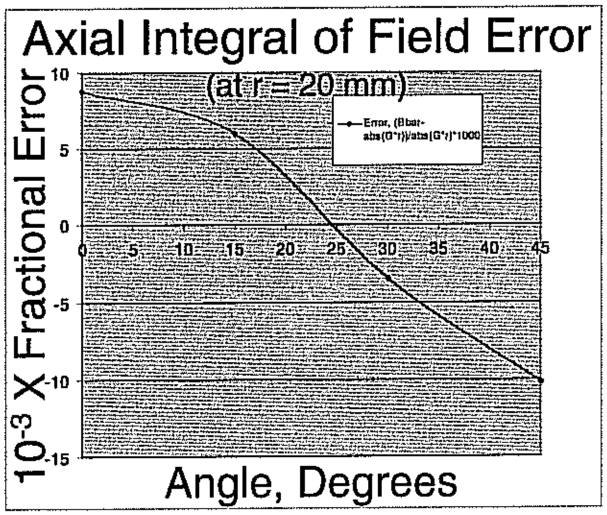

500

S.M. Lund 601

HCX Phase II: Processes influencing beam quality and control have been explored --- Example: Nonlinear applied fields and beam quality

Full 3D magnetic field is resolved as:

$$\vec{B} = \vec{B}_{quad} + \delta\vec{B} \qquad \delta\vec{B} \rightarrow s \cdot \delta\vec{B}$$

Very Strong Space Charge
($\sigma/\sigma_0 = 0.086$)

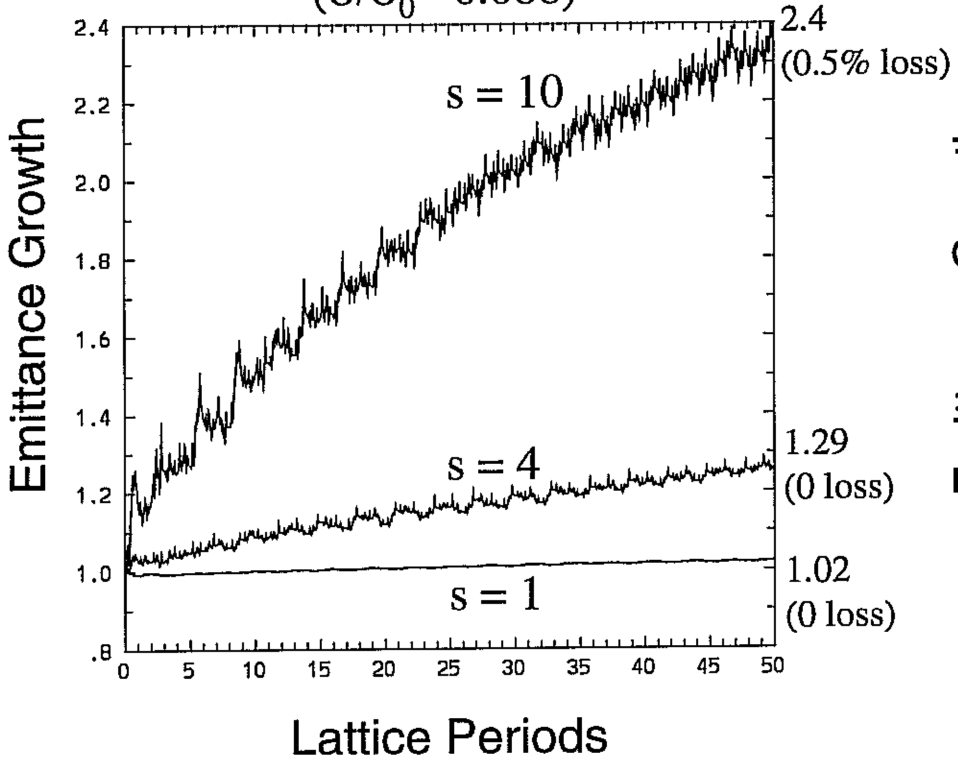

Intermediate Space Charge
($\sigma/\sigma_0 = 0.248$)

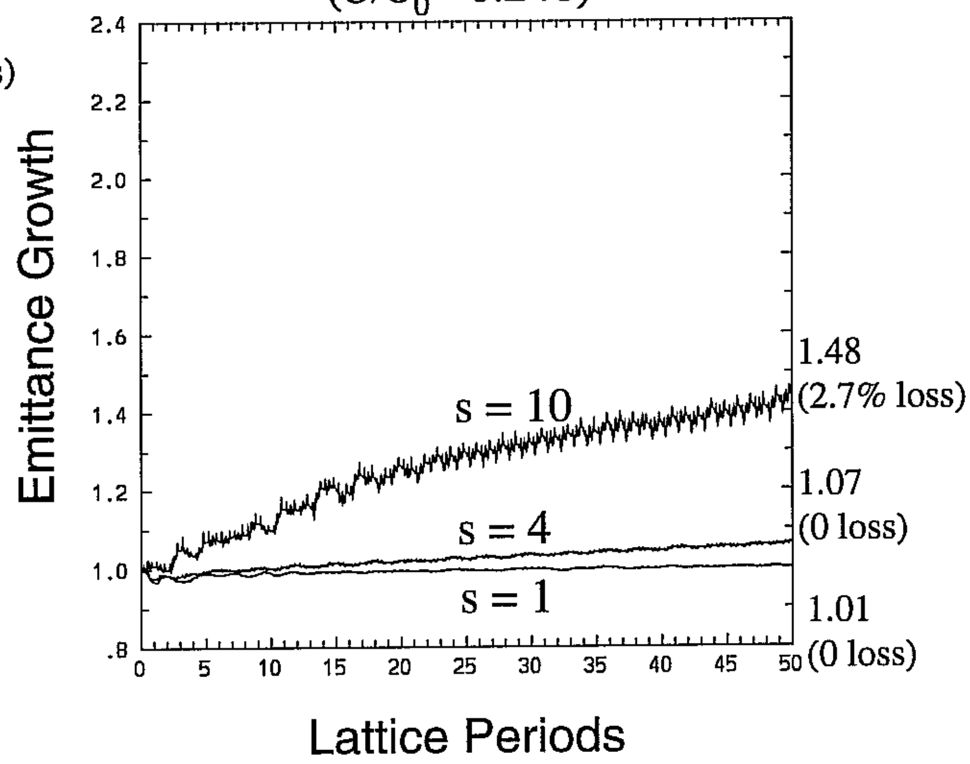

S.M. Lund 6/1/

Initial KV Distribution

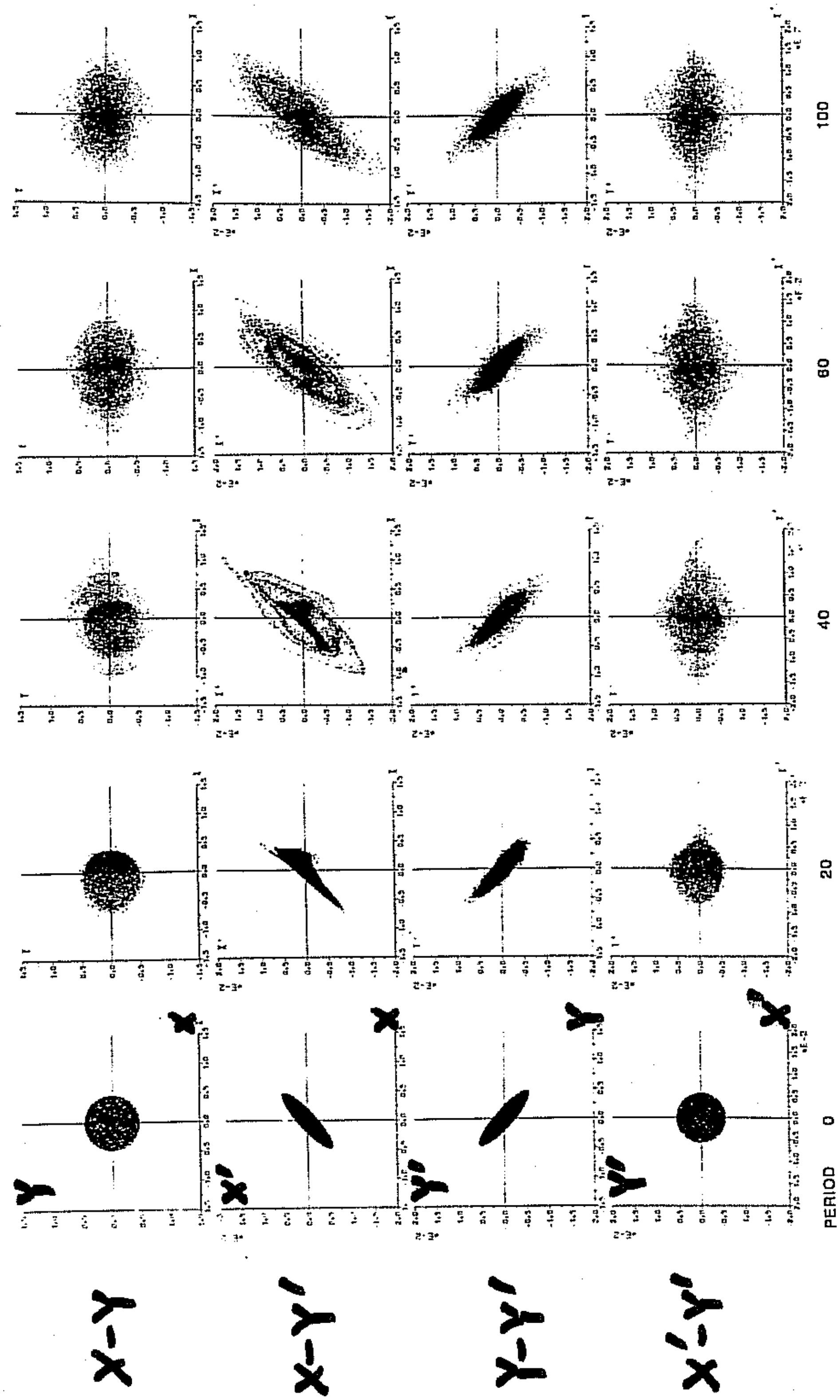

FIGURE 2 Transformation of an initial K-V distribution through the GSI FODO channel at $\sigma_0 = 90°$, $\sigma = 41°$.

J. Struckmeir, J. Klabunde, and M. Reiser, Part. Accel. 15, 47 (1984).

See also Reiser Text, pg 495.

S.M. Lund 63/

Initial Gaussian Distribution

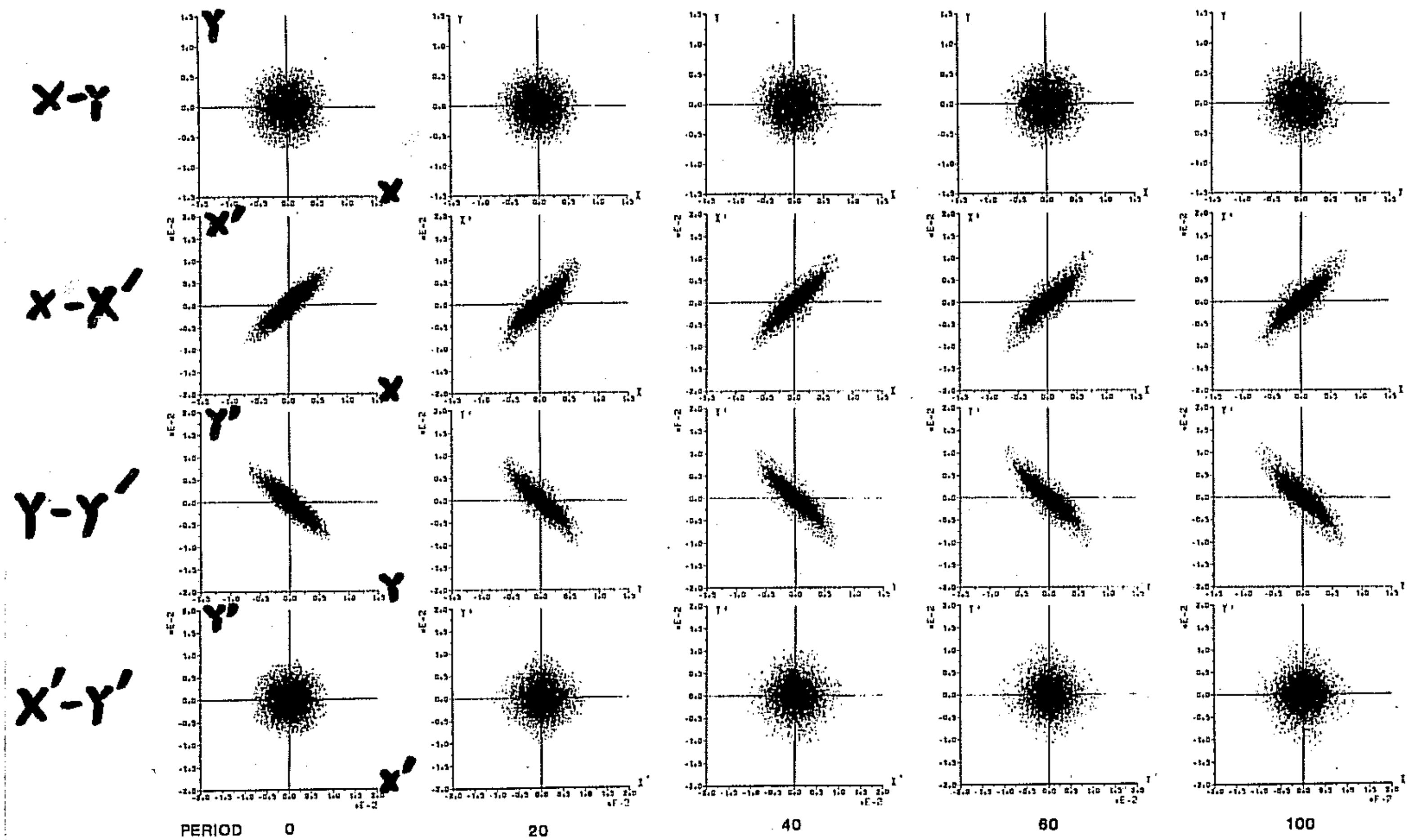

FIGURE 6 Transformation of an initial Gaussian distribution (rms-matched) through the GSI FODO channel at $\sigma_0 = 90°$, $\sigma = 41°$.

J. Struckmeir, J. Klabunde and M. Reiser, Part. Accel. 15, 47 (1984)

S.M. Lund 641

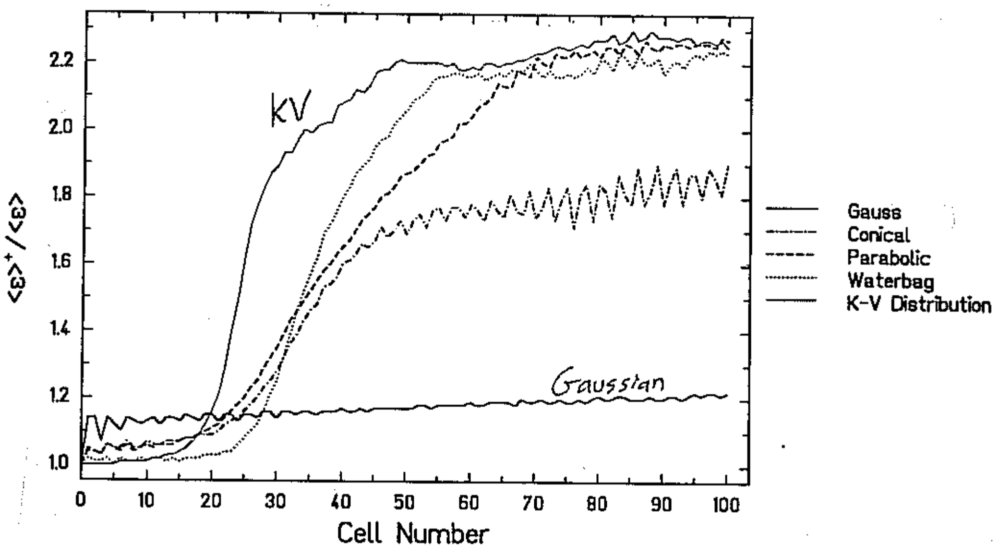

FIGURE 7 Emittance growth factors versus the number of cells obtained from particle simulations for initial K-V, waterbag, parabolic, conical and Gaussian distributions at $\sigma_0 = 90°$, $\sigma = 41°$.

From J. Struckmeier, J. Kabunde, and M. Reiser, Part. Accel. 15 47 (1984).

Distribution Methods – Direct Gridded Solution of Vlasov's Equation.

Consider the Vlasov equation as an example.

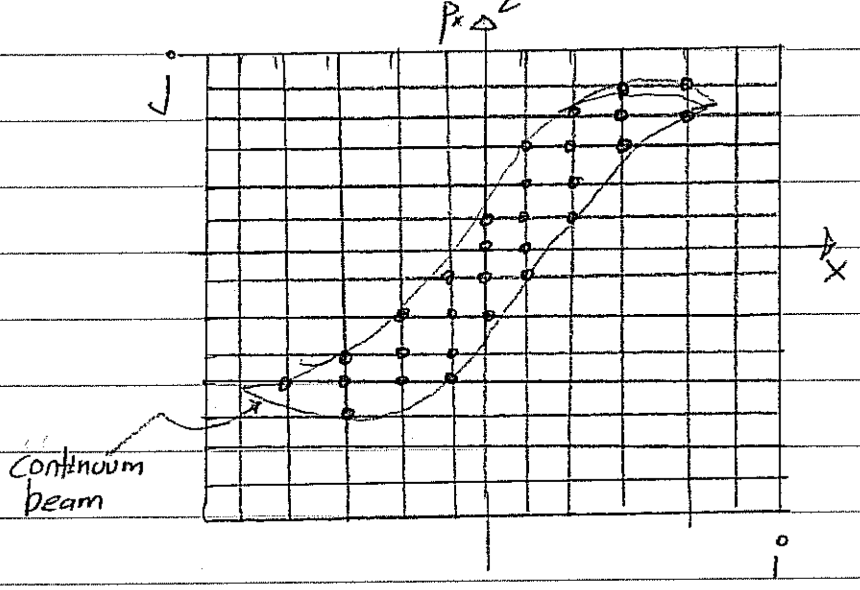

$$f(x_i, p_j, t) = f_{ij}(t)$$

The distribution is advanced at discrete grid points in time.

- Fields are typically solved using a discrete spatial mesh as for the particle methods described before.
  - Deposition on mesh is typically straightforward in Vlasov case (sum over momentum variables.
- The distribution advance cycle is different than for particle methods.
  - Numerical stability is key.
  - Characteristics and "semi-Lagrangian" methods can be employed.
  - Methods for solving for characteristics are familiar from dynamics/plasma physics.

Direct Vlasov Methods:

"Pros"

Reasons for Vlasov simulations:

- Low noise - only discretization effects without statistical effects
- Allows clear analysis of collective effects and tenuous distribution components.

"Cons"

Reasons why Vlasov simulations are presently employed less than PIC:

- Extreme memory requirements for needed grid resolution in multi-dimensional phase space.
  - Beams often have sharp edges in phase space that move in responce to varying applied focusing forces.
- Numerical stability tends to be more difficult than in particle methods.

No time to illustrate Vlasov and other distribution methods in this introductory course. We hope to cover these methods and other numerical fieldsolve techniques in a later expanded version of this class.

However ..... it is easy to generalize from what we have learned!

John Barnard
Steven Lund
USPAS
June 2008

Summary of JB lectures

START WITH MICROSCOPIC PHASE SPACE DENSITY

$$\boxed{N(\underline{x},\underline{v},t) = \sum_{i=1}^{N} \delta(\underline{x}-\underline{X}_i(t))\,\delta(\underline{v}-\underline{V}_i(t))}$$

Klimontovitch Density

$\frac{\partial N}{\partial t}$ + ~~MAXWELLS~~ LORENTZ EQUATIONS ⇒ KLIMONTOVICH EQUATION:

$$\boxed{\frac{\partial N}{\partial t} + v\cdot\nabla_x N(\underline{x},\underline{v},t) - \frac{q}{m}(E^m + v\times B^m)\cdot\nabla_v N(\underline{x},\underline{v},t) = 0}$$

or $\boxed{\frac{dN(\underline{x},\underline{v},t)}{dt} = 0}$

Letting $N = f + \delta f$ $\quad f = \langle N\rangle$ $\quad f = \frac{\int N\,d^3x\,d^3v}{\Delta x^3\,\Delta V^3}$

$E^m = E + \delta E$ $\quad E = \langle E_m\rangle$

$B^m = B + \delta B$ $\quad B = \langle B_m\rangle$ $\quad n^{-1/3} \ll \Delta x \ll \lambda$

PERFORMING LOCAL AVERAGES TO OBTAIN SMOOTH & "SLIKEY" QUANTITIES:

$$\boxed{\frac{\partial f}{\partial t} + \underline{\dot{v}}\cdot\frac{\partial f}{\partial \underline{x}} + \frac{d\underline{v}}{dt}\cdot\frac{\partial f}{\partial \underline{v}} = \frac{\partial f}{\partial t_c}} \sim \frac{f}{\tau_c}$$

We estimated $\frac{|\partial f/\partial t_c|}{|\frac{q\underline{E}}{m}\cdot\partial f/\partial\underline{v}|} \sim \frac{1}{16\lambda_D^3 n_0} \ll 1$

$\lambda_D = V_{TH}/\omega_p$ $\quad V_{th} \equiv \sqrt{\frac{kT}{m}}$ $\quad \omega_p \equiv \sqrt{\frac{q^2 n}{\varepsilon_0 m}}$

$$\frac{\partial f}{\partial t} + \underline{v}\cdot\frac{\partial f}{\partial \underline{x}} + \frac{d\underline{p}}{dt}\cdot\frac{\partial f}{\partial \underline{p}} = 0 \qquad \dot{p} = -\frac{\partial H}{\partial \underline{x}} \;;\; \dot{x} = \frac{\partial H}{\partial \underline{p}}$$

$\boxed{\frac{df}{dt} = 0}$ LIOUVILLES EQUATION (INCOMPRESSIBILITY OF PHASE VOLUME)

CONJUGATE VARIABLES

DEFINE NORMALIZED EMITTANCES PROPORTIONAL TO $\Delta p_z \Delta z \propto \Delta E \Delta t$

$\Delta V_x \Delta x$

$\Delta p_y \Delta y$

SO THAT

$$\varepsilon_{Nx}^2 = \gamma^2\beta^2\left(\langle x^2\rangle\langle x'^2\rangle - \langle x x'\rangle^2\right)$$

⇒ CONSTANT IF FORCES ARE LINEAR IN X & FILAMENTATION IS ABSENT. (LINEAR WITHOUT COUPLING TO Z, OR Y).

WE DERIVED TWO SETS OF PARTICLE EQUATION OF MOTION:

PARAXIAL EQUATION (FOR AXISYMMETRIC SYSTEMS) ($\frac{\partial}{\partial\theta} = 0$)

STARTING WITH THE LORENTZ FORCE EQUATION $\frac{dp}{dt} = q(E + \underline{v} \times \underline{B})$ IN CYL. COORD.

$$\underbrace{\frac{d}{dt}(\gamma m \dot{r})}_{\text{INERTIAL}} - \underbrace{\gamma m r \dot{\theta}^2}_{\text{CENTRIFUGAL}} = q\Big(\underbrace{\frac{V''}{2} r}_{E_r \text{ external (DIVERGENCE OF } E = 0)} + \underbrace{r \dot{\theta} B}_{v_\theta B_z}\Big) + \underbrace{q\left(E_r^{self} + v_z B_\theta^{self}\right)}_{\text{SELF-FIELD}}$$

$$\boxed{\dot{r} \equiv \frac{dr}{dt};\; r' = \frac{dr}{ds} = \frac{\dot{r}}{\beta c}}$$

θ-component:

$$p_\theta = \gamma m r^2 \dot{\theta} + \frac{q B(z) r^2}{2} = \text{constant}$$

$$= \gamma m r^2 \beta c \theta' + \frac{q B r^2}{2} = \text{constant}$$

$$\underbrace{r''}_{\text{INERTIAL}} + \underbrace{\frac{\gamma'}{\beta^2 \gamma} r'}_{\text{ACCELERATION (INERTIAL)}} + \underbrace{\frac{\gamma''}{2\beta^2\gamma} r}_{\text{ER (CONVERGENCE OF FIELD LINES)}} + \underbrace{\left(\frac{\omega_c}{2\gamma\beta c}\right)^2 r}_{v_\theta B_z - \text{CENTRIFUGAL}} - \underbrace{\left(\frac{p_\theta}{\gamma\beta m c}\right)^2 \frac{1}{r}}_{\text{CENTRIFUGAL}} - \underbrace{\frac{q}{\gamma^3 m v_z^2} \frac{\lambda(r)}{2\pi\epsilon_0 r}}_{\text{SELF FIELD}} = 0$$

STATISTICAL AVERAGE OF THIS EQUATION

$$r_b'' + \frac{\gamma'}{\beta^2\gamma} r_b' + \frac{\gamma''}{2\beta^2\gamma} r_b + \left(\frac{\omega_c}{2\gamma\beta c}\right)^2 r_b - \frac{4\langle p_\theta\rangle^2}{(\gamma m \beta c)^2 r_b^3} - \frac{\varepsilon_r^2}{r_b^3} - \frac{Q}{r_b} = 0$$

$$\varepsilon_r^2 \equiv 4\left(\langle r^2\rangle\langle r'^2\rangle - \langle r r'\rangle^2 + \langle r^2\rangle\langle r^2\theta'^2\rangle - \langle r^2\theta'\rangle^2\right); \quad Q = \frac{q\lambda}{2\pi\epsilon_0 \gamma^3 \beta^2 m c^2}$$

$$= \varepsilon_x^2 - 4\langle r^2\theta'\rangle^2 \quad (\text{if } \rho = \rho(r) \text{ only})$$

CARTESIAN EQUATION OF MOTION

J BARNARD

15

EQUATION OF MOTION AGAIN STARTING WITH $\frac{dp}{dt} = q(\underline{E} + \underline{v} \times \underline{B})$

RETURN TO x, y COORDINATES

$$x'' + \frac{1}{\gamma v_z}\frac{d}{ds}(\gamma v_z)x' = \frac{-q}{\gamma^3 m v_z^2}\frac{\partial\varphi}{\partial x} \pm \begin{cases} \frac{qB'}{\gamma m v_z} x & \text{for magnetic quads} \\ \frac{qE'}{\gamma m v_z^2} x & \text{for electric quads} \end{cases}$$

$$\text{Let } \frac{\gamma m v_z}{q} = \frac{p}{q} \equiv [B\rho] \equiv \text{RIGIDITY}$$

$$y'' + \frac{1}{\gamma v_z}\frac{d}{ds}(\gamma v_z)y' = \frac{-q}{\gamma^3 m v_z^2}\frac{\partial\varphi}{\partial y} \mp \begin{cases} \frac{B'}{[B\rho]} y & \text{magnetic} \\ \frac{qE'}{\gamma m v_z^2} y & \text{electric} \end{cases}$$

ENVELOPE EQUATION

$$r_x^2 = 4\langle x^2\rangle; \quad r_y^2 = 4\langle y^2\rangle$$

$$r_x' = \frac{4\langle xx'\rangle}{r_x}$$

$$r_x'' = \frac{4\langle xx''\rangle}{r_x} + \frac{\varepsilon_x^2}{r_x^3}; \qquad \varepsilon_x^2 = 16(\langle x^2\rangle\langle x'^2\rangle - \langle xx'\rangle^2)$$

$$r_y'' = \frac{4\langle yy''\rangle}{r_y} + \frac{\varepsilon_y^2}{r_y^3} \qquad \varepsilon_y^2 = 16(\langle y^2\rangle\langle y'^2\rangle - \langle yy'\rangle^2)$$

for magnetic focusing:

$$r_x'' + \frac{1}{\gamma v_z}\frac{d}{ds}(\gamma v_z)\, r_x' + \frac{4q}{\gamma^3 m v_z^2}\frac{\langle x\frac{\partial\varphi}{\partial x}\rangle}{r_x} \mp \frac{B'}{[B\rho]} r_x - \frac{\varepsilon_x^2}{r_x^3} = 0$$

$$r_y'' + \frac{1}{\gamma v_z}\frac{d}{ds}(\gamma v_z)\, r_y' + \frac{4q}{\gamma^3 m v_z^2}\frac{\langle y\frac{\partial\varphi}{\partial y}\rangle}{r_y} \pm \frac{B'}{[B\rho]} r_x - \frac{\varepsilon_y^2}{r_y^3} = 0$$

(for electric focusing $\frac{B'}{[B\rho]} \rightarrow \frac{qE'}{\gamma m v_z^2}$)

SPACE CHARGE TERM WITH ELLIPTICAL SYMMETRY

NOW DEFOCUSING IN ONE DIRECTION AND FOCUSING IN THE OTHER $\Rightarrow$ RADIAL SYMMETRY SHOULD BE REPLACED BY ELLIPTICAL SYMMETRY: $\rho = \rho\left(\frac{x^2}{r_x^2} + \frac{y^2}{r_y^2}\right)$

CAN BE SHOWN THAT $\left\langle x \frac{\partial \phi}{\partial x} \right\rangle = \frac{-\lambda}{4\pi\epsilon_0} \frac{r_x}{r_x + r_y}$

$$\left\langle y \frac{\partial \phi}{\partial y} \right\rangle = \frac{-\lambda}{4\pi\epsilon_0} \frac{r_y}{r_x + r_y}$$

USE $\phi(x,y) = \frac{-r_x r_y}{4\epsilon_0} \int_0^\infty \frac{\eta(\chi)\, ds}{\sqrt{r_x^2+s}\sqrt{r_y^2+s}}$ to prove, where $\hat{\rho}(\chi) = \frac{d\eta}{d\chi}$

$\rho(x,y) = \hat{\rho}(\chi)\big|_{s=0}$

$\chi = \frac{x^2}{r_x^2+s} + \frac{y^2}{r_y^2+s}$

DEFINING $Q = \frac{2\lambda q}{4\pi\epsilon_0 \gamma^3 m v_z^2}$

$$\Rightarrow \boxed{\begin{aligned} &r_x'' + \frac{1}{\gamma v_z}\frac{d}{ds}(\gamma v_z) r_x' - \frac{2Q}{r_x + r_y} \mp \frac{B'}{[B\rho]} r_x - \frac{\varepsilon_x^2}{r_x^3} = 0 \\ &r_y'' + \frac{1}{\gamma v_z}\frac{d}{ds}(\gamma v_z) r_y' - \frac{2Q}{r_x + r_y} \pm \frac{B'}{[B\rho]} r_y - \frac{\varepsilon_y^2}{r_y^3} \end{aligned}}$$

(for Electric Focusing $\frac{B'}{[B\rho]} \rightarrow \frac{qE'}{\gamma m v_z^2}$).

(ANALOGUE TO CIRCULAR BEAM:

$\left\langle r \frac{\partial \phi}{\partial r} \right\rangle = \frac{-\lambda}{4\pi\epsilon_0}$ PROVED IN HOMEWORK)

ENVELOPE EQUATIONS DERIVED

rms (ENVELOPES DEFINED IN TERMS OF rms QUANTITIES; EMITTANCE

1. PARAXIAL r_b; $\rho(r)$ NOT GUARANTEED TO BE CONSERVED).
2. ELLIPTICAL r_x, r_y; $\rho\left(\frac{x^2}{r_x^2} + \frac{y^2}{r_y^2}\right)$
3. LONGITUDINAL r_z FOR $E_z = \frac{-g}{4\pi\epsilon_0}\frac{\partial\lambda}{\partial z} \propto z$; $[\lambda \propto (1 - 4z^2/r_z^2)]$ $V \propto (z/r_z)$
4. ELLIPSOIDAL rf BUNCHES $r_\perp, r_z$ (ALSO r_x, r_y, r_z. c.f. Wangler, section 9.9).
   (ρ CONSTANT)
5. ELLIPTICAL WITH IMAGES r_x, r_y $\rho\left(\frac{x^2}{r_x^2} + \frac{y^2}{r_y^2}\right)$
6. LARMOR FRAME (PERIODIC SOLENOIDS OR CONTINUOUS FOCUSING) $\tilde{r}_x, \tilde{r}_y$ $\rho(r)$

KINETIC ENVELOPE EQUATIONS (CONSTRAINT EQUATION ON A PARTICULAR DISTRIBUTION FUNCTION; EMITTANCE CONSERVED)

1. KV FOR ELLIPTICAL UNIFORM BEAMS $f(x, x', y, y')$
   [IDENTICAL TO #2 ABOVE]
2. NEUFFER DISTRIBUTION FOR 1D $f(z, z')$
   [IDENTICAL TO #3 ABOVE]

MOMENT EQUATIONS

1. TRANSVERSE WITH CHROMATIC EFFECTS
   $\langle x^2\rangle, \langle x'^2\rangle, \langle xx'\rangle, \langle x^2\delta\rangle, \langle x'^2\delta\rangle, \langle xx'\delta\rangle, \ldots$

Summary of Current Limits From Different Focusing Methods

Einzel Lens

$$Q_{max} \cong \frac{3\pi^2}{8}\left(\frac{q\phi_0}{m v_0^2}\right)^2\left(\frac{r_b}{L}\right)^2$$

Solenoids

$$Q_{max} = \left(\frac{\omega_c r_b}{2\gamma\beta c}\right)^2$$

Quadrupole Focusing

$$Q_{max} \cong \frac{\eta\,\sigma_0}{2\pi}\left(\frac{\sin\frac{\eta\pi}{2}}{\frac{\eta\pi}{2}}\right)\begin{bmatrix}\frac{B r_b}{[B\rho]}\left[\frac{r_b}{r_p}\right] \\ \frac{2qV_q}{\gamma m v_z^2}\left[\frac{r_b^2}{r_p^2}\right]\end{bmatrix}\begin{matrix}\text{Magnetic} \\ \text{Electric}\end{matrix}$$

For Non-Relativistic Beams

$$\lambda_{max} \propto \frac{\phi_0^2}{V}$$

$$\lambda_{max} \propto \frac{q}{m} B^2 r_p^2$$

$$\lambda_{max} \propto \begin{cases} B_i V^{1/2} r_p \\ V_q \end{cases}$$

Note
ϕ_0 = Voltage between Einzel lenses
V_q = Voltage on a quad relative to ground
V = particle energy / q

513

Solenoids: $\log\{\lambda[\mathrm{Cm}^{-1}]\} = -7.0$

Electrostatic quads: $\log\{\lambda[\mathrm{Cm}^{-1}]\} = -5.8$

Magnetic quads: $\log\{\lambda[\mathrm{Cm}^{-1}]\} = -8.9 + \frac{1}{2}\log\{E_{kin}[\mathrm{eV}]\}$

Einzel lenses: $\log\{\lambda[\mathrm{Cm}^{-1}]\} = 0.01 - \log\{E_{kin}[\mathrm{eV}]\}$

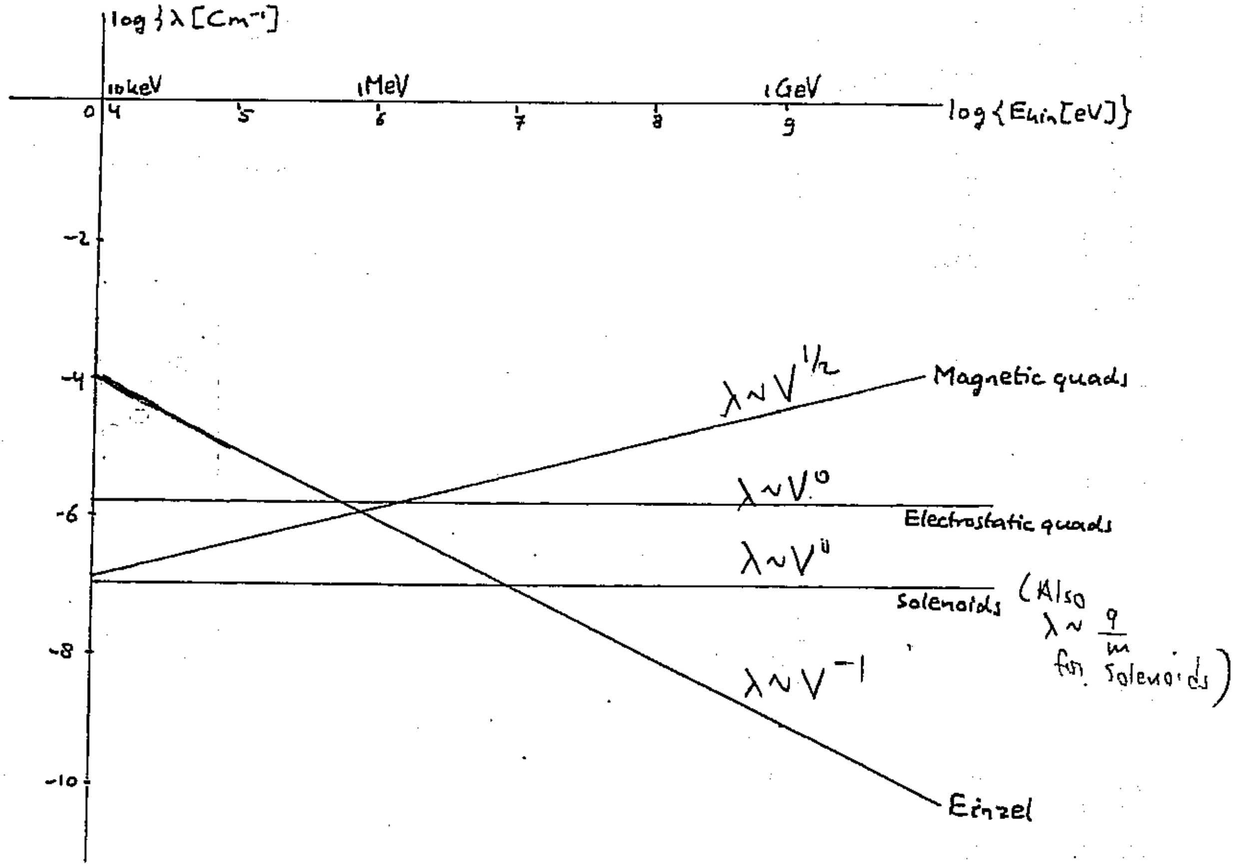

ESTIMATING SPOT SIZE

$$r_x'' + \frac{(\gamma_b\beta_b)'}{\gamma_b\beta_b} r_x + K_x r_x - \frac{2Q}{r_x+r_y} - \frac{\varepsilon_x^2}{r_x^3} = 0$$

$$r_y'' + \frac{(\gamma_b\beta_b)'}{\gamma_b\beta_b} r_y + K_y r_y - \frac{2Q}{r_x+r_y} - \frac{\varepsilon_y^2}{r_y^3} = 0$$

<u>IN CHAMBER</u>: NO EXTERNAL FOCUSING, NO ACCELERATION AND BEAM IS OFTEN CIRCULAR (BY DESIGN)

$$\Rightarrow \quad K_x = K_y = (\gamma_b\beta_b)' = 0 \quad \& \quad r_x = r_y = r_b$$

$\Rightarrow$ ENVELOPE EQUATION IS:

$$r_b'' = \frac{Q}{r_b} + \frac{\epsilon^2}{r_b^3}$$

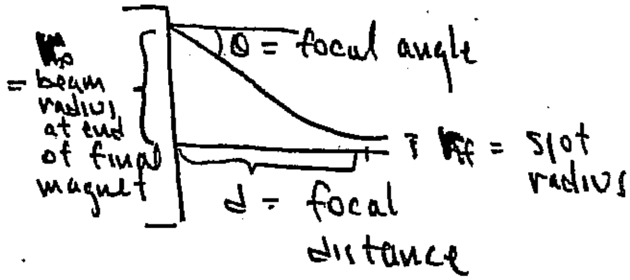

MULTIPLYING BY r_b' & INTEGRATING $\Rightarrow$

$$\frac{r_{bf}'^2}{2} - \frac{r_{bo}'^2}{2} = Q \ln \frac{r_{bf}}{r_{bo}} + \frac{\epsilon^2}{2r_{bo}^2} - \frac{\epsilon^2}{2r_{bf}^2}$$

<u>NOW</u> $r_{bo}' \cong \theta$ $\qquad r_{bf}$ = spot radius

$r_{bf}' = 0$ $\qquad r_{bo} \cong d\theta$ $\qquad r_{bf} << r_{bo}$

$$\Rightarrow \quad \boxed{\theta^2 \cong 2Q \ln\left(\frac{\theta d}{r_{bf}}\right) + \frac{\epsilon^2}{r_{bf}^2}}$$

WHEN $Q = 0$

$$r_{spot}^2 = \frac{\epsilon^2}{\theta^2} + r^2_{\text{CHROMATIC ABERRATION}} + \ldots$$

$$r^2_{\text{CHROMATIC}} = \alpha^2 d^2 \left(\frac{\delta p}{p}\right)^2 \theta^2$$

$\alpha \cong 6$ (system dependent)

LONGITUDINAL DYNAMICS SUMMARY

1D VLASOV EQUATION

$$\frac{\partial \tilde{f}}{\partial s} + z' \frac{\partial \tilde{f}}{\partial z} + z'' \frac{\partial \tilde{f}}{\partial z'} = 0$$

$E_z = \frac{-g}{4\pi\epsilon_0}\frac{\partial \lambda}{\partial z}$ "g-factor" model

$$z'' = \frac{q E_z}{m v_0^2} \; ; \qquad \frac{\partial^2 \phi}{\partial z^2} + \frac{1}{r}\frac{\partial}{\partial r}\left(r \frac{\partial \phi}{\partial r}\right) = -\frac{\rho}{\epsilon_0}$$

CHILD-LANGMUIR IN 1-D DIODE

$\boxed{\text{Ellipsoidal Bunch}}$

LEADS TO FLUID EQUATIONS

$\int(\text{Vlasov Equation})\,dz'$

$$\frac{\partial \lambda}{\partial s} + \frac{\partial}{\partial z}(\lambda \bar{z}') = 0$$

$$\frac{\partial \bar{z}'}{\partial s} + \bar{z}' \frac{\partial \bar{z}'}{\partial z} + \cancel{\frac{1}{\lambda}\frac{\partial}{\partial z}(\lambda \Delta z'^2)} = \frac{q E_z}{m v_0^2}$$

1D E_z: $\Rightarrow$ CHILD LANGMUIR SOLUTION $\leftarrow$ NON-LINEAR SOLUTION TO FLUID EQUATIONS

g-factor: $\Rightarrow$ SPACE-CHARGE WAVES

$\hookrightarrow$ LONGITUDINAL OR RESISTIVE WALL INSTABILITY (IF $E_1 = Z^{\nu} I_1$)

$\Rightarrow$ SPACE-CHARGE RAREFACTION WAVES $\leftarrow$ NON-LINEAR SOLUTION TO FLUID EQNS.

$\Rightarrow$ PARABOLIC BUNCH COMPRESSION $\leftarrow$ NON-LINEAR SOLUTION TO FLUID EQUATIONS

$\Rightarrow$ "EAR" FIELDS

2D PIERCE ELECTRODE

TIME DEPENDENT LAMPEL TIEFENBACK SOLUTION

VLASOV EQUATION ALSO $\Rightarrow$ ENVELOPE EQUATION $\iint$ Vlasov Equation $dz\,dz'$

$$\frac{d^2 r_z}{ds^2} = \frac{\epsilon_z^2}{r_z^3} + \frac{3}{2}\frac{g q Q_c}{4\pi\epsilon_0 m v^2}\frac{1}{r_z^2} - K(r) r_z$$

KINETIC SOLUTION TO VLASOV EQUATION & SATISFYING RMS ENVELOPE EQUATION IS NEUFFER DISTRIBUTION

$$f(z,z') = \frac{3N}{2\pi E_z}\sqrt{1 - \frac{z^2}{r_z^2} - \frac{r_z^2 (z' - r_z' z / r_z)^2}{\epsilon_z^2}}$$

NORMAL MODES

LONGITUDINAL

SPACE-CHARGE WAVES (FLUID)

$\omega = \pm c_s k$ [IN COMOVING BEAM FRAME]

$$c_s = \sqrt{\frac{q g \lambda_0}{4\pi\epsilon_0 m}} = \text{SPACE CHARGE WAVE SPEED}$$

TRANSVERSE

ENVELOPE MODES

CONTINUOUS FOCUSING (LONG BUNCHES)

BREATHING: $k_B^2 = 2k_{\beta 0}^2 + 2k_\beta^2$

QUADRUPOLE $k_Q^2 = k_{\beta 0}^2 + 3k_\beta^2$

(HERE $k_\beta^2 \equiv k_{\beta 0}^2 - \frac{Q}{r_b^2}$)

(ANALOGOUS MODES IN BUNCHED BEAMS)

STEVE LOOKED AT MODES IN PERIODIC SYSTEMS (+ CONTINUOUS FOCUSING

+ KINETIC MODES (GLUCKSTERN MODES)

+ FLUID MODES

INSTABILITIES

1. LONGITUDINAL (RESISTIVE WALL) INSTABILITY
   (FLUID INSTABILITY)

2. ELECTRON – ION INSTABILITY
   (CENTROID INSTABILITY)

STEVE TALKED ABOUT:
3. ENVELOPE INSTABILITIES

STEVE TALKED ABOUT:
4. KINETIC INSTABILITIES
   (DISTRIBUTION FUNCTION DEPENDENT)

5. SINGLE PARTICLE RESONANT INSTABILITIES
   – HALO
   – RING RESONANCES

HALO:

CORE TEST PARTICLE MODEL:

$$x'' = \begin{cases} -\left[k_{\beta 0}^2 - \dfrac{Q}{r_b^2}\right]x & \text{for } r < r_b \\ -\left[k_{\beta 0}^2 - \dfrac{Q}{r^2}\right]x & \text{for } r > r_b \end{cases}$$

$$r_b = r_{b0} + \delta r_b \cos(k_B s + \phi)$$

Gluckstern's phase-amplitude analysis:

$$x'' + \overbrace{\left[k_{\beta 0}^2 - \frac{Q}{r_{b0}^2}\right]}^{k_\beta^2} x = f(x)$$

Non linear + forcing part

$x = A\sin\psi \quad x' = k_\beta A\cos\psi$ ← PHASE/AMPLITUDE

$\psi = k_\beta s + \alpha$ If $f = 0$ A & ϕ would be constant

$\Rightarrow A' = \dfrac{1}{k_\beta r_{b0}} f\cos\psi \qquad \alpha' = \dfrac{-1}{k_\beta r_{b0} A} f\sin\psi$

DEFINE RESONANT PHASE $\Psi_r = 2\psi - k_B s$

AVERAGE OVER ALL NON-RESONANT FREQUENCIES

$$A_r' = \frac{1}{k_\beta r_{b0}} \int_{-\pi}^{\pi} f\cos\psi \frac{d\psi}{2\pi}; \quad \alpha_r' = \frac{-1}{k_\beta A_r}\int_{-\pi}^{\pi}\frac{d\psi}{2\pi} f\sin\psi$$

$\longrightarrow A_r', \Psi_r' \longrightarrow \omega', \Psi_r' \longrightarrow H(\omega, \Psi_r) \longrightarrow$ CORE RESONANT PARTICLE TRAJECTORY & SEPARATRIX

$(\omega = A_r^2)$

Numerically determined frequency and amplitude of particle oscillations: linear rf focusing

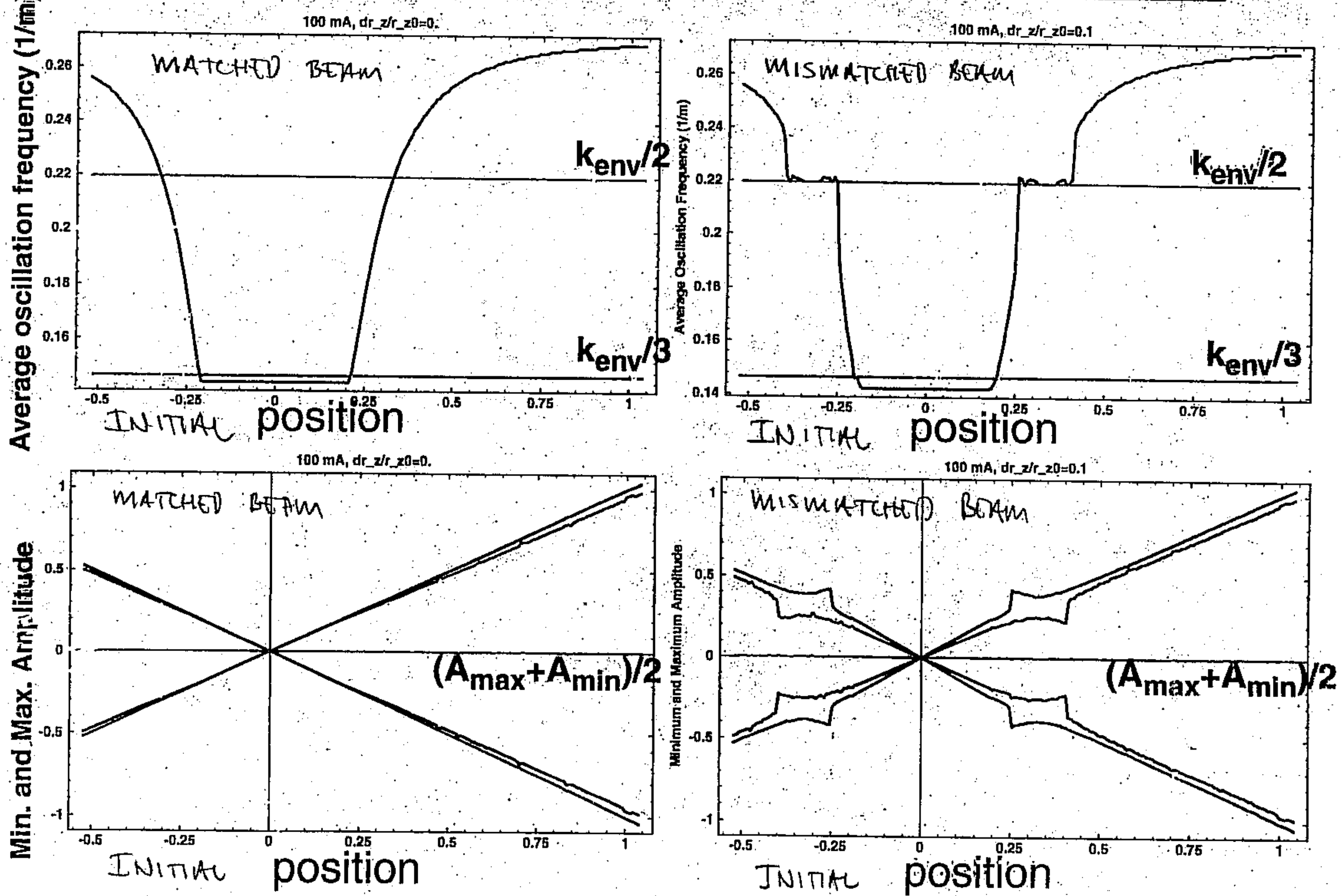

Processes:

1. Coulomb collisons (intra-beam)

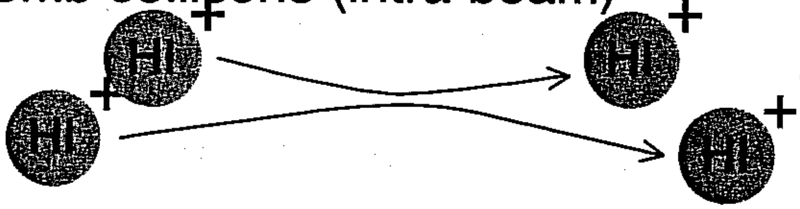

$$\frac{dT_\perp}{dt} = -\frac{1}{2}\frac{dT_\parallel}{dt} = -\frac{(T_\perp - T_\parallel)}{\tau}$$

$$\tau \sim \nu_c^{-1}$$

2. Coulomb collisions with residual gas

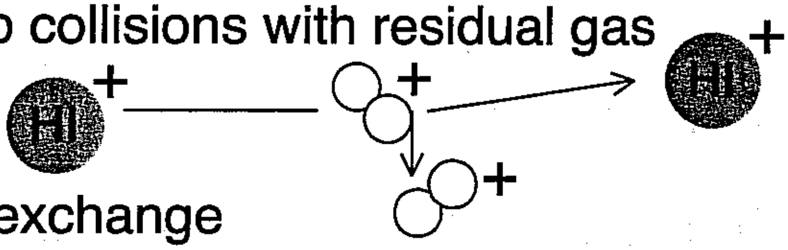

$$\frac{d\sigma_N}{ds} \sim n_g(\quad)$$

3. Charge exchange

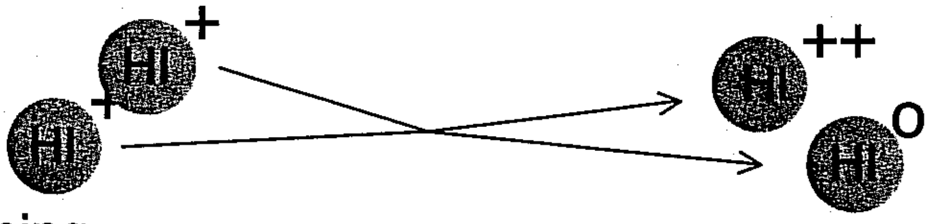

CHARGE CHANGING COLLISIONS

4. Stripping

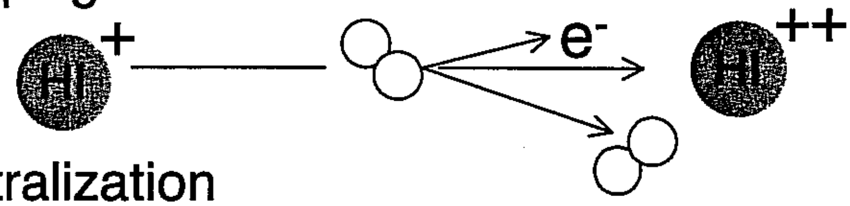

Beam loss

\+

n_{HI} molecules

5. Neutralization

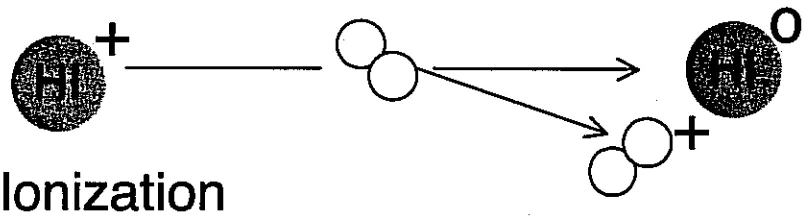

6. Gas Ionization

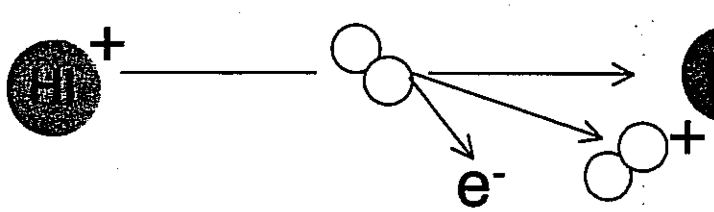

n_g molecules

SUMMARY OF ELECTRON, GAS, PRESSURE, & SCATTERING EFFECTS

1. COULOMB COLLISIONS WITHIN BEAM CAN TRANSFER ENERGY FROM $\perp$ TO $\parallel$ AND PROVIDE LOWER LIMIT ON $T_{\parallel}$, HIGHER THAN FROM ACCELERATIVE COOLING.

2. COULOMB INTERACTIONS WITH RESIDUAL GAS NUCLEI PROVIDE A SOURCE OF EMITTANCE GROWTH (BUT NOT IMPORTANT FOR HIGHER MASS AND LINAC RESIDENCE TIMES).

3. PRESSURE INSTABILITY FROM DESORPTION OF RESIDUAL GAS BY STRIPPED BEAM IONS HITTING WALL OR BEAM-IONIZED RESIDUAL GAS ATOMS, FORCED TO WALL BY E-field OF BEAM. LIMITS CURRENT IN RINGS OR HIGH REP RATE LINAC.

4. ELECTRONS CAN CASCADE AND REACH A "QUASI" EQUILIBRIUM POPULATION OF SIMILAR LINE CHARGE TO THE ION BEAM. ELECTRON-ION TWO STREAM INSTABILITY IS UNSTABLE, AND CAN LEAD TO TRANSVERSE INSTABILITY, SIMILAR TO WHAT IS OBSERVED IN SOME PROTON RINGS.

Inertial Fusion Energy (IFE) power plants of the future will consist of four parts